Hisato Kondoh · Atsushi Kuroiwa
Editors

New Principles in Developmental Processes

Springer

New Principles in Developmental Processes

Hisato Kondoh • Atsushi Kuroiwa
Editors

New Principles in Developmental Processes

Springer

Editors
Hisato Kondoh
Graduate School of Frontier Biosciences
Osaka University
Osaka, Japan

Atsushi Kuroiwa
Graduate School Science
Nagoya University
Nagoya, Japan

ISBN 978-4-431-54633-7 ISBN 978-4-431-54634-4 (eBook)
DOI 10.1007/978-4-431-54634-4
Springer Tokyo Heidelberg New York Dordrecht London

Library of Congress Control Number: 2013957687

Printed on acid-free paper

Springer is part of Springer Science+Business Media (www.springer.com)

Preface

Through modern investigations during the past decade, developmental biology has experienced a revolutionary change. The molecular and cellular processes in live embryos can now be visualized thanks to technologies using fluorescent proteins. The whole-genome information of a wide range of animal species has now become available, confirming the common principles that operate regardless of the particular species. These and other advances in our understanding of developmental processes during embryogenesis and tissue regeneration now allow us to formulate new principles, and it is high time to do so. The stem cell sciences, which branched from developmental biology, also require these new principles to generate a particular tissue by manipulating stem cells.

This book does not aim to cover the entire developmental biology field, which standard textbooks do. Instead, the book highlights representatives of emerging new principles, such as cell competition, tissue asymmetry, a farewell to classical germ layer theory, and various new insights into tissue morphogenesis and specification based on the most modern experimental approaches. The book will thus complement the major textbooks that tend to emphasize a chronological order of events and a comparison of animal models. This book, by contrast, focuses on the commonality of principles underlying diverse developmental processes that take place in different spatiotemporal contexts of development or in phylogenetically distant animal species.

New Principles in Developmental Processes was planned to introduce these new principles to readers working in developmental biology and stem cell biology fields, with an emphasis on genetic and cellular processes. The leading researchers in the new generation of developmental biologists were invited to be the authors who would undertake this task.

We expect two kinds of audiences: an academic audience in the developmental biology field, and a professional audience among those who are involved in stem cell sciences and biomedicine. We hope that the book will be widely read by those at the undergraduate, graduate, and postdoctoral levels as supplementary reading for textbooks because of its unique capability to complement those books.

Osaka, Japan — Hisato Kondoh
Nagoya, Japan — Atsushi Kuroiwa

Contents

Part VI Evolutional Variations Stemming from Common Principles

Part I
Making Cells Unequal in a Tissue to Form Embryos and Organs

Chapter 1
Taxon-Specific Maternal Factors for Germline Specification

Gaku Kumano

Abstract Despite the great diversity of animal forms, many genetic networks controlling developmental processes are remarkably conserved across animal species, such as between flies and mice. In many cases, conserved genetic networks rely on the use of homologous genes, such as Hox genes for the anterior–posterior patterning and NK-class genes for heart development. However, in the case of germline development, although the process itself including global repression of zygotic gene expression is conserved, participating components are often variable and taxon specific. Here I present our recent findings on germline development of the Japanese ascidian *Halocynthia roretzi*, as an example of conserved genetic mechanisms that do not rely on conserved genes.

Keywords Ascidian • Germline segregation • Maternal factor • Taxon-specific • Transcriptional repression

1.1 Germline Specification and the Ascidian Model

Germline development starts from the production of primordial germ cells (PGCs) that differentiate as eggs and sperm in later developmental stages. Metazoan species may be divided into two classes according to the timing and mechanism of the segregation of the germline (Extavour and Akam 2003; Juliano et al. 2010). In one group of metazoan species, the germline is segregated at early embryonic stages. In such cases, a specialized cytoplasm called the germplasm contains essential

G. Kumano (✉)
Asamushi Research Center for Marine Biology, Graduate School of Life Science, Tohoku University, Aomori, Japan
e-mail: kumano@m.tohoku.ac.jp

H. Kondoh and A. Kuroiwa (eds.), *New Principles in Developmental Processes*,
DOI 10.1007/978-4-431-54634-4_1,

maternal factors for germline development and is already localized in the egg. Accordingly, the lineage of cells that inherit the germplasm forms the germline. This type of mechanism to generate the germline is called "preformation." In the other group of metazoan species, PGCs are produced at certain points of ontogenesis without involvement of the maternal germplasm. This latter mechanism to generate the germline is called "epigenesis."

Once the germline is segregated from somatic cell lineages in either way, germline cells exhibit unique features, exemplified by the repression of zygotic gene expression (Nakamura and Seydoux 2008) to maintain their totipotent state. In such animals that develop germline cells by the "preformation" mechanism, such as *Drosophila*, nematodes, and ascidians, a central issue is the function of germplasm-associated maternally derived factors in the germline derivation.

Ascidians are marine invertebrate chordates that belong to the subphylum Urochordata, the sister group of vertebrates. The ascidian tadpole larva represents the basic body plan of all chordates; however, its embryogenesis proceeds with a much smaller number of cells when compared to vertebrates (e.g., approximately 100 cells at the onset of gastrulation in ascidians vs. 10,000 cells at the equivalent stage in frogs), and follows invariant cell lineages. These unique features among chordates make it possible to comprehensively understand cell fate specification mechanisms with one-cell resolution and have attracted many researchers over a century (Kumano and Nishida 2007).

The ascidian germline in its early development constitutes a lineage of cells that are positioned in the posterior end of the embryo at each cell cleavage stage (dark purple in Fig. 1.1a). By the 110-cell stage just before gastrulation starts, the cells in the germline have undergone three consecutive unequal cell divisions, the 8–16, 16–32, and 32–64 cell stages, which produce the smaller germline (B5.2, B6.3, or B7.6) and the larger somatic daughter cells (B5.1, B6.4, or B7.5) at each division (Fig. 1.1a). Through these cell divisions, the germline cells successively inherit a subcellular structure called the centrosome-attracting body (CAB; Fig. 1.1b), which contains germplasm-like structures (Iseto and Nishida, 1999) and deposits a number of maternal mRNAs called *postplasmic/PEM* mRNAs (Fig. 1.1c; Prodon et al. 2007), some of which are known to play roles in germline development. These cells then move inside the body during gastrulation and ultimately are located near the tip of the tail just adjacent to the notochord ventrally at the tailbud stage (Fig. 1.1a).

1.2 A Maternally Deposited Posterior End Mark as an Inhibitor of Gene Expression in Germline Cells

During early ascidian embryogenesis, a germline cell divides to produce the germline and somatic daughter cells, which suggests that loss of a mechanism that is inherited by germline cells leads to the somatic cells.

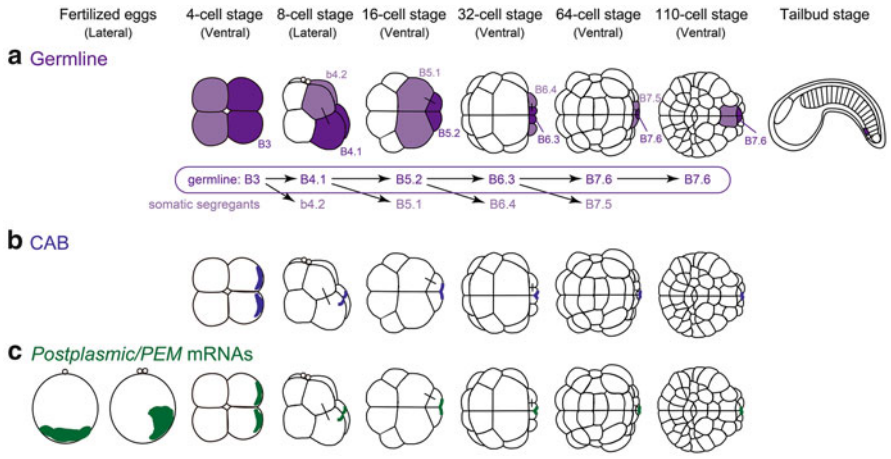

Fig. 1.1 Schematic diagram of ascidian embryos at different developmental stages. Lateral views: fertilized eggs, 8-cell and tailbud stage embryos; vegetal views: 4-cell, 16-cell, 32-cell, 64-cell, and 110-cell stage embryos. Anterior is to the *left*. The germline cells and the siblings (connected by *black lines*) are *colored dark* and *light purple*, respectively (**a**). Blastomeres are numbered according to Conklin (1905). The germline cells divide to produce a germline and somatic daughter cells through the 64-cell stage, but do not divide at the division to the 110-cell stage. They inherit the germplasm-like structure-containing CAB (centrosome-attracting body) whose positions are shown in *blue* in (**b**) and *postplasmic/PEM* mRNAs whose localization is shown in *green* in (**c**)

In our earlier study, we found that a maternal factor posterior end mark (PEM) was involved in *Halocynthia* embryo patterning (Kumano and Nishida 2009). *PEM* is unique to ascidians and belongs to *postplasmic/PEM* mRNAs. The transcripts localize in the germplasm-like CAB during the cleavage stages (Fig. 1.1; Negishi et al. 2007) and are carried by the germline daughter cell while segregating the non-carrier somatic daughters upon cell division during the process to generate posterior somatic cells. The CAB is thought to be the place where *postplasmic/PEM* mRNAs are translated. Consistently, PEM protein is found in the CAB (Negishi et al. 2007), and also in the nuclei of the germline cells (Kumano et al. 2011), where it presumably functions. Knockdown of PEM function in the germline cells by injecting antisense morpholino oligonucleotides (MOs) activated expression of genes characteristic of the somatic cells in the germline, whereas ectopic expression of PEM in the somatic cells by injecting in vitro synthesized *PEM* mRNA inhibited somatic-type gene expression. These observations suggested that PEM confers a germline-characteristic mechanism by globally repressing zygotic gene expression in the germline of the *Halocynthia* embryo.

It is known in *Drosophila* and *Caenorhabditis elegans* that the germline-associated global repression of zygotic gene transcription is mediated by the inhibition of phosphorylation of the RNA polymerase II (RNAP II) C-terminal domain (CTD), which is essential for the transcribed RNA elongation (Nakamura and Seydoux 2008). Even in mouse embryos where germline cells are produced by the "epigenesis"

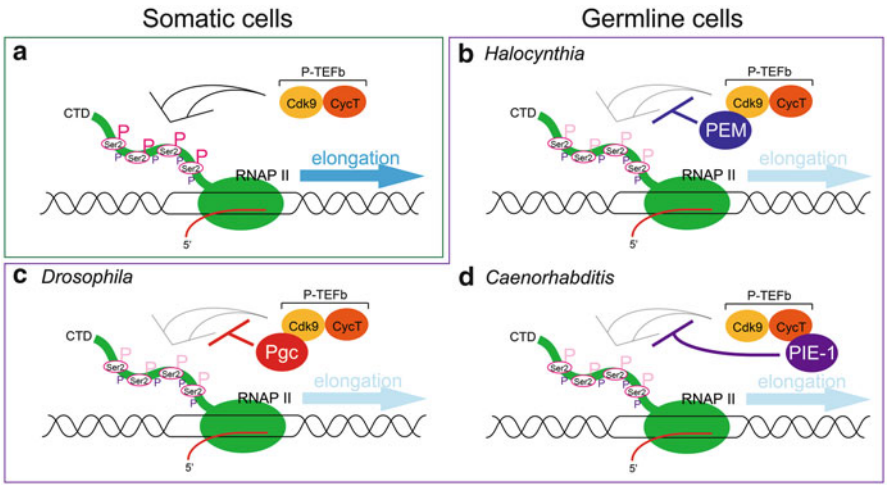

Fig. 1.2 Mechanisms of transcriptional repression during germline specification. (**a)** During mRNA transcription, the P-TEFb complex composed of Cdk9 (*yellow*) and cyclin T (*orange*) phosphorylates CTD-Ser2 (*pink*) of RNAP II (*green*) that has paused after the initiation of transcription. The phosphorylation leads to productive elongation (*light blue arrow*). CTD serine 5 residues that are phosphorylated during transcription initiation are indicated by small purple Ps. (**b)** In *Halocynthia* germline cells, PEM binds to Cdk9 and underphosphorylates CTD-Ser2 to inhibit transcription elongation. (**c)** In *Drosophila* pole (germline) cells, Pgc keeps P-TEFb from being recruited to chromatin by binding to Cdk9 and inhibits RNAP II phosphorylation (Hanyu-Nakamura et al. 2008). (**d)** In *Caenorhabditis* early germline cells (P_2–P_4 blastomeres), PIE-1 binds to cyclin T and prevents P-TEFb from interacting with and phosphorylating CTD-Ser2 (Batchelder et al. 1999; Zhang et al. 2003)

mechanism, RNAP II is temporally underphosphorylated, although it occurs during the PGC migration to the gonad following the first wave of germline gene expression (Seki et al. 2007). Considering these precedences, we analyzed the phosphorylation state of the second serine residues of heptapeptide repeats in the C-terminal domain (CTD-Ser2) of RNAP II in the *Halocynthia* early germline cells by antibody staining. As a result, CTD-Ser2 phosphorylation was very low in these cells (Kumano et al. 2011), consistent with other observations that the *Halocynthia* germline cells lack zygotic gene transcription (Tomioka et al. 2002; Kumano et al. 2011).

We found that PEM is necessary and sufficient for the repression of gene expression in the germline through the regulation of CTD-Ser2 phosphorylation. Knockdown of PEM function resulted in CTD-Ser2 phosphorylation and ectopic gene expression in the germline cells; forced expression of PEM in somatic cells inhibited CTD-Ser2 phosphorylation and zygotic gene expression in these cells (Kumano et al. 2011). We further identified the region of amino acids (aa) 342–426 of PEM that is required for its transcriptional repression activity (Kumano et al. 2011). This aa region is necessary and sufficient for the binding of PEM to CDK9, a component of the P-TEFb complex that phosphorylates CTD-Ser2 during transcriptional elongation (Fig. 1.2a).

PEM has another function to regulate unequal cell divisions that produce smaller germline daughter cells and larger somatic daughters in the posterior end of the cleaving embryos (Negishi et al. 2007) (Fig. 1.1). This function requires aa 258–341 of PEM (Kumano et al. 2011). Therefore, two functions of PEM are borne by two adjacent yet distinct domains of the PEM protein.

Taken together, our observations indicate that PEM, a maternal, locally deposited factor unique to ascidians, represses germline gene expression through binding to the P-TEFb complex and inhibiting CTD-Ser2 phosphorylation (Fig. 1.2b).

1.3 Evolutionary Perspectives

It is interesting to compare the function of PEM in *Halocynthia* embryos with well-characterized cases of global gene silencing in *Drosophila* and *C. elegans* germlines. It is known that maternally localized germplasm factors PIE-1 of *C. elegans* and Pgc of *Drosophila* bind to the P-TEFb complex and underphosphorylate CTD-Ser2 in RNAP II (Fig. 1.2c, d; Seydoux and Dunn 1997; Batchelder et al. 1999; Zhang et al. 2003; Hanyu-Nakamura et al. 2008; Timinszky et al. 2008). PIE-1 and Pgc are relatively new genes in phylogeny and found only in *Caenorhabditis* and *Drosophila*, respectively, similar to PEM in ascidians. This result indicates that different proteins, PIE-1, Pgc, and PEM, are employed in the germline-characteristic global repression of gene expression, by causing CTD-Ser2 underphosphorylation through binding to the P-TEFb complex (Fig. 1.2), thus posing an interesting example of the conservation of the regulatory network without employing homologous gene-coded proteins.

Besides PIE-1, Pgc, and PEM, which fulfill the task of inhibiting CTD-Ser2 phosphorylation, protein factors that regulate the assembly of the germplasm at the top of its hierarchy are also taxon specific. These proteins for germplasm assembly, although divergent, recruit phylogenetically conserved essential components, such as *vasa* and *nanos* gene products.

In *Drosophila*, Oskar has as its function to assemble the germplasm and recruit Vasa and *nanos* (Breitwieser et al. 1996; Ephrussi et al. 1991; Kim-Ha et al. 1995). In *C. elegans*, the germplasm assembly factors PGL-1/3 recruit Vasa (Hanazawa et al. 2011). In zebrafish, Bucky ball recruits *vasa* and *nanos* to organize the germplasm (Bontems et al. 2009). In *Xenopus*, the species-unique Xpat is capable of inducing ectopic germplasm-like structures (Machado et al. 2005). Thus, taxon-specific nonhomologous proteins share molecular functions essential for germline specification (summarized in Table 1.1).

Recently, it was proposed that the “epigenesis”-dependent mechanism is the ancestral form of germline specification, and the “preformation” mechanism via the germplasm has evolved independently in multiple bilaterian lineages from the ancestral “epigenesis” mechanism (Fig. 1.3; Extavour 2007), although it is still controversial (Leclère et al. 2012). This new proposal is consistent with the

Table 1.1 Two classes of germline-characteristic genes

Conserved germline genes			
Gene name	Molecular function	Germline or multipotent stem cell line expression described	References
Vasa	RNA helicase, translational regulator	Ct, Cn, Pl, Mo, An, Ne, Ar, Ec, Ch	Juliano et al. (2010) and Alié et al. (2011)
Nanos	Zinc-finger protein, translational repressor	Cn, Pl, Mo, An, Ne, Ar, Ec, Ch	Juliano et al. (2010)
Piwi	piRNA binding	Po, Ct, Pl, An, Ne, Ar, Ec, Ch	Juliano et al. (2010) and Alié et al. (2011)
Pumilio	Nanos binding, translational repressor	Ne, Ar, Ch	Ewen-Campen et al. (2010)
Tudor	Protein binding	Ar, Ch	Ewen-Campen et al. (2010)
Dazl	RNA-binding protein	Ne, Ar, Ch	Ewen-Campen et al. (2010)
Germ-cell-less	Protein binding	Ar, Ch	Ewen-Campen et al. (2010)
Maelstrom	Unknown	Ar, Ch	Ewen-Campen et al. (2010)
Staufen	RNA binding	Ar, Ch	Ewen-Campen et al. (2010)

Taxon-unique germline genes			
Gene name	Molecular function	Occurrence in genome	References
PEM	Transcriptional repressor	Ascidians	Kumano et al. (2011)
Pgc	Transcriptional repressor	*Drosophila*	Hanyu-Nakamura et al. (2008) and Kumano et al. (2011)
Pie-1	Transcriptional repressor	Nematodes	Kumano et al. (2011)
Bucky ball	Germplasm assembly	Vertebrates	Ewen-Campen et al. (2010)
Oskar	Germplasm assembly	Insects	Ewen-Campen et al. (2010, 2012)
PGL	Germplasm assembly	Nematodes	Hanazawa et al. (2011)
Xpat	Germplasm assembly	*Xenopus*	Machado et al. (2005)

Po Porifera, *Ct* Ctenophora, *Cn* Cnidaria, *Pl* Platyhelminthes, *Mo* Mollusca, *An* Annelida, *Ne* Nematoda, *Ar* Arthropoda, *Ec* Echinodermata, *Ch* Chordata

involvement of taxon-dependent nonhomologous proteins in the same germline specification processes. Genes encoding these proteins could have arisen as novel genes and participated in the "preformation," or, alternatively, they could have derived from preexisting genes by gaining germline roles. In the case of *oskar*, a recent study indicates that it existed earlier than the evolution of the germplasm and had an ancestoral role in neural development (Ewen-Campen et al. 2012). Moreover, the new role of this gene to assemble the germplasm could have occurred

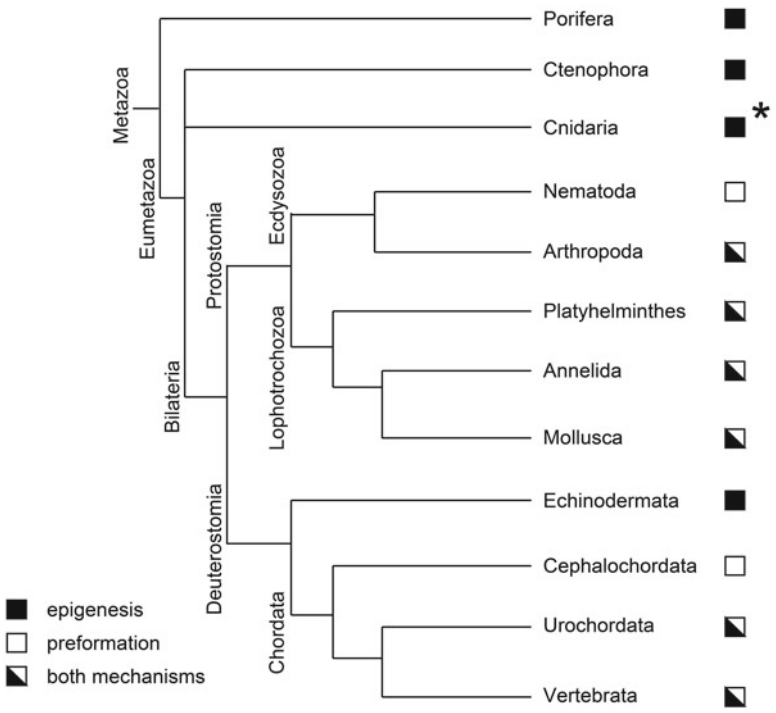

Fig. 1.3 Phylogenetic distribution of germline segregation mechanisms among metazoan species. Epigenesis (*black squares*), preformation (*open squares*), or both mechanisms (*black* and *white squares*) are indicated. See Extavour (2007) for more species. A different distribution pattern may arise as molecular data of more species become available. Note that in *Clytia hemisphaerica*, a cnidarian species, although germline mRNAs are maternally deposited and localized in the egg, germline cells are segregated by the "epigenesis" mechanism (Leclère et al. 2012)

in an evolutionarily conserved gene network, because multiple germplasm genes, such as *nanos*, *pumilio*, and *vasa* (all conserved genes; Table 1.1), are coexpressed with *oskar* in the nervous system in a variety of insect species (Ewen-Campen et al. 2012).

Another interest is why RNAP II is targeted for transcriptional repression in the germline. It would be an efficient way to globally silence gene expression, but may have another reason, namely, that the genes essential for somatic development need to be activated immediately after separation from the germline, in particular, at the fast-developing cell cleavage stages. Transcription that is stalled before the elongation step would enable immediate start of mRNA synthesis after segregation from the germline after cell division. This quick response mechanism has been demonstrated for many developmentally regulated genes in *Drosophila* (Levine 2011). Indeed, in ascidian embryos, some of the transcription factors that are essential for somatic tissue development, for example, *FoxA* and *Not*, are quickly synthesized after the separation from the germline (Kumano et al. 2011).

1.4 Conclusions

Two types of mechanisms exist for germline specification, namely, the "preformation" type that depends on locally deposited maternal factors and is characterized by germline segregation at early stages of development, and the "epigenesis" type, where germline segregation occurs at later stages of ontogenesis. In the former case, two functions are involved in keeping the germline cells, the organization of the germplasm and the germline-specific transcriptional repression via inhibition of RNAP II CTD phosphorylation causing RNAP II stalling. Although these two functions are common to all "preformation"-type species, the proteins that have central roles in these functions are variable and taxon specific. This situation makes a sharp contrast with many other cases where homologous functions are borne by conserved genes. However, this variation of germline-determining genes may be explained by a recently proposed model that the "epigenesis"-type germline segregation mechanism, rather than the "preformation" type, is the ancestral form.

Acknowledgments I thank Dr. H. Nishida's laboratory members for stimulating discussions.

References

Alié A, Leclère L, Jager M, Dayraud C, Chang P, Le Guyader H, Quéinnec E, Manuel M (2011) Somatic stem cells express *Piwi* and *Vasa* genes in an adult ctenophore: ancient association of "germline genes" with stemness. Dev Biol 350:183–197

Batchelder C, Dunn MA, Choy B, Suh Y, Cassie C, Shim EY, Shin TH, Mello C, Seydoux G, Blackwell TK (1999) Transcriptional repression by the *Caenorhabditis elegans* germ-line protein PIE-1. Genes Dev 13:202–212

Bontems F, Stein A, Marlow F, Lyautey J, Gupta T, Mullins MC, Dosch R (2009) Bucky ball organizes germ plasm assembly in zebrafish. Curr Biol 19:414–422

Breitwieser W, Markussen F-H, Horstmann H, Ephrussi A (1996) Oskar protein interaction with Vasa represents an essential step in polar granule assembly. Genes Dev 10:2179–2188

Conklin EG (1905) The organization and cell lineage of the ascidian egg. J Acad Nat Sci 13:1–119

Ephrussi A, Dickinson LK, Lehmann R (1991) Oskar organizes the germ plasm and directs localization of the posterior determinant *nanos*. Cell 66:37–50

Ewen-Campen B, Schwager EE, Extavour CGM (2010) The molecular machinery of germ line specification. Mol Reprod Dev 77:3–18

Ewen-Campen B, Srouji JR, Schwager EE, Extavour CG (2012) *Oskar* predates the evolution of germ plasm in insects. Curr Biol 22:2278–2283

Extavour CGM (2007) Evolution of the bilaterian germ line: lineage origin and modulation of specification mechanisms. Integr Comp Biol 47:770–785

Extavour CG, Akam M (2003) Mechanisms of germ cell specification across the metazoans: epigenesis and preformation. Development 130:5869–5884

Hanazawa M, Yonetani M, Sugimoto A (2011) PGL proteins self associate and bind RNPs to mediate germ granule assembly in *C. elegans*. J Cell Biol 192:929–937

Hanyu-Nakamura K, Sonobe-Nojima H, Tanigawa A, Lasko P, Nakamura A (2008) *Drosophila* Pgc protein inhibits P-TEFb recruitment to chromatin in primordial germ cells. Nature (Lond) 451:730–733

Iseto T, Nishida H (1999) Ultrastructural studies on the centrosome-attracting body: electron-dense matrix and its role in unequal cleavages in ascidian embryos. Dev Growth Differ 41: 601–609

Juliano CE, Swartz SZ, Wessel GM (2010) A conserved germline multipotency program. Development (Camb) 137:4113–4126

Kim-Ha J, Kerr K, Macdonald PM (1995) Translational regulation of *oskar* mRNA by bruno, an ovarian RNA-binding protein, is essential. Cell 81:403–412

Kumano G, Nishida H (2007) Ascidian embryonic development: an emerging model system for the study of cell fate specification in chordates. Dev Dyn 236:1732–1747

Kumano G, Nishida H (2009) Patterning of an ascidian embryo along the anterior-posterior axis through spatial regulation of competence and induction ability by maternally localized PEM. Dev Biol 331:78–88

Kumano G, Takatori N, Negishi T, Takada T, Nishida H (2011) A maternal factor unique to ascidians silences the germline via binding to P-TEFb and RNAP II regulation. Curr Biol 21:1308–1313

Leclère L, Jager M, Barreau C, Chang P, Le Guyader H, Manuel M, Houliston E (2012) Maternally localized germ plasm mRNAs and germ cell/stem cell formation in the cnidarian *Clytia*. Dev Biol 364:236–248

Levine M (2011) Paused RNA polymerase II as a developmental checkpoint. Cell 145:502–511

Machado RJ, Moore W, Hames R, Houliston E, Chang P, King ML (2005) *Xenopus* Xpat protein is a major component of germ plasm and may function in its organization and positioning. Dev Biol 287:289–300

Nakamura A, Seydoux G (2008) Less is more: specification of the germline by transcriptional repression. Development (Camb) 135:3817–3827

Negishi T, Takada T, Kawai N, Nishida H (2007) Localized PEM mRNA and protein are involved in cleavage-plane orientation and unequal cell divisions in ascidians. Curr Biol 17:1014–1025

Prodon F, Yamada L, Shirae-Kurabayashi M, Nakamura Y, Sasakura Y (2007) Postplasmic/PEM RNAs: a class of localized maternal mRNAs with multiple roles in cell polarity and development in ascidian embryos. Dev Dyn 236:1698–1715

Seki Y, Yamaji M, Yabuta Y, Sano M, Shigeta M, Matsui Y, Saga Y, Tachibana M, Shinkai Y, Saitou M (2007) Cellular dynamics associated with the genome-wide epigenetic reprogramming in migrating primordial germ cells in mice. Development (Camb) 134:2627–2638

Seydoux G, Dunn MA (1997) Transcriptionally repressed germ cells lack a subpopulation of phosphorylated RNA polymerase II in early embryos of *Caenorhabditis elegans* and *Drosophila melanogaster*. Development (Camb) 124:2191–2201

Timinszky G, Bortfeld M, Ladurner AG (2008) Repression of RNA polymerase II transcription by a *Drosophila* oligopeptide. PLoS ONE 3:e2506

Tomioka M, Miya T, Nishida H (2002) Repression of zygotic gene expression in the putative germline cells in ascidian embryos. Zool Sci 19:49–55

Zhang F, Barboric M, Blackwell TK, Peterlin BM (2003) A model of repression: CTD analogs and PIE-1 inhibit transcriptional elongation by P-TEFb. Genes Dev 17:748–758

Chapter 2
Establishment of Anterior–Posterior Axis in the Mouse Embryo

Katsuyoshi Takaoka

Abstract The anterior–posterior (A–P) axis is the first established and morphologically discernible axis of the body during mouse development. From embryonic day (E) 4.5 to E6.5 of mouse embryos, the formation of the distal visceral endoderm (DVE) followed by that of the anterior visceral endoderm (AVE) breaks the A–P symmetry of the embryo. The DVE progenitor cells arise in primitive endoderm (PrE) cells of the late blastocyst with an asymmetrical distribution. This asymmetry may contribute to the determination of the A–P axis in later embryos. At E5.5, DVE cells mature, and migrate from the distal tip to the future anterior side. The DVE migration guides the migration of newly formed AVE and trigger the extensive movement of visceral endoderm (VE) cells in a wide area. Our observations revise the earlier model about AVE development, namely, that the AVE is directly derived from the DVE.

Keywords Anterior–posterior axis • AVE • Blastocyst • DVE • Implantation

2.1 Introduction

Vertebrates have three principal body axes: the anterior–posterior (A–P), dorsal–ventral (D–V), and left–right (L–R) axes. In many animal species, the A–P axis is the first morphologically discernible body axis. How and at which stage of development is the A–P axis determined? The answer depends on the animal species. Establishment of the A–P axis is based on early molecular asymmetry. In *Drosophila melanogaster*, the A–P axis is defined during oogenesis by the asymmetrical deposition of maternal mRNAs along two poles of the oocyte (Huynh and St. Johnston 2004).

K. Takaoka (✉)
Developmental Genetics Group, Graduate School of Frontier Biosciences, Osaka University, 1-3 Yamada-oka, Suita, Osaka 565-0871, Japan
e-mail: katsuo@fbs.osaka-u.ac.jp

H. Kondoh and A. Kuroiwa (eds.), *New Principles in Developmental Processes*,
DOI 10.1007/978-4-431-54634-4_2,

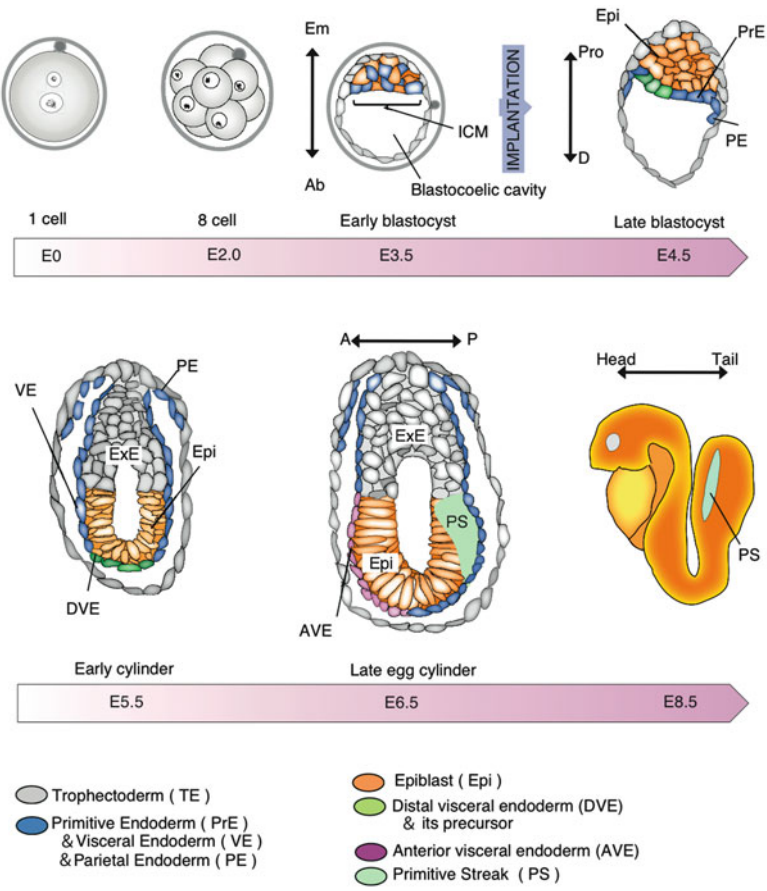

Fig. 2.1 Axis formation of early mouse embryo development. In the early blastocyst, the Em–Ab (embryo–abembryo) axis is defined by the position of the inner cell mass (*ICM*). After the implantation, the Em–Ab axis and the Pro–D axis of the late blastocyst are aligned in the same direction. The proximal side corresponds to the mesometrial side in the uterus. From E5.5 to E6.5, the anterior–posterior (*A–P*) axis of an embryo is established by DVE migration, which is followed by AVE formation. The cell types in the embryos are color coded. *AVE* anterior visceral endoderm, *DVE* distal visceral endoderm, *E* embryonic day, *Epi* epiblast, *Exe* extra-embryonic ectoderm, *PrE* primitive ectoderm, *PE* parietal endoderm, *PS* primitive streak, *VE* visceral endoderm, *Em–Ab* embryonic–abembryonic axis, *Pro–D* proximal–distal axis, *A–P* anterior–posterior axis

In the mouse, the initial process to develop A–P asymmetry has been poorly understood, although several recent reports showed that early A–P molecular asymmetry can be traced back at least to the peri-implantation embryos.

The fertilized mouse egg undergoes cell divisions, increasing the number of blastomeres, and reaches the early blastocyst stage at E3.5 (Fig. 2.1). The early blastocyst is composed of two types of cells: inner cell mass (ICM) and trophectoderm (TE). The ICM contributes to the future embryonic tissues whereas TE contributes

to placental tissues (Yamanaka et al. 2006). The orientation of ICM and its cavity defines the embryonic–abembryonic (Em–Ab) axis of the blastocyst. In the late blastocyst, the Em–Ab axis corresponds to the proximal–distal (Pro–D) axis, in reference to the site of implantation within the mesometrial tissue of the uterus. At this stage, the ICM has contributed to two cell lineages: the PrE and the epiblast (Epi). The PrE first appears as an epithelial monolayer adjacent to the blastocoelic cavity. By E5.5, the PrE gives rise to the VE, lining the surface of the Epi, and to the parietal endoderm (PE), which is located along the TE. A subset of VE cells that are located at the distal tip of the embryo at E5.5 is called the DVE. DVE cells start to migrate toward the future anterior side. At E6.5, AVE cells are indeed located on the anterior side (Rossant and Tam 2009; Takaoka and Hamada 2012). The AVE-derived signals induce head structures on the nearby Epi and primitive streak (PS) on the opposite side; this is followed by the development of head–tail patterning and segmentation in embryos (Tam and Loebel 2007) (Fig. 2.1).

In this chapter, I discuss the mechanisms of A–P axis formation in mouse embryo development concerning cell fate specification, dynamics of cellular arrangements, and effective molecular signaling (Fig. 2.2).

2.2 Origin of DVE in the Blastocyst

DVE cells express several genes such as Nodal antagonists *Lefty1* and *Cerl1* (Meno et al. 1996; Perea-Gomez et al. 2002; Yamamoto et al. 2004), as well as Wnt antagonist *Dkk1* (Kimura-Yoshida et al. 2005). It has been thought that the A–P axis is firmly established when DVE cells located at the distal tip of the embryo migrate toward the future anterior side at E5.5. By this time, the expression domains of the Nodal antagonists *Lefty1* and *Cerl1* in the VE have already been shifted toward the future anterior side. Although the aforementioned asymmetrical cell organization clearly indicates the A–P difference, recent investigations based on fate mapping of *Lefty1*-expressing cells and live imaging of individual cells suggested that DVE cells are derived from *Lefty1*-expressing cells of the late blastocyst (Fig. 2.2). *Lefty1*-expressing cells arise as a small cluster in the PrE of late blastocysts. This asymmetrical expression may determine the future direction of the A–P axis, and the origin of the A–P axis can be traced back to the peri-implantation stage from the egg cylinder stage.

How is asymmetrical *Lefty1* expression induced to a subset of PrE cells? Three possible models can be considered. Expression of *Lefty1* is regulated by Nodal signaling in PrE cells via the activation of an enhancer (APE) located in the upstream region of the *Lefty1* gene, in response to *Nodal*/*Foxh1* signal inputs. Thus, a possible model is that a component of Nodal signaling system is expressed in an asymmetrical manner. However, Nodal ligand, Nodal-downstream transcription factor FoxH1, and Nodal co-receptor Cripto are uniformly expressed in the Epi and VE cells from the late-blastocyst to early-egg cylinder stage. (Takaoka et al. 2006). An unknown factor required for Nodal signaling may be expressed asymmetrically.

Anterior-Posterior patterning (lateral view)
A
P
Cuboidal
Columnar
A. DVE progenitors (section along the middle)
B. Immature DVE cells
C. Mature DVE
D. DVE migration & new AVE formation
E. AVE migration
F. Patterning of epiblast by AVE
E4.2
E5.2
E5.5
E5.7
E6.0
E6.5
section along the middle
Epi
PrE
Pro
D
PE
Late blastocyst
VE
Epi
ExE
PE
DVE
Early cylinder
PS
ExE
Epi
AVE
Late egg cylinder
Trophectoderm (TE)
Primitive Endoderm (PrE) & Visceral Endoderm (VE) & Prietal Endoderm (PE)
Epiblast (Epi)
Primitive Streak (PS)
DVE-lineage cells expressing Lefty1
DVE descendents that have lost Lefty1 expression
AVE progenitors negative for Lefty1 expression
AVE expressing Lefty1
DVE cells migration
AVE cells migration
Patterning of epiblast by AVE
Primitive streak

Fig. 2.2 A–P axis formation during mouse embryo development: origins and migrations of the DVE and the AVE in embryo patterning along the A–P axis. The DVE lineage is shown in *green* and the AVE lineage is shown in *purple cells*; *solid coloring* indicates cells that express *Lefty1*, whereas coloring only in outline indicates cells without Lefty1 expression. (**a**) At E4.2, *Lefty1* is expressed in the DVE progenitors (*green*). (**b**) Immature DVE cells, which maintain *Lefty1* expression but are negative for other DVE markers such as *Cerl1* and *Hex*, are found at the distal tip of the embryo at E5.2. (**c**) At E5.5, matured DVE cells express *Lefty1* and other DVE markers. Shapes of DVE cells change to columnar. DVE cells migrate to the future anterior side of the embryo. (**d**) At E5.7, DVE cells migrate away from the distal tip, and VE cells negative for *Lefty1* expression (*open magenta shapes*) move to the distal tip and become new AVE cells. (**e**) At E6.0, DVE cells that have reached the embryonic/extra-embryonic junction migrate laterally and lose expression of DVE markers, including *Lefty1*. AVE cells remain newly generated at the distal tip and also migrate toward the proximal side. (**f**) At E6.5, the AVE occupies the anterior side of the embryo, and creates A–P patterning in the Epi. *AVE* anterior visceral endoderm, *DVE* distal visceral endoderm, *E* embryonic day, *Epi* epiblast, *Exe* extra-embryonic ectoderm, *PrE* primitive ectoderm, *PS* primitive streak, *VE* visceral endoderm, *Pro–D* proximal–distal axis, *A–P* anterior–posterior axis

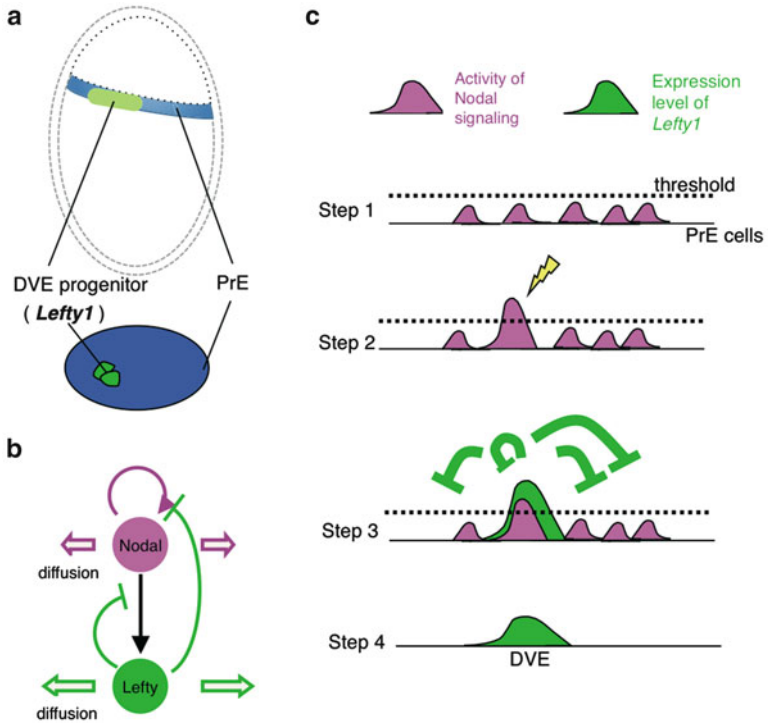

Fig. 2.3 Model for the self-enhancement lateral inhibition (*SELI*) mechanism in DVE formation. (**a**) Observation: *Lefty1*-positive cells (*green*), putative DVE progenitors, appear as a very small population of PrE cells (*blue*). (**b**) Scheme of cross-regulation between Nodal and Lefty 1. Lefty1 (*green*) is induced by Nodal signaling (*magenta*), and Nodal signaling is inhibited by a negative feedback. (**c**) Model: PrE cells have a threshold for the Nodal signaling activity that allows *Lefty1* activation (step 1). By a stochastic mechanism, the activity of Nodal signaling exceeds the threshold in a fraction of PrE cells (*yellow arrows*, step 2). Then, Lefty1 expression is activated in these cells, and the activated Lefty1 inhibits Nodal signaling in other PrE cells (step 3). The DVE is formed (step 4)

The second model assumes crosstalk of these signaling systems with other signaling pathways. Wnt is a candidate signaling system that crosstalks with other systems. The nuclear localization of β-catenin, which is indicative of active Wnt signaling, was observed in late blastocysts detected in a single Epi cell that faces the PrE (Chazaud and Rossant 2006). In addition, investigation on microarray profiling of β-catenin mutant embryos identified Cripto, a Nodal co-receptor, as a β-catenin target gene (Morkel et al. 2003). These results suggest that *Nodal* signaling is readily activated with Wnt signal input.

The third model, the restriction of *Lefty1* expression to a subset of ICM cells, involves a self-enhancement lateral inhibition (SELI) mechanism, which amplifies a small difference of *Nodal* signaling activities into a robust asymmetry, as has been demonstrated for the left–right embryo patterning (Nakamura et al. 2006; Nakamura and Hamada 2012) (Fig. 2.3). Lefty1 is induced by Nodal signaling, and Nodal is

regulated by the *Activin/Nodal* signaling-dependent enhancer of *Nodal* (ASE) in a subset of ICM cells (Granier et al. 2011). These coordinated activities of Nodal and its feedback inhibitor Lefty meet the requirements for the SELI system.

2.3 Maturation of DVE and DVE Migration

From E4.5 to E5.5, expression of *Lefty1* is cell autonomously maintained in the DVE progenitor to mature DVE cells. At E5.5, a greater variety of genes such as *Cerl1*, *Hex*, and *Dkk1* are expressed in the DVE, suggesting that signaling systems change as the DVE cells become mature. In this signaling system, bone morphogenetic protein (BMP) signaling plays an important role. *BMP4*, which is expressed in ExE (extra-embryonic ectoderm) cells, generates a gradient of BMP signaling in the embryonic Epi and VE tissues. The DVE progenitors are confined to the distal tip of embryos corresponding to the BMP signaling-negative portion from E5.2 to E5.5. The BMP signaling thus restricts the DVE region to the distal tip of embryos. Indeed, ExE-removed embryos show an expansion of the DVE region (Rodriguez et al. 2005; Yamamoto et al. 2009) (Fig. 2.4).

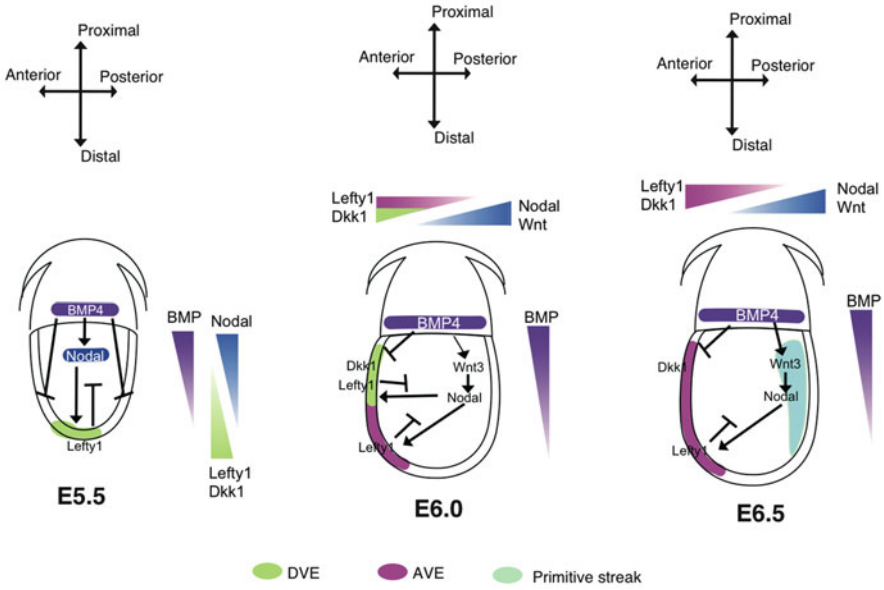

Fig. 2.4 Changes in the network of signaling systems during the developmental stages for DVE migration and AVE formation. Major changes in the spatial organization of the signaling system are caused by the migrations of DVE (*green*) and AVE (*magenta*) cells. After E5.5, the DVE migration transforms the P–D differences in the signaling systems into the A–P differences. At E6.0 and E6.5, signals from the AVE specify the nearby Epi by inhibiting Nodal signaling and Wnt signaling. On the opposite side far from the AVE, Nodal and Wnt signaling remains active, which results in the formation of the primitive streak (*light blue*). Activities of bone morphogenetic protein (*BMP*), Nodal, and Wnt are indicated by *purple* and *blue triangles*, respectively

Alongside their maturation, DVE cells migrate to the future anterior side of the early egg cylinder embryos. Immediately before their migration, three morphological changes take place in the DVE cells. The first is "visceral endoderm thickening" (VET), which makes the entire VE a monolayer of tall columnar cells (Rivera-Perez et al. 2003; Srinivas 2006; Takaoka et al. 2011) (Fig. 2.2).

Second, lamellipodia- and filopodia-like structures are formed in migrating DVE cells (Rakeman and Anderson 2006; Migeotte et al. 2010). In the VE-specific conditional mutant embryo lacking the Rho family GTPase Rac1, a component of WAVE complex (a regulator of the actin cytoskeleton), the lamellipodia- and filopodia-like structures fail to form. As a result, DVE cells fail to migrate away from the distal tip. In *Nap1* mutant embryos also, lacking a component of WAVE complex, DVE cells fail to migrate (Rakeman and Anderson 2006). These observations indicate that dynamic cytoskeletal reorganization regulated by the WAVE complex is required for the correct DVE migration.

Third, at a more macroscopic level, DVE cells form multicellular rosettes. Rosettes of five or more cells, sharing a central vertex, are formed in the simple epithelium of VE during the migration of DVE. Formation of the cellular rosettes depends on PCP signaling, and is supposed to buffer the structural disturbance in cell packing in an epithelium caused by DVE migration (Trichas et al. 2012).

2.4 The Direction of the A–P Axis

At E5.5, DVE cells migrate to the future anterior side. It is a critical issue whether the direction of A–P is determined before the DVE migration. First, several studies suggest that embryos have A–P asymmetry before the DVE migration. One suggestion is that the expression domains of the Nodal antagonists *Lefty1* and *Cerl1* are already shifted toward the future anterior side before E5.5. Forced expression of Nodal antagonist Lefty1 at E5.2 causes asymmetry in Nodal signaling and initiates the migration of DVE (Yamamoto et al. 2004). Similarly, Wnt antagonist and *Dkk1* expression domains change dynamically between before and after DVE migration, and the ectopic activation of *Dkk1* can alter the direction of DVE cell migration (Kimura-Yoshida et al. 2005). These reports suggested that embryos may have A–P pre-patterning before E5.5. However, DVE still migrates unilaterally toward the proximal side in mutant mice that lack both *Lefty1* and *Cerl1* (Perea-Gomez et al. 2002; Yamamoto et al. 2004) or those lacking *Dkk1* (del Barco Barrantes et al. 2003). The lack of migration defects in these mutant embryos may be caused by functional redundancy between Nodal-dependent and Wnt-dependent mechanisms. The process that determines the direction of the A–P axis may involve parallel mechanisms.

2.5 Role of DVE and AVE

Recent investigations have indicated that the descendant of the DVE contributed mainly to the most proximal portion of AVE and VE in the lateral region, but not to the entire AVE (Fig. 2.2). Time-lapse observation of DVE migration and AVE formation showed that the extensive movement of VE cells is initiated by DVE migration at E5.5 (Takaoka et al. 2011). While DVE cells migrate, the majority of AVE cells are newly formed at the distal end, migrate toward the proximal side following DVE migration, and eventually occupy the entire region of the AVE (Takaoka et al. 2011) (Fig. 2.2).

What is the role of the DVE in AVE formation? In DVE-ablated embryos caused by genetic manipulation, AVE cells are newly formed at the distal end but fail to migrate. Under this condition, extensive movement of VE cells does not occur, and the migration of the AVE cells is stalled (Takaoka et al. 2011). For instance, in mutant embryos lacking Cripto, a coreceptor of Nodal, the AVE is formed in the absence of DVE in the absence of DVE but does not migrate at all (Chu and Shen 2010). These observations suggest that the DVE guides the AVE to the anterior side by initiating extensive movement of visceral endoderm cells.

AVE cells function as head organizer by expressing a few signal protein antagonists, that is, Nodal antagonists Lefty1 and Cerl1, and Wnt antagonist Dkk1. Theses antagonists protect nearby Epi cells from posterior-inducing Wnt and Nodal signaling (Fig. 2.4), specifying AVE-underlain Epi to head tissue. In fact, explant culture assays have shown that Epi cells without VE will adopt the posterior identity, whereas implanted AVE cause Epi to assume an anterior identity (Kimura et al. 2000).

2.6 Reinterpretation of Embryo Phenotypes Defective in A–P Axis Formation

It had been believed that the mature DVE is the direct precursor for the entire AVE and its migration toward the future anterior side away from the distal tip is the mechanism of AVE formation (Beddington and Robertson 1999) (Fig. 2.5). However, the recent observation that DVE does not contribute to the major part of AVE renders it necessary to reinterpret the phenotypes of previously reported mutant mouse embryos based on the following four criteria: (1) DVE formation; (2) DVE migration; (3) AVE formation; and (4) AVE migration (Table 2.1).

In *Nodal*-null (Waldrip et al. 1998; Mesnard et al. 2006) and *Smad2*-null (Waldrip et al. 1998) mutants, the Epi is specified to neural tissues precociously, and neither DVE nor AVE forms (Fig. 2.6). In *Cripto*-null (Ding et al. 1998; Chu and Shen 2010) and *Eomes* VE-conditional null embryos, *Cerl1*, a DVE marker, is expressed at very reduced levels or not at all at E5.5. *Cerl1*-positive AVE cells are newly formed close to the distal tip of the mutant embryo from E6.0 to E6.5, but they fail to migrate proximally and remain at the distal tip of the embryo, as in the

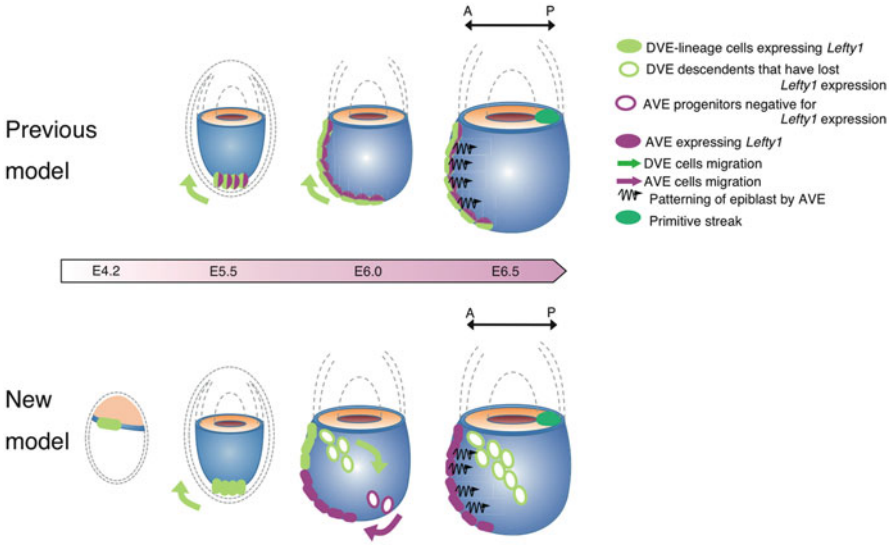

Fig. 2.5 Comparison of previously proposed model and current model concerning the roles of DVE in AVE formation. Previous model (*upper*): The DVE is specified at the distal tip of the embryo at E5.5, then migrates toward the anterior and proximal side to form the AVE. It has been thought that all AVE cells are derived from DVE. New model (*lower*): Origin of the DVE can be traced back to the *Lefty1*-positve primitive endoderm cells. The migration of DVE cells triggers global VE movements, and AVE cells are newly produced at the distal tip. In the proximally located migrating cells, DVE markers are lost. At E6.5, newly formed AVE cells occupy the anterior side of VE cells

DVE-ablated embryo (Takaoka et al. 2011; Morris et al. 2012) (Fig. 2.6). In other mutants also, such as *Otx2*-null (Kimura-Yoshida et al. 2005), *Rac1*-null (Sugihara et al. 1998; Migeotte et al. 2010), and *Pten*-null (Bloomekatz et al. 2012) mutants, the DVE is formed at the distal dip at E5.5, but fails to migrate. Thus, cells that express DVE/AVE markers remain close to the distal tip of the embryo at E6.0 and E6.5 (Fig. 2.6). These observations indicate that the major role of DVE is to guide the AVE migration.

2.7 Conclusion

The A–P axis of mouse embryos is fully established by the directed movement of DVE and AVE cells, the latter known as s head organizer. DVE progenitor cells are distributed on one side of the primitive endoderm cells at E4.2. The direction of the A–P axis of later embryos may depend on this asymmetry. At E5.5, DVE cells that express Nodal antagonists Lefty1 and Cer1, and Wnt antagonist Dkk1,

Table 2.1 Reinterpretation of mutant mouse phenotypes that include defective anterior visceral endoderm (AVE) formation

Gene	Genetic modification	DVE formation at E5.5	DVE migration	AVE formation at E6.5	AVE migration	References
Nodal	Null	No	–	No	–	Brennan et al. (2001), Camus et al. (2006) and Mesnard et al. (2006)
Smad2	Null	No	–	No	–	Nomura and Li (1998) and Brennan et al. (2001)
Cripto	Null	No	–	Yes	No	Ding et al. (1998), Kimura et al. (2001) and Chu and Shen (2010)
Eomes	VE-specific null	Low	No	Yes	No	Nowotschin et al. (2013)
Otx2	Null	Yes	No	Yes	No	Kimura et al. (2000, 2001) and Kimura-Yoshida et al. (2005)
Rac1	VE-specific null	Yes	No	Yes	No	Migeotte et al. (2010)
Lefty1	Null	Expansion	Yes	Yes	Yes	Yamamoto et al. (2004)
Lefty1 Cerl1	Double null	N.D.	N.D.	Yes	Delay	Perea-Gomez et al. (2002) and Yamamoto et al. (2004)

become mature and migrate to the future anterior side. Immediately before their migration, morphological changes occur in the VE cells, namely, visceral endoderm thickening, formation of lamellipodia- and filopodia-like processes, and organization of multicellular rosettes. DVE migration toward the future anterior side has the role of guiding the AVE cells to the anterior side of the egg cylinder embryo, and triggers extensive rearrangement of visceral endoderm cells in a wide area.

Important questions that remain to be answered are these: how are DVE progenitors selected among PrE cells in the blastocyst, and at which stage of development is the direction of DVE migration determined?

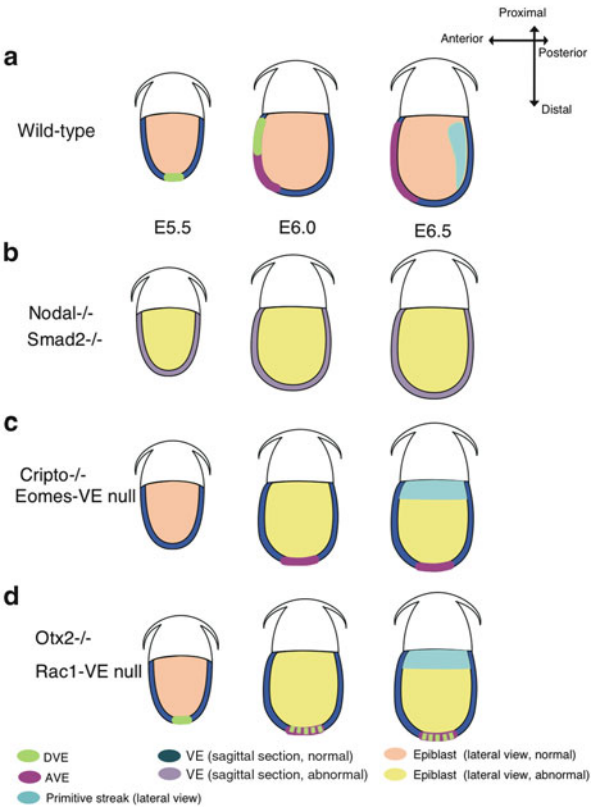

Fig. 2.6 Grouping of mouse mutant phenotypes defective in the A–P axis development. (**a**) Wild-type embryos. (**b**) Precocious neural differentiation occurs in the Epi; thus, the DVE and the AVE fail to form throughout E5.5 and E6.5 stages. (**c**) The DVE does not form at E5.5. The AVE is newly formed at the distal tip at E6.0 but fails to migrate. As a result, Epi cells with posterior identity develop at the proximal side of the embryo. (**d**) The DVE forms at the distal tip of the embryo at E5.5 but fails to migrate. Cells positive for DVE/AVE markers remain at the distal tip at E6.0 and E6.5. As a result, Epi cells with posterior identity develop at the proximal side of the embryo, similar to (**c**)

Acknowledgments We thank members of the Hamada laboratory for discussion.

References

Beddington RS, Robertson EJ (1999) Axis development and early asymmetry in mammals. Cell 96(2):195–209. doi:10.1016/S0092-8674(00)80560-7

Bloomekatz J, Grego-Bessa J, Migeotte I, Anderson KV (2012) Pten regulates collective cell migration during specification of the anterior-posterior axis of the mouse embryo. Dev Biol 364(2):192–201. doi:10.1016/j.ydbio.2012.02.005

Brennan J, Lu CC, Norris DP, Rodriguez TA, Beddington RS, Robertson EJ (2001) Nodal signalling in the epiblast patterns the early mouse embryo. Nature (Lond) 411(6840):965–969. doi:10.1038/35082103

Camus A, Perea-Gomez A, Moreau A, Collignon J (2006) Absence of Nodal signaling promotes precocious neural differentiation in the mouse embryo. Dev Biol 295(2):743–755. doi:10.1016/j.ydbio.2006.03.047

Chazaud C, Rossant J (2006) Disruption of early proximodistal patterning and AVE formation in Apc mutants. Development(Camb) 133(17):3379–3387. doi:10.1242/dev.02523

Chu J, Shen MM (2010) Functional redundancy of EGF-CFC genes in epiblast and extraembryonic patterning during early mouse embryogenesis. Dev Biol 342(1):63–73. doi:10.1016/j.ydbio.2010.03.009

del Barco Barrantes I, Davidson G, Grone HJ, Westphal H, Niehrs C (2003) Dkk1 and noggin cooperate in mammalian head induction. Genes Dev 17(18):2239–2244. doi:10.1101/gad.269103

Ding J, Yang L, Yan YT, Chen A, Desai N, Wynshaw-Boris A, Shen MM (1998) Cripto is required for correct orientation of the anterior-posterior axis in the mouse embryo. Nature (Lond) 395(6703):702–707. doi:10.1038/27215

Granier C, Gurchenkov V, Perea-Gomez A, Camus A, Ott S, Papanayotou C, Iranzo J, Moreau A, Reid J, Koentges G, Saberan-Djoneidi D, Collignon J (2011) Nodal cis-regulatory elements reveal epiblast and primitive endoderm heterogeneity in the peri-implantation mouse embryo. Dev Biol 349(2):350–362. doi:10.1016/j.ydbio.2010.10.036

Huynh JR, St. Johnston D (2004) The origin of asymmetry: early polarisation of the Drosophila germline cyst and oocyte. Curr Biol 14(11):R438–449. doi:10.1016/j.cub.2004.05.040

Kimura C, Yoshinaga K, Tian E, Suzuki M, Aizawa S, Matsuo I (2000) Visceral endoderm mediates forebrain development by suppressing posteriorizing signals. Dev Biol 225(2):304–321. doi:10.1006/dbio.2000.9835

Kimura C, Shen MM, Takeda N, Aizawa S, Matsuo I (2001) Complementary functions of Otx2 and Cripto in initial patterning of mouse epiblast. Dev Biol 235(1):12–32. doi:10.1006/dbio.2001.0289

Kimura-Yoshida C, Nakano H, Okamura D, Nakao K, Yonemura S, Belo JA, Aizawa S, Matsui Y, Matsuo I (2005) Canonical Wnt signaling and its antagonist regulate anterior-posterior axis polarization by guiding cell migration in mouse visceral endoderm. Dev Cell 9(5):639–650. doi:10.1016/j.devcel.2005.09.011

Meno C, Saijoh Y, Fujii H, Ikeda M, Yokoyama T, Yokoyama M, Toyoda Y, Hamada H (1996) Left-right asymmetric expression of the TGF beta-family member lefty in mouse embryos. Nature (Lond) 381(6578):151–155. doi:10.1038/381151a0

Mesnard D, Guzman-Ayala M, Constam DB (2006) Nodal specifies embryonic visceral endoderm and sustains pluripotent cells in the epiblast before overt axial patterning. Development (Camb) 133(13):2497–2505. doi:10.1242/dev.02413

Migeotte I, Omelchenko T, Hall A, Anderson KV (2010) Rac1-dependent collective cell migration is required for specification of the anterior-posterior body axis of the mouse. PLoS Biol 8(8):e1000442. doi:10.1371/journal.pbio.1000442

Morkel M, Huelsken J, Wakamiya M, Ding J, van de Wetering M, Clevers H, Taketo MM, Behringer RR, Shen MM, Birchmeier W (2003) Beta-catenin regulates Cripto- and Wnt3-dependent gene expression programs in mouse axis and mesoderm formation. Development (Camb) 130(25):6283–6294. doi:10.1242/dev.00859

Morris SA, Grewal S, Barrios F, Patankar SN, Strauss B, Buttery L, Alexander M, Shakesheff KM, Zernicka-Goetz M (2012) Dynamics of anterior-posterior axis formation in the developing mouse embryo. Nat Commun 3:673. doi:10.1038/ncomms1671

Nakamura T, Hamada H (2012) Left-right patterning: conserved and divergent mechanisms. Development (Camb) 139(18):3257–3262. doi:10.1242/dev.061606

Nakamura T, Mine N, Nakaguchi E, Mochizuki A, Yamamoto M, Yashiro K, Meno C, Hamada H (2006) Generation of robust left-right asymmetry in the mouse embryo requires a self-enhancement and lateral-inhibition system. Dev Cell 11(4):495–504. doi:10.1016/j.devcel.2006.08.002

Nomura M, Li E (1998) Smad2 role in mesoderm formation, left-right patterning and craniofacial development. Nature (Lond) 393(6687):786–790. doi:10.1038/31693

Nowotschin S, Costello I, Pillisezek A, Kwon GS, Mao CA, Klein WH, Robertson EJ, Hadjantonakis AK (2013) The T-box transcription factor Eomesodermin is essential for AVE induction in the mouse embryos. Genens Dev 27(9):997–1002. doi:10.1101/gad.215152.113

Perea-Gomez A, Vella FD, Shawlot W, Oulad-Abdelghani M, Chazaud C, Meno C, Pfister V, Chen L, Robertson E, Hamada H, Behringer RR, Ang SL (2002) Nodal antagonists in the anterior visceral endoderm prevent the formation of multiple primitive streaks. Dev Cell 3(5):745–756

Rakeman AS, Anderson KV (2006) Axis specification and morphogenesis in the mouse embryo require Nap1, a regulator of WAVE-mediated actin branching. Development (Camb) 133(16):3075–3083. doi:10.1242/dev.02473

Rivera-Perez JA, Mager J, Magnuson T (2003) Dynamic morphogenetic events characterize the mouse visceral endoderm. Dev Biol 261(2):470–487. doi:10.1016/S0012-1606(03)00302-6

Rodriguez TA, Srinivas S, Clements MP, Smith JC, Beddington RS (2005) Induction and migration of the anterior visceral endoderm is regulated by the extra-embryonic ectoderm. Development (Camb) 132(11):2513–2520. doi:10.1242/dev.01847

Rossant J, Tam PP (2009) Blastocyst lineage formation, early embryonic asymmetries and axis patterning in the mouse. Development (Camb) 136(5):701–713. doi:10.1242/dev.017178

Srinivas S (2006) The anterior visceral endoderm-turning heads. Genesis 44(11):565–572. doi:10.1002/dvg.20249

Sugihara K, Nakatsuji N, Nakamura K, Nakao K, Hashimoto R, Otani H, Sakagami H, Kondo H, Nozawa S, Aiba A, Katsuki M (1998) Rac1 is required for the formation of three germ layers during gastrulation. Oncogene 17(26):3427–3433. doi:10.1038/sj.onc.1202595

Takaoka K, Hamada H (2012) Cell fate decisions and axis determination in the early mouse embryo. Development (Camb) 139(1):3–14. doi:10.1242/dev.060095

Takaoka K, Yamamoto M, Shiratori H, Meno C, Rossant J, Saijoh Y, Hamada H (2006) The mouse embryo autonomously acquires anterior-posterior polarity at implantation. Dev Cell 10(4): 451–459. doi:10.1016/j.devcel.2006.02.017

Takaoka K, Yamamoto M, Hamada H (2011) Origin and role of distal visceral endoderm, a group of cells that determines anterior-posterior polarity of the mouse embryo. Nat Cell Biol 13(7):743–752. doi:10.1038/ncb2251

Tam PP, Loebel DA (2007) Gene function in mouse embryogenesis: get set for gastrulation. Nat Rev Genet 8(5):368–381. doi:10.1038/nrg2084

Trichas G, Smith AM, White N, Wilkins V, Watanabe T, Moore A, Joyce B, Sugnaseelan J, Rodriguez TA, Kay D, Baker RE, Maini PK, Srinivas S (2012) Multi-cellular rosettes in the mouse visceral endoderm facilitate the ordered migration of anterior visceral endoderm cells. PLoS Biol 10(2):e1001256. doi:10.1371/journal.pbio.1001256

Waldrip WR, Bikoff EK, Hoodless PA, Wrana JL, Robertson EJ (1998) Smad2 signaling in extra-embryonic tissues determines anterior-posterior polarity of the early mouse embryo. Cell 92(6):797–808

Yamamoto M, Saijoh Y, Perea-Gomez A, Shawlot W, Behringer RR, Ang SL, Hamada H, Meno C (2004) Nodal antagonists regulate formation of the anteroposterior axis of the mouse embryo. Nature (Lond) 428(6981):387–392. doi:10.1038/nature02418

Yamamoto M, Beppu H, Takaoka K, Meno C, Li E, Miyazono K, Hamada H (2009) Antagonism between Smad1 and Smad2 signaling determines the site of distal visceral endoderm formation in the mouse embryo. J Cell Biol 184(2):323–334. doi:10.1083/jcb.200808044

Yamanaka Y, Ralston A, Stephenson RO, Rossant J (2006) Cell and molecular regulation of the mouse blastocyst. Dev Dyn 235(9):2301–2314. doi:10.1002/dvdy.20844

Chapter 3
Cell Competition: The Struggle for Existence in Multicellular Communities

Kei Kunimasa, Shizue Ohsawa, and Tatsushi Igaki

Abstract How the size and shape of organs are determined is one of the most mysterious questions in developmental biology. Organ size and shape are controlled by tissue growth, which is strongly influenced by local homeostatic cell–cell interactions. Studies during the past several years have shown that cells in multicellular communities compete with each other for their existence; cells with higher fitness ("winners") survive and eliminate cells with lower fitness ("losers") by inducing cell death. Accumulating evidence, obtained mainly in *Drosophila*, has revealed that this cellular natural selection, called "cell competition," could have an important role in organ size and shape control in normal development as well as in some pathophysiological conditions such as stem cell regulation and cancer development. In this chapter, we discuss recent insights in cell competition. Elucidation of the mechanism by which cell competition is controlled could create a new dimension for understanding the basic principle of multicellular systems.

Keywords Cell competition • Cell death • Cell–cell interaction • Tissue growth

K. Kunimasa
Laboratory of Genetics, Graduate School of Biostudies, Kyoto University, Kyoto, Japan

Division of Genetics, Kobe University Graduate School of Medicine, Kobe, Japan

S. Ohsawa
Laboratory of Genetics, Graduate School of Biostudies, Kyoto University, Kyoto, Japan

T. Igaki (✉)
Laboratory of Genetics, Graduate School of Biostudies, Kyoto University, Kyoto, Japan

PRESTO, Japan Science and Technology Agency (JST), Saitama, Japan
e-mail: igaki@lif.kyoto-u.ac.jp

H. Kondoh and A. Kuroiwa (eds.), *New Principles in Developmental Processes*,
DOI 10.1007/978-4-431-54634-4_3,

3.1 Introduction

During normal development, cells failing to proliferate or differentiate properly are to be eliminated. There is growing evidence that in multicellular systems cells with lower fitness are eliminated by neighboring cells with higher fitness. The fitter cells ("winners") survive and proliferate at the expense of neighboring less fit cells ("losers"), thus keeping the total cell number unchanged. Such competitive cell–cell interaction is called cell competition (Morata and Ripoll 1975). In recent years, progress has been made in understanding the mechanism of cell competition, especially using *Drosophila* genetics; however, much still remains to be elucidated (Levayer and Moreno 2013; de Beco et al. 2012; Tamori and Deng 2011; Baker 2011; Johnston 2009; Moreno 2008). Although there is no clear definition so far established for cell competition, the essences of cell competition are found to be as follows: (1) losers are eliminated from the cell population in the presence of winners, (2) loser death and winner proliferation occur interdependently, which are distinct from cell autonomous apoptosis or overproliferation. (3) Total cell number or tissue size and shape is unchanged (Fig. 3.1). In this chapter, we provide an overview of recent progress in cell competition research and discuss the physiological role of this cellular communication.

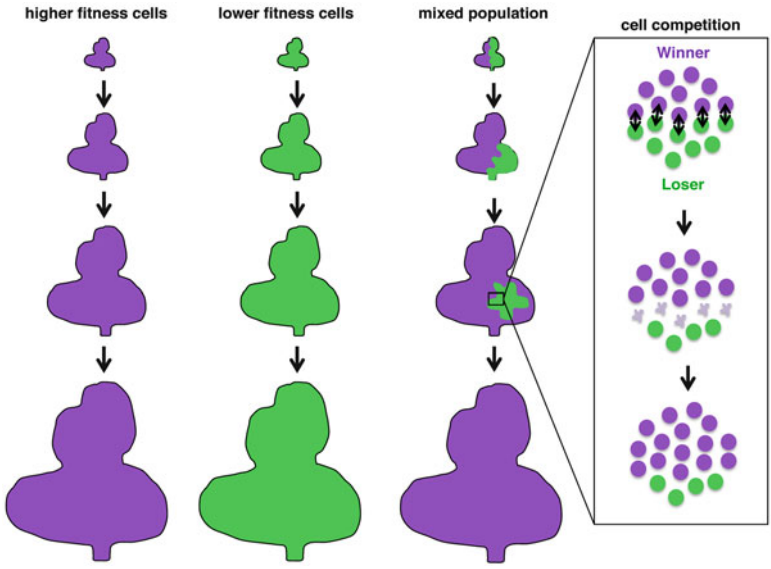

Fig. 3.1 Cell competition during development. Cell competition is triggered by differences in cellular fitness. When the entire tissue is composed of either cells with high fitness or cells with low fitness, cell competition does not occur and the tissue develops normally. However, when the tissue is composed of mixed populations of cells with different cellular fitness, cell competition occurs between these cells, and the cells with higher fitness become winners and eliminate neighboring cells with lower fitness (losers) by inducing cell death. Winners proliferate at the expense of losers, resulting in tissue size and shape remaining unchanged

3.2 Factors That Trigger Cell Competition

3.2.1 Differential Level of Ribosomal Protein

Cell competition was first reported by Morata and Ripoll approximately 40 years ago in the study of a series of *Drosophila* mutants called "*Minutes*." *Minute* heterozygous mutant (*M*/+) flies develop more slowly than wild-type flies, but finally reach normal body size without significant patterning defects (Lambertsson 1998). It was realized later that *Minutes* affect a series of genes encoding ribosomal proteins (Kongsuwan et al. 1985). Morata and Ripoll studied the proliferation dynamics of *M*/+ cells by generating wild-type clones into *M*/+ developing imaginal discs and found that wild-type clones outgrow *M*/+ mutant clones and occupy much of the space in the tissue. *M*/+ clones were found only when wild-type clones were induced relatively late in development. In addition, even in the extreme cases containing a larger *M*/+ clones area, their mosaic wings were of normal size and shape. These observations suggested that elimination of *M*/+ clones depends on their context (the presence of neighbors with higher growth rate) and that wild-type clones grow in compensation for the deficit of *M*/+ clones. Morata and Ripoll used the term "cell competition" to explain this phenomenon (Morata and Ripoll 1975).

This model was subsequently confirmed and elaborated in the studies by Simpson and Morata (Simpson 1979; Simpson and Morata 1981). They explored cell competition more deeply by studying the competition between clones of various *Minutes* mutants and wild-type clones and between the different *Minutes* mutant clones, reporting two important findings. First, cell competition results from differences in relative growth rate between neighboring cells. Slowly dividing cells are eliminated when confronted with cells dividing more rapidly. However, such slower-growing cells are not eliminated when surrounded by other mutant cells with a similar slow growth rate. Clonal analysis revealed that wild-type cells near to *M*/+ clones grow more rapidly and that *M*/+ clones that are not touching wild-type cells are not eliminated. Second, cell competition is position dependent. *M*/+ clone elimination never crosses the borders of developmental compartments, so that losers on one side of the borders are insulated from competitive elimination by winners on the other side (Garcia-Bellido et al. 1973; de la Cova et al. 2004). Because developmental compartments are thought to be units of size control (Crick and Lawrence 1975; Simpson 1976), cell competition may play a crucial role in establishing the normal size and shape of appendages in animals.

Approximately 30 years later, using FLP/FRT mosaic techniques (Golic and Lindquist 1989; Xu and Rubin 1993), actual apoptosis of *M*/+ clones surrounded by wild-type cells was demonstrated. It has been shown that the elimination of *M*/+ clones was driven by relative deficit of Dpp (decapentaplegic; *Drosophila* homologue of bone morphogenetic protein, BMP) pathway activity, which leads to ectopic upregulation of the transcriptional repressor Brinker; this further leads to

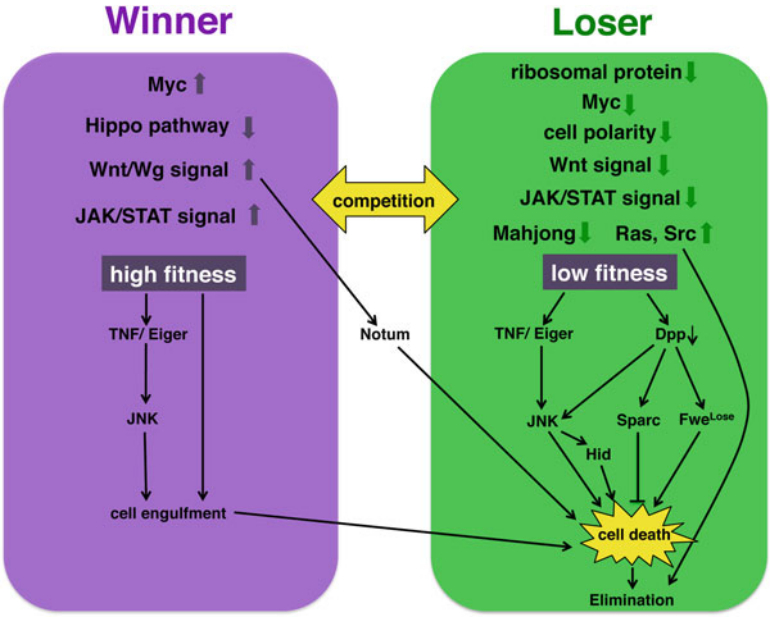

Fig. 3.2 Emerging pathways of cell competition. Factors and signaling pathways regulating cell competition have been reported in the past several years (see text for details)

activation of the c-Jun N-terminal kinase (JNK) pathway and induction of apoptosis (Moreno et al. 2002) (Fig. 3.2). Importantly, it has also been shown in mice that cells that are heterozygous mutants for a ribosomal gene are disproportionately disadvantaged in chimeras during development (Oliver et al. 2004), suggesting that similar cell competition triggered by differential levels of ribosomal proteins occurs in mammals. These observations led to the conclusion that cell competition is a result of local interactions between neighboring cells with different growth rates and suggested that cell competition might act as a quality control mechanism that maximizes tissue fitness by selecting fitter cells.

3.2.2 Differential Level of Myc

The second demonstrated example of cell competition is interactions between cells with different level of the *myc* family of proto-oncogenes (Henriksson and Lüscher 1996). *Drosophila* myc (*dmyc*) mutant flies are small in body size and take longer to develop, as do *Minutes*, but their body parts are appropriately proportioned with no patterning or cell fate specification defects other than the variably penetrant eye phenotype. In the mosaic imaginal tissue containing $dmyc^{-/-}$ clones in otherwise wild-type tissue, the size of $dmyc^{-/-}$ clones is smaller than that of wild-type clones

(Johnston et al. 1999). As with *M*/+ clones, $dmyc^{-/-}$ mutant clones are outcompeted when confronted with wild-type or $dmyc^{-/+}$ clones (Moreno and Basler 2004). In contrast, clones expressing high levels of dMyc behave as "supercompetitors" that eliminate neighboring wild-type clones (Moreno and Basler 2004; de la Cova et al. 2004). Cell death occurring in neighboring wild-type cells was shown to be caused by Dpp deprivation/JNK activation (Moreno and Basler 2004) and induction of the apoptotic activator Hid (de la Cova et al. 2004) (Fig. 3.2). Importantly, cells with two copies of the *dmyc* gene ("wild type") can behave as both winners and losers, as they become winners when confronted with *dmyc* mutant cells but become losers when confronted with cells with four copies of *dmyc* genes (Moreno and Basler 2004). This distinction represents an important feature of cell competition whereby a cell fate is destined by its neighbors. Interestingly, dMyc-overexpressing cells that are also heterozygous for *Minute* do not outcompete surrounding wild-type cells (Moreno and Basler 2004), suggesting that the competitive advantage of dMyc-overexpressing cells could be the result of an active protein synthesis. Importantly, differences in growth rate seem not to be sufficient for inducing cell competition, as cells with different levels of other growth regulators such as PI3K or cyclin D/Cdk4 do not cause cell competition (de la Cova et al. 2004).

3.2.3 Cell Polarity Defects and Oncogenic Mutations

Loss of apico-basal polarity in epithelial cells is often associated with deregulated tissue growth and tumorigenesis (Bilder 2004). *discs large* (*dlg*) (Stewart et al. 1972) and *scribble* (*scrib*) (Bilder and Perrimon 2000), a group of apico-basal polarity genes, were initially identified as members of evolutionally conserved *Drosophila* "neoplastic" tumor suppressors. Scrib localizes to the basolateral cortex, and Dlg directly binds to Scrib and colocalizes with Scrib (Bilder and Perrimon 2000; Dow et al. 2003). Imaginal tissues entirely mutant for *scrib* or *dlg* continue to grow and develop into multilayered tumors (Bilder and Perrimon 2000; Bilder 2004; Brumby and Richardson 2005). Interestingly, when *scrib* or *dlg* mutant clones are surrounded by wild-type tissue, these mutant clones do not overproliferate but are eliminated by JNK-dependent cell death through cell competition (Brumby and Richardson 2003; Igaki et al. 2009; Pagliarini and Xu 2003; Woods and Bryant 1991). Interestingly, also in a mammalian cell culture system, Scrib-knockdown MDCK (Madin–Darby canine kidney) cells that are surrounded by normal MDCK cells cause apoptosis and are extruded from the monolayer culture (Norman et al. 2012). Similarly, mammalian cultured cells with elevated activity of oncogenes, such as Ras and Src, have also been shown to be excluded from the monolayer culture when surrounded by normal cells (Hogan et al. 2009; Kajita et al. 2010) (Fig. 3.2). These observations suggest that cell competition can act as a tumor suppressor that eliminates oncogenic mutant cells from epithelium.

3.2.4 Differential Level of Hippo Signaling

A conserved tumor-suppressor pathway, the Hippo pathway, has been shown to play an important role in cell competition. The core component of the Hippo pathway is a kinase cascade (Hippo-Salvador-Warts) that negatively regulates the transcriptional coactivator Yokie (Yki), which activates the expression of its target genes such as the cell-cycle regulator *cyclin E*, the anti-apoptotic factor *diap1*, and an anti-apoptotic and growth-promoting microRNA *bantam* (Enomoto and Igaki 2011; Yu and Guan 2013; Halder and Johnson 2011; Pan 2010). The role of the Hippo pathway in cell competition was first discovered by a genetic screen in *Drosophila* eye disc for identifying mutations that modulate "*Minute*" cell competition (Tyler et al. 2007). Mutations in the components of the Hippo pathway such as *hippo*, *salvador*, and *warts*, all of which lead to Yki activation, suppress the elimination of *M*/+ clones in competitive mosaics. It has also been shown that cells expressing a higher level of Yki become winners of cell competition (Neto-Silva et al. 2010; Ziosi et al. 2010) (Fig. 3.2). The Hippo pathway is widely recognized as a signaling pathway that regulates organ size. In recent years, a variety of upstream regulators of the Hippo pathway have been identified, including cell polarity (Martin-Belmonte and Perez-Moreno 2012; Yu and Guan 2013), mechanotransduction (Zhao et al. 2012; Yu and Guan. 2013), G protein-coupled receptor (GPCR) signaling (Yu et al. 2012), oncogenic mitochondrial defect (Ohsawa et al. 2012), and an oncoprotein, Src (Enomoto and Igaki 2013). Thus, cell competition could be triggered by various Hippo pathway regulators during normal development.

3.2.5 Loss of Mahjong

Mahjong was identified as an evolutionally conserved Lgl (Lethal giant larvae; an apico-basal polarity protein)-binding protein. It has been shown that cells with no or downregulated expression of Mahjong are eliminated by cell competition when confronted with wild-type cells both in the *Drosophila* imaginal disc and in the mammalian cell culture system (Tamori et al. 2010) (Fig. 3.2). Intriguingly, it has recently been shown that elimination of $mahj^{-/-}$ clones by cell competition occurs even in postmitotic *Drosophila* follicular epithelium. In this case, winner cells undergo "compensatory cellular hypertrophy," in which some wild-type cells become larger in volume than other cells to compensate for lost space created by losers' elimination (Tamori and Deng 2013).

3.2.6 Differential Level of Wg Signaling

Wingless (Wg), a founding member of the Wingless/Int-1 (Wnt) family of secreted proteins, plays important roles as a morphogen in *Drosophila* development (Serrano

and O'Farrell 1997). It has been shown that differences in Wg signal intensity induce competitive cell–cell interactions in wing imaginal discs (Vincent et al. 2011). Local downregulation of Wg signaling causes cell death when confronted with normal cells. On the other hand, local hyperactivation of Wg signaling generates supercompetitors that eliminate neighboring normal cells. *wg* mutant cells cause cell death via JNK activation (Giraldez and Cohen 2003) and Hid induction (Johnston and Sanders 2003), suggesting that Wg-low losers might be eliminated by JNK-dependent cell death. Interestingly, Wg-dependent cell competition has been shown to be independent of dMyc protein level based on the following two observations. First, dMyc is downregulated in Wg-activating supercompetitors, and second, the competitive advantage of Wg-activating cells is not abolished by downregulation of dMyc throughout the tissue or by upregulation of dMyc in neighboring normal cells. Instead, Wg-dependent cell competition is regulated by Notum, a secreted glypican-specific phospholipase. Activation of Wg signaling triggers the expression of Notum, which in turn attenuates the response to Wg in surrounding cells, leading these surrounding cells to cause cell death (Fig. 3.2) (Vincent et al. 2011).

3.2.7 Differential Level of JAK/STAT Signaling

The JAK/STAT pathway is an evolutionarily conserved signaling pathway that promotes tissue growth. In *Drosophila*, unpaired (Upd) (*Drosophila* IL-6-like cytokine) binds to its receptor Domeless, thereby activating the sole Janus kinase Hopscotch and the sole STAT transcription factor Stat92E (Arbouzova and Zeidler 2006). It has been shown that cells lacking Stat92E activity are eliminated when confronted with wild-type cells and that cells with hyperactivated Stat92E become supercompetitors independently of dMyc, Yki, Wg, or ribosomal activity (Rodrigues et al. 2012) (Fig. 3.2). Stat92E activity has also been shown to be involved in the elimination of *scrib* clones. Removal of Stat92E activity from wild-type cells juxtaposed to *scrib* clones results in the failure to eliminate *scrib* clones (Schroeder et al. 2012).

3.3 Stem Cell Competition

Stem cells reside in local microenvironments (niches) that produce signals regulating stem cell divisions and stem cell–niche interactions (Stine and Matunis 2013). There is growing evidence that stem cells compete with each other for their existence within the niche. For example, in the *Drosophila* ovary, each ovariole harbors two to three ovarian germline stem cells (GSCs), which are anchored to stromal cap cells (niche) via E-cadherin-mediated adhesion (Lin 2002). The differentiation-defective GSCs mutant for *bam* (*bag of marbles*) or *bgcn* (*benign gonial cell neoplasm*) outcompete neighboring wild-type GSCs by pushing them out of the niche (Jin et al. 2008) (Fig. 3.3). Such competitive interaction between stem cells would

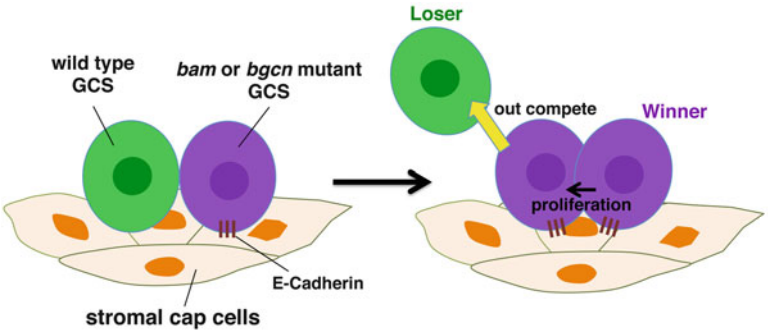

Fig. 3.3 Stem cell competition in *Drosophila* ovary. In *Drosophila* germline stem cell (GSC) competition in the ovary, GSCs adhere to stromal cap cells (niche). GSC mutants for differentiation-promoting gene *bam* or *bgcn* remain in the niche via strong E-cadherin-mediated adhesion and become winners of cell competition. *bam* or *bgcn* mutant GSCs outcompete neighboring wild-type GSCs from the niche

serve as a quality control mechanism to keep fitter stem cells in the niche. Stem cell competition has also been studied in mammalian systems. For example, in the mouse hematopoietic system, hematopoietic stem and progenitor cells compete with each other in response to DNA damage stresses to reconstitute the hematopoietic compartment. In this case, the win–lose decision is made by the level of p53 expression and losers with higher expression of p53 are excluded from the stem cell population by inducing cellular senescence (Bondar and Medzhitov 2010).

3.4 Mechanism of Cell Competition: Common or Diverse?

As already described, cell competition can be triggered by various gene mutations or deregulated signaling cascades. Intriguingly, emerging evidence suggests that some competitive cell–cell interactions share a common mechanism by which cells compare their relative fitness and drive elimination of losers.

3.4.1 Ligand-Capture Mechanism

It has been reported that two adjacent cells compete for the uptake of the Dpp morphogen during cell competition triggered by *Minute* or a differential level of dMyc (Moreno et al. 2002; Moreno and Basler 2004). Because the winners of such cell competition possess higher ribosomal activity than losers, winners could acquire an advantage by capturing extracellular pro-growth ligands (such as Dpp) more efficiently (Morata and Ripoll 1975; Moreno and Basler 2004) (Fig. 3.4a). Ligand-dependent signal transduction can be activated by internalization of ligands through

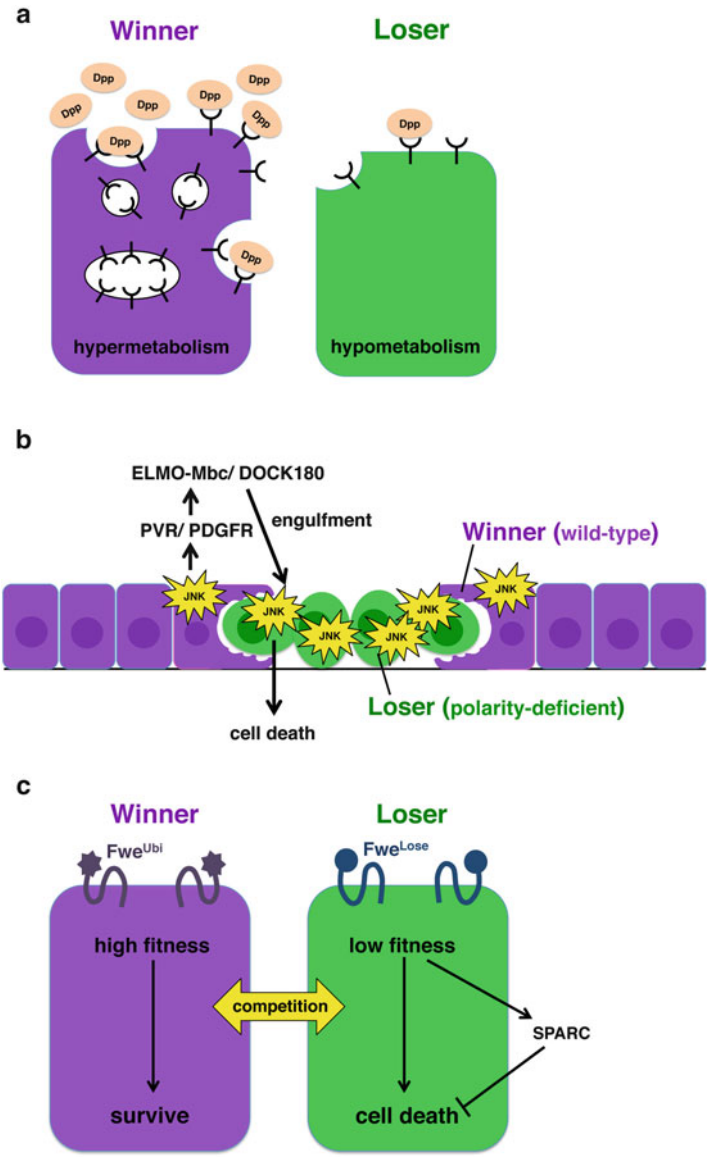

Fig. 3.4 Mechanisms of cell competition. (**a**) Ligand-capture hypothesis. Cells compete for extracellular survival or growth factors such as Dpp (decapentaplegic), and the hypermetabolic winner can capture more survival factors than neighboring the hypometabolic loser, resulting in loser apoptosis. (**b**) Eiger-JNK signaling causes elimination of oncogenic polarity-deficient neighbors. In *Drosophila* imaginal epithelium, clones mutant for neoplastic tumor-suppressor genes such as *scrib* or *dlg* (losers, in *green*) are eliminated by neighboring normal epithelial cells (winners, in *purple*). JNK signaling serves a dual function in this process. JNK signaling in losers promotes losers' apoptosis; JNK signaling in winners promotes elimination of losers through activation of the engulfment pathway. (**c**) The "Flower code" (Fwe code) in cell competition is composed of three Fwe isoforms (Ubi, Lose-A, and Lose-B) that produce a tag to distinguish winners (*purple*) and losers (*green*). Losers tagged with Fwe^{Lose} are eliminated in the presence of winners tagged with Fwe^{Ubi}. SPARC is expressed temporarily in losers to protect them from cell death

endocytosis (Tsukazaki et al. 1998). Interestingly, the small GTPase Rab5, which is required for the formation of endosomes, has been implicated in Dpp-regulated cell competition. Overexpression of Rab5 in *dmyc*-deficient clones blocks their elimination (Moreno and Basler 2004). However, it has also been reported that *Minute* cell competition does not always depend on Dpp signaling (Tyler et al. 2007).

3.4.2 TNF-JNK Signaling

Drosophila tumor necrosis factor (TNF) homologue Eiger and its downstream JNK signaling have been implicated in some types of cell competition. In *scrib* or *dlg* mutant clones that are surrounded by wild-type tissue, Eiger-JNK signaling is activated through elevated endocytic activity, thereby promoting JNK-dependent cell death (Brumby and Richardson 2003; Igaki et al. 2009). JNK signaling has also been shown to regulate cell competition triggered by *Minute*, dMyc, and loss of Mahjong (Moreno et al. 2002; de la Cova et al. 2004; Moreno and Basler 2004; Tamori et al. 2010). However, it has also been reported that cell competition triggered by *Minute* or dMyc can still occur in the absence of JNK activity (de la Cova et al. 2004; Tyler et al. 2007).

3.4.3 Cell Engulfment

It has been reported in *Drosophila* imaginal tissue that dead cells are phagocytosed by neighboring normal epithelial cells during development (Fristrom 1969). In analyzing the fate of losers in cell competition triggered by *Minute* or dMyc, it was found that losers are engulfed by neighboring winners (Li and Baker 2007). Genetic analyses showed that cell competition is blocked in the absence of engulfment by winners (Li and Baker 2007). Similarly, it has been shown that wild-type imaginal cells surrounding *scrib* or *dlg* mutant clones activate JNK signaling, which leads to activation of the PVR-ELMO/Mbc-mediated engulfment pathway, thereby promoting elimination of polarity-deficient neighbors by engulfment (Ohsawa et al. 2011) (Fig. 3.4b). However, it has also been reported that the contribution of cell engulfment by winners is not significant, but circulating phagocytic hemocytes play a role in the clearance of losers' apoptotic bodies during cell competition (Lolo et al. 2012).

3.4.4 Flower Code and Sparc

Microarray analysis of genes changing at early stages of dMyc-induced cell competition identified the *flower* (*fwe*) gene, which was originally identified as a Ca^{2+}

channel associated with synaptic vesicles of photoreceptor nerve terminals (Yao et al. 2009). In *Drosophila*, the *fwe* locus produces three isoforms, fwe^{Ubi}, $fwe^{Lose\text{-}A}$, and $fwe^{Lose\text{-}B}$ (fwe^{Loses}). Fwe^{Ubi} is normally expressed throughout the tissue but downregulated in losers, whereas the other two isoform products, $Fwe^{Lose\text{-}A}$ and $Fwe^{Lose\text{-}B}$, are expressed only in losers. This "flower code" was detected in different types of cell competition triggered by dMyc, *Minute*, or *scrib*. Although uniform upregulation of Fwe^{Ubi} or Fwe^{Loses} in the tissue does not trigger cell competition, relative differences in Fwe^{Ubi} or Fwe^{Loses} expression trigger cell competition; cells with low-level expression of Fwe^{Ubi} or high-level expression of Fwe^{Loses} cause cell death as losers (Rhiner et al. 2010) (Fig. 3.4c). Thus, the Fwe code could be a tag whereby cells identify their relative fitness and determine cellular win–lose fate.

Another early marker of losers of cell competition so far reported is dSparc, the *Drosophila* homologue of the Sparc/Osteonectin protein family. dSparc is a component of the extracellular matrix and found in the basement membrane of both epithelial and endothelial internal organs and tissues (Martinek et al. 2002). dSparc is transiently expressed in losers and protects them from apoptosis during cell competition triggered by dMyc, *Minute*, or *lgl* (Portela et al. 2010) (Fig. 3.4c). It is considered that Fwe and dSparc act in parallel and opposing pathways, as dSparc provides transient protection, whereas the Fwe code promotes cell elimination by labeling cells as losers.

3.5 Concluding Remarks

The concept of cell competition recalls Darwin's theory of evolution, natural selection. In limited environments or niches, various types of cells not only cooperate together but compete with each other for their existence, leading to maintenance of the homeostasis of multicellular systems. In tissues, surviving cells with higher fitness (winners) proliferate and increase their territory at the expense of less fit cells (losers), resulting in the best qualifying tissue. Cell competition can also act as a surveillance system for cellular fitness. As oncogenic cells are eliminated from the epithelium by cell competition, it acts as an intrinsic tumor suppressor mechanism, utilizing the relative differences in cellular fitness. Similarly, elimination of abnormal cells would also be significant for accomplishing normal developmental processes. Future studies for understanding the mechanism of cell competition and for identifying molecules that determine cellular fitness will provide a new dimension in developmental biology.

References

Arbouzova NI, Zeidler MP (2006) JAK/STAT signalling in *Drosophila*: insights into conserved regulatory and cellular functions. Development (Camb) 133(14):2605–2616

Baker NE (2011) Cell competition. Curr Biol 21(1):R11–R15

Bilder D (2004) Epithelial polarity and proliferation control: links from the *Drosophila* neoplastic tumor suppressors. Genes Dev 18(16):1909–1925
Bilder D, Perrimon N (2000) Localization of apical epithelial determinants by the basolateral PDZ protein Scribble. Nature (Lond) 403(6770):676–680
Bondar T, Medzhitov R (2010) p53-mediated hematopoietic stem and progenitor cell competition. Cell Stem Cell 6(4):309–322
Brumby AM, Richardson HE (2003) *scribble* mutants cooperate with oncogenic Ras or Notch to cause neoplastic overgrowth in *Drosophila*. EMBO J 22(21):5769–5779
Brumby AM, Richardson HE (2005) Using *Drosophila melanogaster* to map human cancer pathways. Nat Rev Cancer 5(8):626–639
Crick FH, Lawrence PA (1975) Compartments and polyclones in insect development. Science 189(4200):340–347
de Beco S, Ziosi M, Johnston LA (2012) New frontiers in cell competition. Dev Dyn 241(5):831–841
de la Cova C, Abril M, Bellosta P et al (2004) *Drosophila* myc regulates organ size by inducing cell competition. Cell 117(1):107–116
Dow LE, Brumby AM, Muratore R (2003) hScrib is a functional homologue of the *Drosophila* tumor suppressor Scribble. Oncogene 22(58):9225–9230
Enomoto M, Igaki T (2011) Deciphering tumor-suppressor signaling in flies: genetic link between Scribble/Dlg/Lgl and the Hippo pathways. J Genet Genomics 38(10):461–470
Enomoto M, Igaki T (2013) Src controls tumorigenesis via JNK-dependent regulation of the Hippo pathway in *Drosophila*. EMBO Rep 14(1):65–72
Fristrom D (1969) Cellular degeneration in the production of some mutant phenotypes in *Drosophila melanogaster*. Mol Gen Genet 103(4):363–379
Garcia-Bellido A, Ripoll P, Morata G (1973) Developmental compartmentalization of the wing disk of *Drosophila*. Nat New Biol 245(147):251–253
Giraldez AJ, Cohen SM (2003) Wingless and Notch signaling provide cell survival cues and control cell proliferation during wing development. Development (Camb) 130(26):6533–6543
Golic KG, Lindquist S (1989) The FLP recombinase of yeast catalyze site-specific recombination in *Drosophila* genome. Cell 59(3):499–509
Halder G, Johnson RL (2011) Hippo signaling: growth control and beyond. Development (Camb) 138(1):9–22
Henriksson M, Lüscher B (1996) Proteins of the Myc network: essential regulators of cell growth and differentiation. Adv Cancer Res 68:109–182
Hogan C, Dupre-Crochet S, Norman M et al (2009) Characterization of the interface between normal and transformed epithelial cells. Nat Cell Biol 11(4):460–467
Igaki T, Pastor-Pareja JC, Aonuma H et al (2009) Intrinsic tumor suppression and epithelial maintenance by endocytic activation of Eiger/TNF signaling in *Drosophila*. Dev Cell 16(3):458–465
Jin Z, Kirilly D, Weng C et al (2008) Differentiation-defective stem cells outcompete normal stem cells for niche occupancy in the *Drosophila* ovary. Cell Stem Cell 2(1):39–49
Johnston LA (2009) Competitive interactions between cells: death, growth and geography. Science 324(5935):1679–1682
Johnston LA, Sanders AL (2003) Wingless promotes cell survival but constrains growth during *Drosophila* wing development. Nat Cell Biol 5(9):827–833
Johnston LA, Prober DA, Edgar BA et al (1999) *Drosophila myc* regulates cellular growth during development. Cell 98(6):779–790
Kajita M, Hogan C, Harris AR et al (2010) Interaction with surrounding normal epithelial cells influences signaling pathways and behavior of Src-transformed cells. J Cell Sci 123(Pt 2): 171–180
Kongsuwan K, Yu Q, Vincent A et al (1985) A *Drosophila* minute gene encodes a ribosomal protein. Nature (Lond) 317(6037):555–558
Lambertsson A (1998) The minute genes in *Drosophila* and their molecular functions. Adv Genet 38:69–134

Levayer R, Moreno E (2013) Mechanisms of cell competition: themes and variation. J Cell Biol 200(6):689–698
Li W, Baker NE (2007) Engulfment is required for cell competition. Cell 129(6):1215–1225
Lin H (2002) The stem-cell niche theory: lessons from flies. Nat Rev Genet 3(12):931–940
Lolo FN, Casas-Tinto S, Moreno E (2012) Cell competition time line: winners kill losers, which are extruded and engulfed by hemocytes. Cell Rep 2(3):526–539
Martin-Belmonte F, Perez-Moreno M (2012) Epithelial cell polarity, stem cells and cancer. Nat Rev Cancer 12(1):23–38
Martinek N, Zou R, Berg M et al (2002) Evolutionary conservation and association of SPARC with the basal lamina in *Drosophila*. Dev Genes Evol 212(3):124–133
Morata G, Ripoll P (1975) Minutes: mutants of *Drosophila* autonomously affecting cell division rate. Dev Biol 42(2):211–221
Moreno E (2008) Is cell competition relevant to cancer? Nat Rev Cancer 8(2):141–147
Moreno E, Basler K (2004) dMyc transforms cells into super-competitors. Cell 117(1):117–129
Moreno E, Basler K, Morata G (2002) Cells compete for decapentaplegic survival factor to prevent apoptosis in *Drosophila* wing development. Nature (Lond) 416(6882):755–759
Neto-Silva RM, de Beco S, Johnston LA (2010) Evidence for a growth-stabilizing regulatory feedback mechanism between Myc and Yokie, the *Drosophila* homolog of Yap. Dev Cell 19(4): 507–520
Norman M, Wisniewska KA, Lawrenson K et al (2012) Loss of Scribble causes cell competition in mammalian cells. J Cell Sci 125(pt 1):59–66
Ohsawa S, Sugimura K, Takino K et al (2011) Elimination of oncogenic neighbors by JNK-mediated engulfment in *Drosophila*. Dev Cell 20(3):315–328
Ohsawa S, Sato Y, Enomoto M et al (2012) Mitochondrial defect drives non-autonomous tumor progression through Hippo signaling in *Drosophila*. Nature (Lond) 490(7421):547–551
Oliver ER, Saunders TL, Tarle SA et al (2004) Ribosomal protein L24 defect in belly spot and tail (Bst), a mouse Minute. Development (Camb) 131(16):3907–3920
Pagliarini RA, Xu T (2003) A genetic screen in *Drosophila* for metastatic behavior. Science 302(5648):1227–1231
Pan D (2010) The hippo signaling pathway in development and cancer. Dev Cell 19(4):491–505
Portela M, Casa-Tinto S, Rhiner C et al (2010) *Drosophila* SPARC is a self-protective signal expressed by loser cells during cell competition. Dev Cell 19(4):562–573
Rhiner C, Lopez-Gay JM, Soldini D et al (2010) Flower forms an extracellular code that reveals the fitness of a cell to its neighbors in *Drosophila*. Dev Cell 18(6):985–998
Rodrigues AB, Zoranovic T, Ayala-Camargo A et al (2012) Activated STAT regulates growth and induces competitive interactions independently of Myc, Yokie, Wingless and ribosome biogenesis. Development (Camb) 139(21):4051–4061
Schroeder MC, Chen CL, Gajewski K et al (2012) A non-cell-autonomous tumor suppressor role for Stat in eliminating oncogenic scribble cells. Oncogene. doi:10.1038/onc.2012.476
Serrano N, O'Farrell PH (1997) Limb morphogenesis: connections between patterning and growth. Curr Biol 7(3):R186–R195
Simpson P (1976) Analysis of the compartments of the wing of *Drosophila melanogaster* mosaic for a temperature-sensitive mutation that reduces mitotic rate. Dev Biol 54(1):100–115
Simpson P (1979) Parameters of cell competition in the compartments of wing disc of *Drosophila*. Dev Biol 69(1):182–193
Simpson P, Morata G (1981) Differential mitotic rates and patterns of growth in compartments in *Drosophila* wing. Dev Biol 85(2):299–308
Stewart M, Murphy C, Fristrom JW (1972) The recovery and preliminary characterization of X chromosome mutants affecting imaginal discs of *Drosophila melanogaster*. Dev Biol 27(1):71–83
Stine RR, Matunis EL (2013) Stem cell competition: finding balance in the niche. Trends Cell Biol 23(8):357–364. doi:10.1016/j.tcb.2013.03.001
Tamori Y, Deng WM (2011) Cell competition and its implications for development and cancer. J Genet Genomics 38(10):483–495

Tamori Y, Deng WM (2013) Tissue repair through cell competition and compensatory cellular hypertrophy in postmitotic epithelia. Dev Cell 25(4):350–363

Tamori Y, Bialucha CU, Tian AG et al (2010) Involvement of Lgl and Mahjong/VprBP in cell competition. PLoS Biol 8(7):e1000422

Tsukazaki T, Chiang TA, Davison AF et al (1998) SARA, a FYVE domain protein that recruits Smad2 to the TGFbeta receptor. Cell 95(6):779–791

Tyler DM, Li W, Zhuo N et al (2007) Genes affecting cell competition in *Drosophila*. Genetics 175(2):643–657

Vincent JP, Kolahgar G, Gagliardi M et al (2011) Steep differences in wingless signaling trigger myc-independent competitive cell interactions. Dev Cell 21(2):366–374

Woods DF, Bryant PJ (1991) The disc-large tumor suppressor gene of *Drosophila* encodes a guanylate kinase homolog localized at septate junctions. Cell 66(3):451–464

Xu T, Rubin GM (1993) Analysis of genetic mosaics in developing and adult *Drosophila* tissues. Development (Camb) 117(4):1223–1237

Yao CK, Lin YQ, Ly CV et al (2009) A synaptic vesicle-associated Ca^{2+} channel promotes endocytosis and couples exocytosis to endocytosis. Cell 138(5):947–960

Yu FX, Guan KL (2013) The Hippo pathway: regulators and regulations. Genes Dev 27(4): 355–371

Yu FX, Zhao B, Panupinthu N et al (2012) Regulation of the Hippo-YAP pathway by G-protein-coupled receptor signaling. Cell 150(4):780–791

Zhao B, Li L, Wang L et al (2012) Cell detachment activates the Hippo pathway via cytoskeleton reorganization to induce anoikis. Genes Dev 26(1):54–68

Ziosi M, Baena-Lopez LA, Garoria F et al (2010) dMyc functions downstream of Yokie to promote the supercompetitive behavior of hippo pathway mutant cells. PLoS Genet 6(9):e1001140

Chapter 4
Position-Dependent Hippo Signaling Controls Cell Fates in Preimplantation Mouse Embryos

Hiroshi Sasaki

Abstract During preimplantation mouse development, embryos establish two distinct cell lineages by the time of early blastocyst formation: the trophectoderm (TE) and the inner cell mass (ICM). Historically, the importance of cell position within the embryo (inside–outside model) and apico-basal difference, known as cell polarity (polarity model), were suggested for establishment of the two lineages. In this review, I describe the mechanisms of cell fate specification in preimplantation embryos as an example of cell fate control by position-dependent Hippo signaling. Cell–cell adhesion and cell polarity activate and suppress Hippo signaling, respectively, and their combination establishes position-dependent Hippo signaling. Thus, both inside–outside and polarity models are supported. At the molecular level, phosphorylation of the adherens junctions (AJs)-associated Hippo signal component, angiomotin (Amot), activates Lats protein kinase and triggers Hippo signaling. Although this mechanism operates in the AJs of the apolar inner cells, in the outer cells, cell polarity sequesters Amot from basolateral AJs and inactivates the Hippo pathway. Thus, in preimplantation embryos, the cells utilize positional information for proper cell fate control through Hippo signaling. I also discuss the roles of Hippo signaling in regulation of development.

Keywords Hippo signaling • Preimplantation embryo • Trophectoderm • Inner cell mass • Angiomotin

H. Sasaki (✉)
Department of Cell Fate Control, Institute of Molecular Embryology and Genetics, Kumamoto University, Kumamoto 860-0811, Japan
e-mail: sasaki@kumamoto-u.ac.jp

H. Kondoh and A. Kuroiwa (eds.), *New Principles in Developmental Processes*,
DOI 10.1007/978-4-431-54634-4_4, © Springer Japan 2014

4.1 Historical Models for Cell Fate Control

During preimplantation development, mouse embryos form a cyst-like structure called the blastocyst by 3.5 days post coitus (dpc) (Fig. 4.1a). The early blastocysts consist of two type of cells. The outer epithelial cells are named the trophectoderm (TE), which is required for implantation to the uterus and forms extra-embryonic tissues including the placenta. The inner cells attached to one end of the TE constitute the inner cell mass (ICM). The ICM further differentiates into epiblast and primitive endoderm by 4.5 dpc. The former forms the embryo proper whereas the latter form a second group of extra-embryonic tissues.

Differing from other oviparous vertebrate embryos, development of mouse embryos does not critically depend on the determinants that are localized in the fertilized egg. How do the embryos properly form the two cell types without localized information? Historically, two models have been proposed (Fig. 4.2). The first one is the inside–outside (positional) model proposed by Tarkowski (Tarkowski and Wroblewska 1967). In this model, cell fate is determined by the position of cells within the embryos. In support of this model, forced repositioning of blastomeres of up to 32-cell-stage embryos in the reconstituted embryos readjusted their fates according to their new positions (Suwinska et al. 2008). The second model is the polarity model, in which cell polarity is important for cell fate specification. At the

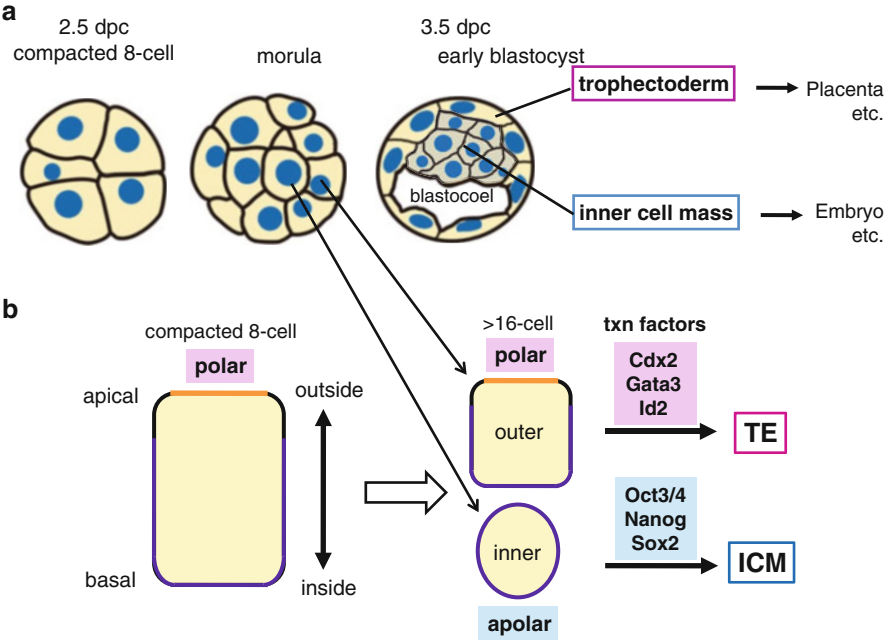

Fig. 4.1 Outline of preimplantation mouse development. (**a**) Schematic presentation of preimplantation development between 8-cell and early blastocyst (~32-cell) stages. (**b**) Relationship among cell position, cell polarity, transcription (txn) factors, and cell fates

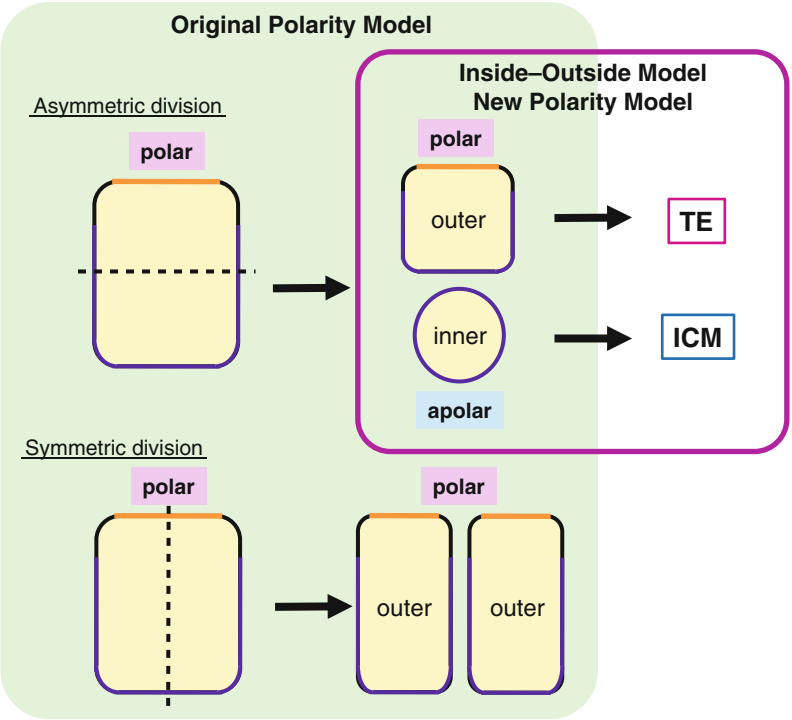

Fig. 4.2 Historical models for cell fate specification. Note that the inside–outside model and the new polarity model are not mutually exclusive

8-cell stage, cell–cell adhesion mediated by E-cadherin increases (Hyafil et al. 1980; Shirayoshi et al. 1983) and each blastomere becomes polarized by acquiring apico-basal differences, which we call cell polarity. This process causes blastomere compaction. In the following cleavages, some of the blastomeres are internalized. The outer cells remain polarized while the inner cells become apolar (Fig. 4.1b). A majority of the inner cells are formed through asymmetrical cell divisions, which form one polar outer cell and one apolar inner cell, from 8 to 16 cells (first wave) and 16 to 32 cells (second wave), and the numbers of inner cells generated in each wave are variable (Fleming 1987; Johnson and Ziomek 1981; Morris et al. 2010; Dietrich and Hiiragi 2007; McDole et al. 2011). In the original polarity model (Johnson and Ziomek 1981), asymmetrical cleavage of the polarized 8-cell stage blastomeres causes differential inheritance, which initiates differential cell fates: the inner cells derived from the bases of polarized cells form the ICM, and the outer cells inheriting the apical surface form the TE. The new version of the polarity model proposes that the presence of cell polarity or apical domain directly controls cell fates in a cell autonomous manner (Niwa et al. 2005; Yamanaka et al. 2006). The original polarity model is not compatible with this model, but the new version of the polarity model is not mutually exclusive with this model, because the inside–outside cell position controls whether the cells have polarity (Fig. 4.2).

4.2 Hippo Signaling Controls Position-Dependent Cell Fates

Cell fates are controlled by expression of the cell type-specific transcription factors. The inner cells gradually increase the expression of a POU family of transcription factor Pou5f1 (also known as Oct3/4), a Sox family of transcription factor Sox2, and a homeodomain protein Nanog (Nichols et al. 1998; Avilion et al. 2003; Chambers et al. 2003; Mitsui et al. 2003), and become ICM (Fig. 4.1b). Sox2 is the first transcription factor that shows selective upregulation in the inner cells as early as the 16-cell stage (Guo et al. 2010). Expression of Nanog and Oct3/4 are initially widespread and restricted to the inner cells from 32-cell to 64-cell stages, respectively (Niwa et al. 2005; Dietrich and Hiiragi 2007; Guo et al. 2010). The outer cells gradually increase the expression of a homeodomain transcription factor Cdx2 and a zinc-finger transcription factor Gata3 (Strumpf et al. 2005; Ralston and Rossant 2008) and become TE (Fig. 4.1b). Expression of both proteins starts from the 8-cell stage. The initial expression pattern appears to be stochastic, but becomes restricted to the outer cells from about the 32-cell stage (Niwa et al. 2005; Dietrich and Hiiragi 2007; Ralston et al. 2010). A helix–loop–helix protein Id2 is the earliest transcription factor that shows outer cell-specific expression at the 16-cell stage (Guo et al. 2010), but the role of Id2 in TE fate specification remains unknown. *Cdx2* mRNAs are localized to the apical domain of blastomeres and asymmetrically inherited to the outer cells (Skamagki et al. 2013). This observation is superficially consistent with the original polarity model, but asymmetrical inheritance of *Cdx2* mRNA is not essential, considering the results of a repositioning experiment (Suwinska et al. 2008). More important is the continued inhibition of Hippo signaling in outer cells, as detailed next.

How is expression of these factors controlled? The key finding was our identification of the TEA domain transcription factor, Tead4, as an upstream regulator of *Cdx2* (Nishioka et al. 2008; Yagi et al. 2007). *Tead4*$^{-/-}$ embryos do not express Cdx2 or Gata3, fail to form blastocoeles, and all the cells follow the ICM fate (Nishioka et al. 2008; Yagi et al. 2007; Ralston et al. 2010). Abnormalities of *Tead4*$^{-/-}$ embryos are more severe than those of *Cdx2*$^{-/-}$ embryos (Nishioka et al. 2008), and Tead4 directly regulates multiple trophoblast genes including *Cdx2* in TS cells (Home et al. 2012). Interestingly, expression of Tead4 is not restricted to the outer cells (Nishioka et al. 2008; Hirate et al. 2012) (Fig. 4.4), but Tead4 exerts its activator function only in the outer cells (Nishioka et al. 2009). Tead proteins are downstream transcription factors of the Hippo signaling pathway in mammals (Ota and Sasaki 2008; Zhao et al. 2008) (Fig. 4.3). The Hippo signaling pathway was originally identified as a tumor suppressor signaling pathway in *Drosophila* (see reviews and references in Yu and Guan 2013; Harvey et al. 2013). Cell–cell adhesion is an important activation signal of this signaling pathway, and activation of the Hippo pathway inactivates Tead function by suppressing nuclear localization of the coactivator protein Yap (Zhao et al. 2007; Ota and Sasaki 2008) (Fig. 4.3). The mouse has two Yap-related proteins, Yap1 and Taz/Wwtr1, and in this review, I describe these proteins as Yap as a whole unless otherwise noted.

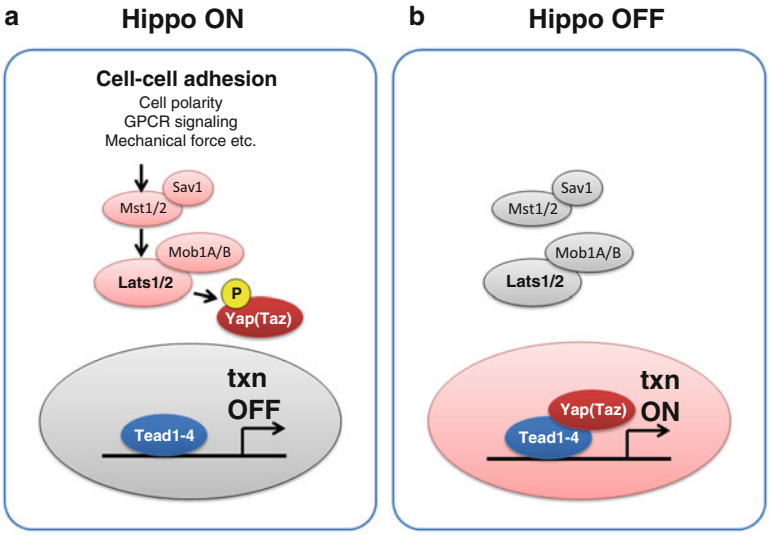

Fig. 4.3 Mammalian Hippo signaling pathway. The core mechanism of the Hippo pathway is regulation of subcellular localization of Yap. The Hippo pathway is regulated by various upstream signals including cell–cell adhesion. (**a**) Activation of the Hippo pathway phosphorylates Yap (and related protein Taz) and prevents its nuclear accumulation. Tead proteins are inactivated and expression of target genes are suppressed. (**b**) When Hippo signaling is inactive, Yap accumulates in the nuclei, Tead becomes activated, and target genes are expressed

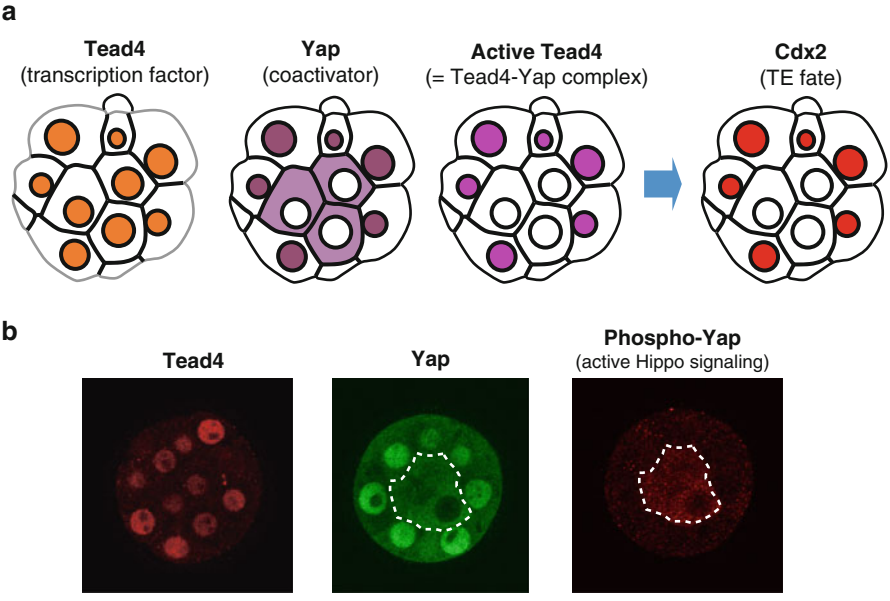

Fig. 4.4 Position-dependent Hippo signaling controls cell fates in preimplantation embryos. (**a**) Schematic presentation of spatial distribution patterns of Tead4, Yap, and Cdx2. (**b**) Confocal images show distribution of Tead, Yap, and phospho-Yap. Note that Hippo signaling revealed by phospho-Yap is stronger in the inner cells

In preimplantation embryos, Yap is present in the nuclei of the outer cells, whereas it is excluded from the nuclei in the inner cells (Nishioka et al. 2009) (Fig. 4.4). In the inner cells, strong activation of the Hippo signaling suppresses nuclear accumulation of Yap and inactivate Tead4-dependent transcription whereas weak Hippo signaling allows nuclear Yap and activates Tead4-dependent transcription in the outer cells (Nishioka et al. 2009). When Hippo signaling is suppressed by reducing or removing the protein kinase Lats1/2, the inner cells also exhibited nuclear Yap and strong Cdx2 expression (Nishioka et al. 2009) and failed to develop into ICM (Lorthongpanich et al. 2013). Thus, the difference in cell position (inside or outside) is reflected in the difference in Hippo signaling, which in turn controls whether cells become TE or ICM. This model is consistent with the inside–outside model.

4.3 Cell Polarity and Cell–Cell Adhesion Cooperate in Establishment of Position-Dependent Hippo Signaling

Establishment of position-dependent Hippo signaling involves differences in cell polarity: the outer and inner cells are polar and apolar, respectively. Disruption of the Par–aPKC system, a key regulator of apico-basal cell polarity (Suzuki and Ohno 2006), results in the activation of the Hippo signal in all cells at about the 32-cell stage (Hirate et al. 2013). This activation depends on cell–cell adhesion because the Hippo signal was not activated when embryos were dissociated (Hirate et al. 2013). These observations indicate a model that, although cell–cell adhesion activates the Hippo signal, polarization in the outer cells blocks its activation (Hirate et al. 2013). This model is consistent with both the inside–outside model and the new version of polarity model (Fig. 4.5). This fact also implies that the critically important information of cell position is whether the cells have apico-basal cell polarity.

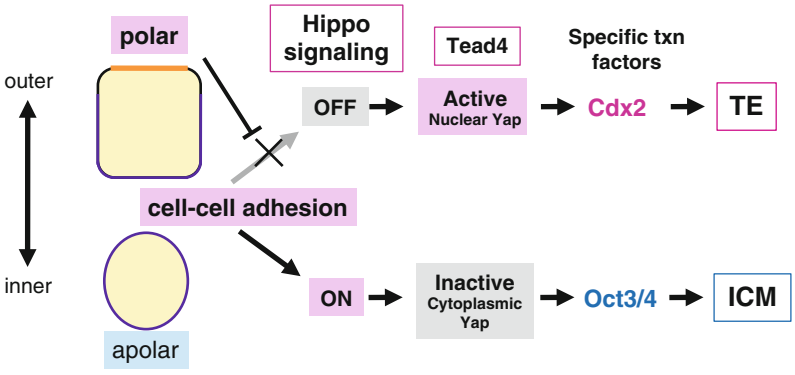

Fig. 4.5 Combination of cell–cell adhesion and cell polarity establishes position-dependent Hippo signaling leading to differential cell fates. Cell–cell adhesion activates whereas cell polarity suppresses the Hippo pathway. Position-dependent differences in cell polarity causes differential Hippo signaling

4.4 Phosphorylation of Angiomotin at Adherens Junctions Activates the Hippo Pathway

Homophilic dimerization of E-cadherins activates the Hippo pathway (Kim et al. 2011). Junction-associated Hippo components angiomotin (Amot) family proteins (Zhao et al. 2011) and Merlin encoded by *Nf2* (Zhang et al. 2010) interact with the E-cadherin–α/β-catenin complex (Hirate et al. 2013; Gladden et al. 2010). In the absence of Amot and a related protein Amotl2 (Amot mutants that are knocked down with Amotl2) or Merlin proteins (maternal and zygotic mutants of *Nf2*), morula cells failed to activate the Hippo pathway, resulting in the development of TE-only blastocyst (Hirate et al. 2013; Cockburn et al. 2013) (Fig. 4.6c). At the adherens junctions (AJs), S176 of Amot is phosphorylated by Lats. This phosphorylation stabilizes interaction of Amot and Lats and activates the Hippo pathway (Fig. 4.7, inner cell). Phosphorylation of S176-Amot is necessary and sufficient for activation of the pathway, indicating that it is a key switching mechanism that turns on the Hippo pathway at the AJs (Hirate et al. 2013).

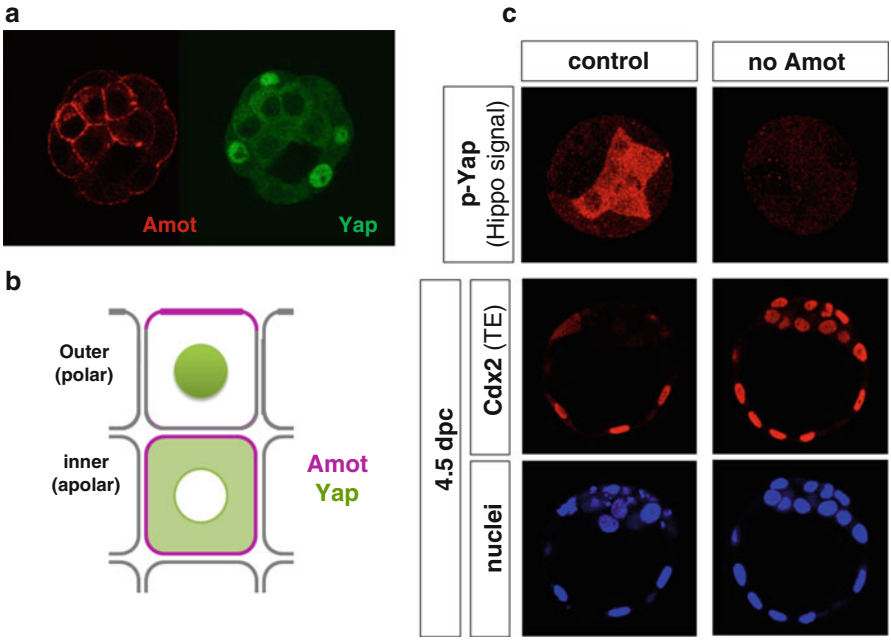

Fig. 4.6 Distribution of Amot regulates position-dependent Hippo signaling. (**a**) Confocal images show distribution of Amot and Yap in a 32-cell stage embryo. (**b**) Schematic representation of position-dependent differential subcellular distribution of Amot and Yap. (**c**) Confocal images show absence of Hippo signaling (p-Yap) and expansion of TE (Cdx2) cells in the embryos lacking Amot and Amotl2 (no Amot)

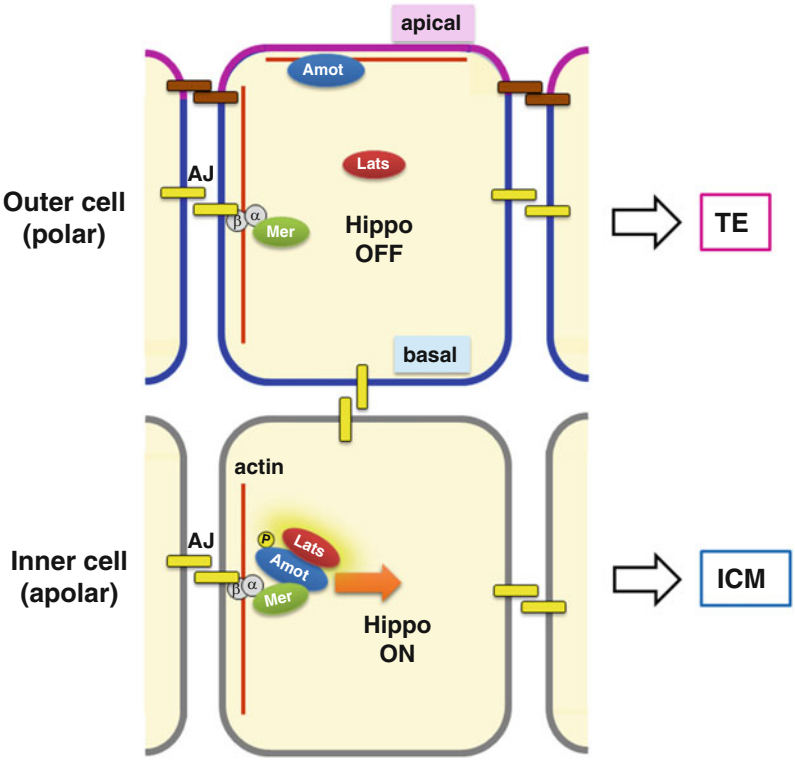

Fig. 4.7 Model of position- and polarity-dependent Hippo signaling in preimplantation mouse embryos. In apolar inner cells, phosphorylation of Amot at AJs activates Lats and Hippo signaling. In polar outer cells, Amot is sequestered from adherens junctions (*AJs*), and the Hippo pathway remains inactive. *Mer* Merlin, *α* α-catenin, *β* β-catenin

4.5 Cell Polarity Controls Hippo Signaling by Restricting Amot Localization to AJs

In preimplantation embryos, Amot shows a striking difference in the distribution between outer (polar) cells and inner (apolar) cells (Hirate et al. 2013; Leung and Zernicka-Goetz 2013) (Fig. 4.6a, b). In the inner cells, Amot is present in all AJs, whereas in the outer cells, Amot is restricted to the apical domain and is absent from basolateral AJs. Such cell position-dependent distribution of Amot is regulated by cell polarity (Hirate et al. 2013). In polarity-disrupted embryos caused by disturbing the Par–aPKC system, Amot is present in all AJs and Hippo signaling is activated in all the cells. Therefore, apolar condition-dependent association of Amot to AJs causes position-dependent Hippo signaling. In the inner apolar cells, presence of Amot in AJs activates Hippo pathway, but in the outer polar cells, Amot is sequestered in the apical membrane, which prevents AJ-dependent activation of the Hippo pathway (Fig. 4.7).

4.6 Cooperation of Hippo Signaling with Other Mechanisms

In spite of the critical importance of Hippo signaling in cell fate specification, Hippo signaling appears not to be the only mechanism. Blastomeres in 4-cell stage embryos already have differences in developmental potential, epigenetic modification, and nuclear retention of Oct3/4 (Piotrowska-Nitsche et al. 2005; Torres-Padilla et al. 2007; Plachta et al. 2011; Tabansky et al. 2013). These differences probably bias cell fates at an early stage. Initial expression of Cdx2 is rather stochastic and is constantly observed in some inner cells (Nishioka et al. 2009; Niwa et al. 2005; Dietrich and Hiiragi 2007), indicating that initial activation of *Cdx2* is not strictly controlled by cell position. Therefore, Hippo signaling probably plays major roles at later stages. Because cell fates are not determined up to the 32-cell stage (Suwinska et al. 2008), continuous operation of position-dependent Hippo signaling from the 16-cell stage onward is likely required to adjust, maintain, and enhance the position-dependent differential cell fates until they are determined.

Recently, it was shown that Tead4 has an antioxidative stress function, and that even *Tead4*$^{-/-}$ embryos can specify TE fate if oxidative stress is alleviated (Kaneko and DePamphilis 2013). It is possible that other unidentified position-dependent signaling systems also exist, and these in cooperation with Hippo signaling specify cell fate.

4.7 Perspective: Hippo Signaling Pathway Functions as a Sensor of Cell Environment

Cell fate control by Hippo signaling is also observed in differentiation of mesenchymal stem cells (MSCs). In this case, elasticity of the extracellular matrix (ECM) controls cell fates: on a stiff ECM, MSCs differentiate into osteoblasts whereas MSCs differentiate into adipocytes on a soft ECM (Engler et al. 2006). Elasticity of substrate controls cell morphology and F-actin, and F-actin regulates Hippo signaling (Dupont et al. 2011; Wada et al. 2011). On a stiff substrate, F-actin promotes nuclear accumulation of Yap, which promotes osteogenesis. On a soft substrate, reduced F-actin causes cytoplasmic localization of Yap, which promotes adipogenesis (Dupont et al. 2011).

In most tissues, Hippo signaling controls cell proliferation. Tead1/2–Yap interaction is required for cell proliferation and suppression of apoptosis in whole embryos as early as 7.5 dpc (Sawada et al. 2008). In heart and liver, Hippo signaling controls organ size. In the heart, Tead1-Yap promotes proliferation of cardiomyocytes and controls heart size (Ota and Sasaki 2008; von Gise et al. 2012). Cross-regulation of Yap, insulin-like growth factor (IGF) signaling and Wnt signaling also contributes to increased cell proliferation in the heart (Xin et al. 2011; Heallen et al. 2011). In the liver, suppression of Hippo signaling or increased nuclear Yap promotes increased liver size and expansion of hepatic progenitor cells (oval cells) (Lee et al.

2010; Dong et al. 2007; Camargo et al. 2007). Similar regulation of stem/progenitor cells by Hippo signaling is also widely observed (reviewed in Hiemer and Varelas 2013). Inactivation of Hippo signaling or increased nuclear Yap in epidermis, intestine, and brain activated proliferation of progenitor cells while compromising their differentiation (Lee et al. 2008; Zhou et al. 2011; Cappello et al. 2013). Nuclear localization of Yap is also required for maintenance of embryonic stem cells (Lian et al. 2010). Hippo signaling also controls cell motility. Increased Tead–Yap activity promotes epithelial–mesenchymal transition of cultured cells (Ota and Sasaki 2008; Overholtzer et al. 2006), and phosphorylation of Amot by Lats inhibits endothelial migration and angiogenesis (Dai et al. 2013).

In summary, upstream stimuli controlling the Hippo pathway are divergent: included are cell–cell adhesion, cell polarity, elasticity of ECM, mechanical force, cytoskeleton, and soluble factors activating various G protein-coupled receptors (GPCR), etc. (Yu and Guan 2013). The Hippo signaling pathway cross-talks with other signaling pathways such as Wnt and TGF-β signaling (Varelas and Wrana 2012). The downstream cellular responses, which include cell differentiation, proliferation, survival and migration, also vary depending on cell types. Taken together, in developing embryos, Hippo signaling pathway likely functions as a sensor of various environmental information that surrounds the cells. The environmental information that controls Hippo signaling will be integrated with other signaling information that cells are receiving, and the cells then make cell type-specific responses to properly form the embryos.

References

Avilion AA, Nicolis SK, Pevny LH, Perez L, Vivian N, Lovell-Badge R (2003) Multipotent cell lineages in early mouse development depend on SOX2 function. Genes Dev 17(1):126–140

Camargo FD, Gokhale S, Johnnidis JB, Fu D, Bell GW, Jaenisch R, Brummelkamp TR (2007) YAP1 increases organ size and expands undifferentiated progenitor cells. Curr Biol 17(23):2054–2060

Cappello S, Gray MJ, Badouel C, Lange S, Einsiedler M, Srour M, Chitayat D, Hamdan FF, Jenkins ZA, Morgan T, Preitner N, Uster T, Thomas J, Shannon P, Morrison V, Di Donato N, Van Maldergem L, Neuhann T, Newbury-Ecob R, Swinkells M, Terhal P, Wilson LC, Zwijnenburg PJ, Sutherland-Smith AJ, Black MA, Markie D, Michaud JL, Simpson MA, Mansour S, McNeill H, Gotz M, Robertson SP (2013) Mutations in genes encoding the cadherin receptor–ligand pair DCHS1 and FAT4 disrupt cerebral cortical development. Nat Genet 45(11):1300–1308. doi:10.1038/ng.2765

Chambers I, Colby D, Robertson M, Nichols J, Lee S, Tweedie S, Smith A (2003) Functional expression cloning of Nanog, a pluripotency sustaining factor in embryonic stem cells. Cell 113(5):643–655

Cockburn K, Biechele S, Garner J, Rossant J (2013) The Hippo pathway member Nf2 is required for inner cell mass specification. Curr Biol 23(13):1195–1201. doi:10.1016/j.cub.2013.05.044

Dai X, She P, Chi F, Feng Y, Liu H, Jin D, Zhao Y, Guo X, Jiang D, Guan KL, Zhong TP, Zhao B (2013) Phosphorylation of angiomotin by Lats1/2 kinases inhibits F-actin binding, cell migration and angiogenesis. J Biol Chem. doi:10.1074/jbc.M113.518019

Dietrich JE, Hiiragi T (2007) Stochastic patterning in the mouse pre-implantation embryo. Development (Camb) 134(23):4219–4231

Dong J, Feldmann G, Huang J, Wu S, Zhang N, Comerford SA, Gayyed MF, Anders RA, Maitra A, Pan D (2007) Elucidation of a universal size-control mechanism in *Drosophila* and mammals. Cell 130(6):1120–1133

Dupont S, Morsut L, Aragona M, Enzo E, Giulitti S, Cordenonsi M, Zanconato F, Le Digabel J, Forcato M, Bicciato S, Elvassore N, Piccolo S (2011) Role of YAP/TAZ in mechanotransduction. Nature (Lond) 474(7350):179–183. doi:10.1038/nature10137

Engler AJ, Sen S, Sweeney HL, Discher DE (2006) Matrix elasticity directs stem cell lineage specification. Cell 126(4):677–689. doi:10.1016/j.cell.2006.06.044

Fleming TP (1987) A quantitative analysis of cell allocation to trophectoderm and inner cell mass in the mouse blastocyst. Dev Biol 119(2):520–531

Gladden AB, Hebert AM, Schneeberger EE, McClatchey AI (2010) The NF2 tumor suppressor, Merlin, regulates epidermal development through the establishment of a junctional polarity complex. Dev Cell 19(5):727–739. doi:10.1016/j.devcel.2010.10.008

Guo G, Huss M, Tong GQ, Wang C, Li Sun L, Clarke ND, Robson P (2010) Resolution of cell fate decisions revealed by single-cell gene expression analysis from zygote to blastocyst. Dev Cell 18(4):675–685. doi:10.1016/j.devcel.2010.02.012

Harvey KF, Zhang X, Thomas DM (2013) The Hippo pathway and human cancer. Nat Rev Cancer 13(4):246–257. doi:10.1038/nrc3458

Heallen T, Zhang M, Wang J, Bonilla-Claudio M, Klysik E, Johnson RL, Martin JF (2011) Hippo pathway inhibits Wnt signaling to restrain cardiomyocyte proliferation and heart size. Science 332(6028):458–461. doi:10.1126/science.1199010

Hiemer SE, Varelas X (2013) Stem cell regulation by the Hippo pathway. Biochim Biophys Acta 1830(2):2323–2334. doi:10.1016/j.bbagen.2012.07.005

Hirate Y, Cockburn K, Rossant J, Sasaki H (2012) Tead4 is constitutively nuclear, while nuclear vs. cytoplasmic Yap distribution is regulated in preimplantation mouse embryos. Proc Natl Acad Sci USA 109(50):E3389–E3390. doi:10.1073/pnas.1211810109

Hirate Y, Hirahara S, Inoue KI, Suzuki A, Alarcon VB, Akimoto K, Hirai T, Hara T, Adachi M, Chida K, Ohno S, Marikawa Y, Nakao K, Shimono A, Sasaki H (2013) Polarity-dependent distribution of angiomotin localizes hippo signaling in preimplantation embryos. Curr Biol. doi:10.1016/j.cub.2013.05.014

Home P, Saha B, Ray S, Dutta D, Gunewardena S, Yoo B, Pal A, Vivian JL, Larson M, Petroff M, Gallagher PG, Schulz VP, White KL, Golos TG, Behr B, Paul S (2012) Altered subcellular localization of transcription factor TEAD4 regulates first mammalian cell lineage commitment. Proc Natl Acad Sci USA 109(19):7362–7367. doi:10.1073/pnas.1201595109

Hyafil F, Morello D, Babinet C, Jacob F (1980) A cell surface glycoprotein involved in the compaction of embryonal carcinoma cells and cleavage stage embryos. Cell 21(3):927–934. doi:10.1016/0092-8674(80)90456-0

Johnson MH, Ziomek CA (1981) The foundation of two distinct cell lineages within the mouse morula. Cell 24(1):71–80

Kaneko KJ, DePamphilis ML (2013) TEAD4 establishes the energy homeostasis essential for blastocoel formation. Development (Camb) 140(17):3680–3690. doi:10.1242/dev.093799

Kim NG, Koh E, Chen X, Gumbiner BM (2011) E-cadherin mediates contact inhibition of proliferation through Hippo signaling-pathway components. Proc Natl Acad Sci USA 108(29): 11930–11935. doi:10.1073/pnas.1103345108

Lee JH, Kim TS, Yang TH, Koo BK, Oh SP, Lee KP, Oh HJ, Lee SH, Kong YY, Kim JM, Lim DS (2008) A crucial role of WW45 in developing epithelial tissues in the mouse. EMBO J 27(8):1231–1242

Lee KP, Lee JH, Kim TS, Kim TH, Park HD, Byun JS, Kim MC, Jeong WI, Calvisi DF, Kim JM, Lim DS (2010) The Hippo–Salvador pathway restrains hepatic oval cell proliferation, liver size, and liver tumorigenesis. Proc Natl Acad Sci USA 107(18):8248–8253. doi:10.1073/pnas.0912203107

Leung CY, Zernicka-Goetz M (2013) Angiomotin prevents pluripotent lineage differentiation in mouse embryos via Hippo pathway-dependent and -independent mechanisms. Nat Commun 4:2251. doi:10.1038/ncomms3251

Lian I, Kim J, Okazawa H, Zhao J, Zhao B, Yu J, Chinnaiyan A, Israel MA, Goldstein LS, Abujarour R, Ding S, Guan KL (2010) The role of YAP transcription coactivator in regulating stem cell self-renewal and differentiation. Genes Dev 24(11):1106–1118. doi:10.1101/gad.1903310

Lorthongpanich C, Messerschmidt DM, Chan SW, Hong W, Knowles BB, Solter D (2013) Temporal reduction of LATS kinases in the early preimplantation embryo prevents ICM lineage differentiation. Genes Dev 27(13):1441–1446. doi:10.1101/gad.219618.113

McDole K, Xiong Y, Iglesias PA, Zheng Y (2011) Lineage mapping the pre-implantation mouse embryo by two-photon microscopy, new insights into the segregation of cell fates. Dev Biol 355(2):239–249. doi:10.1016/j.ydbio.2011.04.024

Mitsui K, Tokuzawa Y, Itoh H, Segawa K, Murakami M, Takahashi K, Maruyama M, Maeda M, Yamanaka S (2003) The homeoprotein Nanog is required for maintenance of pluripotency in mouse epiblast and ES cells. Cell 113(5):631–642

Morris SA, Teo RT, Li H, Robson P, Glover DM, Zernicka-Goetz M (2010) Origin and formation of the first two distinct cell types of the inner cell mass in the mouse embryo. Proc Natl Acad Sci USA 107(14):6364–6369. doi:10.1073/pnas.0915063107

Nichols J, Zevnik B, Anastassiadis K, Niwa H, Klewe-Nebenius D, Chambers I, Scholer H, Smith A (1998) Formation of pluripotent stem cells in the mammalian embryo depends on the POU transcription factor Oct4. Cell 95(3):379–391

Nishioka N, Inoue K, Adachi K, Kiyonari H, Ota M, Ralston A, Yabuta N, Hirahara S, Stephenson RO, Ogonuki N, Makita R, Kurihara H, Morin-Kensicki EM, Nojima H, Rossant J, Nakao K, Niwa H, Sasaki H (2009) The Hippo signaling pathway components Lats and Yap pattern Tead4 activity to distinguish mouse trophectoderm from inner cell mass. Dev Cell 16(3):398–410

Nishioka N, Yamamoto S, Kiyonari H, Sato H, Sawada A, Ota M, Nakao K, Sasaki H (2008) Tead4 is required for specification of trophectoderm in pre-implantation mouse embryos. Mech Dev 125(3–4):270–283

Niwa H, Toyooka Y, Shimosato D, Strumpf D, Takahashi K, Yagi R, Rossant J (2005) Interaction between Oct3/4 and Cdx2 determines trophectoderm differentiation. Cell 123(5):917–929

Ota M, Sasaki H (2008) Mammalian Tead proteins regulate cell proliferation and contact inhibition as a transcriptional mediator of Hippo signaling. Development (Camb) 135:4059–4069

Overholtzer M, Zhang J, Smolen GA, Muir B, Li W, Sgroi DC, Deng CX, Brugge JS, Haber DA (2006) Transforming properties of YAP, a candidate oncogene on the chromosome 11q22 amplicon. Proc Natl Acad Sci USA 103(33):12405–12410

Piotrowska-Nitsche K, Perea-Gomez A, Haraguchi S, Zernicka-Goetz M (2005) Four-cell stage mouse blastomeres have different developmental properties. Development (Camb) 132(3):479–490

Plachta N, Bollenbach T, Pease S, Fraser SE, Pantazis P (2011) Oct4 kinetics predict cell lineage patterning in the early mammalian embryo. Nat Cell Biol 13(2):117–123. doi:10.1038/ncb2154

Ralston A, Cox BJ, Nishioka N, Sasaki H, Chea E, Rugg-Gunn P, Guo G, Robson P, Draper JS, Rossant J (2010) Gata3 regulates trophoblast development downstream of Tead4 and in parallel to Cdx2. Development (Camb) 137(3):395–403. doi:10.1242/dev.038828

Ralston A, Rossant J (2008) Cdx2 acts downstream of cell polarization to cell-autonomously promote trophectoderm fate in the early mouse embryo. Dev Biol 313(2):614–629

Sawada A, Kiyonari H, Ukita K, Nishioka N, Imuta Y, Sasaki H (2008) Redundant roles of Tead1 and Tead2 in notochord development and the regulation of cell proliferation and survival. Mol Cell Biol 28(10):3177–3189

Shirayoshi Y, Okada TS, Takeichi M (1983) The calcium-dependent cell–cell adhesion system regulates inner cell mass formation and cell surface polarization in early mouse development. Cell 35(3 Pt 2):631–638

Skamagki M, Wicher KB, Jedrusik A, Ganguly S, Zernicka-Goetz M (2013) Asymmetric localization of Cdx2 mRNA during the first cell-fate decision in early mouse development. Cell Rep 3(2):442–457. doi:10.1016/j.celrep.2013.01.006

Strumpf D, Mao CA, Yamanaka Y, Ralston A, Chawengsaksophak K, Beck F, Rossant J (2005) Cdx2 is required for correct cell fate specification and differentiation of trophectoderm in the mouse blastocyst. Development (Camb) 132(9):2093–2102

Suwinska A, Czolowska R, Ozdzenski W, Tarkowski AK (2008) Blastomeres of the mouse embryo lose totipotency after the fifth cleavage division: expression of Cdx2 and Oct4 and developmental potential of inner and outer blastomeres of 16- and 32-cell embryos. Dev Biol 322(1):133–144. doi:10.1016/j.ydbio.2008.07.019

Suzuki A, Ohno S (2006) The PAR-aPKC system: lessons in polarity. J Cell Sci 119(Pt 6):979–987. doi:10.1242/jcs.02898

Tabansky I, Lenarcic A, Draft RW, Loulier K, Keskin DB, Rosains J, Rivera-Feliciano J, Lichtman JW, Livet J, Stern JN, Sanes JR, Eggan K (2013) Developmental bias in cleavage-stage mouse blastomeres. Curr Biol 23(1):21–31. doi:10.1016/j.cub.2012.10.054

Tarkowski AK, Wroblewska J (1967) Development of blastomeres of mouse eggs isolated at the 4- and 8-cell stage. J Embryol Exp Morphol 18(1):155–180

Torres-Padilla ME, Parfitt DE, Kouzarides T, Zernicka-Goetz M (2007) Histone arginine methylation regulates pluripotency in the early mouse embryo. Nature (Lond) 445(7124):214–218. doi:10.1038/nature05458

Varelas X, Wrana JL (2012) Coordinating developmental signaling: novel roles for the Hippo pathway. Trends Cell Biol 22(2):88–96. doi:10.1016/j.tcb.2011.10.002

von Gise A, Lin Z, Schlegelmilch K, Honor LB, Pan GM, Buck JN, Ma Q, Ishiwata T, Zhou B, Camargo FD, Pu WT (2012) YAP1, the nuclear target of Hippo signaling, stimulates heart growth through cardiomyocyte proliferation but not hypertrophy. Proc Natl Acad Sci USA 109(7):2394–2399. doi:10.1073/pnas.1116136109

Wada K, Itoga K, Okano T, Yonemura S, Sasaki H (2011) Hippo pathway regulation by cell morphology and stress fibers. Development (Camb) 138(18):3907–3914. doi:10.1242/dev.070987

Xin M, Kim Y, Sutherland LB, Qi X, McAnally J, Schwartz RJ, Richardson JA, Bassel-Duby R, Olson EN (2011) Regulation of insulin-like growth factor signaling by Yap governs cardiomyocyte proliferation and embryonic heart size. Sci Signal 4(196):ra70. doi:10.1126/scisignal.2002278

Yagi R, Kohn MJ, Karavanova I, Kaneko KJ, Vullhorst D, Depamphilis ML, Buonanno A (2007) Transcription factor TEAD4 specifies the trophectoderm lineage at the beginning of mammalian development. Development (Camb) 134(21):3827–3836

Yamanaka Y, Ralston A, Stephenson RO, Rossant J (2006) Cell and molecular regulation of the mouse blastocyst. Dev Dyn 235(9):2301–2314. doi:10.1002/dvdy.20844

Yu FX, Guan KL (2013) The Hippo pathway: regulators and regulations. Genes Dev 27(4):355–371. doi:10.1101/gad.210773.112

Zhang N, Bai H, David KK, Dong J, Zheng Y, Cai J, Giovannini M, Liu P, Anders RA, Pan D (2010) The Merlin/NF2 tumor suppressor functions through the YAP oncoprotein to regulate tissue homeostasis in mammals. Dev Cell 19(1):27–38. doi:10.1016/j.devcel.2010.06.015

Zhao B, Li L, Lu Q, Wang LH, Liu CY, Lei Q, Guan KL (2011) Angiomotin is a novel Hippo pathway component that inhibits YAP oncoprotein. Genes Dev 25(1):51–63. doi:10.1101/gad.2000111

Zhao B, Wei X, Li W, Udan RS, Yang Q, Kim J, Xie J, Ikenoue T, Yu J, Li L, Zheng P, Ye K, Chinnaiyan A, Halder G, Lai ZC, Guan KL (2007) Inactivation of YAP oncoprotein by the Hippo pathway is involved in cell contact inhibition and tissue growth control. Genes Dev 21(21):2747–2761

Zhao B, Ye X, Yu J, Li L, Li W, Li S, Yu J, Lin JD, Wang CY, Chinnaiyan AM, Lai ZC, Guan KL (2008) TEAD mediates YAP-dependent gene induction and growth control. Genes Dev 22:1962–1972

Zhou D, Zhang Y, Wu H, Barry E, Yin Y, Lawrence E, Dawson D, Willis JE, Markowitz SD, Camargo FD, Avruch J (2011) Mst1 and Mst2 protein kinases restrain intestinal stem cell proliferation and colonic tumorigenesis by inhibition of Yes-associated protein (Yap) overabundance. Proc Natl Acad Sci USA 108(49):E1312–E1320. doi:10.1073/pnas.1110428108

Chapter 5
Building Functional Internal Organs from a Naïve Endodermal Sheet

Mitsuru Morimoto

Abstract The organs perform physiological functions with mature tissues composed of variously specialized cell types. Full maturation and proper population balances of these cell types are necessary to generate functional organs and a healthy body. Most of the internal organs are derived from the definitive endoderm (DE), which is a naïve epithelial sheet formed at an early embryonic stage, E7.5, in the mouse. Especially, the anterior pocket of the DE is the foregut known as the origin of functional epithelial cells of many vital internal organs, including the thyroid, thymus, lung, liver and pancreas. I start this review with describing the foregut formation process in the DE and spatial arrangement of the internal organs within this area. Then, I highlight developmental and physiological mechanisms that specify, pattern, and regulate morphogenesis of the lung. Recent advances have begun to define molecular mechanisms that control many of the important processes required for lung organogenesis; however, many questions remain. I, furthermore, focus on airway epithelial development, which generates the bronchial branching structure and many different functional cells. Finally, I discuss a fundamental strategy for regulating the population and localization of various cell types during organogenesis.

Keywords Epithelial patterning • Foregut • Internal organ • Lung • Notch signaling

5.1 Introduction

Organogenesis of the inner organs begins after germ layer formation at the middle stage of embryogenesis. First, endodermal epithelium is assigned an organ cell fate by paracrine signaling from the peripheral mesoderm. The epithelial–mesenchymal

M. Morimoto (✉)
Laboratory for Lung Development, RIKEN Center for Developmental Biology, Kobe, Japan
e-mail: mmorimoto@cdb.riken.jp

H. Kondoh and A. Kuroiwa (eds.), *New Principles in Developmental Processes*,
DOI 10.1007/978-4-431-54634-4_5,

interaction regulates proliferation, selective interaction, and morphological changing of the cells to build unique organ structures. Finally, the organ holds fully differentiated cells to be functionally mature and ready to birth by the late developmental stage. This maturation process is still largely unknown. During the process, cell population and distribution pattern need to be controlled precisely for efficient physiological function. Thus, understanding the fundamental strategy of cell type diversity and its localization throughout organogenesis is important. In the lung, for example, multiciliated cells are numerous in the trachea, which is the most proximal airway, whereas the distal bronchioles include fewer ciliated cells and abundant mucus-providing Clara cells. On the other hand, the ratio between absorptive epithelial and goblet cells is 80:20 in the small intestine. In the colon, however, goblet cells are increased and the ratio becomes 50:50. Although such a region-specific epithelial pattern is related to physiological function of the organs, the molecular mechanism creating this regional distinction is still a black box. Here, I wish to describe early events of internal organ development, especially the respiratory system, in the ventral foregut and discuss the mechanism coordinating epithelial cell type diversity and patterning in the developing organ.

5.2 Formation of the Ventral Foregut from the Definitive Endoderm and Spatial Arrangement of the Internal Organs Within the Foregut

Most of the internal organs arise from the definitive endoderm (DE) with initiation cues by the adjacent mesoderm. These organ cell fates are determined for a short term, within 24 h in the mouse, in the naïve DE. In the developing mouse embryo, by E7.5, the DE is distinguished via expression of *Foxa2* (HNF-3β) in the nascent DE (Sasaki and Hogan 1994; Monaghan et al. 1993; Ang and Rossant 1994) that is induced under Tgfb-Smad3 signaling and GATA6, a transcription factor (Fig. 5.1, left). By E8.0, DE is rapidly organized into a tube along the anterior–posterior (A–P) axis of the embryo and forms pockets of the foregut and hindgut at the anterior and posterior ends. These pockets expand their ventral surfaces toward the midline. These morphogenetic movements and the subsequent deepening of the gut pockets create spatial distinctions between the ventral and dorsal domains of endoderm (Fig. 5.1, right). The ventral foregut cells are exposed to signal ligands—bone morphogenetic proteins (BMPs), fibroblast growth factors (FGFs), transforming growth factor-beta (TGF-β), Wnt2/2b, and retinoic acid (RA)—mainly produced by adjacent lateral plate mesoderm and cardiac mesoderm (Wandzioch and Zaret 2009; Serls et al. 2005; Goss et al. 2009; Chen et al. 2010). Several combinations of these signaling pathways provide various environments in the epithelial sheet. By E8.5 (seven to eight somites), *Nkx2.1*, *Alb1*, and *Pdx1* are activated in the nascent respiratory, hepatocyte, and pancreas progenitors, suggesting determination events have occurred. The results of these patterning events of the gut tubes are now

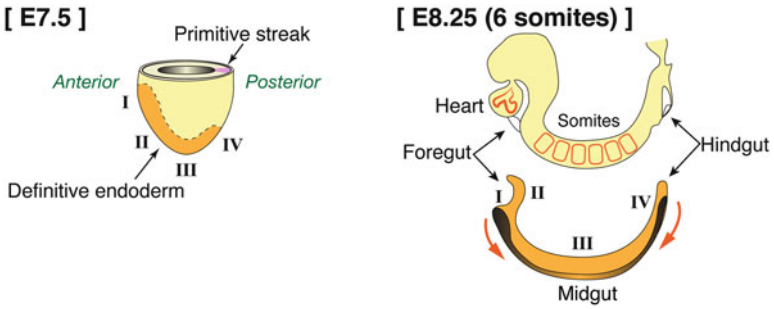

Fig. 5.1 Definitive endoderm and gut tube. *Left*: By E7.5, the late streak stage, the primitive streak extends toward the distal tip of the gastrula and produces mesoderm into an inner layer and a definitive endoderm into an outer layer. The streak-derived definitive endoderm displaces the original visceral endoderm, which becomes extra-embryonic tissue, and forms an single-layered epithelial cup at the bottom of the embryo (*orange*). *Right*: By E8.25, the heart develops rapidly and the more anterior paraxial mesoderm is arranged into paired somite blocks. The endoderm will subsequently fold ventrally in the anterior and posterior regions to form the foregut pocket and hindgut diverticulum, respectively. The embryo is folding in the direction of the arrows both anteriorly and posteriorly (*arrows*) and the open tube will close ventrally. *I*, *II*, *III*, and *IV* indicate the endodermal precursor tissue of the ventral part of the foregut: (*I*), dorsal part of the foregut (*II*), midgut (*III*), and hindgut (*IV*)

loosely divided into organ domains that can be defined by regions of gut endoderm predetermined to contribute to certain organs.

Coincident with this early gut tube formation is a cell morphological differentiation from cuboidal-type endoderm into a columnar epithelium in a part of the endoderm, which will eventually line the respiratory and digestive tracts. Although the endoderm needs further instruction throughout embryogenesis, the basic regional pattern of the endoderm seems to be established during these early stages of development. A current report has proposed that pre-patterning of chromatin states represented by histone modification potentially regulates cell fate selections in the ventral foregut (Xu et al. 2011). In the prospective hepatic progenitors at E8.25 (four to six somites), both the hepatic and pancreas genes are silenced while the *cis-enhancer* element of *Pdx1*, but not hepatic maker, gene is in "poised" state displaying both active modification H3K9, 14 acetylation, and negative modification H3K27 tri-methylation. In the following stage, BMP signaling stimulates the liver gene expression via H3K9 and 14 acetylation. The *Pdx1 cis*-enhancer elements, however, do not respond and still keep the poised state. Alteration of the poised-type histon modifications induced abnormal *Pdx1* expression in the hepatic field and resulted in expansion of the pancreas field at the ventral foregut. These observations indicate that initiation of internal organ development and its spatial relationships are precisely controlled by intercellular signaling under genetic and epigenetic information. At the later stage, those intercellular signals are further reiterated for tissue growth and maturation but most likely do not directly contribute to cell type diversity and patterning.

5.3 Specification of Primary Respiratory Progenitors in Ventral Foregut

The signals that determine and pattern the endoderm derive from adjacent structures of both mesodermal and ectodermal origin, and these signals seem to be both inductive and permissive in nature. We describe some of the better studied examples of cell type diversity in lung epithelium development. Although these studies focus on a particular organ, the conclusions could be extended to the fundamental strategy of cell type diversity of other organs that derive from the other domains of the endoderm. As in the organogenesis of all tissues, formation of the lung is dependent on a myriad of interactions among signaling and receiving molecules that mediate cell proliferation, survival, migration, polarity, differentiation, and function (Morrisey and Hogan 2010). All the airway epithelial cells must experience *Nkx2.1* expression (Kimura et al. 1996; Longmire et al. 2012). Thus, *Nkx2.1* is expected as the master regulator of airway epithelial cells. By E9.0, the homeodomain protein gene *Nkx2.1* (or *Ttf1* or *T/EBP*) is expressed in the prospective thyroid and respiratory field at the anterior from the hepatic field in the ventral foregut, which is the earliest sign of respiratory fate specification from naïve endoderm (Serls et al. 2005). In Nkx2-1 null mutant embryos, although primary lung buds form, the trachea is absent, suggesting that it is essential for the initiation of a subset of the respiratory system (Kimura et al. 1996; Minoo et al. 1999). During the specification, deletion of Wnt ligands Wnt2/2b expressed in lateral plate mesoderm results in complete absence of the primary lung buds with a paucity of *Nkx2.1* expression. Similarly, inactivation of epithelial β-catenin, a key Wnt effector in the canonical Wnt pathway, also leads to the no primary lung buds phenotype. Forced activation of Wnt/β-catenin signaling by means of ectopic expression of a dominant-stable allele of β-catenin in the ventral stomach promotes Nkx2-1 expression (Goss et al. 2009; Harris-Johnson et al. 2009). Tbx5 is also involved in the primary buds formation by regulating Wnt2/2b expression in the mesoderm (Arora et al. 2012).

Studies in mouse foregut cultures strongly indicate that FGFs emanating from the adjacent heart influence the fates of the ventral foregut endoderm in a concentration-dependent manner. A model of foregut specification has been proposed in which different thresholds of FGFs pattern the endoderm into different foregut derivatives, including the liver and lung (Fig. 5.2). If cultured alone, the endoderm adopts a "default" pancreatic fate. Increasing amounts of FGF2 from cardiac mesoderm to the endoderm results first in induction of hepatic, and then of lung or thyroid, fates (Serls et al. 2005; Rossi et al. 2001; Jung et al. 1999). In this system, the induction of lung cell fate appears to involve FGF-receptor 4 (FGFR4) signaling (Serls et al. 2005). Lung development, however, is apparently normal in *Fgfr4*-null mice (Weinstein et al. 1998). Complete absence of both *Wnt2* and *Wnt2b* in mesenchyme surrounding the anterior foregut or absence of β-catenin in the foregut epithelium leads to a loss of specification of lung primordia as seen by the absence of *Nkx2.1* expression. Hence, lung specification is likely to depend on signaling molecules, such as Wnts and FGFs, from the adjacent lateral plate and cardiac mesoderm, and local transcription factors that have yet to be identified.

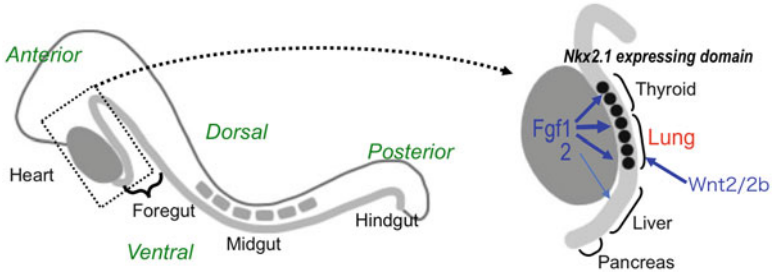

Fig. 5.2 Schematic depictions of key secreted ligands and transcription factors involved in specifying the respiratory progenitors. As the gut tube folds, cardiac FGFs and mesodermal Wnt2/2b signals induce trachea and lung progenitors in the ventral endoderm. Nkx2.1 expression is detected in the primordium thyroid and lung

Following primary lung bud formation, the buds extend into the surrounding mesenchyme and begin the process of branching morphogenesis. The molecular mechanism of branching has been well described in previous reviews (Cardoso and Lu 2006; Morrisey and Hogan 2010), but briefly, elongation of the buds is dependent on the localized expression of FGF10 in the mesoderm overlying the buds and FGFGR2b in the endoderm to stimulate proliferation. No bud extension occurs in mutants lacking *Fgf10*, although the trachea does separate (Min et al. 1998; Sekine et al. 1999). This FGF10–FGFR2b signaling is controlled by a negative feedback loop via BMP4 and Spry2 induction. In addition, the epithelial Shh suppresses mesenchymal FGF10, except for the tip, to limit epithelial proliferation within the distal-most tissue. Between E9.5 and E16.5, the primary buds generate a complex tree-like structure ending in thousands of terminal tubules. Remarkably, during this stage the branching pattern is highly stereotyped and essentially identical between inbred mouse strains (Metzger et al. 2008).

As already described, the primary lung bud formation and following branching process occur on the axis of epithelial–mesenchymal interaction. At E14.5, epithelial cell differentiation begins from the proximal tube coincident with branching formation at the distal tip. Intercellular signaling within the epithelium, rather than an interaction with mesenchyme, has a role in this process. The following sections describe and discuss the epithelial cell type and its differentiation.

5.4 Cell Differentiation and Patterning of the Major Epithelial Cell Types by Notch Signaling

5.4.1 Lung Epithelial Cell Types

The pulmonary system is composed of a tracheal tube, leading to bronchi and bronchioles that provide inhaled gases to saccular alveolar structures in which capillaries come in close apposition to epithelial surfaces to facilitate the exchange of oxygen

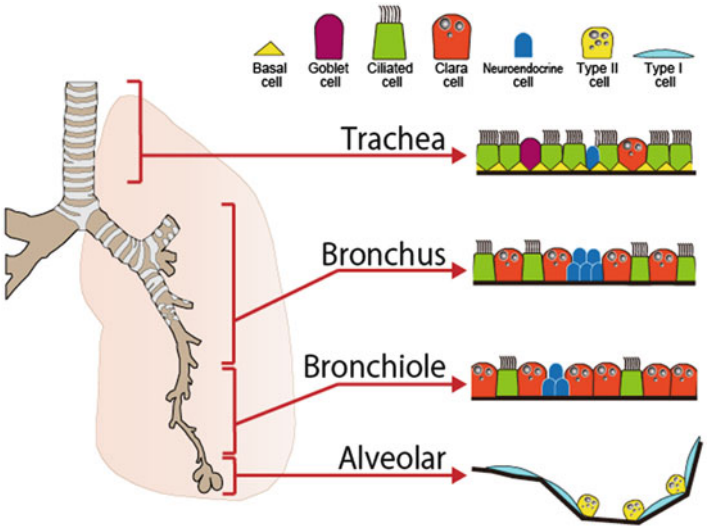

Fig. 5.3 Schematic depiction of relative locations of the various cell types in the mature lung. The epithelium of the conducting airway is composed of seven major cell types. The number and distribution of these cell types are differently arranged in individual airways. These epithelial patterns reflect the functions of the airways. In the trachea–main bronchus epithelium, there are many ciliated cells of which beating multiple cilia establish a flow that will remove a dust particle or phlegm. In contrast, Clara cells are predominantly distributed at the bronchiolar epithelium that maintains inhaled air at the entrance to the alveoli under conditions of high humidity. The alveolar includes AEC1 cells, which are very flat and thin walled, and the much larger cuboidal AEC2 cells providing surfactants. These cell types are closely juxtaposed to each other, and AEC1 cells form intimate interactions with the underlying vascular endothelium

and carbon dioxide required for cellular respiration (Fig. 5.3). These epithelial tissues for ventilation are called the airways, and especially the trachea, bronchi, and bronchioles are known as the conducting airways. This conducting system brings the air from the external environment to the alveoli and functions to protect the lung from debris that could obstruct airways, from entry of pathogens, and from excessive loss of fluids. On the inside of the mammalian airway are seven major epithelial cell types: Clara (secretary) cells, ciliated cells, pulmonary neuroendocrine (NE) cells, basal cells, and goblet cells in the conducting airway, and alveolar epithelial type I and type II cells (AEC1 and 2) (Fig. 5.3). Clara cells are typically marked by synthesis of the secretoglobin family member Scgb1a1 (CC10 or CCSP), whereas ciliated cells express Foxj1 and show more than 200 motile cilia on the apical side. In the postnatal lung, the proportion of ciliated to secretory cells is lower near the distal end of the bronchioles but elsewhere is about 50:50. Ciliated cells occupy the trachea–bronchus epithelium within which the beating multiple cilia establish a flow that will remove a dust particle or phlegm. In contrast, Clara cells are predominantly distributed at the bronchiolar epithelium that maintains inhaled air at the entrance to the alveoli under conditions of high humidity. NE cells express

calcitonin/Pgp9.5/Ascl1 and are found in small clusters at branch points along the airways. The NE cell cluster is called a neuroendocrine body (NEB), which is known as the stem cell niche in severely injured epithelium (Hong et al. 2001). Mucus-producing goblet cells that express Muc5ac, Foxa3, and the secreted ligand anterior gradient 2 (Agr2) are also found in the airways. The number of goblet cells is low in the mouse compared with the human but increases dramatically in response to airway allergens and certain cytokines [e.g., interleukin (IL)-13] and upon down-regulation of Foxa2 (Wan et al. 2004). Recent lineage tracing experiments show that Clara cells can give rise to goblet cells without cell proliferation by a process that requires the transcription factor Spdef (Chen et al. 2009). In the alveoli, these are squamous AEC1 expressing AQP5/T1α and surfactant-producing AEC2. Gas exchange occurs primarily across the attenuated blood–air barrier that is formed by the juxtaposition of AEC1 and microcapillary endothelial cells. The AEC2 functions in the biosynthesis of pulmonary surfactant, which lowers the surface tension within the alveoli, allowing for respiration at normal transpulmonary pressures. In addition, both cell types play important roles in fluid and ion transport.

5.4.2 Epithelial Cell Specification

Lung epithelial tissue acquires mature physiological functions throughout a long-term process. During this process, epithelial tubes build the branching morphology and various cell types in different ratios at individual regions of the conducting airways, as described earlier. Spatiotemporal regulation for the molecular events of these processes is crucial to create the fully functional respiratory system.

During E10.5–16.5, known as the branching stage, the cells in the distal tip of the buds constitute a pool of highly proliferative multipotent progenitor cells: these are maintained by the coordinated activity of signaling factors including Wnts and FGF10 (Okubo and Hogan 2004). Progeny left behind in the stalks by the outgrowth of the epithelium continue to divide and give rise to all the different cell types of the future bronchi and bronchioles. This model was proposed by two groups. Perl et al. found that by using an inducible SP-C-driven Cre system, they could genetically label distal lung epithelium without labeling tracheal and bronchial cells before E8.5 (Perl et al. 2002). Consistent with this, a more recent study using an inducible Id2-CreER^{T2} has shown that cells in the distal tip of the elongating lung branch at E11.5 ultimately contribute to all lung epithelium but not tracheal epithelium cell types.

Following the elongating distal tip, fine-scale differentiation of the respiratory epithelium proceeds in the proximal to distal (P–D) direction. NE and ciliated cells first appear at E14.0–14.5 with detecting expression of Ascl1/Dll1 and Foxj1 (Post et al. 2000; Rawlins et al. 2007; Guha et al. 2012). At that time, these expressions are restricted within the main bronchi while the distal buds are still immature. As the lung buds divide and spread distally, the proximal cells mature into the specialized cell populations just described, and then the Clara cell marker Scgb1a1 is first detected at E15.5. At the beginning of alveologenesis around E17.0, the distal tip

cells rapidly change in shape to flat or round and differentiate into AEC1 or AEC2 that express AQP5/T1α or surfactant protein as the marker. Recently, these airway epithelial cells have been successfully generated from mouse ES cells following the purification of an Nkx2.1^{+} endodermal population in vitro (Longmire et al. 2012), suggesting that the airway epithelial diversity is achieved by cell–cell interaction within epithelial cells.

5.4.3 Multiple Notch Functions Coordinate the Four Epithelial Populations and Patternings in the Developing Lung

Although several transcription factors necessary for formation of particular cell types in the lung have been identified (Wan et al. 2004; Chen et al. 2009; Chen et al. 1998; Que et al. 2009), few signaling pathways involved in the differentiation program and spatial distribution pattern have been implicated. As mentioned in the previous sections, intercellular signaling within epithelial cells could vary and pattern the airway epithelial cells throughout lung development. Evidence demonstrating the importance of Notch signaling in the developing respiratory system is rapidly growing. Mice that are genetically deficient in Hes1, a target of Notch signaling in several biological systems, show hyperplasia-like enlargement of NEB and a decreased number of Clara cells (Ito et al. 2000; Shan et al. 2007). Using the *N1IP*::*CRE* knock-in mouse strain (Vooijs et al. 2007), the cell lineage of Notch1 experienced population has been previously mapped in the developing lung via a Cre recombinase-mediated reporter system (Morimoto et al. 2010). At postnatal day 21, when lung epithelial development is nearly complete, most of the reporter-positive cells converged on the Clara cell fate. These experiments were followed by direct detection of the Notch1 intracellular domain (N1ICD) as an active form Notch1 receptor that revealed that Clara cells are a Notch-active population. Induced expression of a constitutively active N1ICD in lung epithelial cells throughout development promoted mucous metaplasia and remarkably decreased the number of ciliated cells (Guseh et al. 2009). Conditional removal of the core Notch component, such as Pofut1 (a glycosyltransferase for Notch receptors) or Rbpj (a cofactor of canonical Notch signaling), promoted ciliated cell expansion at the expense of Clara cells (Tsao et al. 2009). These genetic data indicate a role for Notch signaling as a suppressor of ciliated cell fate. Clara and ciliated cell fates are determined throughout E14.5–E16.5. During these stages, as described in Sect. 5.4.2, the distal tips preserve stem cells and continuously provide lineage-restricted progenitors. Notch1-active Clara cells and Foxj1-positive ciliated cells were observed through the conducting airway in a "salt-and-pepper" pattern except for the distal tip (Fig. 5.4a, asterisk). Notch activity in Clara cells is stimulated by Jag1 given rise from the ciliated cells (Tsao et al. 2009; Zhang et al. 2013). Thus, cell fate determinations of the Clara cells and ciliated cells occur in a transitional zone located

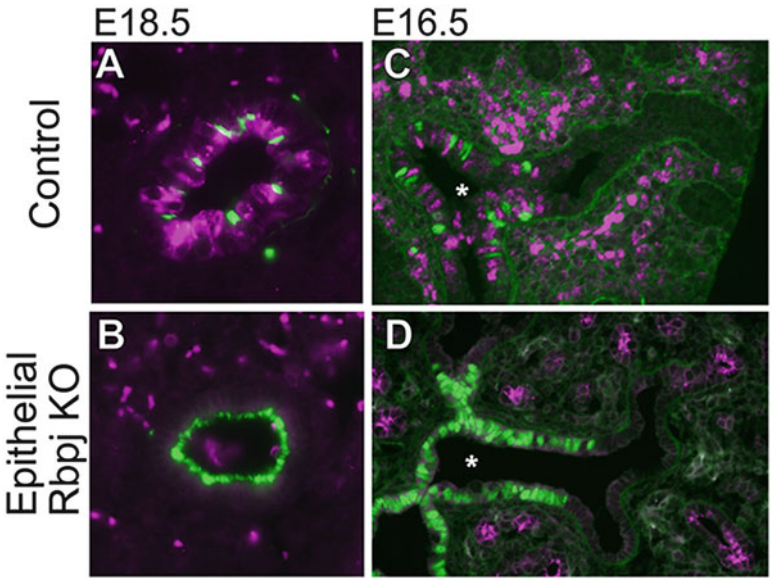

Fig. 5.4 **a**, **b** E18.5 distal conducting airways were stained for acetylated tubulin in ciliated cells (*green*) and CC10 in Clara cells (*magenta*). Ciliated cells occupy these areas, and no Clara cells were detectable in the lung epithelium of the *Rbpj* conditional knockout (KO) mutant (**b**) whereas a predominant distribution of Clara cells was confirmed in the control (**a**). **c**, **d** Clara and ciliated cell fates are delineated from bi-potential progenitors through a lateral inhibition mechanism related to Notch signaling. Immunofluorescence of E16.5 lung for N1ICD (*magenta*) and Foxj1 (*green*) revealed that early Clara and ciliated cells distribute in a "salt-and-pepper" fashion in the proximal epithelium (**c**, *asterisk*). No signal was detected in the distal tip (**c**, *right most*), indicating that undifferentiated progenitors locate in the tip. In Rbpj-deficient epithelium, nearly all proximal epithelial cells were Foxj1 positive (*green*) (**d**, *asterisk*). Staining for the distal tip marker ProSP-C (*magenta*) revealed that the stem cell population was not altered (**d**, *far right*)

between the distal tip stem cells and proximal differentiated daughters. By contrast, nearly all the proximal cells expressed Foxj1 in *Rbpj*-deficient epithelium (Fig. 5.4b, asterisk). The salt-and-pepper distribution of Clara and ciliated cells further suggests a lateral inhibition mechanism, involving activation of Notch signaling in neighbors of nascent ciliated cells at the transition zone.

NE cells appear to be clusters on the bifurcation points of branching bronchioles. The unique location and constant size of the NE clusters prompted us to imagine an existence of a precise regulatory mechanism for NE cell development. The NE cell fate selection presumably involves Notch signaling because the loss of *Hes1* produces enlarged NEB, as already described. Therefore, Notch signaling plays a role in epithelial patterning of Clara, ciliated, and NE cells during lung development. How does Notch signaling control the NEB size? Which of the Notch receptors contributes to the cell fate selections? Stepwise removal of the Notch1/2/3 receptors followed by gene expression and histological analyses identified Notch2 as the primary receptor in Clara/ciliated cell fate selection, with Notch1 and Notch3 making

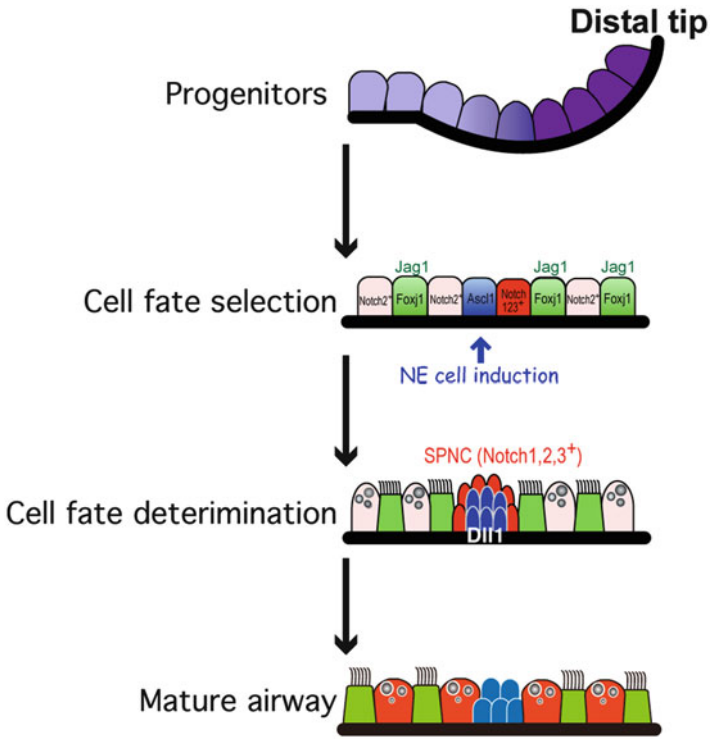

Fig. 5.5 Schematic diagrams of the proposed regulatory mechanisms involved in Notch-dependent cell fate determination during lung epithelial development. During the pseudo-glandular stage, epithelial progenitors (*purple*) located at the distal tip produce descendants that differentiate into Clara (*pink*), ciliated (*green*), SPNC (*red*), and NEC (*blue*) cells (see text for details)

only a minimal contribution to this process (Morimoto et al. 2012). In contrast, all Notch receptors are involved in a redundant manner in NEB size regulation because the Notch1/2/3 triple, but not Notch1/2 double, KO lung epithelium displays NEB hyperplasia that resembles the *Hes1* null phenotype. Given the NE cells express Dll1, another Notch ligand, it is expected that Notch1/2/3 active cells exist that regulate the size of NEB. This Notch active population has been currently identified by two groups (Guha et al. 2012; Morimoto et al. 2012). This novel epithelial population expresses uroplakin3a (Upk3a) and shows immunoreactivity for SSEA-1, and named SSEA-1-positive, Peri-NEC, N1ICD-positive, CC10-negative (SPNC) cells. The SPNC cells appear from E14.5 and cap the NE cell clusters (Fig. 5.5) throughout embryogenesis to regulate the proper cluster size. Lineage tracing of this population revealed its bi-potency for the Clara and ciliated, but not NE, cell fate. The NE cell lineage did not contribute to another airway population, at least during the embryonic stage (Song et al. 2012), suggesting that the SPNC and NE cell lineages never converge. Given that the SSEA-1 immunoreactivity disappears by postnatal day 10, SPNC cells are mainly acting at the fetal stages. The molecular mechanism by which SPNC cells regulate the NEB size should be unveiled in the near future.

In conclusion, the numbers and distribution of the three major lung epithelial cell types are coordinated by two different Notch signaling systems: Jagged1 (ciliated) to the Notch2 canonical signal (Clara) and Dll1 (NE) to all Notch signals contributing to Hes1 expression (SPNC) (Fig. 5.5). Although Notch signaling is reiteratively used to organize the major cell types within a tissue, each step uses different ligands and therefore is either resistant (NEB size regulation, where three Notch genes act with some degree of redundancy) or sensitive (Clara, where the signal relays through one receptor only) to signaling fluctuations throughout airway development. These differences may explain the constant spacing and size of NEB and the patterns of Clara/ciliated cells throughout the conducting airway (Fig. 5.5).

5.5 A Fundamental Strategy for Regulating Population and Localization of Multiple Cell Types by Notch Signaling

Notch signaling was reported previously to be involved in a similar lateral inhibitory process, in which ciliated cells inhibit their neighbors from assuming the same fate. In the zebrafish pronephros, transporting epithelia and multiciliated cells (MCCs) form in a salt-and-pepper pattern (Zhang et al. 2013). It has been shown that zebrafish Jagged2 expression in presumptive MCCs induced activation of zebrafish Notch3 in neighboring cells, blocking MCC fate and driving the alternative transporting epithelial cell fate. In addition, a Hes1-related protein was involved (Ma and Jiang 2007). In *Xenopus*, ciliated cells express Delta ligands to activate Notch signaling and induce Hes-related proteins, inhibiting the selection of ciliated cells by neighboring epidermal cells (Deblandre et al. 1999). Hence, dose and type of Notch signaling are arranged to coordinate the numeric and special balance between functional cell types rather than just generating two alternative cell fates through organogenesis. In airway epithelial patterning, the alternative Clara/ciliated cell fate selection is judged by the Jag1–Notch2 axis while redundant Notch1, 2, 3 functions in SPNC cells shape the NE cell cluster (Zhang et al. 2013; Morimoto et al. 2012). This parallel induction of distinct Notch signals within the epithelium is likely achieved by different affinity between the receptors and ligands. Fringe, a sugar modification enzyme for Notch receptors, promotes Notch1 affinity to Dll1, resulting in inhibition of Jag1-mediated Notch1 activation. Activation of Notch2 is, however, not inhibited by Fringe. If this interpretation is correct, we predict that in L-fringe-deficient mice, Notch1 will be able to rescue Clara cells in Notch2-deficient lung epithelia.

Current improvements of cell reprogramming technology allow us to understand and manipulate the differentiation programs of functional cell type. However, the paucity of our knowledge in tissue building with these various differentiated cell types limits the future use of tissue engineering in a clinical setting. In current research, the organoid culture from a single gut stem cell has recapitulated the U-shape crypt structure and epithelial pattern of intestinal goblet and absorptive cell types (Sato et al. 2011). A complex optic cup tissue structure has been further reconstructed from ES/iPS cells (Eiraku et al. 2011). These discoveries imply that a

latent intrinsic order of tissue-specific stem cells arrange the unique tissue structure and patterning of differentiating cells by a multicellular self-organization fusion. Thus, future study in such a research field would prove fruitful in advancing our understanding of organogenesis and regenerative medicine.

References

Ang SL, Rossant J (1994) HNF-3 beta is essential for node and notochord formation in mouse development. Cell 78(4):561–574

Arora R, Metzger RJ, Papaioannou VE (2012) Multiple roles and interactions of Tbx4 and Tbx5 in development of the respiratory system. PLoS Genet 8(8):e1002866

Cardoso WV, Lu J (2006) Regulation of early lung morphogenesis: questions, facts and controversies. Development (Camb) 133(9):1611–1624

Chen J, Knowles HJ, Hebert JL et al (1998) Mutation of the mouse hepatocyte nuclear factor/forkhead homologue 4 gene results in an absence of cilia and random left-right asymmetry. J Clin Invest 102(6):1077–1082

Chen G, Korfhagen TR, Xu Y et al (2009) SPDEF is required for mouse pulmonary goblet cell differentiation and regulates a network of genes associated with mucus production. J Clin Invest 119(10):2914–2924

Chen F, Cao Y, Qian J et al (2010) A retinoic acid-dependent network in the foregut controls formation of the mouse lung primordium. J Clin Invest 120(6):2040–2048

Deblandre GA, Wettstein DA, Koyano-Nakagawa N et al (1999) A two-step mechanism generates the spacing pattern of the ciliated cells in the skin of *Xenopus* embryos. Development (Camb) 126(21):4715–4728

Eiraku M, Takata N, Ishibashi H et al (2011) Self-organizing optic-cup morphogenesis in three-dimensional culture. Nature (Lond) 472(7341):51–56

Goss AM, Tian Y, Tsukiyama T et al (2009) Wnt2/2b and beta-catenin signaling are necessary and sufficient to specify lung progenitors in the foregut. Dev Cell 17(2):290–298

Guha A, Vasconcelos M, Cai Y et al (2012) Neuroepithelial body microenvironment is a niche for a distinct subset of Clara-like precursors in the developing airways. Proc Natl Acad Sci USA 109(31):12592–12597

Guseh JS, Bores SA, Stanger BZ et al (2009) Notch signaling promotes airway mucous metaplasia and inhibits alveolar development. Development (Camb) 136(10):1751–1759

Harris-Johnson KS, Domyan ET, Vezina CM et al (2009) Beta-catenin promotes respiratory progenitor identity in mouse foregut. Proc Natl Acad Sci USA 106(38):16287–16292

Hong KU, Reynolds SD, Giangreco A et al (2001) Clara cell secretory protein-expressing cells of the airway neuroepithelial body microenvironment include a label-retaining subset and are critical for epithelial renewal after progenitor cell depletion. Am J Respir Cell Mol Biol 24(6):671–681

Ito T, Udaka N, Yazawa T et al (2000) Basic helix-loop-helix transcription factors regulate the neuroendocrine differentiation of fetal mouse pulmonary epithelium. Development (Camb) 127(18):3913–3921

Jung HS, Oropeza V, Thesleff I (1999) Shh, Bmp-2, Bmp-4 and Fgf-8 are associated with initiation and patterning of mouse tongue papillae. Mech Dev 81(1–2):179–182

Kimura S, Hara Y, Pineau T et al (1996) The T/ebp null mouse: thyroid-specific enhancer-binding protein is essential for the organogenesis of the thyroid, lung, ventral forebrain, and pituitary. Genes Dev 10(1):60–69

Longmire TA, Ikonomou L, Hawkins F et al (2012) Efficient derivation of purified lung and thyroid progenitors from embryonic stem cells. Cell Stem Cell 10(4):398–411

Ma M, Jiang YJ (2007) Jagged2a-notch signaling mediates cell fate choice in the zebrafish pronephric duct. PLoS Genet 3(1):e18

Metzger RJ, Klein OD, Martin GR et al (2008) The branching programme of mouse lung development. Nature (Lond) 453(7196):745–750

Min H, Danilenko DM, Scully SA et al (1998) Fgf-10 is required for both limb and lung development and exhibits striking functional similarity to Drosophila branchless. Genes Dev 12(20): 3156–3161

Minoo P, Su G, Drum H et al (1999) Defects in tracheoesophageal and lung morphogenesis in Nkx2.1(−/−) mouse embryos. Dev Biol 209(1):60–71

Monaghan AP, Kaestner KH, Grau E et al (1993) Postimplantation expression patterns indicate a role for the mouse forkhead/HNF-3 alpha, beta and gamma genes in determination of the definitive endoderm, chordamesoderm and neuroectoderm. Development (Camb) 119(3):567–578

Morimoto M, Liu Z, Cheng HT et al (2010) Canonical Notch signaling in the developing lung is required for determination of arterial smooth muscle cells and selection of Clara versus ciliated cell fate. J Cell Sci 123(Pt 2):213–224

Morimoto M, Nishinakamura R, Saga Y et al (2012) Different assemblies of Notch receptors coordinate the distribution of the major bronchial Clara, ciliated and neuroendocrine cells. Development (Camb) 139(23):4365–4373

Morrisey EE, Hogan BL (2010) Preparing for the first breath: genetic and cellular mechanisms in lung development. Dev Cell 18(1):8–23

Okubo T, Hogan BL (2004) Hyperactive Wnt signaling changes the developmental potential of embryonic lung endoderm. J Biol 3(3):11

Perl AK, Wert SE, Nagy A et al (2002) Early restriction of peripheral and proximal cell lineages during formation of the lung. Proc Natl Acad Sci USA 99(16):10482–10487

Post LC, Ternet M, Hogan BL (2000) Notch/Delta expression in the developing mouse lung. Mech Dev 98(1–2):95–98

Que J, Luo X, Schwartz RJ et al (2009) Multiple roles for Sox2 in the developing and adult mouse trachea. Development (Camb) 136(11):1899–1907

Rawlins EL, Ostrowski LE, Randell SH et al (2007) Lung development and repair: contribution of the ciliated lineage. Proc Natl Acad Sci USA 104(2):410–417

Rossi JM, Dunn NR, Hogan BL et al (2001) Distinct mesodermal signals, including BMPs from the septum transversum mesenchyme, are required in combination for hepatogenesis from the endoderm. Genes Dev 15(15):1998–2009

Sasaki H, Hogan BL (1994) HNF-3 beta as a regulator of floor plate development. Cell 76(1): 103–115

Sato T, van Es JH, Snippert HJ et al (2011) Paneth cells constitute the niche for Lgr5 stem cells in intestinal crypts. Nature (Lond) 469(7330):415–418

Sekine K, Ohuchi H, Fujiwara M et al (1999) Fgf10 is essential for limb and lung formation. Nat Genet 21(1):138–141

Serls AE, Doherty S, Parvatiyar P et al (2005) Different thresholds of fibroblast growth factors pattern the ventral foregut into liver and lung. Development (Camb) 132(1):35–47

Shan L, Aster JC, Sklar J et al (2007) Notch-1 regulates pulmonary neuroendocrine cell differentiation in cell lines and in transgenic mice. Am J Physiol Lung Cell Mol Physiol 292(2): L500–L509

Song H, Yao E, Lin C et al (2012) Functional characterization of pulmonary neuroendocrine cells in lung development, injury, and tumorigenesis. Proc Natl Acad Sci USA 109(43): 17531–17536

Tsao PN, Vasconcelos M, Izvolsky KI et al (2009) Notch signaling controls the balance of ciliated and secretory cell fates in developing airways. Development (Camb) 136(13):2297–2307

Vooijs M, Ong CT, Hadland B et al (2007) Mapping the consequence of Notch1 proteolysis in vivo with NIP-CRE. Development (Camb) 134(3):535–544

Wan H, Kaestner KH, Ang SL et al (2004) Foxa2 regulates alveolarization and goblet cell hyperplasia. Development (Camb) 131(4):953–964

Wandzioch E, Zaret KS (2009) Dynamic signaling network for the specification of embryonic pancreas and liver progenitors. Science 324(5935):1707–1710
Weinstein M, Xu X, Ohyama K et al (1998) FGFR-3 and FGFR-4 function cooperatively to direct alveogenesis in the murine lung. Development (Camb) 125(18):3615–3623
Xu CR, Cole PA, Meyers DJ et al (2011) Chromatin "prepattern" and histone modifiers in a fate choice for liver and pancreas. Science 332(6032):963–966
Zhang S, Loch AJ, Radtke F et al (2013) Jagged1 is the major regulator of notch-dependent cell fate in proximal airways. Dev Dyn 242(6):678–86

Part II
Choosing a Fate from Multiple Potencies

Chapter 6
Determination of Stem Cell Fate in Planarian Regeneration

Yoshihiko Umesono

Abstract Planarians have a long history of attracting many biologists for their amazing regenerative ability, which absolutely depends on a unique population of somatic pluripotent stem cells called neoblasts that are distributed throughout the body. After amputation, neoblasts proliferate to form a head blastema at an anterior-facing wound and a tail blastema at a posterior-facing wound, and finally regenerate a whole-body anterior–posterior (A–P) pattern, even from tiny tissue fragments. More than a century ago, Thomas Hunt Morgan, one of the great early investigators of planarian regeneration, proposed that axial patterning is determined by two opposing morphogenetic gradients of formative substances, "head stuff" and "tail stuff," along the A–P axis. However, to date few attempts have been made to assess Morgan's hypothesis. Recent molecular studies using RNA interference (RNAi) have revisited planarian regeneration and revealed key signaling pathways involved in the regulation of neoblast dynamics, including Wnt/β-catenin signaling acting as a posterior tissue determinant (which accordingly fits with the instructive role of the "tail stuff"), during planarian regeneration. One of our recent great advances was identification of extracellular signal-regulated kinase (ERK) signaling that acts as a cell differentiator in the planarian *Dugesia japonica*. Furthermore, we found that interplay between anterior ERK signaling and posterior β-catenin signaling can account for the reconstruction of a complete head-to-tail axis, in which the absence of β-catenin signaling allows neoblasts to achieve the ERK activation necessary for head regeneration. These findings suggest that ERK signaling plays a crucial role in the circuitry of the "head stuff" in Morgan's hypothesis.

Keywords Axial patterning • Planarian • Pluripotent stem cells • Regeneration

Y. Umesono (✉)
RIKEN Center for Developmental Biology, Kobe, Japan

Department of Biophysics, Graduate School of Science, Kyoto University, Kyoto, Japan

Department of Life Systems, Institute of Technology and Science,
The University of Tokushima, Tokushima, Japan
e-mail: umesono.yoshihiko@tokushima-u.ac.jp

H. Kondoh and A. Kuroiwa (eds.), *New Principles in Developmental Processes*,
DOI 10.1007/978-4-431-54634-4_6, © Springer Japan 2014

6.1 Attraction by the Mystery of Planarian Regeneration Over a Century

Planarians belong to an evolutionarily early group of organisms with defined bilateral symmetry, dorsoventral polarity, a central nervous system (CNS) with a simple brain structure, and high regenerative ability (Agata and Umesono 2008; Umesono and Agata 2009; Umesono et al. 2011). They have well-characterized somatic pluripotent stem cells called neoblasts that are distributed throughout the body (Baguñà et al. 1989; Shibata et al. 2010; Wagner et al. 2011). Neoblasts, the only proliferative somatic cells in adults, differentiate to give rise to all missing tissues and organs after injury and during homeostasis (Newmark and Sánchez Alvarado 2000; Salvetti et al. 2000: Orii et al. 2005). The progeny of a single neoblast are capable of rescuing regeneration in animals where neoblasts are ablated by X-ray irradiation, demonstrating the pluripotency of this cell type (Wagner et al. 2011). Because of their unique regenerative capabilities, and the simplicity of their stem cell system, planarians provide an ideal opportunity to analyze stem cell dynamics involved in axial patterning during regeneration.

From the 1890s to early 1900s, Thomas Hunt Morgan devoted his energy to the study of planarian regeneration. After amputation, anterior-facing wounds form a head blastema, and posterior-facing wounds form a tail blastema, a phenomenon known as regeneration polarity. He found that very thin fragments of *Planaria maculata* made by sectioning perpendicular to the anterior–posterior (A–P) axis regenerated bipolar two-headed planarians, termed "Janus heads" (an allusion to the Roman god Janus) (Morgan 1904), and attempted to explain the nature of polarity by positing two opposing morphogenetic gradients of formative substances, "head stuff" and "tail stuff," along the A–P axis (this suggestion provides the first break into the concept of "morphogens") (Morgan 1905; Wolpert 1969; Lawrence 1988). However, he stopped studying regeneration and development and turned to *Drosophila* "genetics" with fruitful outcome (Morgan 1910, 1911a, b, c), causing him to be awarded the Nobel Prize in Physiology or Medicine in 1933.

After many decades, Alvarado and Newmark have developed a method for performing knockdown of the function of a gene by RNA interference (RNAi) in planarians (Sánchez Alvarado and Newmark 1999), which brings our understanding of planarian regeneration to a molecular level. Since then, we have explored the "head stuff" and "tail stuff" per Morgan, by exploiting RNAi.

6.2 MAPK Signaling Pathways Regulate Blastema Formation During Planarian Regeneration

We used a clonal strain of the freshwater planarian *Dugesia japonica* as a model planarian (2–10 mm in body length), one of the most common planarians in Japan. They propagate asexually through fission under laboratory conditions. *D. japonica*

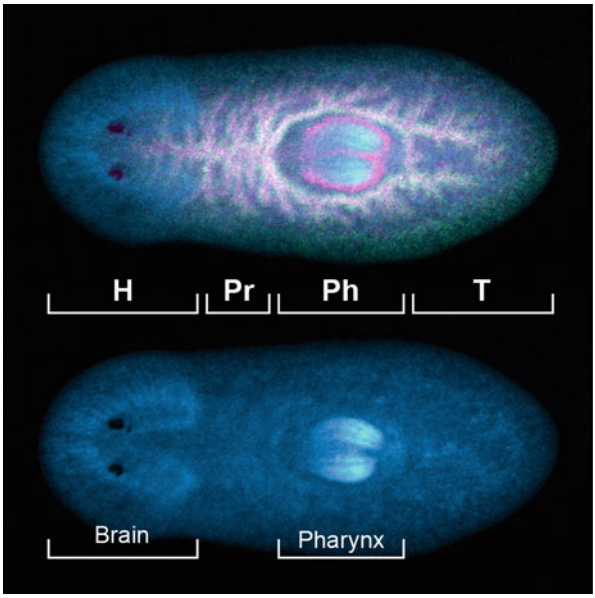

Fig. 6.1 Body structure of the freshwater planarian *Dugesia japonica*. The planarian body is subdivided into at least four regions in an anterior-to-posterior sequence: head containing a brain and eyes (*H*), pre-pharyngeal (*Pr*), pharyngeal containing a pharynx (*Ph*), and tail (*T*) regions. The *upper panel* shows triple staining with anti-AADC antibody (*green*), anti-β-cateninA antibody (*magenta*), and Hoechst 33342 (*cyan*). The *lower panel* shows Hoechst 33342 staining only in the same animal. The digestive system is composed of a three-branched gut, with one anterior branch in the head and pre-pharyngeal regions that is connected with the anterior end of the pharynx, and two posterior branches in the pharyngeal and tail regions, which is well visualized by double staining with anti-AADC (Nishimura et al. 2007) and anti-β-cateninA (because β-cateninA protein is highly accumulated in the epithelial cell membrane of the gut and pharynx). It is known that the *D. japonica* genome possesses at least two *β-catenin* homologue genes (termed *Djβ-cateninA* and *-B*) (Kobayashi et al. 2007; Yazawa et al. 2009). Hoechst 33342 nuclear staining visualizes the brain and pharynx because they are a mass of numerous cells

displays at least four distinct body regions in an anterior-to-posterior sequence: head (H), pre-pharyngeal (Pr), pharyngeal (Ph), and tail (T) regions. The separation between these regions is indicated by the presence of position-specific tissues and organs (Agata et al. 2003; Umesono et al. 2013). A brain and pair of eyes represent landmark morphological structures of the head region (Fig. 6.1). The brain is located on the dorsal side relative to the ventral nerve cords (VNCs) that run through the whole body along the A–P axis (Agata et al. 1998; Umesono and Agata 2009; Umesono et al. 2011). We succeeded in identifying the three *orthodenticle*/*Otx*-related homeobox genes *DjotxA*, *DjotxB*, and *Djotp* in the planarian, whose expression patterns clearly define the brain as a structure distinct from the VNCs (Umesono et al. 1997, 1999). The brain indeed acts as an information-processing center to elicit negative phototaxis (i.e., light avoidance behavior) in response to light signals via the eyes (Inoue et al. 2004; Takano et al. 2007). In the middle portion of the

body, there is a pharynx acting as a mouth and anus (Fig. 6.1). The digestive system is composed of a three-branched gut, with one anterior branch in the head and prepharyngeal regions and two posterior branches in the pharyngeal and tail regions (Fig. 6.1). The anterior gut branch is connected with the anterior end of the pharynx. When double-stranded RNA (dsRNA) for RNAi was incorporated into the gut cavity by injection or feeding via pharynx, dsRNA was effectively transmitted to all the cells that construct a whole individual, including neoblasts (Sánchez Alvarado and Newmark 1999; Rouhana et al. 2013).

D. japonica has high ability to regenerate entire body parts, including a functional brain, from even a tiny tail fragment via activation of neoblasts. In the early process of regeneration, successive phases of wound healing, the formation of a blastema, and differentiation of cells from the blastema (e.g., brain cells from the head blastema), are the events that occur at wounds. The blastema is generally recognized as an unpigmented mass of regenerative cells originated from neoblasts at wounds. However, the cellular state of blastema-forming cells during planarian regeneration has remained unclear. We, therefore, performed detailed analysis of neoblast dynamics involved in the blastema formation of *D. japonica* (Tasaki et al. 2011a, b).

To monitor neoblast dynamics in vivo, we used an mRNA probe of *DjpiwiA*, a *D. japonica* gene of the argonaute family that is specifically expressed in undifferentiated neoblasts and also an antibody against its protein (Yoshida-Kashikawa et al. 2007; Shibata et al. 2010). From around 12 h after amputation, a cluster of *DjpiwiA-positive* neoblasts appeared surrounding the presumptive blastema-forming region at the cut edge and then started to form a blastema (Tasaki et al. 2011a). At around 24 h after amputation, a blastema was well recognized as a mass of cells that are positive for staining with the anti-DjPiwiA antibody (Fig. 6.2a–c). Within a few hours, however, almost all the blastema-forming neoblasts apparently decreased the expression level of *DjpiwiA* mRNA (Fig. 6.2d). At this stage, these blastema-forming cells had no proliferative activity (Tasaki et al. 2011a), as indicated by the absence of staining with both mRNA probe of the gene *D. japonica histone H2B* acting as a marker of proliferating neoblasts (Guo et al. 2006) and anti-phosphohistone H3 antibody acting as a marker of mitotic neoblasts (Newmark and Sánchez Alvarado 2000). Concomitant with the loss of cell proliferation, head blastema-forming cells start to differentiate, as assayed by the expression of some neural genes involved in brain regeneration (Cebrià et al. 2002b). This series of events in neoblast dynamics was commonly observed in both head and tail regeneration. On the basis of these observations, we conclude that a blastema is a mass of neoblast progeny that exits from the proliferative and pluripotent state and simultaneously enters the differentiating state at wounds.

Then, an immediate question is how the formation of blastema is regulated during planarian regeneration. Mitogen-activated protein kinase (MAPK) cascades are an evolutionarily conserved signaling pathway that regulates diverse cellular functions including cell proliferation, differentiation, migration, and stress responses (Nishida and Gotoh 1993; Chang and Karin 2001). The MAPK signaling pathway is induced by various extracellular stimuli, which induce sequential protein phosphorylation reactions that result in the MAPK activation. There are three major

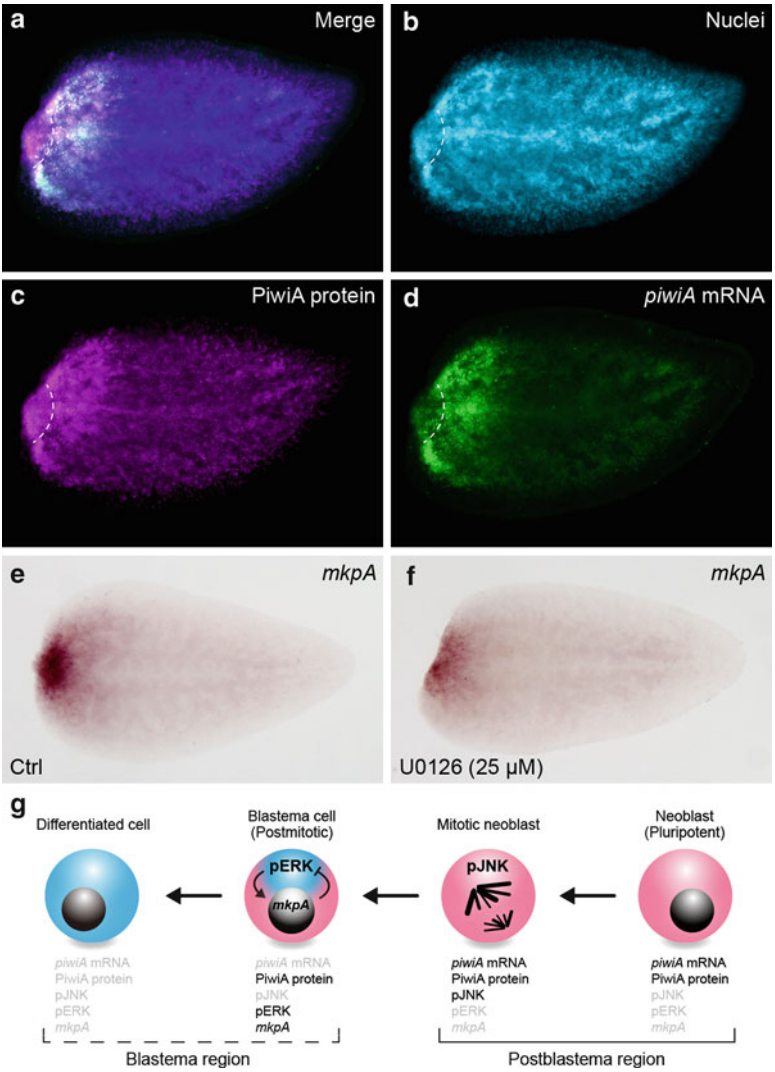

Fig. 6.2 Neoblast dynamics involved in head blastema formation. **a**–**d** Triple staining with *DjpiwiA* gene probe (*green*), anti-DjPiwiA antibody (*magenta*), and Hoechst 33342 nuclear staining (*blue*) at 24 h of head regeneration from a tail fragment. *Dashed lines* indicate the gross border between the head blastema, which recognized a DjPiwiA(+) and *DjpiwiA*(−) region at a wound, and the rest of the body. DjPiwiA(+) and *DjpiwiA*(+) neoblasts are highly accumulated at a position posterior to the blastema (i.e., a collar of strong *DjpiwiA* signal in **d**), the so-called postblastema region, where many mitotic neoblasts are present under the control of JNK activation (Tasaki et al. 2011b). **e**, **f** *DjmkpA* expression at 24 h of head regeneration from tail fragments. **e** *DjmkpA* is strongly expressed in the head blastema. **f** Treatment with the chemical MEK inhibitor U0126, which inactivates ERK signaling, caused drastic decrease of the *DjmkpA* expression at a wound. **g** A summary of the spatial profiles of pJNK, pERK, and *DjmkpA* expression involved in blastema formation. Anterior is to the *left*

subgroups of kinases in the MAPK family: p38, c-Jun N-terminal kinase (JNK), and extracellular signal-regulated kinase (ERK). We found that coordinated action of JNK and ERK signaling pathways is required for the neoblast dynamics involved in blastema formation in *D. japonica* (Tasaki et al. 2011a, b).

JNK is highly activated in mitotic neoblasts via phosphorylation (phosphorylated JNK; pJNK) and is required for accelerating the entry of neoblasts into the M phase in the cell cycle at a position close to wounds, resulting in the generation of neoblast progeny to form a blastema at wounds (Tasaki et al. 2011b). Subsequently, ERK is highly activated in blastema cells via phosphorylation (phosphorylated ERK; pERK) and is required for the exit from their proliferative and pluripotent state and the entry toward the differentiating state (Tasaki et al. 2011a). These blastema cells start to express the *D. japonica* MAPK phosphatase A gene (*DjmkpA*) in response to ERK activation. *DjmkpA* expression is an excellent indicator of ERK phosphorylation, but DjmkpA itself acts as a negative feedback regulator of pERK (Tasaki et al. 2011a; Fig. 6.2e, f). To clarify the role of *DjmkpA* in the circuitry of ERK-dependent cell fate decisions, we examined the effect of *DjmkpA* RNAi on blastema cells sensitized by treatment with a concentration of the chemical MEK inhibitor U0126 that leads to inhibition of the ERK activity at a moderate level (Tasaki et al. 2011a). Treatment with U0126 (5–25 μM) caused differentiation defects of both head and tail regeneration with intensifying severity in a dose-dependent manner. During head regeneration from tail fragments, U0126 (10 μM) caused moderate but clear differentiation defects in the regenerated head, such as reduction in its size with cyclopia or no eyes. Notably, simultaneous action of *DjmkpA* RNAi not only restored the pERK level but also rescued these differentiation defects. These findings suggest that negative feedback regulation of ERK signaling by *DjmkpA* may establish a threshold level of ERK activation for the binary cell fate decisions of blastema cells regarding whether to differentiate in the presence of fluctuations generated by upstream variations of ERK signaling.

More recently, we found that an pERK/*DjmkpA* feedback circuit is also involved in neoblast differentiation necessary for the regeneration of not only the head and tail but also the pre-pharyngeal and pharyngeal regions (Umesono et al. 2013). Here, I summarize neoblast dynamics involved in blastema formation and differentiation in Fig. 6.2g: the pJNK(+) mitotic neoblasts act as a definitive source of the blastema cells, in which an ERK/*DjmkpA* feedback circuit makes the final decision about whether blastema cells undergo differentiation, resulting in regeneration of the head or tail at a wound according to regeneration polarity.

6.3 Wnt/β-Catenin Signaling Modulates ERK Signaling

The next question is how the neoblast cell fates are properly specified to regenerate a whole-body A–P pattern in response to ERK activation. In past years, studies using RNAi promoted understanding of the Wnt/β-catenin and Hedgehog (Hh)

signaling pathways that regulate regeneration polarity in planarians (Gurley et al. 2008; Iglesias et al. 2008; Petersen and Reddien 2008; Adell et al. 2009; Petersen and Reddien 2009; Rink et al. 2009; Yazawa et al. 2009). We found that Hh signaling drives tail regeneration by inducing the expression of *wnt* genes at posterior-facing wounds (Yazawa et al. 2009). As a consequence, β-catenin presumably forms a decreasing activity gradient in the tail-to-head direction (Adell et al. 2010; Almuedo-Castillo et al. 2012). Knockdown of the function of the planarian *β-catenin* gene by RNAi resulted in "Janus heads" at the expense of tail regeneration (Gurley et al. 2008; Iglesias et al. 2008; Petersen and Reddien 2008; Yazawa et al. 2009). This was the first demonstration of Morgan's "Janus heads" via manipulation of a single gene. Conversely, RNAi of the planarian gene *patched*, which encodes a putative receptor of the ligand gene *hedgehog*, caused ectopic activation of Wnt/β-catenin signaling in the anterior blastema and resulted in bipolar two-tailed planarians (so-called Janus tails) at the expense of head regeneration (Rink et al. 2009; Yazawa et al. 2009). These observations suggest that Wnt-dependent posteriorly increasing β-catenin activity fits with the instructive role of the "tail stuff" in Morgan's hypothesis. By contrast, to date no molecules have been reported to function as the " head stuff" in planarians. Our data suggest that Wnt/β-catenin signaling functions as a posterior tissue determinant, in close coordination with ERK activation, during planarian regeneration. Thus, we speculate that unknown links between ERK and posterior Wnt/β-catenin signals might account for the proper types of differentiation of neoblasts along the A–P axis, and tested this possibility during regeneration of *D. japonica*.

To sensitively visualize ERK activation in vivo, we monitored *DjmkpA* expression in regenerating animals treated with RNAi of the *D. japonica β-cateninB* (*Djβ-catB*) gene. During tail regeneration from head fragments, *Djβ-catB* RNAi clearly increased the *DjmkpA* expression level in the presumptive regenerating tail via ERK activation at the expense of tail identity (Umesono et al. 2013; Fig. 6.3a–d). These observations suggest that posterior β-catenin signaling plays a role in decreasing ERK signaling to promote tail regeneration at posterior-facing wounds.

We also found that interplay between the ERK and posterior β-catenin signals is required for the specification and differentiation of pharyngeal cells (Umesono et al. 2013). During head regeneration from tail fragments, *Djβ-catB*(*RNAi*) animals showed roughly normal regeneration of the head and pre-pharyngeal regions but failed to regenerate a pharynx. These knockdown animals had ectopic fusion of the two posterior branches of the gut in the presumptive pharyngeal region at the expense of the pharynx structure, resulting in the transformation of the pharyngeal region into a pre-pharyngeal-like region. Importantly, this phenotype also involves the increase of the ERK activity level along the AP axis. These observations suggest that the posterior β-catenin signaling plays a role in the negative regulation of ERK signaling to decide between pre-pharyngeal versus pharyngeal regeneration.

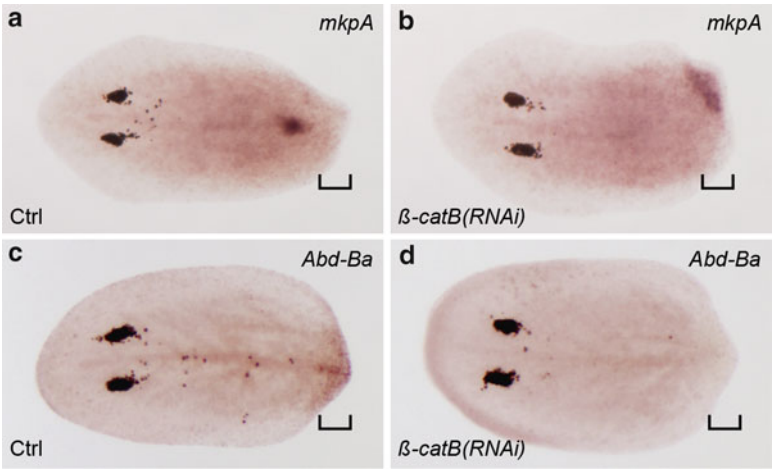

Fig. 6.3 Effects of *Djβ-cateninB* RNAi on extracellular signal-regulated kinase (*ERK*) signaling during tail regeneration. **a** *DjmkpA* expression in control regenerant from head fragment at 3 days of regeneration. Strong *DjmkpA* expression occurred transiently in the tail blastema (Tasaki et al. 2011a), and then decreased at this time (*bracket*). A strong (*dotted*) signal close to the tail blastema indicates *DjmkpA* expression in cells associated with pharynx regeneration. **b** *DjmkpA* expression in *Djβ-catB*(*RNAi*) regenerant from head fragment at 3 days of regeneration. **c** *DjAbd-Ba* expression in control regenerant from head fragment at 3 days of regeneration. *DjAbd-Ba* was specifically expressed in the tail blastema (Nogi and Watanabe 2001). **d** *DjAbd-Ba* expression in *Djβ-catB*(*RNAi*) regenerant from head fragment at 3 days of regeneration. In summary, *Djβ-catB* RNAi caused increase of *DjmkpA* expression and simultaneously repressed expression of *DjAbd-Ba* in the tail blastema. *Brackets* indicate tail blastema. Anterior is to the *left*

6.4 The Gene *Nou-darake* Modulates ERK Signaling

The *D. japonica* gene *nou-darake* (*ndk* means "brains everywhere" in Japanese) encodes a putative transmembrane protein with two extracellular immunoglobulin-like domains related to those of fibroblast growth factor (FGF) receptors, but lacks the cytoplasmic kinase domains characteristic of this receptor family (Cebrià et al. 2002a). We found that *ndk* is specifically expressed in head tissues, including brain cells, under the control of ERK activation (Cebrià et al. 2002a; Umesono et al. 2013; Fig. 6.4a). *ndk* RNAi increased ERK activity levels along the AP axis and induced ectopic differentiation of head tissues, such as eyes and brain cells, predominantly in the pre-pharyngeal region (Fig. 6.4b, c), at the expense of the pre-pharyngeal identity (Cebrià et al. 2002a; Umesono et al. 2013). These observations suggest that *ndk* RNAi caused transformation of the pre-pharyngeal region into a head-like region in a non-cell autonomous manner. In addition, we showed that *ndk* RNAi restored pharynx regeneration in pharynx regeneration-deficient animals induced by pharmacological ERK inhibition at a moderate level (Umesono et al. 2013), supporting the notion of a non-cell autonomous function of *ndk* along the AP axis. It is tempting to

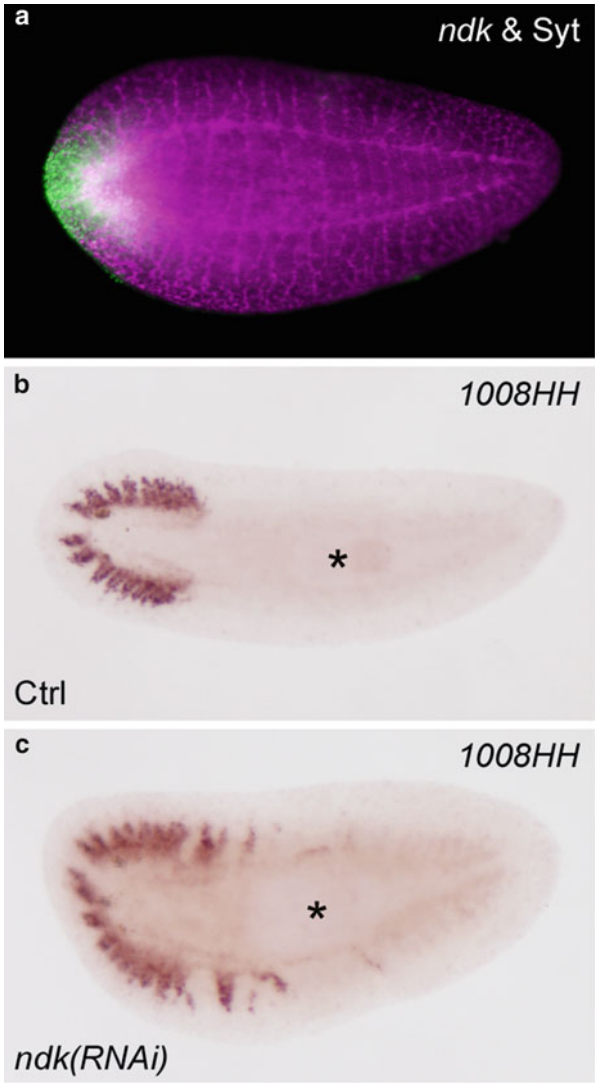

Fig. 6.4 *ndk* RNAi caused ectopic differentiation of brain cells. **a** Double staining with probe for *ndk* (*green*) and anti-synaptotagmin (*Syt*) antibody (*magenta*) that visualizes the neural network (Tazaki et al. 1999). *ndk* was specifically expressed in the regenerating head region, in both brain and non-brain cells, in regenerant from tail fragment at 3 days of regeneration. **b** Expression of *1008HH* (a brain-branch marker gene) in control regenerant from tail fragment at 7 days of regeneration. **c** Expression of *1008HH* in *ndk*(*RNAi*) regenerant from tail fragment at 7 days of regeneration. *Asterisk* indicates pharynx. Anterior is to the *left*

speculate that *ndk* might encode a protein that binds secreted molecules (as yet unidentified) in the head region to delimit their diffusion, so that strong activation of ERK signaling in neoblasts is confined to the head region via these molecules.

6.5 Conclusions and Future Prospects

We showed that globally dynamic activation of ERK signaling along the A–P axis plays a crucial role in the reconstruction of the whole-body A–P patterns via activation of neoblasts during planarian regeneration (Fig. 6.5). Notably, our data suggest

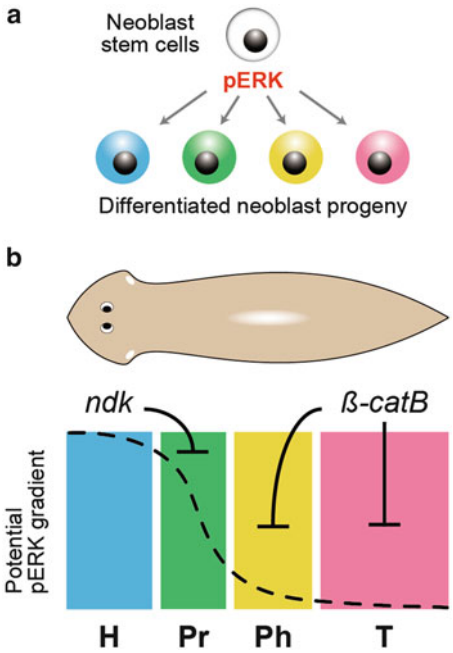

Fig. 6.5 Cell fate determination of neoblasts along the anterior–posterior (A–P) axis during planarian regeneration. **a** Activated ERK (pERK) is required for differentiation of neoblasts to establish the whole-body patterning along the A–P axis. **b** A–P patterning of planarian body is primarily determined by the pERK level and β-catenin signaling. *ndk* expression is activated by ERK signaling, which restricts a high level of ERK signaling to the head region. β-catenin signaling is also involved in the negative regulation of ERK signaling in the pharyngeal and tail regions. *H* head cell, *Pr* pre-pharyngeal cell, *Ph* pharyngeal cell, *T* tail cell

that anterior ERK and posterior β-catenin signals form two opposing activity gradients along the A–P axis (Umesono et al. 2013), in which *ndk* and posterior β-catenin signaling negatively regulate ERK signaling to shape the anterior gradient and posteriorize regenerating tissues in a distinct manner (Fig. 6.5b). Furthermore, *ndk* study implies the existence of secreted molecules (i.e., NDK ligands) acting as an upstream activator of ERK signaling in neoblasts. These observations led us to propose a simple scenario that spatial distribution of NDK ligands along the A–P axis may be translated into the anterior gradient of ERK signaling with the assistance of posterior β-catenin signaling, which plays an instructive role in the circuitry of the "head stuff" in Morgan's hypothesis. One of the best candidates of NDK ligands would be FGF-like ligand molecules, because *ndk* RNAi-induced ectopic brain formation was suppressed by simultaneous inactivation of two planarian FGF receptor genes, *DjFGFR1* and *-2* (Cebrià et al. 2002a). However, no FGF-like ligand molecules have been identified yet in the accumulating expressed sequence tag (EST) and genome sequence data of *D. japonica*, suggesting that the ligand is only distantly related to FGFs at the sequence level. Identification of the FGF receptor

ligands will provide important clues for understanding how ERK signaling is activated in response to injury, and how *ndk* and Wnt/β-catenin signaling regulate ERK signaling for the establishment of the A–P patterning during planarian regeneration.

Acknowledgments This work was supported by a Grant-in-Aid for Scientific Research on Innovative Areas to Y.U. (22124004) and the Naito Foundation.

References

Adell T, Saló E, Boutros M, Bartscherer K (2009) *Smed-Evi/Wntless* is required for beta-catenin-dependent and -independent processes during planarian regeneration. Development (Camb) 136:905–910. doi:10.1242/dev.033761

Adell T, Cebrià F, Saló E (2010) Gradients in planarian regeneration and homeostasis. Cold Spring Harbor Perspect Biol 2:a000505. doi:10.1101/cshperspect.a000505

Agata K, Umesono Y (2008) Brain regeneration from pluripotent stem cells in planarian. Philos Trans R Soc Lond B Biol Sci 363:2071–2078. doi:10.1098/rstb.2008.2260

Agata K, Soejima Y, Kato K, Kobayashi C, Umesono Y, Watanabe K (1998) Structure of the planarian central nervous system (CNS) revealed by neuronal cell markers. Zool Sci 15:433–440. doi:10.2108/zsj.15.433

Agata K, Tanaka T, Kobayashi C, Kato K, Saitoh Y (2003) Intercalary regeneration in planarians. Dev Dyn 226:308–316. doi:10.1002/dvdy.10249

Almuedo-Castillo M, Sureda-Gómez M, Adell T (2012) Wnt signaling in planarians: new answers to old questions. Int J Dev Biol 56:53–65. doi:10.1387/ijdb.113451ma

Baguñà J, Saló E, Auladell C (1989) Regeneration and pattern formation in planarians. Evidence that neoblasts are totipotent stem cells and the source of blastema cells. Development (Camb) 107:77–86

Cebrià F, Kobayashi C, Umesono Y, Nakazawa M, Mineta K, Ikeo K, Gojobori T, Itoh M, Taira M, Sánchez Alvarado A, Agata K (2002a) FGFR-related gene *nou-darake* restricts brain tissues to the head region of planarians. Nature (Lond) 419:620–624. doi:10.1038/nature01042

Cebrià F, Nakazawa M, Mineta K, Ikeo K, Gojobori T, Agata K (2002b) Dissecting planarian central nervous system regeneration by the expression of neural-specific genes. Dev Growth Differ 44:135–146. doi:10.1046/j.1440-169x.2002.00629.x

Chang L, Karin M (2001) Mammalian MAP kinase signalling cascades. Nature (Lond) 410:37–40. doi:10.1038/35065000

Guo T, Peters AH, Newmark PA (2006) A *bruno-like* gene is required for stem cell maintenance in planarians. Dev Cell 11:159–169. doi:10.1016/j.devcel.2006.06.004

Gurley KA, Rink JC, Sánchez Alvarado A (2008) β-Catenin defines head versus tail identity during planarian regeneration and homeostasis. Science 319:323–327. doi:10.1126/science.1150029

Iglesias M, Gomez-Skarmeta JL, Saló E, Adell T (2008) Silencing of *Smed-betacatenin1* generates radial-like hypercephalized planarians. Development (Camb) 135:1215–1221. doi:10.1242/dev.020289

Inoue T, Kumamoto H, Okamoto K, Umesono Y, Sakai M, Sánchez Alvarado A, Agata K (2004) Morphological and functional recovery of the planarian photosensing system during head regeneration. Zool Sci 21:275–283

Kobayashi C, Saito Y, Ogawa K, Agata K (2007) Wnt signaling is required for antero-posterior patterning of the planarian brain. Dev Biol 306:714–724. doi:10.1016/j.ydbio.2007.04.010

Lawrence PA (1988) Background to *bicoid*. Cell 54:1–2

Morgan TH (1904) The control of heteromorphosis in *Planaria maculata*. Arch Entw Mech Org 17:683–695

Morgan TH (1905) "Polarity" considered as a phenomenon of gradation of materials. J Exp Zool 2:495–506
Morgan TH (1910) Sex limited inheritance in *Drosophila*. Science 32:120–122
Morgan TH (1911a) Chromosomes and associative inheritance. Science 34:636–638
Morgan TH (1911b) The origin of five mutations in eye color in *Drosophila* and their modes of inheritance. Science 33:534–537
Morgan TH (1911c) The origin of nine wing mutations in *Drosophila*. Science 33:496–499
Newmark PA, Sánchez Alvarado A (2000) Bromodeoxyuridine specifically labels the regenerative stem cells of planarians. Dev Biol 220:142–153
Nishida E, Gotoh Y (1993) The MAP kinase cascade is essential for diverse signal transduction pathways. Trends Biochem Sci 18:128–131
Nishimura K, Kitamura Y, Inoue T, Umesono Y, Sano S, Yoshimoto K, Inden M, Takata K, Taniguchi T, Shimohama S, Agata K (2007) Reconstruction of dopaminergic neural network and locomotion function in planarian regenerates. Dev Neurobiol 67:1059–1078. doi:10.1002/dneu.20377
Nogi T, Watanabe K (2001) Position-specific and non-colinear expression of the planarian posterior (*Abdominal-B*-like)gene.DevGrowthDiffer43:177–184.doi:10.1046/j.1440-169X.2001.00564.x
Orii H, Sakurai T, Watanabe K (2005) Distribution of the stem cells (neoblasts) in the planarian *Dugesia japonica*. Dev Genes Evol 215:143–157. doi:10.1007/s00427-004-0460-y
Petersen CP, Reddien PW (2008) *Smed-betacatenin-1* is required for anteroposterior blastema polarity in planarian regeneration. Science 319:327–330. doi:10.1126/science.1149943
Petersen CP, Reddien PW (2009) A wound-induced Wnt expression program controls planarian regeneration polarity. Proc Natl Acad Sci USA 106:17061–17066. doi:10.1073/pnas.0906823106
Rink JC, Gurley KA, Elliott SA, Sánchez Alvarado A (2009) Planarian Hh signaling regulates regeneration polarity and links Hh pathway evolution to cilia. Science 326:1406–1410. doi:10.1126/science
Rouhana L, Weiss JA, Forsthoefel DJ, Lee H, King RS, Inoue T, Shibata N, Agata K, Newmark PA (2013) RNA interference by feeding in vitro-synthesized double-stranded RNA to planarians: methodology and dynamics. Dev Dyn 242:718–730. doi:10.1002/dvdy.23950
Salvetti A, Rossi L, Deri P and Batistoni R (2000) An *MCM2*-related gene is expressed in proliferating cells of intact and regenerating planarians. Dev Dyn 218:603–614. doi:10.1002/1097-0177(2000)9999:9999<::AID-DVDY1016>3.0.CO;2-C
Sánchez Alvarado A, Newmark PA (1999) Double-stranded RNA specifically disrupts gene expression during planarian regeneration. Proc Natl Acad Sci USA 96:5049–5054. doi:10.1073/pnas.96.9.5049
Shibata N, Rouhana L, Agata K (2010) Cellular and molecular dissection of pluripotent adult somatic stem cells in planarians. Dev Growth Differ 52:27–41. doi:10.1111/j.1440-169X.2009.01155.x
Takano T, Pulvers JN, Inoue T, Tarui H, Sakamoto H, Agata K, Umesono Y (2007) Regeneration-dependent conditional gene knockdown (Readyknock) in planarian: demonstration of requirement for *Djsnap-25* expression in the brain for negative phototactic behavior. Dev Growth Differ 49:383–394. doi:10.1111/j.1440-169X.2007.00936.x
Tasaki J, Shibata N, Nishimura O, Itomi K, Tabata Y, Son F, Suzuki N, Araki R, Abe M, Agata K, Umesono Y (2011a) ERK signaling controls blastema cell differentiation during planarian regeneration. Development (Camb) 138:2417–2427. doi:10.1242/dev.060764
Tasaki J, Shibata N, Sakurai T, Agata K, Umesono Y (2011b) Role of c-Jun N-terminal kinase activity in blastema formation during planarian regeneration. Dev Growth Differ 53:389–400. doi:10.1111/j.1440-169X.2011.01254.x
Tazaki A, Gaudieri S, Ikeo K, Gojobori T, Watanabe K, Agata K (1999) Neural network in planarian revealed by an antibody against planarian synaptotagmin homologue. Biochem Biophys Res Commun 260:426–432
Umesono Y, Agata K (2009) Evolution and regeneration of the planarian central nervous system. Dev Growth Differ 51:185–195. doi:10.1111/j.1440-169X.2009.01099.x

Umesono Y, Watanabe K, Agata K (1997) A planarian *orthopedia* homolog is specifically expressed in the branch region of both the mature and regenerating brain. Dev Growth Differ 39:723–727

Umesono Y, Watanabe K, Agata K (1999) Distinct structural domains in the planarian brain defined by the expression of evolutionarily conserved homeobox genes. Dev Genes Evol 209:31–39

Umesono Y, Tasaki J, Nishimura K, Inoue T, Agata K (2011) Regeneration in an evolutionarily primitive brain: the planarian *Dugesia japonica* model. Eur J Neurosci 34:863–869. doi:10.1111/j.1460-9568.2011.07819.x

Umesono Y, Tasaki J, Nishimura Y, Hrouda M, Kawaguchi E, Yazawa S, Nishimura O, Hosoda K, Inoue T, Agata K (2013) The molecular logic for planarian regeneration along the anterior-posterior axis. Nature (Lond) 500:73–76. doi:10.1038/nature12359

Wagner DE, Wang IE, Reddien PW (2011) Clonogenic neoblasts are pluripotent adult stem cells that underlie planarian regeneration. Science 332:811–816. doi:10.1126/science.1203983

Wolpert L (1969) Positional information and the spatial pattern of cellular differentiation. J Theor Biol 25:1–47

Yazawa S, Umesono Y, Hayashi T, Tarui H, Agata K (2009) Planarian Hedgehog/Patched establishes anterior-posterior polarity by regulating Wnt signaling. Proc Natl Acad Sci USA 106:22329–22334. doi:10.1073/pnas.0907464106

Yoshida-Kashikawa M, Shibata N, Takechi K, Agata K (2007) DjCBC-1, a conserved DEAD box RNA helicase of the RCK/p54/Me31B family, is a component of RNA-protein complexes in planarian stem cells and neurons. Dev Dyn 236:3436–3450. doi:10.1002/dvdy.21375

Chapter 7
Regulation of Axial Stem Cells Deriving Neural and Mesodermal Tissues During Posterior Axial Elongation

Tatsuya Takemoto

Abstract The vertebrate body axis elongates by extending the posterior end and generating a variety of somatic cells of the trunk (posterior) tissues. Recent studies have demonstrated that the posterior neural plate and posterior paraxial mesoderm are generated from bipotential stem cells, the axial stem cells, which reside in the caudal lateral epiblast of gastrulating embryos. The fate of axial stem cells, neural or mesodermal lineages, depends on the counteracting transcription factors for respective tissues, Sox2 and Tbx6. Tbx6 represses the *Sox2* expression in the axial stem cell-derived mesodermal precursors. In the absence of the *Tbx6* gene, *Sox2* is ectopically expressed in the mesodermal precursors, causing ectopic neural tube development at the expense of paraxial mesoderm. While producing two somatic lineages, axial stem cells are proliferatively maintained by a process that depends on the Wnt-Brachyury regulatory loop; mutant embryos lacking Wnt3a or Brachyury activity prematurely terminate axis elongation as the result of stem cell exhaustion. Although the axial stem cells serve as a cellular source for the neural and paraxial mesoderm tissues of the trunk, at the craniocervical level these tissues are presumably produced via completely different mechanisms. In this chapter, experimental evidence for axial stem cells and their regulation is summarized.

Keywords Axial elongation • Axial stem cell • Sox2 • Tbx6 • Wnt signal

7.1 Introduction

During vertebrate embryogenesis, primordia of anterior tissues (i.e., tissues formed in the anteriormost part of the embryo exemplified by the brain) are established first, and subsequently those of posterior tissues (i.e., tissues posterior to the head) are

T. Takemoto (✉)
Fujii Memorial Institute of Medical Sciences, The University of Tokushima, Tokushima, Japan
e-mail: takemoto.tatsuya@tokushima-u.ac.jp

H. Kondoh and A. Kuroiwa (eds.), *New Principles in Developmental Processes*,
DOI 10.1007/978-4-431-54634-4_7,

generated over time in an anterior-to-posterior sequence. In mouse embryos, the former process occurs between embryonic day (E)6 and E8, and the latter process begins around E8 and continues over the following 5 days until E13. In chick embryos, anterior tissue primordia are generated within the first day of incubation [Hamburger and Hamilton (HH) stage ~5], followed by the generation of posterior tissue primordia over 6 days (ending at HH26). The posterior tissue development initially depends on the primitive streak and the surrounding epiblastic tissues, then the tail bud, which serve as cellular sources for all the posterior tissues.

The primitive streak and neighboring tissues contain several subdomains that generate different types of the posterior tissues (Cambray and Wilson 2007; Wilson et al. 2009; Brown and Storey 2000). The node, which is located on the anterior end of the primitive streak, contains cells that develop into the notochord, ventral neural tube, and the dorsal part of gut endoderm. The cells in the more posterior primitive streak contribute more ventrally and laterally located mesodermal tissues, including paraxial and lateral plate mesoderm. On the other hand, progenitors for posterior neural plate colocate with those for posterior paraxial mesoderm in the epiblast lateral to the anterior 80 % of primitive streak in mouse embryos and anterior 50 % in chick embryos; this region is called the caudal lateral epiblast (CLE). The neural plate cells also emerge from the border between the node and primitive streak (up to 10 % of the streak length), called the node-streak border (NSB), and contribute to the ventral domain of the neural tube. At later stages, descendants of CLE and NSB form the chordoneural hinge (CNH) in the tail bud, which bridges the posterior end of nascent notochord and neural tube, and continue to serve as the progenitors for the neural tube, paraxial mesoderm, and notochord (Fig. 7.1).

Based on cell group tracing experiments using tissue fragment transplantation and cell cluster labeling, a model was proposed in which multipotential stem cells for the entire length of the posterior axis reside in the CLE and NSB (Cambray and Wilson 2007; Wilson et al. 2009). These stem cells have been hypothesized to stay in the developing posterior end of embryos and proliferate throughout axis elongation to supply their descendant cells to multiple somatic tissues.

Recent investigations demonstrated that bipotential stem cells, the “axial stem cells,” reside in the CLE and give rise to both posterior neural plate and paraxial mesoderm (Tzouanacou et al. 2009; Takemoto et al. 2011; Kondoh and Takemoto 2012).

In the following sections, I characterize the axial stem cells and their regulation.

7.2 Evidence for Neuro-Mesodermal Bipotential Axial Stem Cells

The presence of neuro-mesodermal bipotential precursor cells was first indicated by earlier fate map studies using mouse and chick embryos (Cambray and Wilson 2007; Brown and Storey 2000). Using mouse embryos, green fluorescent protein (GFP)-labeled tissue fragments of the E8.5 primitive streak and its lateral region were transplanted homotopically to host embryos (Cambray and Wilson 2007).

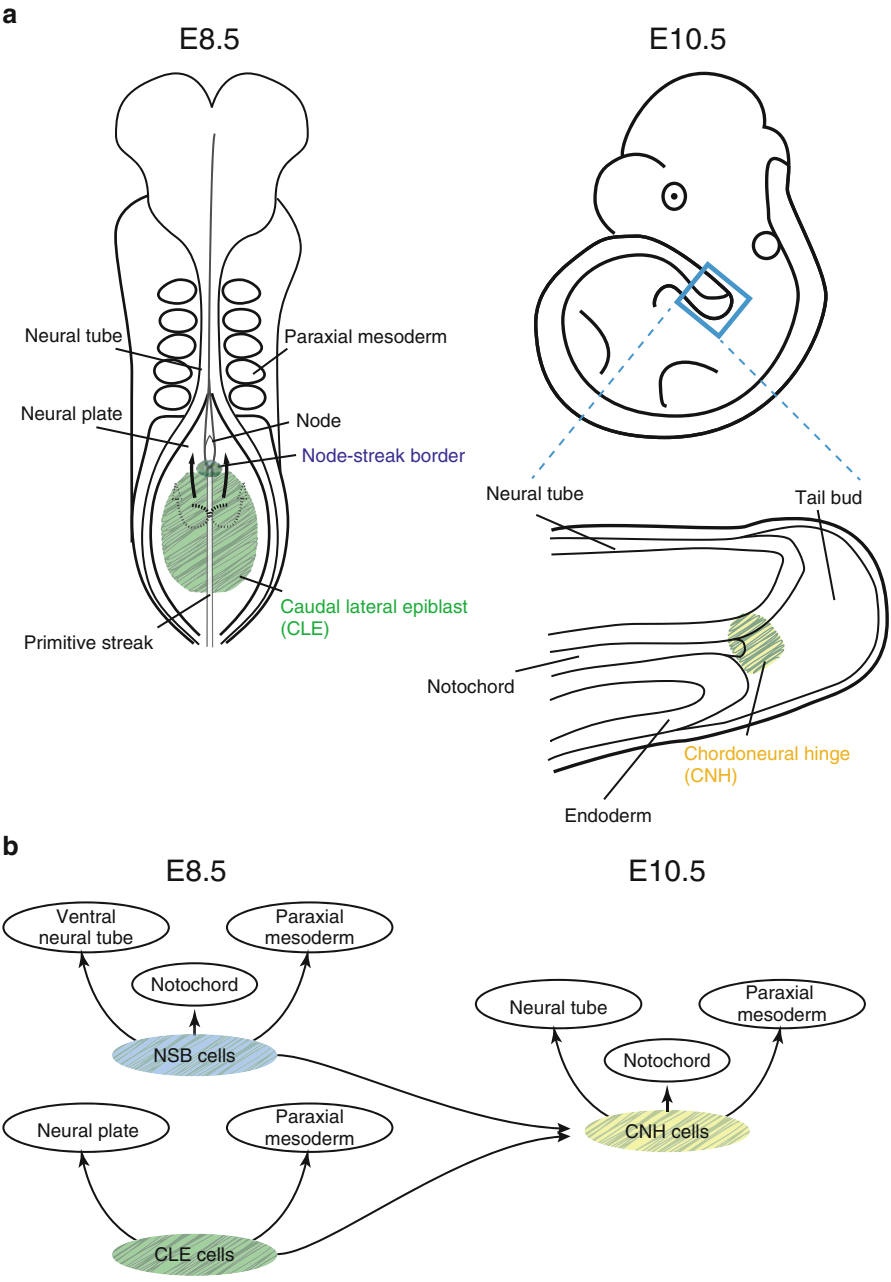

Fig. 7.1 Location of caudal lateral epiblast (*CLE*), node-streak border (*NSB*), and chordoneural hinge (*CNH*) in developing mouse embryo. **a** E8.5 and E10.5 mouse embryos. At E8.5, CLE lies adjacent to the anterior 80 % of the primitive streak. NSB comprises the posterior end of the node and rostral tip of primitive streak. A fraction of cells in both regions later contributes to CNH, which is located posterior to the notochord. **b** A current model of the fate of NSB, CLE, and CNH cells. NSB cells contribute to ventral neural tube, notochord, and dorsal endoderm, and CLE cells give rise to neural tube and paraxial mesoderm. A population of CLE and NSB contribute to CNH, which is the later source for neural and paraxial mesodermal tissues

CLE cells, which are located in the epiblast lateral to the anterior 80 % of primitive streak, contributed to the neural plate and paraxial mesoderm of the trunk, while the fragments derived from other regions of epiblast exclusively gave rise to the neural or mesodermal tissues (Fig. 7.1). The CLE-derived cells are also found in the CNH, a later source for the neural tube, paraxial mesoderm, and notochord. Using chick embryos, Brown and Storey (2000) labeled a few CLE cells of HH6 chick embryos with DiI and traced their fate. The labeled cells contributed to the neural plate and paraxial mesoderm of the trunk and tail. These results raised the possibility that the posterior neural plate and paraxial mesoderm are derived from common precursor cells in the CLE. However, these studies did not have a single cell resolution to test the model (Wilson et al. 2009).

Recent analysis of cellular clones marked by intragenic recombination provided strong evidence for the bipotential precursors giving rise to neural and paraxial mesodermal cells (Tzouanacou et al. 2009). The embryos used for this study carried the *LaacZ* transgene, having intragenic duplication that inactivates the LacZ function. Infrequently occurring intragenic recombination activated the *LacZ* gene, allowing the labeling of clones starting from the recombinant cells. As the recombination frequency was very low, the chance of occurrence of two independent recombinations in an embryo was negligible. Many clones that are estimated to be labeled at E8–E9 stages contributed to both neural tube and paraxial mesoderm for substantial lengths along the posterior axis, demonstrating that neural and paraxial mesodermal tissues at these stages are derived from bipotential axial stem cells (Tzouanacou et al. 2009). However, this retrospective analysis did not determine the localization of the axial stem cells in the embryo or clarify the mechanisms of deriving two different types of cells from individual stem cells (Kondoh and Takemoto 2012).

7.3 Axial Stem Cell Regulation Involving a *Sox2* Enhancer

The nature of axial stem cells and their regulation were revealed by the investigation of *Sox2* regulation (Fig. 7.2).

The *Sox2* gene codes for a transcription factor that is activated when the neural plate develops (Uchikawa et al. 2011; Wood and Episkopou 1999). During

Fig. 7.2 (continued) covering the N1 enhancer-active region represses the *Sox2* activation. A population of axial stem cells is released from BMP-dependent repression by the action of BMP antagonists, Chordin and Noggin, secreted from the node, and activates *Sox2* that causes neural plate development (*blue*). Another population of axial stem cells that have ingressed through the primitive streak activates *Tbx6* (*yellow*). Tbx6 represses *Wnt3a* expression in mesodermal precursors and consequently shuts off N1 activity. These cells develop into paraxial mesoderm. **c** Cross sections of E9 mouse embryos. *Sox2* expression (*blue color*) was visualized by in situ hybridization. In the absence of *Tbx6* gene (*Tbx6* –/–), mouse embryo develops ectopic neural tubes without development of paraxial mesoderm. Removal of N1 enhancer sequence in *Tbx6* mutant embryos resulted in loss of ectopic neural tube formation (*Tbx6* –/–; ΔN1/ΔN1). However, paraxial mesoderm formation is not restored. *NT* neural tube, *PAM* paraxial mesoderm, *eNT* ectopic neural tube

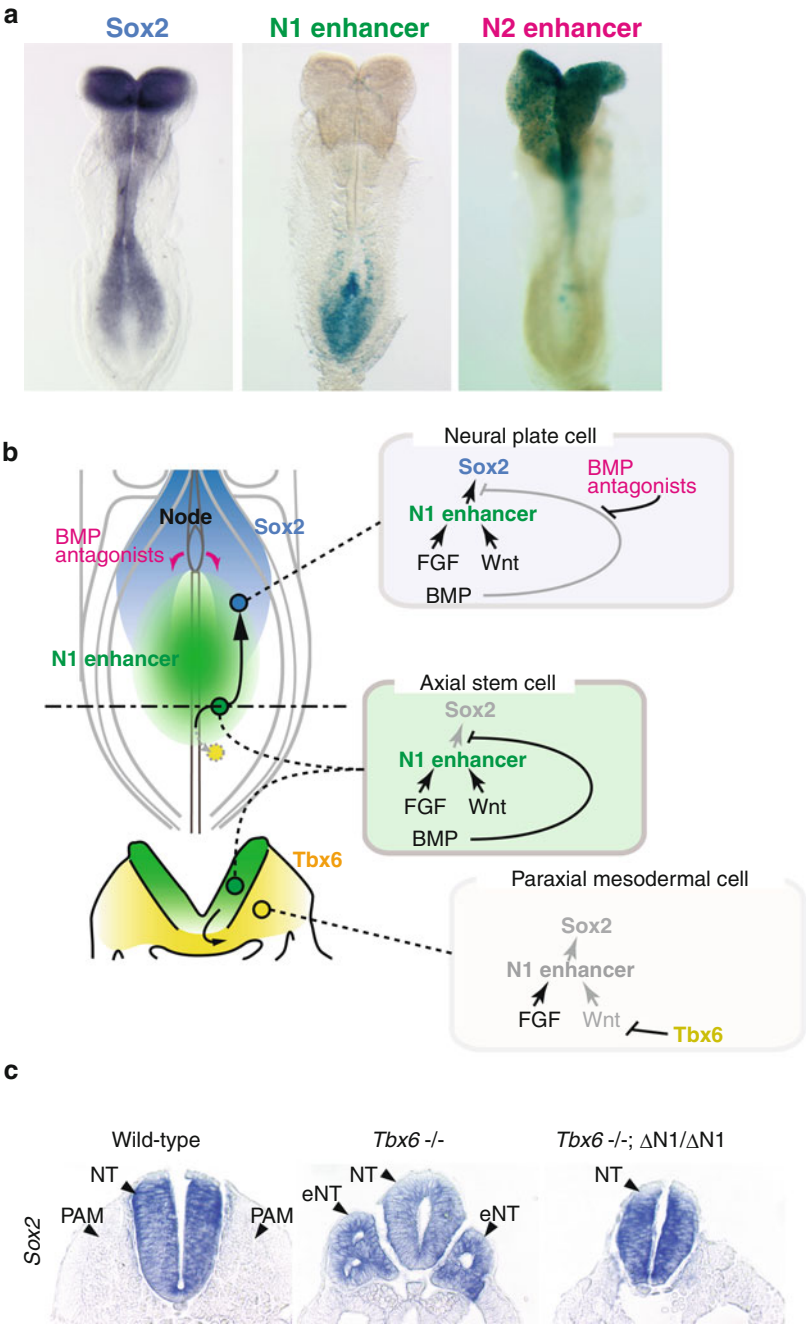

Fig. 7.2 Axial stem cell regulation involving *Sox2* N1 enhancer. **a** Comparison of *Sox2* expression and enhancer activities of N1 and N2 in E8.5 mouse embryos. *Sox2* expression marks the neural plate. N1 enhancer is involved in the activation of *Sox2* in the developing posterior neural plate, while N2 activates *Sox2* in the anterior neural plate. *Sox2* expression was detected by in situ hybridization. Enhancer activities of N1 and N2 were detected by X-gal staining of LacZ reporter expression. **b** Regulation of axial stem cells deriving neural plate and paraxial mesoderm cells. N1 enhancer is activated by Wnt and Fgf signal in axial stem cells in CLE (*green*), but BMP signal

gastrulation stages, *Sox2* is first activated in the forming anterior neural plate, which later gives rise to the brain, then in the forming posterior neural plate, giving rise to the spinal cord.

Sox2 expression in the neural plate is regulated by many enhancers that are distributed in the *Sox2*-encompassing genomic region of a few hundred kilobases (Uchikawa et al. 2003; Kamachi et al. 2009). These enhancers have different yet overlapping spatial and temporal specificities. However, at early developmental stages, only two enhancers, N1 and N2, are activated, which are responsible for the initial activation of *Sox2* in the posterior and anterior neural plate, respectively (Fig. 7.2a) (Iwafuchi-Doi et al. 2011; Takemoto et al. 2006; Uchikawa et al. 2003).

The N1 enhancer is activated by cooperative action of Fgf and Wnt signals in the region of epiblast that flanks anterior primitive streak that corresponds to the CLE. However, N1 activation does not immediately activate *Sox2* expression. The bone morphogenetic protein (BMP) signal emanating from the primitive streak inhibits *Sox2* expression in the CLE, even when the N1 enhancer is activated. *Sox2* starts to be expressed and promotes posterior neural plate development when BMP antagonists Chordin and Noggin secreted from the node quench the inhibitory action of BMP (Fig. 7.2b) (Takemoto et al. 2006).

The fate map studies indicate that CLE cells contribute to both neural plate and paraxial mesoderm of the trunk region. Indeed, a large fraction of N1-activated cells ingress though the primitive streak and become the paraxial mesoderm cells. In these cells, N1 activity is shut off after the ingression. In our chick embryo experiment, a mutation in N1 enhancer (N1 mutE) caused the persistence of N1 activity in the cells after ingression through the primitive streak. This observation suggested that N1-active cells in the CLE are neuro-mesodermal bipotential cells. According to this model, the N1 activity must be shut off for the paraxial mesodermal cells to develop, and the failure of N1 inactivation would cause neural tissue development instead of mesoderm development.

The *Tbx6* gene, which encodes a T-box transcription factor, is involved in the repression of N1 enhancer in the developing paraxial mesodermal cells (Fig. 7.2b) (Takemoto et al. 2011; Kondoh and Takemoto 2012). *Tbx6* is expressed in the paraxial mesodermal precursors that have started ingression through the primitive streak (Chapman et al. 1996). *Tbx6* mutant embryos form ectopic neural tube at the expense of paraxial mesoderm, indicating that Tbx6 represses neural tube development in the mesodermal precursor cells (Chapman and Papaioannou 1998). Tbx6 in fact represses the N1 enhancer in the mesodermal precursors (Takemoto et al. 2011). Without *Tbx6* activity, the N1 enhancer is kept activated even after ingression through the primitive streak, causing ectopic *Sox2* expression in the mesodermal precursors (Fig. 7.2c). These cells with ectopic *Sox2* expression form additional neural tubes at both sides of the primary neural tube, where paraxial mesoderm is normally formed. When the N1 enhancer DNA sequence was deleted from the genome, no ectopic neural tubes developed, indicating that a primary role of Tbx6 is to inactivate the N1 enhancer in mesoderm precursors (Fig. 7.2c). Although ectopic neural tube development was suppressed in the double mutant embryos for *Tbx6* and *Sox2* N1 enhancer, no mesodermal markers were expressed in cells that

were located in the mesodermal position. This observation indicates that Tbx6 has a second important role, to promote mesodermal development in addition to repressing the N1 enhancer. Tbx6 does not bind the N1 enhancer sequence, and its effect on the N1 enhancer is indirect. In Tbx6 mutant embryos, the Wnt3a gene is ectopically activated in the mesodermal precursors, and this presumably causes the mesodermal N1 dysregulation.

In summary, the CLE cells are axial stem cells bipotential for neural plate and paraxial mesodermal cells. The axial stem cells in the CLE are primed for neural development by the activation of the *Sox2* N1 enhancer, but this developmental potential is temporally inhibited by the action of the BMP signal. This time window allows the axial stem cells to determine the developmental pathways, either to neural plate or to paraxial mesoderm (Fig. 7.2). Once the BMP-dependent inhibition is relieved by the BMP antagonists emanating from the node, a population of axial stem cells that have stayed in the epiblastic layer activate *Sox2* expression and develop into neural plate, while another population that have ingressed through the primitive streak activates *Tbx6*, which then represses the N1 enhancer-dependent *Sox2* expression. Although this study did not demonstrate the bipotentiality of axial stem cells at the single-cell level, the results from the single-cell lineage tracing confirmed the bipotentiality of axial stem cells (Tzouanacou et al. 2009)

7.4 Wnt-Brachyury-Dependent Regulation of Axial Stem Cells

As just described, Wnt, fibroblast growth factor (FGF), and BMP signals are involved in the regulation of *Sox2* activation in the axial stem cells. The action of Wnt and FGF signals in the absence of BMP signaling causes the axial stem cell to develop into neural tissue (Takemoto et al. 2006, 2011). However, the action of these signals in regulation of axial stem cells is more complex than the regulation of *Sox2* activation (Fig. 7.3a).

The Wnt signal also participates in the maintenance of axial stem cells and, in addition, in the development of paraxial mesoderm. *Wnt3a* is one of *Wnt* genes that are expressed in the CLE. Inactivation of the *Wnt3a* gene ($Wnt3a^{-/-}$) results in precocious *Sox2* expression in the CLE, the entire loss of *Tbx6* expression, failure of mesodermal development, and premature termination of axis elongation (Takada et al. 1994; Yoshikawa et al. 1997). These observations suggest that in the absence of Wnt3a activity, the axial stem cells readily undergo neural development, which results in the exhaustion of the axial stem cells. In other words, a level of Wnt signal is required for the maintenance of the axial stem cells. In normal embryos, the termination of axis elongation at E13 coincides with the loss of *Wnt3a* expression in the tail bud. A causal relationship between the termination of axial elongation and loss of *Wnt3a* expression is further supported by the study of the *vestigial tail* (*vt*) mutant embryo, which expresses *Wnt3a* at a reduced level (*Wnt3a* hypomorph) (Fig. 7.3b) (Greco et al. 1996). Homozygous *vt* mutant ($Wnt3a^{vt/vt}$) embryos

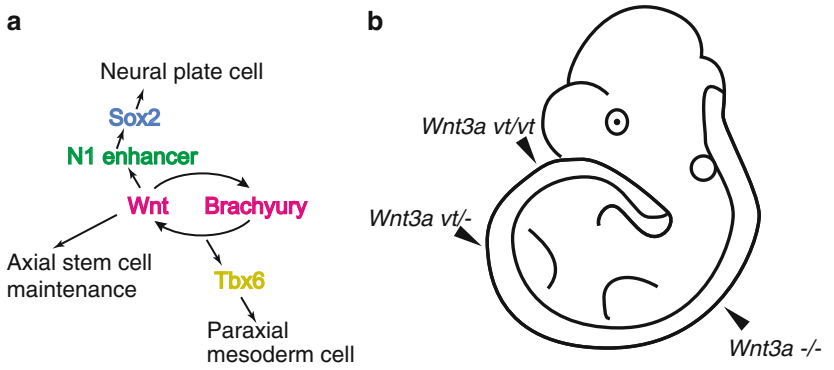

Fig. 7.3 Wnt-Brachyury coregulation in the regulation of axial stem cells. **a** In axial stem cells, Wnt signal and transcription factor Brachyury form a mutual activation loop. Wnt signal regulates *Sox2* expression by activating the N1 enhancer. Wnt signal also regulates the maintenance of axial stem cells and mesodermal development. **b** *Wnt3a* hypomorph mutant embryos terminate axial development at stages that depend on Wnt3a level. *Wnt3a* vt/vt embryos, which express *Wnt3a* at a reduced level, result in tail truncation. *Wnt3a* vt/– embryos with more severe reduction of *Wnt3a* expression terminate axial elongation at the sacral level. *Wnt3a*–/– embryos lack trunk region posterior to somite 6

terminate axis elongation prematurely during tail formation (truncated tail), and the compound heterozygotes for *Wnt3a* null and *vt* alleles ($Wnt3a^{-/vt}$) express *Wnt3a* at much more reduced level and stop axial elongation at an earlier stage than $Wnt3a^{vt/vt}$ (tailless or rumples). *Wnt3a*-null ($Wnt3a^{-/-}$) embryos lack the trunk region posterior to somite 7. These observations suggest that the axial stem cells are exhausted at an earlier stage with the reduction of Wnt signal level (Fig. 7.3b).

The T-box transcription factor gene *Brachyury* is also involved in axial stem cell maintenance. *Brachyury* is expressed strongly in the primitive streak and weakly in the CLE. The phenotype of the *Brachyury* mutant embryo is similar to that of *Wnt3a*, namely, precocious neural development from the CLE, loss of *Tbx6* expression, failure in mesodermal development, and termination of axial elongation after the seventh somite (Chesley 1935; Yamaguchi et al. 1999). In fact, Wnt3a and Brachyury form a mutually activating regulatory loop, where LEF/TCF transcription factors bind the *Brachyury* upstream enhancer and activate the *Brachyury* gene by the Wnt signal input (Fig. 7.3a) (Yamaguchi et al. 1999). Thus, Wnt-Brachyury coregulation plays a central role in axial stem cell maintenance and in mesodermal development.

In the past, *Brachyury* expression tended to be taken as a definitive indication of mesodermal development. However, this model is not supported by the following observations. Tracing the cells that once activated the *Brachyury* gene by use of *Brachyury* enhancer-driven Cre demonstrated that these cells contribute to the neural tube after E9 (Perantoni et al. 2005; Anderson et al. 2013). Furthermore, *Sox2* and *Brachyury* are coexpressed at a low level in the CLE. Thus, Brachyury expression does not determine the future mesodermal fate of cells (Delfino-Machín et al. 2005; Olivera-Martinez et al. 2012; Martin and Kimelman 2012).

An important issue is how the Brachyury-dependent Wnt signal regulates three different processes of axial stem cells: maintenance, neural development, or mesodermal development. A possible mechanism is that the different levels (intensities) of Wnt signal input cause different developmental outputs. A recent study on the zebrafish version of axial stem cells indeed demonstrated that a low-level Wnt signal promotes neural development whereas a high-level Wnt signal directs mesodermal development from the axial stem cells (Martin and Kimelman 2012).

7.5 The Difference in the Mechanisms Deriving Craniocervical and More Posterior Axial Tissues

The axial stem cell system discussed here operates in the production of neural plate and paraxial mesoderm more posterior to the cervical level. *Tbx6* mutant embryos usually have six pairs of somites, although their segmentation is not complete, and ectopic neural tubes at the paraxial position develop only posterior to this level (Takemoto et al. 2011; Chapman and Papaioannou 1998). *Wnt3a* and *Brachyury* mutant embryos also produce the anterior six somite pairs and lack more posterior somites (Yoshikawa et al. 1997). As the first four somites contribute to the occipital domain, the sixth somite corresponds to the second cervical somite. These observations indicate that the axial stem cell-dependent development of neural and mesodermal tissues operates posteriorly to about the seventh somite level, and different mechanisms operate in the production of more anterior mesodermal tissues (Fig. 7.4).

The differences in the derivation of paraxial mesoderm between the axial levels anterior and posterior to the sixth somite may reflect different developmental pathways. Recently, it has been shown that epiblast stem cells (EpiSC), having the character of multipotent epiblast cells, can be derived from early-stage postimplantation embryos (Brons et al. 2007; Tesar et al. 2007). EpiSC can be established from embryos before E8 but not after E8, suggesting that the pluripotent epiblast cells are present only before E8 (Osorno et al. 2012). Cultured EpiSCs can contribute to somatic cells when transplanted into the embryonic epiblast by stage E8, but not in later embryos (Huang et al. 2012). A possible model is that the paraxial mesoderm up to the sixth somite level is derived directly from the pluripotent epiblast rather than through the intermediate axial stem cells.

7.6 Other Stem Cells for Posterior Somatic Tissue Development

I have confined my discussion to the axial stem cells, bipotential for the neural and paraxial mesodermal lineages. However, in developing embryos, other tissues such as axial mesoderm (notochord), lateral plate mesoderm (LPM), intermediate mesoderm (IMM), and endoderm also extend posteriorly. However, the cellular source

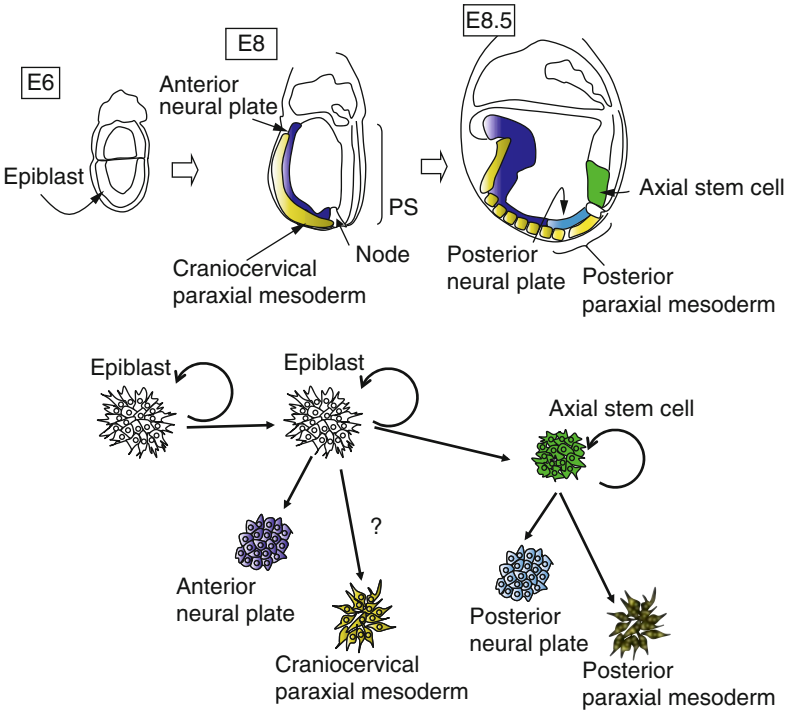

Fig. 7.4 Possible differences of cellular source of neural plate and paraxial mesoderm between the craniocervical and more posterior level. Neural plate and paraxial mesoderm anterior to the sixth somite level develop by E8, possibly from pluripotent epiblast. In contrast, neural plate and paraxial mesoderm at more posterior somite levels are generated from the axial stem cells

and regulatory mechanisms for the axial extension of these tissues have not been fully characterized. In a transplantation experiment, tissue fragments of NSB were shown to give rise to notochord, ventral neural tube, and paraxial mesoderm (Cambray and Wilson 2007), suggesting the presence of stem cells that have different developmental repertoires from the axial stem cells.

7.7 Conclusion

According to a popular model of embryogenesis, embryonic cells are first divided into three germ layers, that is, ectoderm, mesoderm, and endoderm, and this separation of germ layers is the first step of cell lineage specification. According to this model, neural plate is derived from ectoderm, and mesoderm is subdivided into several subdomains including paraxial mesoderm. Thus, the neural plate and paraxial mesoderm have been regarded to be very distant in cell lineages. However, our characterization of axial stem cells revealed that the posterior neural plate and

paraxial mesoderm are directly derived from common precursors, the axial stem cells, thus challenging the classical three germ layers model of cell lineage segregation. This observation is presumably one of many possible examples of cell lineage determination processes deviating from the classical germ layer models. Unbiased and thorough reinvestigation of somatic lineages is anticipated.

References

Anderson MJ, Naiche LA, Wilson CP, Elder C, Swing DA, Lewandoski M (2013) TCreERT2, a transgenic mouse line for temporal control of Cre-mediated recombination in lineages emerging from the primitive streak or tail bud. PLoS ONE 8(4):e62479. doi:10.1371/journal.pone.0062479

Brons IG, Smithers LE, Trotter MW, Rugg-Gunn P, Sun B, de Sousa C, Lopes SM, Howlett SK, Clarkson A, Ahrlund-Richter L, Pedersen RA, Vallier L (2007) Derivation of pluripotent epiblast stem cells from mammalian embryos. Nature (Lond) 448(7150):191–195. doi:10.1038/nature05950

Brown J, Storey K (2000) A region of the vertebrate neural plate in which neighbouring cells can adopt neural or epidermal fates. Curr Biol 10(14):869–872

Cambray N, Wilson V (2007) Two distinct sources for a population of maturing axial progenitors. Development (Camb) 134(15):2829–2840

Chapman D, Papaioannou V (1998) Three neural tubes in mouse embryos with mutations in the T-box gene Tbx6. Nature (Lond) 391(6668):695–697

Chapman D, Agulnik I, Hancock S, Silver L, Papaioannou V (1996) Tbx6, a mouse T-box gene implicated in paraxial mesoderm formation at gastrulation. Dev Biol 180(2):534–542

Chesley P (1935) Development of the short-tailed mutant in the house mouse. J Exp Zool 70(3): 429–459

Delfino-Machín M, Lunn J, Breitkreuz D, Akai J, Storey K (2005) Specification and maintenance of the spinal cord stem zone. Development (Camb) 132(19):4273–4283

Greco TL, Takada S, Newhouse MM, McMahon JA, McMahon AP, Camper SA (1996) Analysis of the vestigial tail mutation demonstrates that Wnt-3a gene dosage regulates mouse axial development. Genes Dev 10(3):313–324

Huang Y, Osorno R, Tsakiridis A, Wilson V (2012) In vivo differentiation potential of epiblast stem cells revealed by chimeric embryo formation. Cell Rep 2(6):1571–1578. doi:10.1016/j.celrep.2012.10.022

Iwafuchi-Doi M, Yoshida Y, Onichtchouk D, Leichsenring M, Driever W, Takemoto T, Uchikawa M, Kamachi Y, Kondoh H (2011) The Pou5f1/Pou3f-dependent but SoxB-independent regulation of conserved enhancer N2 initiates Sox2 expression during epiblast to neural plate stages in vertebrates. Dev Biol 352(2):354–366. doi:10.1016/j.ydbio.2010.12.027, pii: S0012-1606(10)01268-6

Kamachi Y, Iwafuchi M, Okuda Y, Takemoto T, Uchikawa M, Kondoh H (2009) Evolution of non-coding regulatory sequences involved in the developmental process: reflection of differential employment of paralogous genes as highlighted by Sox2 and group B1 Sox genes. Proc Jpn Acad Ser B Phys Biol Sci 85(2):55–68

Kondoh H, Takemoto T (2012) Axial stem cells deriving both posterior neural and mesodermal tissues during gastrulation. Curr Opin Genet Dev 22(4):374–380. doi:10.1016/j.gde.2012.03.006, pii: S0959-437X(12)00044-5

Martin BL, Kimelman D (2012) Canonical Wnt signaling dynamically controls multiple stem cell fate decisions during vertebrate body formation. Dev Cell 22(1):223–232. doi:10.1016/j.devcel.2011.11.001

Olivera-Martinez I, Harada H, Halley PA, Storey KG (2012) Loss of FGF-dependent mesoderm identity and rise of endogenous retinoid signalling determine cessation of body axis elongation. PLoS Biol 10(10):e1001415. doi:10.1371/journal.pbio.1001415

Osorno R, Tsakiridis A, Wong F, Cambray N, Economou C, Wilkie R, Blin G, Scotting PJ, Chambers I, Wilson V (2012) The developmental dismantling of pluripotency is reversed by ectopic Oct4 expression. Development (Camb) 139(13):2288–2298. doi:10.1242/dev.078071

Perantoni AO, Timofeeva O, Naillat F, Richman C, Pajni-Underwood S, Wilson C, Vainio S, Dove LF, Lewandoski M (2005) Inactivation of FGF8 in early mesoderm reveals an essential role in kidney development. Development (Camb) 132(17):3859–3871. doi:10.1242/dev.01945

Takada S, Stark K, Shea M, Vassileva G, McMahon J, McMahon A (1994) Wnt-3a regulates somite and tailbud formation in the mouse embryo. Genes Dev 8(2):174–189

Takemoto T, Uchikawa M, Kamachi Y, Kondoh H (2006) Convergence of Wnt and FGF signals in the genesis of posterior neural plate through activation of the Sox2 enhancer N-1. Development (Camb) 133(2):297–306

Takemoto T, Uchikawa M, Yoshida M, Bell DM, Lovell-Badge R, Papaioannou VE, Kondoh H (2011) Tbx6-dependent Sox2 regulation determines neural or mesodermal fate in axial stem cells. Nature (Lond) 470(7334):394–398. doi:10.1038/nature09729, pii: nature09729

Tesar PJ, Chenoweth JG, Brook FA, Davies TJ, Evans EP, Mack DL, Gardner RL, McKay RD (2007) New cell lines from mouse epiblast share defining features with human embryonic stem cells. Nature (Lond) 448(7150):196–199. doi:10.1038/nature05972

Tzouanacou E, Wegener A, Wymeersch F, Wilson V, Nicolas J (2009) Redefining the progression of lineage segregations during mammalian embryogenesis by clonal analysis. Dev Cell 17(3): 365–376

Uchikawa M, Ishida Y, Takemoto T, Kamachi Y, Kondoh H (2003) Functional analysis of chicken Sox2 enhancers highlights an array of diverse regulatory elements that are conserved in mammals. Dev Cell 4(4):509–519

Uchikawa M, Yoshida M, Iwafuchi-Doi M, Matsuda K, Ishida Y, Takemoto T, Kondoh H (2011) B1 and B2 Sox gene expression during neural plate development in chicken and mouse embryos: universal versus species-dependent features. Dev Growth Differ 53(6):761–771. doi:10.1111/j.1440-169X.2011.01286.x

Wilson V, Olivera-Martinez I, Storey K (2009) Stem cells, signals and vertebrate body axis extension. Development (Camb) 136(10):1591–1604

Wood HB, Episkopou V (1999) Comparative expression of the mouse Sox1, Sox2 and Sox3 genes from pre-gastrulation to early somite stages. Mech Dev 86(1–2):197–201

Yamaguchi T, Takada S, Yoshikawa Y, Wu N, McMahon A (1999) T (Brachyury) is a direct target of Wnt3a during paraxial mesoderm specification. Genes Dev 13:3185–3190

Yoshikawa Y, Fujimori T, McMahon A, Takada S (1997) Evidence that absence of Wnt-3a signaling promotes neuralization instead of paraxial mesoderm development in the mouse. Dev Biol 183(2):234–242

Chapter 8
Tbx1/Ripply3/Retinoic Acid Signal Network That Regulates Pharyngeal Arch Development

Tadashi Okubo

Abstract The main feature of the developing pharynx of the vertebrate embryo is the transient appearance of a series of segmental pharyngeal arches. These arches are divided by internal pouches (endoderm) and external clefts (ectoderm) that together comprise the pharyngeal apparatus. The formation of the pharyngeal arches is essential for the development of many organs at later stages, and the pouches give rise to the rudiments of the thymus, parathyroid glands, and ultimobranchial body. During the development of the arches occur the sequential formation of pharyngeal arch arteries and the precise ingrowth of the axons of cranial nerves. Neural crest cells also migrate through each arch to differentiate in appropriate locations. Therefore, defects in pharyngeal arch development lead to deficits of pharyngeal arch arteries and mislocation or cell death of neural crest cells, which cause later malformations in the derivative organs. This chapter first overviews pharyngeal arch development, and then discusses our present knowledge regarding the genetic factors (Tbx1 and Ripply3) and signaling molecules (retinoic acid) that regulate the formation of the pharyngeal arches and their organ derivatives.

Keywords Organogenesis • Pharyngeal arches • Retinoic acid • Ripply3 • Tbx1

8.1 Overview of Pharyngeal Arch Development

The pharyngeal apparatus of the vertebrate embryo consists of paired pharyngeal arches, with endodermal pouches and corresponding ectodermal clefts between them (Graham and Smith 2001). In the mouse, the first of the pharyngeal arches begins to emerge at embryonic day 8.5 (E8.5), and the last develops by E10.5.

T. Okubo (✉)
Department of Laboratory Animal Science, Kitasato University School of Medicine, Kanagawa, Japan
e-mail: okubo@med.kitasato-u.ac.jp

H. Kondoh and A. Kuroiwa (eds.), *New Principles in Developmental Processes*,
DOI 10.1007/978-4-431-54634-4_8,

In fact, only four pairs of pharyngeal arches are clearly visible and the sixth (and last) is not easily distinguishable (Fig. 8.1a, b). The obvious segmental pattern is transient and is lost by E12.0.

During pharyngeal arch development the cell layer of the ingrowing ectodermal cleft approaches directly the pouch that grows out from the foregut endoderm. In higher vertebrates, the region of direct contact between the pouch and cleft remains intact, but in fishes the corresponding membrane ruptures for the development of the gill slits. In addition to the endodermal and ectodermal epithelia, each arch has distinct mesenchymal populations (Fig. 8.1c). One of these populations constitutes the mesenchymal core, which contains progenitor cells of cartilage and striated muscles. During pharyngeal arch segmentation, pharyngeal arch arteries (PAAs) are formed progressively between the aortic sac and the dorsal aorta (Fig. 8.1c, d). The development of the paired PAAs is important for the formation of the mature cardiovascular system.

8.2 Pharyngeal Arches and Arch-Derived Organogenesis

8.2.1 Contribution to the Cardiovascular System

Significantly, in higher vertebrates, PAAs undergo extensive changes during development, as is illustrated by the dynamic remodeling that takes place during the development of the five pairs of PAAs in the mouse embryo. PAA1–3 appear first by E9.5, and subsequently PAA4–6 are formed by E10.5; PAA1 and PAA2 then regress (Fig. 8.1d, e) (Kaufman 1992; Hiruma et al. 2002). The paired PAA3–6 are initially symmetrical but begin to undergo asymmetrical transformation at around E12.5. PAA3 forms the stem of the common and internal carotid arteries whereas the cranial part of the internal carotid arteries arises from the dorsal aorta. The part of the dorsal aorta between the third and fourth arches disappears bilaterally so that the flow of blood passing through PAA3 is directed toward the head. The left PAA4 contributes to the aortic arch, but the right one becomes the right subclavian artery. The sixth PAAs undergo asymmetrical remodeling; the left PAA6 gives rise to the ductus arteriosus (which connects the pulmonary trunk and dorsal aorta until birth), while the right PAA6 becomes thinner and gives rise to part of the right pulmonary artery. Thus, the left–right patterning of the PAAs is dramatically remodeled by a combination of asymmetrical persistence and regression.

8.2.2 The Cranial Neural Crest Cells That Give Rise to Multiple Tissues

Besides the mesodermal core and vasculature, another important cell type within the pharyngeal arches is the population of neural crest cells that migrates from the

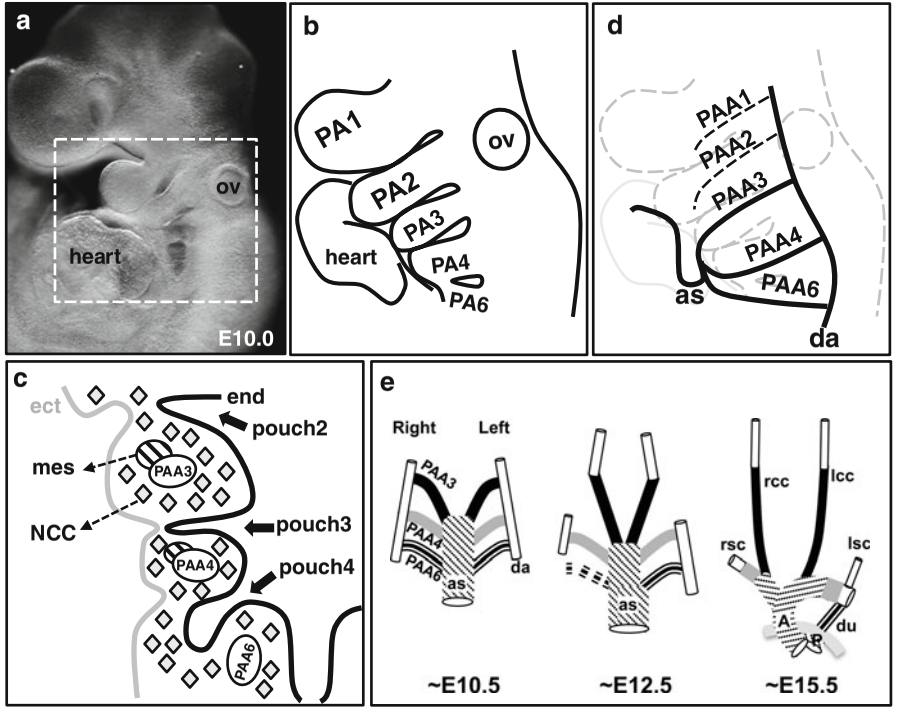

Fig. 8.1 Structure of the pharyngeal arches. **a** Whole-mount view of mouse embryo at embryonic day 10.0 (*E10.0*). *ov* otic vesicle. **b** Diagram of pharyngeal arch (PA). **c** Longitudinal section of pharyngeal arches. *ect* ectoderm, *end* endoderm, *mes* mesoderm, *NCC* neural crest cells. **d** Diagram of pharyngeal arch artery (PAA) pattern. *as* aortic sac, *da* dorsal aorta. **e** Schematic of the remodeling of the pharyngeal arch arteries. *A* aorta, *P* pulmonary trunk, *lcc* and *rcc* left and right common carotid arteries, *lsc* and *rsc* left and right subclavian arteries, *du* ductus arteriosus

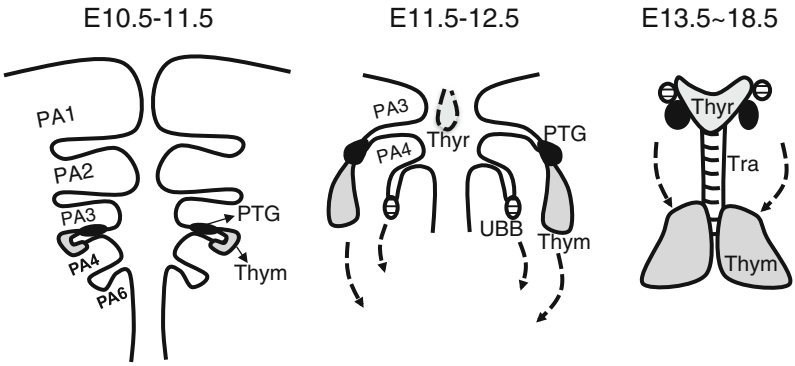

Fig. 8.2 Organ development from pharyngeal pouches. Rudiments of thymus (*Thym*) and parathyroid gland (*PTG*) arise in the third pharyngeal pouch at E10.5–11.5. Rudiment of the ultimobranchial body (*UBB*) arises in the fourth pouch at E11.5–12.5. PTG and UBB move toward the thyroid gland (*Thyr*), and the thymus migrates caudo-medially at E13.5–18.5. *Tra* trachea

dorsal neural tube (Fig. 8.1c) and later gives rise to a variety of differentiated tissues. The fate of the cranial neural crest cells in each arch is diverse. In particular, the subpopulations of cranial neural crest cells that originate from rhombomeres 6–8 emigrate into the third, fourth, and sixth pharyngeal arches, respectively, and contribute to the development of the cardiac outflow tract (Kirby and Waldo 1995; Jiang et al. 2000). A subpopulation of the neural crest cells also contributes to the embryonic thymic capsule and later perivascular cells in the thymus (Foster et al. 2008). Furthermore, pharyngeal arches contain bundles of cranial nerve axons. These cranial nerve axons originate from specific ganglia that are derived from neural crest cells and epibranchial placodes located in the caudo-dorsal region of pharyngeal pouches (Baker and Bronner-Fraser 2001).

8.2.3 Organ Development from Pharyngeal Pouches

The pharyngeal pouches are initially narrow slits, but they become stretched dorsally and ventrally along the pharyngeal cavity. The first pharyngeal pouch generates the tubotympanic recess, which will give rise to the middle ear system. The second pouch-derived tissue is poorly distinguished at early embryonic stages, but will become the palatine tonsil. The third pouch generates two important organs, namely, the parathyroid glands and the thymus from the dorsal and ventral pouches, respectively (Fig. 8.2). Additionally, the fourth pouch produces the ultimobranchial body (UBB), which functions as an endocrine organ for calcium homeostasis.

The rudiments of the parathyroid gland and thymus are clearly separated in the third pouch (Gordon and Manley 2011). These rudiments are composed of endodermal cells that invaginate into the mesenchyme of the pharyngeal arch. The thymus separates from the pharynx by E12.5, and as it grows T-lymphoid progenitor cell

immigration occurs. Finally, the thymus migrates caudo-medially into the superior mediastinum (upper heart) at E14.5 in the mouse (Fig. 8.2). The rudiment of the parathyroid gland and UBB are also pinched off from the third and fourth pouch endoderm, migrate caudally, and are finally incorporated into the thyroid gland (Fig. 8.2) (Kusakabe et al. 2006).

8.3 DiGeorge Syndrome Representing Developmental Defects of the Embryonic Pharyngeal System

8.3.1 Mutations in Tbx1 *Are Associated with DiGeorge Syndrome*

Defects in PAA patterning account for approximately 20 % of congenital cardiovascular malformations and are frequently observed in DiGeorge syndrome (also referred to as velocardiofacial syndrome; incidence, 1 in 3,000 live births). DiGeorge syndrome is most commonly associated with microdeletion of 22q11.2 (Kobrynski and Sullivan 2007; Scambler 2010). Frequent abnormalities include the absence or hypoplasia of thymus, malfunctioning parathyroid glands, and congenital heart defects. Most of these features have been ascribed to haploinsufficiency of TBX1, which is a member of the T-box transcription factor family (Baldini 2005). In the mouse, *Tbx1* is broadly expressed in the pharyngeal region, especially in the pharyngeal endoderm, mesoderm, and ectoderm, but not in the neural crest cells (Vitelli et al. 2002) (Fig. 8.3a). Mouse models, such as *Df1* heterozygotes, which have a deletion of the chromosomal region homologous to the human 22q11.2 deleted region and hence lacking the *Tbx1* gene, and *Tbx1* heterozygotes, recapitulate the major features of the human syndrome (Lindsay et al. 1999, 2001; Jerome and Papaioannou 2001; Merscher et al. 2001). Furthermore, *Tbx1* homozygous mutants show embryonic or perinatal lethality with much more severe phenotypes than heterozygous mutants. Their gross anatomical defects are persistent truncus arteriosus, complete absence of thymus and parathyroid glands, and craniofacial malformations. These defects are thought to result from the lack of distinct segmentation of the caudal pharyngeal arches (loss of PAA3–6 and the corresponding pouches; Fig. 8.4).

Previous studies have analyzed the tissue- and stage-specific requirements for *Tbx1* using cre-loxP-mediated conditional knockout mice (Xu et al. 2005). Mesodermal inactivation of *Tbx1* results in a similar phenotype to that of *Tbx1* homozygous mice with abnormal pharyngeal arch segmentation, severe thymus defects, and persistent truncus arteriosus (Zhang et al. 2006). Endodermal deletion of *Tbx1* also results in defects in the thymus, outflow tract, and pharyngeal arch segmentation (Arnold et al. 2006). These results suggest that *Tbx1* has tissue-specific indispensable functions in both endoderm and mesoderm.

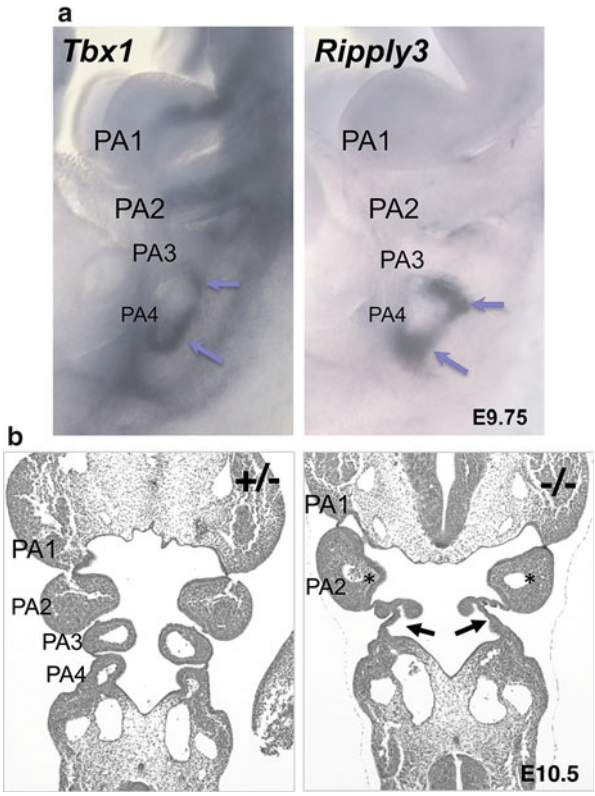

Fig. 8.3 *Ripply3* expression and the knockout phenotype. **a** Expression of *Tbx1* and *Ripply3* in mouse embryos at E9.75, as shown by in situ hybridization of transcripts. *Arrows* indicate third and fourth pouches. *PA1–4* pharyngeal arch from first to fourth. **b** Coronal section of *Ripply3 heterozygous* (+/−) and *homozygous* (−/−) mutant embryos. *Arrows* indicate hypoplastic PA3 and PA4 in *Ripply3*−/− mutant. *Asterisks* show persistent second pharyngeal arch arteries (*PAA2*)

Embryonic development in the mouse is also susceptible to variation in *Tbx1* expression levels. Analysis of compound mutants for members of a *Tbx1* allelic series showed that the specific phenotype is dependent on the dosage of *Tbx1* expression. For example, a level corresponding to about 40 % of wild type seems to be a threshold for the appearance of outflow defects and a transition from hypoplasia to aplasia of the thymus (Zhang and Baldini 2008). Overexpression of *Tbx1* also leads to defects in pharyngeal arch derivatives such as the thymus and outflow tracts (Merscher et al. 2001; Vitelli et al. 2009). These reports suggest that the dosage and timing of *Tbx1* expression are tightly controlled during pharyngeal arch development.

8.3.2 *Identification of a Novel Transcriptional Modulator for* Tbx1

Recently, products of a novel gene family, *Ripply*, were identified as potential transcriptional cofactors for T-box transcription factors in mouse, zebrafish, and *Xenopus* (Kawamura et al. 2005; Morimoto et al. 2007; Kondow et al. 2006; Okubo

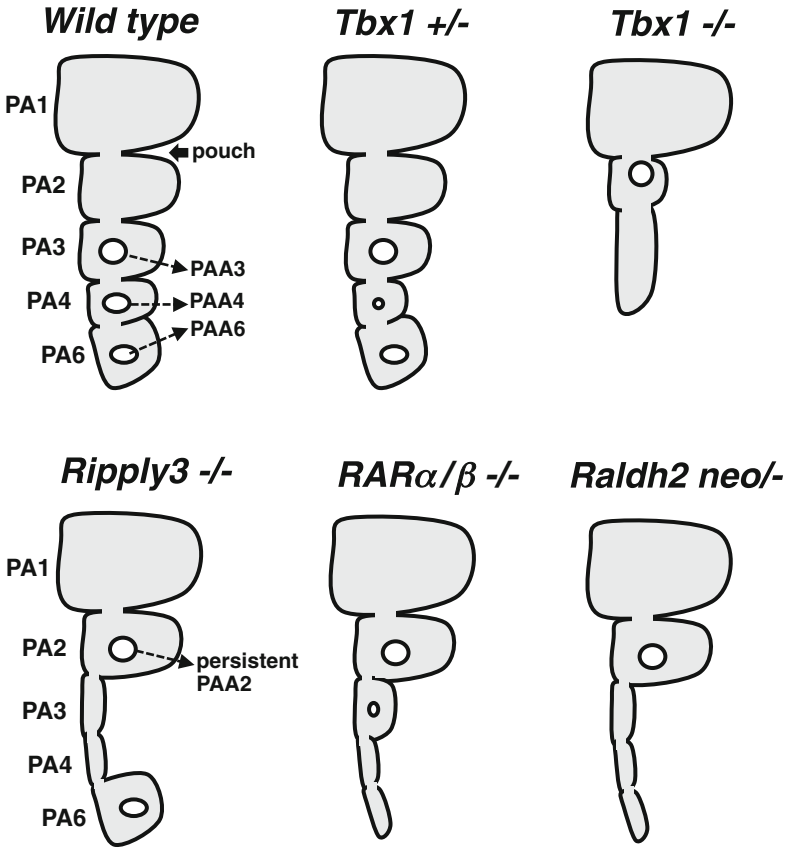

Fig. 8.4 Comparison of various pharyngeal arch phenotypes. Schematic of pharyngeal arch morphology at E10.5 in wild type, *Tbx1*+/–, *Tbx1*–/–, *Ripply3*–/–, *RARα/β*–/– (*double knockout*), and *Raldh2 neo*/– hypomorphic mutants or RA antagonist-treated embryo

et al. 2011). The *Ripply* gene family (*Ripply1*,*2*,*3*) appears to be well conserved among vertebrates, and a *Ripply*-related gene is also found in *Amphioxus* and sea anemones (Janesick et al. 2012). *Ripply1* and 2 are predominantly expressed in the presomatic mesoderm, where they are important for somite segmentation via modulation of T-box factors (Kawamura et al. 2005; Morimoto et al. 2007; Takahashi et al. 2010). In contrast to *Ripply1* and *-2*, *Ripply3* is strongly expressed in the developing pharyngeal arches (endoderm and ectoderm) in a pattern that partially overlaps with that of *Tbx1* (Fig. 8.3a) (Okubo et al. 2011). Biochemical studies suggest that Ripply3 directly interacts with Tbx1 protein as a transcriptional co-repressor and suppresses its transcriptional activity. Ripply proteins contain a highly conserved WRPW motif in the N-terminal and an FPVQ domain in the C-terminal. These motifs are thought to be important for interaction with Groucho/TLE family members and T-box transcription factors, respectively, allowing Ripply proteins to

bridge them (Fisher and Caudy 1998; Kawamura et al. 2005, 2008; Kondow et al. 2006; Okubo et al. 2011).

To investigate the function of *Ripply3*, mice deficient in the gene were generated and their phenotype was analyzed (Okubo et al. 2011). *Ripply3* homozygous mutants exhibit abnormal development of the caudal pharyngeal arches (third and fourth arches are severely hypoplastic and thin) (Fig. 8.3b). As a result, PAA3 and PAA4 are completely absent, neural crest migration is severely reduced, and cell death is increased. These defects in *Ripply3* homozygous mutants directly or indirectly cause abnormal development of the cardiovascular system, thymus, and parathyroid glands, such as failure in the separation of the thymus and parathyroid glands from the pharynx.

8.4 Retinoic Acid Signaling Pathways Involved in Pharyngeal Arch Development

8.4.1 Teratogenic Effects of Abnormal Retinoic Acid Levels on Pharyngeal Arch Development

Retinoic acid (RA), the active derivative of vitamin A, plays an important role in anterior–posterior axis patterning, morphogenesis, and organogenesis (Duester 2008) including, as discussed here, the development of the pharyngeal apparatus. The conditions of embryos with either excess or insufficient levels RA are strongly teratogenic, the most sensitive targets being the pharyngeal arches (Mark et al. 2004). Exposure to excess RA leads to fusion of the first and second pharyngeal arches, abnormal neural crest migration, and aberrant thymus development (Mulder et al. 1998; Matt et al. 2003).

Deficiency of RA also causes abnormalities in pharyngeal arch development. Various defects in the caudal pharyngeal arches are seen in mouse embryos with mutations in genes encoding components of the RA signaling pathway, such as *Retinaldehyde dehydrogenase2* (*Raldh2*) hypomorphs (Vermot et al. 2003), and *RA Receptor* (*RAR*)*α*/*β* double-knockout mutants (Dupe et al. 1999), as well as in mouse embryos treated with an RA antagonist (Wendling et al. 2000). Thus, when RA signaling is genetically or pharmacologically disturbed, the embryos exhibit very hypoplastic caudal pharyngeal arches and absence of the PAAs (Fig. 8.4), resulting in cardiac outflow abnormalities (Mark et al. 2004). Moreover, pharyngeal pouch-derived organs such as the thymus and parathyroid glands are absent or mislocalized in the cervical region (Mulder et al. 1998; Mark et al. 2004; Niederreither et al. 2003). Although maternal RA supplementation partially rescued the phenotype of *Raldh2* homozygous mutant embryos, it could not override the caudal pharyngeal arch defects (Niederreither et al. 1999, 2003). Exogenous RA probably does not fulfill the RA levels required for normal pharyngeal arch development. These results suggest that the caudal pharyngeal arches are highly sensitive to RA levels.

8.4.2 *Involvement of RA Signaling in a Tbx1/Ripply3 Genetic Network*

Given the similarity of the cardiac outflow and thymus defects seen in the RA-deficient phenotype and *Tbx1* mutants (Lindsay et al. 2001; Vermot et al. 2003), we speculate a functional interaction between RA signaling and the Tbx1 pathway. In fact, previous studies have also indicated that the RA signaling system and Tbx1 function are interdependent, mutually modulating the gene expression of the counterparts (Roberts et al. 2006). *Cyp26* genes, which are required for RA catabolism, are downregulated in *Tbx1* null mutants. Conversely, Cyp26 inhibitor treatment induces pharyngeal arch abnormalities in chick embryos with downregulation of *Tbx1* (Roberts et al. 2006), and *Cyp26B1* knockout mouse embryos display an abnormal caudal pharyngeal arch phenotype with upregulation of *Tbx1* and the development of an ectopic thymus (MacLean et al. 2009).

Recently, transcriptomic analysis revealed that *Ripply3* is likely to be a downstream of RA signaling in the *Xenopus* and mouse embryos (Janesick et al. 2012; Paschaki et al. 2013). Janesick et al. demonstrated that RA induces *Ripply3* in preplacodal ectoderm via RARα2. The gain- and loss-of-function studies of *Ripply3* revealed a regulatory gene network via modulation of *Tbx1*, and a negative feedback loop as a downstream factor of RA signaling, resulting in the alteration of preplacodal plate borders and epibranchial placode morphology in the pharyngeal arch region. Indeed, the *Ripply3* homozygous mutant also displays a phenotype reminiscent of RA deficiency, that is, hypoplasia of the third and fourth pharyngeal arches (Figs. 8.3 and 8.4) and abnormal development of the epibranchial placode (Okubo et al., unpublished data). Taken together, these findings suggest that Ripply3 play a critical role downstream of RA as a factor that modulates Tbx1 during the development of the caudal pharyngeal arches.

Although mentioned briefly in this chapter, *fibroblast growth factor 8* (*Fgf8*) is also highly expressed in the pharyngeal arch and anterior heart field (AHF), and the hypomorphic mutant mouse embryo of *Fgf8* displays a DiGeorge syndrome-like phenotype, such as defects of the caudal pharyngeal arch and abnormal cardiac outflow and thymus (Abu-Issa et al. 2002; Frank et al. 2002). However, *Fgf8* seems to be a possible candidate of Tbx1 downstream factor in AHF, but not in the pharyngeal arch (Hu et al. 2004). Therefore, regulation of *Fgf8* via RA/Tbx1/Ripply3 seen in pre-placodal plate (Janesick et al. 2012) may be dependent on the tissues.

8.5 Conclusion

Pharyngeal arch development is a dynamic process, involving a variety of genetic and signaling pathways and reciprocal interactions between cell populations from multiple germ layers. A major advance in the past decade has been the identification of animal models for the study of human congenital defects. Concerning DiGeorge

syndrome, mutations in the *Tbx1* gene cause severe abnormalities in pharyngeal arch development, which recapitulate many aspects of the human phenotype. Imbalance of RA signaling also has a deleterious impact on pharyngeal arch development. Both RA and Tbx1 have a narrow time window of action and tight threshold levels for their proper functions in pharyngeal arch development. Genetic analysis of the Tbx1 and RA signaling pathways indicates that Tbx1 cofactor Ripply3 provides a molecular link between RA signaling and Tbx1 actions. The discovery of the Tbx1/Ripply3/RA signaling network marks a large step toward the understanding of pharyngeal arch development, which has great relevance to congenital birth defects in humans.

References

Abu-Issa R, Smyth G, Smoak I, Yamamura K, Meyers EN (2002) Fgf8 is required for pharyngeal arch and cardiovascular development in the mouse. Development (Camb) 129(19):4613–4625

Arnold JS, Werling U, Braunstein EM, Liao J, Nowotschin S, Edelmann W, Hebert JM, Morrow BE (2006) Inactivation of Tbx1 in the pharyngeal endoderm results in 22q11DS malformations. Development (Camb) 133(5):977–987

Baker CV, Bronner-Fraser M (2001) Vertebrate cranial placodes. I. Embryonic induction. Dev Biol 232(1):1–61

Baldini A (2005) Dissecting contiguous gene defects: TBX1. Curr Opin Genet Dev 15(3): 279–284

Duester G (2008) Retinoic acid synthesis and signaling during early organogenesis. Cell 134(6): 921–931

Dupe V, Ghyselinck NB, Wendling O, Chambon P, Mark M (1999) Key roles of retinoic acid receptors alpha and beta in the patterning of the caudal hindbrain, pharyngeal arches and otocyst in the mouse. Development (Camb) 126(22):5051–5059

Fisher AL, Caudy M (1998) Groucho proteins: transcriptional corepressors for specific subsets of DNA-binding transcription factors in vertebrates and invertebrates. Genes Dev 12(13):1931–1940

Foster K, Sheridan J, Veiga-Fernandes H, Roderick K, Pachnis V, Adams R, Blackburn C, Kioussis D, Coles M (2008) Contribution of neural crest-derived cells in the embryonic and adult thymus. J Immunol 180(5):3183–3189

Frank DU, Fotheringham LK, Brewer JA, Muglia LJ, Tristani-Firouzi M, Capecchi MR, Moon AM (2002) An Fgf8 mouse mutant phenocopies human 22q11 deletion syndrome. Development (Camb) 129(19):4591–4603

Gordon J, Manley NR (2011) Mechanisms of thymus organogenesis and morphogenesis. Development (Camb) 138(18):3865–3878

Graham A, Smith A (2001) Patterning the pharyngeal arches. Bioessays 23(1):54–61

Hiruma T, Nakajima Y, Nakamura H (2002) Development of pharyngeal arch arteries in early mouse embryo. J Anat 201(1):15–29

Hu T, Yamagishi H, Maeda J, McAnally J, Yamagishi C, Srivastava D (2004) Tbx1 regulates fibroblast growth factors in the anterior heart field through a reinforcing autoregulatory loop involving forkhead transcription factors. Development (Camb) 131(21):5491–5502

Janesick A, Shiotsugu J, Taketani M, Blumberg B (2012) RIPPLY3 is a retinoic acid-inducible repressor required for setting the borders of the pre-placodal ectoderm. Development (Camb) 139(6):1213–1224

Jerome LA, Papaioannou VE (2001) DiGeorge syndrome phenotype in mice mutant for the T-box gene, Tbx1. Nat Genet 27(3):286–291

Jiang X, Rowitch DH, Soriano P, McMahon AP, Sucov HM (2000) Fate of the mammalian cardiac neural crest. Development (Camb) 127(8):1607–1616

Kaufman MH (1992) The atlas of mouse development. Academic, London, pp 131–133

Kawamura A, Koshida S, Hijikata H, Ohbayashi A, Kondoh H, Takada S (2005) Groucho-associated transcriptional repressor ripply1 is required for proper transition from the presomitic mesoderm to somites. Dev Cell 9(6):735–744

Kawamura A, Koshida S, Takada S (2008) Activator-to-repressor conversion of T-box transcription factors by the Ripply family of Groucho/TLE-associated mediators. Mol Cell Biol 28(10): 3236–3244

Kirby ML, Waldo KL (1995) Neural crest and cardiovascular patterning. Circ Res 77(2):211–215

Kobrynski LJ, Sullivan KE (2007) Velocardiofacial syndrome, DiGeorge syndrome: the chromosome 22q11.2 deletion syndromes. Lancet 370(9596):1443–1452

Kondow A, Hitachi K, Ikegame T, Asashima M (2006) Bowline, a novel protein localized to the presomitic mesoderm, interacts with Groucho/TLE in *Xenopus*. Int J Dev Biol 50(5):473–479

Kusakabe T, Hoshi N, Kimura S (2006) Origin of the ultimobranchial body cyst: T/ebp/Nkx2.1 expression is required for development and fusion of the ultimobranchial body to the thyroid. Dev Dyn 235(5):1300–1309

Lindsay EA, Botta A, Jurecic V, Carattini-Rivera S, Cheah YC, Rosenblatt HM, Bradley A, Baldini A (1999) Congenital heart disease in mice deficient for the DiGeorge syndrome region. Nature (Lond) 401(6751):379–383

Lindsay EA, Vitelli F, Su H, Morishima M, Huynh T, Pramparo T, Jurecic V, Ogunrinu G, Sutherland HF, Scambler PJ, Bradley A, Baldini A (2001) Tbx1 haploinsufficieny in the DiGeorge syndrome region causes aortic arch defects in mice. Nature (Lond) 410(6824):97–101

Maclean G, Dolle P, Petkovich M (2009) Genetic disruption of CYP26B1 severely affects development of neural crest derived head structures, but does not compromise hindbrain patterning. Dev Dyn 238(3):732–745

Mark M, Ghyselinck NB, Chambon P (2004) Retinoic acid signalling in the development of branchial arches. Curr Opin Genet Dev 14(5):591–598

Matt N, Ghyselinck NB, Wendling O, Chambon P, Mark M (2003) Retinoic acid-induced developmental defects are mediated by RARbeta/RXR heterodimers in the pharyngeal endoderm. Development (Camb) 130(10):2083–2093

Merscher S, Funke B, Epstein JA, Heyer J, Puech A, Lu MM, Xavier RJ, Demay MB, Russell RG, Factor S, Tokooya K, Jore BS, Lopez M, Pandita RK, Lia M, Carrion D, Xu H, Schorle H, Kobler JB, Scambler P, Wynshaw-Boris A, Skoultchi AI, Morrow BE, Kucherlapati R (2001) TBX1 is responsible for cardiovascular defects in velo-cardio-facial/DiGeorge syndrome. Cell 104(4):619–629

Morimoto M, Sasaki N, Oginuma M, Kiso M, Igarashi K, Aizaki K, Kanno J, Saga Y (2007) The negative regulation of Mesp2 by mouse Ripply2 is required to establish the rostro-caudal patterning within a somite. Development (Camb) 134(8):1561–1569

Mulder GB, Manley N, Maggio-Price L (1998) Retinoic acid-induced thymic abnormalities in the mouse are associated with altered pharyngeal morphology, thymocyte maturation defects, and altered expression of Hoxa3 and Pax1. Teratology 58(6):263–275

Niederreither K, Subbarayan V, Dolle P, Chambon P (1999) Embryonic retinoic acid synthesis is essential for early mouse post-implantation development. Nat Genet 21(4):444–448

Niederreither K, Vermot J, Le Roux I, Schuhbaur B, Chambon P, Dolle P (2003) The regional pattern of retinoic acid synthesis by RALDH2 is essential for the development of posterior pharyngeal arches and the enteric nervous system. Development (Camb) 130(11):2525–2534

Okubo T, Kawamura A, Takahashi J, Yagi H, Morishima M, Matsuoka R, Takada S (2011) Ripply3, a Tbx1 repressor, is required for development of the pharyngeal apparatus and its derivatives in mice. Development (Camb) 138(2):339–348

Paschaki M, Schneider C, Rhinn M, Thibault-Carpentier C, Dembele D, Niederreither K, Dolle P (2013) Transcriptomic analysis of murine embryos lacking endogenous retinoic acid signaling. PLoS ONE 8(4):e62274

Roberts C, Ivins S, Cook AC, Baldini A, Scambler PJ (2006) Cyp26 genes a1, b1, and c1 are down-regulated in Tbx1 null mice and inhibition of Cyp26 enzyme function produces a phenocopy of DiGeorge syndrome in the chick. Hum Mol Genet 15(23):3394–3410

Scambler PJ (2010) 22q11 deletion syndrome: a role for TBX1 in pharyngeal and cardiovascular development. Pediatr Cardiol 31(3):378–390

Takahashi J, Ohbayashi A, Oginuma M, Saito D, Mochizuki A, Saga Y, Takada S (2010) Analysis of Ripply1/2-deficient mouse embryos reveals a mechanism underlying the rostro-caudal patterning within a somite. Dev Biol 342(2):134–145

Vermot J, Niederreither K, Garnier JM, Chambon P, Dolle P (2003) Decreased embryonic retinoic acid synthesis results in a DiGeorge syndrome phenotype in newborn mice. Proc Natl Acad Sci USA 100(4):1763–1768

Vitelli F, Morishima M, Taddei I, Lindsay EA, Baldini A (2002) Tbx1 mutation causes multiple cardiovascular defects and disrupts neural crest and cranial nerve migratory pathways. Hum Mol Genet 11(8):915–922

Vitelli F, Huynh T, Baldini A (2009) Gain of function of Tbx1 affects pharyngeal and heart development in the mouse. Genesis 47(3):188–195

Wendling O, Dennefeld C, Chambon P, Mark M (2000) Retinoid signaling is essential for patterning the endoderm of the third and fourth pharyngeal arches. Development (Camb) 127(8): 1553–1562

Xu H, Cerrato F, Baldini A (2005) Timed mutation and cell-fate mapping reveal reiterated roles of Tbx1 during embryogenesis, and a crucial function during segmentation of the pharyngeal system via regulation of endoderm expansion. Development (Camb) 132(19):4387–4395

Zhang Z, Baldini A (2008) In vivo response to high-resolution variation of Tbx1 mRNA dosage. Hum Mol Genet 17(1):150–157

Zhang Z, Huynh T, Baldini A (2006) Mesodermal expression of Tbx1 is necessary and sufficient for pharyngeal arch and cardiac outflow tract development. Development (Camb) 133(18): 3587–3595

Part III
Cells in a Community of Reorganizing Tissues

Chapter 9
Interaction of Epithelial Cells and Basement Membrane in the Regulation of EMT Exemplified in Chicken Embryo Gastrulation

Yukiko Nakaya

Abstract Epithelial–mesenchymal transition (EMT) is a process in which epithelial cells are converted into mesenchymal cells. It plays crucial roles in the formation of complex organs and in tissue repair during animal development. After EMT, cells acquire migratory and invasive properties, which can contribute to organ fibrosis and cancer metastasis. However, the precise cellular mechanisms that govern EMT in various in vivo contexts are poorly understood. Gastrulation is a process through which the three embryonic germ layers are formed. During this process, epithelial cells in the epiblast layer dynamically change their shape and ingress through the primitive streak to become mesoderm or endoderm. EMT occurs during this gastrulation process, and in this chapter, I describe the key principles of EMT and characterize EMT in the primitive streak during chicken gastrulation. Gastrulation EMT is a multistep process that includes the dissociation of cell–cell contact, the loss of epithelial polarity, and the degradation of the basement membrane (BM). Our recent studies indicate that epiblast/BM interaction requires basally localized RhoA activity, and CLASP- and dystroglycan-mediated cortical microtubule anchoring, the disruption of which causes BM degradation during gastrulation EMT.

Keywords BM degradation • Chicken • EMT • Gastrulation • Microtubules

9.1 Introduction

Epithelial–mesenchymal transition (EMT) and mesenchymal–epithelial transition (MET) (Fig. 9.1) play pivotal roles in the tissue rearrangement involved in organ formation during embryogenesis. EMT also occurs when tumor cells metastasize and invade other tissues; after metastasis, tumors colonize foreign tissue via MET.

Y. Nakaya (✉)
Lab for Early Embryogenesis, RIKEN Center for Developmental Biology, Kobe, Japan
e-mail: nakaya@cdb.riken.jp

H. Kondoh and A. Kuroiwa (eds.), *New Principles in Developmental Processes*,
DOI 10.1007/978-4-431-54634-4_9,

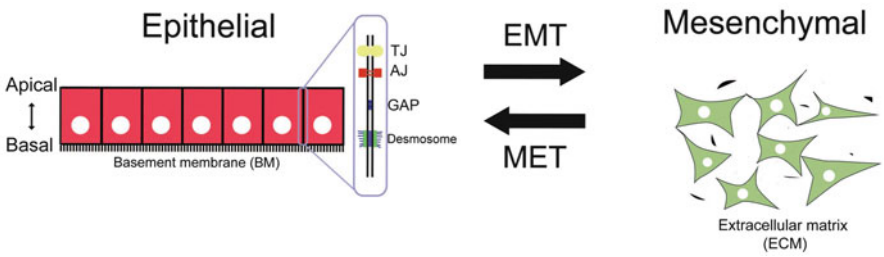

Fig. 9.1 Morphology of epithelial and mesenchymal cells. Structural features that distinguish epithelial and mesenchymal cells. Epithelial cells have apico-basal polarity, show tight cell–cell connections, and are also in contact with the basement membrane (*BM*). Mesenchymal cells have irregular shapes, are loosely connected with surrounding cells, and show high motility in the extracellular matrix (*ECM*). *EMT* epithelial–mesenchymal transition, *MET* mesenchymal–epithelial transition

Because of the importance of EMT in both development and disease, much effort has been made to clarify the initiation cues and transcriptional regulation of EMT (De Craene and Berx 2013; Thiery et al. 2009; Lim and Thiery 2012; Hugo et al. 2007; Acloque et al. 2009; Lopez-Novoa and Nieto 2009; Nakaya and Sheng 2013). However, the precise molecular mechanisms that control the cellular aspects of EMT are not fully understood.

Gastrulation involves large-scale tissue rearrangement including active cell division, extensive cell shape changes, and cell movements to generate the three embryonic germ layers (Chuai et al. 2012; Nakaya and Sheng 2008, 2009; Rohde and Heisenberg 2007; Solnica-Krezel and Sepich 2012). The discovery of EMT in the primitive streak of chicken embryos during gastrulation (Hay 1968) has led to chicken embryos becoming a paradigmatic model of EMT. Gastrulation EMT in the chicken embryo includes a sequence of cellular events such as the disruption of cell–cell adhesion and cell–basement membrane (BM) interaction, the loss of apico-basal polarity, and the reorganization of cytoskeletal proteins, which have all been considered important steps of EMT (Acloque et al. 2009; Hay 1968; Shook and Keller 2003; Nakaya and Sheng 2008, 2009). Here, I briefly characterize EMT/MET and then describe the molecular mechanisms by which cell–BM interaction is regulated during chicken gastrulation.

9.2 The Differences of Epithelial and Mesenchymal Tissues

Cells in an embryo or an organ can be grouped into two types: epithelial and mesenchymal cells. The monolayered epithelial cells have a columnar cell shape and sit on a thin layer of extracellular matrix, the BM (Fig. 9.1). The plasma membrane of epithelial cells consists of three different domains: the apical, the lateral, and the

basal domains. The lateral domain is equipped with components of tight junctions, adherens junctions, gap junctions, and desmosomes, all of which are involved in cell–cell interactions (Fig. 9.1). In contrast, the basal domain mediates attachment of cells to the underlying BM. As these different domains are being established, the membrane proteins are sorted to the apical or basal–lateral membrane domains, resulting in an apico-basal polarization of cells (Schoenenberger and Matlin 1991; Yeaman et al. 1999; Cao et al. 2012).

Mesenchymal cells generally have greater morphological irregularity and higher motility than epithelial cells. They can migrate individually in the extracellular matrix (ECM) (Fig. 9.1). Mesenchymal cells are more elongated than epithelial cells, have a fibroblastic appearance with processes, front end–back end polarity, and invasive motility (Hay 1968, 2005). The origin of mesenchymal cells is often the epithelium, from which cells exit from the BM into the ECM. They lose their apical, lateral, and basal specializations that characterize their parent epithelia. Instead, they form tight contacts between adjacent cells through newly formed processes (England and Wakely 1977; Hay 1968). Mesenchymal cells are mostly derived from mesodermal cells, but some of them originate from the ectoderm layer (e.g., neural crest cells).

9.3 EMT and MET Are Reversible and Important in Organogenesis

Morphological changes of epithelial and/or mesenchymal cells, or a transition between these cell types, are crucial for tissue morphogenesis (Acloque et al. 2009; Shook and Keller 2003; Thiery et al. 2009). The primary EMT is observed during metazoan gastrulation. Mesoderm cells are derived from the epiblast by EMT during gastrulation and are distributed along the entire mediolateral axis of the embryo. These cells then undergo MET, giving rise to transient epithelia that form the notochord, somites, nephritic ducts, splanchnic, and somatic mesoderm. In particular, the somites, balls of epithelial cells, subsequently go through another EMT transition to form the sclerotome, a precursor to the vertebrae (Nakaya et al. 2004; Takahashi et al. 2005), providing an example of how the recurrent EMT/MET process are during organogenesis.

9.4 EMT During Chicken Embryo Gastrulation

At stage 4 (gastrulation stage; full-grown primitive streak), the chicken embryo is shaped as a flat disk, with mesodermal and endodermal cells in the process of being internalized underneath the epiblast layer (Fig. 9.2). During gastrulation, the epiblast cells become competent to respond to EMT-inducing signals, and migrate from the lateral side to the primitive streak, which is supported by the BM (Lawson

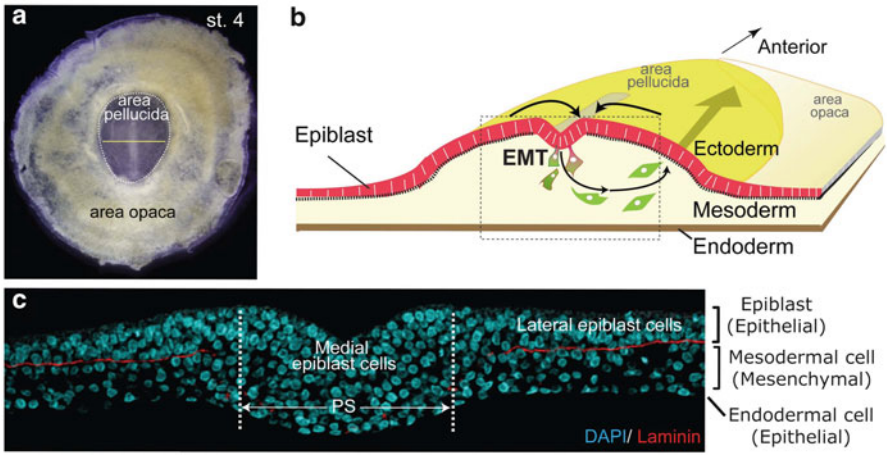

Fig. 9.2 Chicken gastrulation. **a** Isolated stage 4 chick embryo. **b** A schematic schematic diagram of its transverse section. Lateral epiblast cells move toward the primitive streak and undergo EMT to become mesoderm cells. These mesodermal cells then move over a large distance to reach their destination. **c** Transverse section at mid-streak level

and Schoenwolf 2001; Bortier et al. 2001; Hardy et al. 2011) (Fig. 9.2b). They assume a pseudostratified columnar epithelial shape and maintain an apical-basal polarity. Shortly after entering the streak, they become progressively elongated and flask formed, and lose their interaction with BM, while maintaining both tight junctions and adherens junctions (Solursh and Revel 1978; Shook and Keller 2003; Wakely and England 1977). Next, the cells immediately lose their tight junction and the epithelial polarity, undergoing transition from epithelial to mesenchymal cells. This transition, EMT, promotes the ability of cells to migrate away from the streak in the space between the epiblast and the endoderm to form mesoderm (Fig. 9.2b). This progression of the EMT process is paralleled by the change in expression of various proteins. For example, E-cadherin expression observed in the epiblast and nascent mesoderm cells is gradually replaced by N-cadherin expression characterizing mesenchymal mesoderm cells (Fig. 9.3a, c). ZO1, a component of the tight junction, is present in all epiblast cells but is lost in mesoderm cells (Fig. 9.3b), reflecting the absence of tight junction in the mesenchymal cells. Vimentin and snail2, which are commonly expressed in mesenchymal mesoderm cells, are already expressed in the lateral epiblast cells before undergoing EMT, being localized in the basal membrane and nucleus, respectively (Fig. 9.3d, e). Laminin, a BM component, is continuous underneath the lateral epiblast cells, but is fragmented underneath the medial epiblast cells (Fig. 9.3b, e). Thus, EMT during gastrulation in chicken embryo involves multiple cellular events. It is important to note that BM breakdown occurs earlier than the loss of E-cadherin-mediated cell–cell adhesion.

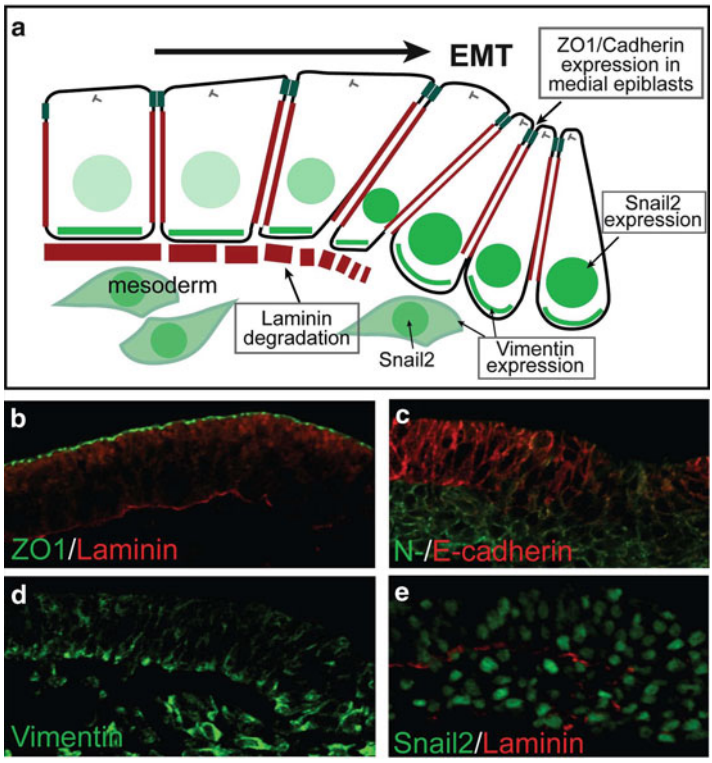

Fig. 9.3 Changes in the distribution of molecules involved in cell–cell contact and EMT. Transverse section of stage 4 embryo at mid-streak level: schematic diagram (**a**); ZO1 (*green*) and laminin (*red*) (**b**); E-cadherin (*red*) and N-cadherin (*green*) (**c**); vimentin (**d**); and Snail2 (*green*) and laminin (*red*) (**e**)

9.5 RhoA Signaling Is Involved in BM Integrity During Gastrulation EMT

BM degradation before EMT-dependent mesoderm formation in chick embryos has been noted (Hay 1968), but the molecular mechanism underlying this process has not been systematically investigated. Small GTPase RhoA is known to regulate the actin and microtubule cytoskeletons that control cell shape and motility and which are also involved in the EMT process (Jaffe and Hall 2005; Ozdamar et al. 2005; Van Aelst and Symons 2002). Indeed, activation of RhoA during gastrulation in mouse embryos results in the suppression of EMT and the failure of mesoderm formation (Fuse et al. 2004). In my study, where RhoA was overexpressed in the medial epiblast cells of gastrulating chicken embryos, laminin expression was maintained in the gastrulating cells, causing mesodermal cell clumps that interfered

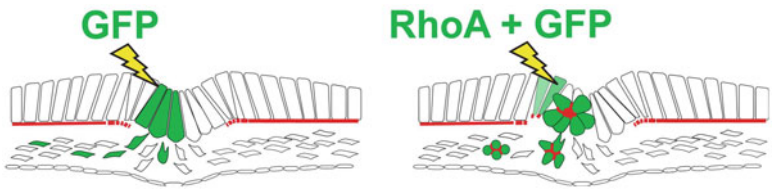

Fig. 9.4 RhoA mis-expression causes EMT defects. *Left:* Electroporation of green fluorescent protein (*GFP*) alone does not affect laminin expression. *Right*: *RhoA* overexpression in the cells on top of the primitive streak causes laminin retention in these cells during EMT

with cell migration as mesoderm (Fig. 9.4). This observation suggests that RhoA function is involved in laminin expression during EMT. A strict basal membrane localization of RhoA-specific GEF (guanine nucleotide-exchanging factor), Net1, was observed in the lateral epiblast cells before EMT, but not in the medial epiblast cells undergoing EMT, suggesting that Net1-dependent activation of RhoA activity at the basal side promotes laminin expression and perhaps secretion. To confirm this, RhoA or Net1 were knocked down, resulting in premature BM breakdown in the lateral epiblast cells. These observations indicate that RhoA activation via Net1 is essential to maintain the BM, which interacts with epiblast cells. The breakdown of BM is mediated by the loss of basally localized Net1 and RhoA activity in the medial epiblast cells, which leads to EMT, causing gastrulation (Fig. 9.6) (Nakaya and Sheng 2008, 2009; Nakaya et al. 2008).

9.6 Changes in Microtubule Organization Are Associated with BM Regulation During Gastrulation EMT

In the fully polarized epithelial cells, microtubules are organized longitudinally along the apico-basal axis with their plus ends oriented basally (Akhmanova et al. 2009; Bacallao et al. 1989; Yeaman et al. 1999; Mimori-Kiyosue 2011). This microtubule organization is also observed in the epiblast cells of gastrulation-stage embryos. However, in the epiblast cells immediately lateral to the primitive streak, there are fewer microtubules in their basal regions, and when these epiblast cells enter the primitive streak, they lose their microtubules in their basal regions (Fig. 9.6) (Nakaya et al. 2008; Nakaya and Sheng 2009). Interestingly, there appears to be a correlation between the timing of the microtubule loss from the basal cortex and the degradation of BM, suggesting that the integrity of the BM is affected by the interaction of microtubules with the basal region. Recently we showed that CLASP (a microtubule plus-end tracking protein) and its binding partner LL5 have a role in anchoring microtubules at the basal cortex of epiblast cells, and that downregulation of CLASP and LL5 causes BM breakdown, which initiates EMT (Fig. 9.6) (Nakaya et al. 2013).

9.7 Dystroglycan Is a Cyto-Linker Connecting the Basal Cell Membrane and BM

From a screen for genes expressed in tissues centered by the primitive streak at stage 4, integrins and dystroglycan were identified as molecules that connect the basal membrane of the epiblast to the BM (Alev et al. 2010; Nakaya et al. 2011). α6 and β1 integrins and dystroglycan are expressed and localized in the basolateral membrane of lateral epiblast cells. However, their basal membrane localization is lost when epiblast cells enter primitive streak. The loss of those proteins from the basal membrane parallels the loss of laminin in the BM that precedes EMT (Nakaya et al. 2008, 2011). These membrane proteins are also known to interact with F-actin and microtubules, and disruption of these cytoskeleton components alters their subcellular localization. When microtubules were disrupted by nocodazole, basal membrane localization of dystroglycan was lost, concomitant with the occurrence of BM breakdown (Fig. 9.5). By contrast, when F-actin was depolymerized by using cytochalacin D, localization of β-dystroglycan in the lateral membrane of lateral epiblast was reduced without affecting its localization in the basal membrane (see Fig. 9.5). These observations indicate that basal membrane localization of β-dystroglycan depends primarily on microtubule organization (Fig. 9.6) (Nakaya

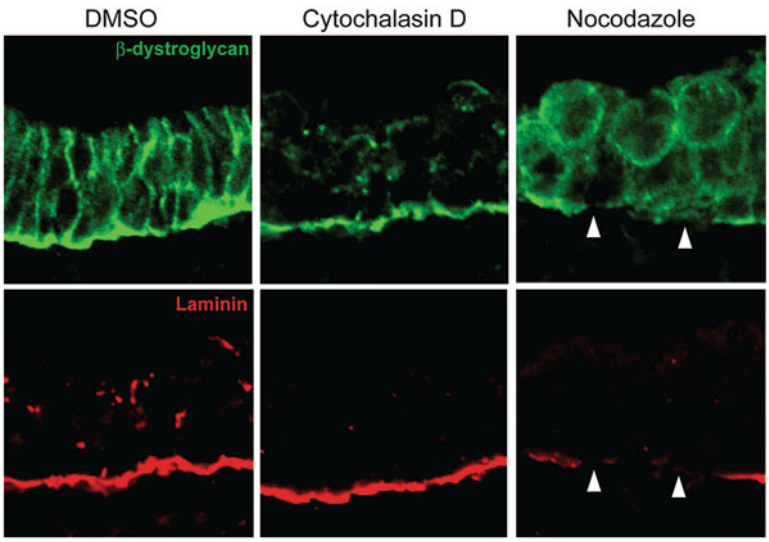

Fig. 9.5 Effect of cytochalasin D and nocodazole on β-dystroglycan localization. All data show lateral epiblast cells. *Left*: In control treatment with DMSO, β-dystroglycan was expressed in the basolateral membrane of cells. *Middle:* Cytochalasin D-treated embryos showed reduced β-dystroglycan expression in lateral membrane, without affecting its localization in basal membrane. *Right:* Nocodazole treatment caused loss of basally localized β-dystroglycan in the epiblast cells, concomitant with the breakdown of underlying laminin (*arrowheads*)

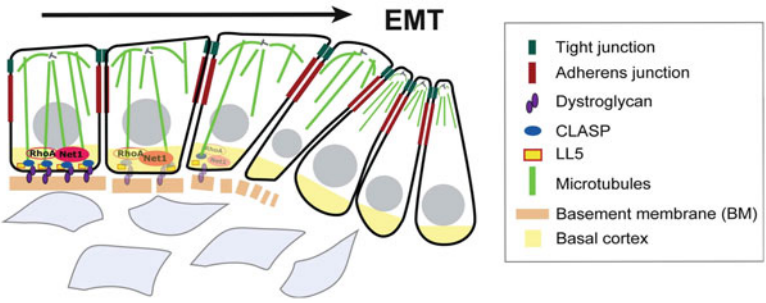

Fig. 9.6 Multiple steps of EMT during chicken embryo gastrulation

et al. 2011). In addition, this basal β-dystroglycan expression has recently been shown to be regulated by CLASP, and there is a physical association between CLASP and β-dystroglycan in epiblast cells before undergoing gastrulation EMT (Nakaya et al. 2013).

9.8 The Nature of Epithelium and EMT Potential

Although EMT occurs at multiple steps of embryonic development, not all epithelial cells have the potential to undergo EMT. For instance, the gastrulating chicken embryo consists of two regions: the area pellucida and the area opaca (Fig. 9.2a, b). In area pellucida, epiblast cells are of columnar epithelium and undergo EMT when they move to the primitive streak. In contrast, the cells in the area opaca are of squamous epithelium and never undergo EMT. Disruption of the microtubules by nocodazole treatment leads to BM breakdown in the epiblast of the area pellucida (Fig. 9.5), whereas the BM remains intact after nocodazole treatment in the area opaca (Nakaya, unpublished data). This result suggests that microtubule organization, distribution, or numbers could be relevant to the potentiality of EMT.

9.9 Significance of Research on Gastrulation EMT

In this chapter, I have described our new findings that the microtubule-dependent establishment of the basal cell membrane affects the integrity of the underlying BM, which is dependent on RhoA activity and the CLASP–dystroglycan complex. Further studies on the underlying molecular mechanisms of BM integrity or its degradation, such as the contribution of some enzymes, will help reveal how EMT processes are regulated.

EMT plays a role in various events during development, in progression of diseases, and in acquisition of stem cell-like characters (Mani et al. 2008; Polyak and Weinberg 2009; Thiery et al. 2009; Lim and Thiery 2012), indicating that EMT/MET is more than a simple morphological phenomenon. The dynamic developmental setting for gastrulation in the chicken not only will reveal the biological context of EMT but will also provide a better understanding of the cellular response of the disease, which is important to design advanced therapies.

Acknowledgments This study was carried out in the laboratory of Dr. Guojun Sheng at RIKEN CDB. I thank Ms. Erike W. Sukowati for supporting most of the experiments and also thank Ms. Hazuki Hiraga and Dr. Guojun Sheng for corrections and critical comments on the manuscript.

References

Acloque H, Adams MS, Fishwick K, Bronner-Fraser M, Nieto MA (2009) Epithelial–mesenchymal transitions: the importance of changing cell state in development and disease. J Clin Invest 119(6):1438–1449. doi:10.1172/JCI38019, pii: 38019

Akhmanova A, Stehbens SJ, Yap AS (2009) Touch, grasp, deliver and control: functional cross-talk between microtubules and cell adhesions. Traffic 10(3):268–274. doi:10.1111/j.1600-0854.2008.00869.x, pii: TRA869

Alev C, Wu Y, Kasukawa T, Jakt LM, Ueda HR, Sheng G (2010) Transcriptomic landscape of the primitive streak. Development (Camb) 137(17):2863–2874. doi:10.1242/dev.053462, pii: dev.053462

Bacallao R, Antony C, Dotti C, Karsenti E, Stelzer EH, Simons K (1989) The subcellular organization of Madin-Darby canine kidney cells during the formation of a polarized epithelium. J Cell Biol 109(6 Pt 1):2817–2832

Bortier H, Callebaut M, van Nueten E, Vakaet L (2001) Autoradiographic evidence for the sliding of the upper layer over the basement membrane in chicken blastoderms during gastrulation. Eur J Morphol 39(2):91–98

Cao X, Surma MA, Simons K (2012) Polarized sorting and trafficking in epithelial cells. Cell Res 22(5):793–805. doi:10.1038/cr.2012.64, pii: cr201264

Chuai M, Hughes D, Weijer CJ (2012) Collective epithelial and mesenchymal cell migration during gastrulation. Curr Genomics 13(4):267–277. doi:10.2174/138920212800793357, pii: CG-13-267

De Craene B, Berx G (2013) Regulatory networks defining EMT during cancer initiation and progression. Nat Rev Cancer 13(2):97–110. doi:10.1038/nrc3447, pii: nrc3447

England MA, Wakely J (1977) Scanning electron microscopy of the development of the mesoderm layer in chick embryos. Anat Embryol (Berl) 150(3):291–300

Fuse T, Kanai Y, Kanai-Azuma M, Suzuki M, Nakamura K, Mori H, Hayashi Y, Mishina M (2004) Conditional activation of RhoA suppresses the epithelial to mesenchymal transition at the primitive streak during mouse gastrulation. Biochem Biophys Res Commun 318(3):665–672. doi:10.1016/j.bbrc.2004.04.076, pii: S0006291X04007934

Hardy KM, Yatskievych TA, Konieczka J, Bobbs AS, Antin PB (2011) FGF signalling through RAS/MAPK and PI3K pathways regulates cell movement and gene expression in the chicken primitive streak without affecting E-cadherin expression. BMC Dev Biol 11:20. doi:10.1186/1471-213X-11-20, pii: 1471-213X-11-20

Hay ED (1968) Organization and fine structure of epithelium and mesenchyme in the developing chick embryo. In: Epithelial–mesenchymal interactions. 18th Hahnemann symposium. Williams & Wilkins, Baltimore

Hay ED (2005) The mesenchymal cell, its role in the embryo, and the remarkable signaling mechanisms that create it. Dev Dyn 233(3):706–720. doi:10.1002/dvdy.20345

Hugo H, Ackland ML, Blick T, Lawrence MG, Clements JA, Williams ED, Thompson EW (2007) Epithelial–mesenchymal and mesenchymal–epithelial transitions in carcinoma progression. J Cell Physiol 213(2):374–383. doi:10.1002/jcp.21223

Jaffe AB, Hall A (2005) Rho GTPases: biochemistry and biology. Annu Rev Cell Dev Biol 21:247–269. doi:10.1146/annurev.cellbio.21.020604.150721

Lawson A, Schoenwolf GC (2001) Cell populations and morphogenetic movements underlying formation of the avian primitive streak and organizer. Genesis 29(4):188–195. doi:10.1002/gene.1023

Lim J, Thiery JP (2012) Epithelial–mesenchymal transitions: insights from development. Development (Camb) 139(19):3471–3486. doi:10.1242/dev.071209, pii: 139/19/3471

Lopez-Novoa JM, Nieto MA (2009) Inflammation and EMT: an alliance towards organ fibrosis and cancer progression. EMBO Mol Med 1(6–7):303–314. doi:10.1002/emmm.200900043

Mani SA, Guo W, Liao MJ, Eaton EN, Ayyanan A, Zhou AY, Brooks M, Reinhard F, Zhang CC, Shipitsin M, Campbell LL, Polyak K, Brisken C, Yang J, Weinberg RA (2008) The epithelial–mesenchymal transition generates cells with properties of stem cells. Cell 133(4):704–715. doi:10.1016/j.cell.2008.03.027, pii: S0092-8674(08)00444-3

Mimori-Kiyosue Y (2011) Shaping microtubules into diverse patterns: molecular connections for setting up both ends. Cytoskeleton (Hoboken) 68(11):603–618. doi:10.1002/cm.20540

Nakaya Y, Sheng G (2008) Epithelial to mesenchymal transition during gastrulation: an embryological view. Dev Growth Differ 50(9):755–766. doi:10.1111/j.1440-169X.2008.01070.x, pii: DGD1070

Nakaya Y, Sheng G (2009) An amicable separation: chick's way of doing EMT. Cell Adh Migr 3(2):160–163, pii: 7373

Nakaya Y, Sheng G (2013) EMT in developmental morphogenesis. Cancer Lett. doi:10.1016/j.canlet.2013.02.037; pii: S0304-3835(13)00163-8

Nakaya Y, Kuroda S, Katagiri YT, Kaibuchi K, Takahashi Y (2004) Mesenchymal–epithelial transition during somitic segmentation is regulated by differential roles of Cdc42 and Rac1. Dev Cell 7(3):425–438. doi:10.1016/j.devcel.2004.08.003, pii: S1534580704002783

Nakaya Y, Sukowati EW, Wu Y, Sheng G (2008) RhoA and microtubule dynamics control cell-basement membrane interaction in EMT during gastrulation. Nat Cell Biol 10(7):765–775. doi:10.1038/ncb1739, pii: ncb1739

Nakaya Y, Sukowati EW, Alev C, Nakazawa F, Sheng G (2011) Involvement of dystroglycan in epithelial–mesenchymal transition during chick gastrulation. Cells Tissues Organs 193 (1–2):64–73. doi:10.1159/000320165, pii: 000320165

Nakaya Y, Sukowati EW, Sheng G (2013) Epiblast integrity requires CLASP and dystroglycan-mediated microtubule anchoring to basal cortex. J Cell Biol 202(4):637–651

Ozdamar B, Bose R, Barrios-Rodiles M, Wang HR, Zhang Y, Wrana JL (2005) Regulation of the polarity protein Par6 by TGF-beta receptors controls epithelial cell plasticity. Science 307(5715):1603–1609. doi:10.1126/science.1105718, pii: 307/5715/1603

Polyak K, Weinberg RA (2009) Transitions between epithelial and mesenchymal states: acquisition of malignant and stem cell traits. Nat Rev Cancer 9(4):265–273. doi:10.1038/nrc2620, pii: nrc2620

Rohde LA, Heisenberg CP (2007) Zebrafish gastrulation: cell movements, signals, and mechanisms. Int Rev Cytol 261:159–192. doi:10.1016/S0074-7696(07)61004-3, pii: S0074-7696(07)61004-3

Schoenenberger CA, Matlin KS (1991) Cell polarity and epithelial oncogenesis. Trends Cell Biol 1(4):87–92, pii: 0962892491900358

Shook D, Keller R (2003) Mechanisms, mechanics and function of epithelial–mesenchymal transitions in early development. Mech Dev 120(11):1351–1383, pii: S0925477303002090

Solnica-Krezel L, Sepich DS (2012) Gastrulation: making and shaping germ layers. Annu Rev Cell Dev Biol 28:687–717. doi:10.1146/annurev-cellbio-092910-154043

Solursh M, Revel JP (1978) A scanning electron microscope study of cell shape and cell appendages in the primitive streak region of the rat and chick embryo. Differentiation 11(3):185–190

Takahashi Y, Sato Y, Suetsugu R, Nakaya Y (2005) Mesenchymal-to-epithelial transition during somitic segmentation: a novel approach to studying the roles of Rho family GTPases in morphogenesis. Cells Tissues Organs 179(1–2):36–42. doi:10.1159/000084507, pii: 84507

Thiery JP, Acloque H, Huang RY, Nieto MA (2009) Epithelial–mesenchymal transitions in development and disease. Cell 139(5):871–890. doi:10.1016/j.cell.2009.11.007, pii: S0092-8674(09)01419-6

Van Aelst L, Symons M (2002) Role of Rho family GTPases in epithelial morphogenesis. Genes Dev 16(9):1032–1054. doi:10.1101/gad.978802

Wakely J, England MA (1977) Scanning electron microscopy (SEM) of the chick embryo primitive streak. Differentiation 7(3):181–186

Yeaman C, Grindstaff KK, Nelson WJ (1999) New perspectives on mechanisms involved in generating epithelial cell polarity. Physiol Rev 79(1):73–98

Chapter 10
Making the Neural Plate to Fold into a Tube

Tamako Nishimura

Abstract Neural tube formation is a critical morphological process for neural development. Its defect causes serious birth defects such as anencephaly and spina bifida. Neural tube formation is initiated by the bending of the neural plate, which is regulated by multiple processes, including planar cell polarity (PCP) signaling, convergent extension, and apical constriction. However, how each event proceeds at the molecular level and how they are coordinated into a sequential movement have not been fully understood. We have explored the mechanisms of neural plate bending, focusing on the role of the remodeling of the adherens junctions (AJ) in neuroepithelial cells. At limited regions of the bending neural plate, neuroepithelial cells apically constrict because of the contraction of actomyosin filaments lining the AJ, which is induced by the recruitment of ROCK/Rho kinase to these sites, and this process is thought to produce a force to bend the plate. We found that this contraction is mediolaterally polarized, and this polarized bending is controlled by a cooperation of PCP signals and actomyosin contraction. Thus, we uncovered a mechanism by which the neural plate bends mediolaterally to form a tube.

Keywords Apical constriction • Celsr1 • Myosin II • Neural plate • PCP

10.1 Introduction

The neural tube is a key precursor of the central nervous system, the brain and spinal cord. At early development following gastrulation, the neural plate invaginates at the midline, rolls up, and becomes a tube structure, the neural tube. Failure in neural tube formation causes serious birth defects, such as anencephaly and spina bifida, which are collectively called neural tube defects (NTDs) (Copp et al. 2003).

T. Nishimura (✉)
Organization of Advanced Science and Technology, Kobe University, Kobe, Japan
e-mail: tnishimura@port.kobe-u.ac.jp

H. Kondoh and A. Kuroiwa (eds.), *New Principles in Developmental Processes*,
DOI 10.1007/978-4-431-54634-4_10,

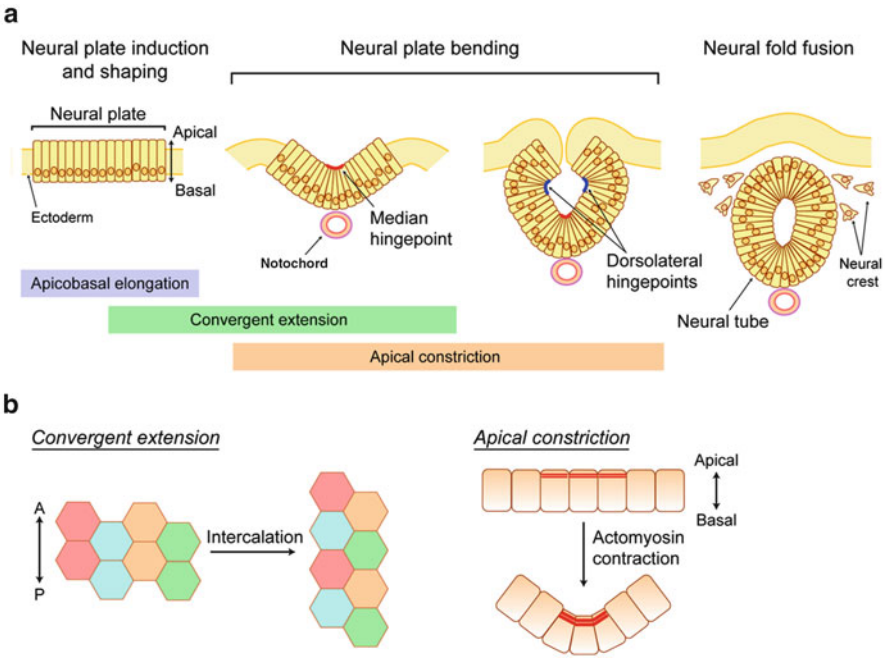

Fig. 10.1 Scheme for neural tube formation. **a** Transverse sections of the neural plates at each developmental stage. **b** Two principal mechanisms for tissue remodeling: convergent extension (*left*) and apical constriction (*right*)

NTDs are the second most human birth defects worldwide, and although the intake of folic acid has successfully decreased its frequency, there are still considerable number of NTDs that cannot be prevented (Wallingford et al. 2013).

Neural tube formation proceeds through four steps: neural plate induction, shaping, bending, and closure (Colas and Schoenwolf 2001) (Fig. 10.1a). The neural plate, induced from dorsal ectoderm, is first thickened apico-basally through microtubules (Suzuki et al. 2010). Then, the neural plate begins to be shaped, such that it is narrowed mediolaterally and elongated anteroposteriorly. This process is mediated through convergent extension, in which cells interdigitate mediolaterally (Fig. 10.1b). While the shaping is underway, bending of the neural plate is initiated. Bending occurs at three specialized portions called hinge points, a single median hinge point at the midline and paired dorsolateral hinge points on the lateral sides. The major driving force for bending is the contraction of actomyosin lining the adherens junctions (AJs) of the neuroepithelial cells, which is called apical constriction (Fig. 10.1b), through which the cell shape is changed from columnar to wedge like. The bending is also accelerated by adjacent nonneuronal tissues to assist the elevation of the neural folds. Eventually, the paired neural folds meet at the midline and are fused.

More than 200 genes are known to influence neural tube closure (Copp and Greene 2010). Among them, planar cell polarity (PCP) signaling regulators, which are extensively studied in *Drosophila* for the orientation of wing hairs or ommatidia, are involved in the neural tube formation (Wallingford 2012). Mutants for PCP core members, such as Celsr1 and Dishevelleds, show severe NTD. In those animals, convergent extension is suppressed, making a widened and shortened neural plate (Wallingford and Harland 2002), whereas neural plate bending at the median hinge point is also impaired (Greene et al. 1998). Regulators for the apical constriction, such as Shroom3 (Hildebrand and Soriano 1999) and Mena/Vasp (Menzies et al. 2004), mediate neural plate bending. Molecules acting on Hedgehog signaling (Ybot-Gonzalez et al. 2002) and BMP signaling (Ybot-Gonzalez et al. 2007) are also involved in the bending. How these functions are spatiotemporally regulated and coordinated is a central issue of neural tube morphogenesis.

In this chapter, I summarize our recent findings on the signaling pathway involved in neural plate bending, focusing on the role of remodeling of AJs of neuroepithelial cells (Nishimura and Takeichi 2009).

10.2 Apical Constriction of Neuroepithelial Cells Is Regulated by Shroom3-Mediated Relocalization of ROCKs to Junctions

Apical constriction of AJs in neuroepithelial cells is a major driving force to bend the neural plate. Shroom3, which was identified using a chemically induced mutant mouse that develops NTDs (Hildebrand and Soriano 1999), localizes around the AJs in the bending neural plate. Overexpression of Shroom3 causes apical constriction of epithelial cells through the activation of myosin II, a component of actomyosin filaments associated with AJs (Haigo et al. 2003; Hildebrand 2005).

To investigate the role of Shroom3 on the apical constriction (Nishimura and Takeichi 2008), we tested several deletion mutants of Shroom3 and found that the C-terminal ASD2 domain, which is characteristic for Shroom family members, is essential for inducing apical constriction and myosin II activation. Pull-down screening using GST-fused ASD2 identified ROCKs (Rho kinases) as ASD2-interacting proteins. ROCKs are known to activate myosin II by phosphorylating and inhibiting myosin phosphatase (Kimura et al. 1996). Overexpression of Shroom3 in cultured epithelial cells changed the localization of endogenous ROCK1 from cytoplasm to AJs (Fig. 10.2a, *left*), and concomitantly activated myosin II there. These observations indicated that Shroom3 causes apical constriction by anchoring ROCKs to AJs and activating myosin II (Fig. 10.2a, *right*).

In chicken embryos also, Shroom3 was localized to AJs of the neural plate, colocalizing with ROCK1 and active myosin II (shown by phosphorylated myosin light

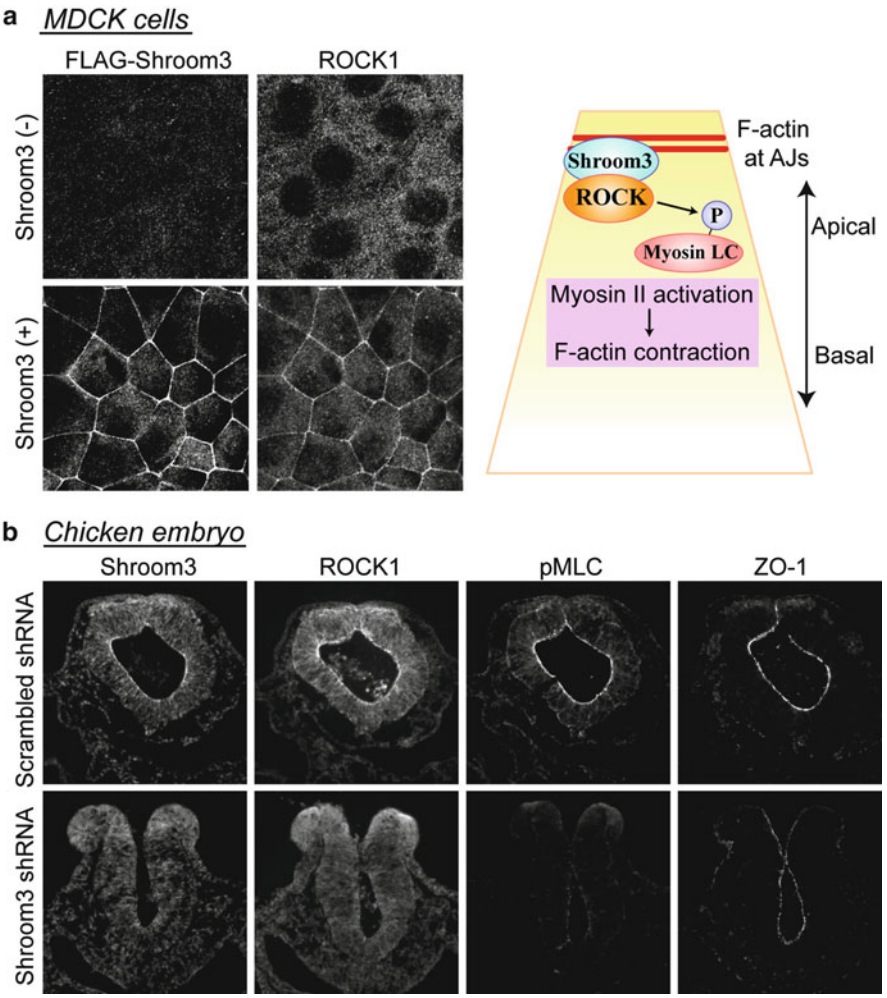

Fig. 10.2 Apical constriction of neuroepithelial cells is regulated by the relocalization of ROCKs to adherens junctions (AJs) by Shroom3. **a** *Left*: Exogenous expression of Shroom3 in MDCK cells recruits endogenous ROCK1 from cytoplasm to AJs. *Right:* Roles of Shroom3 in apical constriction. ROCKs recruited to AJs through Shroom3 activate myosin II by phosphorylation, which facilitates the contraction of F-actin belt lining AJs. **b** Effect of the depletion of Shroom3 on neural plate bending. Chicken embryos were electroporated with plasmid for Shroom3-specific or scrambled shRNA and fixed at stage 9. Serial transverse sections were immunostained as indicated

chain, pMLC) (Fig. 10.2b). When Shroom3 was depleted by electroporating its shRNA plasmids, neural plate bending was impaired, as was shown in Shroom3 mutant mice, and concomitantly ROCK1 localization and myosin II activation at AJs were inhibited (Fig. 10.2b). Thus, Shroom3 recruits ROCKs to AJs of the neural plate, and activates myosin II there, which induces the bending of the plate.

10.3 Polarized Actomyosin Activation Through the PCP Pathway Regulates the Bending of the Neural Plate

10.3.1 Apical Constriction Is Mediolaterally Polarized in the Bending Neural Plate

Although apical constriction is necessary for the bending of the neural plate, this process is not sufficient for the plate to make a tube, as apical constriction could induce a radially bent structure but not necessarily an elongated tube (Jacobson and Gordon 1976). We questioned how apical constriction in the neural plate is controlled to form a tube. To answer this question, we observed the bending neural plate from the apical side using chicken embryos, focusing on the floorplate area, where the bending first occurs. At the apical surface of the neural plate, active myosin II (pMLC) was detected preferentially at the AJs oriented toward the mediolateral axis, and the signals were linearly extended across several cells (Fig. 10.3) (Nishimura et al. 2012). Thick F-actin cables colocalized with the active myosin II, suggesting that these cables are contracting. These observations suggested a mediolaterally polarized apical constriction. To confirm this, we performed in vivo live imaging of neuroepithelial cells by labeling AJs with myosin light chain–EGFP. The AJs of neuroepithelial cells indeed contracted mediolaterally and even elongated anteroposteriorly. Through mathematical modeling, we verified that the mediolateral shortening of individual cell edges leads to the overall pattern of actomyosin cables, which we observed. Thus, in the bending neural plate, apical constriction of the neuroepithelial cells is polarized toward the mediolateral direction.

10.3.2 PCP Signaling and PDZ-RhoGEF Regulate Polarized Actomyosin Contraction at AJs of the Neural Plate

Because PCP signaling is known to be crucial for neural tube formation, we examined the potential role of Celsr1 cadherin, one of the PCP core regulators, in mediolaterally polarized actomyosin contraction. We found that Celsr1 proteins were concentrated at the apical side of the neural tube, and moreover, they colocalized with the mediolaterally contracting actin cables (Fig. 10.4a). When Celsr1 expression was knocked down using specific siRNAs, neural tube formation was severely impaired, as was reported for Celsr1 mutant mice (Curtin et al. 2003). Observation of these neuroepithelial cells from the apical side revealed that the mediolateral actomyosin cables were lost and the apical surface area of individual cells was enlarged (Fig. 10.4b). Inhibition of Dishevelleds, which function downstream of Celsr1 in the PCP regulation, caused analogous results. These findings suggested regulation of the planar-polarized actomyosin contraction by the PCP signals.

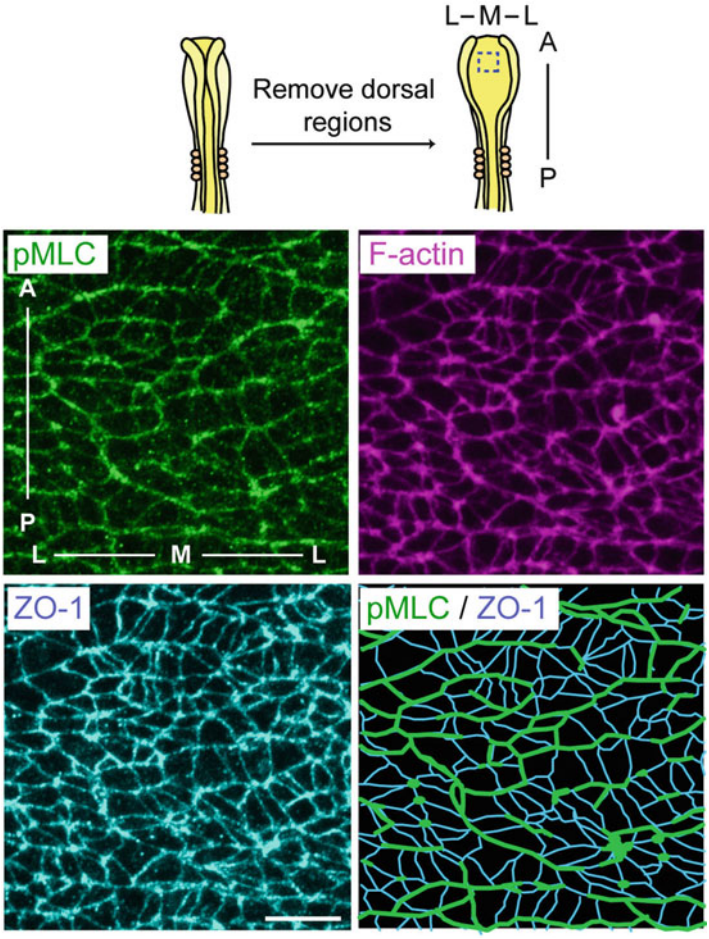

Fig. 10.3 Mediolateral orientation of actomyosin cables at AJs in the bending neural plate. Neural plate of chicken embryo at stage 8 was immunostained and flat mounted. Then, the floorplate region of the neural plate (*dotted square*) was photographed from the apical side. Anterior is oriented toward the *top* and MHP is located at the *center* throughout. *Lower right:* Merged image of pMLC and ZO-1 was traced [this figure, and Figs. 10.4, 10.5, 10.6, and 10.7, are reprinted from Nishimura et al. (2012), pp. 1084–1097, with permission from Elsevier]

In *Drosophila* gastrulation, apical constriction occurs through sequential activation of Gα/Concertina, RhoGEF2, RhoA, ROCK, and myosin II (Hacker and Perrimon 1998). Similarly, in chicken embryos, the transcript of PDZ-RhoGEF, a vertebrate homologue of RhoGEF2, was strongly expressed in the bending neural plate. PDZ-RhoGEF proteins were concentrated at the apical side of the neural tube, and colocalized with the mediolateral actomyosin cables (Fig. 10.4c), as was found for Celsr1. When PDZ-RhoGEF was depleted, neural tube closure was

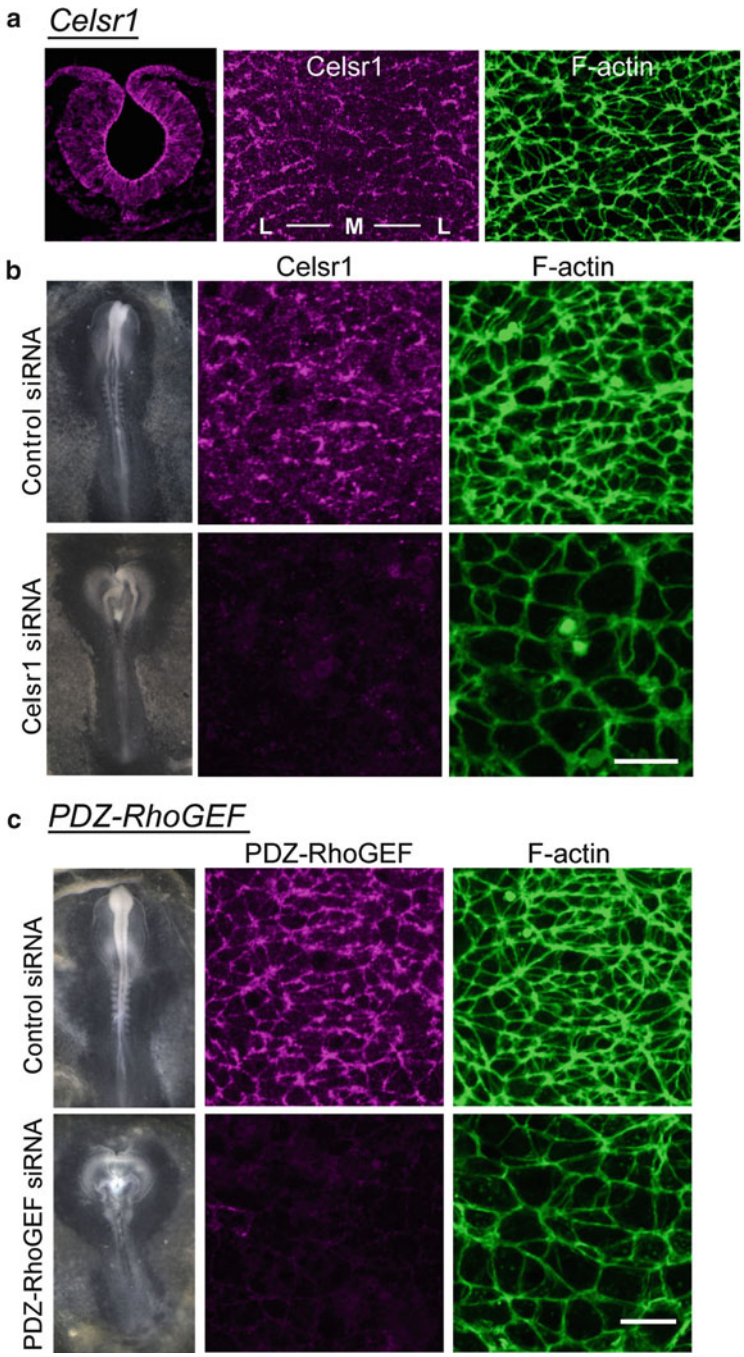

Fig. 10.4 Celsr1 and PDZ-RhoGEF are required for the mediolateral distribution of actomyosin cables at AJs. **a**, **b** Effect of Celsr1 on the distribution of F-actin cables at the apical neural plate. **a** *Left:* Immunostaining for Celsr1 in neural plate section at stage 8. *Right:* Codistribution of Celsr1 and F-actin at AJs in the floorplate region of neural plate. **b** Embryos were electroporated with Celsr1-specific or control siRNAs and fixed at stage 8. *Left:* Whole embryos; *right:* co-staining for Celsr1 and F-actin at the apical neural plate. **c** Effect of PDZ-RhoGEF on the mediolateral distribution of F-actin cables. PDZ-RhoGEF was depleted as described in **b**. *Left:* Whole embryos; *right:* co-staining for PDZ-RhoGEF and F-actin at the apical neural plate

disturbed, the mediolateral actomyosin cables were lost, and the apical surface area of cells was enlarged, just as are PCP-deficient embryos. Thus, PDZ-RhoGEF may work downstream of the PCP pathway for the mediolaterally polarized activation of actomyosin.

10.3.3 DAAM1 Links the PCP Pathway to PDZ-RhoGEF

We examined the role of DAAM1, another PCP regulator that interacts with Dishevelled and regulates convergent extension (Habas et al. 2001). DAAM1 belongs to the formin family, which regulates F-actin polymerization (Chesarone et al. 2010), and is activated by the binding of active RhoA and also by that of Dishevelled to its N- and C-terminal regions, respectively (Liu et al. 2008). We found that DAAM1 was evenly localized at AJs of the neural plate (Fig. 10.5a). Previous reports showed that LARG, an RhoGEF structurally related to PDZ-RhoGEF, interacted with and is activated by mDia, another formin (Kitzing et al. 2007). Thus, we investigated the interaction of DAAM1 with PDZ-RhoGEF and found that they were co-immunoprecipitated (Fig. 10.5b). The interaction occurred through the C-terminal region of DAAM1 and the DH-PH domain of PDZ-RhoGEF. Because the DH-PH domain is known to harbor guanine nucleotide exchange factor (GEF) activity, we examined the influence of DAAM1 on it, and found that the GEF activity was elevated in the presence of DAAM1 (Fig. 10.5c). Therefore, DAAM1 interacts with PDZ-RhoGEF and upregulates its activity. Furthermore, the interaction of DAAM1 and PDZ-RhoGEF was weakened after the depletion of Dishevelled. Thus, the DAAM1–PDZ-RhoGEF interaction is regulated by the upstream PCP regulator, Dishevelled.

10.3.4 PCP Regulators Mediate the Localization of PDZ-RhoGEF and ROCKs to AJs to Facilitate Mediolaterally Polarized Contraction

To confirm the entire signaling pathways from Celsr1 to actomyosin contraction, we performed cell biological studies. When Celsr1 was expressed in epithelial MDCK cells, it was concentrated at cell–cell contacts, as was previously shown for the *Drosophila* homologue Flamingo (Usui et al. 1999). Without Celsr1 expression, Dishevelled was diffusely distributed in cytoplasm. When both Celsr1 and Dishevelled were expressed, Dishevelled became recruited to the cell–cell contacts where Celsr1 was condensed (Fig. 10.6a). This recruitment may be mediated by endogenous Frizzled, as exogenously expressed Frizzled-6 codistributed with Celsr1 and Dishevelled. When DAAM1 was expressed alone, it was distributed evenly along AJs (Fig. 10.6a). When PDZ-RhoGEF was expressed without DAAM1,

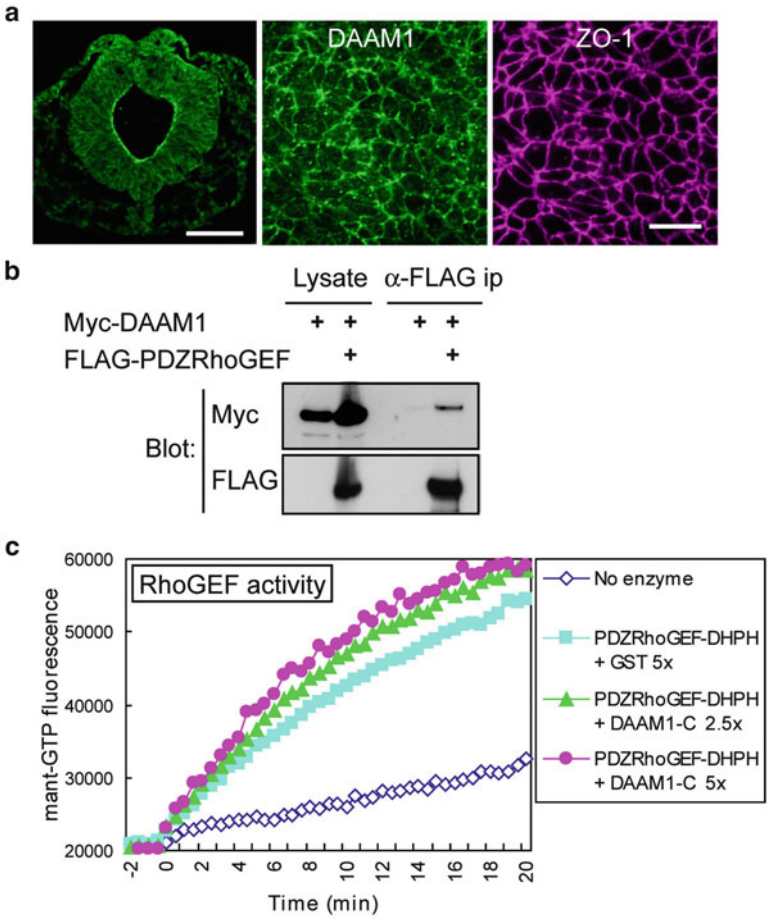

Fig. 10.5 DAAM1 interacts with PDZ-RhoGEF and upregulates its GEF activity. **a** *Left:* Immunostaining for DAAM1 in neural plate section. *Right:* Co-staining for DAAM1 and ZO-1 at the apical neural plate. **b** Interaction of DAAM1 with PDZ-RhoGEF: 293 T cells were cotransfected with plasmids for Myc-tagged DAAM1 and FLAG-tagged PDZ-RhoGEF or Myc-DAAM1 alone, and immunoprecipitated with anti-FLAG antibody. **c** Effects of DAAM1 on RhoGEF activity. PDZ-RhoGEF-DHPH protein was incubated with a 2.5- or 5-fold excess of DAAM1-C (*closed triangles* and *closed circles*, respectively) or GST (*closed squares*) proteins. A mixture containing a fluorogenic substrate (mant-GTP) was added, and the increase in fluorescent intensity was measured

it was mostly localized in the cytoplasm even in the presence of Celsr1 and Dishevelled. In contrast, when PDZ-RhoGEF was expressed together with DAAM1, it was accumulated in the cell–cell contact sites where Celsr1 and Dishevelled colocalized (Fig. 10.6b). Furthermore, at AJs where Celsr1, Dishevelled, and PDZ-RhoGEF colocalized, endogenous ROCK1 was upregulated. Thus, PDZ-RhoGEF is presumably recruited to the Celsr1-Dishevelled-enriched contact sites through DAAM1, and following this step, ROCKs are recruited to the AJs via RhoA.

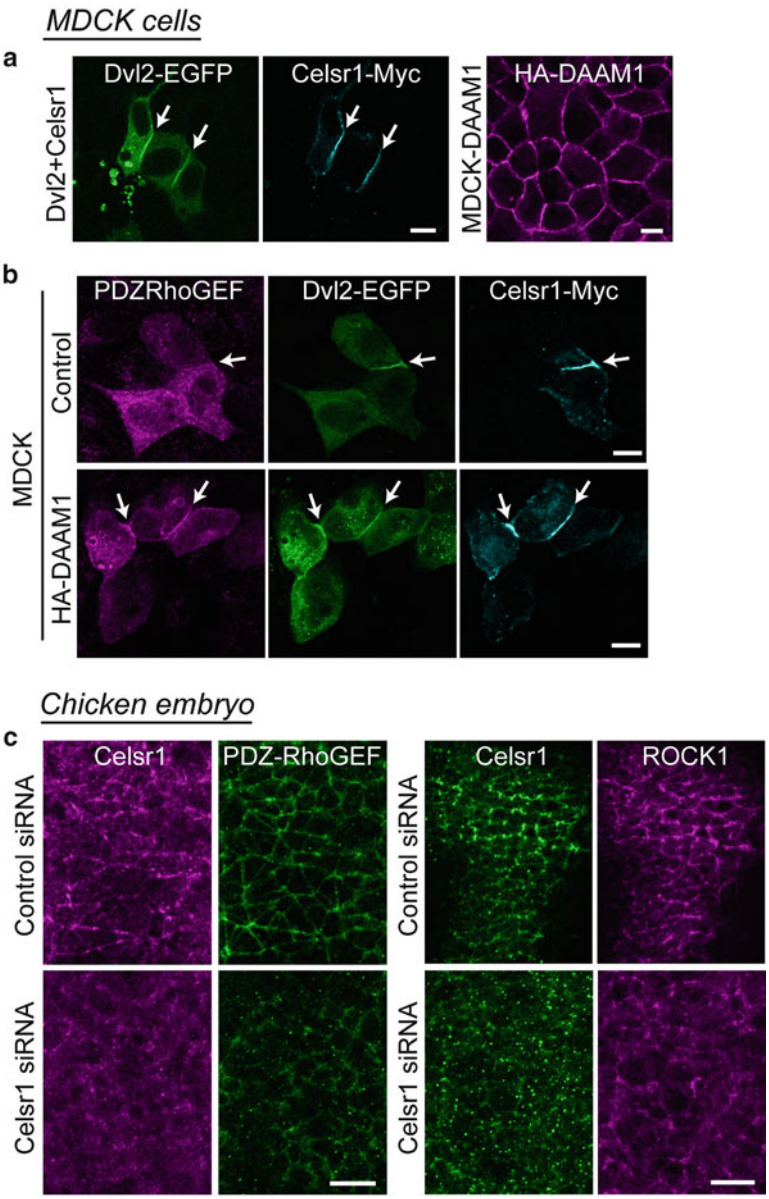

Fig. 10.6 Celsr1-dependent polarized distribution of PDZ-RhoGEF and ROCK1. **a**, **b** Celsr1/Dishevelled/DAAM-dependent recruitment of PDZ-RhoGEF to AJs in MDCK cells. **a** *Left:* Colocalization of Dishevelled-2 (Dvl2-EGFP) and Celsr1 (Celsr1-Myc) at cell–cell junctions when they are coexpressed. *Right:* Distribution of HA-tagged DAAM1 stably expressed in MDCK cells. **b** FLAG-tagged PDZ-RhoGEF was expressed together with Dvl2 and Celsr1 in either MDCK or DAAM1-expressing MDCK cells. *Arrows* point to cell–cell contacts where both Dvl2 and Celsr1 are accumulated. **c** Effects of Celsr1 depletion on the mediolaterally polarized distribution of PDZ-RhoGEF (*left*) or ROCK1 (*right*) at the apical neural plate

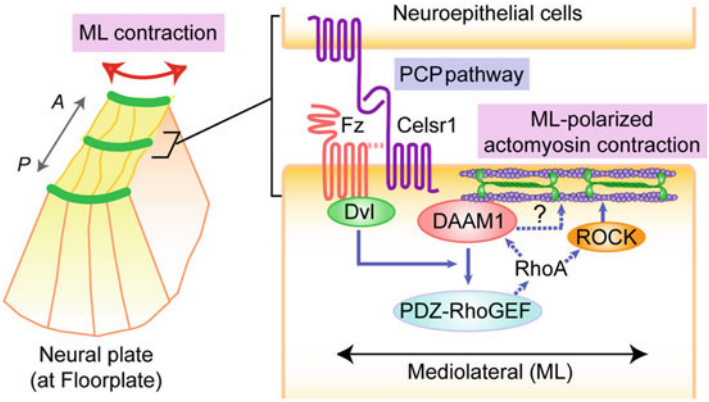

Fig. 10.7 Models of roles of planar cell polarity (PCP) regulators on the mediolaterally polarized contraction of AJs and neural plate bending: summary of present observations. *ML* mediolateral, *Fz* Frizzled. *Arrows* indicate activation of a molecule or promotion of molecular interactions. *Dotted arrows* are hypothetical pathways

Finally, we analyzed the spatial relations of Celsr1, PDZ-RhoGEF, and ROCK in the neural plate. PDZ-RhoGEF and ROCK1 colocalized with Celsr1 at mediolateral AJs. When Celsr1 was depleted, localization of both PDZ-RhoGEF and ROCK1 became diffuse (Fig. 10.6c). On the other hand, neither the depletion of PDZ-RhoGEF nor the inhibition of ROCK changed the polarized distribution of Celsr1. These results suggested that Celsr1 regulates the mediolaterally polarized localization of PDZ-RhoGEF and ROCK at AJs of the neural plate that execute neural plate bending.

Based on the observations described here, we propose the following model of signaling pathway (Fig. 10.7). (1) First, Celsr1 distributes along a subpopulation of AJs oriented toward mediolateral direction, and recruits Dishevelled. (2) Dishevelled then binds and activates DAAM1 at these AJs. (3) DAAM1 interacts with and activates PDZ-RhoGEF there. (4) PDZ-RhoGEF recruits ROCKs to these AJs, possibly by activating RhoA. (5) ROCKs, at the mediolaterally oriented AJs, activate myosin II, which causes the planar-polarized contraction of actomyosins, leading to the bending of the neural plate into a tube.

10.4 Analogy to Other Developmental Processes

Planar-polarized actomyosin contraction coupled with junctional remodeling was originally discovered in the *Drosophila* epithelium undergoing germband extension (Bertet et al. 2004). To elongate a tissue, epithelial cells shrink the dorsoventral AJs to make a four-cell-ordered configuration, and then elongate the anteroposterior AJs. This observation was further expanded by the finding of multicellular rosettes as another intermediate (Blankenship et al. 2006). Multicellular rosette formation

starts with the accumulation of myosin II and F-actin to the dorsoventral AJs over several adjacent cells and their subsequent contraction. This polarized contraction was caused by the asymmetrical localization of ROCK to the dorsoventral junctions under the regulation of AP patterning genes Eve, Runt, and Kruppel (Simoes Sde et al. 2010), not that of the PCP regulators in this case.

As another type of polarized actomyosin contraction, the Fat/Dachsous (Ds)/Four-jointed (Fj) pathway regulates morphogenesis of the dorsal thorax in *Drosophila* (Bosveld et al. 2012). In tissue-wide Ds and Fj gradients, the distribution of Ds at AJs becomes planar polarized, which then polarizes myosin Dachs and produces anisotropic tension. Similar mechanisms also work for the polarized distribution of myosin Dachs in *Drosophila* wing disc, which occurs independently of the core PCP pathway (Brittle et al. 2012).

In *Drosophila* tracheal tube morphogenesis, on the other hand, PCP signals regulate the turnover of E-cadherin through the function of RhoGEF2 and RhoA, promoting cell intercalation in tracheal branches (Warrington et al. 2013). PCP signaling controls the planar-polarized distribution of RhoGEF2, which leads to the polarized E-cadherin turnover.

In vertebrates, analogous mechanisms work for kidney tubule elongation (Lienkamp et al. 2012). In the collecting duct epithelium in mouse and *Xenopus*, multicellular rosettes were observed, and live imaging revealed that rosettes are formed mediolaterally and dissolved perpendicularly, which elongates the tubule. Interestingly, myosin II is activated at the mediolateral AJs, which is required for the elongation, and moreover, the PCP pathway is required for the orientation of the rosette formation.

Collectively, the mechanisms of planar-polarized actomyosin contraction and AJ remodeling may be shared in many morphological processes in various organisms.

10.5 Concluding Remarks

We have shown the signaling cascades involved in the polarized contraction of AJs that leads to the neural plate bending. However, important questions remain unsolved. One is how Celsr1, which determines the direction of contractility, is selectively localized at AJs oriented along the mediolateral axis. In the *Drosophila* wing, Flamingo, an orthologue of Celsr1, couples with Frizzled and is transported along microtubules to the anteroposterior borders (Shimada et al. 2006), although another report showed that the distribution of Frizzled is dependent on Flamingo (Strutt and Strutt 2008). Similarly, in the back skin of mice, Celsr1 localizes to the mediolateral borders, making a complex with Vangl2, and their distributions are interdependent (Devenport and Fuchs 2008). Some secreted ligands, such as Wnts, may regulate this process or, as seen in *Drosophila* germband extension, AP patterning genes might be involved.

Another question is the role of DAAM1. DAAM1 is one of the formins and is involved in normal AJ formation in heart tissues (Li et al. 2011). The contribution

of DAAM1 to neural plate bending may be complex. On one hand, DAAM1 may regulate the basic F-actin organization, which is important for the maintenance of AJ. On the other hand, when DAAM1 receives PCP signals from the Celsr1-Dishevelled system, it may transmit these signals to PDZ-RhoGEF and ROCKs.

Further clarification of the mechanisms underlying neural plate bending will contribute greatly to the understanding of complex morphogenetic processes of the central nervous system and other tubular organs.

Acknowledgments I thank Masatoshi Takeichi for carefully reading this chapter.

References

Bertet C, Sulak L, Lecuit T (2004) Myosin-dependent junction remodelling controls planar cell intercalation and axis elongation. Nature (Lond) 429(6992):667–671

Blankenship JT, Backovic ST, Sanny JS et al (2006) Multicellular rosette formation links planar cell polarity to tissue morphogenesis. Dev Cell 11(4):459–470

Bosveld F, Bonnet I, Guirao B et al (2012) Mechanical control of morphogenesis by Fat/Dachsous/Four-jointed planar cell polarity pathway. Science 336(6082):724–727

Brittle A, Thomas C, Strutt D (2012) Planar polarity specification through asymmetric subcellular localization of Fat and Dachsous. Curr Biol 22(10):907–914

Chesarone MA, DuPage AG, Goode BL (2010) Unleashing formins to remodel the actin and microtubule cytoskeletons. Nat Rev Mol Cell Biol 11(1):62–74

Colas JF, Schoenwolf GC (2001) Towards a cellular and molecular understanding of neurulation. Dev Dyn 221(2):117–145

Copp AJ, Greene ND (2010) Genetics and development of neural tube defects. J Pathol 220(2): 217–230

Copp AJ, Greene ND, Murdoch JN (2003) The genetic basis of mammalian neurulation. Nat Rev Genet 4(10):784–793

Curtin JA, Quint E, Tsipouri V et al (2003) Mutation of Celsr1 disrupts planar polarity of inner ear hair cells and causes severe neural tube defects in the mouse. Curr Biol 13(13):1129–1133

Devenport D, Fuchs E (2008) Planar polarization in embryonic epidermis orchestrates global asymmetric morphogenesis of hair follicles. Nat Cell Biol 10(11):1257–1268

Greene ND, Gerrelli D, Van Straaten HW et al (1998) Abnormalities of floor plate, notochord and somite differentiation in the loop-tail (Lp) mouse: a model of severe neural tube defects. Mech Dev 73(1):59–72

Habas R, Kato Y, He X (2001) Wnt/Frizzled activation of Rho regulates vertebrate gastrulation and requires a novel Formin homology protein Daam1. Cell 107(7):843–854

Hacker U, Perrimon N (1998) DRhoGEF2 encodes a member of the Dbl family of oncogenes and controls cell shape changes during gastrulation in *Drosophila*. Genes Dev 12(2):274–284

Haigo SL, Hildebrand JD, Harland RM et al (2003) Shroom induces apical constriction and is required for hingepoint formation during neural tube closure. Curr Biol 13(24):2125–2137

Hildebrand JD (2005) Shroom regulates epithelial cell shape via the apical positioning of an actomyosin network. J Cell Sci 118(Pt 22):5191–5203

Hildebrand JD, Soriano P (1999) Shroom, a PDZ domain-containing actin-binding protein, is required for neural tube morphogenesis in mice. Cell 99(5):485–497

Jacobson AG, Gordon R (1976) Changes in the shape of the developing vertebrate nervous system analyzed experimentally, mathematically and by computer simulation. J Exp Zool 197(2): 191–246

Kimura K, Ito M, Amano M et al (1996) Regulation of myosin phosphatase by Rho and Rho-associated kinase (Rho-kinase). Science 273(5272):245–248
Kitzing TM, Sahadevan AS, Brandt DT et al (2007) Positive feedback between Dia1, LARG, and RhoA regulates cell morphology and invasion. Genes Dev 21(12):1478–1483
Li D, Hallett MA, Zhu W et al (2011) Dishevelled-associated activator of morphogenesis 1 (Daam1) is required for heart morphogenesis. Development (Camb) 138(2):303–315
Lienkamp SS, Liu K, Karner CM et al (2012) Vertebrate kidney tubules elongate using a planar cell polarity-dependent, rosette-based mechanism of convergent extension. Nat Genet 44(12): 1382–1387
Liu W, Sato A, Khadka D et al (2008) Mechanism of activation of the Formin protein Daam1. Proc Natl Acad Sci USA 105(1):210–215
Menzies AS, Aszodi A, Williams SE et al (2004) Mena and vasodilator-stimulated phosphoprotein are required for multiple actin-dependent processes that shape the vertebrate nervous system. J Neurosci 24(37):8029–8038
Nishimura T, Honda H, Takeichi M (2012) Planar cell polarity links axes of spatial dynamics in neural-tube closure. Cell 149(5):1084–1097
Nishimura T, Takeichi M (2008) Shroom3-mediated recruitment of Rho kinases to the apical cell junctions regulates epithelial and neuroepithelial planar remodeling. Development (Camb) 135(8):1493–1502
Nishimura T, Takeichi M (2009) Remodeling of the adherens junctions during morphogenesis. Curr Top Dev Biol 89:33–54
Shimada Y, Yonemura S, Ohkura H et al (2006) Polarized transport of Frizzled along the planar microtubule arrays in *Drosophila* wing epithelium. Dev Cell 10(2):209–222
Simoes Sde M, Blankenship JT, Weitz O et al (2010) Rho-kinase directs Bazooka/Par-3 planar polarity during *Drosophila* axis elongation. Dev Cell 19(3):377–388
Strutt H, Strutt D (2008) Differential stability of flamingo protein complexes underlies the establishment of planar polarity. Curr Biol 18(20):1555–1564
Suzuki M, Hara Y, Takagi C et al (2010) MID1 and MID2 are required for *Xenopus* neural tube closure through the regulation of microtubule organization. Development (Camb) 137(14): 2329–2339
Usui T, Shima Y, Shimada Y et al (1999) Flamingo, a seven-pass transmembrane cadherin, regulates planar cell polarity under the control of Frizzled. Cell 98(5):585–595
Wallingford JB (2012) Planar cell polarity and the developmental control of cell behavior in vertebrate embryos. Annu Rev Cell Dev Biol 28:627–653
Wallingford JB, Harland RM (2002) Neural tube closure requires Dishevelled-dependent convergent extension of the midline. Development (Camb) 129(24):5815–5825
Wallingford JB, Niswander LA, Shaw GM et al (2013) The continuing challenge of understanding, preventing, and treating neural tube defects. Science 339(6123):1222002
Warrington SJ, Strutt H, Strutt D (2013) The Frizzled-dependent planar polarity pathway locally promotes E-cadherin turnover via recruitment of RhoGEF2. Development (Camb) 140(5): 1045–1054
Ybot-Gonzalez P, Cogram P, Gerrelli D et al (2002) Sonic hedgehog and the molecular regulation of mouse neural tube closure. Development (Camb) 129(10):2507–2517
Ybot-Gonzalez P, Gaston-Massuet C, Girdler G et al (2007) Neural plate morphogenesis during mouse neurulation is regulated by antagonism of BMP signalling. Development (Camb) 134(17):3203–3211

Chapter 11
Contribution of Apoptosis in Cranial Neural Tube Closure Indicated by Mouse Embryo Live Imaging

Yoshifumi Yamaguchi, Naomi Shinotsuka, Keiko Nonomura, and Masayuki Miura

Abstract Many cells die during development through the process called programmed cell death (PCD). Dysregulation of apoptosis, a major form of PCD during development, leads to cranial neural tube closure (NTC) defects such as exencephaly, but the underlying mechanism has remained unclear. Observing cells undergoing apoptosis in the normal developmental process will help elucidate their nature, characteristics, and interaction with surrounding tissues. Using a newly developed transgenic mouse that stably expressed a genetically encoded FRET-based fluorescent reporter for caspase activation, we performed simultaneous time-lapse imaging of apoptosis and morphogenesis in living embryos. This analysis, based on live imaging, indicated that inhibition of caspase activation interfered with and delayed the progression of NTC in the cranial region. The analysis also revealed existence of two types of apoptotic cells during NTC. Based on these results, we propose that cell removal by caspase-mediated apoptosis facilitates NTC and ensues the completion of NTC within a limited developmental time window.

Keywords Apoptosis • Live-imaging • Morphogenesis • Neural tube closure

11.1 Contribution of Programmed Cell Death in Normal Development

Cell death is an integral part of development, because certain numbers of cells actually die at specific regions and stages (Fuchs and Steller 2011; Miura 2011). Such developmentally regulated cell death is called “programmed cell death” (PCD). Well-known examples of PCD include removal of cells from an interdigital

Y. Yamaguchi (✉) • N. Shinotsuka • K. Nonomura • M. Miura
Department of Genetics, Graduate School of Pharmaceutical Sciences, University of Tokyo, Tokyo, Japan
e-mail: bunbun@mol.f.u-tokyo.ac.jp

H. Kondoh and A. Kuroiwa (eds.), *New Principles in Developmental Processes*,
DOI 10.1007/978-4-431-54634-4_11, © Springer Japan 2014

web of developing vertebrate limbs, elimination of developing Mullerian or Wolffian ducts in a sex-dependent manner, and massive cell death in the neural ridge during neural tube closure (NTC).

Recent studies on the conditions where apoptosis, a major form of PCD, is inhibited by genetic and pharmacological means opened up a new avenue to investigate the contribution of PCD in normal development.

11.2 Apoptosis During Neural Tube Closure

Apoptosis is executed by an evolutionary conserved cascade of cysteine proteases called caspases (Fig. 11.1a) (Degterev and Yuan 2008). Apoptotic cells undergo characteristic morphological changes including membrane blebbing, cell shrinkage, cell fragmentation (apoptotic body formation), and chromosomal DNA fragmentation (Fig. 11.1b). DNA fragmentation is mediated by CAD (caspase-activated DNAse) and is detected by TUNEL (terminal deoxynucleotidyl transferase dUTP nick-end labeling). Apoptosis is distinguished from other cell death processes, such as necrosis, in that it does not induce inflammatory responses (Miura 2011) (Fig. 11.1b).

Apoptosis occurs prominently during NTC in birds and mammals. NTC is a dynamic process that provides the basic morphological scaffold for the central

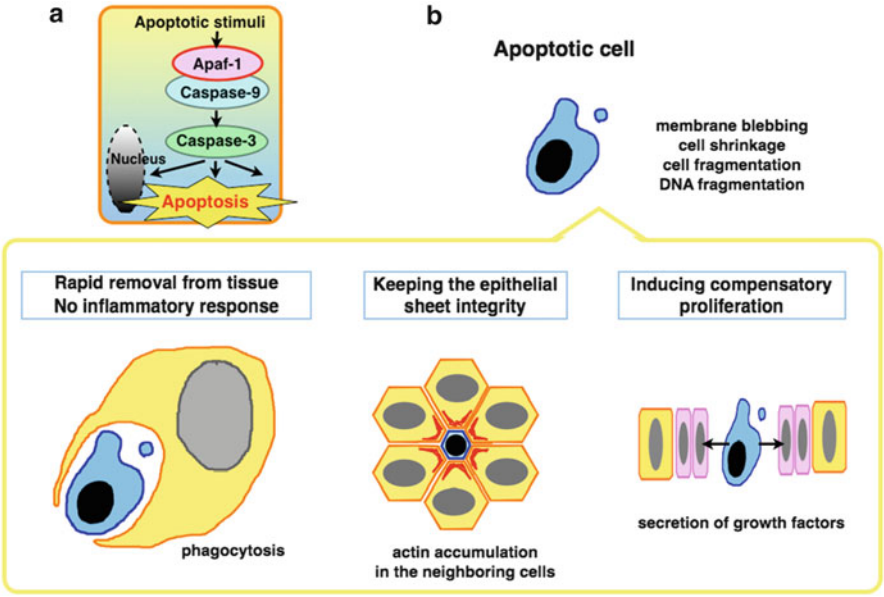

Fig. 11.1 **a** A scheme of apoptotic pathway causing cell death. **b** Features of apoptotic cells in animal bodies (Fuchs and Steller 2011; Miura 2011)

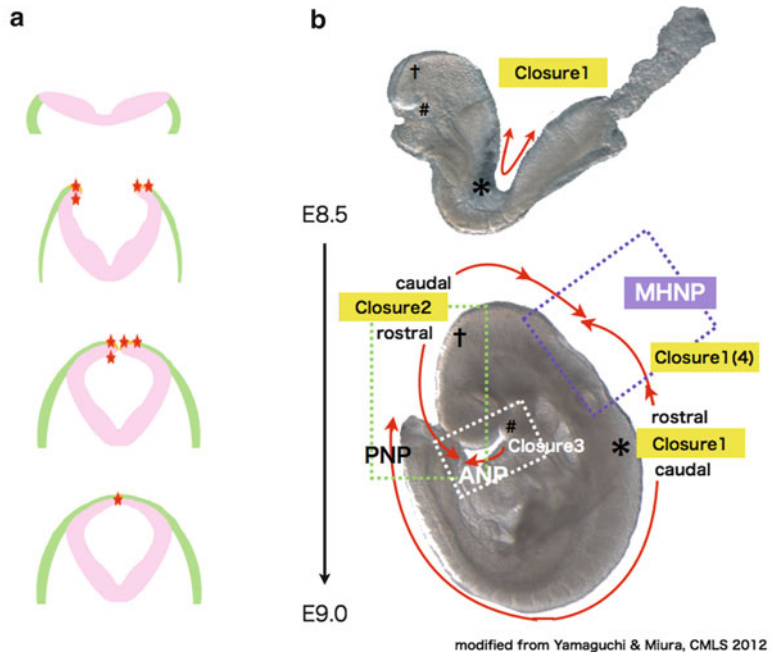

Fig. 11.2 **a** Morphological changes of the cranial neural plates to form the neural tube. The neural plate becomes concave and its ridges are raised to form the neural fold. Along with this continuation, inward flipping of the ridges occurs, resulting in apposition and fusion of the ridges. *Pink* neuroectoderm (neuroepithelium), *green* nonneural ectoderm (surface ectoderm). Locations of apoptotic cells are schematically shown by *red stars*. **b** Multiple start points for neural tube closure (NTC) in the cranial region of mouse embryos. *Top:* Closure 1 occurs bi-directionally occurs from the cervical region (*asterisk*) before embryonic turning in ~E8.5 embryo. *Bottom:* Schematic representation of multiple closures in an E8.75 embryo. The midbrain–hindbrain neuropore (*MHNP*) is closed by merging of caudal closure 2 and rostral closure 1 (closure 4), and ANP by merging of caudal closure 2 and closure 3. *Asterisk* closure 1 start point, *dagger* bi-directional closure 2 start point, # closure 3 start point. Progression of closures is shown by *red arrows*

nervous system. Neural tube defects (NTDs), including exencephaly, anencephaly, open spina bifida, and craniorachischisis, are associated with defects in NTC (Copp and Greene 2010). To generate the neural tube from the neural plate, both sides of the neural plate are raised to form ridges that are bent inwardly until they are apposed, and finally fused to form the roof of the neural tube (Fig. 11.2a). In mammals, NTC begins at multiple axially different points of the neural tube with different timing (Fig. 11.2b) (Copp et al. 2003; Yamaguchi and Miura 2012; Pyrgaki et al. 2010). The cervical region of the neural tube is the first to close (closure I; α in Fig. 11.2b), and the closure extends rostrocaudally from this site. Following the closure of the neural tube at rhombomere (r) 5 and r4 levels, the neural plate at the r3–r2 levels begins to become concave and the dorsal ridges of the neural plates start to flip inwardly. Closure II is initiated at the forebrain–midbrain boundary, and the subsequent neural ridge fusion extend rostrocaudally. The rostrally directed closure

II meets closure III to seal the forebrain region, and the caudally directed closure II meets rostrally directed closure I to seal the midbrain–hindbrain neuropore (MHNP), thus completing the NTC in the cranial region.

During the processes, apoptosis is observed mainly at the neural ridges and the roof plate, before and after the NTC along the entire body axis (Copp et al. 2003; Weil et al. 1997; Nonomura et al. 2013) (Fig. 11.2a). Inhibition of apoptosis with pan-caspase inhibitors in chicken embryos resulted in NTC failure (Weil et al. 1997). Similarly, knockout mice deficient for a component of apoptosis machinery (apaf-1, caspase-3, or caspase-9) resulted in cranial NTD including exencephaly (Yoshida et al. 1998; Kuida et al. 1996, 1998). These observations suggested that apoptosis is important for the completion of the cranial part of NTC. However, another study using cultured mouse embryos that allowed temporally controlled application of caspase inhibitors indicated that inhibition of apoptosis during NTC did not cause any morphological abnormalities (Massa et al. 2009), raising the possibility that apoptosis itself is not be required for the final neural ridge fusion step of NTC. Inhibition of apoptosis thus caused abnormality in other steps of the NTC.

11.3 Live-Imaging of Apoptosis and NTC in Mouse Embryos in Culture

To clarify the contribution of apoptosis in the NTC, it is important to understand how inhibition of apoptosis affects the cellular and tissue processes of NTC. Live imaging of embryonic cells and tissues is essential for this purpose, because NTC is a rapid process and dead cells resulting from apoptosis are lost from the tissue rapidly (Miura 2011).

We took a live-imaging approach by using SCAT3 (sensor for caspase-3 activation based on FRET) (Takemoto et al. 2003) transgenic mice that allowed real-time detection of caspase activation and apoptotic cells during NTC in the cranial region at both tissue and single-cell levels (Fig. 11.3a) (see Sect. 11.5 for details). We first set up an embryo imaging system using a fast-scanning confocal microscope that scans the whole head region of an embryo in ~2 min with *z*-axis image depth of 200–400 μm (Fig. 11.3b) (Yamaguchi et al. 2011). A similar live-imaging system to observe the cranial NTC has also been reported by another group (Pyrgaki et al. 2010; Massarwa and Niswander 2013).

11.4 Impact of Apoptosis Inhibition on the NTC

To investigate how apoptosis contributes to the process of NTC, embryos defective in the apoptotic pathway were analyzed. In these *apaf-1*$^{-/-}$ or *casp-3*$^{-/-}$ mutant embryos, concaving of the neural plate and inward flipping of the neural ridge were compromised. Interestingly, the hindbrain dorsal ridges in *apaf-1*$^{-/-}$ embryos

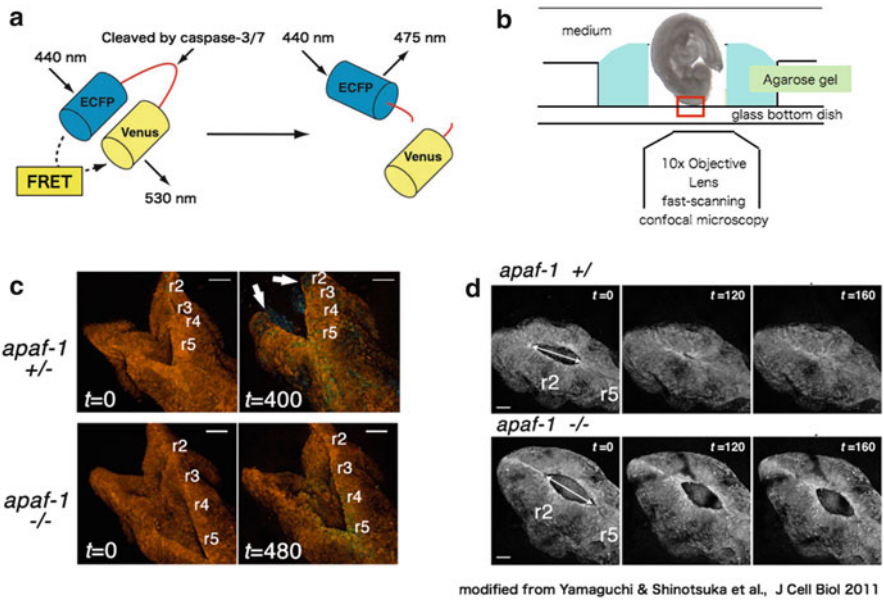

Fig. 11.3 **a** Structure of SCAT3. Linker cleavage by caspase-3 disrupts FRET between ECFP and Venus, leading to decrease of Venus (emission 530 nm)/ECFP (emission 475 nm) fluorescence ratio. **b** A scheme of the culture system to observe NTC in the cranial region with a fast-scanning confocal microscope. **c** Inhibition of apoptosis in *apaf-1*$^{-/-}$ embryos delayed NPC. Imaging with SCAT3 confirmed that there was no apoptotic cell in *apaf-1*$^{-/-}$ embryos. **d** Live-imaging revealed delayed closure in MHNP in an apoptosis-deficient *apaf-1*$^{-/-}$ embryo. © *Yamaguchi and Shinotsuka et al.,* (2011)

showed repeated squeezing motions, yet they failed to complete the neural ridge apposition and fusion (Fig. 11.3c).

Under the condition of reduced concaving of the cranial neural folds and impaired flipping of neural ridges, the contact between the dorsal neural ridges at the site of closure II and subsequent NTC were delayed. The speed of NTC was significantly reduced in embryos treated with the pan-caspase inhibitor zVAD or deficient in *apaf-1* (Fig. 11.3d). This delay in NTC was also confirmed in embryos grown in utero by precise staging of embryos. Thus, the inhibition of caspase activation slowed down NTC at closures I and II.

Then, what impacts does this kinetic difference in the NTC have on embryonic development? Interestingly, some apoptosis-deficient embryos with reduced speed of closure failed in completing the NTC during culture period for live imaging of ~12 h. In an *apaf-1*$^{-/-}$ embryo that was placed in culture at 20 somite stage, when NTC is complete in normal embryos, the hindbrain region remained open at the axial levels from r4 to r2 throughout the culture period. The axial length of MHNP (*L*) decreased and the width of the MHNP increased (Fig. 11.4), suggesting that the force at the contracting neural ridge to fuse the tissue failed to overcome the tissue resistance against bending in the absence of apoptosis. This open neural tube would result in exencephaly, a condition in which the neuroepithelium is exposed to amniotic fluid.

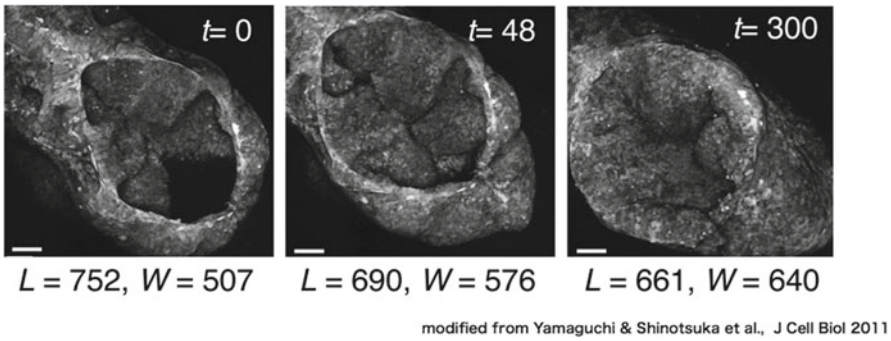

Fig. 11.4 An observation of an *apaf-1*$^{-/-}$ embryo, which was placed in culture at somite 20 when NTC failure was evident. During imaging, the MHNP length (L) decreased, but its width (W) increased, implying the resistance of tissue against the neural tube closure. *L* length of MHNP (μm), *W* width of MHNP at r2 (μm). © *Yamaguchi and Shinotsuka et al.,* (2011)

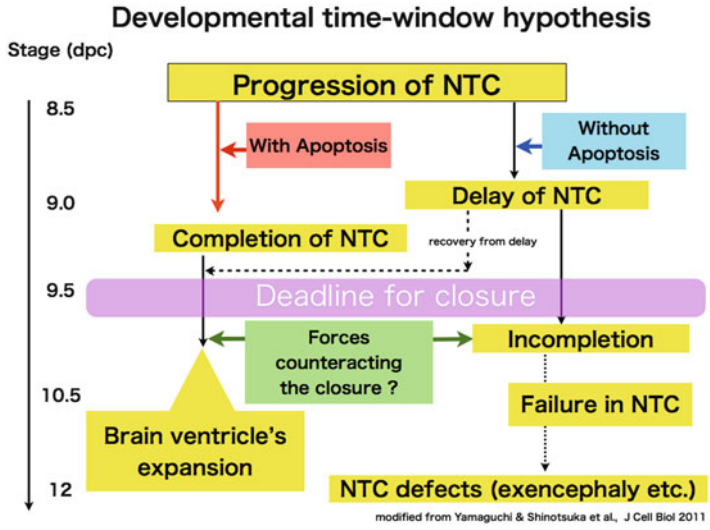

Fig. 11.5 Developmental time-window hypothesis for cranial NTC. NTC must be completed by a developmental deadline (about somite stage 20), when forces derived from neuroepithelial development will not allow the further NTC process to proceed. Any perturbation of NTC process exemplified by the failure in apoptosis delays NTC. Even when closure is delayed, the embryo can develop without NTDs, so long as NTC can be completed before the deadline (shown as "recovery form delay"). However, if closure is not completed by the deadline, cranial NTC ends in failure to close at the MHNP, resulting in cranial NTDs such as exencephaly. © *Yamaguchi and Shinotsuka et al.,* (2011)

Based on these observations, we suggest that there is a strict developmental time window in which the NTC in the cranial region must be completed (Fig. 11.5). This "developmental time-window" hypothesis assumes that neural plate tissue forces, which resist against the generation of tissue curvature and hence

counteract the NTC, start to be reinforced at the end of this time window. Apical constriction driven by actomyosin (Haigo et al. 2003) and apical neural ridge fusion that leads to NTC must be completed before the counteracting forces become strengthened.

The exact contribution of apoptosis to the cranial NTC remains to be elucidated. However, a hint is provided by the case of dorsal closure in *Drosophila* embryos. There, apposing epidermal sheets contact one another and seal with zipper-like dynamics at the midline, and the inhibition or promotion of apoptosis in amnioserosa cells that connect to the lateral epidermis delays or accelerates the dorsal closure process, respectively, suggesting that extrusion of apoptotic cells contribute to dorsal closure by force generation (Toyama et al. 2008). In addition to these physical effects on morphological forces, apoptotic cells can affect their neighbors by releasing signaling molecules, such as Wnts and prostaglandin E2 (Chera et al. 2009; Li et al. 2010) (see Fig. 11.1).

11.5 Measuring Intensity and Kinetics of Signaling Activity in Living Embryos Showing Two Types of Apoptotic Cells

In general, cell death events are difficult to detect, because dying cells are rapidly removed from tissues by engulfment, shedding, or the dispersion of cell debris. To gain insight into the mechanisms of how apoptosis affects the NTC in the cranial region, we utilized SCAT3-transgenic mice to observe occurrence and behaviors of apoptotic cells during the progression of NTC. SCAT3 contains a caspase substrate sequence in its linker region between ECFP and Venus (Fig. 11.3a). The dissociation of ECFP and Venus upon cleavage of the linker lowers FRET and the Venus/ECFP (V/C) fluorescence ratio, and thereby indicates caspase activation in living cells. This analysis showed that at least two types of apoptotic cells exist.

One type of apoptotic cells is conventional type (C-type). After caspase activation indicated by the decrease of V/C fluorescence ratio, the C-type apoptotic cells shrank, became fragmented, and formed apoptotic bodies (Fig. 11.6). The fragmented apoptotic bodies then quickly disappeared, presumably being engulfed by surrounding cells. C-type cells were observed both before and after the completion of NTC at the dorsal midline formed by neural ridge fusion.

Another type is dancing-type (D-type). Immediately after caspase activation, the D-type cells began to protrude from the epithelial layer, became round, and moved actively in the layer. Unexpectedly, these cells were rarely fragmented, and continued to be attached to the cell sheet and “danced” around their original sites. Most of them retained their round shape and moved around during the imaging period (up to ~6 h) (Fig. 11.6). D-type cells appeared mainly in the dorsal ridge of the neural plates and in the boundary domain between the neural plates and surface ectoderm.

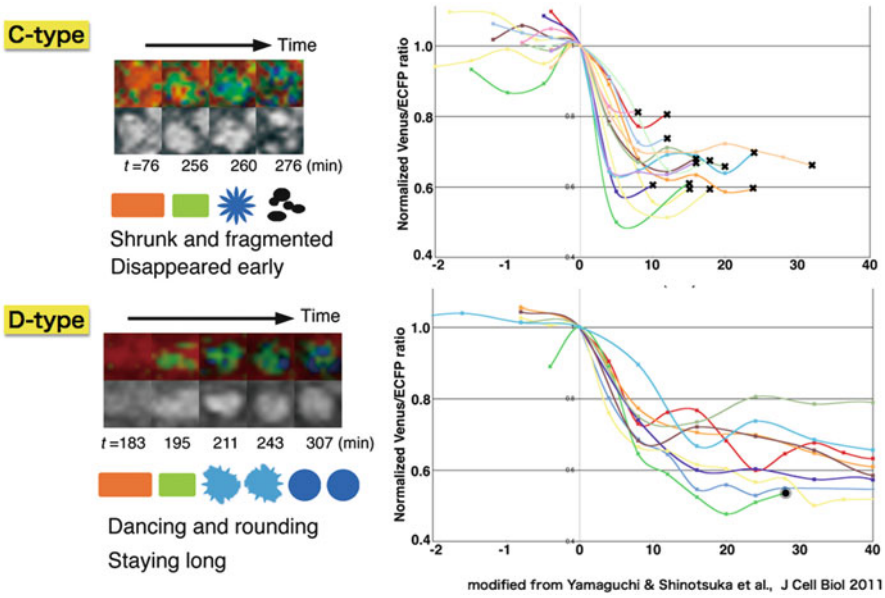

Fig. 11.6 *Left:* Features of caspase activation in C-type and D-type apoptotic cells during cranial NTC. *Right*: Caspase activation kinetics measured with SCAT3 Venus/ECFP ratio in C-type and D-type. Rapid and intense activation of caspases in C-type apoptotic cells resulted in cell fragmentation within about 20 min, whereas relatively mild activation of caspase occurred in D-type and did not lead to cell fragmentation but to rounding of the cells. © *Yamaguchi and Shinotsuka et al.,* (2011)

Another advantages of using SCAT3 other than detecting apoptotic cells is that it enables kinetic measurement of caspase activation by changes of the V/C fluorescence ratio, enabling temporal analysis of the cell dying process starting from caspase activation. This analysis indeed revealed that the C- and D-type cells differed in their kinetics of caspase activity; in C-type cells, the V/C fluorescence ratio decreased quickly in ~10 min, after which the cells underwent cell fragmentation in the following 10–20 min. Thus, in C-type cells, the process from caspase activation to cell fragmentation is very rapid (Fig. 11.6). In contrast, D-type cells exhibited a slower initial decline in the V/C fluorescence ratio, taking ~30 min (Fig. 11.6). The D-type cells never underwent fragmentation.

A difference in activated caspases may explain the mechanism responsible for this kinetic difference between C-type and D-type. Immunohistochemical analysis of fixed embryos indicated that C-type cells had activated caspase-3, whereas D-type cells contained activated caspase-7 in addition to activated caspase-3. It is known that the cleaving (DEVDase) activity of caspase-7 against various substrate peptides including SCAT3 is generally lower than caspase-3 (Walsh et al. 2008). It is possible that the slow kinetics of the V/C fluorescence ratio decline in D-type cells are the result of the activation of caspase-7 in these cells. The activated caspase-7 in D-type cells may compete with caspase-3 for its substrates, reducing the

efficiency of substrate cleavage that otherwise enables the rapid execution of apoptotic change. Thus, the milder caspase activity in the D-type cells might give them time to cleave sufficient amounts of caspase substrates to secrete/expose a "find-me signal," "eat-me signal," or other signals such as growth-promoting signals, before they are eliminated (Grimsley and Ravichandran 2003).

In addition to the supposed delay in the apoptotic process, the D-type apoptotic cells arising from the neural ridge in mammals might be beneficial for the smooth flipping of the neural ridge in a physical manner. Because extrusion of apoptotic D-type cells from the neural ridge resembles behaviors of apoptotic dying cells in fly dorsal closure mentioned in Sect. 11.4, they may contribute to a generating force that promotes either the bending of the neural ridge or the closure of the MHNP, or both.

11.6 Perspective

Recent studies have revealed that cells can choose multiple pathways for their death (Degterev and Yuan 2008; Kroemer et al. 2009). Even when apoptosis is prevented, other forms of cell death represented by caspase-independent cell death and necroptosis can still occur, even though apoptotic cell death is important for the effective clearance of cell debris, which helps maintain immune tolerance and tissue homeostasis (Elliott and Ravichandran 2010). In addition, apoptotic cell debris can also be a cue for muscle cell differentiation and maturation in vitro (Hochreiter-Hufford et al. 2013). In most other developmental processes, however, the mechanism and significance of choosing one form of cell death over another remain to be elucidated (Clarke 1990). Our live-imaging analysis of apoptosis and morphogenesis using SCAT3 transgenic mice distinguished C-type and D-type apoptotic cells that differ in the major active caspases and regional distribution in the closing neural tube. The observation that apoptosis delayed the cranial NTC progression (rostral closure I and caudal closure II) confirmed that apoptosis is a critical cellular event for NTC in the cranial region.

The kinetic analysis of apoptosis during NTC with a live-imaging at tissue and single-cell levels revealed new aspects of NTC regulation. Hundreds of mouse mutants showing NTDs have contributed in revealing the cellular and molecular steps involved in NTC (Copp and Greene 2010; Copp et al. 2003). For example, a disturbance in PCP signaling causes convergence and extension defects that perturb the apposition of the neural ridges, resulting in NTDs in the mouse and other vertebrate models (Wallingford 2006; Wallingford and Harland 2002). In many other mutant cases, however, the mechanistic link between the genetic mutation and NTD remains to be elucidated. Owing to recent technical advances in molecular engineering and imaging devices, the number of reporter genes available for visualizing signaling activity in vivo is increasing (Aoki et al. 2012). Our approach of using SCAT3 transgenic mice to examine caspase activation and apoptosis during NTC is a pioneering study for application of such reporters to NTC analysis.

References

Aoki K, Komatsu N, Hirata E, Kamioka Y, Matsuda M (2012) Stable expression of FRET biosensors: a new light in cancer research. Cancer Sci 103:614–619

Chera S, Ghila L, Dobretz K, Wenger Y, Bauer C, Buzgariu W, Martinou JC, Galliot B (2009) Apoptotic cells provide an unexpected source of Wnt3 signaling to drive hydra head regeneration. Dev Cell 17(2):279–289. doi:10.1016/j.devcel.2009.07.014, pii: S1534-5807(09)00298-6

Clarke PG (1990) Developmental cell death: morphological diversity and multiple mechanisms. Anat Embryol 181(3):195–213

Copp AJ, Greene ND (2010) Genetics and development of neural tube defects. J Pathol 220(2):217–230

Copp AJ, Greene ND, Murdoch JN (2003) The genetic basis of mammalian neurulation. Nat Rev Genet 4(10):784–793

Degterev A, Yuan J (2008) Expansion and evolution of cell death programmes. Nat Rev Mol Cell Biol 9:378–390

Elliott MR, Ravichandran KS (2010) Clearance of apoptotic cells: implications in health and disease. J Cell Biol 189(7):1059–1070. doi:10.1083/jcb.201004096

Fuchs Y, Steller H (2011) Programmed cell death in animal development and disease. Cell 147(4):742–758. doi:10.1016/j.cell.2011.10.033

Grimsley C, Ravichandran KS (2003) Cues for apoptotic cell engulfment: eat-me, don't eat-me and come-get-me signals. Trends Cell Biol 13(12):648–656

Haigo SL, Hildebrand JD, Harland RM, Wallingford JB (2003) Shroom induces apical constriction and is required for hingepoint formation during neural tube closure. Curr Biol 13(24): 2125–2137

Hochreiter-Hufford AE, Lee CS, Kinchen JM, Sokolowski JD, Arandjelovic S, Call JA, Klibanov AL, Yan Z, Mandell JW, Ravichandran KS (2013) Phosphatidylserine receptor BAI1 and apoptotic cells as new promoters of myoblast fusion. Nature (Lond) 497(7448):263–267. doi:10.1038/nature12135

Kroemer G, Galluzzi L, Vandenabeele P, Abrams J, Alnemri ES, Baehrecke EH, Blagosklonny MV, El-Deiry WS, Golstein P, Green DR, Hengartner M, Knight RA, Kumar S, Lipton SA, Malorni W, Nunez G, Peter ME, Tschopp J, Yuan J, Piacentini M, Zhivotovsky B, Melino G (2009) Classification of cell death: recommendations of the Nomenclature Committee on Cell Death 2009. Cell Death Differ 16(1):3–11. doi:10.1038/cdd.2008.150, pii: cdd2008150

Kuida K, Zheng TS, Na S, Kuan C, Yang D, Karasuyama H, Rakic P, Flavell RA (1996) Decreased apoptosis in the brain and premature lethality in CPP32-deficient mice. Nature (Lond) 384(6607):368–372. doi:10.1038/384368a0

Kuida K, Haydar TF, Kuan CY, Gu Y, Taya C, Karasuyama H, Su MS, Rakic P, Flavell RA (1998) Reduced apoptosis and cytochrome c-mediated caspase activation in mice lacking caspase 9. Cell 94(3):325–337, pii: S0092-8674(00)81476-2

Li F, Huang Q, Chen J, Peng Y, Roop D, Bedford J, Li C (2010) Apoptotic cells activate the "phoenix rising" pathway to promote wound healing and tissue regeneration. Sci Signal 3(110):ra13

Massa V, Savery D, Ybot-Gonzalez P, Ferraro E, Rongvaux A, Cecconi F, Flavell R, Greene ND, Copp AJ (2009) Apoptosis is not required for mammalian neural tube closure. Proc Natl Acad Sci USA 106(20):8233–8238

Massarwa R, Niswander L (2013) In toto live imaging of mouse morphogenesis and new insights into neural tube closure. Development (Camb) 140(1):226–236. doi:10.1242/dev.085001

Miura M (2011) Active participation of cell death in development and organismal homeostasis. Dev Growth Differ 53:125–136

Nonomura K, Yamaguchi Y, Hamachi M, Koike M, Uchiyama Y, Nakazato K, Mochizuki A, Sakaue-Sawano A, Miyawaki A, Yoshida H, Kuida K, Miura M (2013) Local apoptosis modulates early mammalian brain development through the elimination of morphogen-producing cells. Deve Cell 27:621–634

Pyrgaki C, Trainor P, Hadjantonakis A, Niswander L (2010) Dynamic imaging of mammalian neural tube closure. Dev Biol 344:941–947

Takemoto K, Nagai T, Miyawaki A, Miura M (2003) Spatio-temporal activation of caspase revealed by indicator that is insensitive to environmental effects. J Cell Biol 160(2):235–243. doi:10.1083/jcb.200207111, pii: jcb.200207111

Toyama Y, Peralta XG, Wells AR, Kiehart DP, Edwards GS (2008) Apoptotic force and tissue dynamics during *Drosophila* embryogenesis. Science 321(5896):1683–1686

Wallingford J (2006) Planar cell polarity, ciliogenesis and neural tube defects. Hum Mol Genet 15(Special No 2):R227–R234

Wallingford J, Harland R (2002) Neural tube closure requires Dishevelled-dependent convergent extension of the midline. Development (Camb) 129:5815–5825

Walsh JG, Cullen SP, Sheridan C, Luthi AU, Gerner C, Martin SJ (2008) Executioner caspase-3 and caspase-7 are functionally distinct proteases. Proc Natl Acad Sci USA 105(35): 12815–12819. doi:10.1073/pnas.0707715105, pii: 0707715105

Weil M, Jacobson MD, Raff MC (1997) Is programmed cell death required for neural tube closure? Curr Biol 7(4):281–284, pii: S0960-9822(06)00125-4

Yamaguchi Y, Miura M (2012) How to form and close the brain: insight into the mechanism of cranial neural tube closure in mammals. Cell Mol Life Sci 70(17):3171–86. doi:10.1007/s00018-012-1227-7

Yamaguchi Y, Shinotsuka N, Nonomura K, Takemoto K, Kuida K, Yosida H, Miura M (2011) Live imaging of apoptosis in a novel transgenic mouse highlights its role in neural tube closure. J Cell Biol 195:1047–1060. doi:10.1083/jcb.201104057

Yoshida H, Kong YY, Yoshida R, Elia AJ, Hakem A, Hakem R, Penninger JM, Mak TW (1998) Apaf1 is required for mitochondrial pathways of apoptosis and brain development. Cell 94(6): 739–750

Part IV
Heterologous Tissue Interactions to Generate a Function

Chapter 12
Secondary Smad1/5/8-Dependent Signaling Downstream of SHH Determines Digit Identity

Takayuki Suzuki

Abstract Digit identity determination is a longstanding question of developmental biology. Through recent embryological and molecular studies, molecular mechanisms that underlie the determination of morphological identity of the digits have been revealed to a certain extent. The first insight into the problem was provided by the discovery of the zone of polarizing activity (ZPA) and its responsible signaling molecule, sonic hedgehog (SHH). However, SHH signaling does not directly determine digit identity. We identified interdigit mesenchymes as the source of signals that activate SMAD1/5/8 in the phalanx-forming region (PFR) cells in a way reflecting the earlier SHH signaling. PFR is located immediately distal to the condensed cartilage of the digit primordium and serves as the zone of cartilage differentiation, and the differential strength of SMAD1/5/8 activation in the PFR was correlated with digit identity.

Keywords Chick • Digit identity • Interdigit tissue • Phalanx-forming region • SMAD1/5/8 activity

12.1 Morphological Digit Identity

Humans have five distinct digits along the anterior–posterior (thumb to little finger) limb axis. In our hands and feet, the thumb/big toe is the widest and shortest among the five digits and has only two phalanges, whereas the little finger is the narrowest and smaller than the middle three digits, and the posterior four digits have three phalanges. These morphological features of individual digits represent "digit identity." To elucidate the mechanisms that endow these morphological features to the digits,

T. Suzuki (✉)
Division of Biological Science, Graduate School of Science,
Nagoya University, Nagoya, Japan
e-mail: suzuki.takayuki@j.mbox.nagoya-u.ac.jp

H. Kondoh and A. Kuroiwa (eds.), *New Principles in Developmental Processes*,
DOI 10.1007/978-4-431-54634-4_12,

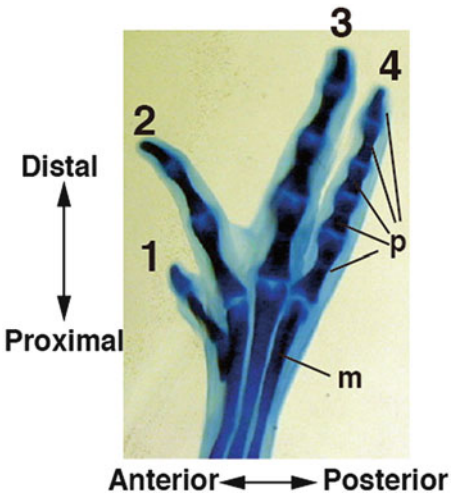

Fig. 12.1 Skeletal pattern of the digits in the chick leg. Four leg digits each have a unique size, shape, and phalange number, two to five for digits *1–4*

we have employed the chick hindlimb bud as a model system. The chick foot has four digits, 1–4, which are easily distinguished (Fig. 12.1). Three major morphological criteria, the number, size, and shape of the phalanges, were used to identify digits that developed under experimental conditions (Suzuki et al. 2008). In the chick foot, digit 1 has two phalanges, digit 2 has three, digit 3 has four, and digit 4 has five. The shapes of the phalanges are clearly different when the cartilages are stained by Victoria blue (Suzuki et al. 2008). Phalanges of digit 4 are shorter than phalanges of other digits. In addition, in all digits, more distally located phalanges are smaller than those of more proximal phalanges. In this way, the number, size, and shape of cartilage in the forming phalanges provide the guide to judge digit identity.

12.2 Involvement of the Zone of Polarizing Activity (ZPA) in the Anteroposterior Differences of the Digits

Hands and feet develop from a cell population of lateral plate mesoderm, called the limb bud, which grows out from the body wall. If we excise cells of posterior edge of the limb bud and graft them to the anterior side, mirror-imaged duplication of posterior digits develops at the grafted side (Saunders and Gasseling 1968). This tissue area has the activity to provide the posterior limb bud character and is called the zone of polarizing activity (ZPA) (Saunders 1972). Later studies have shown that a secreted protein, sonic hedgehog (SHH), expressed in ZPA, provides the limb bud with the posterior character, and hence allows development of digits with posterior identities (Riddle et al. 1993). The effect of SHH protein is concentration- and duration time dependent, that is, use of higher concentration of SHH and longer exposure to SHH promote development of digits with more posterior identity

(Yang et al. 1997). For this reason, SHH was once thought to be a morphogen, which is a secreted molecule-forming gradient in the developing tissues and specifies different cell types in a dose-dependent manner that directly determines the digit identity via its anteroposterior gradient in the limb bud. Transcription factors GLI1, -2, and -3 function downstream of SHH signaling. *Gli3*$^{-/-}$ mice show polydactyly with all digits having posterior-type digit characters, yet with abnormal size and shape of phalanges not typical of a single digit (Litingtung et al. 2002). *Shh*$^{-/-}$;*Gli3*$^{-/-}$ mice also develop a polydactylous hand identical to *Gli3*$^{-/-}$. This result indicates that limbs have potential to form digits without relying on the SHH signaling (Litingtung et al. 2002).

12.3 "Memory" of SHH Signal Strength Contributes to Digit Identity

Digits can form without *Shh*, but SHH signaling affects digit characters in a concentration- and duration time dependent manner. However, the effect of SHH signaling is indirect, as in the chick foot development *Shh* expression is turned off before stage 26 when the digit primordia begin to develop (Dunn et al. 2011). Moreover, when *Shh* expression level was lowered from early limb bud stage by genetic means, digit number was reduced, but individual digits had clear identity (Scherz et al. 2007). These observations suggest the model that limb bud cells retain a molecular "memory" of SHH signaling at the early limb bud stage (Harfe et al. 2004) and that this memory contributes to digit identity more directly than SHH signaling.

12.4 The Interdigit Tissues "Memorize" Earlier SHH Signaling

When interdigit (ID) tissue 2 (ID2) located between digit primordia 2 and 3 (Fig. 12.2a, b), was microsurgically removed, digit 2 developed into digit 1 (Fig. 12.2c, d). Similarly, removal of ID3 caused digit primordium 3 to develop as digit 2 (Fig. 12.2c, e) (Dahn and Fallon 2000). This finding indicates that digit identity has not been determined when the primordia of digit 2 and 3 start to develop, and that activities of ID tissues 2 and 3 are necessary for the digit identities 2 and 3, respectively. In addition, when digit 3 primordium was implanted in the ID2 region, the implanted digit 3 primordium was transformed into digit 2. Conversely, when digit 2 primordium was implanted in the ID3 region, the implanted digit 2 primordium was transformed into digit 3 (Fig. 12.2f–h). These results indicate that the interdigit tissue transmits information to the digit primordia for gaining identity under the influence of earlier SHH signaling.

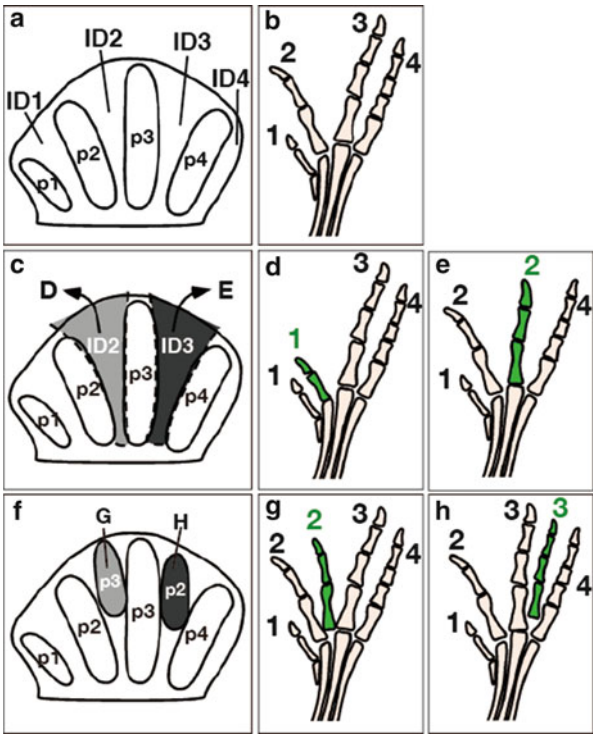

Fig. 12.2 Interdigit tissues contribute to the determination of morphological digit identity. **a** Leg autopod region of normal chick embryos. *p1*, *p2*, *p3*, and *p4*, primordia for digits 1, 2, 3, and 4, respectively; *ID1*, *ID2*, *ID3*, and *ID4*, interdigit tissues 1, 2, 3 and 4, respectively. **b** Normal digit pattern of the chick embryonic leg at stage (St.) 36. **c**, **f** Schematic drawings of microsurgery in the chick leg bud. **c** When ID2 (*D*) or ID3 (*E*) was removed, digit 2 developed as digit 1 (**d**) and digit 3 developed as digit 2 (**e**). **f** When digit 3 primordium (p3) or digit 2 primordium (p2) was implanted in the *ID2* or *ID3* region, they were transformed and developed as digit 2 (**g**) or digit 3 (**h**). The transformed digits are highlighted in green. Anterior is to the left for all panels

12.5 Inquiry into the Nature of the Molecular "Memory" of Earlier SHH Signaling

A simplest model drawn from the results of ID tissue removal experiments is that digit identity is not given to the digit primordia at the beginning, whereas interdigit tissues provide information to digit primordial for their individual identities. By removing interdigit tissues individually at different developmental stages, it was found that the characters (identity) of the digits were determined by stage (St.) 27^{-}, 29^{-}, 30, and 30, for digits 4, 3, 2, and 1, respectively (Suzuki et al. 2008). Removal of interdigit tissues after these stages did not alter the digit characters. As *Shh*

expression is turned off after St. 26, earlier SHH signaling must be in "memory" of certain tissues to more directly determine the digit identity.

When a bead soaked with the bone morphogenetic protein (BMP) antagonist, Noggin, was implanted in ID3, digit 3 was transformed to digit 2, similar to the case of ID3 removal (Dahn and Fallon 2000). Therefore, BMP family proteins were candidate molecules involved in the determination of digit identity. In the interdigit tissues, *Bmp2/4/7* are expressed (Suzuki et al. 2004). However, compound knockout mice with ablation of *Bmp2/4/7* genes specifically in the limb buds did not alter digit characters (Bandyopadhyay et al. 2006). No anteroposterior gradient of expression level was observed in the interdigit tissues for *Bmp2*, *-4*, or *-7* (Suzuki et al. 2004), suggesting participation of other BMP family proteins or graded responses in downstream events. Therefore, other BMP-related molecules are now considered to be involved in the signaling from the interdigit tissues. Strong candidates are GDF5 and GDF6, which are also expressed in the joint region and interdigit tissues. Interestingly, the GDF5 signal is mediated by BMPR1B, and inhibited by Noggin (Seemann et al. 2005; Merino et al. 1999). In addition, $Gdf5^{-/-}$ mice show a similar phalangeal phenotype to $Bmpr1b^{-/-}$ mice; specifically, the proximal and middle phalanges are fused and reduced to a cartilage nodule (Baur et al. 2000; Yi et al. 2000; Settle et al. 2003). Thus, it is possible that Noggin-sensitive members of the BMP family proteins include GDFs that act singly or in combination to determine the digit identity.

12.6 The Target Tissue of Interdigit-Derived Signals

Figure 12.3 illustrates the local tissue arrangements of the distal portion of limb bud that later develops into the autopod (hand and foot). The chick foot autopod consists of four digital rays (DRs), alternating with mesenchymal interdigit tissues. A DR is composed of the proximal condensed (cartilaginous) digit primordium, the noncondensed vascularized mesenchyme, and the distalmost avascular mesenchyme underlying the apical ectodermal ridge (AER).

SMAD1/5/8 are phoshorylated in response to BMP signaling. Phosphorylated SMAD1/5/8 (p-SMAD1/5/8), as detected by immunohistochemistry, was found in the tissue immediately distal to condensed digit primordium in the forming autopod, called the phalanx-forming region (PFR). PFR corresponds to the cell population in the vascularized mesenchyme undergoing condensation and expressing *Sox9* and *Bmpr1b*. The PFR cells dynamically turn over with continuous inflow of cells from avascular mesenchyme underneath the AER and with continuous cell exit by condensation, supporting cartilage elongation. Cells in the PFR receive signaling from the interdigit tissues and develop into a particular phalanx by regulation of cartilage condensation. p-SMAD1/5/8 is also reported for the PFR in mouse autopods (Witte et al. 2010).

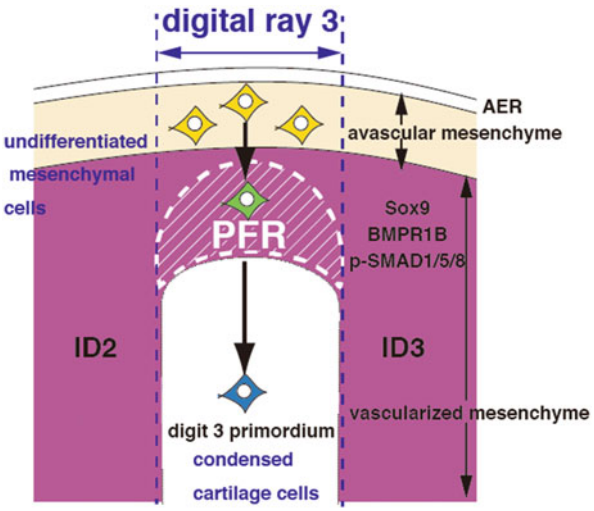

Fig. 12.3 Tissue organization of a digital ray in the developing autopod, taking digital ray 3 as an example. Digital ray 3 is placed between interdigit tissue 2 (*ID2*) and interdigit tissue 3 (*ID3*). A digital ray is composed of the proximal cartilaginous digit primordium, the noncondensed vascularized mesenchyme, and the distalmost avascular mesenchyme underlying the apical ectodermal ridge (*AER*). A phalanx-forming region (*PFR*) of vascularized mesenchyme is located immediately distal to the condensed cartilage of the digit primordium, expresses *Sox9* and *Bmpr1b*, and has the phosphorylated (activated) form of SMAD1/5/8. The PFR cells are in transition from uncondensed mesenchymal cells to condensed cartilaginous cells. Cell loss from the PFR by cartilage differentiation is supplemented by the continuous inflow of cells from the avascular mesenchyme underneath the AER

12.7 A Mechanism Involved in the Differential Signaling by the Interdigit Tissues

The results of ID tissue removal experiments suggested that a more posterior ID tissue provides digital rays with a posterior digit identity, which is in accord with the earlier SHH signal gradient that is higher toward the posterior side. The secondary signal involving BMPs, which act in reflection of the SHH signal memory, would be in gradient, the highest in ID4 and lowest in ID1.

We developed a system to report the SMAD1/5/8 activity that quantitatively reflects BMP-related signaling. We fused a *Xenopus Vent2* promoter that responds to SMAD-mediated signaling to the firefly luciferase gene, and inserted this into a RCAN retrovirus vector with type A envelope. To normalize firefly luciferase activity in infected cells, we inserted CMV promoter-derived *Renilla* luciferase gene into RCAN retrovirus with type B envelope, which guarantees coinfection in the same cells because of the possession of different envelope types. After infection of these viruses in the limb bud tissues with these viruses, we isolated the PFR cells of digits 1, 2, 3, and 4 at different developmental stages, from St. 25 to St. 30. Taking

advantage of this in vivo reporter system, we could quantify SMAD1/5/8 activity level in the PFR of individual digits. We found that among digits 1–3, SMAD1/5/8 activity in the FPR was the highest in digit 3, followed by digit 2 and digit 1, in that order. However, the SMAD1/5/8 activity was not the highest in the digit 4 PFR at all stages; it was the highest only at St. 25 and St. 26 when digit 4 starts to develop. These results are consistent with a BMP signal gradient model for interdigit tissues in particular for PFRs 1–3. Indeed, when we inserted the ID3 tissue on the posterior side of digital ray 1 (DR1), digit 1 was completely transformed to digit 3. In this experiment, the digit 1 PFR showed a high SMAD1/5/8 activity level comparable to digit 3 PFR. This result indicates that if the PFR cells activate SMAD1/5/8 to a higher level, the digit acquires the identity of a more posterior digit. Further, when ID4 (actually external to digit 4) was removed, digit 4 PFR exhibited higher SMAD1/5/8 activity, and digit 4 was transformed to digit 3. This observation suggests that the effect of ID4 is to lower the SMAD1/5/8 activity so that the condition for digit 4 development is met.

12.8 The Current Model of Digit Identity Determination

In the morphogen gradient model, digit primordium is formed as a target tissue of the SHH, and each digit primordium already has positional information to become a particular digit; that is, digit identity has been already decided at the limb bud stage. If the morphogen gradient of SHH works in a concentration- and time dependent fashion, digit identity should be changed to the anterior digit if SHH signaling was inhibited. However, conversely, mouse digits were not transformed to other anterior digits when the timing of *Shh* expression and activity was reduced (Zhu et al. 2008; Scherz et al. 2007). In addition, *Shh* expression in the chick foot is undetectable after St. 26 (Dunn et al. 2011) when digit primordium starts to develop. Therefore, we hypothesized that secondary signaling downstream of SHH directly determines individual digit identity in the autopod.

Our experimental results suggested that the secondary signaling has differential intensities that depend on the anteroposterior positioning of the interdigit tissues, and this difference in signaling intensity determines digit identity (Dahn and Fallon 2000, Suzuki et al. 2008). Further, we identified PFR positioned distally to the digit primordium as the tissue site of receiving signals from the interdigit tissues (Fig. 12.4). At an early stage of autopod development, the PFR cells start as vascularized, noncondensed mesenchyme located immediately distal to the already existing condensed cartilage of metatarsal. The PFR cells express *Sox9* and *Bmpr1b*, activate SMAD1/5/8 by phosphorylation, and themselves serve as precursors for the cartilage. As these cells condense to form cartilage, the PFR is replenished with formerly more distally located avascular mesenchymal cells underlying the AER. In this dynamic sequence of events, the PFR cells are exposed to signals from the interdigit tissues (yellow arrows in Fig. 12.4) that contribute to endow their digit identities (i.e., number, size, and shape of phalanges). Thus, digits have not gained

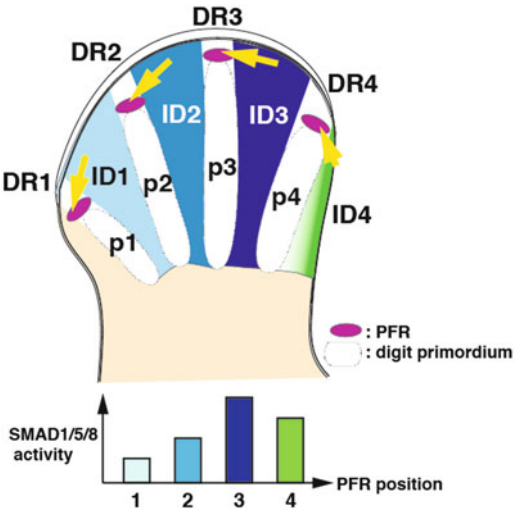

Fig. 12.4 Model of determination of the morphological identity of the digits involving signaling from interdigit tissues. Digital rays (DR1, -2, -3, and -4) each have a PFR shown as an *ellipse* distal to the condensed cartilage of the digit primordium (p1, -2, -3, and -4). PFR cells receive signals from interdigit tissues with domination by the signal from the posterior interdigit (ID1, -2, -3, -4) (shown by *yellow arrows*). Each PFR activates SMAD1/5/8 to a level in response to the strength of signals from the adjoining interdigit tissues and undergoes morphological development unique to the digit

their digit identities when the digital rays start to develop. During development of phalanges, the interdigit tissues send BMP-related signals to the PFR cells for the phalange to undergo morphogenesis unique to a particular digit. An important issue is how PFR cells respond to interdigit signaling and give rise to particular phalangeal morphology including number, size, and shape. In summary, our PFR model assumes that SMAD1/5/8 activation level in the PFR, which reflects the BMP-related signals derived from the interdigit tissues, determines the digit identity.

A related problem is how each digit position is determined. It is suggested that the cumulative activity of HoxA13/HoxD11-13 is involved in the determination of the digit number (Sheth et al. 2012). Usually *Gli3*$^{-/-}$ mice have 6–8 digits (Litingtung et al. 2002). Interestingly, reduction of *hoxA13*/*hoxd11-13* gene expression levels caused more severe polydactyly than *Gli3*-null mutants; for example, *hoxA13*$^{+/-}$;*hoxd11-13*$^{-/-}$;*Gli3*$^{-/-}$ mice show a wider autopod along the anteroposterior axis and have as many as 13 digits that are thinner and narrower than in the wild type. The authors suggested that the reaction–diffusion-type system formulated by Turing (1952) is involved in this process, although the molecular mechanisms downstream of *hoxA13*/*hoxd11-13* genes are still unknown. Previously, it was thought that *Hox* genes are involved in digit identity determination because of nested expression patterns along the digit primordia (Morgan et al. 1992). However, it is likely that cumulative activity of HoxA13/HoxD11–13 regulates digit number

rather than determination of digit identity. It is possible that SHH signaling initially determines the size of the digit-forming field along the anteroposterior axis, and then digit number and positions are determined reflecting the autopod width by the reaction–diffusion-type system downstream of HoxA13/HoxD11–13 activities. Digit-forming positions assign the identity of later developing digits, because each digit PFR receives different levels of Smad1/5/8-activating signaling downstream of SHH, which are derived from posterior-positioned interdigit tissues. Thus, formation of digit primordia at the correct position is critical to receive precise position-dependent information from interdigit tissues and to gain correct digit identity.

Unifying the mechanisms of digit positioning and interdigit activity-dependent digit identity establishment will provide an overall view concerning how the digits are formed in the autopods.

References

Bandyopadhyay A, Tsuji K, Cox K, Harfe BD, Rosen V, Tabin CJ (2006) Genetic analysis of the roles of BMP2, BMP4, and BMP7 in limb patterning and skeletogenesis. PLoS Genet 2:e216

Baur ST, Mai JJ, Dymecki SM (2000) Combinatorial signaling through BMP receptor IB and GDF5: shaping of the distal mouse limb and the genetics of distal limb diversity. Development (Camb) 127:605–619

Dahn RD, Fallon JF (2000) Interdigit regulation of digit identity and homeotic transformation by modulated BMP signaling. Science 289:438–441

Dunn IC, Paton IR, Clelland AK, Sebastian S, Johnson EJ, McTeir L, Windsor D, Sherman A, Sang H, Burt DW, Tickle C, Davey MG (2011) The chicken polydactyly (Po) locus causes allelic imbalance and ectopic expression of Shh during limb development. Dev Dyn 240: 1163–1172

Harfe BD, Scherz PJ, Nissim S, Tian H, McMahon AP, Tabin CJ (2004) Evidence for an expansion-based temporal Shh gradient in specifying vertebrate digit identities. Cell 118:517–528

Litingtung Y, Dahn RD, Li Y, Fallon JF, Chiang C (2002) Shh and Gli3 are dispensable for limb skeleton formation but regulate digit number and identity. Nature (Lond) 418:979–983

Merino R, Macias D, Gañan Y, Economides AN, Wang X, Wu Q, Stahl N, Sampath KT, Varona P, Hurle JM (1999) Expression and function of GDF-5 during digit skeletogenesis in the embryonic chick leg bud. Dev Biol 206:2161–2170

Morgan BA, Izpisúa-Belmonte JC, Duboule D, Tabin CJ (1992) Targeted misexpression of Hox-4.6 in the avian limb bud causes apparent homeotic transformations. Nature 358:236–239

Riddle RD, Johnson RL, Laufer E, Tabin C (1993) Sonic hedgehog mediates the polarizing activity of the ZPA. Cell 75:1401–1416

Saunders JW Jr (1972) Developmental control of three-dimensional polarity in the avian limb. Ann N Y Acad Sci 25:29–42

Saunders JW Jr, Gasseling MT (1968) Ectodermal-mesenchymal interactions in the origin of limb symmetry. In: Fleischmajer R, Billingham RE (eds) Epithelial–mesenchymal interactions. William & Wilkins, Baltimore, pp 78–97

Scherz PJ, McGlinn E, Nissim S, Tabin CJ (2007) Extended exposure to Sonic hedgehog is required for patterning the posterior digits of the vertebrate limb. Dev Biol 308:343–354

Seemann P, Schwappacher R, Kjaer KW, Krakow D, Lehmann K, Dawson K, Stricker S, Pohl J, Plöger F, Staub E, Nickel J, Sebald W, Knaus P, Mundlos S (2005) Activating and deactivating mutations in the receptor interaction site of GDF5 cause symphalangism or brachydactyly type A2. J Clin Invest 115:2373–2381

Settle SH Jr, Rountree RB, Sinha A, Thacker A, Higgins K, Kingsley DM (2003) Multiple joint and skeletal patterning defects caused by single and double mutations in the mouse Gdf6 and Gdf5 genes. Dev Biol 254:116–130

Sheth R, Marcon L, Bastida MF, Junco M, Quintana L, Dahn R, Kmita M, Sharpe J, Ros MA (2012) Hox genes regulate digit patterning by controlling the wavelength of a Turing-type mechanism. Science 338:1476–1480

Suzuki T, Takeuchi J, Koshiba-Takeuchi K, Ogura T (2004) Tbx genes specify posterior digit identity through Shh and BMP signaling. Dev Cell 6:43–53

Suzuki T, Hasso SM, Fallon JF (2008) Unique SMAD1/5/8 activity at the phalanx-forming region determines digit identity. Proc Natl Acad Sci USA 105:4185–4190

Turing AM (1952) The chemical basis of morphogenesis. Phil Trans R Soc Lond B 237(641): 37–72

Witte F, Chan D, Economides AN, Mundlos S, Stricker S (2010) Receptor tyrosine kinase-like orphan receptor 2 (ROR2) and Indian hedgehog regulate digit outgrowth mediated by the phalanx-forming region. Proc Natl Acad Sci USA 107:14211–14216

Yang Y, Drossopoulou G, Chuang PT, Duprez D, Marti E, Bumcrot D, Vargesson N, Clarke J, Niswander L, McMahon A, Tickle C (1997) Relationship between dose, distance and time in Sonic Hedgehog-mediated regulation of anteroposterior polarity in the chick limb. Development (Camb) 124:4393–4404

Yi SE, Daluiski A, Pederson R, Rosen V, Lyons KM (2000) The type I BMP receptor BMPRIB is required for chondrogenesis in the mouse limb. Development (Camb) 127:621–630

Zhu J, Nakamura E, Nguyen MT, Bao X, Akiyama H, Mackem S (2008) Uncoupling Sonic hedgehog control of pattern and expansion of the developing limb bud. Dev Cell 14:624–632

Chapter 13
Deciphering Cerebellar Neural Circuitry Involved in Higher Order Functions Using the Zebrafish Model

Masahiko Hibi and Takashi Shimizu

Abstract The central nervous system (CNS) in vertebrate species is one of the most complex structures in the animal body, containing enormous numbers of neurons that connect to each other through their axons and dendrites to carry out complex tasks. Recent comparative anatomical and functional studies of neural circuits in different vertebrate CNS reveal that, although the structure of the CNS is simpler in lower vertebrates (such as teleosts) than that in mammals, the basic organization of neural circuitry in the CNS is conserved and the formation of neural circuits is controlled by similar or identical mechanisms. In this chapter, we focus on the cerebellum, which is derived from the dorsal part of the most anterior hindbrain and is involved in motor control and higher cognitive/emotional functions. We describe the structure and development processes of the cerebellar neurons and neural circuits in zebrafish and compared them with those in mammals. A variety of techniques and resources is available for zebrafish research on neural development and function, including classical reverse genetics, transgenics, and optogenetics. We discuss how studies on neural circuitry in zebrafish provide us with a general scheme of the formation and function of cerebellar neural circuitry in vertebrate species.

Keywords Cerebellum • Granule cells • Learning • Neural circuitry • Purkinje cells • Zebrafish

M. Hibi (✉) • T. Shimizu
Laboratory of Organogenesis and Organ Function, Bioscience and Biotechnology Center, Nagoya University, Furo, Chikusa, Nagoya, Japan
e-mail: hibi@bio.nagoya-u.ac.jp

H. Kondoh and A. Kuroiwa (eds.), *New Principles in Developmental Processes*,
DOI 10.1007/978-4-431-54634-4_13, © Springer Japan 2014

13.1 Introduction

The cerebellum is a structure derived from the dorsal part of the most anterior hindbrain in the vertebrate central nervous system (CNS). The major function of the cerebellum is considered to be motor control. The cerebellum, however, has connections to the telencephalon and is also implicated in higher cognitive and emotional functions (Ito 2005, 2006, 2008). Compared to neural circuitry in the dorsal telencephalon, the cerebellar neural circuitry has simpler organization, in which two inputs from outside the cerebellum are integrated in the cerebellar neurons to generate outputs (Bell 2002; Bell et al. 2008; Ito 2002a, b). This simple organization has attracted many scientists, who have interest in the roles and development of the cerebellar neural circuitry. However, how it develops and functions is not yet fully understood. Defects in the cerebellum and cerebellar neural circuit in human diseases such as spinocerebellar ataxia cause abnormal motor coordination (Koeppen 2005). Abnormalities in cerebellar neural circuitry have been shown to be involved in pathogenesis of psychological disorders (Fatemi et al. 2002; Tsai et al. 2012). Therefore, elucidation of the function and formation of the cerebellar neural circuitry does not only lead to our better understanding of the brain functions but may also provide some clues for revealing the pathogenesis of related human diseases and establishing therapeutic strategies against these.

13.2 Anatomy

13.2.1 Cerebellar Neurons and Layer Structure

Histological organization of the cerebellar neural circuitry has been well known for over a century, since Ramón y Cajal sketched a section of the chick cerebellum with the Golgi staining method (Sotelo 2008). Comparative anatomical studies revealed basic similarities and species-dependent variations in the cerebellum structure among the vertebrates (Butler and Hodos 1996). The cerebellum contains several types of neurons, which are categorized according to their function (Altman and Bayer 1997; Butler and Hodos 1996) (Fig. 13.1a). The excitatory neurons use glutamate as their major neurotransmitter (glutamatergic neurons): they include the granule cells (GCs), unipolar blush cells, and excitatory projection neurons, which are large neurons in the deep cerebellar nuclei (DCN) in mammals or eurydendroid cells in teleosts. The inhibitory neurons use γ-aminobutyric acid (GABA) and/or glycine (simply called GABAergic neurons), and include Purkinje cells (PCs), Golgi cells, Lugaro cells, candelabrum cells, basket cells, and small neurons in the DCN (Altman and Bayer 1997; Butler and Hodos 1996; Laine and Axelrad 1994; Sillitoe and Joyner 2007; Voogd and Glickstein 1998). In a rough classification, GCs and PCs play major roles in receiving and processing input information; the projection neurons (large neurons in the DCN or eurydendeoid cells) generate

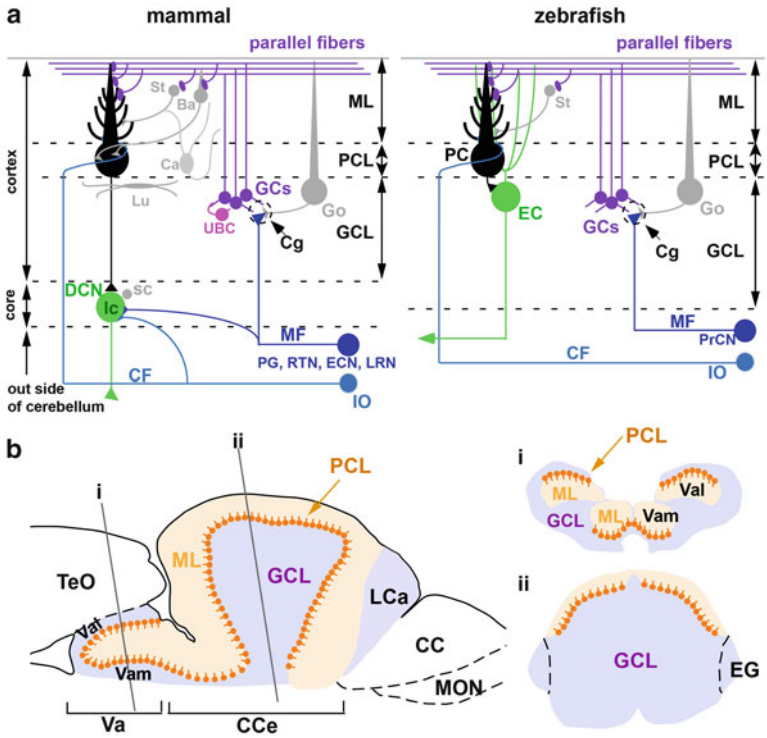

Fig. 13.1 Structure of cerebellum and cerebellar neural circuitry. **a** Schematic representation of cerebellar neural circuitry in mammals and zebrafish. **b** Structure of zebrafish adult cerebellum. Sagittal section image. *i*, *ii* Cross-section images at the levels shown in the *left panel* (*i*, valuvula cerebelli; *ii*, corpus cerebelli). *Ba* basket cell, *Ca* candelabrum cell, *CC* crista cerebellaris, *CCe* corpus cerebelli, *CF* climbing fiber, *Cg* cerebellar glomeruli, *DCN* deep cerebellar nuclei (*lc* large cell, *sc* small cell), *EC* eurydendroid cell (projection neuron), *ECN* external cuneate nuclei, *EG* eminentia granularis, *GCs* granule cells, *GCL* granule cell layer, *Go* Golgi cell, *IO* inferior olive nuclei, *LCa* lobus caudalis cerebelli, *Lu* Lugaro cell, *LRN* lateral reticular nuclei, *MF* mossy fiber, *ML* molecular layer, *PC* Purkinje cell, *PCL* Purkinje cell layer, *PG* pontine gray nuclei, *PrCN* precerebellar nuclei (except IO), *RTN* reticulotegmental nuclei, *St* stellate cells, *Teo* tectum opticum, *UBC* unipolar brush cell, *Va* valvula verebelli, *Vam* medial division of valvula cerebelli, *Val* lateral division of the valvula cerebelli (modified from Hashimoto and Hibi 2012; Hibi and Shimizu 2012)

outputs; and the other neurons (interneurons) function to modify the information transmitted through GCs, PCs, and the projection neurons. In addition to neurons, there are astrocytes, Bergmann glia (radial glia-like astrocytes), and oligodendrocytes in the cerebellum. These cerebellar neurons and glia are arranged in three layers: the molecular layer (ML), Purkinje cell layer (PCL), and granule cell layer (GCL) (Fig. 13.1a, b) from the superficial side. These layers are located over the inner core composed of the white matter (containing myelinated axons) and the DCN in mammals, but there is no white matter or DCN in teleosts. The ML contains dendrites of PCs, axons of GCs, and GABAergic interneurons basket and stellate

cells. The PCL mainly contains the somata of PCs and Bergmann glia, which extend glial processes to the ML and GCL. The GCL contains numerous GCs, eurydendroid cells (in teleosts), and some glutamatergic and GABAergic interneurons. Many of these cerebellar neurons are conserved among vertebrate species; however, a few neuronal types, such as basket cells, are not found in lower vertebrates (Altman and Bayer 1997; Butler and Hodos 1996).

The mammalian cerebellum has ten lobules and each lobule contains the three-layer structure (Altman and Bayer 1997; Butler and Hodos 1996). The teleost cerebellum is composed of three major lobes: the valvula cerebelli (Va, anterior lobe), the corpus cerebelli (CCe, main lobe), and the vestibulo-lateral lobe (caudolateral lobe) that consists of the eminentia granularis (EG) and the lobus caudalis cerebelli (LCa) (Altman and Bayer 1997; Bae et al. 2009; Butler and Hodos 1996; Wullimann et al. 1996) (Fig. 13.1b). In the teleost cerebellum, the anterior and main lobes have the same three-layer structure (ML, PCL, GCL) whereas the caudolateral lobe contains only a GCL.

13.2.2 Cerebellar Neural Circuits

The cerebellar neurons receive excitatory inputs from neurons outside the cerebellum. There are two major afferent inputs, the climbing fibers (CFs) and mossy fibers (MFs) (Fig. 13.1a). The CFs originate exclusively from the contralateral side of inferior olive nuclei (IOs) in the caudoventral hindbrain and innervate the PC dendrites. The MFs originate from neurons in the precerebellar nuclei, including pontine gray (PG) matter nuclei, reticulotegmental nuclei (RTN), the external cuneate nuclei (ECN), and lateral reticular nuclei (LRN), and make synapses with GC dendrites that also contact with Golgi cell axons to form the cerebellar glomeruli. The MF information is conveyed to the dendrites of PCs by the axons of GCs that are aligned parallel to one another (called parallel fibers). The information from CFs and MFs is integrated in the PCs. When the two inputs are simultaneously received by the PCs, a strong CF signal suppresses transmission from parallel fibers by a mechanism called long-term depression (LTD) (Ito 2002a, b, 2006). PCs project their axon to the DCN neurons in mammals and eurydendroid cells in teleosts (also to adjacent PCs, at least at some developmental periods) (Alonso et al. 1992; Altman and Bayer 1997; Butler and Hodos 1996; Meek 1992). In teleosts, eurydendroid cells also receive inputs from GC axons through their dendrites in addition to PC axons, suggesting multiple levels of computation processes. The projection neurons (the DCN neurons and eurydendroid cells) send their axon outside the cerebellum (Ikenaga et al. 2005, 2006; Murakami and Morita 1987).

The cerebellar neural circuits are basically conserved between mammals and teleost species, although there are some differences. In mammals, all GC axons form synapses with the PC dendrites in the cerebellum, whereas GCs in the caudolateral lobe of the teleost cerebellum project their axons ipsilaterally and contralaterally to the dorsal hindbrain crista cerebellaris (see Fig. 13.5a, b). These axons

first form synapses with the dendrites of PCs in the cerebellum and then with the dendrites of crest cells (Purkinje-like cells in the hindbrain), whose soma and dendrites localize in the medial octabolateralis nuleus (MON) and the crista cerebellaris (CC), respectively (Bae et al. 2009; Bell et al. 2008; Mikami et al. 2004). This circuit functions as part of the cerebellum; it is likely involved in processing vestibular information for body balance similarly to the neural circuits in the flocculonodular lobe in the mammalian cerebellum (Altman and Bayer 1997; Bell 2002; Bell et al. 2008). As discussed next, developmental processes of GC axongenesis in the caudolateral lobe is slightly different from that in the anterior and main lobes.

13.3 Development

13.3.1 Establishment of the Cerebellum Domain

The cerebellum domain is determined according to the anteroposterior and dorsoventral neural patterning. The anteroposterior patterning establishes the isthmic organizer, which lies at the junction between the midbrain and hindrain [thus also called the mid–hindbrain boundary (MHB)] and controls the formation of the cerebellum in the most anterior hindbrain (Hidalgo-Sanchez et al. 1999; Joyner et al. 2000; Simeone 2000; Wurst and Bally-Cuif 2001). In the mouse, two homeodomain-containing transcription factors, Otx2 and Gbx2, play an essential role in positioning the isthmic organizer. *Otx2* and *Gbx2* are expressed in a largely complementary fashion in the anterior and posterior neuroectoderm at the end of gastrulation, and the isthmic organizer forms at the boundary of *Otx2* and *Gbx2* expression domains (Simeone et al. 1992; Bally-Cuif and Wassef 1994; Acampora et al. 1997; Suda et al. 1997; Wassarman et al. 1997; Broccoli et al. 1999; Hidalgo-Sanchez et al. 1999; Millet et al. 1999). In zebrafish *gbx1* is expressed earlier than *gbx2* and is involved in the initial positioning of the isthmic organizer (Rhinn et al. 2009). *gbx1* and *gbx2* function redundantly in subsequent development of the cerebellum (Su et al. 2003). At the late gastrula period, the isthmic organizer genes *pax2a*, *wnt1*, *engrailed2a/b* (*eng2a/b*), and fibroblast growth factor 8 (*fgf8*) are expressed. Expression of these genes becomes restricted to the isthmus and mutually dependent during the segmentation period (Wilson et al. 2002). Then other isthmic organizer genes *pax5/8* and *fgf17*, are activated in a way that is dependent on Pax2a and Fgf8 (Lun and Brand 1998; Pfeffer et al. 1998; Reifers et al. 1998, 2000).

Once the isthmic organizer forms, Fgf8 and Wnt family proteins (Wnt1 in mouse, Wnt1/3a/10 in zebrafish) play essential roles in morphogenesis and fate determination of the cerebellum. The Wnt proteins prevent apoptosis, control cell proliferation, and regulate morphogenesis of the midbrain and cerebellum (Dickinson et al. 1994; Buckles et al. 2004). Fgf8 (Fgf8a in zebrafish) is required for development of the isthmic organizer and subsequent formation of the cerebellum (Crossley et al. 1996; Liu et al. 1999; Martinez et al. 1999; Picker et al. 1999; Reifers et al. 1998).

Fgf8 controls fate decision of the cerebellum at least partly through repressing *otx* gene expression (Foucher et al. 2006). The significance of Fgf8 has been emphasized by identification of zebrafish mutant *spiel ohne grenzen* (*spg*), which displays defects in the formation of the isthmus and cerebellum. The *spg* locus encodes the POU domain-containing transcription factor Pou5F1 (Pou2), which is the orthologue of mammalian Oct3/4 and confers competence to respond to Fgf8 (Belting et al. 2001; Burgess et al. 2002; Reim and Brand 2002).

13.3.2 Development of Cerebellar Circuitry

13.3.2.1 Two Neuronal Progenitor Domains: Rhombic Lip and Ventricular Zone

Neurons in the cerebellum are generated from two germinal zones: the upper rhombic lip (URL), which is located at the dorsal surface of the cerebellar primordium, and the cerebellar ventricular zone (VZ), which is located at the roof of the fourth ventricle (Altman and Bayer 1997; Wingate 2001; Wingate and Hatten 1999; Zervas et al. 2004) (Fig. 13.2a, b). The neuronal progenitors in the URL express the bHLH proneural gene *atoh1* (vertebrate homologue of *Drosophila atonal*) and generate glutamatergic excitatory neurons, whereas those in the VZ express another proneural gene *ptf1a* and generate GABAergic inhibitory neurons, in both mammals and teleost species (Alder et al. 1996; Ben-Arie et al. 1997; Hoshino 2006; Hoshino et al. 2005; Kani et al. 2010).

13.3.2.2 Development of GCs and Their Axons

Lineage tracing in mouse reveals that *Atoh1*$^+$ neuronal progenitors in the anterior hindbrain sequentially generate neurons of the tegmental nuclei, the DCN, and then generate the granule cells (Machold and Fishell 2005; Wang et al. 2005; Wilson and Wingate 2006; Wingate 2005). In zebrafish, three *atoh1* genes, *atoh1a*, *atoh1b*, and *atoh1c*, are expressed in overlapped domains of the URL (Adolf et al. 2004; Chaplin et al. 2010; Kani et al. 2010; Koster and Fraser 2001). Lineage tracing with a zebrafish transgenic line expressing EGFP under the control of the *atoh1a* enhancer/promoter also revealed that the URL progenitors generate the tegmental nuclei and GCs in the cerebellum (Kani et al. 2010). The dorsomedial URL progenitors that express *atoh1a* (and *atoh1b*) expand anteriorly and locate in the surface of the anterior and main lobes (Va and CCe) of the cerebellum primordium at the beginning of cerebellar neurogenesis (Fig. 13.2c). A part of these cells starts to express the GC marker Neurod in the superficial domain (Kani et al. 2010) (Fig. 13.2c). Birthdate analysis showed that some Neurod$^+$ immature GCs stop their proliferation and migrate ventrally to the GCL (Kani et al. 2010; Mueller and Wullimann 2002), suggesting the following sequence of events in the development

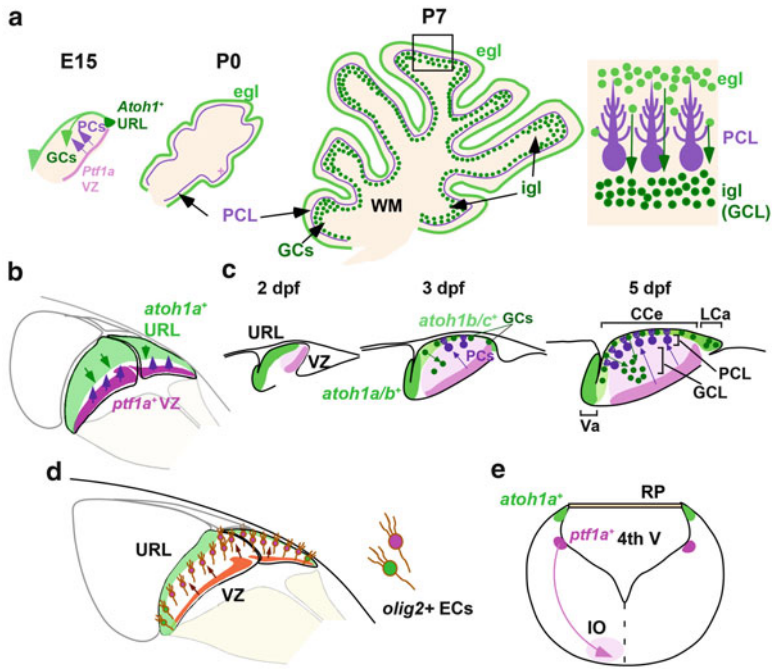

Fig. 13.2 Development of cerebellar neural circuits. **a** Development of mouse cerebellum. **b** Two progenitor zones: upper rhombic lip (*URL*) and ventricular zone (*VZ*). **c** Development of zebrafish cerebellum. **d** Development of *olig*2^{+} eurydendroid cells, the projection neurons in the cerebellum. The majority of *olig*2^{+} eurydendroid cells are derived from VZ and a minor population of them are from URL. **e** Development of IOs. Cross-section image at the posterior caudal hindbrain. *egl* external granule (germinal) layer, *igl* internal granule layer (granule cell layer), *RP* roof plate, *4th V* fourth ventricle. Other abbreviations are described in the legend of Fig. 13.1 (modified from Hashimoto and Hibi 2012; Hibi and Shimizu 2012; Kani et al. 2010)

of GCs in zebrafish: Atoh1^{+} progenitors in the superficial domain → Neurod^{+} proliferating immature GCs in the superficial domain → Neurod^{+} mature postmitotic GCs in the GCL (Hashimoto and Hibi 2012; Hibi and Shimizu 2012; Volkmann et al. 2008) (Fig. 13.2c). These developmental steps leading to GC maturation in the anterior and main lobes are similar to those of GCs in mammalian cerebellum (Fig. 13.2a). There are, however, notable differences between the mammalian and fish cerebella. In mammals, *Atoh1*$^{+}$ proliferating cells form a transient amplification zone, called the external germinal (or granule cell) layer, and their proliferation depends on Sonic hedgehog (Shh), which is produced by PCs (Dahmane and Ruiz i Altaba 1999; Wallace 1999; Wechsler-Reya and Scott 1999) (Fig. 13.2a). In zebrafish, *atoh1*-expressing cells are located along the midline and the caudal edge, but do not form a typical external GCL (Chaplin et al. 2010; Kani et al. 2010). Furthermore, in zebrafish PCs do not produce Shh and GC progenitors do not

respond to Shh signaling (Chaplin et al. 2010). These data suggest that regulation of GC proliferation in zebrafish is different from that in mammals.

In contrast to the URL progenitors in the anterior and main lobes, the URL progenitors in the caudolateral lobe (EG and LCa) initially express *atoh1a*, but later express *atoh1b* and/or *atoh1c* (Kani et al. 2010). The cells located laterally in this domain migrate anterolaterally in a short distance to form EG, but the cells in the caudal edge stay to form LCa (Volkmann et al. 2008). The GC progenitors in the caudolateral lobe do not migrate ventrally but the GCs in this lobe extend their axons ipsilaterally and contralaterally to crest cells, whereas GCs in the main lobe send parallel fibers to PCs (Bae et al. 2009; Volkmann et al. 2008) (see Fig. 13.5a, b). Several molecular markers are differentially expressed in the anterior/main lobe and LCa (Bae et al. 2009). These data indicate that the GC development is differentially regulated between the anterior/main and caudolateral lobes.

13.3.2.3 Development of Purkinje Cells and Their Dendrites

In the mouse cerebellum, the GABAergic neurons, including PCs, are derived from *Ptf1a*-expressing progenitors in the VZ (Hoshino 2006; Hoshino et al. 2005) (Fig. 13.2a). This process is also conserved for zebrafish PCs. Lineage tracing with transgenic fish and birthdate analysis revealed that the *ptf1a*$^+$ progenitors proliferate in the VZ; they stop proliferation and migrate dorsally; they end their migration and differentiate into PCs at the dorsal position (PCL) (Kani et al. 2010) (Fig. 13.2c). Monitoring of *atoh1a*$^+$ and *ptf1a*$^+$ lineages indicated that ventral migration of GCs and dorsal migration of PCs simultaneously take place and the three-layer structure is formed in 5 days post fertilization (dpf) (Bae et al. 2009; Kani et al. 2010).

Studies with transgenic fish expressing fluorescence protein Venus or mCherry specifically in PCs revealed that zebrafish PCs initially have multiple neurites from the soma and subsequently retract all but one, which becomes the primary dendrite (Tanabe et al. 2010). The Golgi apparatus locates to the root of the primary dendrite, and its localization is established in immature PCs having multiple neuritis. Prkci, an atypical protein kinase C (aPKC), cell autonomously controls Golgi localization and thereby regulates the specification of the primary dendrite of PCs (Tanabe et al. 2010) (Fig. 13.3).

13.3.2.4 Development of Projection Neurons

The large (excitatory) neurons in the DCN of the mammalian cerebellum are derived from the *Atoh1*$^+$ URL progenitors and they project their axons outside the cerebellum (Machold and Fishell 2005; Wang et al. 2005; Wilson and Wingate 2006; Wingate 2005). The DCN also contains GABAergic neurons that modulate outputs of the excitatory neurons. In teleost species, eurydendroid cells are the projection neurons in the teleost cerebellum (Bae et al. 2009; Butler and Hodos 1996). In contrast to the DCN in mammals, there is no GABAergic euryndendroid cell population

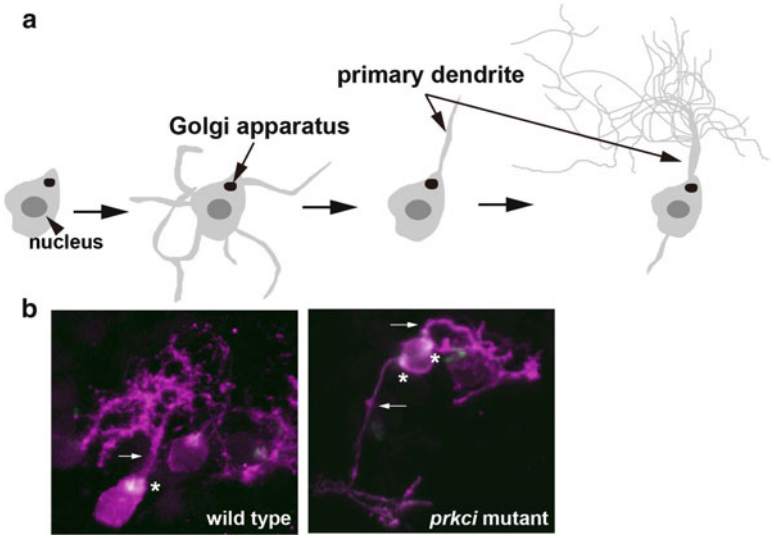

Fig. 13.3 Formation of dendrites of Purkinje cells (PCs). **a** Schematic drawing for development of PC dendrites. **b** Soma and dendrites of PCs and localization of Golgi apparatus in the PCs are visualized in zebrafish 4.5 dpf (days post fertilization) wild-type or *prkci* mutant larvae expressing gap43-mCherry (*magenta*) and Golgi-Venus (*green*). *Asterisks* indicate position of Golgi apparatus; *arrows* indicate position of primary dendrites. PCs have multiple neuritis and retract all but one, which becomes the primary dendrite. Prkci-dependent Golgi localization plays a role in specification of the primary dendrite. In a particular case, a PC has multiple Golgi apparatus and primary dendrites in the *prkci* mutant larvae (modified from Tanabe et al. 2010)

in the teleost cerebellum (Ikenaga et al. 2005). Marker analysis and retrograde labeling revealed two types of eurydendroid cells in zebrafish: *olig2*-expressing eurydendroid cells and calretinin-immunoreactive (Cr-ir$^+$) eurydendroid cells (Bae et al. 2009). *Olig2* is a proneural gene expressed in both eurydendroid cells and oligodendrocytes in zebrafish cerebellum (Bae et al. 2009; McFarland et al. 2008). The majority of *olig2*$^+$ eurydendroid cells (glutamatergic excitatory neurons) are derived from the *ptf1a*$^+$ VZ progenitors; some are derived from the *atoh1a*$^+$ URL progenitors (Bae et al. 2009; Kani et al. 2010) (Fig. 13.2d). These observations suggest that the development of the *olig2*$^+$ eurydendroid cells is distinct from the projection neurons in the DCN. The origin of other eurydendroid cells (Cr-ir$^+$ eurydendroid cells) remains to be clarified.

13.3.2.5 Development of Afferent Fiber Neurons: Mossy and Climbing Fibers

The precerebellar nuclei for MFs are LCN, ECN, RTN, and PG in mice, and they are generated from *Atoh1*$^+$ neural progenitors in the dorsal edge of the posterior hindbrain (rhombomere 6–8), which is called the lower rhombic lip (LRL)

(Landsberg et al. 2005; Rodriguez and Dymecki 2000; Wang et al. 2005; Wilson and Wingate 2006; Wingate 2005). Some of these cells migrate through the extramural migratory stream, cross the ventral midline, and settle in the contralateral side of their origin to form LRN and ECN. Some migrate ventrally but stop at the same side to form RTN and PG. The nature of MF neurons has not been well studied in teleost species. In contrast, development of the precerebellar nuclei IOs for CFs is conserved between mammals and teleost species including zebrafish. The IO neurons originate from *Ptf1a*-expressing neuronal progenitors, which are located more ventrally than the *Atoh1*-expressing cells in the posterior hindbrain (Kani et al. 2010; Yamada et al. 2007). These cells migrate through the intramural migratory stream and stop before the ventral midline (floorplate) to form IO in the ventral hindbrain (Fig. 13.2e). The IO neurons project the CFs contralateraly to PCs. In mammals, there is a clear topographic map of the CFs, in which neurons in a particular region of IOs project their axon to PCs in specific area of the cerebellum (Sugihara 2006; Sugihara et al. 2007; Sugihara and Quy 2007; Sugihara and Shinoda 2004). The topographic map of the CFs is correlated with compartmentalization of the PCs that can be distinguished by several markers including zebrin II (Sugihara et al. 2007; Sugihara and Quy 2007; Sugihara and Shinoda 2004; Apps and Hawkes 2009). The CFs innervate somata and/or proximal dendrites of PCs in zebrafish as observed in developmental stage of mammalian cerebellum (Bae et al. 2009). It is not clarified yet whether a topographic map exists for the CFs in zebrafish.

13.4 Sustained Neurogenesis from Juvenile to Adult Stages in Zebrafish Cerebellum

Cerebellar neurons and glial cells are generated after larval stages in zebrafish (Kani et al. 2010; Kaslin et al. 2009, 2013; Zupanc et al. 2005). GCs, GABAergic neurons including PCs, Bergmann glial cells are generated during the juvenile stage [1–3 months post fertilization (mpf)]. Neurogenesis of these cells declines in transition from juvenile to adult stage (after 3 mpf), but the GCs continue to be generated in the adult cerebellum (Kaslin et al. 2013). There are many proliferating GC progenitors in the ML, and they migrate ventrally to the GCL in both juvenile and adult cerebellum (Kani et al. 2010; Kaslin et al. 2009, 2013; Zupanc et al. 2005) (Fig. 13.4C). *atoh1a/b/c* and *ptf1a* are expressed in the ML and the VZ, respectively, of juvenile and adult cerebellum. BrdU labeling of adult cerebellum revealed that the majority of cells that express *atoh1a*, *atoh1b*, *atoh1c*, or Neurod and a fraction of *ptf1a*-expressing cells maintain proliferation in the adult cerebellum (Kani et al. 2010; Kaslin et al. 2013) (Fig. 13.4A, B). In addition, some of the Bergmann glial cells and Nestin^{+} cells are found to proliferate in the adult cerebellum (Kani et al. 2010; Kaslin et al. 2009). It is not clear which neuronal progenitors or neural stem cells generate cerebellar neurons, particularly GCs, in the adult cerebellum. Studies

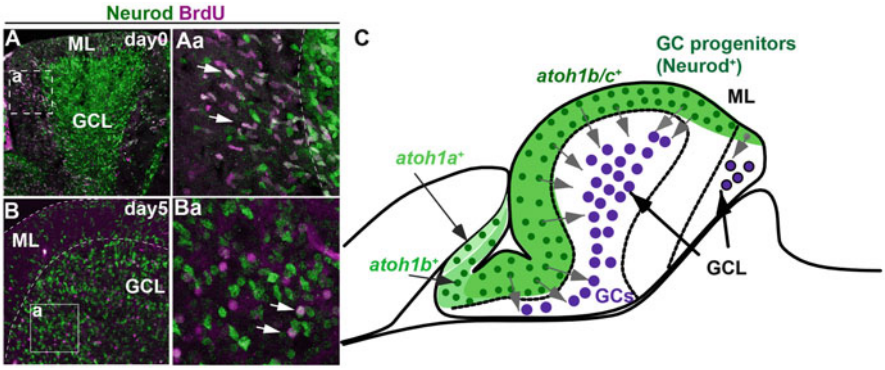

Fig. 13.4 Adult neurogenesis. **A**, **B** Birthdate analysis of granule cells. Adult zebrafish labeled with BrdU for 1 h were fixed immediately (**A**) or 5 days (**B**) after labeling. BrdU-incorporated cells were analyzed with anti-BrdU (*magenta*) and anti-Neurod (*green*) antibodies. Sagittal sections. **Aa**, **Ba** Higher-magnification views of the *boxes* in **A** and **B**. *Arrows* indicate immature GCs in the ML (**A**, **Aa**) and mature GCs in the GCL (**B**, **Ba**). **C** Schematic representation of adult neurogenesis. In juvenile and adult cerebellum, proliferating GC progenitors are located in the ML and potentially express *atoh1* genes and Neurod. They migrate to the GCL for remodeling neural circuitry (modified from Kani et al. 2010)

with a *nestin*:*egfp* transgenic line showed that Nestin:egfp$^+$ cells contain *atoh1c*$^+$ cells and that they are located near the midline (Kaslin et al. 2013), where *atoh1a*/*b* are also expressed. Future studies will clarify whether *atoh1a*/*b*/*c*-expressing cells and Nestin:egfp$^+$ cells represent identical cell populations.

13.5 Function of Cerebellum in Teleosts

13.5.1 Role of Cerebellum in Eyeblink Conditioning and Adaptation of Oculomotor Responses

LTD has been proposed to play a major role in the functions of the cerebellum (Ito 2002a, b, 2006, 2008; Linden and Connor 1993; Jorntell and Hansel 2006). As cerebellum-dependent learning paradigms, eyeblink conditioning and adaptation of the vestibulo-ocular reflex (VOR) have been well investigated. Eyeblink conditioning is a typical classical conditioning paradigm. The repeated pairing of a conditioned stimulus (CS; e.g., a tone or light) and an unconditioned stimulus (US; air puff to the eye) leads to a conditioned response (tone- or light-dependent eyeblinks). The MFs and CFs are proposed to convey information of the CS and US, respectively (Kim and Thompson 1997; Medina et al. 2000). The VOR is a reflexive eye movement that stabilizes images on the retina during head movement. The MFs

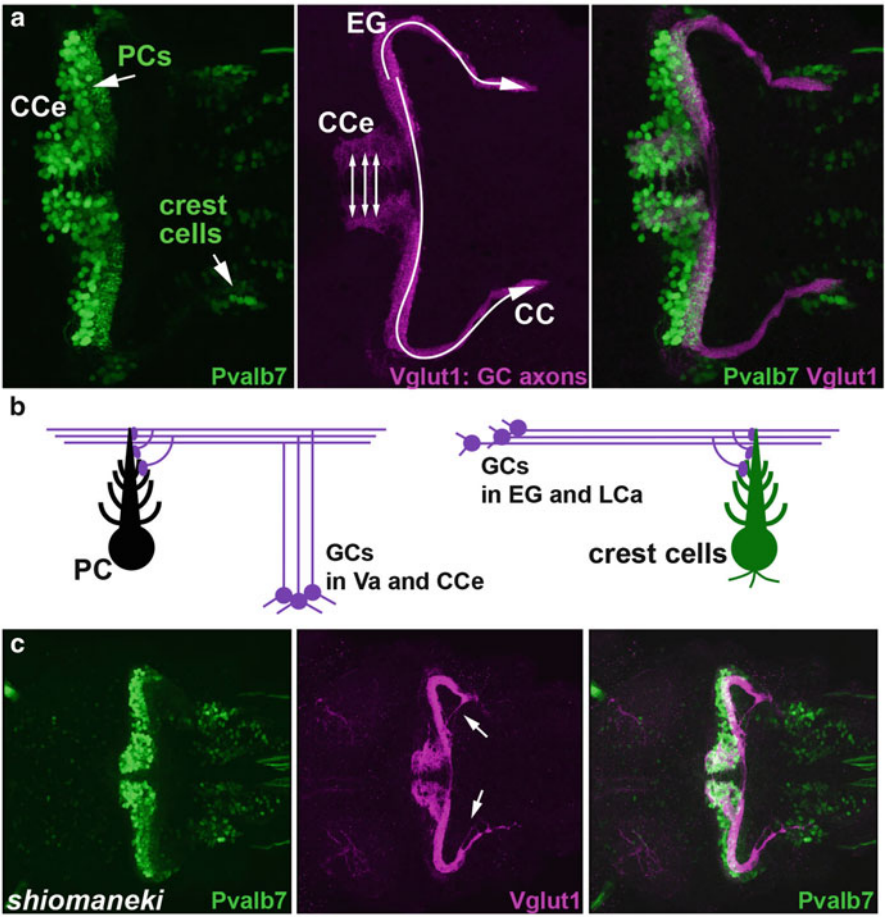

Fig. 13.5 Cerebellar neural circuitry in wild-type and cerebellar mutant larvae. **a** A 5 dpf (days post fertilization) larva was stained with anti-Parvalbumin7 (*green*, a maker for PCs and crest cells) and anti-Vglut1 (*magenta*, a marker of GC axons) antibodies. Dorsal views. **b** Schematic representation of cerebellar neural circuitry at early larval stages. GCs in Va and CCe project axons to the dendrites of PCs, whereas GCs in EG and LCa projects axons to the dendrites of crest cells. **c** *shiomaneki* mutant larvae (5 dpf) show defects in axogenesis of GCs in EG and LCa. The GC axons are short or misrouted (*arrows*) (modified from Bae et al. 2009; Hashimoto and Hibi 2012)

convey information of head and eye movements whereas the CFs transmit information of image motion, known as retinal slips. When information of the retinal slips is continuously provided, the eye movement becomes faster and more efficient to minimize the retinal slips (adaptation of the VOR) (Ito 1982; du Lac et al. 1995; Boyden et al. 2004; Ito 2013). In both eyeblink conditioning and the VOR adaptation, learning depends on the cerebellar neural circuitry. The goldfish is reported to learn an eyeblink-like conditioned response, and cerebellar lesions prevent this learning (Rodriguez et al. 2005; Gomez et al. 2010). Cerebellar lesions in goldfish

also affect VOR adaptation (Pastor et al. 1994, 1997). In zebrafish, the VOR is reported to start at 3 dpf (Mo et al. 2010). The VOR at this stage may not depend on the cerebellar neural circuitry, because that develops at later stages, but rather the cerebellum may be involved in the adaptation process of the VOR. In addition to the VOR, zebrafish larvae express optokinetic response (OKR) (Brockerhoff et al. 1995; Easter and Nicola 1996; Portugues and Engert 2009; Beck et al. 2004; Marsh and Baker 1997), which is a combination of a saccade and smooth-pursuit eye movements that are elicited by moving images. In the OKR, the eyes adapt their positions to moving objects. Similar to VOR, adaptation of the OKR also involves the cerebellum in mammals [reviewed in (Ito 2006)], but the cerebellum dependency of the OKR adaptation has not been well studied in teleost species.

13.5.2 Role of Cerebellum in Other Classical Conditioning

Cerebellum lesions or drug-mediated silencing of the cerebellum function in goldfish also result in impairments in classical fear conditioning, in which repeating the CS (light) and the unconditioned fear stimulus (US, electric shock) leads to bradycardia in response to the conditioned stimulus (Rodriguez et al. 2005; Yoshida and Hirano 2010; Yoshida and Kondo 2012; Yoshida et al. 2004). Early-stage zebrafish larvae move their tail upon a swift touch to a side of the body. When they are trained to associate a light stimulation (CS) with the touch (US), repeated pairing of the CS and US results in an enhanced tail movement upon exposure to the light (conditioned response) (Aizenberg and Schuman 2011). During the conditioning, the CS and US activate different subsets of cerebellar neurons; laser ablation of the main lobe of the cerebellum disrupts acquisition of the conditioned response (Aizenberg and Schuman 2011), suggesting the role of the cerebellar neural circuitry in classical conditioning at the early larval stage. It is, however, also reported that zebrafish start learning in classical conditioning at the late larval stage (4 weeks post fertilization) (Valente et al. 2012). This discrepancy may result from differences in experimental paradigms. Future studies will reveal how early cerebellum-dependent learning initiates and which components in the cerebellar neural circuitry are involved in conditioning in zebrafish.

13.5.3 Role of Cerebellum in Motor Adaptation

Zebrafish modify their motor output during swimming according to visual information (visual feedback) that is obtained from their surrounding. When an early-stage zebrafish larva is paralyzed with a muscle relaxant agent and shown an artificially moving environment, the fish cannot swim but tries to adapt motor output (modify the motoneuron activities for locomotion) to changes in the virtual environment in the brain (fictive swimming). The cerebellar neural circuitry is activated during the

adaptation of fictive swimming, and lesions of the CFs prevent the adaptation (Ahrens et al. 2012), indicating that the cerebellar neural circuits are involved in the visual feedback-dependent motor adaptation in early-stage larvae. All these observations indicate that, as is the mammalian cerebellum, the teleost cerebellum is involved in motor control and learning behaviors.

13.6 Perspectives: What Do Studies with Zebrafish Tell Us?

13.6.1 Unsolved Questions for Development of the Cerebellar Neural Circuitry

There are many questions about the development of the cerebellum and cerebellar neural circuitry that remain to be elucidated. How do the URL and VZ progenitors generate diverse sets of cerebellar neurons? How do the GCs and PCs migrate and develop their axons and dendrites? Interaction of numerous parallel fibers of the GCs and complex dendrites of the PCs is a prerequisite for computation in the cerebellum. Parallel fibers of the GCs are conserved among vertebrate species, but the mechanism controlling the formation of the parallel fibers is not yet well understood. We are beginning to understand how PCs develop the complex dendritic structure in mammals (Fujishima et al. 2012; Kaneko et al. 2011), but the molecular and cellular mechanisms for dendrite formation are not fully understood. A topographic map exists for CFs in mammals, but only a few molecules are shown to be involved in the precise connection of CFs and PCs (Nishida et al. 2002).

13.6.2 Unresolved Questions for Functions of Cerebellar Neural Circuitry

It is more challenging to understand the function of the cerebellar neural circuitry. As described here, the cerebellar neural circuitry is involved in adaptation of motor control and learning (e.g., classical conditioning) in both mammals and zebrafish. In humans, the cerebellum is proposed to be involved in mental activities (Ito 2008). During complex mental activities (e.g., playing chess or Go games), at least part of the cerebellum is activated. Mental disorders, including autism and developmental dyslexia, are known to link to dysfunction of the cerebellum (Ito 2008). These findings suggest that the cerebellum cooperates with the cerebrum to elicit mental activities. We do not know whether the cerebellar neural circuitry also controls complex mental activities in teleost species. It is also not known what kind of information individual components of the cerebellar neural circuitry receive, integrate, and output; and where memory is stored for a long time period in motor control and

learning. Electrophysiological analysis has been used to monitor activities of subsets of neurons and has revealed the roles of individual neurons and their axons/dendrites in motor control by the mammalian cerebellum (reviewed by Ito 2002a). However, imaging of the entire neural circuitry and manipulation of individual components are necessary to completely understand the roles of cerebellar neural circuitry in motor control and learning (and in mental activities).

13.6.3 Techniques to Resolve the Questions in Teleost Species

The morphology-based screening of mutants affecting cerebellum development revealed genes that control activity of the isthmic organizer and formation of the cerebellum, including *pax2a*, *fgf8a*, and *pou5f1* (Brand et al. 1996; Schier et al. 1996). We previously reported isolation of zebrafish mutants that have defects in the formation of cerebellar neurons and neural circuitry (Bae et al. 2009). These mutants can be used for understanding the development and function of the cerebellar neural circuitry.

Many transgenic zebrafish lines are available for studies of development and function of cerebellar neural circuits. Enhancer and/or gene trap screens using transposon systems (Tol2 or Sleeping Beauty) and Gal4-UAS establish transgenic lines that can express the gene of interest in specific neurons (Asakawa et al. 2008; Scott and Baier 2009; Scott et al. 2007; Heap et al. 2013; Ogura et al. 2009). The Gal4-UAS lines and cerebellar neural circuitry-specific promoters can be combined with various systems to monitor and modify the neurons: (1) monitoring of neuronal activities with fluorescent Ca^{2+} indicators (Nakai et al. 2001; Muto et al. 2011, 2013), (2) monitoring of cell polarity and cytoskeletons with fluorescent fusion proteins (Distel et al. 2010; Distel et al. 2011), (3) imaging of neuritis with multicolor fluorescent proteins (brainbow/zebrabow techniques) (Livet et al. 2007; Pan et al. 2013), (4) cell ablation with nitroreductase (Curado et al. 2007; Pisharath et al. 2007), (5) neuronal silencing with tetanus toxin (Asakawa et al. 2008), and (6) neuronal activation and silencing with optogenetic tools, such as channelrhodopsin, halorhodopsin, and archaerhodopsin (Boyden et al. 2005; Douglass et al. 2008; Arrenberg et al. 2009; Kimura et al. 2013; Umeda et al. 2013). Various types of microscopes are now available for Ca^{2+} imaging and manipulating neuronal activities. It is recently reported that a light-sheet microscope can be used for recording neuronal activities from the entire volume of the zebrafish larval brain in vivo at 0.8 Hz (Ahrens et al. 2013). A microscope equipped with a digital micromirror device can be used to activate optogenetic proteins in specific neurons (Kimura et al. 2013). Furthermore, recent genome editing techniques with the TALEN or CRISPR/Cas system enable us to readily knock out genes (Dahlem et al. 2012; Xiao et al. 2013; Hwang et al. 2013; Gaj et al. 2013; Huang et al. 2011; Sander et al. 2011).

13.6.4 Approaches for Understanding the Cerebellar Neural Circuitry

We have undertaken different strategies to resolve the questions for the cerebellar neural circuitry. First, we have been investigating phenotypes of the cerebellar mutants (Bae et al. 2009) and trying to identify genes responsible for these mutants. We have a particular interest in mutants displaying abnormalities in specific cerebellar neurons. *gazami* mutant larvae have normal PCs but strongly reduced GCs and their axons, implying a role of the *gazami* locus in GC development. *shiomaneki* mutant larvae show specific defects in the GC axons to crest cells (but not in the parallel fibers of the GCs; unpublished data) (Fig. 13.5c), suggesting that the *shiomaneki* locus encodes a molecule that is involved in axon guidance of the GCs. We have identified the gene locus for *gazami* and *shiomaneki* mutants (unpublished results). The gene products have not previously be reported to function in development of the cerebellar neural circuitry in mammals. Medaka is another model teleost species that has been used for genetic and behavioral analyses for a long time. A medaka spontaneous mutant *rolling* (*ro*) shows ataxic swimming behaviors and defects in adaption of the OKR (unpublished data); the phenotypes of the *ro* mutant may be comparable to the symptoms seen in human cerebellar defective patients. We have identified the gene responsible for the *ro* mutant, the gene product of which is known to function at various aspects of development and function of neural circuits in mammals (unpublished results). Studies with the zebrafish and medaka mutants may shed light on previously unrecognized mechanisms controlling the development and function of the cerebellar neural circuitry.

We can visualize developmental processes and function of individual components of the cerebellar neural circuits using gene/enhancer trap screening (Asakawa et al. 2008), coupled with fluorescent protein-expressing reporter lines (Kani et al. 2010; Tanabe et al. 2010). Such studies will provide anatomical information (connectome) and reveal molecular mechanisms by which precise neuronal connections are established (e.g., topographic map of the CFs). We can even isolate specific cerebellar circuit neurons by FACS (fluorescence-activated cell sorting) and characterize them in molecular terms. Knockdown (by antisense morpholinos) or knockout (by TALEN or CRISPR/Cas systems) of genes will reveal functions of the newly identified genes. These data will provide us with clues for understanding molecular mechanisms controlling the formation of cerebellar neural circuitry. Comparing the gene expression data from mammalian cerebellum (Furuichi et al. 2011), we will be able to discuss evolution of the cerebellar neural circuits in vertebrate species.

The cerebellar circuit neuron-specific Gal4 lines can also be used for functional analysis. We are setting up analyses of learning behaviors in zebrafish in which the cerebellar neural circuitry is likely involved. We will be able to monitor neuronal activities of cerebellar neural circuits with the fluorescent Ca^{2+} indicators (GCaMPs) and manipulate them with optogenetic tools or cell/neuronal toxins during the learning processes. Combining imaging and electrophysiology techniques, we will be able to determine which cerebellar circuit neurons convey what kind of information

during learning, and which neurons are involved in the learning and memory formation. Using mutants and gene knockout techniques, we will be able to understand molecular mechanisms controlling the function of the cerebellar neural circuitry during learning. We hope to extend these studies to understand the role of more complex functions of the cerebellar neural circuitry, such as mental activities, in the future.

Acknowledgments The authors thank past and current members of the Hibi Laboratory for their contribution to the works cited here. The studies conducted in the Hibi Laboratory have been supported by grants from the Uehara Memorial Foundation (M.H.), Takeda Science Foundation (M.H.), the Naito Foundation Natural Science Scholarship (M.H.), and Grants-in-Aid for Scientific Research from the Ministry of Education, Science, Sports and Technology (M.H., T.S.)

References

Acampora D, Avantaggiato V, Tuorto F, Simeone A (1997) Genetic control of brain morphogenesis through Otx gene dosage requirement. Development (Camb) 124(18):3639–3650

Adolf B, Bellipanni G, Huber V, Bally-Cuif L (2004) Atoh1.2 and beta3.1 are two new bHLH-encoding genes expressed in selective precursor cells of the zebrafish anterior hindbrain. Gene Expr Patterns 5(1):35–41. doi:10.1016/j.modgep.2004.06.009, pii: S1567-133X(04)00093-6

Ahrens MB, Li JM, Orger MB, Robson DN, Schier AF, Engert F, Portugues R (2012) Brain-wide neuronal dynamics during motor adaptation in zebrafish. Nature (Lond) 485(7399):471–477. doi:10.1038/nature11057

Ahrens MB, Orger MB, Robson DN, Li JM, Keller PJ (2013) Whole-brain functional imaging at cellular resolution using light-sheet microscopy. Nat Methods 10(5):413–420. doi:10.1038/nmeth.2434

Aizenberg M, Schuman EM (2011) Cerebellar-dependent learning in larval zebrafish. J Neurosci 31(24):8708–8712. doi:10.1523/JNEUROSCI.6565-10.2011

Alder J, Cho NK, Hatten ME (1996) Embryonic precursor cells from the rhombic lip are specified to a cerebellar granule neuron identity. Neuron 17(3):389–399, pii: S0896-6273(00)80172-5

Alonso JR, Arevalo R, Brinon JG, Lara J, Weruaga E, Aijon J (1992) Parvalbumin immunoreactive neurons and fibres in the teleost cerebellum. Anat Embryol (Berl) 185(4):355–361

Altman J, Bayer SA (1997) Development of the cerebellar system in relation to its evolution, structure, and function. CRC, Boca Raton

Apps R, Hawkes R (2009) Cerebellar cortical organization: a one-map hypothesis. Nat Rev Neurosci 10(9):670–681. doi:10.1038/nrn2698

Arrenberg AB, Del Bene F, Baier H (2009) Optical control of zebrafish behavior with halorhodopsin. Proc Natl Acad Sci USA 106(42):17968–17973. doi:10.1073/pnas.0906252106

Asakawa K, Suster ML, Mizusawa K, Nagayoshi S, Kotani T, Urasaki A, Kishimoto Y, Hibi M, Kawakami K (2008) Genetic dissection of neural circuits by Tol2 transposon-mediated Gal4 gene and enhancer trapping in zebrafish. Proc Natl Acad Sci USA 105(4):1255–1260. doi:10.1073/pnas.0704963105

Bae YK, Kani S, Shimizu T, Tanabe K, Nojima H, Kimura Y, Higashijima S, Hibi M (2009) Anatomy of zebrafish cerebellum and screen for mutations affecting its development. Dev Biol 330(2):406–426. doi:10.1016/j.ydbio.2009.04.013, pii: S0012-1606(09)00245-0

Bally-Cuif L, Wassef M (1994) Ectopic induction and reorganization of Wnt-1 expression in quail/chick chimeras. Development (Camb) 120(12):3379–3394

Beck JC, Gilland E, Tank DW, Baker R (2004) Quantifying the ontogeny of optokinetic and vestibuloocular behaviors in zebrafish, medaka, and goldfish. J Neurophysiol 92(6):3546–3561. doi:10.1152/jn.00311.2004

Bell CC (2002) Evolution of cerebellum-like structures. Brain Behav Evol 59(5–6):312–326
Bell CC, Han V, Sawtell NB (2008) Cerebellum-like structures and their implications for cerebellar function. Annu Rev Neurosci 31:1–24. doi:10.1146/annurev.neuro.30.051606.094225
Belting HG, Hauptmann G, Meyer D, Abdelilah-Seyfried S, Chitnis A, Eschbach C, Soll I, Thisse C, Thisse B, Artinger KB, Lunde K, Driever W (2001) Spiel ohne grenzen/pou2 is required during establishment of the zebrafish midbrain-hindbrain boundary organizer. Development (Camb) 128(21):4165–4176
Ben-Arie N, Bellen HJ, Armstrong DL, McCall AE, Gordadze PR, Guo Q, Matzuk MM, Zoghbi HY (1997) Math1 is essential for genesis of cerebellar granule neurons. Nature (Lond) 390(6656):169–172. doi:10.1038/36579
Boyden ES, Katoh A, Raymond JL (2004) Cerebellum-dependent learning: the role of multiple plasticity mechanisms. Annu Rev Neurosci 27:581–609. doi:10.1146/annurev.neuro.27.070203.144238
Boyden ES, Zhang F, Bamberg E, Nagel G, Deisseroth K (2005) Millisecond-timescale, genetically targeted optical control of neural activity. Nat Neurosci 8(9):1263–1268. doi:10.1038/nn1525
Brand M, Heisenberg CP, Jiang YJ, Beuchle D, Lun K, Furutani-Seiki M, Granato M, Haffter P, Hammerschmidt M, Kane DA, Kelsh RN, Mullins MC, Odenthal J, van Eeden FJ, Nusslein-Volhard C (1996) Mutations in zebrafish genes affecting the formation of the boundary between midbrain and hindbrain. Development (Camb) 123:179–190
Broccoli V, Boncinelli E, Wurst W (1999) The caudal limit of Otx2 expression positions the isthmic organizer. Nature (Lond) 401(6749):164–168. doi:10.1038/43670
Brockerhoff SE, Hurley JB, Janssen-Bienhold U, Neuhauss SC, Driever W, Dowling JE (1995) A behavioral screen for isolating zebrafish mutants with visual system defects. Proc Natl Acad Sci USA 92(23):10545–10549
Buckles GR, Thorpe CJ, Ramel MC, Lekven AC (2004) Combinatorial Wnt control of zebrafish midbrain-hindbrain boundary formation. Mech Dev 121(5):437–447. doi:10.1016/j.mod.2004.03.026, pii: S0925477304000747
Burgess S, Reim G, Chen W, Hopkins N, Brand M (2002) The zebrafish spiel-ohne-grenzen (spg) gene encodes the POU domain protein Pou2 related to mammalian Oct4 and is essential for formation of the midbrain and hindbrain, and for pre-gastrula morphogenesis. Development (Camb) 129(4):905–916
Butler AB, Hodos H (1996) Comparative vertebrate neuroanatomy: evolution and adaptation. Wiley-Liss, New York
Chaplin N, Tendeng C, Wingate RJ (2010) Absence of an external germinal layer in zebrafish and shark reveals a distinct, anamniote ground plan of cerebellum development. J Neurosci 30(8):3048–3057. doi:10.1523/JNEUROSCI.6201-09.2010
Crossley PH, Martinez S, Martin GR (1996) Midbrain development induced by FGF8 in the chick embryo. Nature (Lond) 380(6569):66–68. doi:10.1038/380066a0
Curado S, Anderson RM, Jungblut B, Mumm J, Schroeter E, Stainier DY (2007) Conditional targeted cell ablation in zebrafish: a new tool for regeneration studies. Dev Dyn 236(4):1025–1035. doi:10.1002/dvdy.21100
Dahlem TJ, Hoshijima K, Jurynec MJ, Gunther D, Starker CG, Locke AS, Weis AM, Voytas DF, Grunwald DJ (2012) Simple methods for generating and detecting locus-specific mutations induced with TALENs in the zebrafish genome. PLoS Genet 8(8):e1002861. doi:10.1371/journal.pgen.1002861
Dahmane N, Ruiz i Altaba A (1999) Sonic hedgehog regulates the growth and patterning of the cerebellum. Development (Camb) 126(14):3089–3100
Dickinson ME, Krumlauf R, McMahon AP (1994) Evidence for a mitogenic effect of Wnt-1 in the developing mammalian central nervous system. Development (Camb) 120(6):1453–1471
Distel M, Hocking JC, Volkmann K, Koster RW (2010) The centrosome neither persistently leads migration nor determines the site of axonogenesis in migrating neurons in vivo. J Cell Biol 191(4):875–890. doi:10.1083/jcb.201004154

Distel M, Jennifer CH, Koster RW (2011) In vivo cell biology using Gal4-mediated multicolor subcellular labeling in zebrafish. Commun Integr Biol 4(3):336–339. doi:10.4151/cib.4.3.15037
Douglass AD, Kraves S, Deisseroth K, Schier AF, Engert F (2008) Escape behavior elicited by single, channelrhodopsin-2-evoked spikes in zebrafish somatosensory neurons. Curr Biol 18(15):1133–1137. doi:10.1016/j.cub.2008.06.077, pii: S0960-9822(08)00959-7
du Lac S, Raymond JL, Sejnowski TJ, Lisberger SG (1995) Learning and memory in the vestibulo-ocular reflex. Annu Rev Neurosci 18:409–441. doi:10.1146/annurev.ne.18.030195.002205
Easter SS Jr, Nicola GN (1996) The development of vision in the zebrafish (*Danio rerio*). Dev Biol 180(2):646–663
Fatemi SH, Halt AR, Realmuto G, Earle J, Kist DA, Thuras P, Merz A (2002) Purkinje cell size is reduced in cerebellum of patients with autism. Cell Mol Neurobiol 22(2):171–175
Foucher I, Mione M, Simeone A, Acampora D, Bally-Cuif L, Houart C (2006) Differentiation of cerebellar cell identities in absence of Fgf signalling in zebrafish Otx morphants. Development (Camb) 133(10):1891–1900. doi:10.1242/dev.02352
Fujishima K, Horie R, Mochizuki A, Kengaku M (2012) Principles of branch dynamics governing shape characteristics of cerebellar Purkinje cell dendrites. Development (Camb) 139(18):3442–3455. doi:10.1242/dev.081315
Furuichi T, Shiraishi-Yamaguchi Y, Sato A, Sadakata T, Huang J, Shinoda Y, Hayashi K, Mishima Y, Tomomura M, Nishibe H, Yoshikawa F (2011) Systematizing and cloning of genes involved in the cerebellar cortex circuit development. Neurochem Res 36(7):1241–1252. doi:10.1007/s11064-011-0398-1
Gaj T, Gersbach CA, Barbas CF 3rd (2013) ZFN, TALEN, and CRISPR/Cas-based methods for genome engineering. Trends Biotechnol 31(7):397–405. doi:10.1016/j.tibtech.2013.04.004
Gomez A, Duran E, Salas C, Rodriguez F (2010) Cerebellum lesion impairs eyeblink-like classical conditioning in goldfish. Neuroscience 166(1):49–60. doi:10.1016/j.neuroscience.2009.12.018, pii: S0306-4522(09)02051-X
Hashimoto M, Hibi M (2012) Development and evolution of cerebellar neural circuits. Dev Growth Differ 54(3):373–389. doi:10.1111/j.1440-169X.2012.01348.x
Heap LA, Goh CC, Kassahn KS, Scott EK (2013) Cerebellar output in zebrafish: an analysis of spatial patterns and topography in eurydendroid cell projections. Front Neural Circuits 7:53. doi:10.3389/fncir.2013.00053
Hibi M, Shimizu T (2012) Development of the cerebellum and cerebellar neural circuits. Dev Neurobiol 72(3):282–301. doi:10.1002/dneu.20875
Hidalgo-Sanchez M, Millet S, Simeone A, Alvarado-Mallart RM (1999) Comparative analysis of Otx2, Gbx2, Pax2, Fgf8 and Wnt1 gene expressions during the formation of the chick midbrain/hindbrain domain. Mech Dev 81(1–2):175–178
Hoshino M (2006) Molecular machinery governing GABAergic neuron specification in the cerebellum.Cerebellum5(3):193–198.doi:10.1080/14734220600589202,pii:U0771321MJN0N232
Hoshino M, Nakamura S, Mori K, Kawauchi T, Terao M, Nishimura YV, Fukuda A, Fuse T, Matsuo N, Sone M, Watanabe M, Bito H, Terashima T, Wright CV, Kawaguchi Y, Nakao K, Nabeshima Y (2005) Ptf1a, a bHLH transcriptional gene, defines GABAergic neuronal fates in cerebellum. Neuron 47(2):201–213. doi:10.1016/j.neuron.2005.06.007, pii: S0896-6273(05)00485-X
Huang P, Xiao A, Zhou M, Zhu Z, Lin S, Zhang B (2011) Heritable gene targeting in zebrafish using customized TALENs. Nat Biotechnol 29(8):699–700. doi:10.1038/nbt.1939
Hwang WY, Fu Y, Reyon D, Maeder ML, Tsai SQ, Sander JD, Peterson RT, Yeh JR, Joung JK (2013) Efficient genome editing in zebrafish using a CRISPR-Cas system. Nat Biotechnol 31(3):227–229. doi:10.1038/nbt.2501
Ikenaga T, Yoshida M, Uematsu K (2005) Morphology and immunohistochemistry of efferent neurons of the goldfish corpus cerebelli. J Comp Neurol 487(3):300–311. doi:10.1002/cne.20553
Ikenaga T, Yoshida M, Uematsu K (2006) Cerebellar efferent neurons in teleost fish. Cerebellum 5(4):268–274. doi:10.1080/14734220600930588, pii: H82731V07J781700
Ito M (1982) Cerebellar control of the vestibulo-ocular reflex–around the flocculus hypothesis. Annu Rev Neurosci 5:275–296. doi:10.1146/annurev.ne.05.030182.001423

Ito M (2002a) Historical review of the significance of the cerebellum and the role of Purkinje cells in motor learning. Ann N Y Acad Sci 978:273–288

Ito M (2002b) The molecular organization of cerebellar long-term depression. Nat Rev Neurosci 3(11):896–902. doi:10.1038/nrn962

Ito M (2005) Bases and implications of learning in the cerebellum: adaptive control and internal model mechanism. Prog Brain Res 148:95–109. doi:10.1016/S0079-6123(04)48009-1, pii: S0079612304480091

Ito M (2006) Cerebellar circuitry as a neuronal machine. Prog Neurobiol 78(3–5):272–303. doi:10.1016/j.pneurobio.2006.02.006, pii: S0301-0082(06)00023-2

Ito M (2008) Control of mental activities by internal models in the cerebellum. Nat Rev Neurosci 9(4):304–313. doi:10.1038/nrn2332

Ito M (2013) Error detection and representation in the olivo-cerebellar system. Front Neural Circuits 7:1. doi:10.3389/fncir.2013.00001

Jorntell H, Hansel C (2006) Synaptic memories upside down: bidirectional plasticity at cerebellar parallel fiber–Purkinje cell synapses. Neuron 52(2):227–238. doi:10.1016/j.neuron.2006.09.032, pii: S0896-6273(06)00770-7

Joyner AL, Liu A, Millet S (2000) Otx2, Gbx2 and Fgf8 interact to position and maintain a mid-hindbrain organizer. Curr Opin Cell Biol 12(6):736–741, pii: S0955-0674(00)00161-7

Kaneko M, Yamaguchi K, Eiraku M, Sato M, Takata N, Kiyohara Y, Mishina M, Hirase H, Hashikawa T, Kengaku M (2011) Remodeling of monoplanar Purkinje cell dendrites during cerebellar circuit formation. PLoS One 6(5):e20108. doi:10.1371/journal.pone.0020108

Kani S, Bae YK, Shimizu T, Tanabe K, Satou C, Parsons MJ, Scott E, Higashijima S, Hibi M (2010) Proneural gene-linked neurogenesis in zebrafish cerebellum. Dev Biol 343(1–2):1–17. doi:10.1016/j.ydbio.2010.03.024, pii: S0012-1606(10)00207-1

Kaslin J, Ganz J, Geffarth M, Grandel H, Hans S, Brand M (2009) Stem cells in the adult zebrafish cerebellum: initiation and maintenance of a novel stem cell niche. J Neurosci 29(19):6142–6153. doi:10.1523/JNEUROSCI.0072-09.2009

Kaslin J, Kroehne V, Benato F, Argenton F, Brand M (2013) Development and specification of cerebellar stem and progenitor cells in zebrafish: from embryo to adult. Neural Dev 8(1):9. doi:10.1186/1749-8104-8-9

Kim JJ, Thompson RF (1997) Cerebellar circuits and synaptic mechanisms involved in classical eyeblink conditioning. Trends Neurosci 20(4):177–181, pii: S0166223696100813

Kimura Y, Satou C, Fujioka S, Shoji W, Umeda K, Ishizuka T, Yawo H, Higashijima S (2013) Hindbrain V2a neurons in the excitation of spinal locomotor circuits during zebrafish swimming. Curr Biol 23(10):843–849. doi:10.1016/j.cub.2013.03.066

Koeppen AH (2005) The pathogenesis of spinocerebellar ataxia. Cerebellum 4(1):62–73

Koster RW, Fraser SE (2001) Direct imaging of in vivo neuronal migration in the developing cerebellum. Curr Biol 11(23):1858–1863, pii: S0960-9822(01)00585-1

Laine J, Axelrad H (1994) The candelabrum cell: a new interneuron in the cerebellar cortex. J Comp Neurol 339(2):159–173. doi:10.1002/cne.903390202

Landsberg RL, Awatramani RB, Hunter NL, Farago AF, DiPietrantonio HJ, Rodriguez CI, Dymecki SM (2005) Hindbrain rhombic lip is comprised of discrete progenitor cell populations allocated by Pax6. Neuron 48(6):933–947. doi:10.1016/j.neuron.2005.11.031, pii: S0896-6273(05)01043-3

Linden DJ, Connor JA (1993) Cellular mechanisms of long-term depression in the cerebellum. Curr Opin Neurobiol 3(3):401–406

Liu A, Losos K, Joyner AL (1999) FGF8 can activate Gbx2 and transform regions of the rostral mouse brain into a hindbrain fate. Development (Camb) 126(21):4827–4838

Livet J, Weissman TA, Kang H, Draft RW, Lu J, Bennis RA, Sanes JR, Lichtman JW (2007) Transgenic strategies for combinatorial expression of fluorescent proteins in the nervous system. Nature (Lond) 450(7166):56–62. doi:10.1038/nature06293

Lun K, Brand M (1998) A series of no isthmus (noi) alleles of the zebrafish pax2.1 gene reveals multiple signaling events in development of the midbrain-hindbrain boundary. Development (Camb) 125(16):3049–3062

Machold R, Fishell G (2005) Math1 is expressed in temporally discrete pools of cerebellar rhombic-lip neural progenitors. Neuron 48(1):17–24. doi:10.1016/j.neuron.2005.08.028, pii: S0896-6273(05)00703-8

Marsh E, Baker R (1997) Normal and adapted visuooculomotor reflexes in goldfish. J Neurophysiol 77(3):1099–1118

Martinez S, Crossley PH, Cobos I, Rubenstein JL, Martin GR (1999) FGF8 induces formation of an ectopic isthmic organizer and isthmocerebellar development via a repressive effect on Otx2 expression. Development (Camb) 126(6):1189–1200

McFarland KA, Topczewska JM, Weidinger G, Dorsky RI, Appel B (2008) Hh and Wnt signaling regulate formation of olig2+ neurons in the zebrafish cerebellum. Dev Biol 318(1):162–171. doi:10.1016/j.ydbio.2008.03.016, pii: S0012-1606(08)00227-3

Medina JF, Garcia KS, Nores WL, Taylor NM, Mauk MD (2000) Timing mechanisms in the cerebellum: testing predictions of a large-scale computer simulation. J Neurosci 20(14):5516–5525

Meek J (1992) Comparative aspects of cerebellar organization. From mormyrids to mammals. Eur J Morphol 30(1):37–51

Mikami Y, Yoshida T, Matsuda N, Mishina M (2004) Expression of zebrafish glutamate receptor delta2 in neurons with cerebellum-like wiring. Biochem Biophys Res Commun 322(1): 168–176. doi:10.1016/j.bbrc.2004.07.095, pii: S0006-291X(04)01588-8

Millet S, Campbell K, Epstein DJ, Losos K, Harris E, Joyner AL (1999) A role for Gbx2 in repression of Otx2 and positioning the mid/hindbrain organizer. Nature (Lond) 401(6749):161–164. doi:10.1038/43664

Mo W, Chen F, Nechiporuk A, Nicolson T (2010) Quantification of vestibular-induced eye movements in zebrafish larvae. BMC Neurosci 11:110. doi:10.1186/1471-2202-11-110

Mueller T, Wullimann MF (2002) Expression domains of neuroD (nrd) in the early postembryonic zebrafish brain. Brain Res Bull 57(3–4):377–379, pii: S0361923001006943

Murakami T, Morita Y (1987) Morphology and distribution of the projection neurons in the cerebellum in a teleost, *Sebastiscus marmoratus*. J Comp Neurol 256(4):607–623. doi:10.1002/cne.902560413

Muto A, Ohkura M, Kotani T, Higashijima S, Nakai J, Kawakami K (2011) Genetic visualization with an improved GCaMP calcium indicator reveals spatiotemporal activation of the spinal motor neurons in zebrafish. Proc Natl Acad Sci USA 108(13):5425–5430. doi:10.1073/pnas.1000887108

Muto A, Ohkura M, Abe G, Nakai J, Kawakami K (2013) Real-time visualization of neuronal activity during perception. Curr Biol 23(4):307–311. doi:10.1016/j.cub.2012.12.040

Nakai J, Ohkura M, Imoto K (2001) A high signal-to-noise Ca(2+) probe composed of a single green fluorescent protein. Nat Biotechnol 19(2):137–141. doi:10.1038/84397

Nishida K, Flanagan JG, Nakamoto M (2002) Domain-specific olivocerebellar projection regulated by the EphA-ephrin-A interaction. Development (Camb) 129(24):5647–5658

Ogura E, Okuda Y, Kondoh H, Kamachi Y (2009) Adaptation of GAL4 activators for GAL4 enhancer trapping in zebrafish. Dev Dyn 238(3):641–655. doi:10.1002/dvdy.21863

Pan YA, Freundlich T, Weissman TA, Schoppik D, Wang XC, Zimmerman S, Ciruna B, Sanes JR, Lichtman JW, Schier AF (2013) Zebrabow: multispectral cell labeling for cell tracing and lineage analysis in zebrafish. Development (Camb) 140(13):2835–2846. doi:10.1242/dev.094631

Pastor AM, de la Cruz RR, Baker R (1994) Cerebellar role in adaptation of the goldfish vestibuloocular reflex. J Neurophysiol 72(3):1383–1394

Pastor AM, De la Cruz RR, Baker R (1997) Characterization of Purkinje cells in the goldfish cerebellum during eye movement and adaptive modification of the vestibulo-ocular reflex. Prog Brain Res 114:359–381

Pfeffer PL, Gerster T, Lun K, Brand M, Busslinger M (1998) Characterization of three novel members of the zebrafish Pax2/5/8 family: dependency of Pax5 and Pax8 expression on the Pax2.1 (noi) function. Development (Camb) 125(16):3063–3074

Picker A, Brennan C, Reifers F, Clarke JD, Holder N, Brand M (1999) Requirement for the zebrafish mid-hindbrain boundary in midbrain polarisation, mapping and confinement of the retinotectal projection. Development (Camb) 126(13):2967–2978

Pisharath H, Rhee JM, Swanson MA, Leach SD, Parsons MJ (2007) Targeted ablation of beta cells in the embryonic zebrafish pancreas using *E. coli* nitroreductase. Mech Dev 124(3):218–229. doi:10.1016/j.mod.2006.11.005, pii: S0925-4773(06)00215-2

Portugues R, Engert F (2009) The neural basis of visual behaviors in the larval zebrafish. Curr Opin Neurobiol 19(6):644–647. doi:10.1016/j.conb.2009.10.007

Reifers F, Bohli H, Walsh EC, Crossley PH, Stainier DY, Brand M (1998) Fgf8 is mutated in zebrafish acerebellar (ace) mutants and is required for maintenance of midbrain-hindbrain boundary development and somitogenesis. Development (Camb) 125(13):2381–2395

Reifers F, Adams J, Mason IJ, Schulte-Merker S, Brand M (2000) Overlapping and distinct functions provided by fgf17, a new zebrafish member of the Fgf8/17/18 subgroup of Fgfs. Mech Dev 99(1–2):39–49, pii: S0925477300004755

Reim G, Brand M (2002) Spiel-ohne-grenzen/pou2 mediates regional competence to respond to Fgf8 during zebrafish early neural development. Development (Camb) 129(4):917–933

Rhinn M, Lun K, Ahrendt R, Geffarth M, Brand M (2009) Zebrafish gbx1 refines the midbrain-hindbrain boundary border and mediates the Wnt8 posteriorization signal. Neural Dev 4:12. doi:10.1186/1749-8104-4-12

Rodriguez CI, Dymecki SM (2000) Origin of the precerebellar system. Neuron 27(3):475–486, pii: S0896-6273(00)00059-3

Rodriguez F, Duran E, Gomez A, Ocana FM, Alvarez E, Jimenez-Moya F, Broglio C, Salas C (2005) Cognitive and emotional functions of the teleost fish cerebellum. Brain Res Bull 66 (4–6):365–370. doi:10.1016/j.brainresbull.2004.11.026, pii: S0361-9230(05)00038-9

Sander JD, Cade L, Khayter C, Reyon D, Peterson RT, Joung JK, Yeh JR (2011) Targeted gene disruption in somatic zebrafish cells using engineered TALENs. Nat Biotechnol 29(8): 697–698. doi:10.1038/nbt.1934

Schier AF, Neuhauss SC, Harvey M, Malicki J, Solnica-Krezel L, Stainier DY, Zwartkruis F, Abdelilah S, Stemple DL, Rangini Z, Yang H, Driever W (1996) Mutations affecting the development of the embryonic zebrafish brain. Development (Camb) 123:165–178

Scott EK, Baier H (2009) The cellular architecture of the larval zebrafish tectum, as revealed by gal4 enhancer trap lines. Front Neural Circuits 3:13. doi:10.3389/neuro.04.013.2009

Scott EK, Mason L, Arrenberg AB, Ziv L, Gosse NJ, Xiao T, Chi NC, Asakawa K, Kawakami K, Baier H (2007) Targeting neural circuitry in zebrafish using GAL4 enhancer trapping. Nat Methods 4(4):323–326. doi:10.1038/nmeth1033

Sillitoe RV, Joyner AL (2007) Morphology, molecular codes, and circuitry produce the three-dimensional complexity of the cerebellum. Annu Rev Cell Dev Biol 23:549–577. doi:10.1146/annurev.cellbio.23.090506.123237

Simeone A (2000) Positioning the isthmic organizer where Otx2 and Gbx2meet. Trends Genet 16(6):237–240, pii: S0168-9525(00)02000-X

Simeone A, Acampora D, Gulisano M, Stornaiuolo A, Boncinelli E (1992) Nested expression domains of four homeobox genes in developing rostral brain. Nature (Lond) 358(6388): 687–690. doi:10.1038/358687a0

Sotelo C (2008) Viewing the cerebellum through the eyes of Ramon y Cajal. Cerebellum 7(4): 517–522. doi:10.1007/s12311-008-0078-0

Su CY, Kemp HA, Moens CB (2013) Cerebellar development in the absence of Gbx function in zebrafish. Dev Biol doi: 10.1016/j.ydbio.2013.10.026, pii: S0012-1606(13)00581-2

Suda Y, Matsuo I, Aizawa S (1997) Cooperation between Otx1 and Otx2 genes in developmental patterning of rostral brain. Mech Dev 69(1–2):125–141

Sugihara I (2006) Organization and remodeling of the olivocerebellar climbing fiber projection. Cerebellum 5(1):15–22. doi:10.1080/14734220500527385

Sugihara I, Quy PN (2007) Identification of aldolase C compartments in the mouse cerebellar cortex by olivocerebellar labeling. J Comp Neurol 500(6):1076–1092. doi:10.1002/cne.21219

Sugihara I, Shinoda Y (2004) Molecular, topographic, and functional organization of the cerebellar cortex: a study with combined aldolase C and olivocerebellar labeling. J Neurosci 24(40): 8771–8785. doi:10.1523/JNEUROSCI.1961-04.2004

Sugihara I, Marshall SP, Lang EJ (2007) Relationship of complex spike synchrony bands and climbing fiber projection determined by reference to aldolase C compartments in crus IIa of the rat cerebellar cortex. J Comp Neurol 501(1):13–29. doi:10.1002/cne.21223

Tanabe K, Kani S, Shimizu T, Bae YK, Abe T, Hibi M (2010) Atypical protein kinase C regulates primary dendrite specification of cerebellar Purkinje cells by localizing Golgi apparatus. J Neurosci 30(50):16983–16992. doi:10.1523/JNEUROSCI.3352-10.2010

Tsai PT, Hull C, Chu Y, Greene-Colozzi E, Sadowski AR, Leech JM, Steinberg J, Crawley JN, Regehr WG, Sahin M (2012) Autistic-like behaviour and cerebellar dysfunction in Purkinje cell Tsc1 mutant mice. Nature (Lond) 488(7413):647–651. doi:10.1038/nature11310

Umeda K, Shoji W, Sakai S, Muto A, Kawakami K, Ishizuka T, Yawo H (2013) Targeted expression of a chimeric channelrhodopsin in zebrafish under regulation of Gal4-UAS system. Neurosci Res 75(1):69–75. doi:10.1016/j.neures.2012.08.010

Valente A, Huang KH, Portugues R, Engert F (2012) Ontogeny of classical and operant learning behaviors in zebrafish. Learn Mem 19(4):170–177. doi:10.1101/lm.025668.112

Volkmann K, Rieger S, Babaryka A, Koster RW (2008) The zebrafish cerebellar rhombic lip is spatially patterned in producing granule cell populations of different functional compartments. Dev Biol 313(1):167–180. doi:10.1016/j.ydbio.2007.10.024, pii: S0012-1606(07)01438-8

Voogd J, Glickstein M (1998) The anatomy of the cerebellum. Trends Neurosci 21(9):370–375, pii: S0166-2236(98)01318-6

Wallace VA (1999) Purkinje-cell-derived Sonic hedgehog regulates granule neuron precursor cell proliferation in the developing mouse cerebellum. Curr Biol 9(8):445–448, pii: S096098229980195X

Wang VY, Rose MF, Zoghbi HY (2005) Math1 expression redefines the rhombic lip derivatives and reveals novel lineages within the brainstem and cerebellum. Neuron 48(1):31–43. doi:10.1016/j.neuron.2005.08.024, pii: S0896-6273(05)00699-9

Wassarman KM, Lewandoski M, Campbell K, Joyner AL, Rubenstein JL, Martinez S, Martin GR (1997) Specification of the anterior hindbrain and establishment of a normal mid/hindbrain organizer is dependent on Gbx2 gene function. Development (Camb) 124(15):2923–2934

Wechsler-Reya RJ, Scott MP (1999) Control of neuronal precursor proliferation in the cerebellum by Sonic hedgehog. Neuron 22(1):103–114, pii: S0896-6273(00)80682-0

Wilson LJ, Wingate RJ (2006) Temporal identity transition in the avian cerebellar rhombic lip. Dev Biol 297(2):508–521. doi:10.1016/j.ydbio.2006.05.028, pii: S0012-1606(06)00867-0

Wilson SW, Brand M, Eisen JS (2002) Patterning the zebrafish central nervous system. Results Probl Cell Differ 40:181–215

Wingate RJ (2001) The rhombic lip and early cerebellar development. Curr Opin Neurobiol 11(1):82–88, pii: S0959-4388(00)00177-X

Wingate R (2005) Math-Map(ic)s. Neuron 48(1):1–4. doi:10.1016/j.neuron.2005.09.012, pii: S0896-6273(05)00779-8

Wingate RJ, Hatten ME (1999) The role of the rhombic lip in avian cerebellum development. Development (Camb) 126(20):4395–4404

Wullimann MF, Rupp B, Reichert H (1996) Neuroanatomy of the zebrafish brain: a topological atlas. Birkhäuser, Basel

Wurst W, Bally-Cuif L (2001) Neural plate patterning: upstream and downstream of the isthmic organizer. Nat Rev Neurosci 2(2):99–108

Xiao A, Wang Z, Hu Y, Wu Y, Luo Z, Yang Z, Zu Y, Li W, Huang P, Tong X, Zhu Z, Lin S, Zhang B (2013) Chromosomal deletions and inversions mediated by TALENs and CRISPR/Cas in zebrafish. Nucleic Acids Res 41(14):e141. doi:10.1093/nar/gkt464

Yamada M, Terao M, Terashima T, Fujiyama T, Kawaguchi Y, Nabeshima Y, Hoshino M (2007) Origin of climbing fiber neurons and their developmental dependence on Ptf1a. J Neurosci 27(41):10924–10934. doi:10.1523/JNEUROSCI.1423-07.2007

Yoshida M, Hirano R (2010) Effects of local anesthesia of the cerebellum on classical fear conditioning in goldfish. Behav Brain Funct 6:20. doi:10.1186/1744-9081-6-20

Yoshida M, Kondo H (2012) Fear conditioning-related changes in cerebellar Purkinje cell activities in goldfish. Behav Brain Funct 8:52. doi:10.1186/1744-9081-8-52

Yoshida M, Okamura I, Uematsu K (2004) Involvement of the cerebellum in classical fear conditioning in goldfish. Behav Brain Res 153(1):143–148. doi:10.1016/j.bbr.2003.11.008

Zervas M, Millet S, Ahn S, Joyner AL (2004) Cell behaviors and genetic lineages of the mesencephalon and rhombomere 1. Neuron 43(3):345–357. doi:10.1016/j.neuron.2004.07.010, pii: S0896627304004283

Zupanc GK, Hinsch K, Gage FH (2005) Proliferation, migration, neuronal differentiation, and long-term survival of new cells in the adult zebrafish brain. J Comp Neurol 488(3):290–319. doi:10.1002/cne.20571

Chapter 14
Primitive Erythroblast Cell Autonomously Regulates the Timing of Blood Circulation Onset via a Control of Adherence to Endothelium

Atsuo Iida

Abstract Blood circulation is essential for the maintenance of life. It starts from the early embryonic stage and continues throughout the entire lifetime. However, it remains unclear how the circulation of blood starts in early development. This chapter introduces an active mechanism involving the primitive erythroblasts for the onset of blood circulation by monitoring fluorescently labeled blood precursors and blood vessels in transgenic zebrafish. The earliest erythroblasts are generated in the extravascular region and enter into the vascular tube by interacting with the endothelial cells. They continue to adhere to the vascular lumen and are not released into the bloodstream soon after the invasion. ADAM8, a membrane-bound metalloprotease expressed in the erythroblasts, mediates the onset of blood circulation by an abrogation of blood–vessel contact. In *adam8*-depleted embryos, the erythroid cells fail to detach from the vascular lumen and stagnate. Biochemical assay indicates that ADAM8 is an active protease that cleaves the membrane-anchored cell adhesion molecules such as PSGL-1. These findings suggest that the primitive erythroblasts have a cell autonomous function in regulating the timing of the onset of blood circulation.

Keywords ADAM8 • Blood circulation • Proteolysis • Zebrafish

14.1 Primitive Hematopoiesis and Onset of Blood Circulation in Vertebrates

In almost all animals, the cardiovascular system is critical to the maintenance of life. Blood circulation, particularly, functions as the central component of the system that carries oxygen throughout the body. The supply of oxygen by the

A. Iida (✉)
Institute for Frontier Medical Sciences, Kyoto University, Kyoto, Japan
e-mail: atsuo@frontier.kyoto-u.ac.jp

H. Kondoh and A. Kuroiwa (eds.), *New Principles in Developmental Processes*,
DOI 10.1007/978-4-431-54634-4_14,

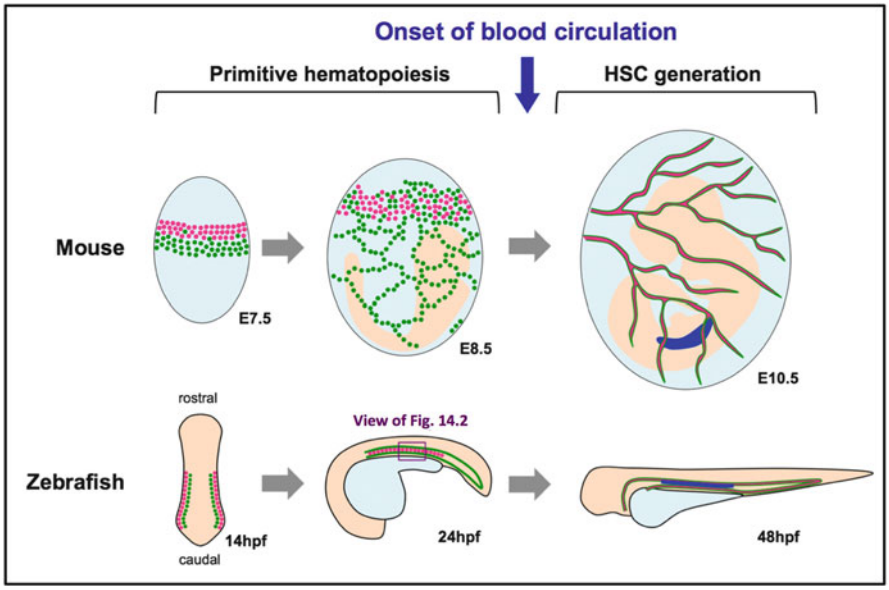

Fig. 14.1 The early hematopoietic system is conserved among vertebrates. Generation of primitive erythroblasts (*magenta*) and endothelial cells (*green*) from mesodermal cells is followed by differentiation of the endothelial cells into the vasculature and release of the erythroblasts into circulation. The hematopoietic stem cells (*HSC*) are generated in the aortic lumen (*blue*) after the onset of blood circulation. *E* embryonic day

circulating erythrocytes is already initiated at birth and continues for the entire lifetime. Despite its importance, how blood circulation starts during early development is mostly unknown. The circulatory system is composed of vasculatures, blood cells, and cardiac components. In the mouse, the first endothelial cells and hematopoietic cells arise in the blood island of the extra-embryonic yolk sac at embryonic (E) day 7.5, and the heartbeat-dependent circulating blood is observed around the E8.5 stage (Palis et al. 1999). The hematopoietic system that arose on the yolk sac is called the primitive hematopoiesis. In addition, vertebrates have another hematopoietic system. The definitive hematopoiesis initiates at a later stage of the primitive process during development and involves the generation of all types of hematopoietic cells from the hematopoietic stem cells (HSC) present in the adult bone marrow. Recently, time-lapse imaging has revealed that the first "definitive" hematopoietic cell is generated from the lumen of the dorsal aorta of the aorta-gonad-mesonephros (AGM) region at E9.5 (Boisset et al. 2010) when the blood circulation is already initiated. Thus, the initially circulated erythroblasts are derived from primitive hematopoiesis (Fig. 14.1). The primitive hematopoiesis-derived cells that undergo differentiation into predominantly erythrocytes and some myeloid lineage cells are directly generated from the mesodermal precursor cells and not via HSC. Additionally, mesodermal cells also give rise to the endothelial cells, which form the vascular plexus on the yolk sac. Thus, the primitive erythroblast is the first circulated blood cell that enters into the blood vessel and initiates circulation on

the yolk sac at E8–9. Previous studies have reported the behavior of primitive erythroblast in live embryos using whole embryo culture methods (Jones et al. 2002; Lucitti et al. 2007). However, there still are many questions to be solved about the behavior of these cells, such as the "pathways for entrance into the vasculature" or the "required factors for the circulation onset" in mammalian development. Native cell behaviors in the embryo in the mother's body are not easy to observe in current mammalian models. Thus, we used zebrafish as a model for these studies, because their eggs are fertilized and developed outside the mother's body.

14.2 Zebrafish, a Model for Live Imaging of Primitive Hematopoiesis

The zebrafish is a powerful tool that may be applied to such investigations because of the experimental advantages that it offers, such as (1) a transparent body in early development, (2) transgenic technologies for labeling specific cell lineages, and (3) a hematopoietic system similar to mammals. In zebrafish, the first erythroid cells generate the lateral plate mesoderm, which is bordered by endothelial cells (Davidson and Zon 2004). The mesodermal cells migrate together to the midline of the body and are called the intermediate cell mass (ICM); the endothelial cells form the first vascular tubes (Jin et al. 2005). The erythroblasts enter into the vascular tubes and start circulating through the plasma flow (Fig. 14.1). Although these events correspond to the primitive hematopoiesis and vascular formation in the blood island of the yolk sac in the mouse, the actual behavior of the living cells has not been previously reported. Recent advances in genetic engineering and innovations of the high-power microscope have allowed the development of high-resolution live imaging using zebrafish. Using a transgenic zebrafish in which blood vessel and erythroid precursor cell are labeled with green fluorescent protein (GFP) and red fluorescent protein (RFP), endothelial and hematopoietic cell behavior can be tracked in the living embryo (Lawson and Weinstein 2002; Kitaguchi et al. 2009).

14.3 Live Imaging of Onset of Blood Circulation in Zebrafish

Time-lapse imaging revealed the behavior of erythroblasts and endothelial cells before the onset of blood circulation. The early erythroblasts generated in the ICM were clustered in the ventral region of the dorsal aorta (DA) at 20–22 h post fertilization (hpf). A portion of the endothelial cells segregated into the ventral region of the DA, where they were organized into the posterior cardinal vein (PCV) at 23–24 hpf (Herbert et al. 2009; see also Fig. 14.2). Advanced vessel formation led to the localization of the ventral erythroblasts into the subaortic region, which is present between the DA and the PCV. Then, the erythroblasts gradually migrated into the lumen of both vascular tubes. Even though intravascular erythroid precursors were accumulated in the vasculature, circulation did not commence immediately after the invasion. Only upon nearly complete invasion by the erythroblasts were they synchronously released

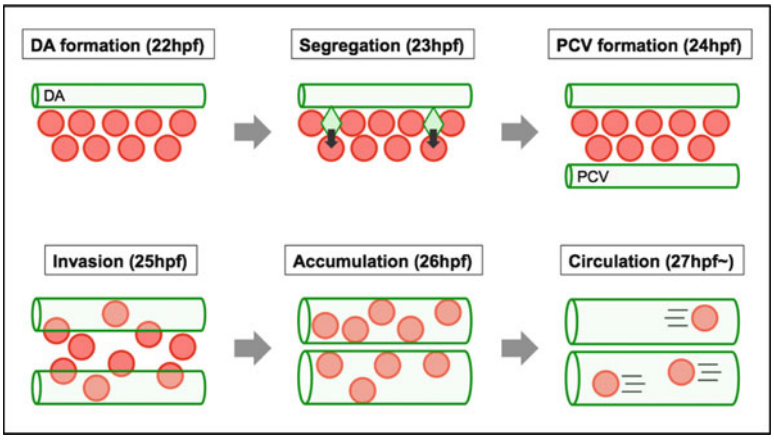

Fig. 14.2 Formation of blood vessels and onset of blood circulation in zebrafish. Formation of blood vessels (*upper*) and behavior of the primitive erythroblasts (*lower*) in the intermediate cell mass (*ICM*) region of zebrafish embryo (*purple square* in Fig. 14.1) are illustrated. First, the dorsal aorta (*DA*) appears in the dorsal region of the erythroblast [22 hours past fertilization (hpf)]. Some endothelial cells segregate ventrally and form the posterior cardinal vein (*PCV*) (23 and 24 hpf). After formation of the vessels, the erythroblasts enter both (26 hpf). The intravascular erythroblasts accumulate in the vasculature briefly (27 hpf) and then start circulating (~28 hpf)

into the flow and was circulation initiated (Figs. 14.2 and 14.3a). These results suggest that the timing of the onset of primitive blood circulation is strictly controlled. Interaction between the endothelial cells and the erythroblasts was observed during the invasion and the accumulation stages. High-resolution imaging of the erythroblasts revealed that most of them are attached to the lumen of the blood vessels via tiny membrane protrusions after the invasion (Fig. 14.3b). Further, electron microscopy confirmed contact of the erythroblast with the vessel lumen during and after invasion into the vasculature. Membrane protrusions belonging to the erythroblasts were observed in the live imaging as well as the electron micrographs, which suggested the involvement of integrin-mediated focal adhesion between erythroblasts and the vasculature (Fig. 14.2c). Indeed, the focal adhesion protein vinculin was strongly localized at the blood–vessel interface in the subaortic region and only weakly in the lumen of vessels before the onset of blood circulation. The vinculin signal decreased after the initiation of blood circulation, implying that the onset of blood circulation is associated with an abrogation of the blood–vessel adhesion (Iida et al. 2010).

14.4 Requirement of Intravascular Proteolysis for Blood Circulation

Intravascular proteolysis is one of the mechanisms involved in the abrogation of the heterologous cell–cell interactions. A metal chelator 1,10-orthophenanthroline and an active site-binding hydroxamate GM6001 are commonly used inhibitors for

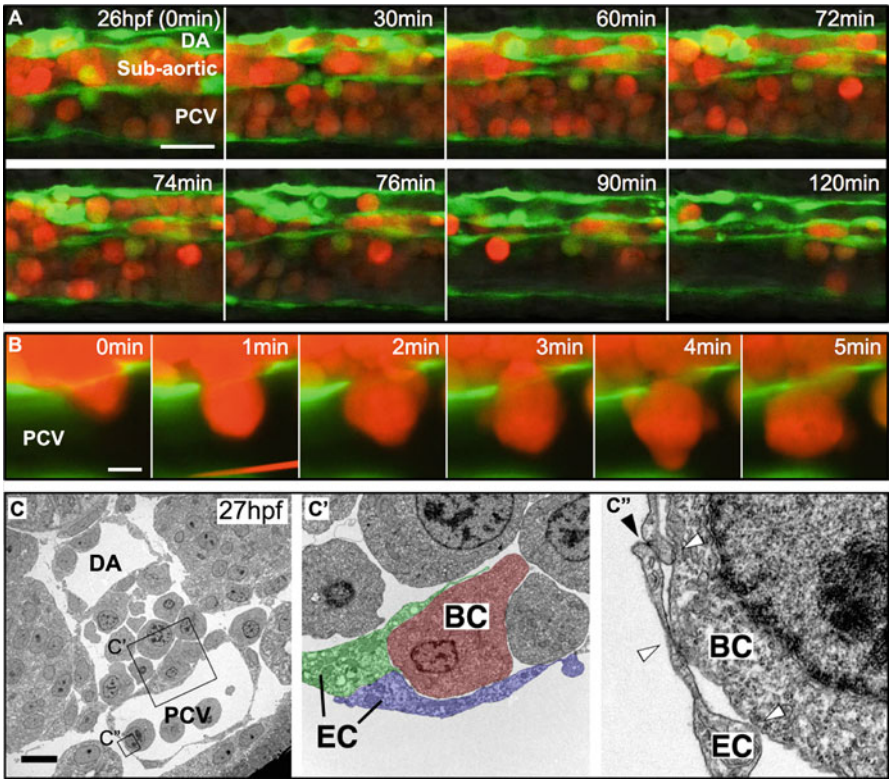

Fig. 14.3 Interaction of the primitive blood cells with the endothelial cells before the onset of circulation. (**a**) Time-lapse images capture the initiation of blood circulation with representative live-imaging stills from a key moment when primitive blood starts to flow in an embryo. On significant vessel formation at around 26 hpf (0 min), RFP^+ cells in the subaortic region become prominently motile and begin invasion into the DA and posterior cardinal vein (*PCV*) one after another. Sequential blood invasion into the DA (72 min) is followed by the sudden onset of circulation in the DA (74 min). Finally, most of the RFP^+ cells in the vasculature start to flow all at once (76 min). *Bar* 25 μm. (**b**) Time-lapse images of invasion into the PCV in the wild-type embryo. An erythroid cell adheres to the PCV with protrusions post invasion. *Bar* 5 μm. (**c**) Representative electron micrographs of transverse section of embryos at 27 hpf show erythroid cells in the subaortic region, in the PCV, and during invasion through the endothelial cell layer. *Bar* 10 μm. **c** Electron micrograph of transverse section of embryo shows aorta, cardinal vein, and subaortic region between them. *Black boxes* indicate areas shown enlarged in **c′** and **c″**. **c′** Enlargement of **c** shows an invading erythroid cell (*BC*, blood cell) surrounded firmly by endothelial cells (*EC*). *BC* blood cell. **c″** Enlargement of **c** shows erythroid cell tethered to the lumen of the PCV. *White arrowheads* point to blood–vessel contact; *black arrowhead* points to vessel–vessel contact

metalloproteases, including matrix metalloproteases (MMP) and "a disintegrin and metalloproteinases" (ADAMs) (Arribas et al. 1996; Moss and Rasmussen 2007). Injecting these solutions into the vasculature at the pre-circulation stage, when the plasma flow has already occurred, resulted in a partial accumulation of erythroblasts in the vasculature post circulation (Iida et al. 2010). These results indicated that

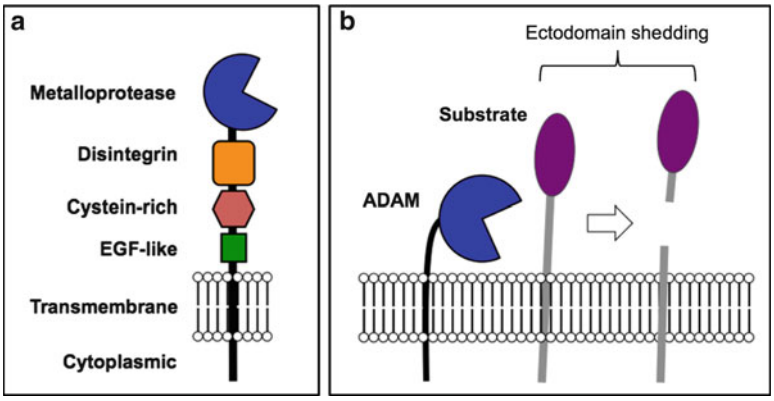

Fig. 14.4 Membrane metalloproteases release the extracellular domain of membrane-bound proteins. **a** Typical ADAM protease possesses an amino-terminal metalloprotease domain, followed by a disintegrin domain, a cysteine-rich region, an EGF-like repeat, a transmembrane domain, and a cytoplasmic domain. **b** ADAM is implicated in the ectodomain shedding of membrane-bound proteins, such as adhesion molecules or growth factors. A cleaved extracellular domain is released from the cell surface in response to ectodomain shedding

intravascular metalloproteases play some role in the abrogation of the blood–vessel interaction in the lumen of the vasculature.

ADAM family proteases are candidates for the detachment of blood from the vessel wall because of their demonstrated role in the ectodomain shedding of various cell adhesion molecules such as E-, N-, and VE-cadherin, L-selectin, and P-selectin glycoprotein ligand-1 (PSGL-1) (Edwards et al. 2008; see also Fig. 14.4). In circulatory systems, ADAM10 regulates the functions of a VE-cadherin-dependent endothelial cell and in vitro leukocyte transendothelial migration (Schulz et al. 2008). ADAM8 is another candidate protease for the blood–vessel interaction, which is distributed in the hematopoietic tissues of mammals such as peripheral blood, bone marrow, and thymus. ADAM8 expressed in neutrophils catalyzes L-selectin shedding (Gómez-Gaviro et al. 2007). However, the in vivo physiological functions of ADAM8 proteases are mostly unknown. In the development of zebrafish, the *adam8* transcript was highly expressed in the primitive erythroblasts located in the subaortic region, which were low in the intravascular erythroid cells (Iida et al. 2010). In the *adam8* knockdown embryo using morpholino antisense oligonucleotides, primitive erythroblasts stagnated in the vasculature without apparent abnormalities in vascular formation and blood invasion (Fig. 14.5a–d). Moreover, normal heartbeat and plasma flow were also initiated in *adam8*-deficient fish and the resulting phenotype was similar to that from the foregoing inhibitor assay. Thus, zebrafish *adam8* regulates the timing of onset of blood circulation without involvement in the development of the cardiovascular system. The erythroblasts lacking *adam8* express *gata1* and *α-e1-globin* transcripts (Iida et al. 2010), and undergo differentiation into *o*-dianisidine-positive mature erythroid cells that possess the ability to carry oxygen. These results suggest that *adam8* is required for blood circulation rather than the cell fate determination of erythroid precursors.

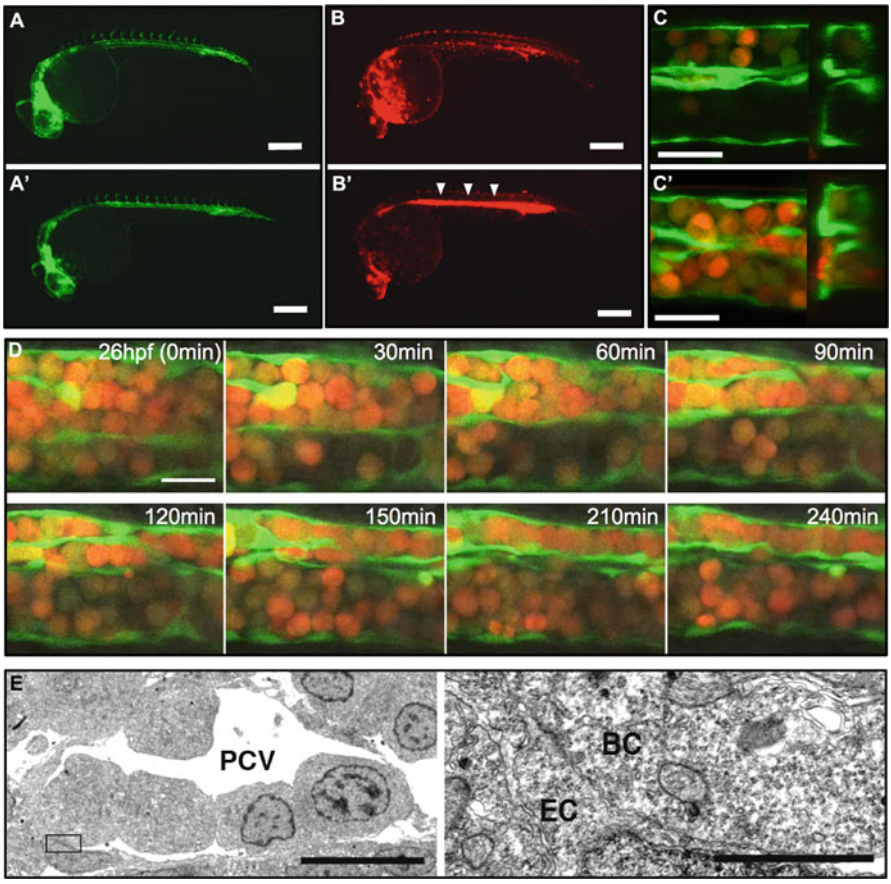

Fig. 14.5 ADAM8 is essential for the onset of primitive blood circulation. (**a**, **b)** Representative images of live embryos injected with control (**a**, **b**) and *adam8* morpholino oligo (**a′**, **b′**) observed by stereomicroscopy at 30 hpf. An accumulation of RFP^+ erythroblasts in the trunk is evident in *adam8* knockdown fish (*white arrowheads*). *Bars* 250 μm. **c** Representative Z-stack images of the control (**c**) and adam8 knockdown embryos (**c′**) at 30 hpf. Intravascular blood accumulation is apparent in the *adam8* knockdown fish. *Bars* 25 μm. (**d)** Time-lapse image captures the failure of onset of blood circulation in *adam8* knockdown fish at 26–30 hpf. (**e)** Representative electron micrographs of transverse section of *adam8* morphants at 27 hpf. Erythroid cells adhere to the endothelial cells in the lumen of the PCV. *Bars* 10 μm (*left panel*); 1 μm (*right panel*)

Overexpression of protease-defective ADAM8 (EQ mutant) in primitive erythroblasts resulted in the inhibition of the onset of blood circulation, albeit without failure in vascular formation or heartbeat, similar to the knockdown assay (Iida et al. 2010). These dominant negative effects not only indicated the autonomous role of ADAM8 in the erythroblasts but also suggested a requirement for ADAM8 metalloprotease activity in the abrogation of blood–vessel adhesion. Moreover, the *adam8* knockdown embryo exhibited remarkable adhesion between erythroid cells and the lumen of the vasculature in electron micrographs (Fig. 14.5e) and displayed

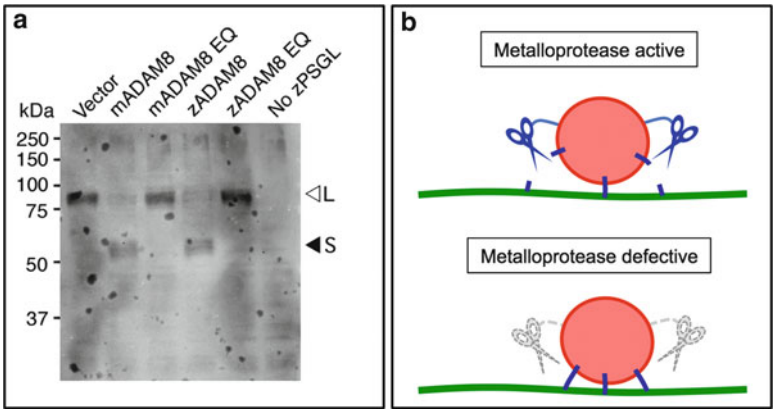

Fig. 14.6 Onset of blood circulation depends on metalloprotease. **a** Mouse ADAM8 (mADAM8), protease-defective mADAM8 (mADAM8 EQ), zebrafish ADAM8 (zADAM8), zADAM8 EQ, or empty vector cDNA was coexpressed with zebrafish PSGL-1-HA in HEK-293T cells. Ectodomain shedding was assessed by Western blotting for HA. Signals for long forms (*L*) were decreased and those for short forms (*S*) were increased significantly by expression of mADAM8 and zADAM8, but not by expression of EQ mutants. **b** This cartoon indicates the function of ADAM8 present on the erythroid cell. ADAM8 cleaves the adhesion molecules responsible for the blood–vessel contact (*upper*). Loss of this function results in strong adherence of the erythroid cells to the vascular lumen (*lower*)

an increase in vinculin signal on the surface of erythroid cells (Iida et al. 2010). These results suggest a critical role of ADAM8 as a protease in disrupting the blood–vessel adhesion at the onset of blood circulation.

L-selectin has been previously reported as a substrate for ADAM8 (Gómez-Gaviro et al. 2007); however, the *l-selectin ortholog gene* has not yet been identified in the zebrafish genome. Another candidate for adhesion substrate molecule is the P-selectin glycoprotein ligand-1 (PSGL-1), which is a major mucin-type adhesion protein present in mammalian blood. PSGL-1 existing on a leukocyte is required to act as a ligand for E-, L-, and P-selectin present on an endothelial cell for "leukocyte rolling," resulting from the loose interaction between blood cells and vascular lumen (McEver and Cummings 1997; Ley et al. 2007). Furthermore, recombinant soluble PSGL-1 accelerates thrombolysis and prevents occlusion (Kumar et al. 1999), and some metalloproteases such as mocarhagin, BASE, or ADAM10 are known to degrade PSGL-1 (De Luca et al. 1995; Lichtenthaler et al. 2003). In the zebrafish embryo, the *psgl-1* ortholog gene is ubiquitously expressed, including the ICM region. Biochemical assay indicates that murine and zebrafish PSGL-1 are shed by both murine and zebrafish ADAM8 depending on their protease activity in cultured mammalian cells (Fig. 14.6a). Thus, ADAM8 is an active metalloprotease that can shed the ectodomain of a cell adhesion molecule such PSGL-1 (Fig. 14.6b).

14.5 Conclusion

This chapter describes the significance of heterologous cell–cell interactions occurring between primitive hematopoietic cells and endothelial cells during development of the cardiovascular system. The primitive erythroblasts interacting with the endothelial cells pass through three states to initiate blood circulation in zebrafish: (1) invasion through the endothelial cell layer, (2) "idling" or pausing on the lumen of the vasculature, and (3) an almost simultaneous release into circulation. This dissection revealed the role of ADAM8 in the progression from idling to the release of blood cells. ADAM8 contributed to the onset of blood circulation via cleavage of cell adhesion molecules such as PSGL-1. In the case of loss of this function, the erythroblasts stagnated in the vasculature and were unable to enter into the bloodstream at an appropriate time. Based on these findings, we propose that the onset of primitive blood circulation is regulated not only passively by blood flow or cardiovascular development but also by the autonomous proteolysis catalyzed by ADAM8 in the blood cell (Fig. 14.7).

Why does the onset of primitive blood circulation require an autonomous regulation in addition to heartbeat-dependent passive control? First, proteolysis allows the segregation of the population of blood cells to be released into the circulation from

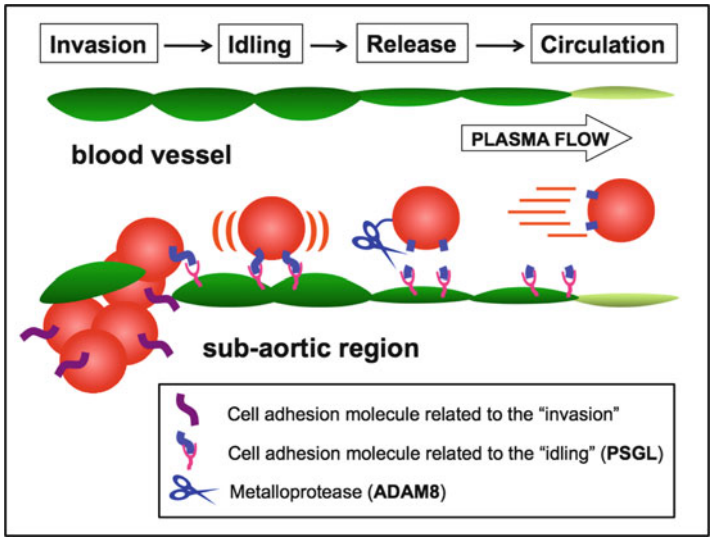

Fig. 14.7 A working hypothesis on the onset of primitive blood circulation. Initially, primitive erythroblasts in the subaortic region enter the vasculature with the aid of an endothelial cell adherent ("Invasion"). The intravascular erythroid cells are not released into the bloodstream upon invasion as they keep adhering to endothelial cells ("Idling"). On near completion of the invasion or the maturation of the vascular system, the blood–vessel adhesion is abrogated by ectodomain shedding of the adhesion molecules such a PSGL-1 by ADAM8 ("Proteolysis"). Subsequently, the erythroid cells are released into plasma flow ("Circulation")

those retained on the vasculature, as a portion of the erythroid precursors remain attached to the vessels after the start of blood circulation in wild-type embryos (Fig. 14.3a: 90 min). Moreover, another population of erythroid precursors located in the posterior blood island is likely to remain adhered to endothelial cells. Second, the onset of blood circulation is required to be strictly associated with development of the circulatory organ to prevent any leakage or congestion before the completion of vasculogenesis. The vascular diameter actually narrows during the erythroblast invasion and expands afterward (Fig. 14.3a).

Similar cell autonomous, proteolysis-dependent mechanisms responsible for the release into circulation may be used by various blood cell types in other vertebrates. The primitive erythroid cells in mice move from the blood island to the embryo proper in a stepwise pattern and not gradually (McGrath et al. 2003). *Adam8* is also expressed in adult hematopoietic tissues such as bone marrow and thymus in mice (The FANTOM Consortium 2005). All the outlined evidence supports the hypothesis that has been put forth. Although *Adam8*-deficient mice survive without major developmental defects (Kelly et al. 2005), whether primitive or definitive blood circulation is affected in these mice remains elusive.

As described, oviparous animals including the zebrafish have some advantages for developmental biology and cell biology compared to viviparous animals such as mice. In this study, we identified the synchronous circulation onset of the primitive erythrocytes in zebrafish development. On the other hand, the definitive blood cells generated from the HSCs might be serially released into the blood flow throughout a lifetime. Recently, the HSC could be visualized and traced in zebrafish (Bertrand et al. 2010; Kissa and Herbomel 2010). In the future, we would like to reveal the blood cell behavior and significance of interactions to the extracellular niches, including endothelial cells, using such vertebrate models.

References

Arribas J, Coodly L, Vollmer P et al (1996) Diverse cell surface protein ectodomains are shed by a system sensitive to metalloprotease inhibitors. J Biol Chem 271:11376–11382

Bertrand JY, Chi NC, Santoso B et al (2010) Haematopoietic stem cells derive directly from aortic endothelium during development. Nature (Lond) 464:108–111

Boisset JC, van Cappellen W, Andrieu-Soler C et al (2010) In vivo imaging of haematopoietic cells emerging from the mouse aortic endothelium. Nature (Lond) 464:116–120

Davidson AJ, Zon LI (2004) The 'definitive' (and 'primitive') guide to zebrafish hematopoiesis. Oncogene 23:7233–7246

De Luca M, Dunlop LC, Andrews RK (1995) A novel cobra venom metalloproteinase, mocarhagin, cleaves a 10-amino acid peptide from the mature N terminus of P-selectin glycoprotein ligand receptor, PSGL-1, and abolishes P-selectin binding. J Biol Chem 270:26734–26737

Edwards DR, Handsley MM, Pennington CJ (2008) The ADAM metalloproteinases. Mol Aspects Med 29:258–289

Gómez-Gaviro M, Domínguez-Luis M, Canchado J et al (2007) Expression and regulation of the metalloproteinase ADAM-8 during human neutrophil pathophysiological activation and its catalytic activity on L-selectin shedding. J Immunol 178:8053–8063

Herbert SP, Huisken J, Kim TN et al (2009) Arterial-venous segregation by selective cell sprouting: an alternative mode of blood vessel formation. Science 326:294–298
Iida A, Sakaguchi K, Sato K et al (2010) Metalloprotease-dependent onset of blood circulation in zebrafish. Curr Biol 20:1110–1116
Jin SW, Beis D, Mitchell T et al (2005) Cellular and molecular analyses of vascular tube and lumen formation in zebrafish. Development (Camb) 132:5199–209
Jones EA, Crotty D, Kulesa PM et al (2002) Dynamic in vivo imaging of postimplantation mammalian embryos using whole embryo culture. Genesis 34:228–235
Kelly K, Hutchinson G, Nebenius-Oosthuizen D et al (2005) Metalloprotease-disintegrin ADAM8: expression analysis and targeted deletion in mice. Dev Dyn 232:221–231
Kissa K, Herbomel P (2010) Blood stem cells emerge from aortic endothelium by a novel type of cell transition. Nature (Lond) 464:112–115
Kitaguchi T, Kawakami K, Kawahara A (2009) Transcriptional regulation of a myeloid-lineage specific gene lysozyme C during zebrafish myelopoiesis. Mech Dev 126:314–323
Kumar A, Villani MP, Patel UK et al (1999) Recombinant soluble form of PSGL-1 accelerates thrombolysis and prevents reocclusion in a porcine model. Circulation 99:1363–136
Lawson ND, Weinstein BM (2002) In vivo imaging of embryonic vascular development using transgenic zebrafish. Dev Biol 248:307–318
Ley K, Laudanna C, Cybulsky MI et al (2007) Getting to the site of inflammation: the leukocyte adhesion cascade updated. Nat Rev Immunol 7:678–689
Lichtenthaler SF, Dominguez DI, Westmeyer GG et al (2003) The cell adhesion protein P-selectin glycoprotein ligand-1 is a substrate for the aspartyl protease BACE1. J Biol Chem 278: 48713–48719
Lucitti JL, Jones EAV, Huang C et al (2007) Vascular remodeling of the mouse yolk sac requires hemodynamic force. Development (Camb) 134:3317–3326
McEver RP, Cummings RD (1997) Perspectives series: cell adhesion in vascular biology. Role of PSGL-1 binding to selectins in leukocyte recruitment. J Clin Invest 100:485–491
McGrath KE, Koniski AD, Malik J et al (2003) Circulation is established in a stepwise pattern in the mammalian embryo. Blood 101:1669–1676
Moss ML, Rasmussen FH (2007) Fluorescent substrates for the proteinases ADAM17, ADAM10, ADAM8, and ADAM12 useful for highthroughput inhibitor screening. Anal Biochem 366: 144–148
Palis J, Robertson S, Kennedy M et al (1999) Development of erythroid and myeloid progenitors in the yolk sac and embryo proper of the mouse. Development (Camb) 126:5073–5084
Schulz B, Pruessmeyer J, Maretzky T et al (2008) ADAM10 regulates endothelial permeability and T-Cell transmigration by proteolysis of vascular endothelial cadherin. Circ Res 102: 1192–1201
The FANTOM Consortium (2005) The transcriptional landscape of the mammalian genome. Science 309:1559–1563

Chapter 15
Limb Regeneration: Reconstitution of Complex Organs Using Specific Tissue Interactions

Akira Satoh

Abstract Limb regeneration in amphibians has been investigated for a long time because we still have not found a way to regenerate our body parts. Urodele amphibians generally have the ability to regenerate most of their organs. Limb regeneration has been investigated as a representative phenomenon of their high regeneration ability. Limb amputation in urodele amphibians causes regeneration blastema formation. A regeneration blastema is composed of undifferentiated cells called blastema cells. This blastema induction mechanism is the issue that has been the focus of study for a long time. Nerve tissue is known to be key for successful blastema formation and limb regeneration. Despite the importance of the nerve tissue in limb regeneration, its molecular description is not well established. Recently, a brand-new experimental system called an accessory limb model (ALM) was reported that is designed to reveal minimum and necessary tissue interaction including nerves. In this chapter, necessary tissue interactions for blastema induction in the ALM and related molecular descriptions are given.

Keywords Accessory limb model (ALM) • Apical epithelial/epithelium cap (AEC) • Blastema • Dedifferentiation • Limb regeneration • Nerve factor

15.1 Background of a Brand-New Experimental System in Urodele Amphibian Limb Regeneration

The history of amphibian limb regeneration is relatively long, spanning more than 240 years. The first study of amphibian limb regeneration was published in 1769 by Spallanzani (1769). The reason why amphibian limb regeneration has been studied for such a long time is very simple: we humans cannot regenerate our limbs and

A. Satoh (✉)
Okayama University, Research Core for Interdisciplinary Sciences (RCIS), Okayama, Japan
e-mail: satoha@cc.okayama-u.ac.jp

H. Kondoh and A. Kuroiwa (eds.), *New Principles in Developmental Processes*,
DOI 10.1007/978-4-431-54634-4_15, © Springer Japan 2014

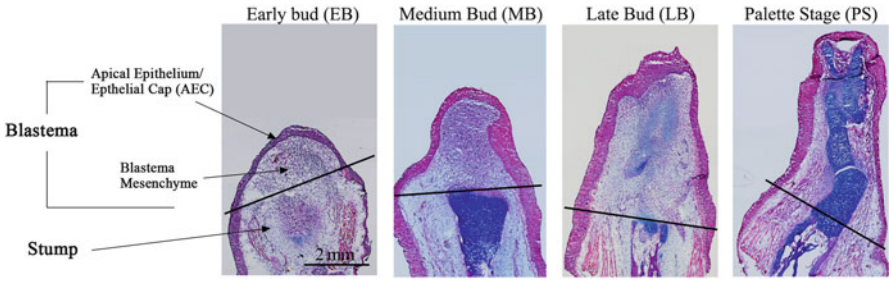

Fig. 15.1 Histology of the regeneration blastema in the amputated limbs. *Black lines* indicate the approximate border of the blastemas (regenerations). Cartilage is visualized by Alcian blue

amphibians can. The mystery is still outstanding so far and many scientists are still eagerly challenging it.

Blastema induction mechanism is the one of the biggest unsolved issues in this field. A regeneration blastema is the structure that forms after limb amputation in regenerative animals. In the early phases, a blastema consists of undifferentiated mesenchymal cells called blastema cells and an epithelial structure called the apical epithelium/epidermal cap (AEC) (Fig. 15.1). Later, undifferentiated blastemal mesenchyme differentiates into limb tissues, such as cartilaginous cells. Blastema cells are derived from varied limb tissues. It is noteworthy that dermis-derived blastema cells show a certain grade of multipotency in limb regeneration (Hirata et al. 2010; Kragl et al. 2009). Induction of such undifferentiated (and multipotent) blastema cells from fully differentiated limb tissues is the unique phenomenon of limb regeneration, and great effort has been expended to understand the underlying mechanisms. However, research effort on the issues always faces difficulties. The limb is a heavily complex structure with many kinds of tissues. When a limb is damaged, multiple tissues run their own healing programs, and, of course, wounding itself causes complex reactions such as inflammation. It is quite hard to approach such a complex structure with current biological techniques. Simplifying the experimental system is essential before investigating the molecular mechanisms of blastema induction.

The accessory limb model (ALM) is designed to solve the complexity in limb regeneration. Only skin wounding and nerve rerouting from many kinds of tissues results in blastema induction in the ALM (Endo et al. 2004; Satoh et al. 2007). Minimizing necessary tissues for limb induction is indeed simplifying limb regeneration study. The blastema induced by skin wounding plus nerve rerouting fundamentally possesses limb-forming ability (Fig. 15.2). To be precise, an induced limb in the ALM would not be properly be called “a regenerate,” because an original limb is largely intact. In the case of an amputated limb, a transverse cut damages all limb tissues, and all the stump tissues contribute to blastema formation and regenerate a complete replica of an original limb (Fig. 15.2a). On the other hand, accessory limb surgery basically damages only skin and nerves, suggesting a much more limited tissue contribution. Furthermore, an induced limb is usually not a complete replica of its stump limb (Fig. 15.2b–d); the induced limb lacks a proximal region.

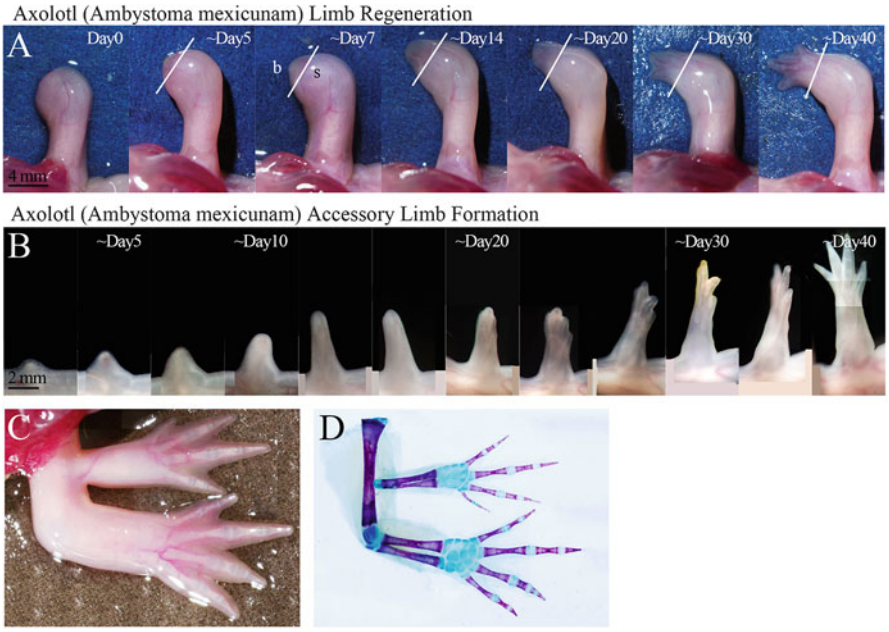

Fig. 15.2 Comparison of accessory limb formation and limb regeneration. (**a**) Regular limb regeneration process in an amputated limb. The limb is amputated at the lower arm level. b: blastema. s: stump. White lines in A indicate the border of the blastema. (**b**) Process of the accessory limb formation. (**c**) Accessory limb. Left panel shows dorsal view of the induced accessory limb. Right panel shows skeletal pattern visualized by Alizarin Red and Alcian blue. The accessory limb can be induced by only skin wounding and nerve deviation. (**d**) bone and cartilage are visualized by Alizarin red and Alcian blue

An accessory limb induced at the middle of the upper limb does not have half an upper limb (Fig. 15.2c, d). Although some differences are observable in the ALM and regular limb regeneration, it is still possible to use the ALM as a substitute and better experimental model for an amputated limb because a blastema in the ALM result in a patterned limb from greatly limited tissues.

15.2 Early Events of ALM Limb Regeneration

Nerve and skin wounds are sufficient to initiate limb regeneration responses in the ALM as mentioned (Endo et al. 2004; Satoh et al. 2007). A summary of accessory limb induction is shown in Fig. 15.3. Initially, a piece of skin is removed. Such simple skin wounding results in skin healing but does not result in limb regeneration (Fig. 15.3, right column). In this process, surrounding epidermis migrates to the wound, and dermal collagen deposition follows immediately (Carlson et al. 1998; Satoh et al. 2008a, b, 2012a; Seifert et al. 2012b). However, if nerves are rerouted to

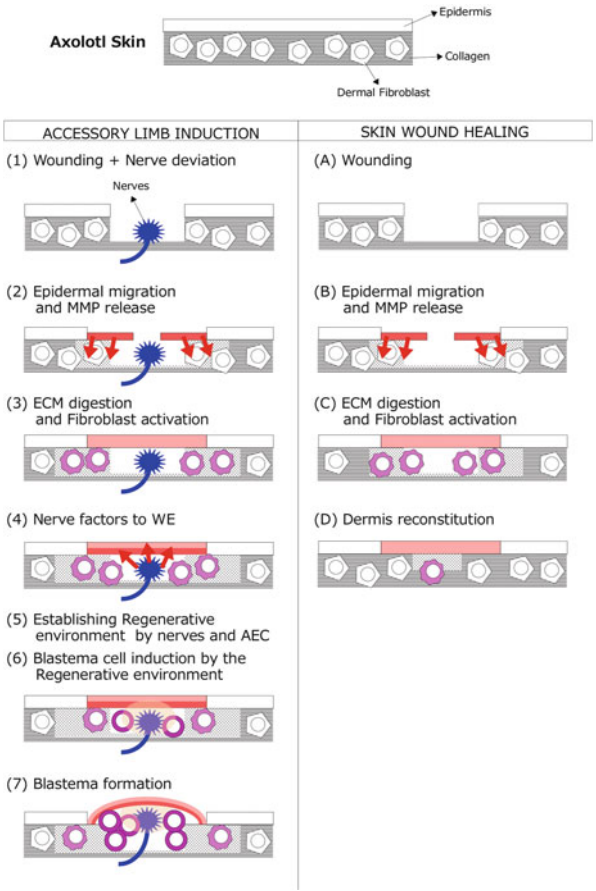

Fig. 15.3 Diagrams for comparison of accessory limb induction and skin wound healing. Axolotl skin consists of dermis and epidermis. *1*, *A* Dermal fibroblasts exist in dermal collagen. Skin wounding damages in both dermis and epidermis. *1* Immediately after skin wounding, nerve is deviated to the wound. *2*, *B* Surrounding epidermis migrates to cover the wound surface and the migrating epidermis (epithelium) expresses matrix metalloproteinases (*MMPs*). The epithelium/epidermis over the wound is called wound epithelium/epidermis (*WE*). *3*, *C* Extracellular matrix (*ECM*) is digested by MMPs and fibroblasts are activated. *4* Nerves are expected to secrete some factors to specify WE to regeneration a specific epithelium called the apical epithelial/epithelium cap (*AEC*). *D* Without the nerve deviation, dermal fibroblasts start reconstituting dermis. *5*, *6* Interaction between AEC and nerves creates regenerative environment and induces blastema cells. *7* Blastema is induced by nerve deviation and skin wounding

the wound, completely different responses are activated (Fig. 15.3, left column). The rerouted nerve ends interact with the overlying epidermis to create an appropriate environment for limb regeneration. In the nerve presence, overlying epidermis/epithelium is transformed into regeneration-specific epidermis known as the AEC (Satoh et al. 2008b, 2012a). In particular, the basal layer of AEC appears to play an important role in AEC regulation of the blastema, and the basal layer of AEC shows

specific gene expression patterns. For example, Fgf8, Sp9, Fgf receptor 2 (Fgfr2), fibronectin, and thrombospondin-1[1] are upregulated in this basal layer of AEC (Christensen et al. 2002; Han et al. 2001; Poulin et al. 1993; Satoh et al. 2008b; Whited et al. 2011). Furthermore, keratin 5 and cell proliferation are negatively regulated in the basal layer (Moriyasu et al. 2012; Satoh et al. 2012a). Functions of such basal layer-specific regulation are still under investigation. Interaction between nerves and AEC leads to accumulation of mesenchymal cells. Fibroblasts and other cells migrate and accumulate around the regenerative field created by nerves and AEC (Endo et al. 2004; Gardiner et al. 1986). Subsequently, a regeneration blastema consisting of undifferentiated cells is formed (Figs. 15.2b and 15.3(7)). Such regeneration blastemas in the ALM have been considered equivalent to developing limb buds (Muneoka and Bryant 1982; Satoh et al., 2007). These regeneration ALM blastemas mimic limb developmental processes to restore the limb in an adequate environment (Fig. 15.2). These sequential regeneration processes are initiated by only skin wounding and nerve rerouting in the axolotl limb.

15.3 Seeking Nerve Factors as a Trigger of Limb Regeneration

The presence of nerves is crucial for successful limb regeneration as just indicated. Nerves control regeneration-specific regulation in early regeneration phases. However, the molecular mechanisms of nerve regulation in the early phases are unclear. The importance of nerves in limb regeneration was first recognized in 1823 (Todd 1823), and some candidate nerve factors have since been reported (Makanae and Satoh 2012; Nye et al. 2003). Presumably, not a single but multiple nerve factors are involved in the regulation of limb regeneration.

A couple of potential nerve factors have been reported so far. Fibroblast growth factors (FGFs) have been reported as the nerve factor by some independent research groups (Dungan et al. 2002; Mullen et al. 1996; Satoh et al. 2008b, 2011). If limb regeneration recapitulates limb development, Fgfs are likely to be central regulators because they play critical roles in limb induction during development (Capdevila and Izpisua Belmonte 2001). Fgf2 and Fgf10, which can induce limb bud formation in chick embryos (Cohn et al. 1995; Ohuchi et al. 1997; Yonei-Tamura et al. 1999), are expressed in axolotl dorsal root ganglia that project axons to limbs (Mullen et al. 1996; Satoh et al. 2011). Furthermore, repeated application of Fgf2 and Fgf8, instead of nerves, to wounded skin can induce regeneration blastemas (Satoh et al. 2011). Given those facts, it is very likely that Fgfs from nerves trigger limb regeneration. On the other hand, anterior gradient (*AG*)[2] was reported as an exclusive

[1] Thrombospondin-1 (TSP-1), the founding member of the thrombospondin family, is released by human platelets in response to thrombin.

[2] Anterior gradient (AG): synonym is XAG2. AG is expressed in the cement gland of a *Xenopus* tadpole.

nerve molecule that could replace nerves in limb regeneration (Kumar et al. 2007). The AG is reportedly a regulator of gland development in other species (Sive and Bradley 1996), AG functions in limb development have not been described yet in any species. Therefore, the detailed molecular mechanisms of AG regulation in limb regeneration are uncertain and unpredictable. Fgfs and AG are indeed good candidates as the nerve factor for successful limb regeneration. However, this still remains controversial; further molecular analysis is needed.

What are the nerve functions? It is strongly suggested that the roles of nerves in early phases of regeneration involve interactions with overlying epidermis/epithelium and induction of AEC (Makanae and Satoh 2012). AEC is considered an equivalent structure to the apical ectodermal ridge (AER) in higher vertebrates. So, nerve function in AEC induction may be assumed from AER studies. Reportedly, AER is induced and maintained by Fgf signaling (Sun et al. 2002). From this point of view, it is easy to imagine the interaction between nerves and AEC because nerves can be a source of Fgfs. Actually, nerve rerouting to wounded skin induces Sp9, one of the AEC marker genes, in the overlying wound epithelium (Satoh et al. 2008). It is also known that continuous inputs from nerves are important for maintenance of AEC (Satoh et al. 2012a), which is consistent with the necessity of Fgfs for AER maintenance in higher vertebrates (Martin 1998; Ohuchi et al. 1997). Although nerve functions in AEC induction and maintenance can be assumed from AER functions of chick/mouse limb development, the molecular details of nerve functions in AEC induction and maintenance have not been described at all.

Maintenance of blastema cell proliferation is also one of the predictive nerve functions. In collaboration with AEC, nerve factors reportedly promote mitosis (Boilly and Albert 1988). Candidate nerve factors, such as Fgfs, AG, Ggf, substance P, and transferrin, are reported to act as mitogens for blastema cells (Albert et al. 1987; Kiffmeyer et al. 1991; Globus 1988; Wang et al. 2000; Nye et al. 2003). However, direct evidence that the nerve secretes those factors to blastema cell to promote cell proliferation has not been reported so far.

Identification of nerve factors has been a long-standing issue in this field, the efforts consuming several decades. Poor genetic information and limited useful molecular biological techniques make the identification of nerve factors difficult. But, nerve factors must be identified at any cost, because “anything’s possible if you’ve got enough nerve!”

15.4 Dedifferentiation of Dermal Fibroblasts in Limb Regeneration

The regenerative environment induces blastemas comprising undifferentiated blastema cells. A blastema was considered to consist of homogeneous and multipotent stem-like cells. However, a recent study clearly indicates that the blastema consists of heterogeneous cell populations (Kragl et al. 2009). For example, muscle-derived blastema cells participate only in muscle formation in limb regeneration (Kragl

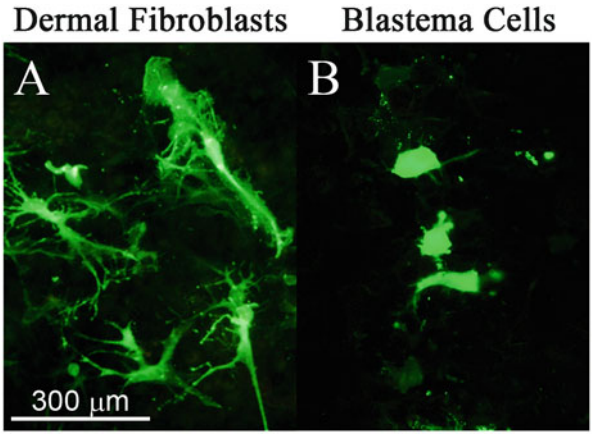

Fig. 15.4 Cell morphology of axolotl fibroblasts and blastema cells. **a** Dermal fibroblasts in axolotl akin were visualized by electroporation with the green fluorescent protein (*GFP*) expression vector. GFP plasmids were electroporated into axolotl limb skin, and GFP fluorescence was captured by fluorescent microscope. **b** Blastema cells with GFP expression vector. The same procedure as above visualizes blastema cells. Blastema cells are typically rounded and compact cells as compared to dermal fibroblasts

et al. 2009). On the other hand, dermis-derived blastema cells can redifferentiate into varied tissues within the limits of connective tissue lineages, such as cartilage (Hirata et al. 2010; Kragl et al. 2009). Generating such undifferentiated and multipotent blastema cells from fully differentiated tissues has been studied for a long time and is yet unresolved.

As mentioned earlier, dermal fibroblast-derived blastema cells are the only population that can participate in varied tissues in limb regeneration. In mature skin, dermal fibroblasts maintain skin homeostasis and collagen fibers. Upon skin damage, dermal fibroblasts immediately start regenerating dermal collagen matrices. In the case of higher vertebrates, the regenerated collagen fibers are disorganized, resulting in scar formation. Axolotl skin wound healing is basically the same but is scarless (Levesque et al. 2010). In axolotl scarless wound healing, the emergence of blastema cells has been disputed. However, as already mentioned, nerves in wounded skin suppress collagen deposition and convert wound healing to blastema formation (Satoh et al. 2012b). It is known that dermal fibroblasts migrate to the regenerative field (Gardiner et al. 1986). In the ALM, dermal fibroblasts start migrating from day 3 to 5 after the establishment of nerve–AEC interactions (Endo et al. 2004; Satoh et al. 2008b). In an intact limb, axolotl dermal fibroblasts are relatively larger and take typical fibroblastic shape in vivo (Fig. 15.4a). During and after migration, however, dermal fibroblasts are thought to be reprogrammed/dedifferentiated to form undifferentiated blastema cells, which are small and rounded (Fig. 15.4b). Such dermis-derived blastema cells can participate in varied cell types within the connective tissue lineage.

Dedifferentiation of dermal fibroblasts in limb regeneration is still debated because the existence of multipotent stem cells in dermis cannot be denied. However, the cell contribution from the dermis is quite large in a blastema. It is unlikely that such a large population of multipotent stem cells is maintained in the axolotl dermis. Rather, dermal fibroblasts are dedifferentiated during limb regeneration and generate a large number of blastema cells. The dedifferentiation mechanisms are a mystery. But if such dedifferentiation mechanisms are programmed in their genome, it can be called an "endogenous reprogramming" system. Such an endogenous reprogramming system should be worthwhile studying.

15.5 Wound Healing Versus Epimorphic Regeneration

Tissue regeneration and epimorphic regeneration offer mutually interesting comparisons. It is still unknown whether these are independent reactions. Higher vertebrates undoubtedly possess tissue regeneration capability. For example, we can restore muscle damage and bone fracture. Actually, relatively smaller (local) damage can be restored via the tissue regeneration system. How do regenerative animals restore such smaller damages? Needless to say, they can regenerate a whole limb with the epimorphic regeneration ability. Do they use the epimorphic regeneration system in smaller damage repair, such as a bone fracture? Or, do they have a tissue regeneration system and use it depending on the situation? This is an important issue in comparing the regeneration ability of amphibians with that of higher vertebrates.

ALM can provide a good comparative environment between the epimorphic and tissue regeneration. As mentioned, simple skin peeling results in skin healing without extra limb formation (Endo et al. 2004; Seifert et al. 2012b). In such skin peeling, exposed inner tissues are immediately covered by migrating epidermis. Subsequently, fibroblasts gather, restore collagens, and reconstitute the dermis (Figs. 15.3 and 15.5) (Satoh et al. 2008a, 2012b). In such a skin-healing process, emergence of blastema cells has been disputed. However, nerve-deviated skin wounds and simple skin wounds show a different gene expression pattern in ALM (Satoh et al. 2007). Thus, it is considered that wounded skin (dermis) is restored by activated dermal fibroblasts, which are not dedifferentiated as the same level as blastema cells.

Bone fracture/excision is also used as a comparative experimental system. Interestingly, axolotls cannot regenerate relatively tiny bone excisions although they can regenerate an entire limb (Goss 1956; Hutchison et al. 2007). When axolotl bones of 2–4 mm of the radius or tibia are excised, the damaged bone is not restored. Although such excision damage is not restorable, some restoration reactions can be observed (Satoh et al. 2010a), as in higher vertebrates. The damaged bone forms cartilaginous calluses similar to those in humans, which can join if the excision is small. However, if the distance between the ends of the damaged bone exceeds a certain length, calluses from the ends cannot join and an excision gap remains. In these bone-healing processes accompanying callus formation, whether the gap is

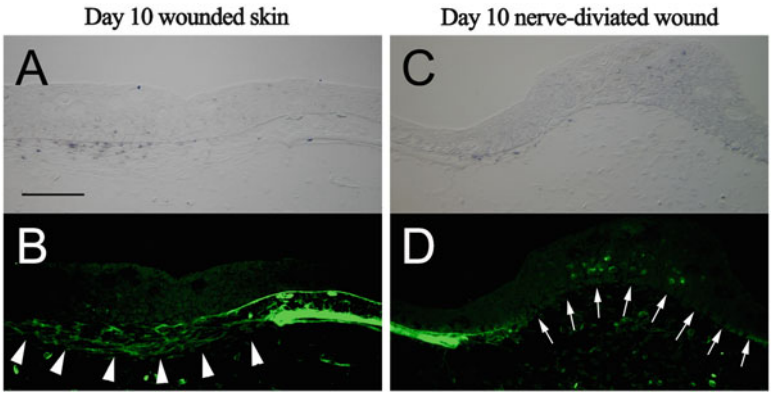

Fig. 15.5 Dermis reconstitution and blastema formation. **a**, **b** Simple skin wounding. Type I collagen reconstitution is visualized by immunofluorescence. *Arrowheads* indicate type I collagen expression. **c**, **d** Type I collagen deposition is inhibited in the regenerative environment. *Arrows* indicate border of blastema epithelium (from Satoh et al. 2008a)

joined or not, blastema cells are not formed because of the lack of the regenerative environment (no AEC and insufficient nerves) (Satoh et al. 2010a). Therefore, the bone damage is thought to be restored in a blastema-independent way. Basically, such a bone-healing process can progress without the nerve presence although the speed of healing is somewhat slowed down (Satoh et al. 2010a). Considering nerve importance in limb regeneration, the bone-healing process is not related to epimorphic regeneration. Experimentally, it is possible to force an epimorphic regeneration system to participate in the bone-healing process (tissue regeneration). In this case, blastema cells are induced or grafted in the bone excision site. The blastema cells not only heal the damaged bone but also can fill the gap, which the usual bone-healing system cannot do (Satoh et al. 2010a). Thus, a bone excision experiment in urodele amphibians is also a useful experimental system to compare epimorphic with tissue regeneration systems.

Epimorphic and tissue regeneration are very likely to be used differently depending on situations in urodele amphibians. Tissue regeneration has been studied in higher vertebrates and much knowledge has been accumulated. Generally, tissue regeneration is a "stem cell-based" system. For example, muscle damage is restored by myogenic stem cells called muscle satellite cells (Yusuf and Brand-Saberi 2012). On the other hand, it is believed that epimorphic regeneration is achieved by dedifferentiated cells (blastema cells) in cooperation with stem cells. Specifically, a fibroblast-derived mesenchymal blastema that eventually reforms the cartilaginous skeleton and associated connective tissues forms a blueprint that guides the growth of nerves and the migration of stem cells, such as myogenic cells (Gardiner et al. 2002). These two regeneration systems should be studied separately and simultaneously to bridge the gap between amphibian regeneration capability and that of higher vertebrates.

15.6 Regeneration in Nonregenerative Animals

Can mammalians become regenerative animals? As we focus on the evolution of regeneration abilities, it is evident that lower organisms retained higher regenerative capacity than the higher organisms. Invertebrates, such as a planarian, show very strong regenerative abilities (Agata et al. 2003). Among vertebrates, an ancestral fish, *Polypterus*, shows remarkable regenerative abilities (Cuervo et al. 2012) and, similar to axolotls, they can regenerate their lobed fins. Anuran amphibians, which are so-called higher vertebrates compared to urodele amphibians, are a curious population in terms of limb regeneration ability: they have half-regenerative abilities (Suzuki et al. 2006). The frog *Xenopus laevis* can initiate regeneration responses and form regeneration blastemas. However, the blastema cannot mimic redevelopmental processes, resulting in hypomorphic regeneration (Fig. 15.6, upper row) (Yokoyama 2008). Because of this characteristic regeneration capability, frogs have been considered a regenerative intermediate between higher and lower organisms. Mice and humans, of course, cannot regenerate limbs. However, it is known that the tips of the digits of mice and humans can regenerate (Fig. 15.6, lower row) (Han et al. 2005; Muller et al. 1999). If approximately one third of a terminal phalange is cut, the lost digit tip is restored with all necessary tissues. Moreover, some regenerative responses can be induced when mouse limbs are amputated, even at the lower arm level (Ide 2012; Yu et al. 2012). Thus, regeneration reactions have been described in many animals. As more such clarification of differences in regeneration

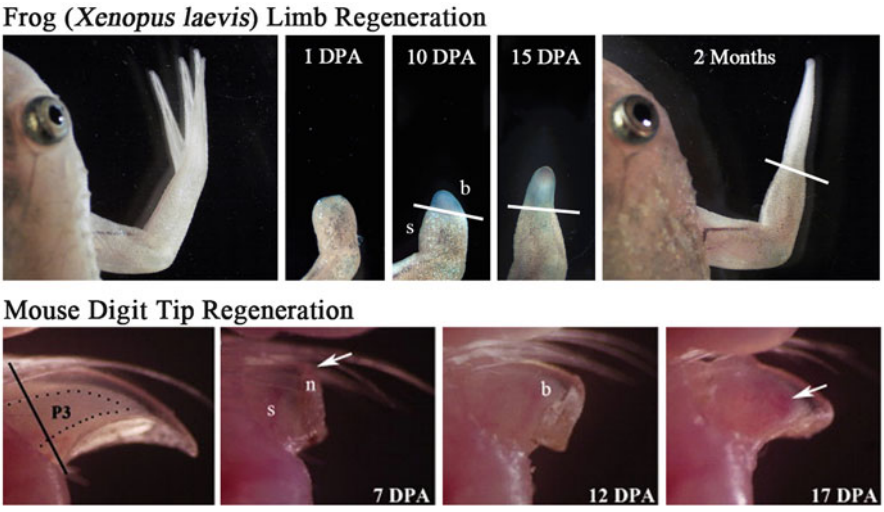

Fig. 15.6 Limb/digit regeneration in "higher" vertebrates. *Upper row:* Limb regeneration in a *Xenopus* frog. *Xenopus*, an anuran amphibian, cannot restore a complete limb after amputation: a cartilaginous spike is restored instead of a limb. *DPA* days post amputation. *Lower row*: Mouse digit tip regeneration. Even mice digit tips can be regenerated after amputation. *P3* terminal phalange, *s* stump, *b* blastema (Bottom Column; modified from Fernando et al. 2010)

responses in regenerative and nonregenerative animals is achieved, it will be possible to find key regulations that determine regeneration ability.

A roadmap to successful mammalian limb regeneration has been proposed (Han et al. 2005). Organ regeneration ability has decreased during evolution. Considering the cause of the loss of regeneration ability, some possibilities can be raised. (1) Key molecules in the genome are deleted or its functions are transformed. (2) Suppression mechanisms are developed. (3) Epigenetic status is changed. Regarding the loss of key molecules or functions, it would be understandable if we find the responsible molecules by comparative analysis. For the suppression mechanisms, gene suppression technology has been developed. Therefore, it would be possible to determine such suppression mechanisms after their identification. Differences in epigenetic status were first reported by Yakushiji et al. (2007). They compared the DNA methylation level of a certain domain of the genome in both regenerative and nonregenerative animals. The DNA methylation level is much higher in nonregenerative animals, suggesting that the epigenetic status is different. It is still unknown whether such differences in epigenetic regulation are correlated to their regeneration ability. Also, editing epigenetic status is quite difficult at this moment; further technological breakthrough is needed. Anyway, clarification of the differences in regenerative and nonregenerative animals and "step-by-step" research achievements are the only way to make our organs become regenerative.

The ALM is surely a superior experimental system for the study of amphibian limb regeneration. However, it is also true that there are many difficulties to studying at the same level as in other model organisms. Lack of biological technology and genetic information are the main issues obstructing direct comparative analysis between urodele amphibians and higher vertebrates. Therefore, technological breakthrough and finer genomic information should be demanded to develop limb regeneration study of urodele amphibians further. With daily technological advances, we can optimistically expect to overcome current hurdles in the near future and find the crucial cascade that determines regeneration capability.

References

Agata K, Tanaka T, Kobayashi C, Kato K, Saitoh Y (2003) Intercalary regeneration in planarians. Dev Dyn 226(2):308–316. doi:10.1002/dvdy.10249

Albert P, Boilly B, Courty J, Barritault D (1987) Stimulation in cell culture of mesenchymal cells of newt limb blastemas by EDGF I or II (basic or acidic FGF). Cell Differ 21(1):63–68

Boilly B, Albert P (1988) Blastema cell proliferation in vitro: effects of limb amputation on the mitogenic activity of spinal cord extracts. Biol Cell 62(2):183–187

Capdevila J, Izpisua Belmonte JC (2001) Patterning mechanisms controlling vertebrate limb development. Annu Rev Cell Dev Biol 17:87–132. doi:10.1146/annurev.cellbio.17.1.87

Carlson MR, Bryant SV, Gardiner DM (1998) Expression of Msx-2 during development, regeneration, and wound healing in axolotl limbs. J Exp Zool 282(6):715–723

Christensen RN, Weinstein M, Tassava RA (2002) Expression of fibroblast growth factors 4, 8, and 10 in limbs, flanks, and blastemas of *Ambystoma*. Dev Dyn 223(2):193–203. doi:10.1002/dvdy.10049

Cohn MJ, Izpisua-Belmonte JC, Abud H, Heath JK, Tickle C (1995) Fibroblast growth factors induce additional limb development from the flank of chick embryos. Cell 80(5):739–746

Cuervo R, Hernandez-Martinez R, Chimal-Monroy J, Merchant-Larios H, Covarrubias L (2012) Full regeneration of the tribasal *Polypterus* fin. Proc Natl Acad Sci USA 109(10):3838–3843. doi:10.1073/pnas.1006619109

Dungan KM, Wei TY, Nace JD, Poulin ML, Chiu IM, Lang JC, Tassava RA (2002) Expression and biological effect of urodele fibroblast growth factor 1: relationship to limb regeneration. J Exp Zool 292(6):540–554. doi:10.1002/jez.10077

Endo T, Bryant SV, Gardiner DM (2004) A stepwise model system for limb regeneration. Dev Biol 270(1):135–145. doi:10.1016/j.ydbio.2004.02.016

Fernando WA, Leininger E, Simkin J, Li N, Malcom CA, Sathyamoorthi S, Han M, Muneoka K (2011) Wound healing and blastema formation in regenerating digit tips of adult mice. Dev Biol 350(2):301–310. doi:10.1016/j.ydbio.2010.11.035

Gardiner DM, Muneoka K, Bryant SV (1986) The migration of dermal cells during blastema formation in axolotls. Dev Biol 118(2):488–493

Gardiner DM, Endo T, Bryant SV (2002) The molecular basis of amphibian limb regeneration: integrating the old with new. Semin Cell Dev Biol 13(5):345–352

Globus M (1988) A neuromitogenic role for substance P in urodele limb regeneration. In: Inoue S, et al (eds) Regeneration and development. Okada, Maebashi

Goss RJ (1956) The relation of bone to the histogenesis of cartilage in regenerating forelimbs and tails of adult *Trituris viridescens*. J Morphol 98:89–123

Han MJ, An JY, Kim WS (2001) Expression patterns of Fgf-8 during development and limb regeneration of the axolotl. Dev Dyn 220(1):40–48, doi:10.1002/1097-0177(2000)9999:9999<::AID-DVDY1085>3.0.CO;2-8

Han M, Yang X, Taylor G, Burdsal CA, Anderson RA, Muneoka K (2005) Limb regeneration in higher vertebrates: developing a roadmap. Anat Rec B New Anat 287(1):14–24. doi:10.1002/ar.b.20082

Hirata A, Gardiner DM, Satoh A (2010) Dermal fibroblasts contribute to multiple tissues in the accessory limb model. Dev Growth Differ 52(4):343–350. doi:10.1111/j.1440-169X.2009.01165.x

Hutchison C, Pilote M, Roy S (2007) The axolotl limb: a model for bone development, regeneration and fracture healing. Bone (NY) 40(1):45–56. doi:10.1016/j.bone.2006.07.005

Ide H (2012) Bone pattern formation in mouse limbs after amputation at the forearm level. Dev Dyn 241(3):435–441. doi:10.1002/dvdy.23728

Kiffmeyer WR, Tomusk EV, Mescher AL (1991) Axonal transport and release of transferrin in nerves of regenerating amphibian limbs. Dev Biol 147(2):392–402

Kragl M, Knapp D, Nacu E, Khattak S, Maden M, Epperlein HH, Tanaka EM (2009) Cells keep a memory of their tissue origin during axolotl limb regeneration. Nature (Lond) 460(7251):60–65. doi:10.1038/nature08152

Kumar A, Godwin JW, Gates PB, Garza-Garcia AA, Brockes JP (2007) Molecular basis for the nerve dependence of limb regeneration in an adult vertebrate. Science 318(5851):772–777. doi:10.1126/science.1147710

Levesque M, Villiard E, Roy S (2010) Skin wound healing in axolotls: a scarless process. J Exp Zool B Mol Dev Evol 314(8):684–697. doi:10.1002/jez.b.21371

Makanae A, Satoh A (2012) Early regulation of axolotl limb regeneration. Anat Rec 295(10):1566–1574. doi:10.1002/ar.22529

Martin GR (1998) The roles of FGFs in the early development of vertebrae limbs. Genes Dev 12:1571–1586. doi:10.1101/gad.12.11.1571

Moriyasu M, Makanae A, Satoh A (2012) Spatiotemporal regulation of keratin 5 and 17 in the axolotl limb. Dev Dyn 241(10):1616–1624. doi:10.1002/dvdy.23839

Mullen LM, Bryant SV, Torok MA, Blumberg B, Gardiner DM (1996) Nerve dependency of regeneration: the role of Distal-less and FGF signaling in amphibian limb regeneration. Development (Camb) 122(11):3487–3497

Muller TL, Ngo-Muller V, Reginelli A, Taylor G, Anderson R, Muneoka K (1999) Regeneration in higher vertebrates: limb buds and digit tips. Semin Cell Dev Biol 10(4):405–413. doi:10.1006/scdb.1999.0327

Muneoka K, Bryant SV (1982) Evidence that patterning mechanisms in developing and regenerating limbs are the same. Nature (Lond) 298(5872):369–371

Nye HL, Cameron JA, Chernoff EA, Stocum DL (2003) Regeneration of the urodele limb: a review. Dev Dyn 226(2):280–294. doi:10.1002/dvdy.10236

Ohuchi H, Nakagawa T, Yamamoto A, Araga A, Ohata T, Ishimaru Y, Yoshioka H, Kuwana T, Nohno T, Yamasaki M, Itoh N, Noji S (1997) The mesenchymal factor, FGF10, initiates and maintains the outgrowth of the chick limb bud through interaction with FGF8, an apical ectodermal factor. Development (Camb) 124(11):2235–2244

Poulin ML, Patrie KM, Botelho MJ, Tassava RA, Chiu IM (1993) Heterogeneity in the expression of fibroblast growth factor receptors during limb regeneration in newts (*Notophthalmus viridescens*). Development (Camb) 119(2):353–361

Satoh A, Gardiner DM, Bryant SV, Endo T (2007) Nerve-induced ectopic limb blastemas in the axolotl are equivalent to amputation-induced blastemas. Dev Biol 312(1):231–244. doi:10.1016/j.ydbio.2007.09.021

Satoh A, Graham GMC, Bryant SV, Gardiner DM (2008) Neurotrophic regulation of epidermal dedifferentiation during wound healing and limb regeneration in the axolotl (*Ambystoma mexicanum*). Dev Biol 319(2):321–335. doi:10.1016/j.ydbio.2008.04.030

Satoh A, Bryant SV, Gardiner DM (2008a) Regulation of dermal fibroblast dedifferentiation and redifferentiation during wound healing and limb regeneration in the axolotl. Dev Growth Differ 50(9):743–754. doi:10.1111/j.1440-169X.2008.01072.x

Satoh A, Graham GM, Bryant SV, Gardiner DM (2008b) Neurotrophic regulation of epidermal dedifferentiation during wound healing and limb regeneration in the axolotl (*Ambystoma mexicanum*). Dev Biol 319(2):321–335. doi:10.1016/j.ydbio.2008.04.030

Satoh A, Cummings GM, Bryant SV, Gardiner DM (2010a) Neurotrophic regulation of fibroblast dedifferentiation during limb skeletal regeneration in the axolotl (*Ambystoma mexicanum*). Dev Biol 337(2):444–457. doi:10.1016/j.ydbio.2009.11.023

Satoh A, Makanae A, Hirata A, Satou Y (2011) Blastema induction in aneurogenic state and Prrx-1 regulation by MMPs and FGFs in *Ambystoma mexicanum* limb regeneration. Dev Biol 355(2):263–274. doi:10.1016/j.ydbio.2011.04.017

Satoh A, Bryant SV, Gardiner DM (2012a) Nerve signaling regulates basal keratinocyte proliferation in the blastema apical epithelial cap in the axolotl (*Ambystoma mexicanum*). Dev Biol 366(2):374–381. doi:10.1016/j.ydbio.2012.03.022

Satoh A, Hirata A, Makanae A (2012b) Collagen reconstitution is inversely correlated with induction of limb regeneration in *Ambystoma mexicanum*. Zool Sci 29(3):191–197. doi:10.2108/zsj.29.191

Seifert AW, Monaghan JR, Voss SR, Maden M (2012b) Skin regeneration in adult axolotls: a blueprint for scar-free healing in vertebrates. PloS One 7(4):e32875. doi:10.1371/journal.pone.0032875

Sive H, Bradley L (1996) A sticky problem: the *Xenopus* cement gland as a paradigm for anteroposterior patterning. Dev Dyn 205(3):265–280. doi:10.1002/(SICI)1097-0177(199603)205:3<265::AID-AJA7>3.0.CO;2-G

Spallanzani L (1769) An essay on animal reproductions. Reproductions of the legs in the aquatic salamander. Becket and de Hondt, London

Sun X, Mariani FV, Martin GR (2002) Functions of FGF signalling from the apical ectodermal ridge in limb development. Nature (Lond) 418(6897):501–508. doi:10.1038/nature00902

Suzuki M, Yakushiji N, Nakada Y, Satoh A, Ide H, Tamura K (2006) Limb regeneration in *Xenopus laevis* froglet. Sci World J 6(suppl 1):26–37. doi:10.1100/tsw.2006.325

Todd TJ (1823) On the process of reproduction of the members of the aquatic salamander. Q J Sci Lit Arts 16:84–96

Wang L, Marchionni MA, Tassava RA (2000) Cloning and neuronal expression of a type III newt neuregulin and rescue of denervated, nerve-dependent newt limb blastemas by rhGGF2. J Neurobiol 43(2):150–158

Whited JL, Lehoczky JA, Austin CA, Tabin CJ (2011) Dynamic expression of two thrombospondins during axolotl limb regeneration. Dev Dyn 240(5):1249–1258. doi:10.1002/dvdy.22548

Yakushiji N, Suzuki M, Satoh A, Sagai T, Shiroishi T, Kobayashi H, Sasaki H, Ide H, Tamura K (2007) Correlation between Shh expression and DNA methylation status of the limb-specific Shh enhancer region during limb regeneration in amphibians. Dev Biol 312(1):171–182. doi:10.1016/j.ydbio.2007.09.022

Yokoyama H (2008) Initiation of limb regeneration: the critical steps for regenerative capacity. Dev Growth Differ 50(1):13–22. doi:10.1111/j.1440-169X.2007.00973.x

Yonei-Tamura S, Endo T, Yajima H, Ohuchi H, Ide H, Tamura K (1999) FGF7 and FGF10 directly induce the apical ectodermal ridge in chick embryos. Dev Biol 211(1):133–143. doi:10.1006/dbio.1999.9290

Yu L, Han M, Yan M, Lee J, Muneoka K (2012) BMP2 induces segment-specific skeletal regeneration from digit and limb amputations by establishing a new endochondral ossification center. Dev Biol 372(2):263–273. doi:10.1016/j.ydbio.2012.09.021

Yusuf F, Brand-Saberi B (2012) Myogenesis and muscle regeneration. Histochem Cell Biol 138(2):187–199. doi:10.1007/s00418-012-0972-x

Part V
New Players in Signaling Systems

Chapter 16
Context-Dependent Bidirectional Modulation of Wnt/β-Catenin Signaling

Tohru Ishitani

Abstract Wnt/β-catenin signaling is an evolutionarily conserved signaling system that controls cell proliferation, fate specification, differentiation, survival, and death. This signaling system is used repeatedly during embryogenesis and organogenesis and has diverse context-dependent functions in different aspects. Extensive investigations during the past three decades have clarified the core components that mediate Wnt/β-catenin signaling in all cells. However, to understand the mechanisms by which Wnt/β-catenin signaling exerts context-specific roles, it is also important to identify the context-dependent modulators of Wnt/β-catenin signaling. Recently, we and others discovered that Nemo-like kinase (NLK) and dimerization partner 1 (DP1) can regulate Wnt/β-catenin signaling positively and negatively in a cellular context-dependent manner and demonstrated that they play essential roles in embryonic development by fine-tuning cellular response to Wnt/β-catenin signaling. In this chapter, I summarize the function of the context-dependent bidirectional Wnt/β-catenin signaling modulators, with particular focus on NLK and DP1, and discuss the significance of the bidirectional modulation in embryonic development.

Keywords Bidirectional modulation • Context-dependent • Dimerization partner 1 • Nemo-like kinase • Wnt/β-catenin signaling

16.1 Introduction

The evolutionarily conserved Wnt/β-catenin signaling system is repetitively used during embryogenesis and organogenesis (Clevers 2006; Logan and Nusse 2004). For example, Wnt/β-catenin signaling determines the axis and pattern in the early

T. Ishitani (✉)
Division of Cell Regulation Systems, Medical Institute of Bioregulation, Kyushu University, Fukuoka, Japan
e-mail: tish@bioreg.kyushu-u.ac.jp

H. Kondoh and A. Kuroiwa (eds.), *New Principles in Developmental Processes*,
DOI 10.1007/978-4-431-54634-4_16,

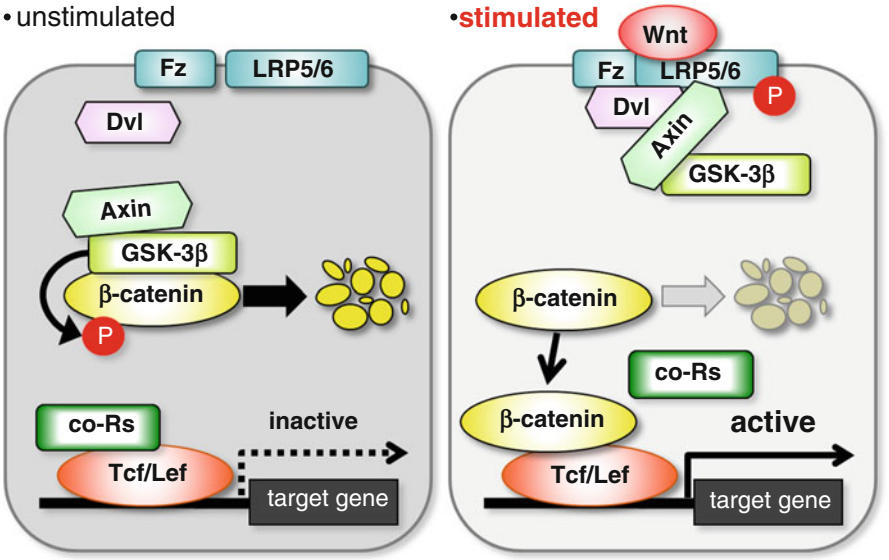

Fig. 16.1 Core components of Wnt/β-catenin signaling pathway. In unstimulated conditions, cytoplasmic β-catenin is phosphorylated by GSK-3β within a degradation complex. The phosphorylation of β-catenin promotes its ubiquitination and subsequent proteasomal degradation. In the nucleus, Tcf/Lef interacts with corepressors (co-Rs). Binding of Wnt to Fz and LRP5/6 stimulates the recruitment of Dvl, Axin, and GSK-3β to the membrane and induces the phosphorylation of LRP5/6. As a result, accumulated β-catenin enters into the nucleus where it forms complexes with Tcf/Lef, which then activate gene expression

embryo and regulates the fate of progenitor and stem cells during the development and maintenance of multiple organs (Logan and Nusse 2004; Wang and Wynshaw-Boris 2004). Thus, Wnt/β-catenin signaling plays distinct roles in different contexts.

Wnt/β-catenin signaling transduces its signal via regulating the stability of β-catenin protein (Fig. 16.1). In unstimulated cells, the levels of cytoplasmic β-catenin are kept low by a degradation complex that includes Axin and glycogen synthase kinase 3β (GSK-3β). GSK-3β catalyzes the phosphorylation of β-catenin, which promotes its ubiquitination and subsequent proteasomal degradation (Clevers 2006; Logan and Nusse 2004). In the absence of stimulation, the Tcf/Lef-family of transcription factors represses the expression of Wnt/β-catenin signaling target genes by interacting with transcriptional corepressors, such as histone deacetylase 1 (HDAC1) and Groucho (Arce et al. 2006, 2009). The Wnt/β-catenin signaling pathway is activated when the secreted glycoprotein Wnt binds to the cell-surface Frizzled (Fz) receptor and its coreceptor LRP5/6. This Wnt-bound receptor complex recruits the cytoplasmic protein Dishevelled (Dvl), which in turn brings the Axin-GSK-3β complex to the membrane and induces the phosphorylation of LRP5/6. Phosphorylated LRP5/6 promotes the dissociation of the β-catenin degradation complex (Davidson et al. 2005; Zeng et al. 2005, 2008). This series of events

results in the accumulation of cytoplasmic β-catenin (Niehrs and Shen 2010). The increased β-catenin concentration drives its migration into the nucleus where it forms complexes with Tcf/Lef, which then activate gene expression. Thus, the core machinery of the Wnt/β-catenin signaling pathway is becoming clear. However, to understand how Wnt/β-catenin signaling exhibits diverse context-dependent functions, it is also important to make clear the context-dependent machinery that regulates Wnt/β-catenin signaling only in specific biological events. We recently discovered that Nemo-like kinase (NLK) and dimerization partner 1 (DP1) have context-dependent positive and negative roles in the regulation of Wnt/β-catenin signaling. Here, I summarize the function of NLK and DP1 in the Wnt/β-catenin signaling pathway. I also introduce some other context-dependent bidirectional modulators and discuss the importance of the contextual regulation of Wnt/β-catenin signaling.

16.2 Roles of NLK in Wnt/β-Catenin Signaling

16.2.1 Roles of LIT-1/NLK in Caenorhabditis elegans

NLK is an evolutionarily conserved serine/threonine kinase. In 1999, we identified NLK as a negative regulator of Tcf/Lef in *Caenorhabditis elegans* mesoderm–endoderm specification (Meneghini et al. 1999). At the eight-cell stage of *C. elegans* embryogenesis, the Tcf/Lef homologue POP-1 represses the expression of genes required for endoderm induction in the MS cell, which generates mesoderm. On the other hand, in the E cell that generates endoderm, signaling induced by a Wnt-related protein, MOM-2, which is secreted from the P2 cell, negatively regulates POP-1 via a β-catenin-related protein WRM-1 to promote mesoderm formation (Lin et al. 1995; Thorpe et al. 1997) (Fig. 16.2). We discovered that the NLK homologue LIT-1 is also required for nuclear export of POP-1 in E cells (Meneghini et al. 1999). Analysis using genetics, cell biology, and biochemistry by us and other laboratories revealed that LIT-1/NLK forms a ternary complex with WRM-1/β-catenin and POP-1/Tcf and induces the nuclear export of POP-1 by phosphorylating it in the E cell (Meneghini et al. 1999; Rocheleau et al. 1999) (Fig. 16.2). In short, LIT-1/NLK negatively regulates POP-1/Tcf to positively regulate Wnt/β-catenin signaling in E cells.

However, in the fate specification of gonadal precursor cells, Z1 and Z4, LIT-1 seems to cooperate with POP-1 (Herman 2001; Siegfried and Kimble 2002; Siegfried et al. 2004). Z1/Z4 cells generate the precursors of distal tip cells (DTCs), which control germline proliferation, by asymmetrical division. The loss of function of any one of the *wrm-1*, *pop-1*, and *lit-1* genes results in a symmetrical Z1/Z4 division, causing a lack of DTCs (Siegfried and Kimble 2002), which suggests that WRM-1/β-catenin, LIT-1/NLK, and POP-1/Tcf collaborate in the Z1/Z4 division. The detailed mechanisms of this collaboration have been unclear. Thus, the mode of POP-1/Tcf activity regulation by LIT-1/NLK is context dependent.

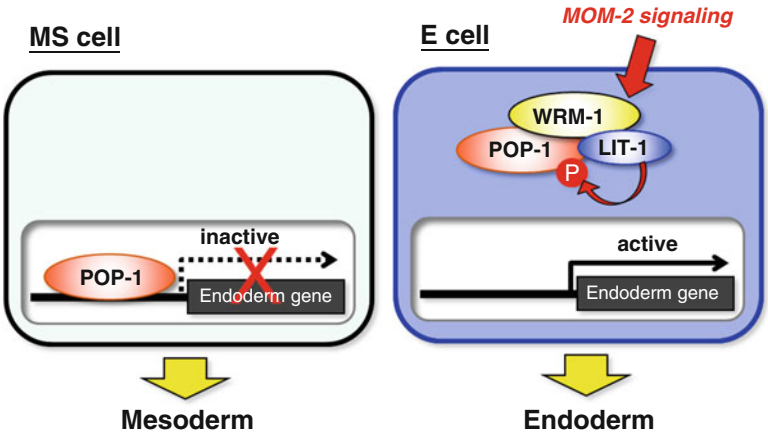

Fig. 16.2 Roles of LIT-1/NLK in the regulation of Wnt/β-catenin signaling in early embryogenesis of *Caenorhabditis elegans*. In the MS cell, POP-1 represses the expression of endoderm-specific genes to promote mesoderm formation. In the E cell, MOM-2 signaling stimulates the formation of a ternary complex consisting of LIT-1/NLK, WRM-1, and POP-1 and promotes LIT-1-mediated POP-1 phosphorylation in the E cell. Phosphorylation of POP-1 induces the nuclear export of POP-1 and the consequent transcriptional activation of POP-1-repressed genes, resulting in the E cell generating endoderm

16.2.2 Contextual Dual-Mode Tcf/Lef Regulation by NLK in Vertebrates

16.2.2.1 The Negative Regulation of Tcf/Lef in HEK293 and HeLa Cells

Does vertebrate NLK also have a context-dependent role in Tcf/Lef regulation? We first discovered that NLK negatively regulates Tcf/Lef activity in the human embryonic kidney cell line HEK293 and the human cervical cancer cell line HeLa (Fig. 16.3a). Vertebrates have four Tcf/Lef family members: Tcf7/Tcf1, Tcf7L1/Tcf3, Tcf7L2/Tcf4, and Lef1. NLK could phosphorylate Tcf7L1, Tcf7L2, and Lef1, but not Tcf7 (Ishitani et al. 1999; T. Ishitani, unpublished observations). Overexpression of NLK inhibited Tcf/Lef-mediated transcription in both HEK293 and HeLa cells (Ishitani et al. 1999, 2003). In addition, the Tcf7L2 and Lef1 proteins phosphorylated by NLK in HEK293 cells lacked DNA-binding activity in gel-shift assays (Ishitani et al. 1999; T. Ishitani, unpublished observations). Moreover, NLK overexpression reduced binding of Lef1 to its target gene, the *Axin2* promoter, in HeLa cells (Ota et al. 2012). Thus, NLK-mediated phosphorylation of Tcf/Lef inhibits Tcf/Lef activity by blocking their binding to the target genes (Fig. 16.3a).

16.2.2.2 The Positive Regulation of Lef1 in Neural Progenitor Cells

On the other hand, we recently discovered that NLK positively regulates Lef1 activity in vertebrate neural tissues (Ota et al. 2012). In many types of cells, the binding of

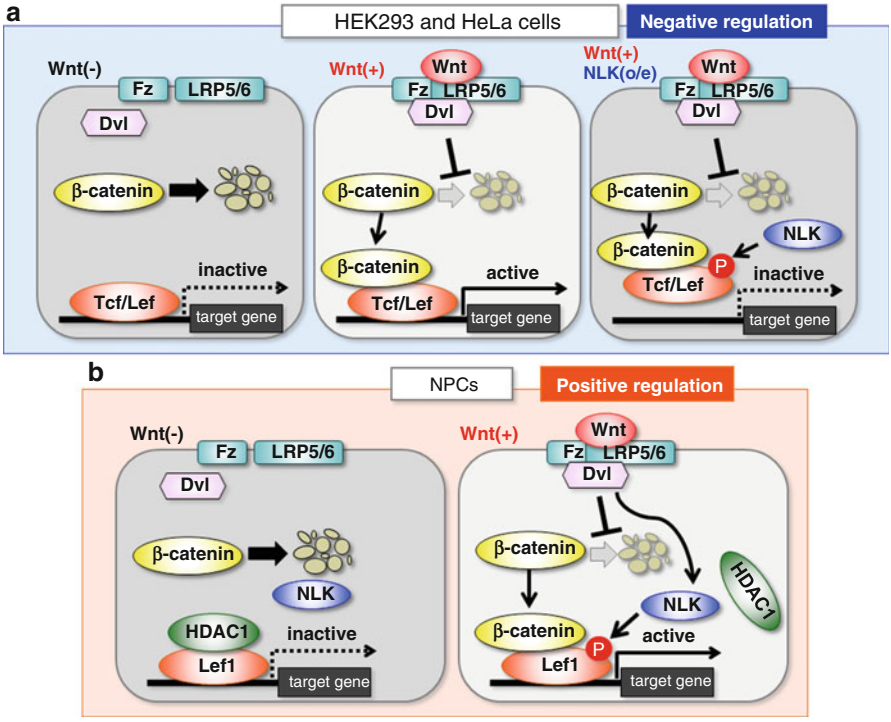

Fig. 16.3 Cell context-dependent bidirectional modulation of Wnt/β-catenin signaling by NLK. In the absence of Wnt, β-catenin is destabilized and Tcf/Lef represses target gene expression in all cell types (*left panels* in **a** and **b**). In NPCs, but not in HEK293 or HeLa cells, HDAC1 strongly inhibits Lef1 transcriptional activity (*left panels* in **a** and **b**). Binding of Wnt to the receptor induces the stabilization of β-catenin via Dvl in all cell types (*middle panel* in **a** and *right panel* in **b**). In HEK293 and HeLa cells, stabilized β-catenin forms a complex with Tcf/Lef, resulting in the activation of target gene expression (*middle panel* in **a**). NLK overexpression (o/e) inhibits Tcf/Lef-mediated gene expression by blocking its DNA-binding activity (*right panel* in **a**). In NPCs, Wnt-activated Dvl promotes Wnt/β-catenin signaling target gene expression via formation of the β-catenin-Lef1 complex and phosphorylation of Lef1 by NLK and the consequent dissociation of Lef1 from HDAC1 (*right panel* in **b**)

β-catenin with Tcf/Lef is sufficient for the activation of Tcf/Lef-mediated transcription. Actually, in HeLa and HEK293 cells, overexpression of the constitutive stable β-catenin mutant, β-cateninΔN, with Lef1 induced both the association of β-cateninΔN with Lef1 and the activation of Lef1-mediated transcription (Ishitani et al. 1999, 2003; Ota et al. 2012). Interestingly, we found that, in the neural progenitor cell (NPC)-like mammalian cell lines, mouse neuro-2a, and rat PC12 cells, overexpression of β-cateninΔN with Lef1 was insufficient for the activation of Lef1-mediated transcription (Ota et al. 2012). Moreover, coexpression of NLK with both β-cateninΔN and Lef1 efficiently activated Lef1-mediated transcription in these cells, whereas coexpression of NLK with Lef1 without β-cateninΔN could not activate it (Ota et al. 2012). These results suggest that both β-catenin stabilization and NLK activation are required for promoting Lef1-mediated transcription in these cells.

We also found that HDAC1 strongly bound to Lef1 and inhibited its transcription activity in NPC-like mammalian cells, and that overexpression of NLK disrupted this interaction through phosphorylation of Lef1, thereby promoting Lef1 activity (Ota et al. 2012). Furthermore, we showed that, in these cell lines, either Wnt-3a treatment or Dvl1 overexpression activated NLK kinase activity, which in turn induced Lef1 phosphorylation and transcriptional activation. RNAi-mediated NLK knockdown inhibited Wnt-3a- and Dvl1-induced phosphorylation and transcriptional activation of Lef1. These data suggest that Dvl has two functions that serve to activate Lef1-mediated transcription in the Wnt signaling pathway in these cells (Fig. 16.3b). One is β-catenin stabilization, and the other is NLK activation, resulting in Lef1 phosphorylation. Phosphorylated Lef1 dissociates from HDAC1 and activates transcription by forming a complex with β-catenin.

We also discovered that this Wnt–Dvl–NLK–Lef1 pathway functions in the developing midbrain tectum of zebrafish (Ota et al. 2012). Zebrafish Nlk2 is expressed in head tissues from the pharyngula stage. MO (morpholino)-mediated knockdown of a zebrafish NLK homologue Nlk2 decreased Lef1 phosphorylation, Lef1-mediated gene expression, and cell proliferation in the presumptive midbrain tectum at pharyngula stage, resulting in a reduction in midbrain tectum size. The phenotype caused by Nlk2 knockdown was suppressed by expression of a Lef1 mutant that mimics the constitutively phosphorylated state or by co-knockdown of HDAC1. Knockdown of either Lef1 or Wnt1 resulted in phenotypes similar to those caused by Nlk2 knockdown (Ota et al. 2012). These findings suggest that Nlk2 is required for Wnt/β-catenin signaling through Lef1 phosphorylation and for the abrogation of HDAC1-mediated Lef1 inhibition in the zebrafish midbrain tectum.

Thus, NLK has two effects in Wnt/β-catenin signaling: the first is the inhibition of Tcf/Lef DNA-binding activity in HeLa and HEK293 cells, and the second is the release of HDAC1 from the Lef1 transcriptional complex in NPCs (Fig. 16.3a, b). The molecular mechanisms underlying this context-dependent function of NLK have yet to be characterized. Interestingly, we found that the inhibitory effect of HDAC1 on Lef1-mediated transcription in HEK293 and HeLa cells was weaker than that in NPCs (Ota et al. 2012). This difference may explain why NLK-mediated inhibition of HDAC1 is not required for the activation of Tcf/Lef-mediated transcription in HeLa and HEK293 cells. We also found that Lef1 phosphorylation by NLK affected the binding of Lef1 to its target gene promoter in HeLa cells, but not in NPCs, and that the Lef1 phosphorylation level in HeLa cells was much higher than that of Lef1 in NPCs (Ota et al. 2012). These observations suggest that additional phosphorylation probably results in the dissociation of Lef1 from DNA. Based on these observations, comparison of the Lef1-binding proteins and Lef1 phosphorylation sites in these cells may help to elucidate this mechanism.

16.2.2.3 Speculation About the Significance of Bidirectional Regulation by NLK

In many type of cells, NLK is not required for the activation of Wnt/β-catenin signaling. And yet, why does the developing midbrain tectum use the

Nlk2-dependent "special" Wnt signaling system? In small teleost fishes, the early phase of the midbrain tectum grows very rapidly (Nguyen et al. 1999). It is noteworthy that, in the transgenic zebrafish carrying a Tcf/Lef-dependent Wnt/β-catenin signaling reporter TOPdGFP (Dorsky et al. 2002), the reporter activity in developing midbrain tectum at the pharyngula stage was much stronger than that in the other Wnt/β-catenin-active areas (Ota et al. 2012; Shimizu et al. 2012), and this midbrain reporter activity was dramatically reduced by Nlk2 knockdown (Ota et al. 2012). These observations suggest that the Nlk2-dependent pathway can induce relatively strong activation of Tcf/Lef-mediated transcription. This strong activation is likely to enable the rapid growth of midbrain tectum. Interestingly, Nlk2 knockdown downsized not only midbrain tectum but also other organs/tissues, including eye and limb, in zebrafish embryos (T. Ishitani, unpublished observations), suggesting the possibility that these tissues/organs may also utilize the Nlk2-dependent Wnt signaling system for its growth.

On the other hand, the developmental roles of the negative regulation in vertebrates remain unclear. Until now, we found that knockdown of a *Xenopus* NLK homologue NLK1 augmented Tcf/Lef-mediated transcription in neurula-stage posterior dorsal tissues (Kim et al. 2012) and that Nlk2 knockdown enhanced the activity of Tcf/Lef-driven reporter in several differentiating cells in zebrafish embryos (T. Ishitani, unpublished observations), indicating that the negative regulation occurs in vivo. These observations also suggest that NLK modulates Wnt/β-catenin signaling bidirectionally, depending on the situation, in vertebrate development. Such fine tuning may underlie the context-dependent functions of Wnt/β-catenin signaling.

16.3 Roles of DP1 in Wnt/β-Catenin Signaling

16.3.1 Molecular Mechanisms of DP1-Mediated Bidirectional Modulation of Wnt/β-Catenin Signaling

DP1 is known to function as a binding protein of the E2F transcription factor (van den Heuvel and Dyson 2008). Recently, an international collaboration team (including the author) discovered that DP1 is a context-dependent Wnt/β-catenin signaling modulator, essential for anterior–posterior (AP) neural patterning. First, we found that overexpression of DP1 augmented Wnt-3a-induced β-catenin stabilization and Tcf/Lef-mediated transcription in HEK293T cells, whereas DP1 RNAi reduced both of these (Kim et al. 2012). These results suggest that DP1 positively regulates the Wnt/β-catenin signaling induced by a Wnt ligand. However, surprisingly, DP1 overexpression inhibited Dvl or β-catenin overexpression-induced Tcf/Lef-mediated transcription (Kim et al. 2012). Furthermore, Dvl-induced Tcf/Lef-mediated transcription was enhanced by DP1 siRNA treatment (Kim et al. 2012). These findings raise the possibility that DP1 may positively regulate Wnt/β-catenin signaling in the presence of a Wnt ligand and negatively regulate in its absence.

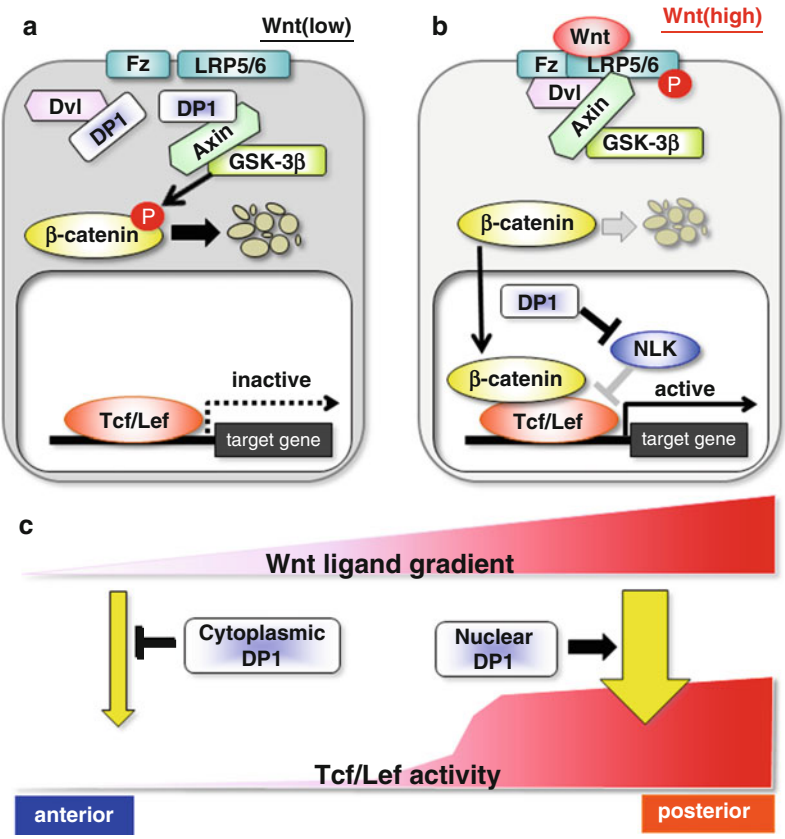

Fig. 16.4 Cell context-dependent bidirectional modulation of Wnt/β-catenin signaling by DP1. **a** In the "Wnt-low" condition, DP1 keeps the signaling activity at low level by blocking Dvl–Axin interaction. **b** In the "Wnt-high" condition, DP1 positively regulates the signaling through suppression of NLK activity. **c** Wnt ligands secreted form the posterior tissues generate a Wnt ligand gradient in the neural plate. In the "Wnt-high" posterior neural plate, nuclear DP1 boosts Wnt/β-catenin signaling activity. In the "Wnt-low" anterior neural plate, cytoplasmic DP1 attenuates signaling activity. By this dual activity, DP1 translates a slight gradient of Wnt ligand into a steep gradient of Tcf/Lef activity

Further analyses revealed the molecular mechanisms of DP1-mediated positive and negative regulation of Wnt/β-catenin signaling. We found that DP1 associated with both Dvl and Axin in the cytoplasm and competed with Dvl for Axin binding to promote β-catenin degradation in the absence of a Wnt ligand (Kim et al. 2012) (Fig. 16.4a). On the other hand, in the presence of a Wnt ligand, DP1 binds to and inhibits the kinase activity of NLK and consequently cancels NLK-mediated Tcf/Lef inhibition (Kim et al. 2012) (Fig. 16.4b). These regulatory mechanisms were independent from E2F (Kim et al. 2012). Taken together, these results suggest that DP1 has a positive role in the nucleus in the presence of a Wnt ligand, whereas in its absence DP1 has a negative role in the cytoplasm.

16.3.2 A Dual Role of DP1 in AP Neural Patterning

What are the physiological significances of the dual regulation by DP1? In vertebrate early embryogenesis, a gradient of Wnt activity, which is generated by Wnt ligands produced form the posterior tissues, determines the AP pattern of future regions of the central nervous system (CNS) (Fig. 16.4c). Posterior neural marker genes are induced by strong activation of Wnt/β-catenin signaling (Kiecker and Niehrs 2001). In contrast, repression of Wnt/β-catenin signaling is essential for anterior neural marker expression (Lagutin et al. 2003). Interestingly, endogenous DP1 protein was concentrated in the nucleus of posterior neural plate of *Xenopus* embryos at the early neurula stage, whereas it was localized in the cytoplasm in the anterior neural plate (Kim et al. 2012). It is possible that DP1 may boost the Wnt/β-catenin signaling activity in the nucleus of the "Wnt-high" posterior neural plate, whereas it may attenuate the signaling activity in the cytoplasm of the "Wnt-low (or Wnt-free)" anterior neural plate. Consistent with this idea, injection of DP1 MO reduced expression of both anterior and posterior neural markers. In addition, DP1 MO enhanced active β-catenin level and Tcf/Lef-mediated transcription in the anterior neural plate, whereas it reduced Tcf/Lef-mediated transcription in the posterior neural plate. Furthermore, DP1 MO-induced reduction of Tcf/Lef-mediated transcription in the posterior neural plate was reversed by coinjection with NLK1 MO (Kim et al. 2012). Taken together, these results suggest that DP1 plays a dual role during *Xenopus* AP neural patterning. One function is the negative regulation of Wnt/β-catenin signaling via blocking β-catenin activation in the cytoplasm of anterior neural plate cells, and the other is the positive regulation of signaling through suppression of NLK activity in the nucleus of posterior neural plate cells. By this dual activity, DP1 translates a slight gradient of Wnt ligand into a steep gradient of Tcf/Lef activity and consequently sharpens the resulting pattern (Fig. 16.4c).

16.4 Other Context-Dependent Bidirectional Modulators

Several bidirectional modulators of Wnt/β-catenin signaling have been discovered by functional experiments in *Xenopus* and zebrafish embryos. Among them, the transmembrane receptor Kremen, which can interact with LRP6 and a secreted Wnt antagonist Dkk1, controls Wnt/β-catenin signaling activity in a manner similar to that of DP1. In the most anterior region of neural plate where Wnt level is low and Dkk1 is present, Kremen negatively regulates Wnt/β-catenin signaling through ternary complex formation with LRP6 and Dkk1 and consequently promotes anterior CNS development (Davidson et al. 2002). On the other hand, in the lateral neural plate where Dkk1 is absent and Wnt level is high, Kremen directly binds to LRP6 and enhances Wnt/β-catenin signaling to promote neural crest induction, for which high Wnt/β-catenin activity is required (Hassler et al. 2007). Thus, similar to DP1, Kremen strengthens Wnt/β-catenin signaling in Wnt high-activity tissues and weakens it in Wnt low-activity tissues (Fig. 16.5a).

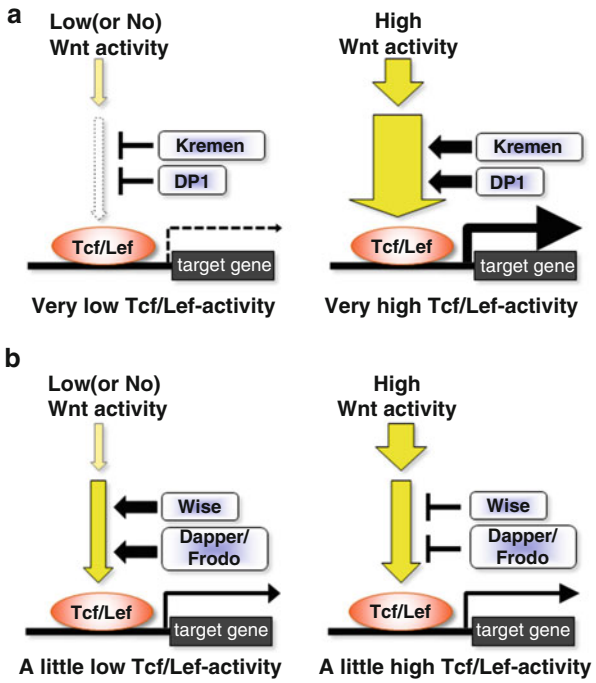

Fig. 16.5 Effects of context-dependent bidirectional modulators on Wnt/β-catenin signaling. **a** DP1 and Kremen weaken Tcf/Lef-mediated transcription in the Wnt activity-high condition and weaken it in the Wnt activity-low (or no) condition. Consequently, the difference of the signaling activity between these two conditions is amplified. **b** Dapper/Frodo and Wise act as an activator in the absence of Wnt activity and functions as an inhibitor in the presence of Wnt activity. These actions may reduce the difference in signaling activity

Wise and Dapper/Frodo regulate Wnt/β-catenin signaling in a manner different from that of DP1 and Kremen. Wise is a secreted LRP6-binding protein. Wise overexpression induced the nuclear accumulation of β-catenin and Wnt target gene expression in *Xenopus* animal cap assays, whereas it inhibited the axis-inducing activity of Wnt8 in *Xenopus* axis-duplication assays (Itasaki et al. 2003). From these observations, it is thought that Wise acts as an inhibitor in the presence of Wnt and functions as an activator in the absence of Wnt. However, the molecular mechanism underlying this dual function is poorly understood. Dapper/Frodo was first identified as a Dvl antagonist that inhibits the Tcf/Lef-mediated transcription induced by overexpression of Wnt or Dvl in *Xenopus* embryos (Cheyette et al. 2002; Gloy et al. 2002). However, knockdown of Dapper/Frodo reduced the constitutively active Tcf/Lef mutant-induced transcription in *Xenopus* embryos (Hikasa and Sokol 2004) and enhanced the brain anteriorization phenotype of Wnt8 knockdown zebrafish embryos (Waxman et al. 2004). Based on these results, Hikasa and Sokol (2004) proposed that Dapper/Frodo functions as a positive regulator in the absence of

Wnt-Dvl signaling. However, the mechanisms of this positive regulation remain unclear. Thus, DP1 and Kremen amplify the difference of Wnt signaling activity while Dapper/Frodo and Wise appear to lessen this (Fig. 16.5b). This amplification and decrease must contribute to the variation of the cellular response to Wnt ligands in developing tissues and organs.

16.5 Conclusion

Recent studies have revealed many new modulators that can control Wnt/β-catenin signaling positively and negatively in a context-dependent manner. However, because of the complexity of their functions, the molecular mechanisms by which they activate or inhibit Wnt/β-catenin signaling and in what context they act as activators or inhibitors of Wnt/β-catenin signaling remain poorly understood. Against that background, we and others have succeeded to clarify some of the mechanisms using a combination of functional and biochemical experiments in mammalian culture cells and in simple model animals, such as zebrafish and *Xenopus*. Accordingly, it is also becoming clear that contextual bidirectional Wnt/β-catenin signaling modulation supports Wnt/β-catenin signaling to exert context-dependent actions. For instance, DP1 and Kremen boost Wnt/β-catenin signaling in Wnt-high tissues to promote the gene expression for which strong activation of Wnt/β-catenin signaling is required, whereas they suppress basal signaling in low-Wnt tissues to induce gene expression for which a low level of Wnt/β-catenin signaling is essential. NLK is likely to intensify Wnt/β-catenin signaling to accelerate cell proliferation only in a specific rapidly growing tissue. Therefore, I believe firmly that analysis of context-dependent bidirectional modulation must contribute to the clarification of the molecular mechanisms by which Wnt/β-catenin signaling directs distinct actions to cells in different contexts. Similar to Wnt/β-catenin signaling, other cell signaling pathways including BMP and Shh are also used repetitively during embryonic development and have diverse context-dependent functions in different aspects. Hence, such analysis will also contribute to the discovery of a new general principle underlying the cell signaling systems controlling embryonic development.

As already mentioned, the study of context-dependent bidirectional modulation has been very challenging work. However, the recent progress of technology has enabled every researcher to handle this effort. By OMICS technology, we can compare gene expression, protein levels, posttranslational modifications, intermolecular interactions, and epigenetic modification in different contexts. In addition, model animals are good systems for investigating the in vivo roles of context-dependent bidirectional regulators in each context. Recently, our group generated a highly sensitive Wnt/β-catenin signaling reporter-transgenic zebrafish (Shimizu et al. 2012). Such in vivo signal visualization enables analyzing the function and regulation of cell signaling in each aspect of embryonic development. Thus, the mechanisms underlying context-dependent function and regulation of cell signaling are within our reach. Now is the time to tackle this subject!

References

Arce L, Pate KT, Waterman ML (2009) Groucho binds two conserved regions of LEF-1 for HDAC-dependent repression. BMC Cancer 9:159–172

Arce L, Yokoyama NN, Waterman ML (2006) Diversity of LEF/TCF action in development and disease. Oncogene 25(57):7492–7504

Cheyette BN, Waxman JS, Miller JR et al (2002) Dapper, a Dishevelled-associated antagonist of beta-catenin and JNK signaling, is required for notochord formation. Dev Cell 2(4):449–461

Clevers H (2006) Wnt/β-catenin signaling in development and disease. Cell 127(3):469–480

Davidson G, Mao B, del Barco Barrantes I et al (2002) Kremen proteins interact with Dickkopf1 to regulate anteroposterior CNS patterning. Development (Camb) 129(24):5587–5596

Davidson G, Wu W, Shen J et al (2005) Casein kinase 1 gamma couples Wnt receptor activation to cytoplasmic signal transduction. Nature (Lond) 438(7069):867–872

Dorsky RI, Sheldahl LC, Moon RT (2002) A transgenic Lef1/β-catenin-dependent reporter is expressed in spatially restricted domains throughout zebrafish development. Dev Biol 241(2):229–237

Gloy J, Hikasa H, Sokol SY (2002) Frodo interacts with Dishevelled to transduce Wnt signals. Nat Cell Biol 4(5):351–357

Hassler C, Cruciat CM, Huang YL et al (2007) Kremen is required for neural crest induction in *Xenopus* and promotes LRP6-mediated Wnt signaling. Development (Camb) 134(23):4255–4263

Herman M (2001) C. elegans POP-1/TCF functions in a canonical Wnt pathway that controls cell migration and in a noncanonical Wnt pathway that controls cell polarity. Development (Camb) 128(4):581–590

Hikasa H, Sokol SY (2004) The involvement of Frodo in TCF-dependent signaling and neural tissue development. Development (Camb) 131(19):4725–4734

Ishitani T, Ninomiya-Tsuji J, Nagai S et al (1999) The TAK1-NLK-MAPK-related pathway antagonizes signalling between β-catenin and transcription factor TCF. Nature (Lond) 399(6738):798–802

Ishitani T, Ninomiya-Tsuji J, Matsumoto K (2003) Regulation of lymphoid enhancer factor 1/T-cell factor by mitogen-activated protein kinase-related Nemo-like kinase-dependent phosphorylation in Wnt/β-catenin signaling. Mol Cell Biol 23(4):1379–1389

Itasaki N, Jones CM, Mercurio S et al (2003) Wise, a context-dependent activator and inhibitor of Wnt signalling. Development (Camb) 130(18):4295–4305

Kiecker C, Niehrs C (2001) A morphogen gradient of Wnt/beta-catenin signalling regulates anteroposterior neural patterning in Xenopus. Development (Camb) 128(21):4189–4201

Kim WT, Kim H, Katanaev VL et al (2012) Dual functions of DP1 promote biphasic Wnt-on and Wnt-off states during anteroposterior neural patterning. EMBO J 31(16):3384–3397

Lagutin OV, Zhu CC, Kobayashi D, Topczewski J, Shimamura K, Puelles L, Russell HR, McKinnon PJ, Solnica-Krezel L, Oliver G (2003) Six3 repression of Wnt signaling in the anterior neuroectoderm is essential for vertebrate forebrain development. Genes Dev 17(3):368–379

Lin R, Thompson S, Priess JR (1995) pop-1 encodes an HMG box protein required for the specification of a mesoderm precursor in early *C. elegans* embryos. Cell 83(4):599–609

Logan CY, Nusse R (2004) The Wnt signaling pathway in development and disease. Annu Rev Cell Dev Biol 20:781–810

Meneghini MD, Ishitani T, Carter JC et al (1999) MAP kinase and Wnt pathways converge to downregulate an HMG-domain repressor in *Caenorhabditis elegans*. Nature (Lond) 399(6738):793–797

Nguyen V, Deschet K, Henrich T et al (1999) Morphogenesis of the optic tectum in the medaka (*Oryzias latipes*): a morphological and molecular study, with special emphasis on cell proliferation. J Comp Neurol 413(3):385–404

Niehrs C, Shen J (2010) Regulation of Lrp6 phosphorylation. Cell Mol Life Sci 67(15):2551–2562

Ota S, Ishitani S, Shimizu N et al (2012) NLK positively regulates Wnt/β-catenin signalling by phosphorylating LEF1 in neural progenitor cells. EMBO J 31(8):1904–1915

Rocheleau CE, Yasuda J, Shin TH et al (1999) WRM-1 activates the LIT-1 protein kinase to transduce anterior/posterior polarity signals in *C. elegans*. Cell 97(6):717–726

Shimizu N, Kawakami K, Ishitani T (2012) Visualization and exploration of Tcf/Lef function using a highly responsive Wnt/β-catenin signaling-reporter transgenic zebrafish. Dev Biol 370(1):71–85

Siegfried KR, Kimble J (2002) POP-1 controls axis formation during early gonadogenesis in *C. elegans*. Development (Camb) 129(2):443–453

Siegfried KR, Kidd AR 3rd, Chesney MA et al (2004) The sys-1 and sys-3 genes cooperate with Wnt signaling to establish the proximal-distal axis of the *Caenorhabditis elegans* gonad. Genetics 166(1):171–186

Thorpe CJ, Schlesinger A, Carter JC et al (1997) Wnt signaling polarizes an early *C. elegans* blastomere to distinguish endoderm from mesoderm. Cell 90(4):695–705

van den Heuvel S, Dyson NJ (2008) Conserved functions of the pRB and E2F families. Nat Rev Mol Cell Biol 9(9):713–724

Wang J, Wynshaw-Boris A (2004) The canonical Wnt pathway in early mammalian embryogenesis and stem cell maintenance/differentiation. Curr Opin Genet Dev 14(5):533–539

Waxman JS, Hocking AM, Stoick CL et al (2004) Zebrafish Dapper1 and Dapper2 play distinct roles in Wnt-mediated developmental processes. Development (Camb) 131(23):5909–5921

Zeng X, Tamai K, Doble B et al (2005) A dual-kinase mechanism for Wnt co-receptor phosphorylation and activation. Nature (Lond) 438(7069):873–877

Zeng X, Huang H, Tamai K et al (2008) Initiation of Wnt signaling: control of Wnt coreceptor Lrp6 phosphorylation/activation via frizzled, dishevelled and axin functions. Development (Camb) 135(2):367–375

Chapter 17
The Role of Tsukushi as an Extracellular Signaling Coordinator

Kunimasa Ohta

Abstract Temporal and spatial coordination of multiple signaling pathways is essential for finely tuned cellular regulation in development. Extracellular signaling molecules that function in a concentration-dependent manner, collectively called "morphogens," and their inhibitors both play pivotal roles in the regulation of embryogenesis. Understanding concerning the coordination of these signal molecule-dependent pathways has been mainly about the mechanisms of intracellular crosstalk. Small leucine-rich proteoglycan (SLRP) family proteins modulate various cellular processes, that is, cellular proliferation, growth, differentiation, survival, and adhesion. In this chapter, I discuss signal coordination at the extracellular level by this family of proteins that interact with a variety of signaling molecules, as exemplified by Tsukushi (TSK). We discovered a novel SLRP family member, TSK, which is expressed and secreted in several specific tissue areas where embryonic organogenesis is ongoing. TSK binds nodal/Vg1/TGF-β1, BMP4/chordin, FGF8, Frizzled4, and Delta and modulates their downstream intracellular signaling pathways, indicating multiple regulatory functions of TSK during development.

Keywords Multiple signaling pathways • SLRP • Soluble molecule • Tsukushi

17.1 Introduction

The exchange of information between cells is essential for embryonic development and homeostasis in multicellular organisms. Signaling molecules that are released from a group of cells travel to target cells and bind to their surface receptors to exert their effects. Improper deployment of signaling molecules can lead to

K. Ohta (✉)
Department of Developmental Neurobiology, Graduate School of Life Sciences, Kumamoto University, Kumamoto, Japan
e-mail: ohta9203@gpo.kumamoto-u.ac.jp

H. Kondoh and A. Kuroiwa (eds.), *New Principles in Developmental Processes*,
DOI 10.1007/978-4-431-54634-4_17, © Springer Japan 2014

developmental defects and cause diseases (Muller and Schier 2011). Many important extracellular signaling molecules such as Wnts, Hedgehog (Hh), fibroblast growth factors (FGFs), and their downstream signaling cascades have now been itemized and characterized, demonstrating evolutionary conservation of their actions. Importantly, they are employed repeatedly at different stages of development. Growing evidence indicates that virtually all developmental events are regulated by cooperation of multiple signaling pathways. Some extracellular regulators interact with multiple signaling molecules, for example, Cerberus interacting with Wnt, Nodal, and bone morphogenetic (BMP) (Piccolo et al. 1999) and follistatin interacting with activin and BMP (Fainsod et al. 1997), suggesting that these extracellular signaling molecules function to integrate multiple signaling processes, but this has remained only as a model.

We carried out a signal sequence trap screening using a chick lens library and isolated five cDNAs encoding novel secreted proteins (Mu et al. 2003). One of these cDNA clones (clone 179) encoded a new member of the small leucine-rich proteoglycan family (SLRP) of 369 amino acid residues. To date, 17 proteins have been assigned to the SLRP family (Schaefer and Iozzo 2008; Dellett et al. 2012). An SLRP protein binds various cell-surface receptors, growth factors, cytokines, and other extracellular matrix components, suggesting a potential role to coordinate diverse cellular functions (Dellett et al. 2012). We named this new SLRP protein of our discovery "Tsukushi" (TSK), from the observation that the expression pattern in blastoderm-stage chick embryos (Fig. 17.1a) looks like a shoot of the horsetail plant (*Equisetum*), "Tsukushi" in Japanese (Fig. 17.1b) (Ohta et al. 2004). At the amino-acid sequence level, chick Tsukushi (C-TSK) shares 59 % identity with *Xenopus* Tsukushi (X-TSK) and 53–54 % identity with zebrafish, mouse, and human TSKs. Our studies indicate that TSKs function as signaling coordinators by interacting with multiple extracellular signaling molecules. The multiple roles of TSK during the development are reviewed in this chapter.

17.1.1 TSK Promotes Organizer Formation by Inhibiting BMP Signaling

During early chick development (stage 3), the middle portion of the primitive streak functions as "the node-inducing center" that corresponds to the Nieuwkoop center in *Xenopus* (Joubin and Stern 1999). Induced Hensen's node corresponds to amphibian Spemann organizer. BMP4 is present at low levels in the entire embryonic epiblast (area pellucida) and extraembryonic epiblast (area opaca) (Faure et al. 2002). At later stages, BMPs are more strongly expressed over the posterior primitive streak and encircle the area pellucida, excluding the areas in and surrounding the node (Joubin and Stern 1999). In contrast to BMPs, BMP antagonist chordin (Sasai et al. 1994) is expressed in the anterior tip of the forming primitive streak and subsequently localizes to Hensen's node (Streit et al. 1998). This inhibition of BMP signaling by chordin and other BMP antagonists is a critical step in the formation of the primitive streak and induction of Hensen's node (Joubin and Stern 1999).

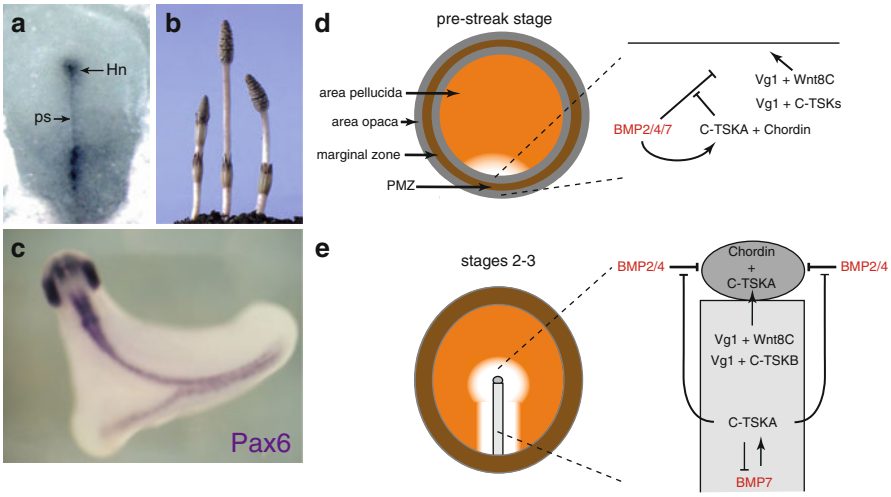

Fig. 17.1 Molecular interaction of Tsukushi (*TSK*) during chick gastrulation. (**a**, **b**) We identified a unique secreted bone morphogenetic protein (*BMP*) inhibitor, which is expressed in the primitive streak and Hensen's node (*Hn*) during chick gastrulation (**a**). We named this factor "Tsukushi" (*TSK*) because its expression pattern in chick embryos is similar to the shape of the shoot of the horsetail plant, "Tsukushi" in Japanese (**b**). **c** C-TSK mRNA was injected into a ventral vegetal blastomere, embryos were cultured, and in situ hybridization was performed with Pax6. (**d**, **e**) Successive stages in the development of the chick embryo are shown on the *left*; the sequential molecular signaling steps are shown on the *right*. (**d**) Just before gastrulation, Wnt8C and C-TSK are expressed all around the marginal zone, and Vg1 in PMZ. C-TSKA collaborates with chordin to decrease BMP activity in PMZ. (**e**) At stages 2–3, the primitive streak starts to form under the influence of Vg1 + Wnt8C and Vg1 + C-TSKB. The Vg1 + Wnt8C and Vg1 + C-TSKB signaling cascade synergize to induce the organizer in the central area where the C-TSKA + chordin serves to keep BMP expression clear of the center. C-TSKA also inhibits the activity of BMP7 expressed in the posterior primitive streak

Alternative splicing of C-TSK transcripts generates two isoforms, C-TSKA, (originally reported form of C-TSK) and C-TSKB, that differ in their C-terminal region (Ohta et al. 2006). All TSK orthologues in zebrafish, *Xenopus*, mouse, and human have only the TSKB isoform. The C-TSKA isoform is a strong BMP antagonist (Fig. 17.1c). Its expression becomes progressively restricted to Hensen's node and the anterior primitive streak during gastrulation (Ohta et al. 2004), similar to other BMP antagonists. In contrast, the C-TSKB isoform is a much weaker antagonist, and is expressed mainly in the middle portion of the primitive streak (Ohta et al. 2006).

C-TSK isoforms presumably play two different roles in the primitive streak formation. At pre-streak stage (Fig. 17.1d), C-TSK expression is detectable in the area opaca, the posterior marginal zone (PMZ), and Koller's sickle. Of the two isoforms, C-TSKA cooperates with chordin to decrease BMP activity in the posterior epiblast (Ohta et al. 2004), whereas both C-TSKA and C-TSKB augment Vg1 activity in the PMZ, thus facilitating induction of the primitive streak. At primitive streak stages (Fig. 17.1e), both C-TSKA and C-TSKB are initially expressed throughout the primitive streak. However, as the primitive streak reaches its full extension, the

expression of C-TSKA becomes restricted to the anterior part of the streak and Hensen's node, whereas C-TSKB expression becomes enriched in the middle portion of the primitive streak. Thus, C-TSKA is involved in counteracting BMP2/4 signals spreading from the periphery in cooperation with chordin (Ohta et al. 2004), whereas C-TSKB promotes node-inducing activity by positively regulating Vg1 activity (Ohta et al. 2006).

17.1.2 TSK Controls Neural Crest Specification by Inhibiting BMP Signaling, Being Modulated by Notch Signaling Strength

Vertebrate neural crest cells arise at the border between the neural plate and the epidermis in the embryonic ectoderm. A gradient of BMP activity in the ectoderm, weaker around the neural plate periphery, is produced by interactions between BMPs expressed in the ectoderm and the BMP inhibitors secreted from the axial mesoderm, resulting in a specific BMP signaling level that directs specification of the neural crest cells (Nguyen et al. 1998; Marchant et al. 1998; LaBonne and Bronner-Fraser 1998). However, the neural crest is not produced from the anterior-most portion of the neural plate (Hopwood et al. 1989; Mayor et al. 1995), which is not readily explained by the BMP signal gradient alone and suggests involvement of additional factor(s) in these anteroposterior differences (Villanueva et al. 2002).

Recently, the Notch signaling pathway has also been shown to be important in neural crest specification by regulating the expression of BMP signaling molecules at the lateral edge of the neural plate (Glavic et al. 2004). X-TSK is expressed in the prospective cranial neural crest at the early neurula stage (Fig. 17.2a) (Kuriyama et al. 2006). In the migrating cranial neural crest, X-TSK is expressed in the mandibular and the anterior and posterior branchial crest segments (Fig. 17.2b). During gastrulation, X-TSK is expressed in the whole-animal ectoderm and in the dorsal mesoderm (Ohta et al. 2004). Dorsal midline signals, such as chordin, Noggin, and X-TSK, bind to BMPs and directly inhibit their activity in the dorsal ectoderm (phase I in Fig. 17.2i), leading to the specification of the neural plate at these stages (Sasai and De Robertis 1997). Subsequently, X-TSK expression is downregulated in the presumptive neural plate, although it is even augmented in the ectoderm flanking the neural plate (phase II in Fig. 17.2i). At these stages, in the presumptive neural crest region, X-TSK controls BMP activity through direct binding to BMPs, and it also downregulates BMP transcription, possibly via modulation of the Notch signaling pathway (Fig. 17.2j). Our gain- and loss-of-function experiments with X-TSK in isolated animal caps suggest that X-TSK modulates X-delta-1 activity in a dose-dependent manner, by activating it at lower X-TSK levels and repressing it at higher X-TSK levels (Kuriyama et al. 2006). Acting via simultaneous modulation of BMP and Notch signaling, TSK regulates the establishment of a pre-neural crest region expressing Hairy2A and Msx1. Monsoro-Burq et al. (2005) reported that Msx1 and XWnt-8-dependent posteriorizing effect converge on Pax3. In turn, Pax3

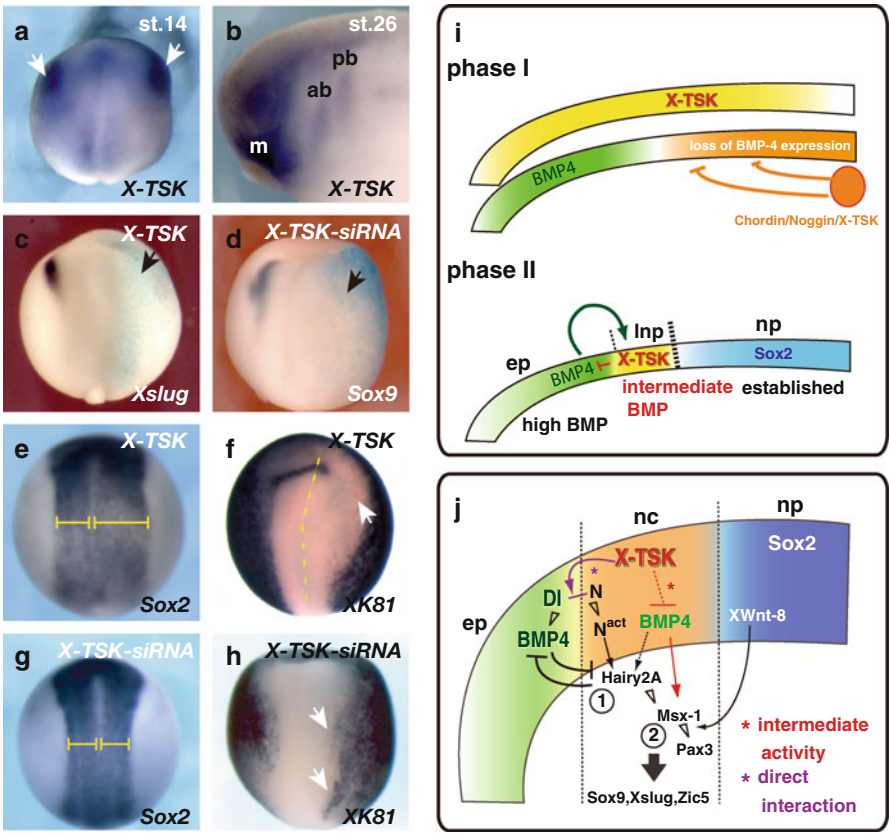

Fig. 17.2 Molecular interaction of TSK during neural crest specification. (**a**) Bilateral expression of X-TSK outside the neural plate (*arrows*). Dorsal view: anterior is upward. (**b**) X-TSK expression was observed in mandibular (*m*) neural crest, anterior branchial (*ab*) crest, and posterior branchial (*pb*) crest. (**c**) The neural crest marker Xslug disappeared with X-TSK overexpression (*arrow*). (**d**) The neural crest marker Sox9 disappeared with X-TSK siRNA (*arrow*). (**e**) Sox2 expression expanded laterally in the X-TSK-injected side (*right side*). (**f**) Epidermal keratin expression disappeared at the anterior border on the X-TSK-injected side (*arrow*). (**g**) Sox2 expression was not disturbed in the X-TSK-siRNA-injected embryo. (**h**) Epidermal keratin was activated in the X-TSK-siRNA-injected side (*arrows*). (**i**) A model of sequential steps for neural crest specification. Phase I: During gastrulation, midline BMP antagonists inhibit BMP4 expression and specify the neural plate (*np*: *orange*). After this, X-TSK expression is repressed in the presumptive neural plate, while it is maintained in the lateral ectoderm by BMP4 signaling (*green*). Phase II: At a later stage, X-TSK expression is upregulated in the lateral neural crest region (*lnp*: *yellow*), which has intermediate levels of BMP signaling. (**j**) Molecular network of neural crest (*nc*) specification. X-TSK inhibits BMP4 (*red asterisk*) and modulates Notch signaling via direct binding to X-delta-1 (*purple asterisk*). Notch signaling can regulate the expression of BMP4, and BMP and Notch signaling interact to control the expression of Hairy2A and Msx1. Finally, caudalizing signals such as XWnt-8 converge to this network downstream of Msx1, to control the activation of Pax3 expression and neural crest cell specification

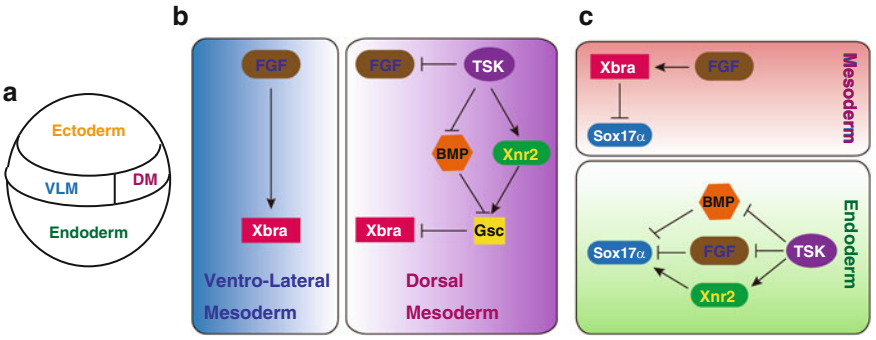

Fig. 17.3 Molecular interaction of TSK during germ layer formation. (**a**) Schematic drawing of X-TSK expression in ectoderm, dorsal mesoderm (*DM*), and endoderm of *Xenopus* embryo. (**b**) Model of X-TSK function in germ layer formation and patterning: dorsal–ventral mesoderm patterning. X-TSK in dorsal mesoderm inhibits BMP signaling and activates Xnr2 signals to promote dorsal mesoderm formation. Further, X-TSK inhibits expression of ventrolateral mesoderm (*VLM*) marker Xbra, through inhibition of FGF signaling. (**c**) Model of X-TSK function in endoderm formation. X-TSK coordinates inhibition of FGF and BMP signals with activation of Xnr2 signaling to induce endoderm formation, as marked by Sox17α. Again, X-TSK inhibits expression of ventrolateral mesoderm marker Xbra, through inhibition of BMP and FGF signaling, and contributes to the distinction between endoderm- and mesoderm-specific gene expression

cooperates with ZicR1 (Zic1) to activate neural crest markers (Sox9, Xslug, and Zic5), resulting in the specification of the neural crest (Monsoro-Burq et al. 2005) (Fig. 17.2j). Furthermore, some FGFs such as FGF8 are expressed in the anterior neural border from early neurula stages (Lupo et al. 2005), suggesting that the presence of higher levels of X-TSK in the anterior neural border, compared with the neural crest itself, might be an additional mechanism to restrict the boundaries of the neural crest domain.

17.1.3 TSK Is Involved in Germ Layer Formation by the Inhibition of BMP and FGF Signaling and the Enhancement of Xnr2 Signaling

During blastula stages of amphibian development, the germ layers are formed along the primary animal–vegetal axis of the embryo: the pigmented animal pole develops into ectoderm, the yolk-rich vegetal pole develops into endoderm, and the equatorial region develops into mesoderm (Schohl and Fagotto 2003). Germ layer formation appears to rely on inductive interactions, which are generated by prelocalized maternal determinants (Schohl and Fagotto 2003). Multiple signaling pathways initiated by extracellular molecules must be finely coordinated to produce the required output and to achieve appropriate germ layer specification (Darras et al. 1997).

X-TSK is expressed in ectoderm, endoderm, and dorsal mesoderm during early stages of *Xenopus* development, suggesting a role for X-TSK in germ layer formation and patterning (Fig. 17.3a) (Morris et al. 2007). Our functional analyses

show that X-TSK has activity to expand the region of Gsc expression marking the organizer, via BMP signal inhibition and *Xenopus* nodal-related protein (Xnr) signal activation (Morris et al. 2007). Additionally, X-TSK inhibits expression of ventrolateral mesoderm markers through inhibition of FGF signaling. Moreover, X-TSK expression in the dorsal mesoderm contributes to organizer formation through BMP signaling inhibition and activates the dorsal mesoderm-specific gene regulatory network (Fig. 17.3b). For the endoderm to develop, X-TSK interacts with Xnr2 and enhances Smad2 activity downstream of Xnr2. In addition, X-TSK has two more activities: binding and inhibition of FGF8b and BMP. It is known that strong activation of nodal signaling plays a major role in endoderm development (Schier 2003). Thus, X-TSK organizes endoderm development through its action of Xnr2 activation, FGF-MAPK inhibition, and BMP inhibition (Fig. 17.3c). In conclusion, through regulation of these multiple factors, TSK coordinates formation of the endoderm and patterning of mesoderm during early *Xenopus* embryogenesis (Morris et al. 2007).

17.1.4 TSK Is Involved in Ciliary Body Formation in the Eye by Inhibiting Wnt Signaling

Multipotent stem/progenitor cells have been isolated from the ciliary body (CB) at the anterior margin of the adult mouse retina and shown to possess characteristics of stem cells (Tropepe et al. 2000). Several lines of evidence suggest that Wnt signaling promotes proliferation of neural retinal stem cells. Wnt proteins released from the signaling cells bind to the Frizzled (Fzd)/low-density lipoprotein receptor-related protein complex on the cell surface of target cells, eliciting these Wnt receptor complexes to transduce the signal intracellularly (Logan and Nusse 2004).

In the chick embryonic eye, Wnt2b is localized to the anterior tip of the optic cup, and C-TSKB is expressed in the adjacent ciliary/iris epithelium, whereas Fzd4 is expressed in both the ciliary and the iris epithelia (Fig. 17.4a) (Ohta et al. 2011). In the mouse eye, the TSK gene is expressed in the retinal layers, CB, and lens epithelium, and its expression then continues in the prospective CB until adulthood (Fig. 17.4b) (Ohta et al. 2011). In the anterior parts of the eye, the β-catenin-dependent Wnt signaling pathway is mainly activated by the Wnt2b ligand and transduced through the Fzd4 receptor (Kubo et al. 2005). Interestingly, TSK directly binds to the cysteine-rich domain of Fzd4 and competes with Wnt2b for binding to the same domain, thus preventing Wnt activation of β-catenin-dependent signaling (Ohta et al. 2011). The expression of both Wnt2b and Fzd4 in embryonic (E) 15.5 day eyes is augmented and regionally expanded in the future CB area of TSK KO mice compared with WT mice (Fig. 17.4c). Targeted inactivation of the TSK gene in mice causes expansion of the CB (Ohta et al. 2011). These observations indicate that TSK is an important component of the Wnt signal pathway controlling CB development (Fig. 17.4d) (Ohta et al. 2011).

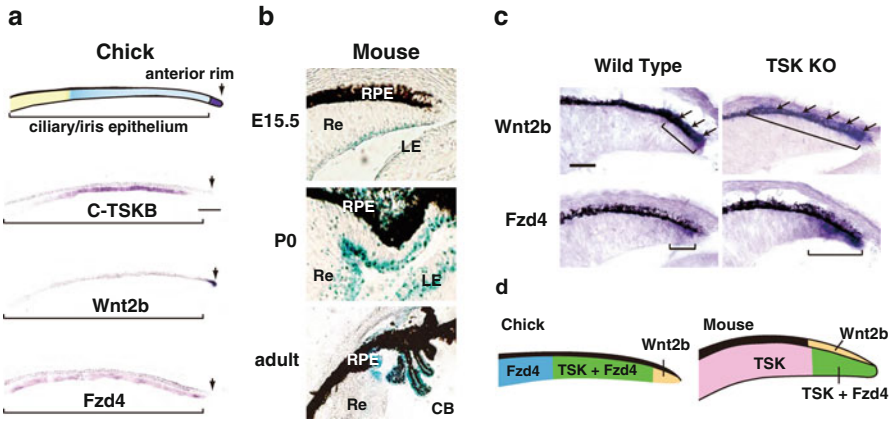

Fig. 17.4 Molecular interaction of TSK during peripheral eye formation. (**a**) Schematic drawing of the peripheral region of a chick E6 eye and in situ hybridizations showing mRNA expression patterns of C-TSKB, Wnt2b, and Fzd4. (**b**) M-TSK is expressed in the anteriormost tip of the developing mouse optic cup and the mature CB. *RPE* retinal pigmented epithelium, *CB* ciliary body, *Re* retina, *LE* lens epithelium. (**c**) Expression of Wnt2b and Fzd4 in the E15.5 peripheral retina. Note that the expression of Wnt2b (*arrows*) and Fzd4 in M-TSK KO mice is expanded in both the pigmented epithelium and the nonpigmented epithelium compared with WT mice. (**d**) During early retinal development, Wnt2b (*yellow*) expressed in the tip of the retina (chick) and the peripheral pigmented epithelium (mouse) acts on the nonpigmented cells expressing Fzd4 and TSK (*green*) to cause proliferation. TSK regulates this effect by inhibiting Wnt2b activity

17.1.5 TSK Augments Transforming Growth Factor (TGF)-β Signaling Activity During the Hair Cycle

The hair follicle is a complex mini-organ with repeated regeneration and degeneration processes known as hair cycles. Hair follicular stem cells (HFSCs) are located in the hair follicle bulge area (Blanpain and Fuchs 2006). The HFSC population is composed of multipotent keratinocyte stem cells that are responsible for the cyclic generation of hair follicles and, during wound healing, for transient cell supply to interfollicular epidermis and sebaceous glands (Oshima et al. 2001). Several signaling molecules of the Wnt, BMP, Shh, and TGF-β signaling cascades are involved in the normal hair follicle cycle (Alonso and Fuchs 2006).

TSK is expressed in restricted areas of the hair follicle during hair growth and the hair cycle (Fig. 17.5a) (Niimori et al. 2012). We demonstrated that TSK secreted from lower follicle (bulb) directly binds to TGF-β1 outside the cell. Skin pigmentation after depilation was different between wild-type (WT) and TSK knockout (KO) mice; the skin color of WT mice is gray (anagen stage), whereas that of TSK KO mice is pink (telogen stage) (Fig. 17.5b). TGF-β signaling has been reported to be important for the homeostasis of hair follicles and

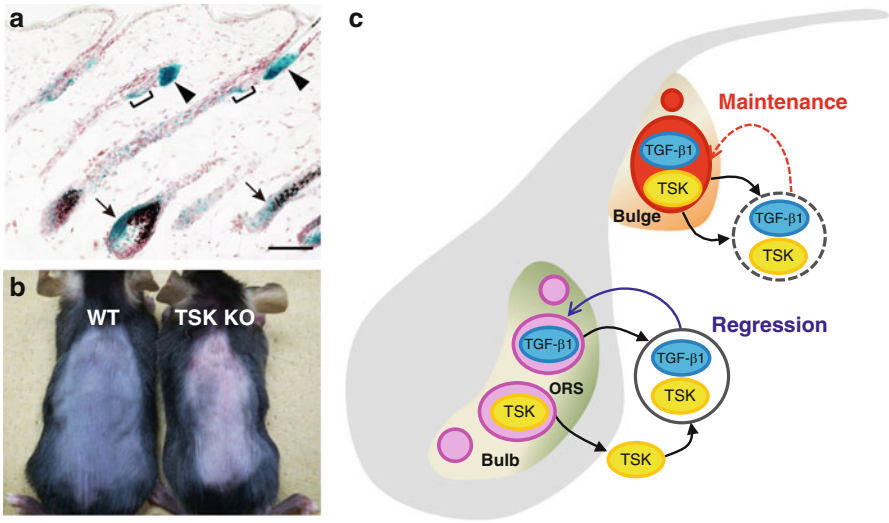

Fig. 17.5 Molecular interaction of TSK during hair cycling. (**a**) M-TSK is expressed in the bulge cells (*brackets*), sebaceous glands (*arrowheads*), and bulb (*arrows*) at P30. (**b**) The wild-type (*WT*) mouse shows a *gray color* after depilation, which indicates the hair growth state, although the M-TSK knockout (*KO*) mouse shows a *pink color*, which indicates that the hair follicles are in a resting state. (**c**) A schematic model of M-TSK and TGF-β1 during the hair cycle. M-TSK is secreted from the lower follicle (bulb), binds to TGF-β1 outside the cell, and causes cell regression. HFSCs are localized in the hair follicle bulge area M-TSK may maintain HFSCs that are TGF-β dependent. *ORS* outer root sheath

causes the phosphorylation of Smad2/3 (Yang et al. 2009). The expression of pSmad2/3 is detected in the bulge area at the telogen stage of WT mice but was not detected in TSK KO mice (Niimori et al. 2012). Therefore, we suggest that TSK secreted by bulge cells induces the anagen phase of the hair cycle by enhancing TGF-β activity after secretion (Fig. 17.5c).

17.1.6 TSK Is Involved in Neural Circuit Formation

In the developing mouse brain, TSK is expressed in the olfactory bulb, anterior olfactory nucleus, neocortex, and piriform cortex (Ito et al. 2010). In the TSK KO mice, nerve fibers fail in crossing the midline in the anterior commissure position, and the adult brain lacks the anterior commissure (Ito et al. 2010). Presumably related to this KO mouse phenotype, TSK has axon guidance activity by inhibiting neurite outgrowth of anterior olfactory neurons and cortical neurons in vitro (Hossain et al. 2013). TSK also induced growth cone collapse when applied to these cultured neurons (Hossain et al. 2013), demonstrating involvement of TSK in the neuronal circuit formation.

17.2 Conclusion

TSK directly binds several signaling molecules in the extracellular space through protein–protein interactions. TSK functions as an extracellular modulator of signaling cascades by enhancing or inhibiting their activity during early embryonic development. Figure 17.6 cartoons multiple and context-dependent functions of TSK. In the case of *Xenopus* neural crest specification, X-TSK augments X-delta-1 activity when X-TSK expression is low, whereas it represses X-delta-1 activity when the X-TSK expression level is high, ensuring a range of X-delta-1-dependent signaling (Kuriyama et al. 2006). In more complex situations, TSK protein simultaneously binds to multiple signaling molecules to modulate the integrated outputs. One such example is that TSK binds both BMP and its antagonist chordin and potentiates chordin BMP inhibitory activity during organizer formation (Ohta et al. 2004). Thus, TSK modulates the balance of multiple signaling pathways depending on the context of developmental processes.

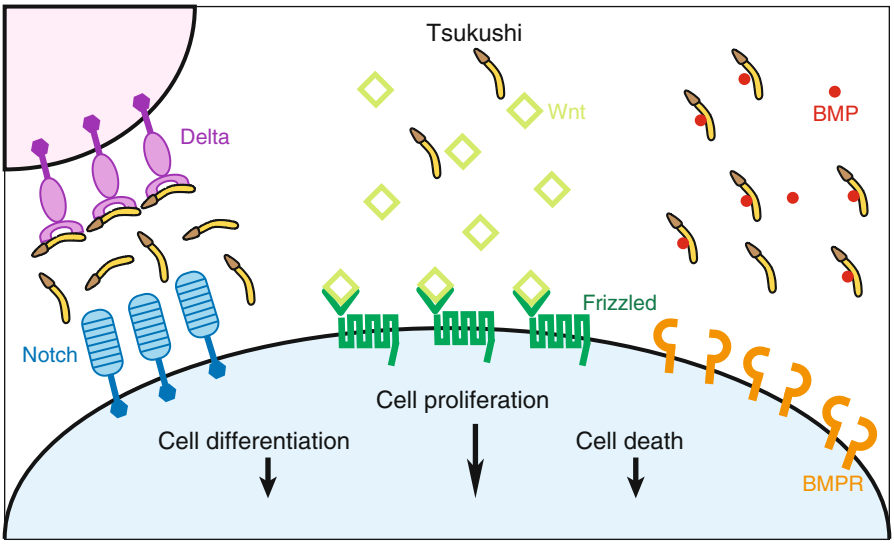

Fig. 17.6 Dynamic regulation of extracellular signaling network. The signaling molecules that localized the extracellular region create a microenvironment through combinatory potentiation of multiple signaling activities, then extracellular signals are activated or repressed at the correct time and place. For example, *blue cells* and *purple cells* express cell membrane protein Notch, Frizzled, and bone morphogenetic protein receptor (*BMPR*) and Delta, respectively. TSK localized at the extracellular region binds to BMP and Delta and inhibits their signaling cascades, but in the central area, as TSK concentration is low, Wnt binds to Frizzled, resulting in cell proliferation. Thus, TSK coordinates extracellular signaling networks that determine the several biological processes during development

References

Alonso L, Fuchs E (2006) The hair cycle. J Cell Sci 119(Pt 3):391–393. doi:10.1242/jcs02793

Blanpain C, Fuchs E (2006) Epidermal stem cells of the skin. Annu Rev Cell Dev Biol 22:339–373. doi:10.1146/annurev.cellbio.22.010305.104357

Darras S, Marikawa Y, Elinson RP, Lemaire P (1997) Animal and vegetal pole cells of early *Xenopus* embryos respond differently to maternal dorsal determinants: implications for the patterning of the organiser. Development (Camb) 124(21):4275–4286

Dellett M, Hu W, Papadaki V, Ohnuma S (2012) Small leucine rich proteoglycan family regulates multiple signalling pathways in neural development and maintenance. Dev Growth Differ 54(3):327–340. doi:10.1111/j.1440-169X.2012.01339.x

Fainsod A, Deissler K, Yelin R, Marom K, Epstein M, Pillemer G, Steinbeisser H, Blum M (1997) The dorsalizing and neural inducing gene follistatin is an antagonist of BMP-4. Mech Dev 63(1):39–50

Faure S, de Barbara Santa P, Roberts DJ, Whitman M (2002) Endogenous patterns of BMP signaling during early chick development. Dev Biol 244(1):44–65. doi:10.1006/dbio.2002.0579

Glavic A, Silva F, Aybar MJ, Bastidas F, Mayor R (2004) Interplay between Notch signaling and the homeoprotein Xiro1 is required for neural crest induction in *Xenopus* embryos. Development (Camb) 131(2):347–359. doi:10.1242/dev.00945

Hopwood ND, Pluck A, Gurdon JB (1989) A *Xenopus* mRNA related to *Drosophila* twist is expressed in response to induction in the mesoderm and the neural crest. Cell 59(5):893–903

Hossain M, Ahmed G, Naser IB, Shinmyo Y, Ito A, Riyadh MA, Felemban A, Song X, Ohta K, Tanaka H (2013) The combinatorial guidance activities of draxin and Tsukushi are essential for forebrain commissure formation. Dev Biol 374(1):58–70. doi:10.1016/j.ydbio.2012.11.029

Ito A, Shinmyo Y, Abe T, Oshima N, Tanaka H, Ohta K (2010) Tsukushi is required for anterior commissure formation in mouse brain. Biochem Biophys Res Commun 402(4):813–818. doi:10.1016/j.bbrc.2010.10.127

Joubin K, Stern CD (1999) Molecular interactions continuously define the organizer during the cell movements of gastrulation. Cell 98(5):559–571

Kubo F, Takeichi M, Nakagawa S (2005) Wnt2b inhibits differentiation of retinal progenitor cells in the absence of Notch activity by downregulating the expression of proneural genes. Development (Camb) 132(12):2759–2770. doi:10.1242/dev.01856

Kuriyama S, Lupo G, Ohta K, Ohnuma S, Harris WA, Tanaka H (2006) Tsukushi controls ectodermal patterning and neural crest specification in *Xenopus* by direct regulation of BMP4 and X-delta-1 activity. Development (Camb) 133(1):75–88. doi:10.1242/dev.02178

LaBonne C, Bronner-Fraser M (1998) Neural crest induction in *Xenopus*: evidence for a two-signal model. Development (Camb) 125(13):2403–2414

Logan CY, Nusse R (2004) The Wnt signaling pathway in development and disease. Annu Rev Cell Dev Biol 20:781–810. doi:10.1146/annurev.cellbio.20.010403.113126

Lupo G, Liu Y, Qiu R, Chandraratna RA, Barsacchi G, He RQ, Harris WA (2005) Dorsoventral patterning of the *Xenopus* eye: a collaboration of Retinoid, Hedgehog and FGF receptor signaling. Development (Camb) 132(7):1737–1748. doi:10.1242/dev.01726

Marchant L, Linker C, Ruiz P, Guerrero N, Mayor R (1998) The inductive properties of mesoderm suggest that the neural crest cells are specified by a BMP gradient. Dev Biol 198(2):319–329

Mayor R, Morgan R, Sargent MG (1995) Induction of the prospective neural crest of *Xenopus*. Development (Camb) 121(3):767–777

Monsoro-Burq AH, Wang E, Harland R (2005) Msx1 and Pax3 cooperate to mediate FGF8 and WNT signals during *Xenopus* neural crest induction. Dev Cell 8(2):167–178. doi:10.1016/j.devcel.2004.12.017

Morris SA, Almeida AD, Tanaka H, Ohta K, Ohnuma S (2007) Tsukushi modulates Xnr2, FGF and BMP signaling: regulation of *Xenopus* germ layer formation. PLoS ONE 2(10):e1004. doi:10.1371/journal.pone.0001004

Mu H, Ohta K, Kuriyama S, Shimada N, Tanihara H, Yasuda K, Tanaka H (2003) Equarin, a novel soluble molecule expressed with polarity at chick embryonic lens equator, is involved in eye formation. Mech Dev 120(2):143–155

Muller P, Schier AF (2011) Extracellular movement of signaling molecules. Dev Cell 21(1):145–158. doi:10.1016/j.devcel.2011.06.001

Nguyen M, Park S, Marques G, Arora K (1998) Interpretation of a BMP activity gradient in *Drosophila* embryos depends on synergistic signaling by two type I receptors, SAX and TKV. Cell 95(4):495–506

Niimori D, Kawano R, Felemban A, Niimori-Kita K, Tanaka H, Ihn H, Ohta K (2012) Tsukushi controls the hair cycle by regulating TGF-beta1 signaling. Dev Biol 372(1):81–87. doi:10.1016/j.ydbio.2012.08.030

Ohta K, Lupo G, Kuriyama S, Keynes R, Holt CE, Harris WA, Tanaka H, Ohnuma S (2004) Tsukushi functions as an organizer inducer by inhibition of BMP activity in cooperation with chordin. Dev Cell 7(3):347–358. doi:10.1016/j.devcel.2004.08.014

Ohta K, Kuriyama S, Okafuji T, Gejima R, Ohnuma S, Tanaka H (2006) Tsukushi cooperates with VG1 to induce primitive streak and Hensen's node formation in the chick embryo. Development (Camb) 133(19):3777–3786. doi:10.1242/dev.02579

Ohta K, Ito A, Kuriyama S, Lupo G, Kosaka M, Ohnuma S, Nakagawa S, Tanaka H (2011) Tsukushi functions as a Wnt signaling inhibitor by competing with Wnt2b for binding to transmembrane protein Frizzled4. Proc Natl Acad Sci USA 108(36):14962–14967. doi:10.1073/pnas.1100513108

Oshima H, Rochat A, Kedzia C, Kobayashi K, Barrandon Y (2001) Morphogenesis and renewal of hair follicles from adult multipotent stem cells. Cell 104(2):233–245

Piccolo S, Agius E, Leyns L, Bhattacharyya S, Grunz H, Bouwmeester T, De Robertis EM (1999) The head inducer Cerberus is a multifunctional antagonist of Nodal, BMP and Wnt signals. Nature (Lond) 397(6721):707–710. doi:10.1038/17820

Sasai Y, De Robertis EM (1997) Ectodermal patterning in vertebrate embryos. Dev Biol 182(1):5–20. doi:10.1006/dbio.1996.8445

Sasai Y, Lu B, Steinbeisser H, Geissert D, Gont LK, De Robertis EM (1994) *Xenopus* chordin: a novel dorsalizing factor activated by organizer-specific homeobox genes. Cell 79(5):779–790

Schaefer L, Iozzo RV (2008) Biological functions of the small leucine-rich proteoglycans: from genetics to signal transduction. J Biol Chem 283(31):21305–21309. doi:10.1074/jbc.R800020200

Schier AF (2003) Nodal signaling in vertebrate development. Annu Rev Cell Dev Biol 19:589–621. doi:10.1146/annurev.cellbio.19.041603.094522

Schohl A, Fagotto F (2003) A role for maternal beta-catenin in early mesoderm induction in *Xenopus*. EMBO J 22(13):3303–3313. doi:10.1093/emboj/cdg328

Streit A, Lee KJ, Woo I, Roberts C, Jessell TM, Stern CD (1998) Chordin regulates primitive streak development and the stability of induced neural cells, but is not sufficient for neural induction in the chick embryo. Development (Camb) 125(3):507–519

Tropepe V, Coles BL, Chiasson BJ, Horsford DJ, Elia AJ, McInnes RR, van der Kooy D (2000) Retinal stem cells in the adult mammalian eye. Science 287(5460):2032–2036

Villanueva S, Glavic A, Ruiz P, Mayor R (2002) Posteriorization by FGF, Wnt, and retinoic acid is required for neural crest induction. Dev Biol 241(2):289–301. doi:10.1006/dbio.2001.0485

Yang L, Wang L, Yang X (2009) Disruption of Smad4 in mouse epidermis leads to depletion of follicle stem cells. Mol Biol Cell 20(3):882–890. doi:10.1091/mbc.E08-07-0731

Chapter 18
Divergent Roles of Heparan Sulfate in Regulation of FGF Signaling During Mammalian Embryogenesis

Isao Matsuo, Chiharu Kimura-Yoshida, and Kayo Shimokawa

Abstract Heparan sulfate proteoglycans, composed of heparan sulfate (HS) glycosaminoglycan chains and core proteins, are distributed at the cell surface as well as in the extracellular matrix (ECM). HS chains play crucial yet divergent roles in regulation of fibroblast growth factor (FGF) signaling extracellularly: as an essential cofactor for ligand–receptor dimerization at the cell surface, positive and negative modulators of stable dimer formation, as a key mediator of active movement of ligands, and as a spatial barrier for passive diffusion in the ECM. These divergent functions are mediated by the local HS structures, for example, chain length and sulfation level, and by the spreading of unanchored HS chains after enzymatic cleavage by proteinases and heparanases. In this way, FGF signaling activity modified by HS participates in multiple cellular processes including cell proliferation, differentiation, survival, and migration during embryonic development. In this chapter, we highlight the essential and cell nonautonomous roles of the cell-surface HS in activation of FGF signaling during mouse extra-embryonic ectoderm development.

Keywords Chimeric analysis • *Ext2* • Extra-embryonic ectoderm • Fibroblast growth factor (FGF) • Heparan sulfate proteoglycans (HSPGs)

18.1 Introduction

Heparan sulfate proteoglycans (HSPGs) are composed of a specific core protein covalently linked with one or more heparan sulfate (HS) glycosaminoglycan chains (Perrimon and Bernfield 2000; Bishop et al. 2007; Bülow and Hobert 2006; Varki et al. 2009) (Fig. 18.1). HSPGs are divided into three major classes based on their

I. Matsuo (✉) • C. Kimura-Yoshida • K. Shimokawa
Department of Molecular Embryology, Osaka Medical Center and Research Institute for Maternal and Child Health, Osaka Prefectural Hospital Organization, Osaka, Japan
e-mail: imatsuo@mch.pref.osaka.jp

H. Kondoh and A. Kuroiwa (eds.), *New Principles in Developmental Processes*,
DOI 10.1007/978-4-431-54634-4_18,

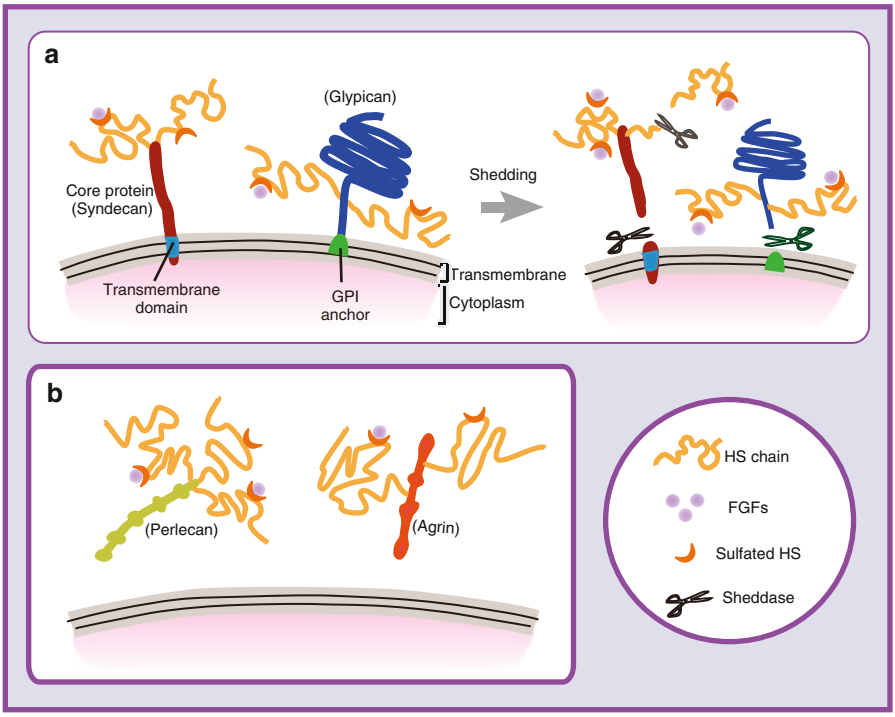

Fig. 18.1 Schematic representation of structures and localization of heparan sulfate proteoglycans (*HSPGs*). (**a**) Transmembrane-type and glycerophosphatidylinositide (*GPI*)-anchored type HSPGs. HS chains are covalently linked to core proteins. The two types of HSPGs, transmembrane type (syndecan) and GPI-anchored type (glypican), are tethered initially at the cell surface. These cell-surface HSPGs are occasionally cleaved by proteinases and heparanases. In addition, notum specifically cleaves the extracellular domain of GPI-linked core proteins. By "shedding," i.e., by sheddases cleavage, extracellular domains of HSPGs and HS chains are released from the cell surface into the extracellular matrix (*ECM*). (**b**) ECM-associated HSPSs. Secreted-type HSPGs such as perlecan and agrin are localized in the ECM, including the basement membrane

core-protein structure, transmembrane type (e.g., syndecans), glycerophosphatidylinositide (GPI)-anchored type (e.g., glypicans), and secreted extracellular matrix (ECM) type (e.g., perlecan and agrin) (Fig. 18.1). The transmembrane and GPI-anchored types are localized on the cell surface, but can also be released to the extracellular space and ECM by sheddase cleavage, such as a proteinase, a heparanase, or notum (pectinacetylesterase) depending on the context of cells. The ECM-type HSPG is solely secreted into the ECM such as the basement membrane during embryogenesis. Therefore, the cellular localization of HS chains is primarily dependent on the distribution of the linked core proteins (Fig. 18.1). During their synthesis, HS chains are initially assembled on serine residues of core proteins by a series of glycosyltransferases and modification enzymes in the Golgi apparatus. HS chains elongate by addition of disaccharide units consisting of *N*-acetylglucosamine and

glucuronic acid (generally 25–100 repeat units in length), being catalyzed by the heterodimer complex of Ext1 (exostosin glycosyltransferase 1) and Ext2 proteins (Perrimon and Bernfield 2000; Bishop et al. 2007; Bülow and Hobert 2006; Varki et al. 2009). Resultant long linear HS chains are further subjected to a series of modification reactions by several sulfotransferases and an epimerase, thereby generating a diversity of HS structures.

Mammalian 22 fibroblast growth factor (FGF) proteins can be classified into three groups: paracrine FGFs (also named canonical FGFs), hormonal FGFs (also endocrine FGFs), and intracrine FGFs (reviewed in Beenken and Mohammadi 2009; Dorey and Amaya 2010; Itoh and Ornitz 2011). Among these, paracrine FGFs comprising five subfamilies (i.e., FGF1/2/5, FGF3/4/6, FGF8/17/18, FGF7/10/22, and FGF9/16/20) have relatively high affinities to HS and thus can be retained locally by HS chains (Asada et al. 2009). Consequently, paracrine FGF–FGFR dimerization stabilized by HS chains directs tyrosine kinase activation of the FGF receptor (FGFR) (Yayon et al. 1991; Rapraeger et al. 1991; Schlessinger et al. 2000; Pellegrini et al. 2000), which controls multiple cellular events such as cell proliferation, differentiation, migration, and survival during mammalian development (Dorey and Amaya 2010; Lanner and Rossant 2010). In contrast, hormonal FGFs (FGF15/19/21/23) have a lower affinity to HS and can travel for longer distances through the bloodstream in an endocrine fashion to bind FGFRs with the aid of an α- or β-Klotho coreceptor at the cell surface of target organs (Kuro-o 2008; Goetz et al. 2012). Finally, intracrine FGFs (FGF11/12/13/14) are not secreted and bind to the sodium channel independently of FGFRs (Goldfarb 2012).

In addition to the crucial roles of HS in a FGF–FGFR ternary complex formation, HS chains modulate the signaling activity of diffusible growth factors such as FGF, bone morphogenetic protein (BMP), transforming growth factor (TGF)-β, Wnt, and Shh by controlling their extracellular stabilization, movement, and retention at the cell surface as well as in the ECM during development (Perrimon and Bernfield 2000; Bishop et al. 2007; Yan and Lin 2009; Matsuo and Kimura-Yoshida 2013). Consistent with an essential role of HS chains in the FGF–FGFR complex formation, the mouse gene for the synthesis of the glycosaminoglycan chains is required for proper activation of FGF signaling during normal mammalian development (García-García and Anderson 2003). However, it has not been clarified how the molecular distribution and subsequent signal activation of FGFs are spatially and temporally controlled in the ECM and on the cell surface. This chapter highlights our recent findings on the roles of HS in the extracellular distribution of paracrine FGFs and subsequent signaling activation during mammalian embryonic development.

18.2 HS Is Required for the Local Retention of FGF Ligands on the Cell Surface

To determine how HS chains regulate the activity of FGF signaling, we have analyzed the *Ext2* null mutant mouse, which was originally identified by a transgene-inserted mutation showing early embryonic lethality (Shimokawa et al. 2011).

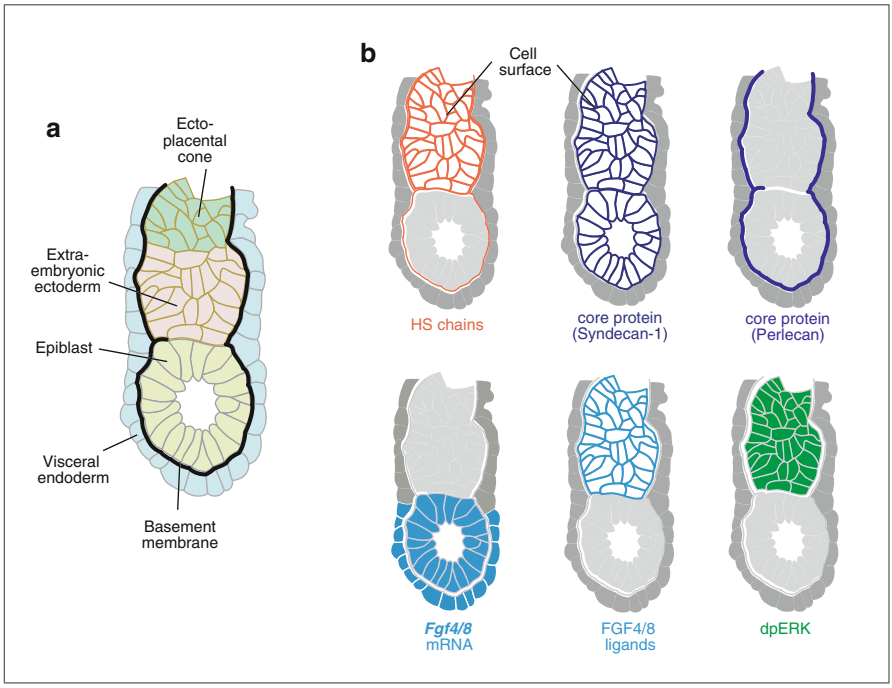

Fig. 18.2 Distribution of fibroblast growth factors (*FGFs*), heparin sulfate (*HS*), and core proteins in extra-embryonic ectoderm. (**a**) Schematic representation of mouse embryonic structures at embryonic (*E*) day 5.5, illustrating the tissue layers and basement membranes (*ECM*). (**b**) Schematic representations of local distribution of HS chains, core proteins, Fgf transcripts, FGF, and dp-ERK activity in the wild-type embryos at E5.5

As the Ext1–Ext2 protein complex catalyzes HS elongation, disaccharide analysis with high-sensitive fluoromeric post-column HPLC demonstrated that disaccharides of HS were undetectable but those of chondroitin sulfate were normally present in *Ext2*-deficient embryos (Shimokawa et al. 2011). At the tissue level, *Ext2*-deficient embryos fail to develop an extra-embryonic ectoderm and mesoderm properly (Stickens et al. 2005; Shimokawa et al. 2011). To elucidate the role of HS in mouse extra-embryonic ectoderm development where FGF signaling is thought to be involved (Corson et al. 2003), we tested whether HS chains are essential for FGF signaling activation. Then, we have analyzed expression of downstream targets of the FGF signaling pathway, for example, the diphosphorylated form of extracellular signal-regulated kinase (ERK) (dp-ERK), *Dusp6*/*Mpk3*, and *Sprouty4*. In the wild-type embryos, expression of these FGF targets was upregulated in the extra-embryonic ectoderm specifically at embryonic (E) day 5.5, although their expression was severely reduced in the HS-deficient *Ext2* null mutant embryos (Fig. 18.2). To assure that *Ext2*-deficient abnormities are brought about by the lack of HS chains, we exploited the in vitro explant assay. In vitro explant studies using wild-type and mutant embryo tissues revealed that reduced FGF signaling caused

by *Ext2* deficiency was partly restored by addition of heparin in the culture medium (Shimokawa et al. 2011). These findings together suggest that HS chains are essential for FGF signaling activation in the extra-embryonic ectoderm of the mouse embryo.

To investigate how HS chains are involved in FGF signaling activation in more detail, we examined the tissue distributions of *Ext2* transcripts, HS, FGF4/8 ligands, FGFR2, and syndecan-1, one of the major core proteins of cell-surface HSPGs (Fig. 18.2). HS chains as well as *Ext2* transcripts were abundantly expressed in the extra-embryonic ectoderm of the wild-type embryo at E5.5. Notably, cell surface-tethered HS were prominently expressed in the extra-embryonic ectoderm but was expressed at a low level in the epiblast although ECM-associated HS was distributed throughout the basement membrane (Shimokawa et al. 2011) (Fig. 18.2). As expected, however, neither *Ext2* transcripts nor HS chains were detectable in the *Ext2*-deficient embryos. To investigate whether HS chains are involved in local distribution of FGF ligands, we analyzed the expression of *Fgf* transcripts as well as FGF proteins in the E5.5 wild-type embryos during extra-embryonic ectoderm. Unexpectedly, although the *Fgf4* gene was transcribed in the epiblast and *Fgf8* in the epiblast and visceral endoderm, both FGF4/8 proteins were exclusively localized in the extra-embryonic ectoderm. Coincidentally, these FGF proteins appeared to be colocalized with cell-surface HS chains as well as the syndecan-1 core protein, but not with ECM-associated HS chains in the basement membrane such as perlecan (Fig. 18.2) (Shimokawa et al. 2011). In the HS-deficient embryos, however, local retention of the FGF4/8 protein in the extra-embryonic ectoderm was lost despite normal transcription of both *Fgf4* and *Fgf8* genes (Shimokawa et al. 2011). These findings strongly suggest that although ECM-associated HS chains also contribute to the regulation of FGF spreading in other biological systems (see later: Sect. 18.6), cell surface-tethered HS expression is crucial for the local retention of FGF ligands on the cell surface during mouse extra-embryonic ectoderm development.

18.3 HS Chains Can Spread FGF Signaling Activation Within a Short Range in a Cell Nonautonomous Manner

It has been suggested that HS chains regulate the activity of growth factors in both a cell autonomous and non-cell autonomous manner (Häcker et al. 2005). To assess this alternative mechanism, we have analyzed FGF signaling activity in chimeric embryos consisting of wild-type and HS-deficient cells by means of embryonic stem cell (ES) injection in blastocysts and eight-cell aggregation (Fig. 18.3a). The basic idea of the analysis is that in either types of chimeric embryos cell surface-tethered HS (e.g., syndecan-attached HS) is localized exclusively on the cell surface of the wild-type cells while ECM-associated HS (e.g., Perlecan-attached HS) secreted from the wild-type cells reach the basement membrane that surrounds HS-deficient cells as well (Figs. 18.1 and 18.3a).

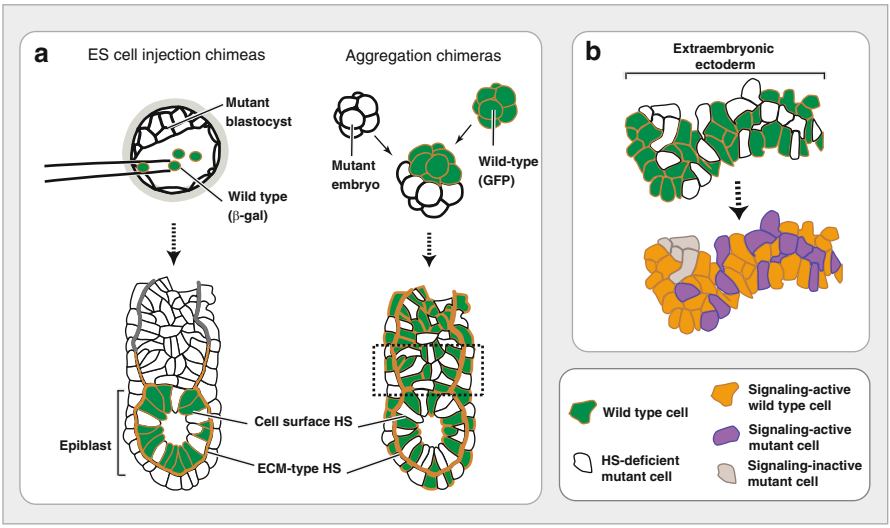

Fig. 18.3 Chimeric analyses on the cell autonomy of HS chains for FGF signaling activation. (**a**) Two distinct strategies for generating chimeric embryos. *Top left:* Embryonic stem (*ES*) cell injection into blastocysts. *Top right:* Aggregation of eight-cell stage embryos. *Below:* Diagrams for distribution of HS chains in the two types of chimeric embryos derived from the ES cell injection and aggregation with *Ext2*-deficient embryos. (**b**) Diagrams for distribution of wild-type and HS-deficient cells showing FGF signaling activity in the extra-embryonic ectoderm in aggregation chimera

When wild-type ES cells that were marked by β-galactosidase (βgal) expression were injected into HS-deficient blastocysts, extra-embryonic ectoderm was exclusively derived from HS-deficient cells but the epiblast contained wild-type cells in addition to mutant cells (Tam and Rossant 2003) (Fig. 18.3a). Then, the distribution of HS in the chimeric embryos was visualized with the antibody specific for HS chains whereas FGF signaling activation was monitored by testing dp-ERK and Err-β induction in the HS-deficient cells. In this assay, only those HS-deficient cells of the extra-embryonic ectoderm that were in close proximity to the wild-type epiblast cells activated FGF signaling (Shimokawa et al. 2011). Given that ECM-associated HS chains were abundantly found throughout the basement membrane irrespective of cellular genotypes, FGF signaling activation may be primarily mediated by cell surface-tethered HS but not ECM-derived HS.

To confirm the nonautonomous role of HS chains for FGF signaling activation, we generated aggregation chimera in which the wild-type and HS-deficient cells are distributed in a salt-and-pepper manner (Fig. 18.3a). As examined with HS-specific antibody, mutant cells failed to express HS chains at their cell surface while wild-type cells expressed cell surface-tethered HS, whereas ECM-associated HS chains were distributed throughout the basement membrane (Fig. 18.3a). Analysis of HS expression and FGF signaling markers together revealed that mutant cells in the

vicinity of the wild-type cells activated FGF signaling, as indicated by dp-ERK immunostaining, similar to the wild-type cells (Fig. 18.3b). In addition, a fraction of HS-deficient mutant cells did not express dp-ERK. Considering the fact that ECM-associated HS chains were abundantly distributed throughout the basement membrane, FGF signaling mainly depends on cell surface-tethered HS but not ECM-derived HS. These findings indicated that HS functions in a cell nonautonomous manner for FGF signaling activation in the extra-embryonic ectoderm and that signaling activation occurs only within a short distance, mainly mediated by cell surface-tethered HS.

18.4 FGF Signaling Activation Is Mediated by Proteolytic Cleavage of HSPGs

The spreading of HS has been proposed to be mediated by enzymatic cleavage of HSPGs, planar transcytosis, and/or cytoneme (filopodia) (Häcker et al. 2005; Yan and Lin 2009) (Fig. 18.4a). Several lines of evidence, as indicated next, argue that the first mechanism account for the HS spreading. Notably, cleavage of HSPGs by several secreted serine proteinases can modulate FGF signaling for a long distance in the extracellular space (Bülow and Hobert 2006; Yan and Lin 2009) (Fig. 18.4a). A secreted serine protease, xHtrA1, can cleave cell surface-tethered HSPGs including biglycan, syndecan-4, and glypican-4 and spread over HS for tissue posteriorization, mesoderm induction, and neuronal differentiation through long-range FGF signaling activation in *Xenopus* embryos (Hou et al. 2007). In addition, several hypothetical functions of HS cleavage by endoglycosidases such as a heparanase are implicated: HS chains can travel at a long distance by removal of core proteins, growth factors bound to HS chains can be released from core proteins for signaling activation or inactivation, and removal of HS chains can affect interactions between HSPGs and other ECM-associated proteins (Reiland et al. 2004; Patel et al. 2007) (Fig. 18.4a).

To further clarify the short-range spreading mechanism of FGF with HS, we have used several chemical inhibitors for the foregoing specific processes of HS movement. Specific inhibitors for a serine protease strongly reduced the FGF signal activation in the extra-embryonic ectoderm. However, inhibitors of a heparanase, a metalloproteinase, and other proteinases, except the serine protease, did not reduce FGF signaling activity (Table 18.1). Correspondingly, expression of mouse *Htra1*, a serine proteinase, was specifically found in the extra-embryonic ectoderm (Fig. 18.4b). *HtraI* expression was still observed in the *Ext2*- and *Fgf8*-deficient embryos in which FGF signaling is reduced, suggesting the possible involvement of HtraI in FGF signaling spreading of *Ext2*-dificient and wild-type chimeric embryos as described above (Fig. 18.3b). These results support the hypothesis that shedding, that is, cleavage of HSPGs by a serine protease such as Htra1, allows diffusion of cell-surface-bound FGFs together with HS chains, thereby facilitating FGF signaling in a non-cell autonomous manner. In contrast, because both planar transcytosis and

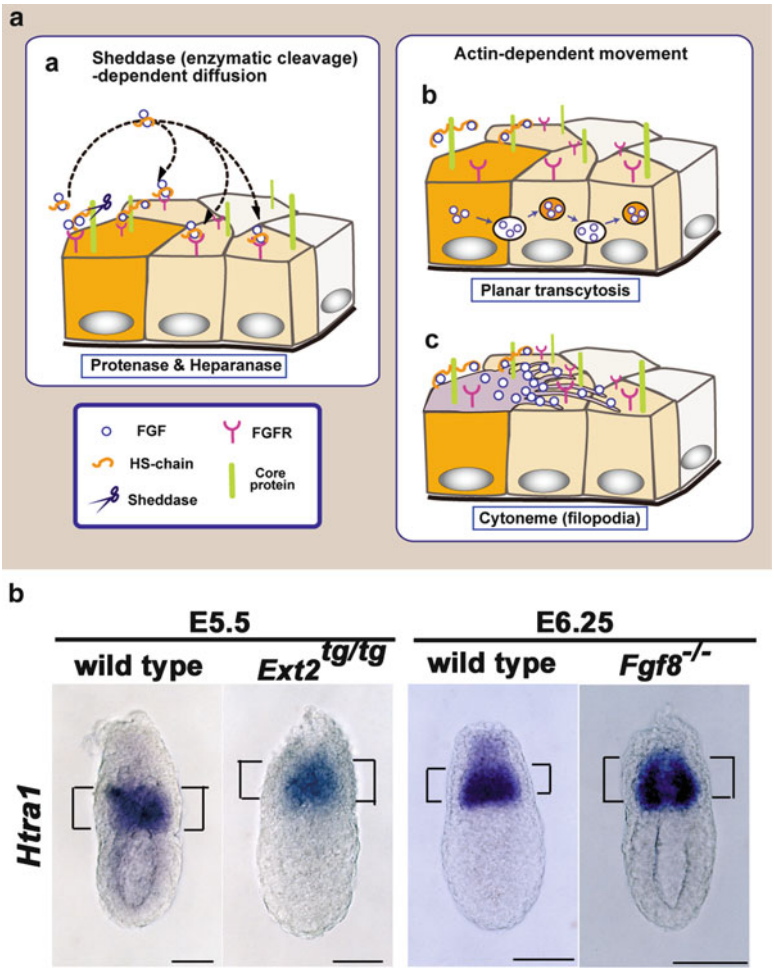

Fig. 18.4 Proposed models for short-range spreading of FGF signaling activation via HS chains. (**a**) Three proposed models of the regulation of FGF spread: (*a*) sheddase-dependent diffusion, (*b*) planar transcytosis, and (*c*) cytoneme (filopodia)-dependent process. The latter two mechanisms depend on the F-actin cytoskeleton. The experimental evidence is in support of the first mechanism; however, as cytocalasin D that depolymerizes F-actin did not affect FGF spreading, the latter two mechanisms are ruled out. (**b**) Spatial distribution of *Htra1* transcripts, encoding a serine protease, during extra-embryonic ectoderm development in the wild-type, *Ext2* (HS chains) -deficient, and *Fgf8-deficient* embryos indicated by whole-mount in situ hybridization

cytoneme are dependent on the actin cytoskeleton, we treated the embryo with cytochalasin D, an inhibitor of actin filament polymerization, and found that the cytochalasin treatment did not reduce dp-ERK expression in the extra-embryonic ectoderm (Table 18.1) (Shimokawa et al. 2011). This finding suggests that FGF signal activation is independent of actin-dependent transcytosis- or cytoneme-mediated processes.

Table 18.1 Summary of fibroblast growth factor (FGF) signaling activity treated with specific inhibitors

Chemical inhibitors	Inhibitory effects	FGF signaling activity[a]
Cytochalasin D	Actin polymerization	+
Benzamide	Serine protease	–
Phenylmethylsulfonyl fluoride	Serine protease	–
E-64	Cystein protease	+
Chymostatin	Chymotripsin, papain, cysteine protease	+
Pepstatin A	Aspartic protease	+
Calpain inhibitor I	Calpain, cathepsin	+
OGT2115	Heparanase	+
GM6001	Metalloproteinase (ECM protein cleavage)	+

[a]– and + denote, respectively, that dp-ERK expression is reduced or not reduced significantly

18.5 HS Modulates FGF Signaling in a Spatially and Temporally Specific Manner

Long and linear HS chains are further modified by *N*-, 2-*O*-, 6-*O*-, and 3-*O*-sulfotransferases and epimerized by GlcA C5 epimerase locally and consecutively in the Golgi apparatus. The produced sulfated patterns of HS in terms of overall sulfation levels and specific sulfated moieties appear to affect the affinity for FGF ligands and subsequent signaling activity (Patel et al. 2008; Pan et al. 2008; Qu et al. 2011; Pye et al. 1998; Escobar Galvis et al. 2007). Indeed, extensively sulfated HS chains can enhance FGF signaling activity; moreover, distinct sulfation patterns appear to modulate different aspects of FGF10-mediated gland morphogenetic processes (Patel et al. 2008; Pan et al. 2008; Qu et al. 2011). Heavily sulfated HS chains appear to promote the formation of ternary complexes with FGF–FGFR (Escobar Galvis et al. 2007). In the extracellular space, sulfated HS chains are occasionally and partially desulfated by endosulfatases (Dhoot et al. 2001). It is known that desulfation of HS through two 6-*O*-endosulfatases, Sulf1 and Sulf2, stabilizes the formation of Wnt and Frizzled receptor complexes (Dhoot et al. 2001). For FGF signaling, desulfation of HS chains tends to downregulate FGF signaling activity (Settembre et al. 2008; Otsuki et al. 2010; Wang et al. 2004; Jastrebova et al. 2010). In addition, the overall size or length of HS disaccharide units, which is mediated by Ext1/Ext2 heterodimer, is likely to affect FGF signaling activation; shorter HS chains can form a ternary complex with FGF–FGFR more efficiently than longer HS chains (Patel et al. 2008; Jastrebova et al. 2010). Thus, these fine structures of HS chains in terms of both sulfated patterns and overall length appear to modulate FGF signaling activity.

In addition to these alterations of fine HS structures, the spatiotemporal changes of HS chains can further control FGF signaling in development (Allen and Rapraeger 2003; David et al. 1992). Elongation and modifications of HS chains appear to be

regulated spatially and temporally in a dynamic fashion. Paralleling *Ext2* mRNA expression in the extra-embryonic ectoderm, expression of cell-surface HS was upregulated in the extra-embryonic ectoderm of the E5.5 embryo (Shimokawa et al. 2011), with coincident increase of FGFR-dependent dp-ERK expression (Corson et al. 2003; Shimokawa et al. 2011) (Fig. 18.2). At the same developmental stages, HS modification enzymes are expressed in a cell- or tissue-specific manner, resulting in heterogeneous distribution of varied forms of sulfated HS chains (Higginson et al. 2012; Nagamine et al. 2012). Indeed, expression studies with several monoclonal antibodies recognizing different HS structures have indicated that the fine structures of cell surface-tethered HS chains are also different from those of ECM-associated chains (Allen and Rapraeger 2003; David et al. 1992). The cell-surface HS was recognized by specific monoclonal antibodies of 3G10 and JM403 but not those of 10E4, HepSS-1, and NAH46 in the most anterior neuroectoderm at E7.5 where FGF signaling was potentially active (Shimokawa et al. 2011). According to the preference of epitope recognition by these monoclonal antibodies (van den Born et al. 2005), cell-surface HS appear to be predominately desulfated compared with ECM HS. Concurrently, correct sulfation patterns of HS chains are crucial to normal embryogenesis such as mesoderm induction, angiogenesis, and endochondral ossification (Wang et al. 2004; Settembre et al. 2008). These lines of evidence support the model that spatiotemporally controlled diversity of HS structures participates in the modulation of FGF signaling activity during development.

18.6 ECM HS Chains Modulate FGF Distribution for Signaling Activation Negatively and Positively

In this chapter, we have highlighted the important roles of cell-surface HS chains in FGF signaling. Although we have not shown these in detail here, ECM-associated HS chains have additional unique roles (Matsuo and Kimura-Yoshida 2013). The ECM-associated HS modulate FGF signaling negatively or positively depending on their cellular context (Yan and Lin 2009). HS chains in the ECM are thought to disturb movement of FGF ligands for a long distance as a barrier and restrict distribution to the surrounding produced cells. Notably, FGF9 and FGF20 ligands undergo a reversible homodimerization, and monomer ligands display much lower affinity for HS than dimer ligands, so that monomers can spread over and activate FGF signaling at a greater distance than dimers (Harada et al. 2009; Kalinina et al. 2009). Similarly, mesenchyme-specific knockout of glycosaminoglycan chains supports that ECM-associated HS chains from perlecan can restrict the movement of FGF ligands as a diffusion barrier (Qu et al. 2012). In addition, ECM-associated HS chains are also considered to activate FGF signaling rather directly (Yan and Lin 2009). The ECM-associated HSPGs perlecan and agrin can form ternary complexes with FGF–FGFR dependently of HS chains and promote cartilage development and neurite outgrowth, respectively (Chuang et al. 2010; Kim et al. 2003). However, it is still unclear whether the these two distinct functions of ECM-associated HSPGs

are contributed by their structural differences of HS chains or their distribution in the extracellular space. To address this issue, a technical breakthrough to detect endogenous FGF ligands and highly divergent HS structures might be required (Uchimura et al. 2010; Duchesne et al. 2012).

18.7 Conclusion

To date, FGF signaling activation has been considered to be primarily regulated by the local expression of FGFs and FGFRs, and the HS chain had been believed to express rather ubiquitously during development (Häcker et al. 2005; Mohammadi et al. 2005; Yan and Lin 2009). However, recent studies, including those by our group, suggest that the spatiotemporal regulation of FGF signaling activity can be also established through the local affinity of HS chains for FGFs during development, which is affected by length, sulfation levels, and sulfation patterns of HS as well as their expression levels. Considering that cell-surface HS chains can retain FGFs and spread FGF signaling activity over a short range, the spatiotemporally regulated expression of cell-surface HS chains may control the stable formation of the FGF–FGFR dimer complex and confine signaling activation to target fields. Such a cell nonautonomous function of HS may be important to synchronize the developmental progress within a local area.

References

Allen BL, Rapraeger AC (2003) Spatial and temporal expression of heparan sulfate in mouse development regulates FGF and FGF receptor assembly. J Cell Biol 163:637–648

Asada M, Shinomiya M, Suzuki M et al (2009) Glycosaminoglycan affinity of the complete fibroblast growth factor family. Biochim Biophys Acta 1790:40–48

Beenken A, Mohammadi M (2009) The FGF family: biology, pathophysiology and therapy. Nat Rev Drug Discov 8:235–253

Bishop JR, Schuksz M, Esko JD (2007) Heparan sulphate proteoglycans fine-tune mammalian physiology. Nature (Lond) 446:1030–1037

Bülow HE, Hobert O (2006) The molecular diversity of glycosaminoglycans shapes animal development. Annu Rev Cell Dev Biol 22:375–407

Chuang CY, Lord MS, Melrose J et al (2010) Heparan sulfate-dependent signaling of fibroblast growth factor 18 by chondrocyte-derived perlecan. Biochemistry 49:5524–5532

Corson LB, Yamanaka Y, Lai KM et al (2003) Spatial and temporal patterns of ERK signaling during mouse embryogenesis. Development (Camb) 130:4527–4537

David G, Bai XM, Van der Schueren B et al (1992) Developmental changes in heparan sulfate expression: in situ detection with mAbs. J Cell Biol 119:961–975

Dhoot GK, Gustafsson MK, Ai X et al (2001) Regulation of Wnt signaling and embryo patterning by an extracellular sulfatase. Science 293:1663–1666

Dorey K, Amaya E (2010) FGF signalling: diverse roles during early vertebrate embryogenesis. Development (Camb) 137:3731–3742

Duchesne L, Octeau V, Bearon RN et al (2012) Transport of fibroblast growth factor 2 in the pericellular matrix is controlled by the spatial distribution of its binding sites in heparan sulfate. PLoS Biol 10:e1001361

Escobar Galvis ML, Jia J, Zhang X et al (2007) Transgenic or tumor-induced expression of heparanase upregulates sulfation of heparan sulfate. Nat Chem Biol 3:773–778
García-García MJ, Anderson KV (2003) Essential role of glycosaminoglycans in Fgf signaling during mouse gastrulation. Cell 114:727–737
Goetz R, Ohnishi M, Kir S et al (2012) Conversion of a paracrine fibroblast growth factor into an endocrine fibroblast growth factor. J Biol Chem 287:29134–29146
Goldfarb M (2012) Voltage-gated sodium channel-associated proteins and alternative mechanisms of inactivation and block. Cell Mol Life Sci 69:1067–1076
Häcker U, Nybakken K, Perrimon N (2005) Heparan sulphate proteoglycans: the sweet side of development. Nat Rev Mol Cell Biol 6:530–541
Harada M, Murakami H, Okawa A et al (2009) FGF9 monomer-dimer equilibrium regulates extracellular matrix affinity and tissue diffusion. Nat Genet 41:289–298
Higginson JR, Thompson SM, Santos-Silva A et al (2012) Differential sulfation remodelling of heparan sulfate by extracellular 6-*O*-sulfatases regulates fibroblast growth factor-induced boundary formation by glial cells: implications for glial cell transplantation. J Neurosci 32:15902–15912
Hou S, Maccarana M, Min TH et al (2007) The secreted serine protease xHtrA1 stimulates long-range FGF signaling in the early *Xenopus* embryo. Dev Cell 13:226–241
Itoh N, Ornitz DM (2011) Fibroblast growth factors: from molecular evolution to roles in development, metabolism and disease. J Biochem 149:121–130
Jastrebova N, Vanwildemeersch M, Lindahl U et al (2010) Heparan sulfate domain organization and sulfation modulate FGF-induced cell signaling. J Biol Chem 285:26842–26851
Kalinina J, Byron SA, Makarenkova HP et al (2009) Homodimerization controls the fibroblast growth factor 9 subfamily's receptor binding and heparan sulfate-dependent diffusion in the extracellular matrix. Mol Cell Biol 29:4663–4678
Kim MJ, Cotman SL, Halfter W et al (2003) The heparan sulfate proteoglycan agrin modulates neurite outgrowth mediated by FGF-2. J Neurobiol 55:261–277
Kuro-o M (2008) Endocrine FGFs and Klothos: emerging concepts. Trends Endocrinol Metab 19:239–245
Lanner F, Rossant J (2010) The role of FGF/Erk signaling in pluripotent cells. Development (Camb) 137:3351–3360
Matsuo I, Kimura-Yoshida C (2013) Extracellular modulation of fibroblast growth factor signaling through heparan sulfate proteoglycans in mammalian development. Curr Opin Genet Dev 23(4):399–407
Mohammadi M, Olsen SK, Ibrahimi OA (2005) Structural basis for fibroblast growth factor receptor activation. Cytokine Growth Factor Rev 16:107–137
Nagamine S, Tamba M, Ishimine H et al (2012) Organ-specific sulfation patterns of heparan sulfate generated by extracellular sulfatases Sulf1 and Sulf2 in mice. J Biol Chem 287: 9579–9590
Otsuki S, Hanson SR, Miyaki S (2010) Extracellular sulfatases support cartilage homeostasis by regulating BMP and FGF signaling pathways. Proc Natl Acad Sci USA 107:10202–10207
Pan Y, Carbe C, Powers A et al (2008) Bud specific N-sulfation of heparan sulfate regulates Shp2-dependent FGF signaling during lacrimal gland induction. Development (Camb) 135:301–310
Patel VN, Knox SM, Likar KM et al (2007) Heparanase cleavage of perlecan heparan sulfate modulates FGF10 activity during ex vivo submandibular gland branching morphogenesis. Development (Camb) 134:4177–4186
Patel VN, Likar KM, Zisman-Rozen S et al (2008) Specific heparan sulfate structures modulate FGF10-mediated submandibular gland epithelial morphogenesis and differentiation. J Biol Chem 283:9308–9317
Pellegrini L, Burke DF, von Delft F et al (2000) Crystal structure of fibroblast growth factor receptor ectodomain bound to ligand and heparin. Nature (Lond) 407:1029–1034
Perrimon N, Bernfield M (2000) Specificities of heparan sulphate proteoglycans in developmental processes. Nature (Lond) 404:725–728

Pye DA, Vives RR, Turnbull JE et al (1998) Heparan sulfate oligosaccharides require 6-*O*-sulfation for promotion of basic fibroblast growth factor mitogenic activity. J Biol Chem 273:22936–22942

Qu X, Carbe C, Tao C et al (2011) Lacrimal gland development and Fgf10-Fgfr2b signaling are controlled by 2-*O*- and 6-*O*-sulfated heparan sulfate. J Biol Chem 286:14435–14444

Qu X, Pan Y, Carbe C et al (2012) Glycosaminoglycan-dependent restriction of FGF diffusion is necessary for lacrimal gland development. Development (Camb) 139:2730–2739

Rapraeger AC, Krufka A, Olwin BB (1991) Requirement of heparan sulfate for bFGF-mediated fibroblast growth and myoblast differentiation. Science 252:1705–1708

Reiland J, Sanderson RD, Waguespack M et al (2004) Heparanase degrades syndecan-1 and perlecan heparan sulfate: functional implications for tumor cell invasion. J Biol Chem 279:8047–8055

Schlessinger J, Plotnikov AN, Ibrahimi OA et al (2000) Crystal structure of a ternary FGF-FGFR-heparin complex reveals a dual role for heparin in FGFR binding and dimerization. Mol Cell 6:743–750

Settembre C, Arteaga-Solis E, McKee MD et al (2008) Proteoglycan desulfation determines the efficiency of chondrocyte autophagy and the extent of FGF signaling during endochondral ossification. Genes Dev 22:2645–2650

Shimokawa K, Kimura-Yoshida C, Nagai N et al (2011) Cell surface heparan sulfate chains regulate local reception of FGF signaling in the mouse embryo. Dev Cell 21:257–272

Stickens D, Zak BM, Rougier N et al (2005) Mice deficient in Ext2 lack heparan sulfate and develop exostoses. Development (Camb) 132:5055–5068

Tam PP, Rossant J (2003) Mouse embryonic chimeras: tools for studying mammalian development. Development (Camb) 130:6155–6163

Uchimura K, Lemjabbar-Alaoui H, van Kuppevelt TH et al (2010) Use of a phage display antibody to measure the enzymatic activity of the Sulfs. Methods Enzymol 480:51–64

van den Born J, Salmivirta K, Henttinen T et al (2005) Novel heparan sulfate structures revealed by monoclonal antibodies. J Biol Chem 280:20516–20523

Varki A, Cummings RD, Esko JD et al (eds) (2009) Essentials of glycobiology, 2nd edn. Cold Spring Harbor Laboratory Press, Cold Spring Harbor

Wang S, Ai X, Freeman SD et al (2004) QSulf1, a heparan sulfate 6-*O*-endosulfatase, inhibits fibroblast growth factor signaling in mesoderm induction and angiogenesis. Proc Natl Acad Sci USA 101:4833–4838

Yan D, Lin X (2009) Shaping morphogen gradients by proteoglycans. Cold Spring Harbor Perspect Biol 1:a002493

Yayon A, Klagsbrun M, Esko JD et al (1991) Cell surface, heparin-like molecules are required for binding of basic fibroblast growth factor to its high affinity receptor. Cell 64:841–848

Chapter 19
Cooperation of Signaling for Tissue Interaction and *Hox* Genes in Tissue Precursor Patterning

Yo-ichi Yamamoto-Shiraishi

Abstract During organogenesis, the positional organization of tissue precursors is an important process that relies on locally regulated cell fate determination. Two distinct systems are known to be involved in the positioning of tissue precursors, that is, gross positioning according to the *Hox* code and locally refined positioning by the signals derived from earlier-formed tissues. We investigated the functional cooperation of the intertissue signaling and *Hox* gene activities for the precise pattern formation of tissue precursors. We found that bone morphogenetic protein (BMP) and Wnt signaling interplay with *Hox* genes for tendon precursor patterning during limb morphogenesis. Organogenesis of the gut tube also showed the cooperation of platelet-derived growth factor (PDGF) signaling from earlier-formed tissues and the *Hox* genes in the formation of the longitudinal smooth muscle layer. Cooperation of gross tissue positioning by *Hox* genes and local positioning by the signals from neighboring tissues that formed earlier is presumably a common mechanism for tissue patterning to organize a functional organ.

Keywords BMP • Hox • Tendon • Tissue interaction • Wnt

19.1 Introduction

Our body has many organs that exert unique functions consequent to organized arrangements of component tissues. Positioning and pattern formation of the tissue precursors in a developing organ are important issues in this regard. During the development of tissue precursors, undifferentiated multipotent cells develop into

Y. Yamamoto-Shiraishi (✉)
Division of Biological Science, Graduate School of Science,
Nagoya University, Nagoya, Japan
e-mail: shiraishi.yo-ichi@h.mbox.nagoya-u.ac.jp

H. Kondoh and A. Kuroiwa (eds.), *New Principles in Developmental Processes*,
DOI 10.1007/978-4-431-54634-4_19,

various tissue precursors depending on their positioning in the organ primordium. What mechanisms are employed in the position-dependent differentiation of multipotent cells? The answer is the combination of the gross positioning system according to the *Hox* code in the organ primordium and locally refined regulation using signals derived from earlier-formed tissues.

In the developing central nervous system, somites, lateral plate mesoderm, and digestive tract, *Hox* genes are expressed sequentially along the anteroposterior (AP) axis according to their order in the *Hox* clusters (Krumlauf 1994; Sakiyama et al. 2001; Yokouchi et al. 1995b). In the limb mesenchyme, the *Abd-B* genes belonging to the *Hoxa* or *Hoxd* cluster are expressed in a nested fashion along the proximodistal (PD) or the AP axis (Nelson et al. 1996; Yokouchi et al. 1991). The pattern of precursors of limb cartilages, the templates of skeleton derived from the limb bud mesenchyme, is autonomously formed according to the *Hox* code (Yokouchi et al. 1995a). On the other hand, the patterning of muscle masses to form the limb muscles is regulated by the signals from other tissues. Muscle masses, derived from the somites and migrating into the limb bud, split according to the signal from surrounding limb mesenchyme, and form the position-specific pattern (Hashimoto et al. 1999).

The pattern of a tissue needs to be precisely controlled by the combination of the *Hox* code and signals derived from neighboring tissues that developed earlier, which would enable the intricate pattern formation of tissue precursors. However, reports have been limited that demonstrate the cooperative regulation of tissue precursor patterning by these two systems.

We recently reported that *Hox* genes expressed in tissue precursors and the signals from the neighboring tissues that were formed earlier cooperate for the limb tendon precursor patterning (Yamamoto-Shiraishi and Kuroiwa 2013). In this chapter, I discuss a tissue precursor patterning mechanism that involves cooperation of *Hox* activity-dependent regulation that provides gross positional frameworks to the tissue precursors and the locally refined tissue positioning regulated by the signals from preexisting tissues.

19.2 Cooperative Regulation of Limb Tendon Precursor Patterning by *Hox* Genes and Inter-Tissue Signaling

Locomotor system of the limb consists of bone, muscle, and tendon. Tendons connect bone and muscle physically and transmit the force (Fig. 19.1a). Dorsal tendons function for the extension and ventral tendons for flexion of the limb. For these functions, limb tendons are located between the bones and the dorsal/ventral skin (Fig. 19.1a). Limbs consist of the stylopod (upper arm/thigh), zeugopod (lower arm/lower leg), and autopod (hand/foot). Tendons of zeugopodal muscles run into the autopod and have their insertion sites on the distal autopodal skeletal elements. Although they are a very simple string-like tissue in the zeugopod, they bifurcate in a complex pattern in the autopod (Fig. 19.1b). In addition, many shorter tendons are

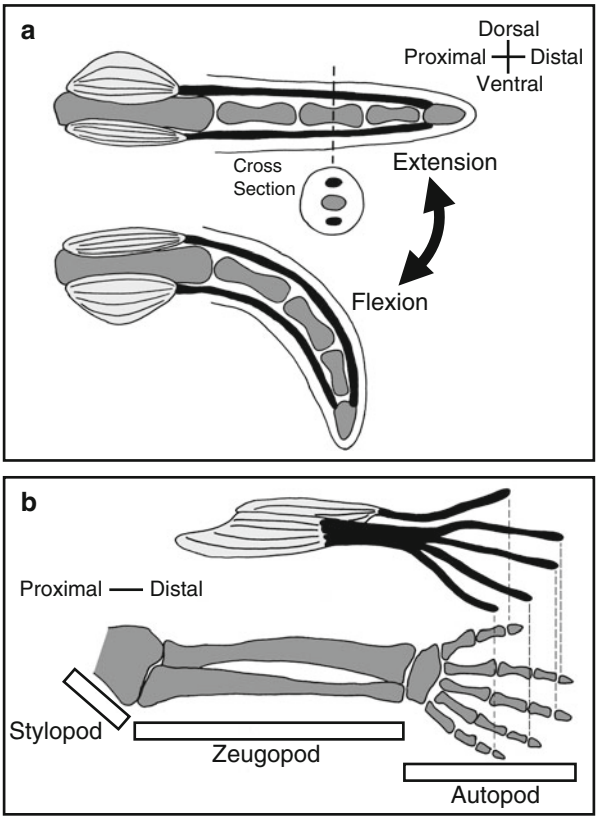

Fig. 19.1 Pattern of the limb tendon. **a** Limb tendons (*black thick lines*) connect the muscles (*light gray*) and bones (*dark gray*) and are located between the bones and dorsal/ventral skin (*outline*). *Dotted line* indicates level of cross section. Tendons function for the extension and flexion of the limb. **b** Morphology of the tendons of zeugopodal muscles (part). Many tendons are contained in the autopod (illustrations by Shiori Yamamoto)

associated with the autopodal muscles (Baumel et al. 1993; Greene 1963). Therefore, there are more tendons in the autopod than in the zeugopod. The intricate organization of tendon requires precise patterning of its precursors. Tendon precursors are derived from limb bud mesenchyme and induced in a position-specific manner.

19.2.1 Signaling and Tissue Interaction That Control Tendon Precursor Patterning

Mechanisms of limb tendon precursor induction have been investigated using *Scleraxis* (*Scx*) and *Six2* as the specific markers for the tendon precursor cells (Schweitzer et al. 2001; Edom-Vovard et al. 2002; Yamamoto-Shiraishi and Kuroiwa 2013).

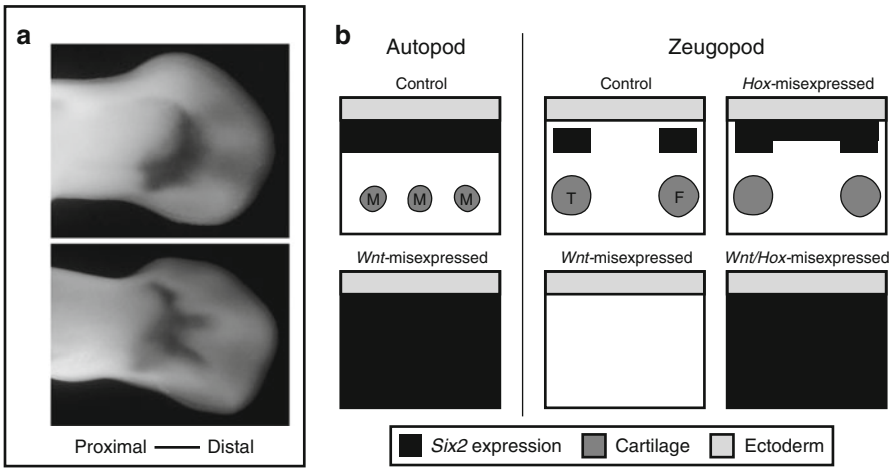

Fig. 19.2 Expression regulation of a tendon precursor-specific gene, *Six2*. **a** *Six2* expression marks the tendon precursor of HH stage 26 (*upper panel*) and 30 (*lower panel*) chick hindlimb. **b** As shown in "Control" panels, *Six2* expression (*black*) is restricted between the surface ectoderm (*light gray*) and cartilages (*dark gray*) in both autopod and zeugopod and is affected by viral misexpression of the ectodermal *Wnt* and/or autopodal *Hox*. *Wnt* alone or *Wnt*/*Hox* misexpression caused the loss of limb cartilage. Muscle masses are omitted in the schemes. *M* metatarsals, *T* tibia, *F* fibula

The tendon precursors expressing these marker genes together are located on the dorsal and ventral sides of the metacarpal/metatarsal region of the autopod and zeugopod of HH stage 26 chick hindlimb (Fig. 19.2a). Later, the dorsal and ventral expression of the marker genes expands distally along the digital cartilages (Fig. 19.2a). Neither *Scx* nor *Six2* is ever expressed in the peripheral mesenchyme and interdigital mesenchyme, where bone morphogenetic proteins (BMPs) are expressed. When BMP were locally administered, expression of *Scx* and *Six2* disappeared, indicating that BMPs repress the tendon precursor marker expressions (Schweitzer et al. 2001; Yamamoto-Shiraishi and Kuroiwa 2013).

The distal expansion of marker expression along digits was suggestive of the function of limb cartilage on tendon precursor-specific gene expression. We tested the possibility of *Six2* induction by cartilage by two surgical operations: first, ectopic cartilage formation following limb tissue incision, and second, extra-cartilage grafting. After making incisions between digits and interdigital tissue, ectopic digits with phalangeal cartilage are formed from the residual interdigital mesenchyme (Omi and Ide 1996). In the ectopic digits, *Six2* was expressed between the ectoderm and the phalangeal cartilage. In the second operation, the grafting of a piece of sternum cartilage into limb mesenchyme also caused ectopic *Six2* expression around the graft. These results suggest that the limb cartilage induces mesenchymal *Six2* expression to cause tendon development via diffusible factor(s). A BMP antagonist, Noggin, is expressed in the cartilage (Brunet et al. 1998; Capdevila and Johnson 1998; Merino et al. 1998; Pathi et al. 1999). The local administrations of

Noggin caused the ectopic expressions of *Scx* (Schweitzer et al. 2001) and *Six2* (Yamamoto-Shiraishi and Kuroiwa 2013). Therefore, these results indicate that BMP represses and cartilage-derived Noggin induces tendon precursor-specific gene expression in the limb.

Tendon precursor-specific gene expressions are restricted to the mesenchyme between the cartilage and surface ectoderm. Therefore, it is possible that limb ectoderm is involved in the regulation of tendon precursor-specific gene expression. Surgical removal of dorsal or ventral ectoderm resulted in the loss of *Scx* and *Six2* expression in the underlying mesenchyme (Schweitzer et al. 2001; Yamamoto-Shiraishi and Kuroiwa 2013), indicating that limb ectoderm is required for tendon precursor-specific gene expressions. Limb ectoderm specifically expresses members of *Wnt* gene family, including *Wnt6* (Geetha-Loganathan et al. 2005, 2010; Rodriguez-Niedenfuhr et al. 2003) and *Wnt7a* (Dealy et al. 1993). When sFRP-2, a potent inhibitor of Wnts, was locally administered, *Six2* expression in the region was downregulated, suggesting the involvement of Wnts in the *Six2* expression regulation. Then, to ascertain whether ectodermal Wnts function as positive regulators of *Six2* expression, we misexpressed ectodermal *Wnt*s in the limb bud via replication-competent retrovirus vector RCAS-BP(A) (Petropoulos and Hughes 1991). Viral misexpression of ectodermal *Wnt* caused the loss of limb cartilage and ectopic *Six2* expression in the entire autopodal mesenchyme except the peripheral region where BMP level is high (Fig. 19.2b). The ectopic *Six2* expression caused by *Wnt* misexpression in the autopod indicates that ectodermal Wnts positively regulate tendon precursor-specific gene expression. Recently, it was reported that loss of function of *Wntless* and *beta-catenin* both cause the loss of *Scx* expression in the limb tendon precursor (Zhu et al. 2012). Wntless is required for the secretion of various Wnts, and beta-catenin is a crucial mediator of the canonical Wnt pathway. This report supports our finding that ectodermal Wnts are involved in limb tendon precursor-specific gene regulation.

Tendon is physically connected with muscle. Research using *Scx* and tenascin, another marker for tendon precursor, showed that muscle is necessary not for the formation but for the maintenance of distal limb tendons (Kardon 1998; Schweitzer et al. 2001; Edom-Vovard et al. 2002). Edom-Vovard et al. (2002) reported that *fibroblast growth factor 4* (*Fgf4*) is expressed in muscle and involved in maintenance of the tendon.

19.2.2 Hox *Genes Controlling Tendon Precursor Patterning*

When we observed *Six2* expression in the *Wnt*-misexpressed limb, we found that ectopic *Six2* expression was restricted to the autopodal mesenchyme and never observed in the zeugopodal mesenchyme (Fig. 19.2b). These findings suggested the involvement of autopod-specific factor(s) in the regulation of *Six2* expression. The possibility was considered that autopodal *Hox* genes regulate *Six2* expression in the tendon precursor. To test this, we analyzed the function of autopod-specific *Hox* genes.

When we compared the expression of *Six2* and *Hox* genes in the autopod, the expression domains of *Six2* and *Hoxa-13* overlapped and shared the same proximal expression boundary. In addition, the *Six2* expression domain partially overlapped that of *Hoxd-13* in the distal autopod.

To analyze autopodal *Hox* gene functions, *Hoxa-13* or *Hoxd-13* was misexpressed in the limb mesenchyme using the retrovirus vector or electroporation technique. In the *Hox*-misexpressed zeugopod, ectopic *Six2* expression was observed in the mesenchyme near the ectoderm (Fig. 19.2b). Conversely, to analyze the requirement of autopodal *Hox* expression for autopodal *Six2* expression, we analyzed *Six2* expression in *Hox* mutant mice. In the autopod of the quadruple loss-of-function mutant of *Hoxa-13*, *d-13*, *d-12*, and *d-11* (Fromental-Ramain et al. 1996; Zakany et al. 1997), the dorsal expression of *Six2* was completely lost, indicating the necessity of autopodal *Hox* genes for the dorsal *Six2* expression. These results suggest that autopodal *Hox* genes regulate the tendon precursor-specific gene expression.

19.2.3 Regulation of Tendon Precursor Patterning by the Cooperation of BMP/Wnt Signaling and Hox *Genes*

As already described, limb tendon precursor-specific gene expression is regulated by the autopodal *Hox* genes and the signals derived from earlier-formed tissues. The next question is how these mechanisms cooperate.

Ectopic *Six2* expression in the *Hox*-misexpressed zeugopod was restricted to the mesenchyme adjacent to the ectoderm (Fig. 19.2b), suggesting the cooperation of *Hox* genes and Wnt signaling. To test this possibility, we analyzed *Six2* expression in the *Wnt3a/Hoxa-13* co-misexpressing limb. For the co-misexpression of *Wnt3a/Hoxa-13*, we injected a mixture of two viruses. In the co-misexpressed zeugopod, ectopic *Six2* expression was observed in the mesenchyme located far from the ectoderm (Fig. 19.2b), indicating the cooperative function of *Hox* and Wnt signaling.

Then, how do *Hox* genes and BMP signaling interact? The following observations provide a clue. First, in the *Wnt*-misexpressed autopod, in spite of cartilage loss, ectopic *Six2* expression was observed in the entire mesenchyme (Fig. 19.2b) except the peripheral region where the BMP level is high. Second, in the *Hox*-misexpressed zeugopod, ectopic *Six2* expression was observed on the mesenchyme located far from the cartilage (Fig. 19.2b). Third, the *Hox* mutant limb showed the loss of dorsal *Six2* expression, and *Bmp4* expression in the dorsal mesenchyme is more intensive than that in ventral mesenchyme in the chicken limb bud (Geetha-Loganathan et al. 2006), suggesting higher BMP signaling in the dorsal mesenchyme than in the ventral mesenchyme. These observations suggest that autopodal *Hox* genes function to override a certain level of BMP signaling to permit autopodal *Six2* expression. Although *Hoxa-13* is expressed in the entire autopodal mesenchyme, *Six2* is never expressed in the interdigital mesenchyme or the peripheral mesenchyme, where the BMP level is high. Therefore, the autopodal *Hox* genes alone are not sufficient to permit *Six2* expression in the region that receives high-level BMP signaling. So how do the autopodal *Hox* genes regulate *Six2* expression?

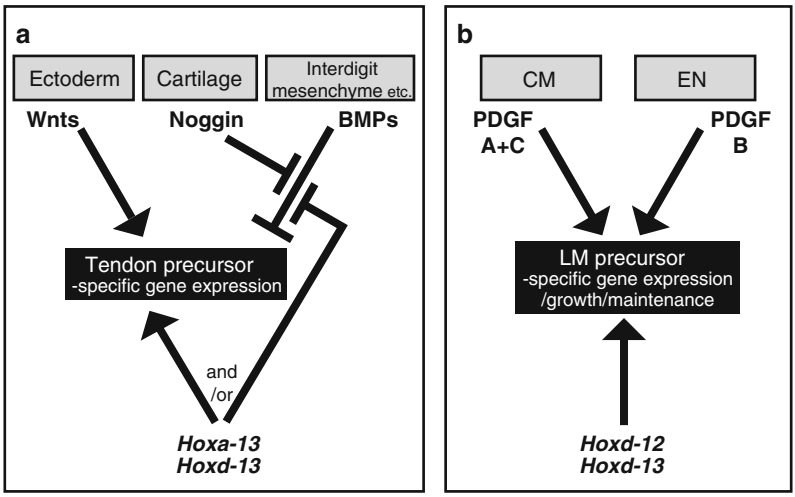

Fig. 19.3 Models for the tissue precursor patterning cooperatively regulated by *Hox* genes and signaling for tissue interactions. **a** Limb tendon precursor patterning. **b** Patterning of precursor of longitudinal smooth muscle layer in rectum. *LM* longitudinal smooth muscle, *CM* circular smooth muscle, *EN* enteric neuron

One possibility is direct transcriptional regulation. Another is that they modulate the function(s) of receptor-regulated Smads (R-Smads), the effectors of BMP and transforming growth factor (TGF)-β/activin signaling. Hoxa-13 and Hoxd-13 interact with the MH2 domain of R-Smads, including two BMP-regulated Smads, Smad5 and Smad1, and antagonize Smad-mediated transcriptional activation (Williams et al. 2005). These molecular interactions may explain the repression of BMP signaling by Hoxa-13 and Hoxd-13 in *Six2* regulation in the limb mesenchyme.

The analysis of the specific marker gene expressions suggests that the patterning of limb tendon precursors is cooperatively regulated by *Hox* genes and intertissue signaling (Fig. 19.3a). In this patterning process, autopodal *Hox* genes first permit the induction of many more tendon precursor cells in the autopod than in the zeugopod, and signaling for tissue interactions determines the precise position, shape, and timing of the precursor formation.

19.3 Regulation of Rectum Smooth Muscle Layer Morphogenesis by *Hox* Genes and Signaling Mediating Tissue Interactions

The regulation of tissue morphology by *Hox* genes and signaling for tissue interactions are not restricted to limb tendon formation. Similar regulation is observed in smooth muscle layer formation in the gut.

The smooth muscle layer of the gut tube consists of a circular smooth muscle layer, enteric neuron, and longitudinal smooth muscle layer. As well as interstitial

cells of Cajal, the pacemakers, longitudinal smooth muscle is derived from the peripheral mesenchyme. Gene expression specific to the longitudinal smooth muscle lineage is induced by platelet-derived growth factor (PDGF) signals from the circular smooth muscle and enteric neuron that form at an earlier stage (Kurahashi et al. 2008). Experimental inhibition of PDGF signaling causes increase of the interstitial cells of Cajal and the repression of longitudinal smooth muscle formation, indicating that PDGF signals from the underlying tissues are necessary for longitudinal smooth muscle precursor induction. The thickness of the longitudinal smooth muscle layer varies along the AP axis of the gut tube. For example, the longitudinal smooth muscle layer of rectum is thicker than that of sigmoid, a more anterior part of the gut tube. *Hoxd-12* and *Hoxd-13* are expressed in the developing rectum, and the loss-of-function mutation of each of these *Hox* genes results in the abnormally thin longitudinal smooth muscle layer (Kondo et al. 1996). The thickness of the longitudinal smooth muscle layer of the *Hox* mutant rectum resembles that of sigmoid. Therefore, *Hoxd-12* and *Hoxd-13* regulate rectum-specific longitudinal smooth muscle layer morphogenesis. During rectum development, *Hoxd-12* and *Hoxd-13* may be involved in the induction, growth, and maintenance of longitudinal smooth muscle precursor. These data show that morphogenesis of the longitudinal smooth muscle layer in the rectum is also regulated by *Hox* genes and signaling for tissue interaction, similar to limb tendon development (Fig. 19.3b).

19.4 Conclusion

Morphogenesis of limb tendons and the rectum longitudinal smooth muscle layer represents a paradigm of tissue patterning wherein the gross tissue positioning mechanism involving *Hox* gene activities and refined tissue positioning by the signals emanating from neighboring tissues cooperate. The scheme, namely, that *Hox* genes provide a fundamental framework and pre-formed tissues provide cues for the precise positioning of later-developing tissues, can be widely applied to histogenesis, for example, ligament, fascia, and tendon sheath in the muscle–bone complex. Precise determination of the signaling molecules and *Hox* genes that function in individual tissues not only will lead to a full understanding of organogenesis but also will open an avenue to the future of regenerative medicine.

Acknowledgments This chapter was originally published as Yamamoto-Shiraishi and Kuroiwa (2013).

References

Baumel JJ, King AS, Breazile JE, Evans HE, Vanden Berge JC (1993) Handbook of avian anatomy: nomina anatomica avium. Nuttall Ornithological Club, Cambridge

Brunet LJ, McMahon JA, McMahon AP, Harland RM (1998) Noggin, cartilage morphogenesis, and joint formation in the mammalian skeleton. Science 280:1455–1457

Capdevila J, Johnson RL (1998) Endogenous and ectopic expression of Noggin suggests a conserved mechanism for regulation of BMP function during limb and somite patterning. Dev Biol 197:205–217

Dealy CN, Roth A, Ferrari D, Brown AM, Kosher RA (1993) Wnt-5a and Wnt-7a are expressed in the developing chick limb bud in a manner suggesting roles in pattern formation along the proximodistal and dorsoventral axes. Mech Dev 43:175–186

Edom-Vovard F, Schuler B, Bonnin MA, Teillet MA, Duprez D (2002) Fgf4 positively regulates Scleraxis and Tenascin expression in chick limb tendons. Dev Biol 247:351–366

Fromental-Ramain C, Warot X, Messadecq N, LeMeur M, Dolle P, Chambon P (1996) Hoxa-13 and Hoxd-13 play a crucial role in the patterning of the limb autopod. Development (Camb) 122:2997–3011

Geetha-Loganathan P, Nimmagadda S, Prols F, Patel K, Scaal M, Huang R, Christ B (2005) Ectodermal Wnt-6 promotes Myf5-dependent avian limb myogenesis. Dev Biol 288:221–233

Geetha-Loganathan P, Nimmagadda S, Huang R, Scaal M, Christ B (2006) Expression pattern of BMPs during chick limb development. Anat Embryol (Berl) 211(suppl 1):87–93

Geetha-Loganathan P, Nimmagadda S, Christ B, Huang R, Scaal M (2010) Ectodermal Wnt6 is an early negative regulator of limb chondrogenesis in the chicken embryo. BMC Dev Biol 10:32

Greene EC (1963) Anatomy of the rat. Transactions of the American Philosophical Society, new series, vol XXVII. American Philosophical Society, Philadelphia

Hashimoto K, Yokouchi Y, Yamamoto M, Kuroiwa A (1999) Distinct signaling molecules control Hoxa-11 and Hoxa-13 expression in the muscle precursor and mesenchyme of the chick limb bud. Development (Camb) 126:2771–2783

Kardon G (1998) Muscle and tendon morphogenesis in the avian hind limb. Development (Camb) 125:4019–4032

Kondo T, Dolle P, Zakany J, Duboule D (1996) Function of posterior *HoxD* genes in the morphogenesis of the anal sphincter. Development (Camb) 122:2651–2659

Krumlauf R (1994) *Hox* genes in vertebrate development. Cell 78:191–201

Kurahashi M, Niwa Y, Cheng J, Ohsaki Y, Fujita A, Goto H, Fujimoto T, Torihashi S (2008) Platelet-derived growth factor signals play critical roles in differentiation of longitudinal smooth muscle cells in mouse embryonic gut. Neurogastroenterol Motil 20:521–531

Merino R, Ganan Y, Macias D, Economides AN, Sampath KT, Hurle JM (1998) Morphogenesis of digits in the avian limb is controlled by FGFs, TGFbetas, and Noggin through BMP signaling. Dev Biol 200:35–45

Nelson CE, Morgan BA, Burke AC, Laufer E, DiMambro E, Murtaugh LC, Gonzales E, Tessarollo L, Parada LF, Tabin C (1996) Analysis of *Hox* gene expression in the chick limb bud. Development (Camb) 122:1449–1466

Omi M, Ide H (1996) Effects of digit tissue on cell death and ectopic cartilage formation in the interdigital zone in chick leg buds. Dev Growth Differ 38:419–428

Pathi S, Rutenberg JB, Johnson RL, Vortkamp A (1999) Interaction of Ihh and BMP/Noggin signaling during cartilage differentiation. Dev Biol 209:239–253

Petropoulos CJ, Hughes SH (1991) Replication-competent retrovirus vectors for the transfer and expression of gene cassettes in avian cells. J Virol 65:3728–3737

Rodriguez-Niedenfuhr M, Dathe V, Jacob HJ, Prols F, Christ B (2003) Spatial and temporal pattern of Wnt-6 expression during chick development. Anat Embryol (Berl) 206:447–451

Sakiyama J, Yokouchi Y, Kuroiwa A (2001) *HoxA* and *HoxB* cluster genes subdivide the digestive tract into morphological domains during chick development. Mech Dev 101:233–236

Schweitzer R, Chyung JH, Murtaugh LC, Brent AE, Rosen V, Olson EN, Lassar A, Tabin CJ (2001) Analysis of the tendon cell fate using *Scleraxis*, a specific marker for tendons and ligaments. Development (Camb) 128:3855–3866

Williams TM, Williams ME, Heaton JH, Gelehrter TD, Innis JW (2005) Group 13 HOX proteins interact with the MH2 domain of R-Smads and modulate Smad transcriptional activation functions independent of HOX DNA-binding capability. Nucleic Acids Res 33:4475–4484

Yamamoto-Shiraishi Y, Kuroiwa A (2013) Wnt and BMP signaling cooperate with Hox in the control of Six2 expression in limb tendon precursor. Dev Biol 377:363–374

Yokouchi Y, Sasaki H, Kuroiwa A (1991) Homeobox gene expression correlated with the bifurcation process of limb cartilage development. Nature (Lond) 353:443–445

Yokouchi Y, Nakazato S, Yamamoto M, Goto Y, Kameda T, Iba H, Kuroiwa A (1995a) Misexpression of Hoxa-13 induces cartilage homeotic transformation and changes cell adhesiveness in chick limb buds. Genes Dev 9:2509–2522

Yokouchi Y, Sakiyama J, Kuroiwa A (1995b) Coordinated expression of Abd-B subfamily genes of the *HoxA* cluster in the developing digestive tract of chick embryo. Dev Biol 169:76–89

Zakany J, Fromental-Ramain C, Warot X, Duboule D (1997) Regulation of number and size of digits by posterior *Hox* genes: a dose-dependent mechanism with potential evolutionary implications. Proc Natl Acad Sci USA 94:13695–13700

Zhu X, Zhu H, Zhang L, Huang S, Cao J, Ma G, Feng G, He L, Yang Y, Guo X (2012) Wls-mediated Wnts differentially regulate distal limb patterning and tissue morphogenesis. Dev Biol 365:328–338

Part VI
Evolutional Variations Stemming from Common Principles

Chapter 20
Molecular and Cellular Bases of Sexual Flexibility in Vertebrates

Minoru Tanaka

Abstract Vertebrates display sexual flexibility at cellular and tissue levels. Some vertebrates even exhibit sex reversal during their natural life. This flexibility of sexuality can be understood as an adaptation to their environment to maximize efficiency of reproduction. Recent analyses reveal that sexual flexibility is underlain by antagonistic mechanisms that lead to either female or male development. In medaka, germ cells have the capability to induce the ovary, which antagonizes testicular development led by somatic cells. In mouse, the male versus female antagonism operates in the somatic cells rather than between germ cells and somatic cells. The molecular and cellular players responsible for the antagonistic mechanisms are different between the two species. In either species, however, the imbalance in the antagonistic mechanisms to establish one sex results in sex reversal at cellular or organismal levels.

Keywords Fate decision • Germ cells • Gonad • Sex determination and differentiation

20.1 Variety in Sexual Reproduction

Mammals, such as we humans, do not change sex throughout their life. During embryogenesis, the first organ that exhibits sex is the gonad. The gonad forms as a sexually bipotential organ, called the gonadal primordium, and then develop into either testis or ovary during embryogenesis. Recent analyses, however, have shown that only a single mutation can reverse sex opposite to the originally determined sex.

M. Tanaka (✉)
Laboratory of Molecular Genetics for Reproduction, National Institute for Basic Biology (NIBB), Aichi, Japan
e-mail: mtanaka@nibb.ac.jp

H. Kondoh and A. Kuroiwa (eds.), *New Principles in Developmental Processes*,
DOI 10.1007/978-4-431-54634-4_20,

Indeed, determination of sex is more flexible than what we may envision. Some species of teleost fish change sex in their natural life (Devlin and Nagahama 2002). In these species, sex determination and the subsequent ovarian or testicular formation, called sex differentiation, occur multiple times. For examples, the black porgy (*Acanthopagrus schlegeli*) develops a testis and behaves as a male for the first couple of years whereas the ovary develops later in life (Wu et al. 2010). The timing of sex reversal is temporally determined, suggesting that sex reversal in this fish species is genetically regulated. On the other hand, several species of wrasse (Labridae) show a bidirectional sex reversal (Kuwamura et al. 2011). Once sex reversed, an individual may even return to the original sex in these species. In this case, sex reversal is thought to be triggered by visual input.

These observations tell us that vertebrate species take their strategy of sexual development as suitable for their reproduction. Thus, some questions arise: Do the different species develop their own mechanism of sexual development or are there any common core features of sex determination and differentiation that are shared by a variety of species?

One common feature deduced from many examples is that ovarian and testicular developments are mutually exclusive processes. Some species develop both testicular-specified and ovarian-specified primordia in a gonad but only the primordium of one sex or the other develops into a functional gonad. These observations collectively suggest the presence of some antagonistic mechanism that allows only one sex to develop while repressing another. In this chapter, I discuss male versus female antagonistic mechanisms, with emphasis on the differences in the contribution of germ cells to sexual development in medaka and mouse.

20.2 Regulation of Gonadal Sex at the Tissue Level in Medaka

Recent genetic and developmental experiments using the teleost fish medaka unveiled the sexual antagonistic mechanism at the tissue level. The core players are the germ cells. The germ cells develop into sperm or oocytes and convey genetic information to the next generation. The vertebrate germ cells have been regarded to be neutral concerning sex differentiation and to adopt the sex determined by the gonadal somatic cells. In contrast to this view, experiments using medaka showed that the germ cells make a critical contribution to female sex determination in the gonad.

Gonochorism refers to the state in which an individual has a single sex throughout life with all organs belonging to the same sexual identity. Medaka is a representative of gonochoristic vertebrates and has a sex-determining gene, *DMY/dmrt1bY*, on the Y chromosome (an XY/XX type) (Matsuda et al. 2002; Nanda et al. 2002). *DMY/dmrt1bY* is expressed in supporting cells that surround germ cells in the gonadal primordium and direct supporting cells to differentiate male-supporting cells, the Sertoli cells. The Sertoli cells then act on the other cells to form the testis. Germ cells, which are of different origin from the gonadal somatic cells, migrate

toward the prospective gonadal region and colonize in the gonadal primordia (Kurokawa et al. 2006; Nakamura et al. 2006). Under the condition where gonad primordia develop without colonization of germ cells as a consequence of the failure of the germ cells in proliferation or migration, XX gonads develop into male type rather than into an ovary (Kurokawa et al. 2007). Under such conditions, *Foxl2*, normally expressed in female-supporting cells (granulosa cell), is expressed only transiently and is subsequently repressed as *dmrt1* expression starts. The gonadal somatic cells that develop in a germ cell-less gonad exhibit male characteristics, without showing any intermediate cellular states between male and female (Kurokawa et al. 2007; Tanaka et al. 2008). Thus, colonization by germ cells is necessary for ovarian development in medaka (Saito and Tanaka 2009).

Importance of germ cells in ovarian development is supported by the phenotype of the mutant medaka, *hotei* (Morinaga et al. 2004; Morinaga et al. 2007). The mutants are characterized by hyperproliferation of germ cells and exhibit male-to-female conversion in a fraction of the XY fish. The mutational defect lies in the type II receptor of anti-Müllerian hormone (AMH), a member of the transforming growth factor (TGF)-β superfamily. In wild-type medaka, both the receptor gene, *amhrII*, and the ligand gene, *amh*, are expressed in the supporting cells surrounding germ cells. The chimera analysis of gonads having both mutant and wild-type cells indicated that AMH signaling occurs between the supporting cells but does not directly act on the germ cells. When the germ cells are experimentally depleted from the mutant, male-to-female sex reversal no longer happens even in the *hotei* mutant. This result indicates that male-to-female sex reversal involves the germ cell populations in the gonad (Nakamura et al. 2012a). The developing ovary in the XY *hotei* mutant expresses male-specific genes simultaneously with female-specific genes. Although further analysis is required, germ cells may override the male pathway occurring in the supporting cells (Nakamura et al. 2012a). The studies of germ cell-excess *hotei* mutant and germ cell-deficient experimental medaka indicate a pivotal contribution of germ cells in ovarian development from the initially sexually neutral gonad (Tanaka et al. 2008).

Even the reduction of germ cells is sufficient for inhibiting ovarian development and causes XX gonads to develop into functional testis and the fish to develop male secondary sex characteristics. Such a case is found in the *sox9b* mutant XX medaka, as is discussed in the next section (Nakamura et al. 2012b).

The role of germ cells in ovarian development is also suggested for zebrafish (Siegfried and Nüsslein-Volhard 2008; Dranow et al. 2013). The zebrafish is not a typical gonochoristic fish. All the gonads first possess oocyte-containing follicles but a gonad without an abundance of germ cells loses the follicles and differentiates into a testis, whereas the gonad with abundant germ cells develops into an ovary (Takahashi 1977; Uchida et al. 2002).

Thus, in several fish species, without a sufficient supply of germ cells, the gonadal somatic cells develop the male phenotype without dependence on the Y chromosome. The sex determination gene on the medaka Y chromosome may function to enhance the intrinsic male bias of the somatic cells. The ovary develops when sufficiently abundant germ cells counteract the male bias of gonadal somatic cells (Kurokawa et al. 2007; Tanaka et al. 2008; Saito and Tanaka 2009).

20.3 Regulation of Gonadal Sex at the Cellular Level in the Mouse

Studies using the medaka have demonstrated the antagonistic interaction between germ cells and gonadal somatic cells in the sexual development of the gonads. An imbalance of the interaction caused by mutations or experimental manipulation results in sex reversal in medaka. In mammals, however, such an interaction between the germ cells and somatic cells in sexual differentiation has not been demonstrated. Rather, sex-associated mechanisms in the supporting somatic cells are the major issue.

Similar to the medaka, the mouse is a gonochoristic vertebrate. The gene responsible for male determination is *Sry* on the Y chromosome. Following Sry activation in the precursor of supporting cells, Sry and SF1 synergistically activate autosomal *Sox9* (Sekido and Lovell-Badge 2008) (Fig. 20.1), which then activates *Fgf9* expression. The Fgf9 signal in turn enhances *Sox9* in the supporting cell precursors through a positive feedback mechanism (Kim et al. 2006). This *Sox9–Fgf9* regulatory loop promotes the differentiation of the supporting cells into Sertoli cells (Bowles et al. 2010).

During this initial stage of supporting cell development toward Sertoli cells, the genes involved in Wnt signaling, such as *Wnt4* and *Rspo1* for female development, are repressed by the action of the *Sox9–Fgf9* loop. In the female gonad lacking the Sry activation, Wnt4 activity shuts off the Fgf9–Sox9 loop for male gonad development and allows the female gonad development of the supporting cell precursors (Vainio et al. 1999; Parma et al. 2006; Maatouk et al. 2008; Chassot et al. 2011) (Fig. 20.1). Initially indifferent supporting cells develop into either male or female gonad cells by virtue of the antagonistic mechanism between *Sox9* and *Wnt4* (Brennan and Capel 2004). Gene expression analyses using microarray and RNA sequencing indicated that many genes critical for female and male development are already expressed in the "indifferent gonad" cells, albeit at low levels (Jameson et al. 2012; Yamaguchi et al. 2012).

The aforementioned antagonistic regulations operate not in individual cells but at the tissue level. Actually, mouse chimera with XX and XY cells exhibit the complete male phenotype when a major fraction of supporting cells is XY. In such chimeric testis in the adult, seminiferous tubules are predominated by XY-Sertoli cells but also contain XX-Sertoli cells (Burgoyne et al. 1988), indicating that the regulation for Sertoli cells development is non-cell autonomous. Prostaglandin may also take a part in the antagonistic mechanism as a factor involved in the non-cell autonomously male gonad regulation. Prostaglandin enhances the nuclear localization of Sox9 protein independent of Fgf9 (Moniot et al. 2009).

The antagonistic mechanism has also been analyzed in the mature ovary (Fig. 20.1). Foxl2 is a forkhead transcriptional factor that is expressed in granulosa cells but not in Sertoli cells. Conditional disruption of *Foxl2* in granulosa cells causes the transformation from granulosa cells to Sertoli-like cells that express *Sox9*. Following *Sox9* expression, oocytes die and the follicular structures turn into the testicular cord-like

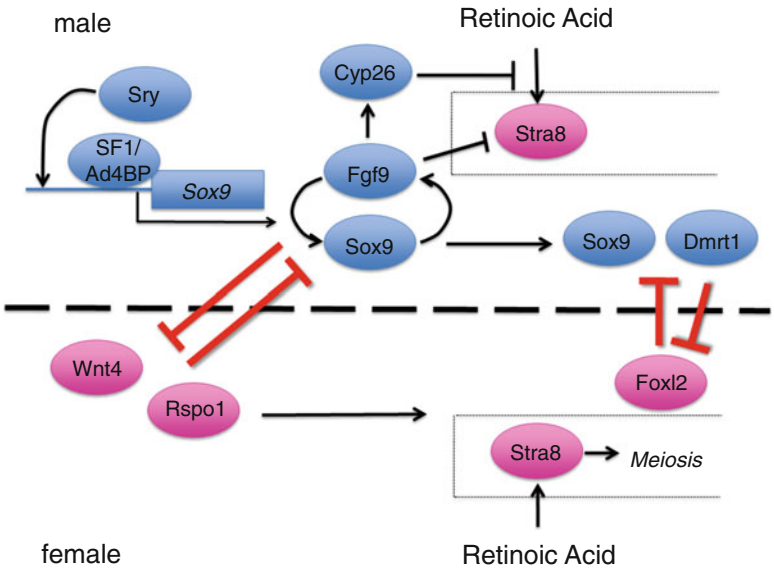

Fig. 20.1 Antagonistic mechanism ensures the sexual bipotential state in mouse gonads. *Sry* expression triggers a positive feedback loop of *Sox9*/*Fgf9* and antagonizes the feminizing signal, *Wnt4*/*Rspo1*. Without Sry activation, *Wnt4*/*Rspo1* represses establishment of positive feedback. The antagonistic mechanism between *Wnt4*/*Rspo1* and *Sox9*/*Fgf9* thus leads to either ovarian or testicular development. The mechanism links to the female-specific promotion of meiosis in germ cells through regulation of action of retinoic acid and *Stra8*. In adult ovarian (granulosa)/testicular (Sertoli) supporting cells, the bipotential state is retained by an additional antagonistic mechanism with *Foxl2* versus *Sox9*/*Dmrt1*. *Thick red lines* indicate the antagonistic mechanisms, which could cause the sex reversal at tissue or cellular levels. *Dotted lines* indicate the events occurring in germ cells in the developing gonads

structure. Therefore, *Foxl2* is critical for suppression of the Sertoli cell developmental program in granulosa cells (Uhlenhaut et al. 2009). Conversely, in Sertoli cells, *Dmrt1* participates in the suppression of expression of *Foxl2* and other genes that are involved in granulosa cell development (Matson et al. 2011).

All these studies indicate that the function of Sertoli and granulosa cells is not fixed but is maintained as the result of the antagonistic relationship between regulation toward female or male development.

20.4 Comparison of Mouse and Medaka

In both mouse and medaka gonads, counteraction between two opposing regulations that leads to male- or female-type development determines the sex of the gonad. Let us compare the molecular mechanisms involved in the male versus female counteraction between mouse and medaka.

The mouse has a single *Sox9* gene whereas the medaka has two *sox9* genes, *sox9a* and *sox9b* (Klüver et al. 2005), the latter being expressed in the supporting cells of the gonad. The homozygous *sox9b* mutants die at an early larval stage, but by then morphologically normal gonads have developed with germ cells surrounded by supporting cells (Nakamura et al. 2012b). However, germ cell numbers are reduced in both homozygous and heterozygous mutant gonads, and the deposition of extracellular matrix (ECM) enclosing the supporting cells is defective in such gonads. This ECM defect is considered to cause germ cell loss. As expected from the reduction of germ cells in the gonad, *sox9b* mutant XX fish often display female-to-male sex reversal in contrast with the XY male-to-female sex reversal in mammalian *Sox9* mutants (Vidal et al. 2001). This female-to-male sex reversal in the medaka *sox9b* mutant is rescued by the increase of germ cells effected by introduction of the heterozygous *hotei* mutation. This result indicates that *sox9b* is not involved in an initial stage of male gonad development. In support of this, an increase of *sox9b* gene copies by transgene introduction does not affect the sexual phenotype of XX medaka (Nakamura et al. 2012b). Interestingly, a recent study in the mouse indicates that testicular development proceeds in the absence of Sox9 function, if the feminizing gene, *Rspo1*, is ablated (Lavery et al. 2012). This finding suggests that, even in mouse, Sox9 function is dispensable, insofar as the female developmental pathway is inhibited.

The *fgf9* gene, the Sox9 partner in the positive-feedback loop for Sertoli development in mouse, is not found in the medaka genome (Forconi et al. 2013). Therefore, the Sox9–Fgf9 positive feedback loop is not a universal system and may be functionally replaced by *DMY/dmrt1bY* functions in medaka.

The action of the AMH signal is also different between mouse and medaka. In the mouse, AMH acts on Müllerian duct regression after the gonadal sex is determined (Klattig and Englert 2007), but in medaka, Müllerian duct-equivalent tissue is not present and the AMH signal is required for the genetically determined sex to be properly developed (Nakamura et al. 2012a).

These comparisons reveal that the antagonistic mechanisms function in both species ensuring either female or male development in both mouse and medaka. However, the molecular mechanisms, especially in the initial process triggering ovarian or testicular development, are not conserved between the two species.

20.5 How Is the Sex of Germ Cells Regulated?

In the female mouse, all germ cells enter cystic division to produce meiotic oocytes in embryos (Pepling et al. 1999). The cystic division and the following meiotic entry do not occur in testicular development during embryogenesis. Prenatal meiosis per se does not represent feminization of germ cells because meiosis is the event common to both oogenesis and spermatogenesis. The core mechanism that regulates the sex determination of germ cells currently is totally unknown in vertebrates. Early entry into meiosis in the mouse developing ovary is, however, often taken as

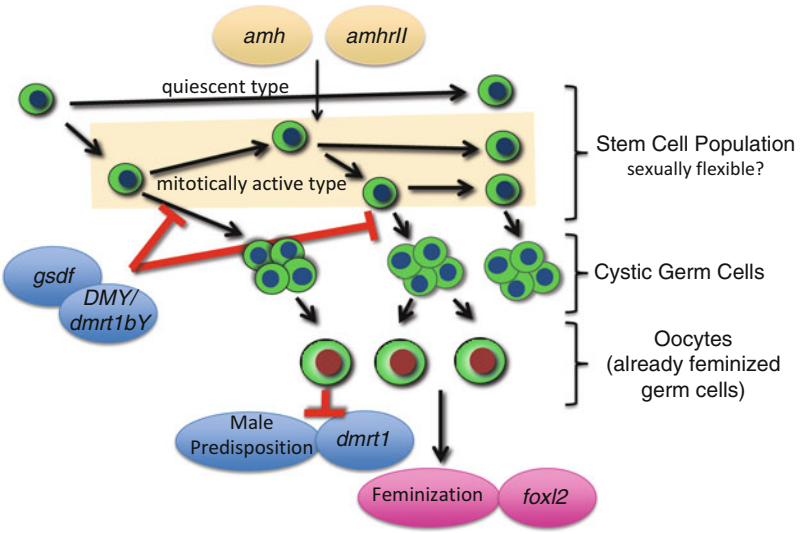

Fig. 20.2 Antagonistic mechanism ensures sexual bipotential state in the developing gonad of medaka. *Green cells* are germ cells. In contrast to mammals, both female and male gonads, even in their mature state, maintain a stem cell population of germ cells. In the XX female, a fraction of the mitotically active stem cell population commits to cystic division. These germ cells are feminized at some point before or during cystic division and form oocytes. During this process germ cells repress the male pathway of somatic cells and promote feminization of somatic cells to form follicles and maintain aromatase expression. The *DMY/dmrt1bY* and *gsdf* expressing in the somatic cells of XY medaka inhibit the commitment to cystic germ cells (Saito et al. 2007). Defect in intercellular antagonism causes complete sex reversal (*thick red lines*). The AMH signal regulates proliferation of the mitotically active stem cell population (Nakamura et al. 2012a). Loss of the AMH signal in XY gonads causes dysregulation of commitment to cystic division, resulting in many oocytes and ovarian formation

an indication of female germ cell development. The *Stra8* is critical for promotion of the meiosis and is upregulated by female-specific action of retinoic acid (Bowles et al. 2006; Koubova et al. 2006). In male developing gonads, the *Stra8* upregulation is repressed by both *Nos2* in germ cells and *Fgf9* from Sertoli cells (Bowles et al. 2010; Saga 2010) (Fig. 20.1).

In the medaka also, meiosis proceeds in developing female gonads, much earlier than that in male gonadal development, which occurs 1 month after hatching. In contrast to the mouse, however, *Nos2* expression is not detected in germ cells of the developing gonads but is detected in germline stem cells of the mature gonads (Aoki et al. 2009; Nakamura et al. 2010) (Fig. 20.2). In addition, *Stra8* is not found in the medaka genome. Therefore, the *Nos2/Fgf9-Stra8* mechanism is unlikely to function during the formation of ovary in medaka.

Given that early meiotic entry is a good indication of feminization of germ cells, when does the commitment to meiotic events occur? In mouse, XY/XX reaggregate experiments showed that the ovarian or testicular fate of germ cells is fixed and does not change in response to the surrounding somatic cells after E13.5. The germ cells

isolated from the XY gonad before E12.5 enter meiosis (McLaren 2000; Adams and McLaren 2002). By contrast, in fish the reciprocal transplantation of XY germ cells from mature testis to XX ovary somatic environment, and vice versa, demonstrates that either germ cell can develop into oocytes or sperm in accordance with the sex of gonadal somatic cells (Shinomiya et al. 2002; Yoshizaki et al. 2010; Wong et al. 2011). These observations suggest that the sex of germ cells in mature testis and ovary of teleost is still flexible and can adjust the developmental state to the surrounding somatic cells in the adult gonad. Alternatively, the germ cells may be kept in a sexually indifferent status even in the adult testicular or ovarian environment.

In addition to the difference in germ cell dependence of gonadal sex differentiation, medaka and mouse gonads differ in the maintenance of germline stem cells. As already mentioned, mouse germ cells all commit to oogenesis during early ovarian development to form oocytes. Therefore, it is generally accepted that active germline stem cells that keep producing oocytes are not present in the adult ovary (Lei and Spradling 2013). In contrast, in both testicular and ovarian development in medaka, some fraction of germ cells is kept dividing as a self-renewal population (Saito et al. 2007) (Fig. 20.2), and even germline stem cells are proved to be present in mature ovary (Nakamura et al. 2010). Concerning details, two types of germline stem cell populations are found, quiescent and mitotically active populations, and the AMH signal regulates the latter (Nakamura et al. 2012a) (Fig. 20.2).

In summary, germ cells in medaka seem to be flexible in choosing sperm or oocyte development whereas the prenatal meiotic entry of germ cells in mammals, often regarded as germ cell feminization, is in part regulated by a mammalian-specific antagonistic mechanism in somatic cells. In contrast to the mouse, a self-renewal stem type of germ cells persists in the medaka developing ovary. AMH regulates the mitotically active stem type of germ cells, and dysregulation causes an excessive number of germ cells in the *hotei* mutant with a male-to-female sex-reversal phenotype (Fig. 20.2).

20.6 Hormonal Control of Sex at the Organismal Level

Hormonal control is the mechanism that establishes sexual identity at the organismal level. Evidence indicates the contribution of sex steroid hormones to organismal sex reversal. In mutant mice that lack both estrogen receptors, ERα and ERβ, *Foxl2* expression is not maintained in the granulosa cells, concomitant with gradual increase of *Amh* and *Sox9* expression, which destroys oocytes (Couse et al. 1999; Dupont et al. 2000). Foxl2 and ERα/β together bind to an *Sox9* enhancer sequence and repress the enhancer, thus inhibiting transformation of granulosa cells into Sertoli cells (Uhlenhaut et al. 2009). Following *Sox9* expression, follicular structures turn into seminiferous tubule-like structures. These observations indicate that estrogen is involved in the repression of male development.

In medaka, administration of estrogen to XY embryos and larvae causes not only phenotypic females but also ovary formation. The effect of estrogen has been

repeatedly reported since Yamamoto's pioneering studies of inducing sex reversal in medaka (e.g., Yamamoto 1975; Hagino et al. 2001; Kobayashi et al. 2011). Interestingly the studies showed that a low dose of administration often induces an ovary located posteriorly to a testis in XY medaka. In the orange-red variety of medaka, gonadogenesis proceeds in an anteroposterior gradient of development. Therefore, a posterior part may be more indifferent and is sensitive to a low dose of estrogen. Conversely, the blockage of estrogen signal by the aromatase (estrogen-producing enzyme) inhibitor results in formation of a testis. The studies also describe frequent occurrence of rudimental gonads devoid of germ cells in sex-reversed XX males, especially when a high dose of androgen is administered (Yamamoto 1958). Although the molecular function of androgen in sex differentiation is unclear, the female-to-male sex reversal can be explained by direct or indirect action of androgen on germ cells and the subsequent loss of germ cells. Thus, the action of sex steroid hormones seems integrated in the antagonistic mechanism in medaka. The gonad is in a bipotential state capable of responding to sex steroid hormone(s).

Although the granulosa cells are a major source of estrogen in the mouse ovary, theca cells seem a primary source of estrogen in the medaka because the theca cells are the first steroidogenic cells that express aromatase during ovarian development (Nakamura et al. 2009), and aromatase is not detected in the granulosa cells until oocytes become fully grown in the mature ovary. Consistent with the importance of germ cells in medaka ovarian formation, estrogen secretion is dependent on the presence of germ cells in the gonad. If germ cells are removed from the gonadal primordium, the theca cells gradually lose the expression of aromatase (Kurokawa et al. 2007; Nakamura et al. 2009). This loss indicates that the development of theca cells initiates independently of the signal from germ cells but that maintenance requires the presence of germ cells, presumably female-committed germ cells.

20.7 Conclusions

Throughout evolution, sexual reproduction has been adopted as a means to generate offspring. By development of sexually distinct gametes, sperm and oocytes are produced in testis and ovary, respectively. Besides sex-specific gonadal development, sexual differentiation occurs at the organismal level via hormonal regulation.

Although not a focus in this chapter, the sex-determining genes are variable among vertebrate species (Kikuchi and Hamaguchi 2013; Marshall Graves 2013). Vertebrate species seem to have developed specific mechanisms to trigger ovarian or testicular development to optimize reproduction efficiency according to life cycle or environment. The basis of this variation is the male/female bipotential (indifferent) state of the gonad. In support of this, many sex determination genes are originated from the players involved in the bipotential state (DM domain genes in medaka, chick, and *Xenopus laevis*; sox genes in mammals and some species of medaka; TGF-β genes in medaka and pufferfish) (Table 20.1).

Table 20.1 A variety of sex determination genes

Species	Inheritance mode	Gene name
Mammals	XY/XX	*Sry* (1–3)
Chicken	ZZ/ZW	*Dmrt1* (4)
Xenopus laevis	ZZ/ZW	*DM-W* (5)
Medaka *(Oryzias latipes*)	XY/XX	*DMY/dmrt1bY* (6, 7)
Medaka (*Oryzias luzonensis*)	XY/XX	*gsdfY* (allelic) (8)
Trout (*Oncorhynchus mykiss*)	XY/XX	*Irf9* (9)
Pufferfish (*Takifuga rubripes*)	XY/XX	$amhrII^{Y}$ (allelic) (10)
Patagonian pejerrey (*O. hatcheri*)	XY/XX	*Amhy* (11)

(1) Sinclair et al. (1990); (2) Gubbay et al. (1990); (3) Koopman et al. (1991); (4) Smith et al. (2009); (5) Yoshimoto et al. (2010); (6) Matsuda et al. (2002); (7) Nanda et al. (2002); (8) Myosho et al. (2012); (9) Yano et al. (2012); (10) Kamiya et al. (2012); (11) Hattori et al. (2012)

The antagonistic mechanism underlying the bipotential state is different between medaka and mouse. In medaka, the presence of germline stem cells seems critical for the bipotential state. Unless instructed to develop into sperm, the stem cell population produces daughter germ cells that develop into oocytes. During this process, the germ cells provide an effect on somatic cells to organize the ovarian tissues. In contrast, the bipotentiality is primarily regulated by supporting cells in germ cells. Many players in the antagonistic mechanism functioning in mouse somatic cells are not present in the medaka genome.

The bipotential state is also seen at an organismal level by steroid hormones. The different layers of hierarchy from genetic to organismal levels ensure flexibility of sex differentiation and thus allow organisms to maximize chances of reproduction.

References

Adams IR, McLaren A (2002) Sexually dimorphic development of mouse primordial germ cells: switching from oogenesis to spermatogenesis. Development (Camb) 129:1155–1164

Aoki Y, Nakamaura S, Ishikawa Y, Tanaka M (2009) Expresssion and systenic analysis of four *nanos* genes in medaka. Zool Sci 26:112–118

Bowles J, Knight D, Smith C, Wilhelm D, Richman J, Mamiya S, Yashiro K, Chawengsaksophak K, Wilson MJ, Rossant J, Hamada H, Koopman P (2006) Retinoid signaling determines germ cell fate in mice. Science 312:596–600

Bowles J, Feng CW, Spiller C, Davidson TL, Jackson A, Koopman P (2010) FGF9 suppresses meiosis and promotes male germ cell fate in mice. Dev Cell 19:440–449

Brennan J, Capel B (2004) One tissue, two fates: molecular genetic events that underlie testis versus ovary development. Nat Rev Genet 5:509–521

Burgoyne PS, Buehr M, Koopman P, Rossant J, McLaren A (1988) Cell-autonomous action of the testis-determining gene: Sertoli cells are exclusively XY in XX–XY chimaeric mouse testes. Developmen (Camb) 102:443–450

Chassot AA, Gregoire EP, Lavery R, Taketo MM, de Rooij DG, Adams IR, Chaboissier MC (2011) RSPO1/β-catenin signaling pathway regulates oogonia differentiation and entry into meiosis in the mouse fetal ovary. PLoS ONE 6:e25641

Couse JF, Hewitt SC, Bunch DO, Sar M, Walker VR, Davis BJ, Korach KS (1999) Postnatal sex reversal of the ovaries in mice lacking estrogen receptors α and β. Science 286:2328–2331

Devlin RH, Nagahama Y (2002) Sex determination and sex differentiation in fish: an overview of genetic, physiological, and environmental influences. Aquaculture 208:191–364

Dranow DB, Tucker RP, Draper BW (2013) Germ cells are required to maintain a stable sexual phenotype in adult zebrafish. Dev Biol 376:43–50

Dupont S, Krust A, Gansmuller A, Dierich A, Chambon P, Mark M (2000) Effect of single and compound knockouts of estrogen receptors α (ERα) and β (ERβ) on mouse reproductive phenotypes. Development (Camb) 127:4277–4291

Forconi M, Canapa A, Barucca M, Biscotti MA, Capriglione T, Buonocore F, Fausto AM, Makapedua DM, Pallavicini A, Gerdol M, De Moro G, Scapigliati G, Olmo E, Schartl M (2013) Characterization of sex determination and sex differentiation genes in *Latimeria*. PLoS ONE 8:e56006

Gubbay J, Collignon J, Koopman P, Capel B, Economou A, Münsterberg A, Vivian N, Goodfellow P, Lovell-Badge R (1990) A gene mapping to the sex-determining region of the mouse Y chromosome is a member of a novel family of embryonically expressed genes. Nature (Lond) 346(6281):245–250

Hagino S, Kagoshima M, Ashida S (2001) Effects of ethynylestradiol, diethylstilbestrol, 4-t-penthylphenol, 17β-estradiol, methyltestosterone and flutamide on sex reversal in S-rR strain medaka (*Oryzias latipes*). Environ Sci 8:75–87

Hattori RS, Murai Y, Oura M, Masuda S, Majhi SK, Sakamoto T, Fernandino JI, Somoza GM, Yokota M, Strüssmann CA (2012) A Y-linked anti-Müllerian hormone duplication takes over a critical role in sex determination. Proc Natl Acad Sci USA 109:2955–2959

Jameson SA, Natarajan A, Cool J, DeFalco T, Maatouk DM, Mork L, Munger SC, Capel B (2012) Temporal transcriptional profiling of somatic and germ cells reveals biased lineage priming of sexual fate in the fetal mouse gonad. PLoS Genet 8:e1002575

Kamiya T, Kai W, Tasumi S, Oka A, Matsunaga T, Mizuno N, Fujita M, Suetake H, Suzuki S, Hosoya S, Tohari S, Brenner S, Miyadai T, Venkatesh B, Suzuki Y, Kikuchi K (2012) A trans-species missense SNP in Amhr2 is associated with sex determination in the tiger pufferfish, Takifugu rubripes (fugu). PLoS Genet 8:e1002798

Kikuchi K, Hamaguchi S (2013) Novel sex-determining genes in fish and sex chromosome evolution. Dev Dyn 242:339–353

Kim Y, Kobayashi A, Sekido R, DiNapoli L, Brennan J, Chaboissier MC, Poulat F, Behringer RR, Lovell-Badge R, Capel B (2006) Fgf9 and Wnt4 act as antagonistic signals to regulate mammalian sex determination. PLoS Biol 4:e187

Klattig J, Englert C (2007) The Müllerian duct: recent insights into its development and regression. Sex Dev 1:271–278

Klüver N, Kondo M, Herpin A, Mitani H, Schartl M (2005) Divergent expression patterns of *Sox9* duplicates in teleosts indicate a lineage specific subfunctionalization. Dev Genes Evol 215:297–305

Kobayashi H, Iwamatsu T, Shibata Y, Ishihara M, Kobayashi Y (2011) Effects of co-administration of estrogen and androgen on induction of sex reversal in the medaka *Oryzias latipes*. Zool Sci 28:355–359

Koopman P, Gubbay J, Vivian N, Goodfellow P, Lovell-Badge R (1991) Male development of chromosomally female mice transgenic for Sry. Nature (Lond) 351(6322):117–121

Koubova J, Menke DB, Zhou Q, Capel B, Griswold MD, Page DC (2006) Retinoic acid regulates sex-specific timing of meiotic initiation in mice. Proc Natl Acad Sci USA 103:2474–2479

Kurokawa H, Aoki Y, Nakamura S, Ebe Y, Kobayashi D, Tanaka M (2006) Time-lapse analysis reveals different modes of primordial germ cell migration in the medaka *Oryzias latipes*. Dev Growth Differ 48:209–221

Kurokawa H, Saito D, Nakamura S, Katoh-Fukui Y, Ohta K, Aoki Y, Baba T, Morohashi K, Tanaka M (2007) Germ cells are essential for sexual dimorphism in the medaka gonad. Proc Natl Acad Sci USA 104:16958–16963

Kuwamura T, Suzuki S, Kadota T (2011) Reversed sex change by widowed males in polygynous and protogynous fishes: female removal experiments in the field. Naturwissenschaften 98:1041–1048

Lavery R, Chassot AA, Pauper E, Gregoire EP, Klopfenstein M, de Rooij DG, Mark M, Schedl A, Ghyselinck NB, Chaboissier MC (2012) Testicular differentiation occurs in absence of R-spondin1 and Sox9 in mouse sex reversals. PLoS Genet 8:e1003170

Lei L, Spradling A (2013) Female mice lack adult germ-line stem cells but sustain oogenesis using stable primordial follicles. Proc Natl Acad Sci USA 110:8585–8590

Maatouk DM, DiNapoli L, Alvers A, Parker KL, Taketo MM, Capel B (2008) Stabilization of beta-catenin in XY gonads causes male-to-female sex-reversal. Hum Mol Genet 17:2949–2955

Marshall Graves JA (2013) How to evolve new vertebrate sex determining genes. Dev Dyn 242:354–359

Matson CK, Murphy MW, Sarver AL, Griswold MD, Bardwell VJ, Zarkower D (2011) DMRT1 prevents female reprogramming in the postnatal mammalian testis. Nature (Lond) 476:101–104

Matsuda M, Nagahama Y, Shinomiya A, Sato T, Matsuda C, Kobayashi T, Morrey CE, Shibata N, Asakawa S, Shimizu N, Hori H, Hamaguchi S, Sakaizumi M (2002) *DMY* is a Y-specific DM-domain gene required for male development in the medaka fish. Nature (Lond) 417(6888):559–563

McLaren A (2000) Germ and somatic cell lineages in the developing gonad. Mol Cell Endocrinol 163:3–9

Moniot B, Declosmenil F, Barrionuevo F, Scherer G, Aritake K, Malki S, Marzi L, Cohen-Solal A, Georg I, Klattig J, Englert C, Kim Y, Capel B, Eguchi N, Urade Y, Boizet-Bonhoure B, Poulat F (2009) The PGD2 pathway, independently of FGF9, amplifies SOX9 activity in Sertoli cells during male sexual differentiation. Development (Camb) 136:1813–1821

Morinaga C, Tomonaga T, Sasado T, Suwa H, Niwa K, Yasuoka A, Henrich T, Watanabe T, Deguchi T, Yoda H, Hirose Y, Iwanami N, Kunimatsu S, Okamoto Y, Yamanaka T, Shinomiya A, Tanaka M, Kondoh H, Furutani-Seiki M (2004) Mutations affecting gonadal development in medaka, *Oryzias latipes*. Mech Dev 121:829–839

Morinaga C, Saito D, Nakamura S, Sasaki T, Asakawa S, Shimizu N, Mitani H, Furutani-Seiki M, Tanaka M, Kondoh H (2007) The *hotei* mutation of medaka in the anti-Mullerian hormone receptor causes the dysregulation of germ cell and sexual development. Proc Natl Acad Sci USA 104:9691–9696

Myosho T, Otake H, Masuyama H, Matsuda M, Kuroki Y, Fujiyama A, Naruse K, Hamaguchi S, Sakaizumi M (2012) Tracing the emergence of a novel sex-determining gene in medaka, Oryzias luzonensis. Genetics 191(1):163–170

Nakamura S, Kobayashi D, Aoki Y, Yokoi H, Ebe Y, Wittbrodt J, Tanaka M (2006) Identification and lineage tracing of two populations of somatic gonadal precursors in medaka embryos. Dev Biol 295:678–688

Nakamura S, Kurokawa H, Asakawa S, Shimizu N, Tanaka M (2009) Two distinct types of theca cells in the medaka gonad: germ cell-dependent maintenance of *cyp19a1*-expressing cells. Dev Dyn 238:2652–2657

Nakamura S, Kobayashi K, Nishimura T, Higashijima S, Tanaka M (2010) Identification of germ-line stem cells in the ovary of the teleost medaka. Science 328:1561–1563

Nakamura S, Watanabe I, Nishimura T, Picard J-Y, Toyoda A, Taniguchi Y, di Clemente N, Tanaka M (2012a) Hyperproliferation of mitotically active germ cells dues to defective anti-Müllerian hormone signaling mediates sex reversal in medaka. Development (Camb) 139:2283–2287

Nakamura S, Watanabe I, Nishimura T, Toyoda A, Taniguchi Y, Tanaka M (2012b) Analysis of medaka *sox9* orthologue reveals a conserved role in germ cell maintenance. PLoS ONE 7:e29982

Nanda I, Kondo M, Hornung U, Asakawa S, Winkler C, Shimizu A, Shan Z, Haaf T, Shimizu N, Shima A, Schmid M, Schartl M (2002) A duplicated copy of DMRT1 in the sex-determining region of the Y chromosome of the medaka, *Oryzias latipes*. Proc Natl Acad Sci USA 99(18):11778–11783

Parma P, Radi O, Vidal V, Chaboissier MC, Dellambra E, Valentini S, Guerra L, Schedl A, Camerino G (2006) R-spondin1 is essential in sex determination, skin differentiation and malignancy. Nat Genet 38:1304–1309

Pepling ME, de Cuevas M, Spradling AC (1999) Germline cysts: a conserved phase of germ cell development? Trends Cell Biol 9:257–262

Saga Y (2010) Function of Nanos2 in the male germ cell lineage in mice. Cell Mol Life Sci 67:3815–3822

Saito D, Tanaka M (2009) Comparative aspects of gonadal differentiation in medaka: a conserved role of developing oocytes in sexual canalization. Sex Dev 3:99–107

Saito D, Morinaga C, Aoki Y, Nakamura S, Mitani H, Furutani-Seiki M, Kondoh H, Tanaka M (2007) Proliferation of germ cells during gonadal sex differentiation in medaka: insights from germ cell depleted mutant *zenzai*. Dev Biol 310:280–290

Sekido R, Lovell-Badge R (2008) Sex determination involves synergistic action of SRY and SF1 on a specific Sox9 enhancer. Nature (Lond) 453:930–934

Shinomiya A, Shibata N, Sakaizumi M, Hamaguchi S (2002) Sex reversal of genetic females (XX) induced by the transplantation of XY somatic cells in the medaka, *Oryzias latipes*. Int J Dev Biol 46:711–717

Siegfried KR, Nüsslein-Volhard C (2008) Germ line control of female sex determination in zebrafish. Dev Biol 324:277–287

Sinclair AH, Berta P, Palmer MS, Hawkins JR, Griffiths BL, Smith MJ, Foster JW, Frischauf AM, Lovell-Badge R, Goodfellow PN (1990) A gene from the human sex-determining region encodes a protein with homology to a conserved DNA-binding motif. Nature (Lond) 346(6281):240–244

Smith CA, Roeszler KN, Ohnesorg T, Cummins DM, Farlie PG, Doran TJ, Sinclair AH (2009) The avian Z-linked gene DMRT1 is required for male sex determination in the chicken. Nature (Lond) 461(7261):267–271

Takahashi H (1977) Juvenile hermaphroditism in the zebrafish, *Brachydanio rerio*. Bull Fac Fish Hokkaido Univ 28:57–65

Tanaka M, Saito D, Morinaga C, Kurokawa H (2008) Cross talk between germ cells and gonadal somatic cells is critical for sex differentiation of the gonads in the teleost fish, medaka (*Oryzias latipes*). Dev Growth Differ 50:273–278

Uchida D, Yamashita M, Kitano T, Iguchi T (2002) Oocyte apoptosis during the transition from ovary-like tissue to testes during sex differentiation of juvenile zebrafish. J Exp Biol 205:711–718

Uhlenhaut NH, Jakob S, Anlag K, Eisenberger T, Sekido R, Kress J, Treier AC, Klugmann C, Klasen C, Holter NI, Riethmacher D, Schütz G, Cooney AJ, Lovell-Badge R, Treier M (2009) Somatic sex reprogramming of adult ovaries to testes by FOXL2 ablation. Cell 139:1130–1142

Vainio S, Heikkilä M, Kispert A, Chin N, McMahon AP (1999) Female development in mammals is regulated by Wnt-4 signalling. Nature (Lond) 397:405–409

Vidal VPI, Chaboissier MC, de Rooij DG, Schedl A (2001) *Sox9* induces testis development in XX transgenic mice. Nat Genet 28:216–217

Wong TT, Saito T, Crodian J, Collodi P (2011) Zebrafish germline chimeras produced by transplantation of ovarian germ cells into sterile host larvae. Biol Reprod 84:1190–1197

Wu GC, Tomy S, Lee MF, Lee YH, Yueh WS, Lin CJ, Lau EL, Chang CF (2010) Sex differentiation and sex change in the protandrous black porgy, *Acanthopagrus schlegeli*. Gen Comp Endocrinol 167:417–421

Yamaguchi S, Hong K, Liu R, Shen L, Inoue A, Diep D, Zhang K, Zhang Y (2012) Tet1 controls meiosis by regulating meiotic gene expression. Nature (Lond) 492:443–447

Yamamoto T (1958) Artificial induction of functional sex-reversal in genotypic females of the medaka (*Oryzias latipes*). J Exp Zool 137:227–263

Yamamoto T (1975) Induced intersex. In: Medaka (killifish): biology and strains. Keigaku, Tokyo, pp 214–222

Yano A, Guyomard R, Nicol B, Jouanno E, Quillet E, Klopp C, Cabau C, Bouchez O, Fostier A, Guiguen Y (2012) An immune-related gene evolved into the master sex-determining gene in rainbow trout, Oncorhynchus mykiss. Curr Biol 22:1423–1428

Yoshimoto S, Ikeda N, Izutsu Y, Shiba T, Takamatsu N, Ito M (2010) Opposite roles of DMRT1 and its W-linked paralogue, DM-W, in sexual dimorphism of Xenopus laevis: implications of a ZZ/ZW-type sex-determining system. Development (Camb) 137(15):2519–2526

Yoshizaki G, Ichikawa M, Hayashi M, Iwasaki Y, Miwa M, Shikina S, Okutsu T (2010) Sexual plasticity of ovarian germ cells in rainbow trout. Development (Camb) 137:1227–1230

Chapter 21
Differential Use of Paralogous Genes via Evolution of *Cis*-Regulatory Elements for Divergent Expression Specificities

Haruki Ochi, Akane Kawaguchi, and Hajime Ogino

Abstract Recent accumulation of genome sequences indicates that vertebrate genomes retained many duplicate genes, called paralogues, after whole-genome duplications (WGDs) occurring in the early stages of chordate evolution. Although paralogous gene pairs probably had the same expression patterns immediately after WGDs, they often showed distinct expression patterns in modern vertebrates. Nucleotide sequence changes in noncoding genomic regions, including *cis-regulatory* elements (CRE) such as enhancers and silencers, are the primary cause of the divergent paralogue expression. Such CRE evolution can be classified as follows: (1) enhancer innovation, (2) silencer innovation, and (3) ancestral CRE degeneration. In this chapter, we first show examples of the degeneration of ancestral CREs, with reference to the duplication–degeneration–complementation model, and subsequently introduce recently discovered evidence for silencer innovation and conservation of ancestral pleiotropic enhancers. Finally, we discuss the possible involvement of enhancer innovation in the divergent paralogue expression.

Keywords Evolution of *cis*-regulatory element • Paralogue • Whole-genome duplication

H. Ochi (✉)
Faculty of Medicine, Yamagata University, Yamagata, Japan
e-mail: harukiochi@med.id.yamagata-u.ac.jp

A. Kawaguchi
Graduate School of Biological Sciences, Nara Institute of Science and Technology, Nara, Japan

H. Ogino
Department of Animal Bioscience, Nagahama Institute of Bio-Science and Technology, Shiga, Japan

H. Kondoh and A. Kuroiwa (eds.), *New Principles in Developmental Processes*,
DOI 10.1007/978-4-431-54634-4_21,

21.1 Introduction

It is widely accepted that two rounds of whole-genome duplication (WGD) occurred in the stem lineage of extant modern vertebrates, followed by a third round in the teleost lineage (Jaillon et al. 2004). WGDs have produced many paralogous gene pairs from the set of ancestral genes (Koonin 2005). Classic studies hypothesized that one copy of such a paralogous pair would have one of two fates: evolution of a novel function, known as neofunctionalization, or accumulation of deleterious mutations and disappearance from the genome, known as nonfunctionalization (Ohno 1970). However, whole-genome sequencing of several chordates has revealed that paralogous pairs are often retained without significant changes in their coding sequences (Dehal and Boore 2005). Gene disruption experiments showed that some of these genes were functionally redundant in overlapping expression domains (Bouchard et al. 2000).

The functional conservation of such paralogous genes can be explained on the basis of their essential role in other unique expression domains. The paralogous genes often have multiple expression domains; some are shared between paralogous pairs, while others are not. Such expression differences are probably caused by mutations in *cis*-regulatory elements (CREs), including enhancers, silencers, and promoters, after WGD. The evolutionary changes in CREs leading to phenotypic diversification in fruit flies have been previously reviewed (Wray et al. 2002; Carroll 2008; Stern and Orgogozo 2008). In this chapter, we focus on recent investigations on the evolution of CREs responsible for the divergent expression of paralogs in vertebrates. After briefly summarizing the definition and function of CREs, we discuss the mechanisms of CRE innovation and degeneration following WGDs.

21.2 Classification of CREs

In this review, we use the term CREs to refer to only genomic DNA sequences for transcriptional regulation of a flanking gene, that is, enhancers, silencers, and promoters, although a broader definition of CREs may include untranslated exon sequences that operate in translational regulation. The definition of "promoter" is often ambiguous and is sometimes used to indicate a 5′-flanking sequence that includes not only a basal promoter but also enhancers. The basal promoter is a genomic region that initiates transcription of an associated gene but only produces basal level transcription when acting alone (Ong and Corces 2011) (Fig. 21.1). In this chapter, a promoter refers to a basal promoter. General transcription factors (GTFs), such as TATA-binding proteins (TBPs) and TBP-associated factors, bind to the promoter. This GTF complex formation on the promoter is required for transcriptional initiation, following which RNA polymerase initiates mRNA

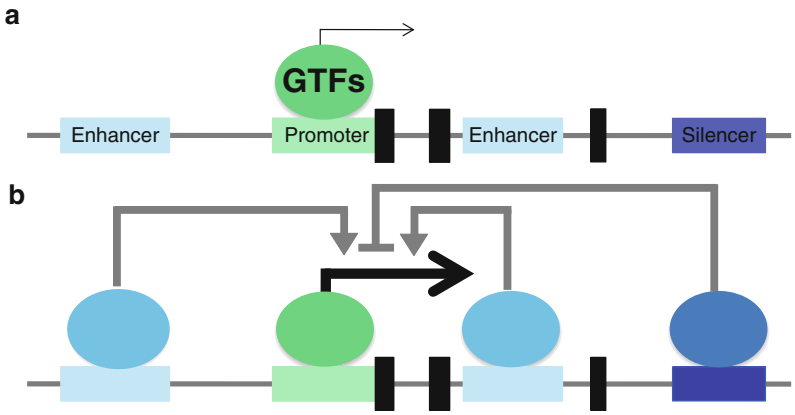

Fig. 21.1 *Cis*-regulatory element (*CRE*) for mRNA transcription. (**a)** Promoters are located near the transcription start site (*green box*). A promoter alone produces basal transcription levels. (**b)** In contrast, enhancers (*light blue*) and silencers (*dark blue*) are located upstream and/or downstream of the gene and/or in introns. The combination of enhancers and silencers produces tissue-specific transcription. Exons are shown in *black*

synthesis. Most GTFs are broadly expressed in vertebrate tissues and organs (Xiao et al. 2006; Huss et al. 2008). In contrast, several transcription factors binding to enhancers show tissue-dependent expression. These transcription factors recruit coactivators that interact with GTFs and activate mRNA transcription from the flanking basal promoter in a tissue-specific manner (Ong and Corces 2011) (Fig. 21.1). Silencers perform the function, which is opposite to that of enhancers, and are bound by transcriptional repressors that recruit corepressors and repress mRNA transcription (Susan and Michael 1996; Courey and Jia 2001; Gaston and Jayaraman 2003). Similar to transcriptional activators, several repressors show restricted expression in particular tissues and organs. Given that both enhancers and silencers contribute to the tissue specificity of transcription, they are probably involved in the evolution of gene expression patterns. Although enhancer evolution has been extensively discussed (Carroll 2008), silencer evolution has gained less attention.

21.2.1 Monospecific and Multispecific Enhancers

It is possible to classify enhancers into the following two types: monospecific enhancers, which drive expression only in a single or extremely narrow range of tissues, and multispecific enhancers, which drive expression in multiple tissues.

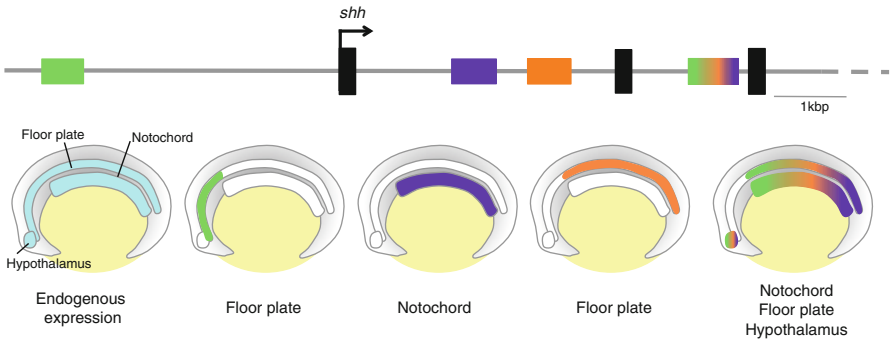

Fig. 21.2 Monospecific and multispecific enhancers. In zebrafish, *sonic hedgehog* (*shh*) is expressed in the floor plate, notochord, and hypothalamus at the three-somite stage (*light blue*). Enhancers, indicated in *green*, *purple*, and *orange*, are only active in one tissue. These *cis-regulatory* elements are categorized as monofunctional enhancers. The enhancer in the second intron is active in all tissues showing endogenous *shh* expression. This enhancer that drives multi-tissue gene expression is categorized as a multispecific enhancer. Diagram of the zebrafish *shh* locus shows the position of the enhancers in the *upper panel*. Schematic endogenous expression of *shh* and enhancer activities are shown in the *lower panel*

This distinction is critical for understanding the divergent paralogue expression. Analysis of enhancers of the zebrafish gene, *sonic hedgehog* (*shh*), provide a good example (Ertzer et al. 2007). Shh is a secreted signaling molecule expressed in the notochord, floor plate, and hypothalamus of zebrafish at the three-somite stage (Fig. 21.2). *Cis*-regulatory reporter assays using zebrafish have identified four zebrafish *shh* enhancers; one upstream of the gene, two in the first intron, and one in the second intron (Fig. 21.2). The upstream and first intronic enhancers are monospecific, with activities in the anterior floor plate (green box), notochord (purple box), and posterior floor plate (orange box), respectively. In contrast, the enhancer in the second intron is a multispecific enhancer, which is active in all *shh*-expressing tissues including the floor plate, notochord, and hypothalamus (Fig. 21.2).

21.3 Evolution of CREs

The evolution of CREs will depend on the following events: (1) enhancer innovation, (2) silencer innovation, and (3) ancestral CRE degeneration. Although it is believed that enhancer innovation has contributed to the divergent expression of paralogous genes, it is difficult to distinguish between real innovation and the remnant of an ancestral enhancer in several cases. However, we have good examples of degeneration of ancestral enhancers and silencer innovation. First, we discuss enhancer degeneration and silencer innovation, and subsequently focus on enhancer innovation.

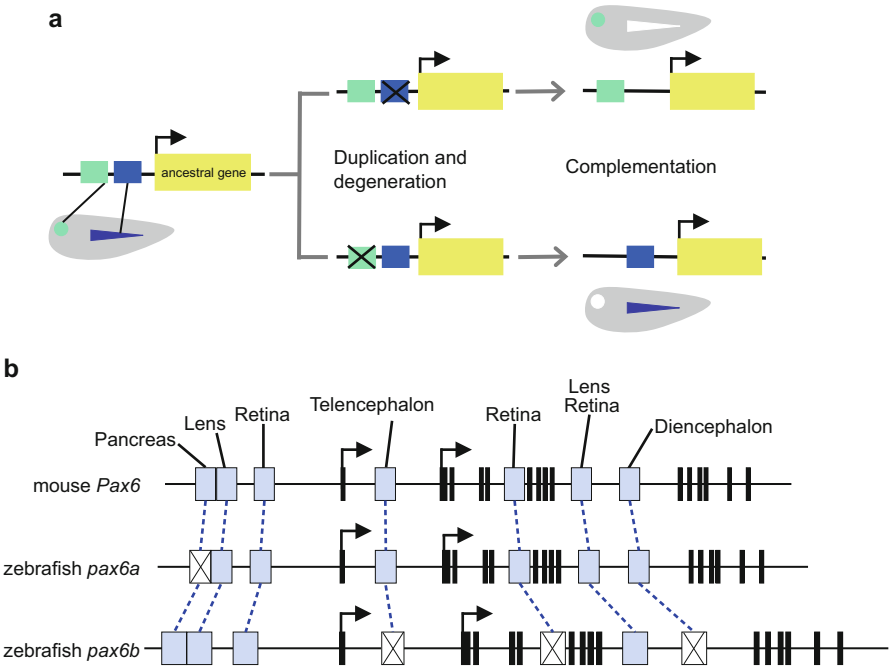

Fig. 21.3 (**a**) Differential utilization of paralogous genes by degeneration of an ancestral enhancer. Schematic representation of the duplication–degeneration–complementation (DDC) model, which assumes that ancestral genes have multiple tissue-specific enhancers (*green* and *blue*). After gene duplication, these tissue-specific enhancers complementarily degenerate from each of the duplicated loci, but one enhancer copy remains in each of the paralogues. (**b**) A comparison between the mouse *Pax6* locus and zebrafish *pax6a* and *pax6b* loci provides substantial evidence for the DDC model

21.3.1 Differential Utilization of Paralogous Genes via Ancestral Enhancer Degeneration: The Duplication–Degeneration–Complementation Model

The duplication–degeneration–complementation (DDC) model was first proposed by Allan Force and John Postlethwait to explain how both copies of duplicate genes can be preserved in a genome over a long evolutionary period (Force et al. 1999). This model hypothesizes that the ancestral gene has multiple tissue-specific enhancers (Fig. 21.3). After gene duplication, these tissue-specific enhancers complementarily degenerate from each of the duplicated loci (Fig. 21.3). At least one enhancer copy remains in each of the paralogues, resulting in complementary gene expression patterns that cover the original range of expression of the progenitor gene (Fig. 21.3). A comparison of the mouse *Pax6* locus and zebrafish *pax6a* and *pax6b* loci supports the DDC model (Kleinjan et al. 2008). A WGD event, which occurred

in the ancestral teleost, produced two *pax6* genes, *pax6a* and *pax6b*, whereas mammals have only one *Pax6* gene. Therefore, it is possible to postulate that the mouse *Pax6* locus, which possesses multiple tissue-specific enhancers such as those in the pancreas, lens, retina, telencephalon, and diencephalon, is of the ancestral type (Fig. 21.3) (Kleinjan et al. 2004; Williams et al. 1998; Xu et al. 1999; Kammandel et al. 1999). Kleinjan and colleagues observed that some enhancers (pancreas, telencephalon, and intronic retinal enhancers) were complementarily lost from zebrafish *pax6a* and *pax6b* loci and that this enhancer degeneration produced the differences in their expression patterns (Kleinjan et al. 2004) (Fig. 21.3). Another example of the DDC model is provided by zebrafish *engrailed2a* (*eng2a*) and *eng2b* genes, a pair of orthologues of mammalian *Engrailed2* (*En2*). Mouse *En2* is expressed in the somites, anterior hindbrain, jaw muscles, and midbrain–hindbrain boundary (MHB) (Postlethwait et al. 2004). In contrast, *eng2a* and *eng2b* are specifically expressed in the somites and anterior hindbrain, respectively, although they show overlapping expression in part of the MHB and jaw muscle (Fjose et al. 1992). A comparative genome sequence analysis of zebrafish *eng2a*, *eng2b*, and human *EN2* genes identified an array of conserved noncoding sequences (CNSs), which may function as enhancers (Woolfe et al. 2005; Postlethwait et al. 2004). As observed in the zebrafish *pax6a* and *pax6b* loci, some CNSs were complementarily lost from the zebrafish *eng2a/eng2b* loci (Postlethwait et al. 2004). This complementary degeneration of CNSs is probably responsible for differential expression, although experimental evidence for the enhancer activity of these CNSs has not been provided.

21.3.2 Differential Utilization of Paralogous Genes via Silencer Innovation

The significance of transcriptional repression during embryonic development and homeostasis has been extensively discussed (Susan and Michael 1996; Courey and Jia 2001). Direct evidence for the contribution of silencer evolution to the divergent expression patterns of paralogous genes was provided by our recent analysis of CREs in *pax8* and *pax2* (Ochi et al. 2012). These two genes, in addition to *pax5*, are considered to have arisen from a single ancestral gene following WGD1 and WGD2. *pax8* is primarily expressed in the kidney, ear, and thyroid gland during development, whereas *pax2* is expressed not only in the *pax8*-expressing tissues but also in other tissues such as the eye, pharyngeal arches, MHB, hindbrain, and spinal cord (Dressler et al. 1990; Heller and Brändli 1997).

Our comparative genome sequence analysis and the transgenic *Xenopus* assay revealed that *pax8* is associated with four conserved enhancers that drive multispecific *pax2*-like expression. Furthermore, one of these *pax8* enhancers shares remarkable sequence similarity with a CNS identified in the *pax2* locus (Fig. 21.4a). This pair of CNSs in *pax2* and *pax8* loci was probably generated by WGD, still retaining the ancestral regulatory mode (Fig. 21.4b). A more restricted expression pattern of the *pax8* gene than that generated by the multispecific enhancers suggests

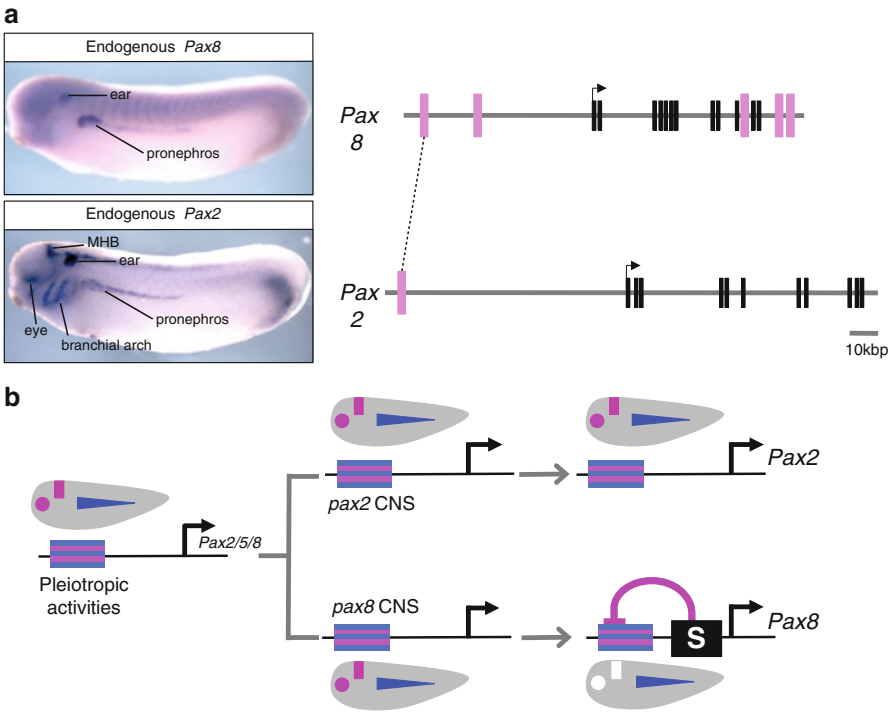

Fig. 21.4 Differential utilization of paralogous genes by silencer innovation. (**a**) Diagram of vertebrate *pax8* and *pax2* loci shows the position of conserved noncoding sequences (*CNSs*). *Magenta* and *black boxes* indicate CNSs and exons, respectively. For *pax2*, only one CNS, paralogous to the *pax8*-CNS, is shown. Endogenous expression of *pax8* and *Pax2* is shown on the *left*. (**b**) The amphioxus *pax2/5/8* promoter shows pleiotropic activities in most of the tissues that are homologous to vertebrate *pax2*-expressing tissues. Vertebrate *pax2* and *pax8* inherited the multispecific enhancer, and *pax8* acquired the tissue-specific silencer following whole-genome duplications. The silencer results in the divergent expression of paralogues

the presence of tissue-specific silencer(s). A silencer was identified in the proximal promoter region (Fig. 21.4b). To investigate the evolutionary origin of this silencer, we investigated the genome of the cephalochordate amphioxus, which diverged from the vertebrate lineage before WGDs occurred. Amphioxus has a single orthologue called *pax2/5/8*. This ancestral-type gene shows multispecific expression in tissues orthologous to vertebrate *pax2*-expressing tissues (Kozmik et al. 1999), and as expected, our transgenic experiment demonstrated that its promoter drives *pax2-like* expression. Thus, vertebrate *Pax8* has uniquely acquired tissue-specific silencers after WGDs. Although the paralogous pair *Pax2* and *Pax8* provides the only substantial evidence that acquisition of tissue-specific silencers caused differential utilization of paralogous genes, several paralogous gene pairs, such as *Otx1*/*Otx2*

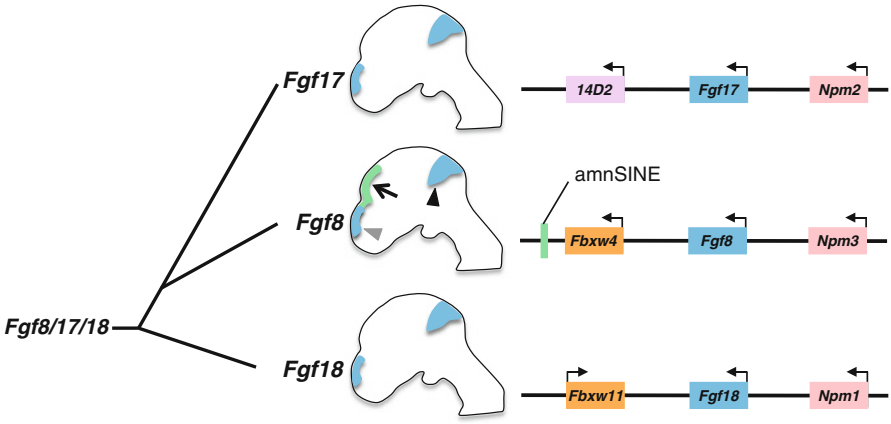

Fig. 21.5 Differential utilization of paralogous genes by enhancer innovation. Vertebrate fibroblast growth factors (*Fgf*) *8*, *Fgf17*, and *Fgf18* were derived from a single ancestral *Fgf8/17/18* gene through gene duplication events. *Fgf8*, *Fgf17*, and *Fgf18* are all expressed in the midbrain–hindbrain boundary and the telencephalic commissural plate (*black arrowhead* and *gray arrowhead*, respectively), whereas *Fgf8* is uniquely expressed in the diencephalon (*green shading*, *black arrow*). Schematic genome structures surrounding *Fgf8*, *Fgf17*, and *Fgf18* are shown on the *right*

and *Irx1/Irx3*, retain duplicated CNSs in their loci (McEwen et al. 2006). Therefore, it is possible that silencer innovations for divergent expression of paralogues have frequently occurred after WGD.

21.3.3 Differential Utilization of Paralogous Genes via Enhancer Innovation

One way to alter gene expression is by the acquisition of an enhancer. A growing body of evidence shows that genes have acquired novel expression domains by the following process: (1) nucleotide sequence changes produce novel transcription-binding motifs (Gompel et al. 2005), (2) preexisting enhancers relocate through genome rearrangement and enhance transcription of surrounding genes (Cande et al. 2009), and (3) genome-integrated retrotransposons become enhancers for surrounding genes (Sasaki et al. 2008). The enhancer innovations for gene expression divergence in fruit flies have been demonstrated and extensively discussed (Borok et al. 2010). However, it is not easy to distinguish cases of genuine enhancer innovation and the remnant of an ancestral enhancer in vertebrate paralogous genes. Nevertheless, divergent expression of mammalian fibroblast growth factor 8 (*Fgf8*), *Fgf17*, and *Fgf18*, which was probably produced by two rounds of WGD, may indicate the relationship between enhancer innovation and divergent expression of paralogs (Itoh and Ornitz 2008) (Fig. 21.4). A detailed expression analysis of *Fgf8*, *Fgf17*, and *Fgf18* shows that *Fgf8* transcripts predominate in the diencephalon hypothalamus at E10.5 of mouse embryos, whereas *Fgf17* and *Fgf18* are not expressed (Maruoka et al. 1998) (Fig. 21.5). Sasaki et al. (2008) discovered that an

amniota-specific short interspersed element (amnSINE), a type of retrotransposon, is integrated 178 kb downstream of *Fgf8*. Reporter analysis using transgenic mice revealed that this *Fgf8*-associated amnSINE functions as an enhancer in the lateral diencephalon and hypothalamus where endogenous *FGF8* is expressed (Sasaki et al. 2008; Maruoka et al. 1998). Therefore, unique expression of endogenous *Fgf8* in these tissues may have been produced by amnSINE in the *Fgf8* locus. Because it remains a possibility that the ancestral gene, *Fgf8/17/18*, possessed an enhancer that could have activated transcription in the diencephalon hypothalamus, future studies need to precisely address whether unique expression of *Fgf8* has been caused by the acquisition of a novel enhancer at the *Fgf8* locus, by the acquisition of novel silencers at the *Fgf17* and *Fgf18* loci, or by the degeneration of ancestral enhancers.

21.4 Conclusion

Massive quantities of genomic data and an increasing number of functional characterizations of CREs strongly support the model that the divergent expression of paralogues is caused by changes in the *cis*-regulatory sequence. The contribution of such changes in CRE to morphological innovations in vertebrates still remains unknown. However, there are certain indications that divergent expression of paralogues possibly contributed to the acquisition of unique vertebrate traits. One example is the correlation between the elongated body shape of reptiles and the intergenic region of *Hox* genes (Di-Poï et al. 2010). A comparison of the genomic sequences has shown that the intergenic regions of the posterior *HoxD* in reptiles are considerably longer than those of other corresponding vertebrate elements (Di-Poï et al. 2010). Because retrotransposons are highly integrated in this region, these genomic elements may have altered *HoxD* gene expression following the evolution of body shape (Di-Poï et al. 2010). An enhancer that may have contributed to the innovation of the placenta has also been shown by analysis of coelacanth CNS. Comparative genome sequence analysis and a reporter assay revealed that the coelacanth *Hoxa14* proximal promoter region, which is highly conserved in humans, mice, chickens, and horn sharks, drives reporter expression in the extra-embryonic regions of mice and extra-embryonic area vasculosa of the chick embryo, although humans, mice, and chickens have no *Hoxa14*. Horn shark *Hoxa14* has become a pseudogene (Amemiya et al. 2013). Based on these observations, those authors postulated that *Hoxa14* proximal promoter have somehow contributed to the evolution of the placenta (Amemiya et al. 2013). The genomic regions shown here may have altered vertebrate morphology during evolution, although it remains to be seen whether such genomic regions are really responsible for the formation of the elongated reptile body and placenta. A genetic engineering experiment, such as interchanging CREs between different species, may suggest future approaches to understand whether innovated CREs are responsible for morphological or biological innovations in the vertebrate (Cretekos et al. 2008). A genetically modified mouse, in which *paired related homeobox 1* (*Prx1*) expression is controlled by the corresponding element obtained from bat, has elongated forearm bones.

This morphological change partially explains the long bone in the wings of bats (Cretekos et al. 2008). Future analyses, such as replacement and deletion of *cis*-regulatory sequences in paralogous loci, may elucidate whether the divergence of *cis*-regulatory sequences between paralogues has produced morphological or biological innovations in vertebrates.

References

Amemiya CT, Alföldi J, Lee AP, Fan S, Philippe H, Maccallum I, Braasch I, Manousaki T, Schneider I, Rohner N et al (2013) The African coelacanth genome provides insights into tetrapod evolution. Nature (Lond) 496:311–316

Borok MJ, Tran DA, Ho MCW, Drewell R (2010) Dissecting the regulatory switches of development: lessons from enhancer evolution in *Drosophila*. Development (Camb) 137:5–13

Bouchard M, Pfeffer P, Busslinger M (2000) Functional equivalence of the transcription factors Pax2 and Pax5 in mouse development. Development (Camb) 127:3703–3713

Cande JD, Chopra VS, Levine M (2009) Evolving enhancer-promoter interactions within the tinman complex of the flour beetle, *Tribolium castaneum*. Development (Camb) 136:3153–3160

Carroll SB (2008) Evo-devo and an expanding evolutionary synthesis: a genetic theory of morphological evolution. Cell 134:25–36

Courey AJ, Jia S (2001) Transcriptional repression: the long and the short of it. Genes Dev 15:2786–2796

Cretekos CJ, Wang Y, Green ED, Martin JF, Rasweiler JJ 4th, Behringer RR (2008) Regulatory divergence modifies limb length between mammals. Genes Dev 22:141–151

Dehal P, Boore JL (2005) Two rounds of whole genome duplication in the ancestral vertebrate. PLoS Biol 3:e314

Di-Poï N, Montoya-Burgos JI, Miller H, Pourquié O, Milinkovitch MC, Duboule D (2010) Changes in Hox genes' structure and function during the evolution of the squamate body plan. Nature (Lond) 464:99–103

Dressler GR, Deutsch U, Chowdhury K, Nornes HO, Gruss P (1990) Pax2, a new murine paired-box-containing gene and its expression in the developing excretory system. Development (Camb) 109:787–795

Ertzer R, Müller F, Hadzhiev Y, Rathnam S, Fischer N, Rastegar S, Strähle U (2007) Cooperation of sonic hedgehog enhancers in midline expression. Dev Biol 301:578–589

Fjose A, Njølstad PR, Nornes S, Molven A, Krauss S (1992) Structure and early embryonic expression of the zebrafish engrailed-2 gene. Mech Dev 39:51–62

Force A, Lynch M, Pickett FB, Amores A, Yan YL, Postlethwait J (1999) Preservation of duplicate genes by complementary, degenerative mutations. Genetics 151:1531–1545

Gaston K, Jayaraman P (2003) Transcriptional repression in eukaryotes: repressors and repression mechanisms. Cell Mol Life Sci 60:721–741

Gompel N, Prud B, Wittkopp PJ, Kassner VA, Carroll SB (2005) Chance caught on the wing: *cis-regulatory* evolution and the origin of pigment patterns in *Drosophila*. Nature (Lond) 433:481–487

Heller N, Brändli AW (1997) *Xenopus* Pax-2 displays multiple splice forms during embryogenesis and pronephric kidney development. Mech Dev 69:83–104

Huss JW, Orozco C, Goodale J, Wu C, Batalov S, Vickers TJ, Valafar F, Su AI (2008) A gene wiki for community annotation of gene function. PLoS Biol 6:e175

Itoh N, Ornitz DM (2008) Functional evolutionary history of the mouse Fgf gene family. Dev Dyn 237:18–27

Jaillon O, Aury JM, Brunet F, Petit JL, Stange-Thomann N, Mauceli E, Bouneau L, Fischer C, Ozouf-Costaz C, Bernot A, Nicaud S, Jaffe D, Fisher S, Lutfalla G, Dossat C, Segurens B, Dasilva C, Salanoubat M, Levy M, Boudet N, Castellano S, Anthouard V, Jubin RCH (2004) Genome duplication in the teleost fish *Tetraodon nigroviridis* reveals the early vertebrate protokaryotype. Nature (Lond) 431:946–957

Kammandel B, Chowdhury K, Stoykova A, Aparicio S, Brenner S, Gruss P (1999) Distinct *cis-essential* modules direct the time-space pattern of the Pax6 gene activity. Dev Biol 205:79–97

Kleinjan DA, Seawright A, Childs AJ, Van Heyningen V (2004) Conserved elements in Pax6 intron 7 involved in (auto)regulation and alternative transcription. Dev Biol 265:462–477

Kleinjan DA, Bancewicz RM, Gautier P, Dahm R, Schonthaler HB, Damante G, Seawright A, Hever AM, Yeyati PL, Van Heyningen V et al (2008) Subfunctionalization of duplicated zebrafish pax6 genes by *cis*-regulatory divergence. PLoS Genet 4:e29

Koonin EV (2005) Orthologs, paralogs, and evolutionary genomics. Annu Rev Genet 39:309–338

Kozmik Z, Holland ND, Kalousova A, Paces J, Schubert M, Holland LZ (1999) Characterization of an amphioxus paired box gene, AmphiPax2/5/8: developmental expression patterns in optic support cells, nephridium, thyroid-like structures and pharyngeal gill slits, but not in the midbrain–hindbrain boundary region. Development (Camb) 126:1295–1304

Maruoka Y, Ohbayashi N, Hoshikawa M, Itoh N, Hogan BL, Furuta Y (1998) Comparison of the expression of three highly related genes, Fgf8, Fgf17 and Fgf18, in the mouse embryo. Mech Dev 74:175–177

McEwen GK, Woolfe A, Goode D, Vavouri T, Callaway H, Elgar G (2006) Ancient duplicated conserved noncoding elements in vertebrates: a genomic and functional analysis. Genome Res 16:451–465

Ochi H, Tamai T, Nagano H, Kawaguchi A, Sudou N, Ogino H (2012) Evolution of a tissue-specific silencer underlies divergence in the expression of pax2 and pax8 paralogues. Nat Commun 3:848

Ohno S (1970) Evolution by gene duplication. Springer, Berlin

Ong CT, Corces VG (2011) Enhancer function: new insights into the regulation of tissue-specific gene expression. Nat Rev Genet 12:283–293

Postlethwait J, Amores A, Cresko W, Singer A, Yan YL (2004) Subfunction partitioning, the teleost radiation and the annotation of the human genome. Trends Genet 20:481–490

Sasaki T, Nishihara H, Hirakawa M, Fujimura K, Tanaka M, Kokubo N, Kimura-Yoshida C, Matsuo I, Sumiyama K, Saitou N et al (2008) Possible involvement of SINEs in mammalian-specific brain formation. Proc Natl Acad Sci USA 105:4220–4225

Stern DL, Orgogozo V (2008) The loci of evolution: how predictable is genetic evolution? Evolution 62:2155–2177

Susan G, Michael L (1996) Transcriptional repression in development. Curr Opin Cell Biol 8:358–364

Williams SC, Altmann CR, Chow RL, Hemmati-Brivanlou A, Lang RA (1998) A highly conserved lens transcriptional control element from the Pax-6 gene. Mech Dev 73:225–229

Woolfe A, Goodson M, Goode DK, Snell P, McEwen GK, Vavouri T, Smith SF, North P, Callaway H, Kelly K et al (2005) Highly conserved non-coding sequences are associated with vertebrate development. PLoS Biol 3:e7

Wray GA, Hahn MW, Abouheif E, Balhoff JP, Pizer M, Rockman MV, Romano LA (2002) The evolution of transcriptional regulation in eukaryotes. Mol Biol Evol 20:1377–1419

Xiao L, Kim M, DeJong J (2006) Developmental and cell type-specific regulation of core promoter transcription factors in germ cells of frogs and mice. Gene Expr Patterns 6:409–419

Xu PX, Zhang X, Heaney S, Yoon A, Michelson AM, Maas RL (1999) Regulation of Pax6 expression is conserved between mice and flies. Development (Camb) 126:383–395

Chapter 22
Fins and Limbs: Emergence of Morphological Differences

Tohru Yano, Haruka Matsubara, Shiro Egawa, Koun Onodera, and Koji Tamura

Abstract Paired appendages (fins and limbs) are regarded as distinct morphologies by classification of skeletal patterns. On the basis of sequential orientation and articulation of tetrapod limb bones, we can understand that stylopodial/zeugopodial skeletal elements are present in an extinct and extant basal sarcopterygian (coelacanth and lungfish) fin and that only nonhomologous radial bones exist in a zebrafish fin. From these phylogenetic views, morphological differences between fins and limbs and paleontological discoveries of limb-like fins of basal sarcopterygians emphasize both the homologous skeletal elements and tetrapodomorph evolution. During embryogenesis, on the other hand, initial fin development requires apical ectodermal ridge (AER) signals as does tetrapod limb development, and then the AER itself starts to transform into a fin-specific structure, the apical fold (AF). *HoxD* genes are involved in fish fin development as in tetrapod limb development, but the resultant skeletal patterns of fins are very different from those of limbs as a result of differences in regulation of genes such as *HoxD*. From these developmental aspects, we can understand that both fins and limbs develop by common mechanisms, including fibroblast growth factors (FGFs) from the AER and *Hox* genes, and that alteration of basic mechanisms by heterochronic/heterometric change in

T. Yano (✉)
Department of Developmental Biology and Neurosciences, Graduate School of Life Sciences, Tohoku University, Sendai, Japan

Present Affiliation: Department of Anatomy, The Jikei University School of Medicine, Tokyo, Japan
e-mail: tohruyano@jikei.ac.jp

H. Matsubara • S. Egawa • K. Tamura
Department of Developmental Biology and Neurosciences, Graduate School of Life Sciences, Tohoku University, Sendai, Japan

K. Onodera
Department of Developmental Biology and Neurosciences, Graduate School of Life Sciences, Tohoku University, Sendai, Japan

Present Affiliation: Graduate School of Biostudies, Kyoto University, Kyoto, Japan

H. Kondoh and A. Kuroiwa (eds.), *New Principles in Developmental Processes*,
DOI 10.1007/978-4-431-54634-4_22, © Springer Japan 2014

expression of AER/AF signals and *Hox* gives rise to morphological differences among paired appendages. In this chapter, we describe homology and difference in several research fields (genome commonality/difference, developmental commonality/difference, and anatomical or paleontological correspondence/difference) and especially explain a scenario of fin-to-limb evolution.

Keywords Endoskeleton • Exoskeleton • Fin • Limb

22.1 Introduction

Paired appendages in vertebrates, the fins and limbs, are organs for locomotion. In the vertebrate lineage, paired appendages evolved from fins to limbs (Fig. 22.1). Chondrichthyans and actinopterygians possess paired fins (pectoral and pelvic), and tetrapods (amphibians, reptiles, birds, and mammals) possess limbs (fore and hind). These paired appendages are classified into fins or limbs, not by locomotive function (for example, mudskippers creep on the bog by using fins, and whales swim in the sea by using flipper-like limbs), but by skeletal patterns and the cellular properties of bones. There are differences in skeletal patterns, not only between fins and limbs, but also among fins. For understanding the mechanism for paired appendage

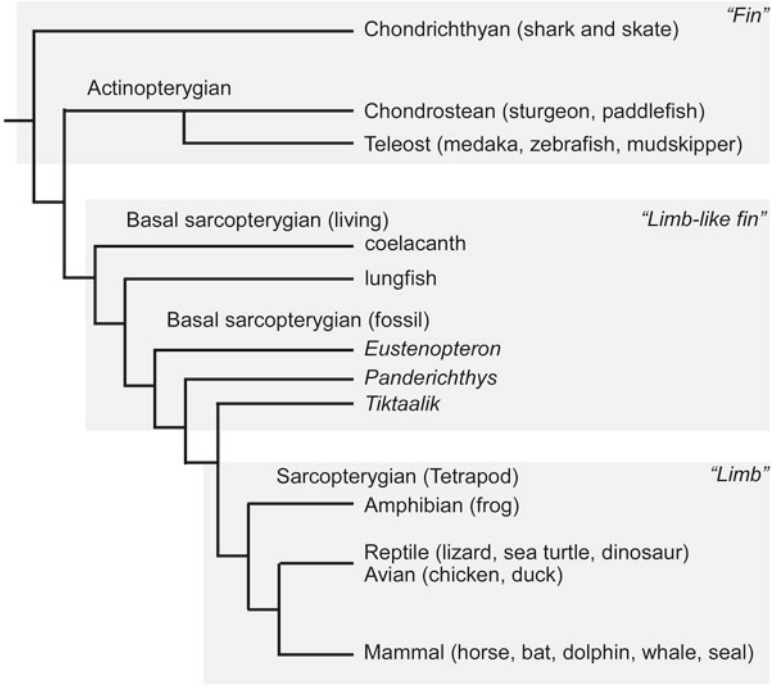

Fig. 22.1 Phylogenic tree of vertebrates that possess paired appendages

evolution from fin to limb, we here overview common principles of paired appendage development, focusing on the cellular properties of the skeleton, and introduce evolutional alterations of the developmental mechanisms (roles of ectodermal structures and regulation of Hox genes) in fins and limbs.

22.2 We Can Understand Homology and Differences Between Fin and Limb from the Point of View of Development

The skeleton in vertebrates can be classified into endoskeleton and exoskeleton according to developmental mechanisms. The endoskeleton is located deep inside the body and functions as a supporting structure, and it is mainly formed by the replacement from cartilage (endochondral ossification). Both fins and limbs consist of endoskeletons, although the morphological patterns are different (Yano and Tamura 2013) (Fig. 22.2). The limb endoskeleton is mainly formed from the proximal to distal direction during embryogenesis, giving rise to three skeletal domains (from proximal to distal, one long bone in the stylopod, two long bones in the zeugopod, and many short and long bones in the autopod) (Fig. 22.2a). On the other hand, the fin endoskeleton is not composed of three clear domains along the proximal–distal axis, and there are many radial bones only at the base of the fin. The exoskeleton is formed underneath the skin and protects/supports the body on the surface; it is formed not through a cartilaginous intermediate but by direct ossification of mesenchymal cells. Fin exoskeletal components, which are formed at distal to radial bones, are characteristic of a fin skeleton. The fin exoskeleton consists of lepidotrichia and is formed within the fin ray (the distalmost fin structure with membrane-like epithelium and mesenchymal supports). In chondrichthyans, ceratotrichia (collagenous fibrils) are formed in the fin ray region. Vertebrates in the water (fish) may have evolved into tetrapods, land vertebrates (amphibians), in the Devonian period (about 4 billion years ago). There are several fossils of basal sarcopterygians that possess characteristic appendages (limb-like fins). Limb-like fins consist of both a fin ray (with an exoskeleton) and an endoskeleton with incomplete three skeletal domains (Boisvert et al. 2008; Shubin et al. 2006). Importantly, the existence of fin rays with an exoskeleton is a good criterion for classification as a fin, and the lateral appendage in basal sarcopterygians is categorized as not a limb but a limb-like fin (Shubin et al. 2006).

22.2.1 Cellular Property of Fin Mesenchyme Tells Us the Scenario of Fin-to-Limb Evolution

An understanding of the mechanisms of endoskeleton and exoskeleton formation in fin development is important for elucidating the story of paired appendage evolution in gnathostomes. In limbs, the endoskeleton consists of lateral plate mesoderm

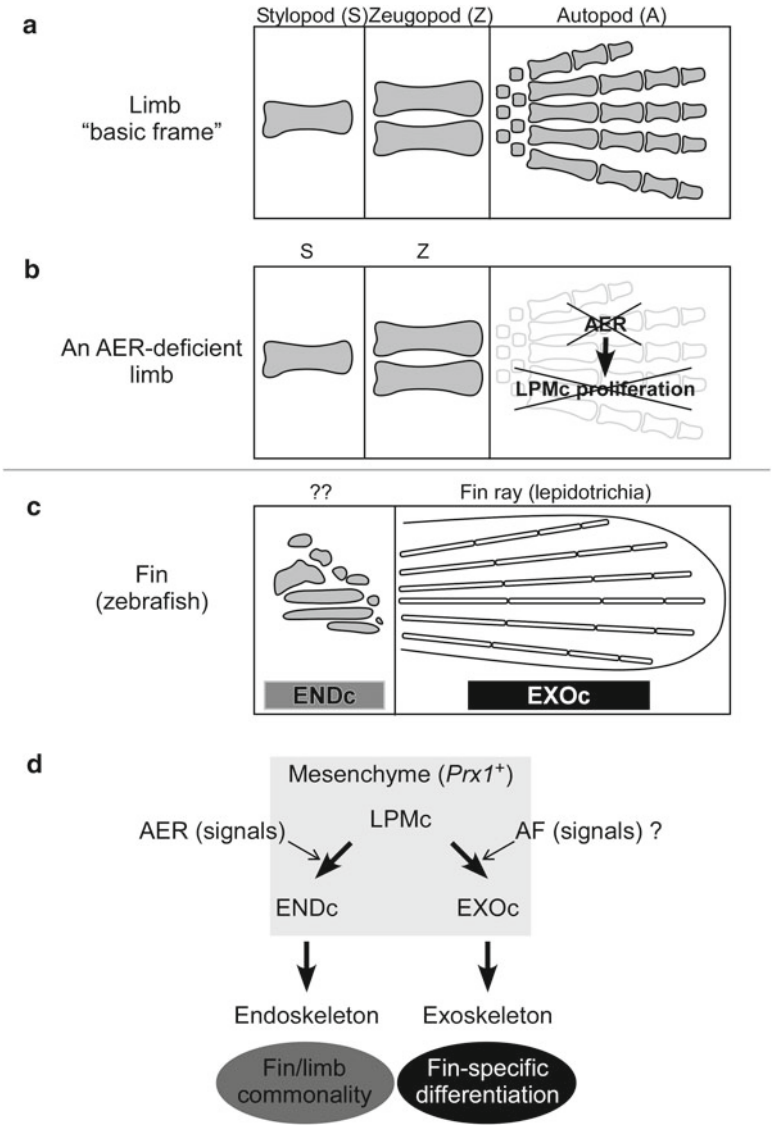

Fig. 22.2 Developmental-morphological diagrams of the fin and limb. **a** Typical skeletal pattern of the limb. *S* stylopod (humerus/femur), *Z* zeugopod (radius/tibia and ulna/fibula), *A* autopod (carpal/tarsal bones, metacarpal/metatarsal bones, and phalanges). *Gray components* represent individual endoskeletal bones, abbreviated. **b** When the functional apical ectodermal ridge (*AER*) is lost [e.g., at stages of stylopod/zeugopod formation], the limb bud stops developing and lateral plate mesoderm (*LPM*)-derived mesenchymal cells (*LPMc*) do not construct the distal part of the limb. **c** In zebrafish, there are four proximal radials and about eight distal radials, into which the endoskeleton-forming cells (*ENDc*) differentiate. The AER transforms into the AF at early stages of development, and LPMc contribute to the formation of lepidotrichia (*black-outlined rods*) as exoskeleton-forming cells (*EXOc*). **d** Scheme of skeletal differentiation

(LPM)-derived mesenchymal cells (LPMc). Although the paired fin endoskeleton also consists of LPMc, there have been various theories regarding the developmental origin of exoskeleton-forming cells (EXOc). For several decades, EXOc (which form lepidotrichia) in the paired fin were believed to be derived from neural crest cells (Hall 2005; Smith et al. 1994; Witten and Huysseune 2007), and it has long been suggested that loss of the fin ray skeleton during fin-to-limb evolution was caused by loss of the ability of skeletogenesis in trunk neural crest cells.

Paired-related homeobox 1 (*Prrx1*) is expressed in the undifferentiated mesodermal cells (LPMc) of the limb/fin bud and is extinguished when the LPMc initiate condensation and form the endoskeleton (Cserjesi et al. 1992; Hernández-Vega and Minguillón 2011). Mouse *Prrx1* limb bud enhancer is widely used to mark the LPMc of zebrafish, frog, and mouse (Martin and Olson 2000; Suzuki et al. 2007; Yano and Tamura 2013). We found that the *Prrx1* enhancer is active not only in the endoskeleton-forming cells (ENDc) but also in the EXOc during pectoral fin development of zebrafish (Yano and Tamura 2013). This observation suggests that the EXOc also originates from the mesoderm of the fin bud. Our recent study on cell lineage analysis of LPMc directly confirmed that the EXOc are derived not from neural crest cells but from the LPMc (Shimada et al. 2013). This finding indicates that both the endoskeleton and exoskeleton in paired fins are formed from the same type of mesenchymal cells, LPMc. This finding also raised the possibility of the presence of a unique system that switches the direction of the differentiation pathway of LPMc from ENDc to EXOc in zebrafish.

22.2.2 AER and AF Are Crucial for Causing Morphological Differences Between Fins and Limbs

In gnathostome development, a part of the LPM grows, protrudes, and forms the primordium of a paired appendage (fin bud or limb bud). The budding position is defined as a *Fgf10*-expressing region in the LPM (Norton et al. 2005; Ohuchi et al. 1997; Yonei-Tamura et al. 1999). Ectodermal cells receiving the Fgf10 signal form the apical ectodermal ridge (AER), which is a thickened epidermal structure at the distal edge of the limb/fin primordium at the dorsal–ventral boundary. The AER acts as one of the important signaling centers for fin or limb development, and it secretes FGFs that induce proliferation of LPMc (Grandel et al. 2000; Mariani and Martin 2003).

During limb development, the AER exists throughout the patterning stage of the limb endoskeleton until formation of digital tips in the autopod. During fin development, on the other hand, the AER starts to elongate distally then forms the fin ray, leaving the endoskeletal region proximally. This transformed AER is called the apical fold (AF), and the AF consists of two layered (back-to-back) epidermal sheets (Dane and Tucker 1985). Migrating LPMc (as EXOc) invade into a slit of the AF epidermal sheets, and the EXOc in the AF region differentiate into osteocytes,

giving rise to lepidotrichia in the fin ray. As the formation of lepidotrichia is a characteristic feature of the fin, the epithelial transformation from the AER to the AF and subsequent migration of EXOc are crucial events for development of the characteristic fin structure (Fig. 22.2c). However, there were no experimental data that confirmed the model of a relationship between the AER–AF transition and skeletal morphology of paired appendages (Thorogood 1991). To understand the details of the AF structure and roles of the AER/AF in fin development, we investigated AF morphogenesis in the developing fin bud. At later stages of fin development, the AF grows distally with little proliferation of ectodermal cells, but the ectodermal AF cells change their shape from sphere morphology to a tile-like morphology (Yano et al. 2012). It is likely that the presumptive fin ray region (filled with EXOc) is stretched distally during the AF morphogenesis. Interestingly, this region stops stretching and developing when the distal portion of the AF is removed. Inhibition of AF signals [Fgf signals and *transcription factor 7* (*tcf7*)] causes shrinkage of the presumptive fin ray region (Yano et al. 2012). Malformation of the ectodermal AF cells also can be seen in *ectodysplasin receptor* (*edar*) mutant fish, which exhibit loss of the exoskeleton (Harris et al. 2008). These findings suggest that the AF is important for formation of the fin ray region. Moreover, when AF formation is blocked by repeated ablation of the AF, the AER continues to interact with the endoskeletal region, causing excess mesenchymal proliferation and additional formation of an endoskeleton (Yano et al. 2012). In tetrapod limb development, exposure to AER signals causes mesenchymal proliferation, and the deposition/formation of endoskeleton is stopped by AER removal (Mariani and Martin 2003; Fig. 22.2b). Our findings suggest that change in timing of AER–AF transition is important for formation of endoskeleton and exoskeleton in fin development and that AF regulation is different from the AER regulation against LPMc (Fig. 22.2c). The heterochronic change in AER–AF transition and the AF loss (continuous secretion of AER signals) may be key factors for skeletal diversification of paired fins and fin-to-limb evolution.

22.3 Correlations Between Genome, Developmental Mechanisms, and Morphology Can Explain Tetrapodomorph Evolution

Our recent findings indicated that skeletons in both paired fins and limbs are formed from LPMc, as described in the previous section (Shimada et al. 2013; Yano et al. 2012; Yano and Tamura 2013), suggesting that LPMc can differentiate into both an endoskeleton and an exoskeleton. Fin ray loss and digit formation occurred during evolution from fish to tetrapods, but we can consider that both of these were caused concurrently by regulation of the differentiation of LPMc. On the basis of these new findings, we next describe correlations between genome, developmental mechanisms, and morphology in fin-to-limb evolution with focus on Hox gene regulation.

In vertebrate appendage development, expression and function of Hox genes are common and important principles in endoskeletal formation along the proximal–distal

and anterior–posterior axes, but regulations on their expression are different in fins and limbs (Ahn and Ho 2008; Tamura et al. 2008; Fig. 22.3). *HoxD* genes play important roles in skeletal patterning of the appendage endoskeleton. At later stages of limb development, *Hoxd-11–13* expression domains are seen in the digit-forming region regulated by *HoxD* genomic sequences (enhancers) (Tarchini et al. 2006) (Fig. 22.3a). Interestingly, a tetrapod-specific *cis*-regulatory element of *HoxD* (CsC; conserved sequence C) does not exist in the zebrafish genome. To elucidate CsC activation, Freitas et al. (2012) demonstrated reporter assays by using transgenic fish and showed that CsC could drive the reporter gene expression at only the distal part of the endoskeleton-forming region [corresponding to the region of "HoxD (late)" in Fig. 22.3b]. Freitas et al. (2012) suggest that there are transcription factors that can interact with CsC and give rise to the *HoxD* expression in zebrafish, although CsC is missing in zebrafish. It is a possibility that the *HoxD* activation by CsC is important for formation of the limb-like skeleton in mice limbs, because the expression pattern of the CsC reporter gene is similar to that of the *Hoxd-13* gene, which is at a tetrapod-specific region (digit region). By using zebrafish embryos, Freitas et al. (2012) also showed that overexpression of *Hoxd-13a* caused proliferation of LPMc in the AF region. Because the authors showed that the AF thickening by *Hoxd-13a* overexpression did not occur over the AER–AF transition stage (late stages), excessive proliferation of LPMc may be caused from AER-forming stages (early stages) or by a sufficient amount of Hoxd-13 protein. Therefore, spatiotemporal (heterochronic; Sakamoto et al. 2009) or quantitative (heterometric; Freitas et al. 2012) regulation of *HoxD* expression from AER-forming stages (early stages) may be important for proliferation of LPMc as well as AER/AF regulation against LPMc (as described in the previous section). Production of many LPMc may be necessary for stylopod–zeugopod partition (early stages; reviewed by Yano and Tamura 2013) and autopod/digit formation (late stages) in tetrapodomorph evolution (Fig. 22.3c).

Correlation between AER/AF function and endoskeleton/exoskeleton formation can explain the morphological feature of basal sarcopterygian appendages. In the coelacanth, there are several radial bones distal to the predicted stylopod/zeugopod, and an exoskeleton [consisting of camptotrichia (white rods in Fig. 22.4a)] forms in the fin ray. Despite well-developed endoskeleton in the coelacanth paired fin, however, CsC does not exist in the coelacanth genome (Amemiya et al. 2013). It is possible that many LPMc proliferate at AER-forming stages in coelacanth fin development and that incomplete stylopod/zeugopod/autopod compartments are formed before LPMc differentiate into EXOc by AER–AF transition. Anatomical observations have also suggested a limb-like skeletal pattern in the lungfish lateral appendage (Coates et al. 2002). In contrast to the fin skeleton of the coelacanth, there are many radial bones in the region distal to the zeugopod domain (approximately corresponding to the autopod domain in tetrapod limbs) (Fig. 22.4b, c). In lungfish fin development, *Hoxd-13* is expressed at this radial bone region. It is possible that *Hoxd-13* expression in the autopod domain is regulated by CsC in the lungfish genome and that much proliferation of LPMc occurs. Other studies revealed that AER–AF transition also occurred in the developing lungfish fin bud, and exoskeletal components (camptotrichia) existed in the fin ray (Hodgkinson et al. 2009;

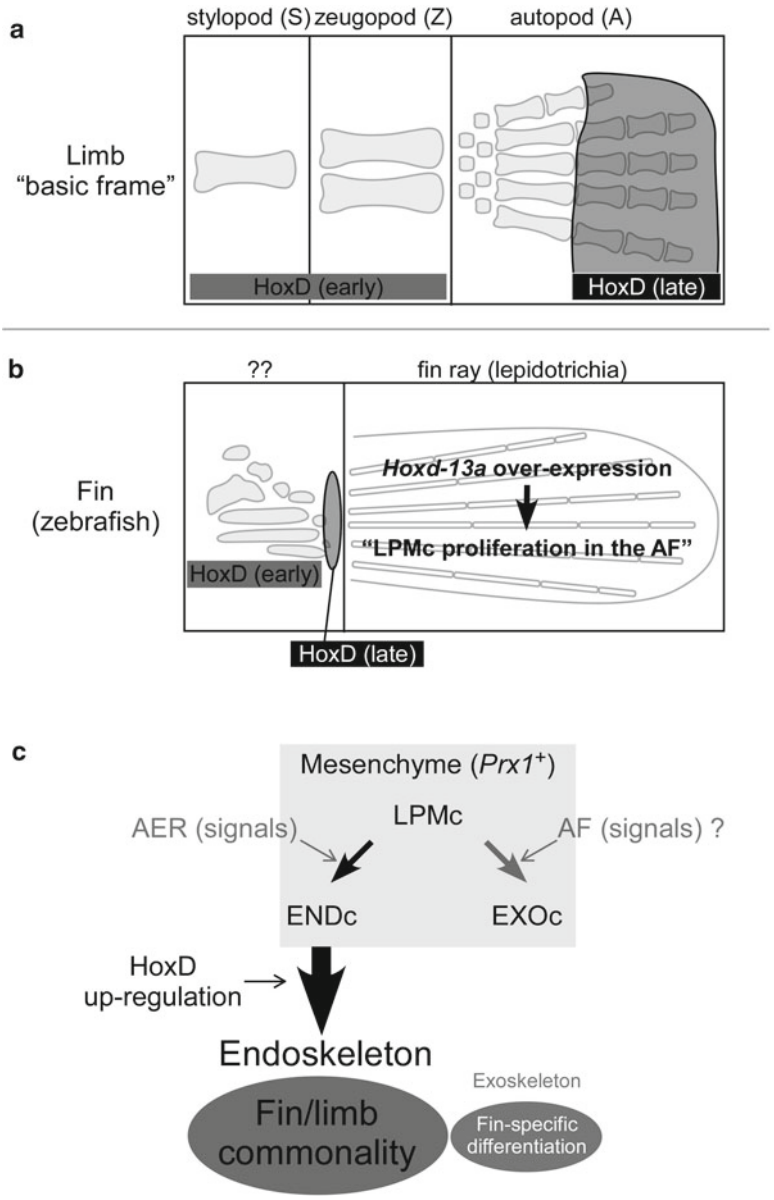

Fig. 22.3 Developmental-morphological diagrams of HoxD regulation in paired appendages. **a** Typical skeletal pattern of the limb. In the timing of stylopod/zeugopod development, *HoxD* genes are expressed (early phase), and the late phase of HoxD regulation mechanisms starts to work at the timing of digit formation (enclosed in *black line*). *Hoxd-13* is expressed at the digit-forming region in tetrapod limb development. **b** In zebrafish, there is a region regulated by the late phase of HoxD enhancer (CsC) at the distal and posterior edges of the endoskeletal region. Freitas et al. (2012) have shown that *Hoxd-13a* overexpression caused proliferation of LPMc. **c** Scheme of skeletal differentiation regulated by HoxD

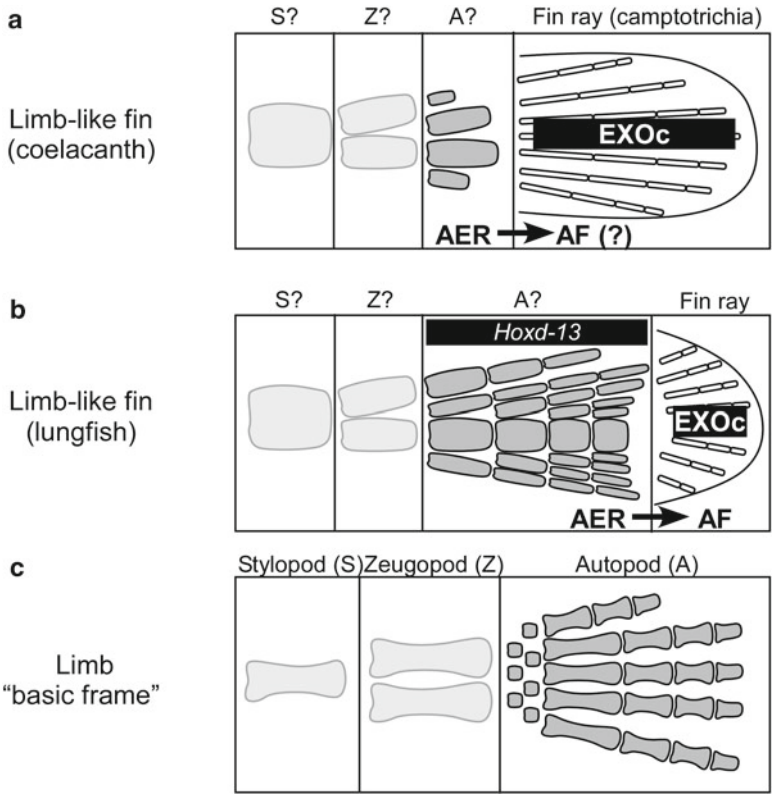

Fig. 22.4 Developmental-morphological diagrams of paired appendage diversification. **a** In the coelacanth fin, camptotrichia are formed in the fin ray. **b** In the lungfish, there are many endoskeletal elements distal to the zeugopod domain. *Hoxd-13* mRNA is expressed in this endoskeletal region. **c** Typical skeletal pattern of the limb. *Hoxd-13* is expressed in the digit-forming region in tetrapod limbs

Johanson et al. 2007). In this sense, it is also possible that the later timing of AER–AF transition causes much proliferation of LPMc and addition of many radial bones. Taken together, the heterometric change in *HoxD* expression (Freitas et al. 2012) and the heterochronic change in AER–AF transition (Thorogood 1991; Yano et al. 2012) may bring about skeletal diversification in the autopod.

22.4 Conclusion

As for the formation of a paired appendage skeleton, we can understand that fins and limbs develop with shared developmental mechanisms of endoskeleton formation. These mechanisms are changeable by genomic evolution, and consequently

morphological differences of paired appendages in gnathostomes occur. In this review, we have shown that differences between the endoskeleton and exoskeleton are caused by alteration of the differentiation of LPMc, alteration of the developmental cue from the apical thickened epidermis (AER and AF), and alteration of *Hox* expression. To elucidate fin-to-limb evolution and paired appendage diversification, we need to investigate several issues further. (1) We need to find molecular mechanisms of the differentiation of LPMc. By elucidation of developmental mechanisms of both endoskeleton and exoskeleton formed by homogenous LPMc, we can understand how LPMc are distributed to endoskeleton and exoskeleton among the skeletal variation of paired appendages. (2) We need to find an AER/AF factor as a determinant of skeletogenesis. Especially, it is important to find AF-specific signals that control fin ray formation and exoskeleton formation. Finally, we need to find genomic alteration near genes of AF signals to understand gnathostome evolution. (3) We need to elucidate the synergistic roles of Hox and AER/AF factors in fin and limb development. We do not yet know whether either Hox regulation or the function of AER/AF is the direct determinant for morphological differences between fin and limb. By using transgenic analyses, for instance, we need to investigate roles of Hox in AER/AF formation and the roles of AER/AF in Hox regulation in fish fin development.

References

Ahn D, Ho RK (2008) Tri-phasic expression of posterior Hox genes during development of pectoral fins in zebrafish: implications for the evolution of vertebrate paired appendages. Dev Biol 322(1):220–233. doi:10.1016/j.ydbio.2008.06.032

Amemiya CT, Alfoldi J, Lee AP, Fan S, Philippe H, Maccallum I, Braasch I, Manousaki T, Schneider I, Rohner N, Organ C, Chalopin D, Smith JJ, Robinson M, Dorrington RA, Gerdol M, Aken B, Biscotti MA, Barucca M, Baurain D, Berlin AM, Blatch GL, Buonocore F, Burmester T, Campbell MS, Canapa A, Cannon JP, Christoffels A, De Moro G, Edkins AL, Fan L, Fausto AM, Feiner N, Forconi M, Gamieldien J, Gnerre S, Gnirke A, Goldstone JV, Haerty W, Hahn ME, Hesse U, Hoffmann S, Johnson J, Karchner SI, Kuraku S, Lara M, Levin JZ, Litman GW, Mauceli E, Miyake T, Mueller MG, Nelson DR, Nitsche A, Olmo E, Ota T, Pallavicini A, Panji S, Picone B, Ponting CP, Prohaska SJ, Przybylski D, Saha NR, Ravi V, Ribeiro FJ, Sauka-Spengler T, Scapigliati G, Searle SM, Sharpe T, Simakov O, Stadler PF, Stegeman JJ, Sumiyama K, Tabbaa D, Tafer H, Turner-Maier J, van Heusden P, White S, Williams L, Yandell M, Brinkmann H, Volff JN, Tabin CJ, Shubin N, Schartl M, Jaffe DB, Postlethwait JH, Venkatesh B, Di Palma F, Lander ES, Meyer A, Lindblad-Toh K (2013) The African coelacanth genome provides insights into tetrapod evolution. Nature (Lond) 496(7445):311–316. doi:10.1038/nature12027

Boisvert CA, Mark-Kurik E, Ahlberg PE (2008) The pectoral fin of *Panderichthys* and the origin of digits. Nature (Lond) 456(7222):636–638. doi:10.1038/nature07339

Coates MI, Jeffery JE, Rut M (2002) Fins to limbs: what the fossils say. Evol Dev 4(5):390–401

Cserjesi P, Lilly B, Bryson L, Wang Y, Sassoon DA, Olson EN (1992) MHox: a mesodermally restricted homeodomain protein that binds an essential site in the muscle creatine kinase enhancer. Development (Camb) 115(4):1087–1101

Dane PJ, Tucker JB (1985) Modulation of epidermal cell shaping and extracellular matrix during caudal fin morphogenesis in the zebra fish *Brachydanio rerio*. J Embryol Exp Morphol 87:145–161

Freitas R, Gomez-Marin C, Wilson JM, Casares F, Gomez-Skarmeta JL (2012) Hoxd13 contribution to the evolution of vertebrate appendages. Dev Cell 23(6):1219–1229. doi:10.1016/j.devcel.2012.10.015

Grandel H, Draper BW, Schulte-Merker S (2000) dackel acts in the ectoderm of the zebrafish pectoral fin bud to maintain AER signaling. Development (Camb) 127(19):4169–4178

Hall BK (2005) Bones and cartilage: developmental and evolutionary skeletal biology. Elsevier Academic, London

Harris MP, Rohner N, Schwarz H, Perathoner S, Konstantinidis P, Nusslein-Volhard C (2008) Zebrafish eda and edar mutants reveal conserved and ancestral roles of ectodysplasin signaling in vertebrates. PLoS Genet 4(10):e1000206. doi:10.1371/journal.pgen.1000206

Hernández-Vega A, Minguillón C (2011) The Prx1 limb enhancers: targeted gene expression in developing zebrafish pectoral fins. Dev Dyn 240(8):1977–1988. doi:10.1002/dvdy.22678

Hodgkinson VS, Ericsson R, Johanson Z, Joss J (2009) The apical ectodermal ridge in the pectoral fin of the Australian lungfish (*Neoceratodus forsteri*): keeping the fin to limb transition in the fold. Acta Zool 90:253–263. doi:10.1111/j.1463-6395.2008.00349.x

Johanson Z, Joss J, Boisvert CA, Ericsson R, Sutija M, Ahlberg PE (2007) Fish fingers: digit homologues in sarcopterygian fish fins. J Exp Zool B Mol Dev Evol 308(6):757–768. doi:10.1002/jez.b.21197

Mariani FV, Martin GR (2003) Deciphering skeletal patterning: clues from the limb. Nature (Lond) 423(6937):319–325. doi:10.1038/nature01655

Martin JF, Olson EN (2000) Identification of a *prx1* limb enhancer. Genesis 26(4):225–229. doi:10.1002/(SICI)1526-968X(200004)26:4<225::AID-GENE10>3.0.CO;2-F

Norton WH, Ledin J, Grandel H, Neumann CJ (2005) HSPG synthesis by zebrafish Ext2 and Extl3 is required for Fgf10 signalling during limb development. Development (Camb) 132(22):4963–4973. doi:10.1242/dev.02084

Ohuchi H, Nakagawa T, Yamamoto A, Araga A, Ohata T, Ishimaru Y, Yoshioka H, Kuwana T, Nohno T, Yamasaki M, Itoh N, Noji S (1997) The mesenchymal factor, FGF10, initiates and maintains the outgrowth of the chick limb bud through interaction with FGF8, an apical ectodermal factor. Development (Camb) 124(11):2235–2244

Sakamoto K, Onimaru K, Munakata K, Suda N, Tamura M, Ochi H, Tanaka M (2009) Heterochronic shift in Hox-mediated activation of sonic hedgehog leads to morphological changes during fin development. PLoS One 4(4):e5121. doi:10.1371/journal.pone.0005121

Shimada A, Kawanishi T, Kaneko T, Yoshihara H, Yano T, Inohaya K, Kinoshita M, Kamei Y, Tamura K, Takeda H (2013) Trunk exoskeleton in teleosts is mesodermal in origin. Nat Commun 4:1639. doi:10.1038/ncomms2643

Shubin NH, Daeschler EB, Jenkins FA Jr (2006) The pectoral fin of *Tiktaalik roseae* and the origin of the tetrapod limb. Nature (Lond) 440(7085):764–771. doi:10.1038/nature04637

Smith M, Hickman A, Amanze D, Lumsden A, Thorogood P (1994) Trunk neural crest origin of caudal fin mesenchyme in the zebrafish *Brachydanio rerio*. Proc R Soc Lond B Biol Sci 256(1346):137–145

Suzuki M, Satoh A, Ide H, Tamura K (2007) Transgenic *Xenopus* with prx1 limb enhancer reveals crucial contribution of MEK/ERK and PI3K/AKT pathways in blastema formation during limb regeneration. Dev Biol 304(2):675–686. doi:10.1016/j.ydbio.2007.01.019

Tamura K, Yonei-Tamura S, Yano T, Yokoyama H, Ide H (2008) The autopod: its formation during limb development. Dev Growth Differ 50(suppl 1):S177–S187. doi:10.1111/j.1440-169X.2008.01020.x

Tarchini B, Duboule D, Kmita M (2006) Regulatory constraints in the evolution of the tetrapod limb anterior–posterior polarity. Nature (Lond) 443(7114):985–988. doi:10.1038/nature05247

Thorogood P (1991) The development of the teleost fin and implications for our understanding of tetrapod evolution. Developmental patterning of the vertebrate limb. Plenum, London, pp 347–354

Witten PE, Huysseune A (2007) Mechanisms of chondrogenesis and osteogenesis in fins. In: Witten PE, Huysseune A, Hall B (eds) Fins into limbs: evolution, development, and transformation. University of Chicago Press, Chicago, pp 79–92

Yano T, Tamura K (2013) The making of differences between fins and limbs. J Anat 222(1):100–113. doi:10.1111/j.1469-7580.2012.01491.x

Yano T, Abe G, Yokoyama H, Kawakami K, Tamura K (2012) Mechanism of pectoral fin outgrowth in zebrafish development. Development (Camb) 139(16):2916–2925. doi:10.1242/dev.075572

Yonei-Tamura S, Endo T, Yajima H, Ohuchi H, Ide H, Tamura K (1999) FGF7 and FGF10 directly induce the apical ectodermal ridge in chick embryos. Dev Biol 211(1):133–143. doi:10.1006/dbio.1999.9290

Chapter 23
The Turtle Evolution: A Conundrum in Vertebrate Evo-Devo

Naoki Irie*, Hiroshi Nagashima*, and Shigeru Kuratani

Abstract Because of their unique morphology, turtles have raised profound questions as to their evolutionary origin. In striking contrast to the body plan of other tetrapods, the shoulder girdle of turtles sits inside the rib cage, which comprises the dorsal shell, or carapace. By this topological change of the skeletal elements, the carapace has been regarded as an example of evolutionary novelty that violates the ancestral body plan of tetrapods. In this chapter, we first overview the phylogenetic positioning of turtles, and then review how turtles evolved their unique body plan. In brief, three points have been clarified by recent studies. (1) Turtles have birds/crocodilians (or archosaurians) affinity of evolutionary origin. (2) During embryogenesis, the turtle also establishes the vertebrate basic body plan, as in other vertebrates, followed by the late developmental stages of generating turtle-specific structures, such as folding of the lateral body wall to make the apparent inside-out topology of shoulder girdle against ribs. (3) One of the causal factors of folding appears to be the concentric growth of carapacial margin, which involves an ancestral gene expression cascade in a new location. These reports allow us to hypothesize the

*Author contributed equally with all other contributors.

N. Irie
Laboratory for Evolutionary Morphology, RIKEN Center for Developmental Biology, 2-2-3 Minatojima-minami, Chuo, Kobe, Hyogo 650-0047, Japan

Department of Biological Sciences, Graduate School of Science, University of Tokyo, Tokyo, Japan
e-mail: irie@biol.s.u-tokyo.ac.jp

H. Nagashima
Division of Gross Anatomy and Morphogenesis, Department of Regenerative and Transplant Medicine, Niigata University, Niigata, Japan
e-mail: nagahiro@med.niigata-u.ac.jp

S. Kuratani (✉)
Laboratory for Evolutionary Morphology, RIKEN Center for Developmental Biology, 2-2-3 Minatojima-minami, Chuo, Kobe, Hyogo 650-0047, Japan
e-mail: saizo@cdb.riken.jp

H. Kondoh and A. Kuroiwa (eds.), *New Principles in Developmental Processes*,
DOI 10.1007/978-4-431-54634-4_23, © Springer Japan 2014

stepwise, not necessarily saltatory, evolution of turtles, consistent with the recent finding of a transitional fossil animal, *Odontochelys*, that did not have the carapace but already possessed the plastron.

Keywords Development • Evolution • Phylogeny • Phylotype • Turtle

23.1 Introduction

Turtles have long been regarded not only as the most primitive extant amniotes but also as animals that evolved abruptly without any intermediate morphology. Their skull does not possess any temporal fenestrae (representing the anapsid state), a character that was once hypothesized to be a hallmark of basal amniotes and their ancestral amphibians (Romer 1956; reviewed by Tsuji and Müller 2009). The trunk of turtles, on the other hand, shows an extensively derived feature. The turtle shell is composed of dorsal and ventral moieties; the ventral moiety is referred to as a plastron, consisting of nine dermal elements corresponding to clavicle, interclavicle, and gastralia in other amniotes (Fig. 23.1b–d). The dorsal shell, termed the carapace, comprises the thoracic vertebrae, ribs, and dermal bones surrounding the axial skeleton (Fig. 23.1a). In many turtle species, these bony shells are covered by keratinous scutes, whereas in some species, such as the soft-shelled turtles, the scutes and the peripheral dermal bones are lost.

The outstanding feature in the turtle flank is not the shell itself, but the resultant body plan of turtles (Burke 2009). Turtle ribs, rather than growing ventrally, grow laterally to form the carapace, and the uniqueness of the turtles is that their shoulder girdle composed of scapula and coracoid is housed inside the ribcage. This inside-out morphology appears to have been established by violating the basic rules of the vertebrate body plan, thus regarded as a typical example of evolutionary novelties (Hall 1998; Rieppel 2001; Gilbert et al. 2001, 2008).

Lack of any transitional patterns to explain this turtle-specific topological change, as well as the absence of intermediate fossils, have led biologists to assume that turtles emerged by saltatory evolution (reviewed by Nagashima et al. 2012a). In this section, we overview the evolutionary origin of turtles by introducing studies aimed to clarify the phylogenetic position of turtles, followed by studies focused on the body plan evolution of turtles.

Fig. 23.1 (continued) (*epi*) is homologized with clavicle, entplastron (*ent*) with interclavicle, and other dermal bones with gastralia. **c**, **d** Comparison of body plan between other amniotes (**c**) and turtles (juvenile of Chinese soft-shelled turtle, *Pelodiscus sinensis*) (**d**). Note that scapula (*sc*) and coracoid (*cor*) are outside of the ribs in other amniotes and inside the ribs in turtles. *ca* carapace, *c* clavicle, *cos* costal plate, *g* gastralia, *hyo* hyoplastron, *hypo* hypoplastron, *ic* interclavicle, *neu* neural plate, *nu* nuchal plate, *pe* peripheral plate, *pl* plastron, *py* pygal plate, *r* dorsal ribs, *spy* suprapygal plate, *v* dorsal vertebrae, *xiphi* xiphiplastron (figure modified from Nagashima et al. 2012a)

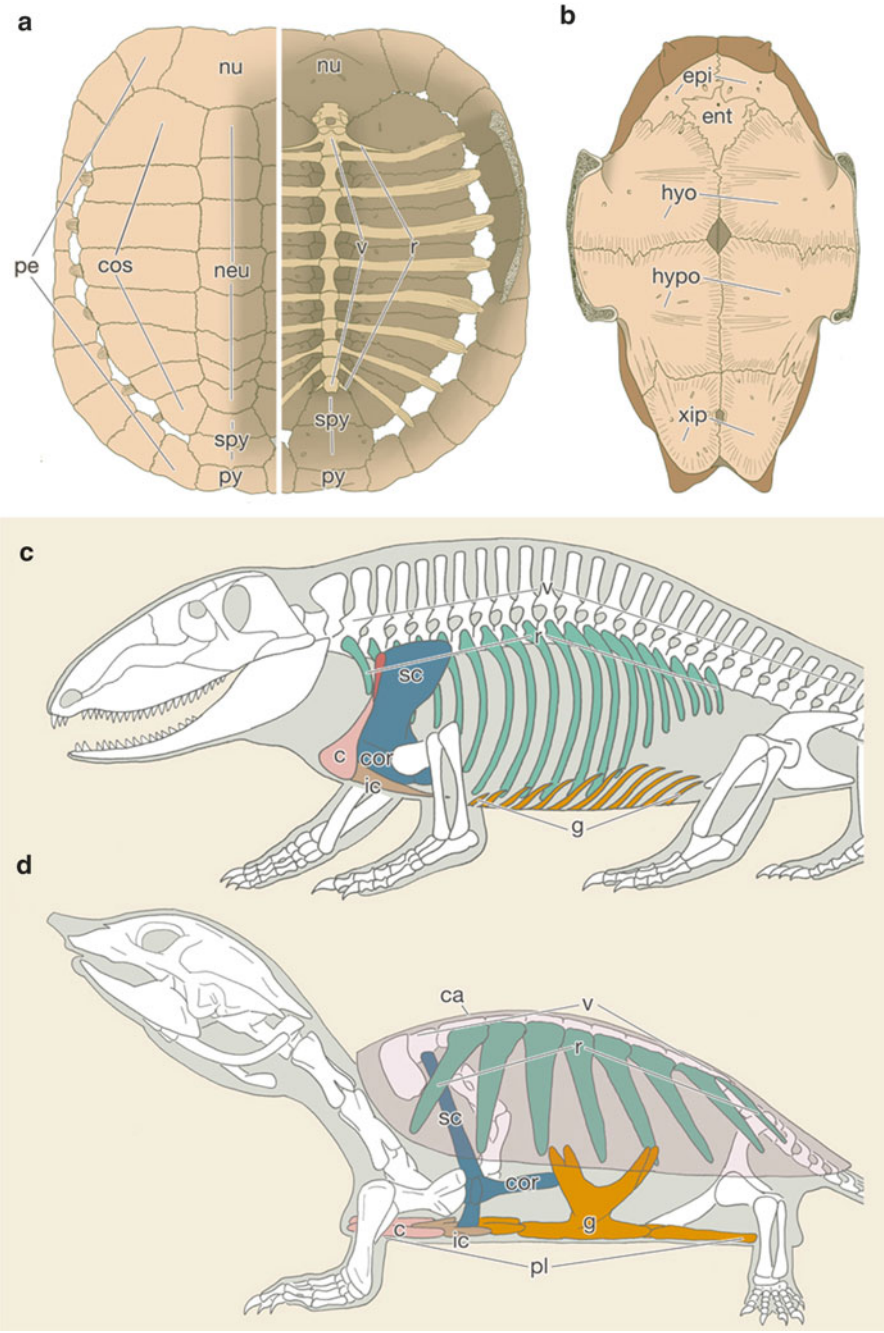

Fig. 23.1 The turtle shell and body plan of turtles. **a**, **b** Turtle shell. **a** Dorsal (*left*) and ventral (*right*) views of the carapacial skeleton of *Chinemys reevesii*. The carapace is formed by ribs (*r*), vertebrae (*v*), and dermal bones arranged peripherally. **b** Dorsal view of the plastron. Epiplastron

23.2 Phylogenetic Position of Turtles

When and where did turtles come into being? Historically, three major hypotheses have been proposed for the phylogenetic origin of turtles. Largely based on the skull morphology, the earliest hypothesis relegated turtles to early-diverged reptiles, called anapsids, located basal to Diapsida (Tsuji and Müller 2009; Kuratani et al. 2011). Meanwhile, with almost every accessible element from egg, embryo, and adult morphology, Rieppel and de Braga (1996) proposed the turtle as a sister group with the lizard–snake–tuatara (Lepidosauria) clade (Fig. 23.2). As the third hypothesis, first by molecular phylogenetic analysis with rRNA (Hedges et al. 1990), and other molecular studies (Caspers et al. 1996; Crawford et al. 2012), it was alleged that turtles are closely related to a lineage including crocodilians and birds (Archosauria) (Fig. 23.2). What confused researchers was that controversy arose even among the molecular-based approaches. Based on the existence or absence of miRNAs,

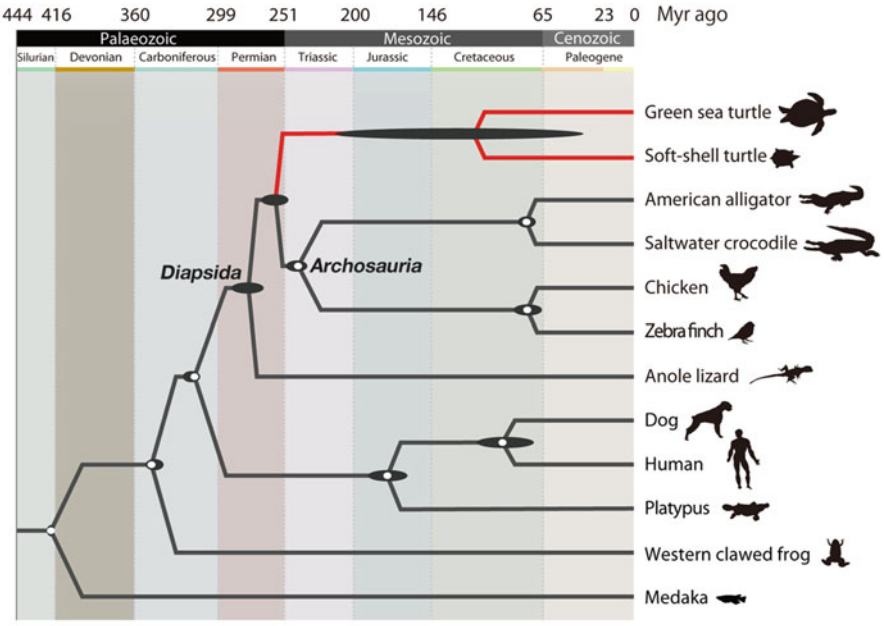

Fig. 23.2 The common ancestor of turtles arose around 267.9–248.3 million years ago, splitting from archosaurians. Molecular phylogenetic analysis based on genome-wide data (1,113 orthologous genes from 12 vertebrate species) supported that turtles are a sister group of archosaurians. Molecular clock analysis, calibrated with fossil records (*white dots* in each branching node) supported that the split occurred around 267.9–248.3 million years ago, the period that overlaps or followed shortly after the Permian extinction event (Chen and Benton 2012). The *black ellipses* on the nodes indicate the 95 % credibility intervals of the estimated posterior distributions of the divergence times (figure modified from Wang et al. 2013)

Lyson et al. (2012) reported that the turtles are a sister group of Lepidosauria. For this study, however, Hedges (2012) draws cautionary attention that the phylogenetic analysis using miRNA is yet to be established to obtain significant results. Finally, recent studies that reported the draft genome sequences of turtles (*Pelodiscus sinensis* and *Chelonia mydas*, by Wang et al. 2013; *Chelonia picta*, by Shaffer et al. 2013), robustly supported the archosaurian affinity of turtles (Fig. 23.2).

These molecular phylogenetic studies are already making some impact on paleontological study, and some paleontologists are reexamining the morphological characters to reconcile morphological data with molecular results (Rieppel 2000). For example, morphology of the vormer (Damiani and Modesto 2001), temporal region (Müller 2003), and carotid circulation (Müller et al. 2011) are suggested not to support a turtle–anapsids relationship. The presence of a laterosphenoid ossification in a basal turtle is proposed to unite turtles to Archosauria (Bhullar and Bever 2009). In the archosauromorph lineage, Merck (1997) found the Euryapsida (Helveticosaurus, Sauropterygia, and Ichthyosauria)–Thalattosauria clade, to which turtles are suggested to be a sister group (Rieppel and de Braga 1996).

Although the ancestor did not possess the complete dorsal shell such as that in existing turtles, the oldest known fossil turtle, *Odontochelys* (Li et al. 2008), showed that the turtle ancestor already existed 220 million years ago. Consistent with this oldest fossil record, Wang et al. (2013), based on their genome-wide dataset including two turtle species (Chinese soft-shelled turtle and green sea turtle), estimated that the common ancestor of turtles already existed before the emergence of *Odontochelys*. According to the estimate based on genome-wide analysis, turtles split from the lineage of archosaurians at around 267.9–248.3 million years ago. Interestingly, the period coincides with the one of the largest mass extinction events on this planet, called the Permian-Triassic extinction event (Chen and Benton 2012). However, whether this extinction event has a certain role in the evolution of the turtle ancestor awaits further investigation.

23.3 Body Plan Development and Evolution of Turtles

How did turtles evolve their unique body plan after splitting from the archosaurians (the group consisting of birds/crocodilians)? Substantial contribution has been made to this question by recent comparative embryonic studies.

Despite the uniqueness of the turtle body plan, recent studies clarified that turtles also follow the general rule for embryonic evolution of vertebrates, or the developmental hourglass model (Fig. 23.3) (Duboule 1994; Irie and Kuratani 2011; Wang et al. 2013), to produce their unique body. The model explains that vertebrate embryos pass through the conserved bottleneck-like period, the period that shows the basic vertebrate body plan (called the phylotypic period), and then specialize afterward. Meanwhile, earlier to, or later than, this phylotypic period, divergent characteristics appear among different species. Actually, the midembryonic stages

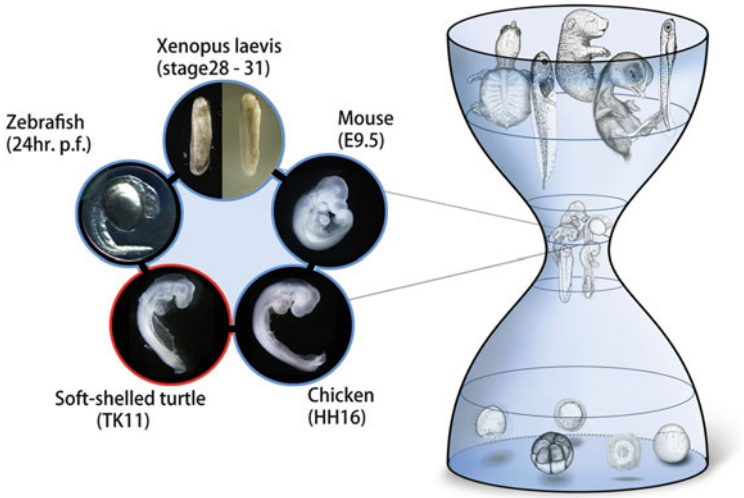

Fig. 23.3 Turtles also follow the developmental hourglass model during embryogenesis. The hourglass model (*right*), first proposed by Duboule (1994), explains that vertebrate embryogenesis is rather divergent during early and late stages whereas midembryonic stages show maximum similarity both in morphology and in whole embryonic gene expression profile. The bottleneck period, called the vertebrate phylotypic period, becomes the source of the vertebrate basic body plan found among adult vertebrates. The horizontal width of the hourglass model represents the evolutionary divergence among vertebrate embryos, and embryogenesis flows upward in this drawing. Recent molecular studies (Irie and Kuratani 2011; Wang et al. 2013) identified that pharyngular embryos are the stages that show most conservation among vertebrates

of turtles and chicken (e.g., stage TK11 of turtle and stage HH16 of chicken) appear somewhat more similar to each other than the earlier and later embryonic stages (Fig. 23.4). Furthermore, quantitative evidence was obtained from the study that took advantage of whole embryonic gene expression profiles (Wang et al. 2013), showing that maximal similarity between turtle and chicken embryos appears in the pharyngula stages (Fig. 23.4; red dashed circles). Direct inference of this observation suggests that turtles, similar to other vertebrates, develop their body first by establishing the vertebrate basic body plan, and then modify the developmental trajectory to obtain the turtle-specific morphological patterns. Actually, the first sign of a turtle-specific character, the carapacial ridge (CR; Figs. 23.4 and 23.5) (Burke 1989), appears after this phylotypic period (see following section). These studies as a whole tell us that the turtle body plan evolved by adding major changes to the embryonic stages after the vertebrate phylotypic period during evolution. Actually, Wang et al. reported that genes that potentially explain the turtle-specific features, such as genes involved in ossification, extracellular matrix reorganization, and collagen, show increasing expression only in the later phase of turtle embryogenesis (Wang et al. 2013).

Finally, the reason why turtles still adhere to the conservation of the vertebrate phylotypic period is not clear; however, some researchers attribute this to a particularly complex signaling network working in this embryonic period (e.g., Hox colineality, interdependent molecular signals: Duboule 1994; Raff 1996).

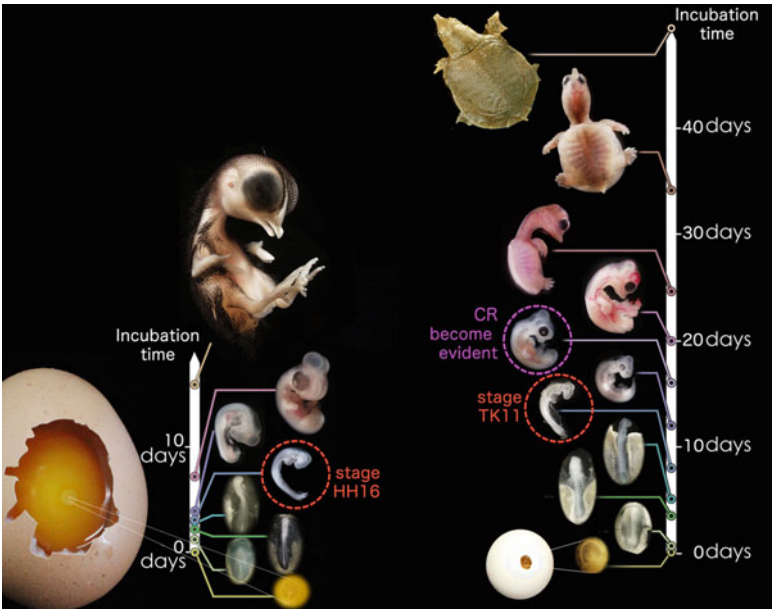

Fig. 23.4 External appearances of chicken and Chinese soft-shelled turtle embryos. Soft-shelled turtle embryogenesis shows a rather different morphology of the gastrula but soon converges to show similar morphology with the chicken at around the pharyngula stage. Actually, chicken stage HH 16 (Hamburger and Hamilton 1951) and turtle stage TK 11 (Tokita and Kuratani 2001) show the most similar gene expression profile compared to other developmental stages (*dashed circles*). These embryos show striking similarity in morphology as well, despite the fact that these two species split more than 250 million years ago, with almost twice the time for embryogenesis. *White arrows* show the direction and relative length of time needed for embryogenesis. Size of embryos not to scale

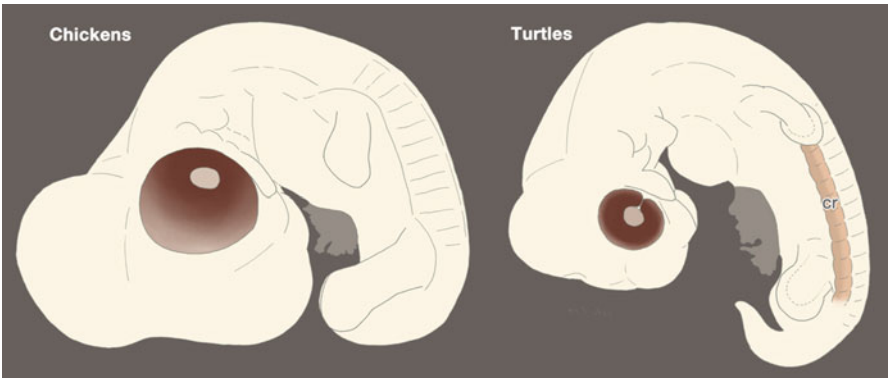

Fig. 23.5 Development of the carapacial ridge in turtle embryos. Comparison of the external morphology of embryos of stage 26 chicken and stage 14 *Pelodiscus sinensis*. In turtle embryos, the most ventral part of the axial part swells and makes a longitudinal ridge, which represents the carapacial ridge (*cr*)

23.4 Carapacial Ridge

As mentioned earlier, the CR appears after the phylotypic period as a longitudinal ridge on the lateral aspect of the flank of turtle embryos (Fig. 23.5). The CR forms the leading edge of the developing carapace, and functions to make the turtle-specific rostrocaudally expanded pattern of ribs through accelerated growth of the carapacial margin (Figs. 23.5 and 23.6) (Burke 1989, 1991; Nagashima et al. 2007).

Morphologically, the embryonic body is composed of the dorsomedially located axial part and the ventrolaterally lateral body wall. The dermal mesenchyme of the former is derived from somites and that of the latter from the somatic mesoderm. The CR develops at the ventrolateral edge of the axial domain and delineates a boundary between the two kinds of dermal mesenchyme with its ventral edge through its development, which indicates the uniqueness of the structure among amniote embryos, because such a structure does not appear in other amniote embryos (Figs. 23.5 and 23.6) (reviewed by Kuratani et al. 2011).

Although the precise molecular mechanism involved in CR development is yet to be clarified, some studies have provided intriguing insights. Through a subtractive

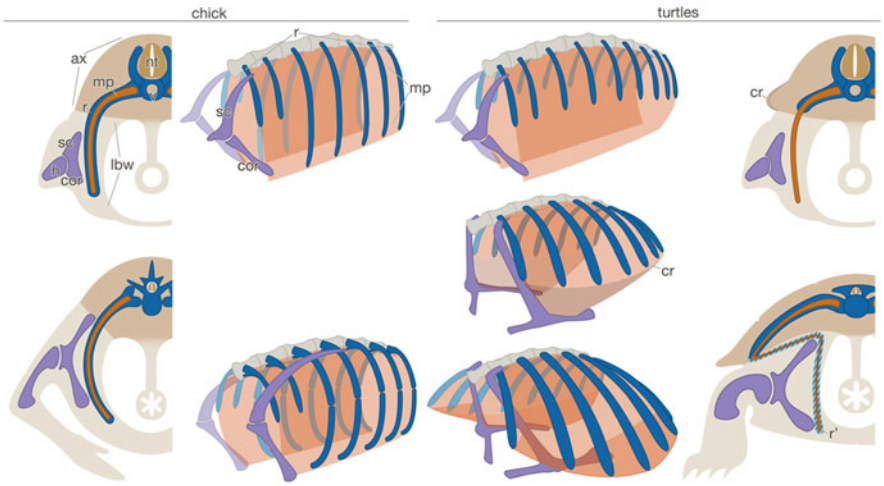

Fig. 23.6 A scheme representing trunk development in the chicken (*left*) and turtle (*right*). Plates at both *lateral ends* are transverse views; those in the *middle columns* are lateral view. From top to bottom, development proceeds as follows. *Top:* Both animals have nearly identical morphology at an early developmental stage. Note that turtle ribs (*r*) are morphologically shorter than those of chicken but grow along the the muscle plate (*mp*) as do chicken ribs. *Middle* and *bottom:* Chicken development proceeds without a major change in morphology from the initial state. The folding process occurring in the late developmental stage of turtles does not change the topological relationship between the ribs, muscle plate, and shoulder girdle from that at the beginning of development. Note that only the body folding is different between the animals. *Shaded domain* (*r′*) in transverse view of turtles (*bottom*) represents undeveloped ribs in the lateral body wall, which are expected to be found along the muscle plate as are those in chicken. *ax* axial domain, *h* humerus, *lbw* lateral body wall, *nt* neural tube, *v* vertebrae (figure modified from Nagashima et al. 2012a)

cDNA screening method, Kuraku et al. (2005) identified four genes specifically expressed in the CR, which include *cellular retinoic acid-binding protein* (*Crabp*)-*I*, *Sp-5*, *lymphocyte enhancer factor* (*Lef*)-*1*, and *Apcdd-1*. All these genes are components of, or are related to, the canonical Wnt signaling pathway (Kuratani et al. 2011). Actually, localization of β-catenin in nuclei of the CR epidermis (Kuraku et al. 2005) and arrest of CR formation after the inhibition of Lef-1 activity suggest that the Lef-1/β-catenin complex is involved in CR development as a transcriptional activator of the signal cascade (Nagashima et al. 2007).

Recently, based on comprehensive in situ hybridization screening that took advantages of turtle genomes, one of the upstream factors, *Wnt 5a* expression, was discovered in the CR mesenchyme (Wang et al. 2013). The reason why the subtractive cDNA method between the CR and the lateral body wall failed to detect this gene is that the gene was also expressed in the body wall. As another upstream molecule, hepatocyte growth factor (HGF) expressed at the vicinity of the CR is suggested; inactivation of HGF function leads to degradation of the CR (Kawashima-Ohya et al. 2011). Consistent with this, carcinoma studies have found regulation of the canonical Wnt pathway by HGF (Nelson and Nusse 2004). In chicken and mouse embryos, expressions of the orthologous genes are not observed at the corresponding site, reconfirming the novel nature of the CR. Many of the genes are commonly expressed in the limb bud of the amniote embryos including turtles, indicating that some of the gene cascade functioning in limb development would be secondarily recruited to invent the CR (Kuratani et al. 2011; also see Gilbert et al. 2001, 2008).

23.5 Positional Change of Ribs and Scapula

One of the differences between turtle ribs and those of other amniotes is the relative lengths of the ribs: the turtle ribs are morphologically shorter than those of other amniotes, because turtle ribs are arrested in the axial domain, never penetrating into the lateral body wall as in many other amniotes (axial arrest of the ribs; Fig. 23.6) (Burke 1989; Nagashima et al. 2007; Kuratani et al. 2011).

As the cause for the truncation of turtle ribs, a turtle-specific expression pattern of *Hox* genes and unique features of Myf5 have been proposed (Ohya et al. 2005, 2006; Nagashima et al. 2012a, b). Especially, transcriptional factor Myf5 is involved not only in myogenic activity but also in inductive activity of ribs (Nagashima et al. 2012b), which would explain both rib truncation and the characteristic meager development of muscle plates, elongated myotomes, in turtles (Nagashima et al. 2005).

At first glance, turtle ribs appear to take different trajectories from those in other amniotes because they grow laterally and superficially. The turtle ribs, however, are along the muscle plate as are chicken and mouse ribs (Fig. 23.6), reflecting that the ribs are induced by the muscle plate. Hence, it is convincing to suppose that if turtles would have long ribs, they would be found along the muscle plate in the lateral body wall, indicating that the muscle plate can be regarded as “the latent ribcage.”

The shoulder girdle of turtles initially develops rostral to the ribs and outside the muscle plate or "the latent ribcage" as that in other amniotes (Fig. 23.6). Although chicken and mouse development proceed without much modification of this pattern, in turtles, the CR renders some of the rostral ribs fanned out rostrally to cover the scapula caudodorsally (Fig. 23.6). During this process, the shoulder girdle remains outside the muscle plate, which is now severely folded inward in the lateral body wall (Fig. 23.6). Thus, turtles change the spatial relationship between the ribs and shoulder girdle by folding the lateral body wall inward after skeletal development, and this process does not alter the body plan of amniotes (Nagashima et al. 2009).

These developmental findings highlight and fill the saltatory evolutionary gap once believed to be present in turtle evolution; namely, axial arrest, fanned-out expansion of ribs, and encapsulation of the scapula would have occurred in the ancestral animals of turtles successively. Illustrating this, a previously unknown fossil, *Odontochelys*, has intermediate morphology linking turtles and the ancestral animals (Li et al. 2008). This animal did not have a complete carapace but did have the plastron. The ribs were already arrested axially but did not show a flabellate pattern, so the scapula was still situated rostral to the ribs. This pattern is reminiscent of the morphological pattern of turtle embryos before the folding process. Thus, morphogenesis of *Odontochelys* would have been completed at this developmental stage and would not have acquired developmental programs to expand the ribs and to encase the shoulder girdle. Turtle evolution would have been achieved by secondarily adding the folding process in the late developmental phase of *Odontochelys-like* ancestral animals (Nagashima et al. 2009).

23.6 Perspective

Our studies have suggested that stepwise changes of the developmental program have caused the evolution of turtles. By comparative genomics as well as analyses of gene regulations, it could become possible in the near future to ascertain the net elements that are truly relevant to the modification of the animal body plan, especially through construction of a turtle-like developmental phenocopy by means of functional assays on model animals. By understanding the creation of animals such as turtles, which apparently violate the developmental constraints specific to vertebrates, we will be able eventually to correlate the DNA sequence and evolving morphology of animals. For this reason, turtles potentially provide very intriguing and promising aspects for the study of evolutionary developmental biology.

References

Bhullar B-AS, Bever GS (2009) An archosaur-like laterosphenoid in early turtles (Reptilia: Pantestudines). Breviora 518:1–11

Burke AC (1989) Development of the turtle carapace: implications for the evolution of a novel bauplan. J Morphol 199:363–378

Burke AC (1991) The development and evolution of the turtle body plan. Inferring intrinsic aspects of the evolutionary process from experimental embryology. Am Zool 31:616–627
Burke AC (2009) Turtles……again. Evol Dev 11:622–624
Caspers GJ, Reinders GJ, Leunissen JA, Wattel J, de Jong WW (1996) Protein sequences indicate that turtles branched off from the amniote tree after mammals. J Mol Evol 42:580–586
Chen Z-Q, Benton MJ (2012) The timing and pattern of biotic recovery following the end-Permian mass extinction. Nat Geosci 5:375–383
Crawford NG, Faircloth BC, McCormack JE, Brumfield RT, Winker K, Glenn TC (2012) More than 1000 ultraconserved elements provide evidence that turtles are the sister group of archosaurs. Biol Lett 8:783–786
Damiani RJ, Modesto JP (2001) The morphology of the pareiasaurian vomer. N Jb Geol Paläont Mh 7:423–434
Duboule D (1994) Temporal colinearity and the phylotypic progression: a basis for the stability of a vertebrate bauplan and the evolution of morphologies through heterochrony. Development (Camb) 1994:135–142
Gilbert SF, Loredo GA, Brukman A, Burke AC (2001) Morphogenesis of the turtle shell: the development of a novel structure in tetrapod evolution. Evol Dev 3:47–58
Gilbert SF, Cebra-Thomas JA, Burke AC (2008) How the turtle gets its shell. In: Wyneken J, Godfrey MH, Bels V (eds) Biology of turtles. CRC, Boca Raton, pp 1–16
Hall BK (1998) Evolutionary developmental biology, 2nd edn. Chapman & Hall, London
Hamburger V, Hamilton HL (1951) A series of normal stages in the development of the chick embryo. J Morphol 88:49–92
Hedges SB (2012) Amniote phylogeny and the position of turtles. BMC Biol 10:64
Hedges SB, Moberg KD, Maxson LR (1990) Tetrapod phylogeny inferred from 18S and 28S ribosomal RNA sequences and a review of the evidence for amniote relationships. Mol Biol Evol 7:607–633
Irie N, Kuratani S (2011) Comparative transcriptome analysis reveals vertebrate phylotypic period during organogenesis. Nat Commun 2:248
Kawashima-Ohya Y, Narita Y, Nagashima H, Usuda U, Kuratani S (2011) Hepatocyte growth factor is crucial for development of the carapace in turtles. Evol Dev 13:260–268
Kuraku S, Usuda R, Kuratani S (2005) Comprehensive survey of carapacial ridge-specific genes in turtle implies co-option of some regulatory genes in carapace evolution. Evol Dev 7:3–17
Kuratani S, Kuraku S, Nagashima H (2011) Evolutionary developmental perspective for the origin of the turtles: the folding theory for the shell based on the developmental nature of the carapacial ridge. Evol Dev 13:1–14
Li C, Wu X, Rieppel O, Wang L, Zhao L (2008) An ancestral turtle from the Late Triassic of southwestern China. Nature (Lond) 45:497–501
Lyson TR, Sperling EA, Heimberg AM, Gauthier JA, King BL et al (2012) MicroRNAs support a turtle + lizard clade. Biol Lett 8:104–107
Merck JW (1997) A phylogenetic analysis of the euryapsid reptiles. Unpublished Ph.D. dissertation, University of Texas at Austin
Müller J (2003) Early loss and multiple return of the lower temporal arcade in diapsid reptiles. Naturwissenschaften 90:473–476
Müller J, Sterli J, Anquetin J (2011) Carotid circulation in amniotes and its implications for turtle relationships. N Jb Geol Paläont Abh 261:289–297
Nagashima H, Uchida K, Yamamoto K, Kuraku S, Usuda R, Kuratani S (2005) Turtle-chicken chimera: an experimental approach to understanding evolutionary innovation in the turtle. Dev Dyn 232:149–161
Nagashima H, Kuraku S, Uchida K, Ohya YK, Narita Y, Kuratani S (2007) On the carapacial ridge in turtle embryos: its developmental origin, function, and the chelonian body plan. Development (Camb) 134:2219–2226
Nagashima H, Sugahara F, Takechi M, Ericsson R, Kawashima-Ohya Y, Narita Y, Kuratani S (2009) Evolution of the turtle body plan by the folding and creation of new muscle connections. Science 325:193–196

Nagashima H, Kuraku S, Uchida K, Kawashima-Ohya Y, Narita Y, Kuratani S (2012a) Body plan of turtles: an anatomical, developmental and evolutionary perspective. Anat Sci Int 87:1–13

Nagashima H, Kuraku S, Uchida K, Kawashima-Ohya Y, Narita Y, Kuratani S (2012b) Origin of the turtle body plan: the folding theory to illustrate turtle-specific developmental repatterning. In: Brinkman DB, Holroyd PA, Gardner JD (eds) Morphology and evolution of turtles: origin and early diversification. Springer, Dordrecht

Nelson WJ, Nusse R (2004) Convergence of Wnt, β-catenin, and cadherin pathways. Science 303:1483–1487

Ohya YK, Kuraku S, Kuratani S (2005) Hox code in embryos of Chinese soft-shelled turtle *Pelodiscus sinensis* correlates with the evolutionary innovation in the turtle. J Exp Zool 304B:107–118

Ohya YK, Usuda R, Kuraku S, Nagashima H, Kuratani S (2006) Unique features of Myf-5 in turtles: nucleotide deletion, alternative splicing and unusual expression pattern. Evol Dev 8:415–423

Raff A (1996) The shape of life: genes, development, and the evolution of animal form. University of Chicago Press, Chicago

Rieppel O (2000) Turtles as diapsid reptiles. Zool Scr 29:199–212

Rieppel O (2001) Turtles as hopeful monsters. Bioessays 23:987–991

Rieppel O, de Braga M (1996) Turtles as diapsid reptiles. Nature (Lond) 384:453–455

Romer AS (1956) Osteology of the reptiles. University of Chicago Press, Chicago

Shaffer HB, Minx P, Warren DE, Shedlock AM, Thomson RC, Valenzuela N et al (2013) The western painted turtle genome, a model for the evolution of extreme physiological adaptations in a slowly evolving lineage. Genome Biol 14:R28

Tokita M, Kuratani S (2001) Normal embryonic stages of the Chinese soft-shelled turtle *Pelodiscus sinensis*. Zool Sci 18:705–715

Tsuji LA, Müller J (2009) Assembling the history of the Parareptilia: phylogeny, diversification, and a new definition of the clade. Fossil Rec 12:71–81

Wang Z, Pascual-Anaya J, Zadissa A, Li W, Niimura Y, Huang Z et al (2013) The draft genomes of soft-shell turtle and green sea turtle yield insights into the development and evolution of the turtle-specific body plan. Nat Genet. doi:10.1038/ng.2615

Name Index

H. Kondoh and A. Kuroiwa (eds.), *New Principles in Developmental Processes*,
DOI 10.1007/978-4-431-54634-4, © Springer Japan 2014

Subject Index

H. Kondoh and A. Kuroiwa (eds.), *New Principles in Developmental Processes*,
DOI 10.1007/978-4-431-54634-4, © Springer Japan 2014